

Toward On-Demand Peptide Synthesis:
Development and Application of Enantioselective Syntheses of Unnatural α -Amino Amides

By

Kenneth E. Schwieter

Dissertation

Submitted to the Faculty of the
Graduate School of Vanderbilt University
in partial fulfillment of the requirements
for the degree of

DOCTOR OF PHILOSOPHY

in

CHEMISTRY

December 2016

Nashville, Tennessee

Approved:

Jeffrey N. Johnston, Ph.D.

Gary A. Sulikowski, Ph.D.

Nathan D. Schley, Ph.D.

Robert H. Carnahan, Ph.D.

To my Mom

ACKNOWLEDGMENTS

This document is not solely the work of one person, but of the many people who supported me and contributed to my success in both graduate school and all other aspects of my life. I am incredibly grateful for all of the support and contributions.

First, I would like to thank my advisor Dr. Jeffrey Johnston for his mentorship and support for the past six years. His wealth of knowledge, problem solving skills, and never-ending work ethic have served as an inspiration. I would not be the chemist I am today if he had not invested so much of his time and resources in me. He has also assisted me in putting out many Microsoft Word formatting fires, and for this I am eternally grateful.

I would also like to acknowledge the many members of the Johnston group, past and present, that I have had the pleasure to work with and learn from: Tyler Davis and Mark Dobish for welcoming me to the lab and showing me what it takes to succeed in graduate school, Sergey Tsukanov for being a great friend and providing endless entertainment, and Matt Knowe for always being willing to talk soccer. Additionally, I would like to acknowledge Marta Wenzler and Emilianne Limbrick for constant lunchtime entertainment.

I would like to thank my Ph. D. committee for their guidance and help throughout this process: Prof. Gary Sulikowski, Prof. Nathan Schley, Prof. Robert Carnahan, and Prof. Piotr Kaszynski. My research would not have been possible without support from the departmental staff, specifically Don Stec and Markus Voehler for maintaining the NMR facilities and providing the necessary assistance. This work would also not be possible without the financial support provided by the NIH (GM 063557).

I reserve my greatest gratitude for my parents, Ed and Ann. They have always supported me in all aspects of my life. I can never thank them enough for everything they have done for me. Without their love, I would not be the person I am today. They always stressed the importance of education and I owe my inspiration for coming to graduate school to them. I would also like to recognize my brother Andy and my sister Juliann for their never-ending love and support. I would also like to thank my in-laws, Ed and Linda, for welcoming me to their family and supporting me through this journey.

Finally, I would like to thank my wife, Bethany. She is an amazing, talented, and loving woman who has endlessly supported me through the ups and downs of this process. Without her love and support (and cooking), none of this would be possible. I am eternally grateful for everything she has done, and I could not imagine life without her.

TABLE OF CONTENTS

	Page
ACKNOWLEDGMENTS	iii
LIST OF FIGURES	vi
LIST OF SCHEMES.....	viii
LIST OF TABLES.....	xi
 Chapter	
I. Development of Umpolung Amide Synthesis Substoichiometric in NIS.....	1
1.1 Importance and Synthesis of Amides.....	1
Coupling Reagents in Amide Bond Synthesis	1
Peptide Synthesis	3
Catalytic Amide Bond Formation	5
1.2 Umpolung Amide Synthesis	10
1.3 Umpolung Amide Synthesis Substoichiometric in NIS.....	12
II. Organocatalyzed Enantioselective Synthesis of α -Alkyl Unnatural α -Amino Amides.....	16
2.1 Importance and Synthesis of Unnatural Amino Acids.....	16
Catalytic Asymmetric Synthesis of Unnatural Alkyl Amino Acids	19
2.2 The aza-Henry Reaction	23
Alkyl Imines as Electrophiles in the Enantioselective aza-Henry Reaction	25
Bromonitromethane Additions.....	28
Chiral Proton Catalysis	31
2.3 Bis(Amidine) Catalyzed Bromonitromethane Addition to Alkyl <i>N</i> -Tosyl-Imines.....	31
Previous Efforts	33
Additions of Bromonitromethane to Alkyl <i>N</i> -Tosyl-Imines.....	35
Umpolung Amide Synthesis with <i>N</i> -Tosyl Bromonitroalkanes	42
2.4 Bis(Amidine)-Catalyzed Bromonitromethane Additions to Alkyl <i>N</i> -Boc Imines.....	46
2.5 Catalytic Enantioselective Synthesis of D-Amino Amides using a Phase Transfer Catalyzed aza-Henry Addition and Umpolung Amide Synthesis	48
Background: Palomo's Phase Transfer Catalyzed aza-Henry Reaction	48
Phase Transfer Catalyzed aza-Henry with Bromonitromethane	49
2.6 Enantioselective Addition of Bromonitromethane to Aliphatic <i>N</i> -Boc Aldimines Using a Homogeneous Bifunctional Chiral Organocatalyst	57

III. Oxidative Amidation of Primary Nitroalkanes	63
3.1 Nitroalkane to Carbonyl Transformation	63
Nef Reaction	63
Kornblum Chemistry	65
3.2 One-pot Oxidative Amidation of Primary Nitroalkanes	66
Investigation of Nitrolic Acid Intermediate	66
Discovery of a One-pot Oxidative Amidation of Primary Nitroalkanes	67
Comparison with Hayashi Protocol	71
IV. Synthesis of a Fluorinated Feglymycin Derivative, Ffeglymycin	76
4.1 Feglymycin: Isolation and Background	76
Isolation and Structure Determination	76
Biological Activity	77
4.2 Süßmuth's Synthesis of Feglymycin	78
4.3 Previous Efforts Towards the Synthesis of Feglymycin	82
4.4 Synthesis of Ffeglymycin and other Derivatives	87
Synthesis of Ffeglymycin.....	87
Efforts Towards the Synthesis of other Feglymycin Analogues.....	96
V. Umpolung Amide Synthesis: Mechanistic Investigation	101
5.1 UmAS: Current Mechanistic Understanding	101
Hayashi-Lear: Nitroalkane Amidation Mechanism	103
5.2 UmAS: Mechanistic Investigation	105
Dihalonoalkane vs. Monohalonoalkane	105
N-Iodamine and other Electrophilic Amine Sources	109
Kinetic Studies	114
Investigating the Tetrahedral Intermediate: Preliminary and Future Work	115
VI. Experimentals	119

LIST OF FIGURES

Figure 1. Important molecules containing amide bonds	1
Figure 2. Mechanism of epimerization during amide bond synthesis	2
Figure 3. Amide formation using DCC.....	2
Figure 4. Epimerization suppressants	2
Figure 5. Coupling reagents based on benzotriazoles.....	3
Figure 6. Coupling reagents that generate acid halides.....	3
Figure 7. Peptide ligation methods	4
Figure 8. Proposed catalytic cycle for boronic acid catalyzed amidation	6
Figure 9. Comparison of polarity in amide bond forming reactions.....	10
Figure 10. Anaerobic and aerobic pathways of UmAS.....	11
Figure 11. UmAS: competing anaerobic and aerobic pathways to amide	12
Figure 12. Correlation of electrophilic halogen loading and amide yield under anaerobic conditions	14
Figure 13. Proposed synthesis of alkyl unnatural amino amides	16
Figure 14. Unnatural amino acid publications by year	16
Figure 15. Unnatural amino acid containing therapeutics	17
Figure 16. Stapled peptides.....	18
Figure 17. Unnatural amino acids used in bioorthogonal labeling	18
Figure 18. Fluorescent labeling of Hpg containing protein	19
Figure 19. Commercial availability of unnatural amino acids.....	19
Figure 20. Bis(Amidine) catalysis	31
Figure 21. Enantioselective nitrocyclopropanation reactions using bromonitromethane	31
Figure 22. Imine tautomerization.....	32
Figure 23. <i>N</i> -Boc alkyl imines as electrophiles in the aza-Henry reaction	33
Figure 24. Difference between expected and observed product dr based on partially racemized unreacted starting material, and evidence for racemization prior to, and competitive with UmAS.....	44
Figure 25. UmAS: sulfonyl protecting group screen	46
Figure 26. Catalyst screen: quinoline 4-position	48
Figure 27. Proposed mechanism of Palomo's phase transfer catalyzed aza-Henry reaction	49
Figure 28. Proposed bromine transfer from bromonitromethane to nitromethane aza-Henry adduct	51
Figure 29. Screen of bromonium sources in proposed bromine transfer reaction	51
Figure 30. NMR experiments probing bromonitromethane decomposition	54
Figure 31. Recrystallized β -amino α -bromonitroalkanes.....	60
Figure 32. Strategy for oxidative amidation of primary nitroalkanes	63
Figure 33. Nitromethane vs. bromonitromethane in enantioselective transformations	63
Figure 34. Comparison of Hayashi-Lear and Schwieter-Johnston Protocols Across Platforms (NIS/acetonitrile vs. DBTCE/NIS/dimethoxyethane) using Nitroalkane 91.	72
Figure 35. ^1H NMR (CDCl_3) of 90.	73
Figure 36. Comparison of Hayashi-Lear and Schwieter-Johnston Protocols Across Platforms (NIS/acetonitrile vs. DBTCE/NIS/dimethoxy ethane) using Nitroalkane 304.	74
Figure 37. ^1H NMR (CDCl_3) of 306 (from Hayashi-Lear work).	75
Figure 38. Structure of feglymycin	76
Figure 39. Results of feglymycin alanine scan	82
Figure 40. Feglymycin model target peptide with 2,4-difluorophenylglycine residues	85
Figure 41. Targeted feglymycin analogues	96
Figure 42. Current mechanistic understanding of UmAS	103
Figure 43. Alternative mechanism for UmAS proposed by Hayashi.....	103
Figure 44. Bromonium transfer between dibromonitroalkane and bromonitroalkane	107
Figure 45. Crystal structures of NIS-amine complexes	109
Figure 46. Crystal structure of morpholine-iodine complex	110

Figure 47. Hammett plot for UmAS	115
Figure 48. Strategies for investigating the existence of the tetrahedral intermediate	116

LIST OF SCHEMES

Scheme 1. Solid-phase peptide synthesis.....	3
Scheme 2. Proposed mechanism for KAHA.....	5
Scheme 3. Yamamoto's boronic acid catalyzed amidation	5
Scheme 4. Hall's boronic acid catalyzed amidation	6
Scheme 5. Whiting's boronic acid catalyzed amidation with amino acids	7
Scheme 6. Wolf's amidation of aldehydes.....	7
Scheme 7. Amidation of α -functionalized aldehydes	8
Scheme 8. Milstein's direct amidation of alcohols	8
Scheme 9. Hong's amidation of alcohols and nitriles.....	9
Scheme 10. Umpolung Amide Synthesis.....	10
Scheme 11. Access to chiral bromonitroalkanes and their use in UmAS	12
Scheme 12. UmAS: halonium turnover	14
Scheme 13. O'Donnell's phase transfer catalyzed alkylation of glycine.....	20
Scheme 14. Corey and Lygo's phase transfer catalyzed alkylations of glycine	20
Scheme 15. Maruoka's phase transfer catalyzed alkylation of glycine	21
Scheme 16. Strategy for synthesis of α -amino acids via asymmetric hydrogenation.....	21
Scheme 17. First asymmetric hydrogenation of α,β -dehydro- α -amino acids	21
Scheme 18. Burk's asymmetric hydrogenation of DAA's.....	22
Scheme 19. Asymmetric hydrogenation of fluoro iminoesters.....	22
Scheme 20. Metal-free asymmetric hydrosilylation of an iminoester	22
Scheme 21. First catalytic asymmetric organocatalyzed Strecker reaction	23
Scheme 22. Jacobsen's asymmetric organocatalyzed Strecker reaction.....	23
Scheme 23. First report of the aza-Henry reaction	24
Scheme 24. First report of the aza-Henry reaction using preformed imines.....	24
Scheme 25. Diastereoselective base-promoted aza-Henry reaction.....	24
Scheme 26. First enantioselective aza-Henry reaction	25
Scheme 27. Jørgensen's enantioselective aza-Henry reaction employing silyl nitronates	25
Scheme 28. First enantioselective organocatalyzed aza-Henry reaction	25
Scheme 29. First phase transfer catalyzed enantioselective aza-Henry reactions of <i>N</i> -carbamoyl alkyl imines.....	26
Scheme 30. Catalysts employed in phase transfer catalyzed aza-Henry reactions	26
Scheme 31. Zhao's phase transfer catalyzed aza-Henry reaction	27
Scheme 32. Ellman's nitroethane additions to <i>N</i> -Boc aldimines.....	27
Scheme 33. Chiral ammonium betaine catalyzed aza-Henry reaction.....	28
Scheme 34. Guanidine-thiourea catalyzed aza-Henry reaction	28
Scheme 35. Iminophosphorane catalyzed aza-Henry addition of nitromethane to ketimines	28
Scheme 36. Bromonitromethane in NaI catalyzed Henry reaction.....	29
Scheme 37. First enantioselective Henry reaction	29
Scheme 38. Indium catalyzed debrominative Henry and aza-Henry reaction	29
Scheme 39. Bromonitromethane in NaI catalyzed aza-Henry reaction	29
Scheme 40. Bromonitromethane in nitroaziridination reaction	30
Scheme 41. Bromonitromethane in nitrocyclopropanation reaction.....	30
Scheme 42. First enantioselective nitrocyclopropanation reaction using bromonitromethane.....	30
Scheme 43. Chiral proton catalyzed aza-Henry additions	32
Scheme 44. PBAM•HOTf catalyzed bromonitromethane addition to an alkyl <i>N</i> -tosyl imine	33
Scheme 45. Catalyst backbone modifications: additions of bromonitromethane to alkyl <i>N</i> -tosyl imines..	35
Scheme 46. Synthesis of <i>N</i> -tosyl protected alkyl imine.....	36
Scheme 47. Preparation of 2-chloro-4-methoxyquinoline	36
Scheme 48. Synthesis of ⁴ MeO-StilbBAM.....	36

Scheme 49. Efforts to repeat initial results	37
Scheme 50. Catalyst screen in additions of bromonitromethane to alkyl <i>N</i> -tosyl imines.....	38
Scheme 51. Effect of temperature on additions of bromonitromethane to alkyl <i>N</i> -tosyl imines	39
Scheme 52. Slow addition of bromonitromethane to alkyl <i>N</i> -tosyl imines	40
Scheme 53. Concentration effects on additions of bromonitromethane to alkyl <i>N</i> -tosyl imines.....	40
Scheme 54. Initial attempt at Umpolung Amide Synthesis using alkyl <i>N</i> -tosyl α -bromonitroalkanes.....	42
Scheme 55. Proposed mechanism of retro aza-Henry	42
Scheme 56. UmAS reaction using free amine as coupling partner and base.....	42
Scheme 57. Correlation between expected and observed product dr based on starting material ee	43
Scheme 58. UmAS reaction temperature study	43
Scheme 59. Palomo's phase transfer catalyzed aza-Henry reaction	48
Scheme 60. Initial attempts at phase transfer catalyzed addition of bromonitromethane to <i>N</i> -Boc aldimines	49
Scheme 61. Nitromethane as an additive in the phase transfer catalyzed addition of bromonitromethane to <i>N</i> -Boc aldimines	50
Scheme 62. Probing effect of additive on addition of bromonitromethane to <i>N</i> -Boc aldimines	53
Scheme 63. Cinchona alkaloid derived catalysts in nitromethane addition to <i>N</i> -Boc aldimines.....	55
Scheme 64. Other cinchona alkaloid derived catalyst in phase transfer catalyzed addition of bromonitromethane to <i>N</i> -Boc aldimines	56
Scheme 65. Iterative synthesis of a tripeptide containing unnatural amino acids.....	56
Scheme 66. One-pot procedure for BAM-catalyzed addition of bromonitromethane to <i>N</i> -Boc aldimines	57
Scheme 67. Two-pot procedure for BAM-catalyzed addition of bromonitromethane to <i>N</i> -Boc aldimines	57
Scheme 68. Synthesis of two tripeptides featuring substituent and configurational diversity.....	62
Scheme 69. Synthesis of a peptide effective in reversal of P-glycoprotein-mediated resistance to carfilzomib.....	62
Scheme 70. Mechanism of traditional Nef reaction	64
Scheme 71. Base promoted Nef reaction with molecular oxygen as proposed by Hayashi.....	64
Scheme 72. Kornblum's proposed mechanism for the conversion of nitroalkanes to carboxylic acids.....	65
Scheme 73. Mioskowski's proposed mechanism for the conversion of nitroalkanes to carboxylic acids.....	65
Scheme 74. Investigation of Kornblum's conditions for amide synthesis	66
Scheme 75. Investigation of nitrolic acid as amide precursor	66
Scheme 76. Comparison of nitroalkane and α -bromonitroalkane under standard UmAS conditions	67
Scheme 77. Comparison of nitroalkane and α -bromonitroalkane under standard UmAS conditions	67
Scheme 78. Hayashi-Lear oxidative amidation of nitroalkanes	71
Scheme 79. Synthesis of 3,5-dihydroxyphenylglycine.....	78
Scheme 80. Süssmuth's retrosynthetic analysis of feglymycin	79
Scheme 81. Synthesis of hexapeptide 313 for the preparation of feglymycin (Süssmuth).....	80
Scheme 82. Synthesis of heptapeptide 312 for the preparation of feglymycin (Süssmuth).....	81
Scheme 83. Final peptide fragment coupling in the synthesis of feglymycin (Süssmuth).....	81
Scheme 84. Retrosynthetic analysis of feglymycin	83
Scheme 85. Preparation of building blocks for synthesis of feglymycin	83
Scheme 86. Challenges in preparation of tetrapeptide 329	84
Scheme 87. Completion of tetrapeptide 329	84
Scheme 88. Efforts toward the synthesis of hexapeptide 328.....	85
Scheme 89. Key steps in the synthesis of peptide fragments 349 and 350.....	86
Scheme 90. Peptide fragment condensations for synthesis of feglymycin model peptide.....	87
Scheme 91. Retrosynthetic analysis of Ffeglymycin	88
Scheme 92. Synthesis of building blocks for the synthesis of Ffeglymycin.....	89

Scheme 93. Comparison of catalytic and stoichiometric NIS in UmAS couplings in the synthesis of Ffeglymycin	90
Scheme 94. Synthesis of tetrapeptide 349	90
Scheme 95. Synthesis of hexapeptide 356	91
Scheme 96. Synthesis of tripeptide 354.....	92
Scheme 97. Final deprotection to provide Ffeglymycin.....	95
Scheme 98. Synthesis of α -bromonitroalkanes for feglymycin analogues.....	97
Scheme 99. Synthesis of tetrapeptide containing a 3,5-difluorophenylglycine residue.....	97
Scheme 100. Synthesis of tripeptide containing a 3,5-difluorophenylglycine residue	98
Scheme 101. Attempted synthesis of hexapeptide containing 3,5-difluorophenylglycine residues ..	99
Scheme 102. Attempted synthesis of hexapeptide containing 3,5-dibromophenylglycine residues	100
Scheme 103. Early UmAS experiments probing halamine intermediacy	101
Scheme 104. Experiments probing for carbonyl intermediates in UmAS	102
Scheme 105. Isotopic labeling experiments probing UmAS mechanism	102
Scheme 106. Hayashi's key experiments: NIS-amine complex	104
Scheme 107. Hayashi's key experiments: diiodonitroalkane	104
Scheme 108. UmAS reaction pathways	105
Scheme 109. Comparison of bromonitroalkane and dibromonitroalkane in UmAS	106
Scheme 110. Competition experiments between bromonitroalkanes and dibromonitroalkanes in UmAS	107
Scheme 111. Possible mechanisms of halonium transfer and experiments to probe them during bromonitroalkane amidation	108
Scheme 112. Attempted preparation of <i>N</i> -iodamine with α -methyl benzylamine	109
Scheme 113. Attempts at preparing <i>N</i> -iodomorpholine.....	110
Scheme 114. Iodomorpholine compounds in UmAS.....	111
Scheme 115. UmAS with other electrophilic amine sources.....	111
Scheme 116. Possible pathways of oxadiazole formation	112
Scheme 117. Oxadiazole formation: optimal conditions and mechanistic investigation.....	113
Scheme 118. UmAS: probing formation of acyl halide intermediate.....	114
Scheme 119. Attempted synthesis of α -amino nitroalkanes	116
Scheme 120. Attempted bromination of α -amino nitro compounds	117
Scheme 121. Preliminary results with radical traps in UmAS.....	117

LIST OF TABLES

Table 1. Investigation of NIS reagent loading	13
Table 2. UmAS substoichiometric in NIS substrate scope	15
Table 3. Catalyst screen in bromonitromethane addition to alkyl <i>N</i> -tosyl imines	34
Table 4. Counterion effects in the PBAM catalyzed additions of bromonitromethane to alkyl <i>N</i> -tosyl imines	34
Table 5. Solvent screen of additions of bromonitromethane to alkyl <i>N</i> -tosyl imines	37
Table 6. Concentration and catalyst loading screen in addition of bromonitromethane to alkyl <i>N</i> -tosyl imines	38
Table 7. Catalyst loading in additions of bromonitromethane to alkyl <i>N</i> -tosyl imines	41
Table 8. Substrate scope of additions of bromonitromethane to alkyl <i>N</i> -tosyl imines	41
Table 9. Screen of bases in UmAS reaction.....	43
Table 10. Solvent screen for UmAS reaction	44
Table 11. Base screen for UmAS reaction.....	45
Table 12. Bromonitromethane addition to <i>N</i> -Boc alkyl imines	47
Table 13. Counter-ion screen.....	47
Table 14. Base screen in phase transfer catalyzed addition of bromonitromethane to <i>N</i> -Boc aldimines ...	50
Table 15. Nitromethane additive in the phase transfer catalyzed aza-Henry reaction.....	52
Table 16. Effect of different nitroalkane additives on the phase transfer catalyzed addition of bromonitromethane to <i>N</i> -Boc aldimines	53
Table 17. Substrate scope for the phase transfer catalyzed addition of bromonitromethane to <i>N</i> -Boc aldimines	55
Table 18. Catalyst screen for BAM-catalyzed addition of bromonitromethane to <i>N</i> -Boc aldimines	58
Table 19. Counterion screen for BAM-catalyzed addition of bromonitromethane to <i>N</i> -Boc aldimines	58
Table 20. Catalyst loading in BAM-catalyzed addition of bromonitromethane to <i>N</i> -Boc aldimines	59
Table 21. Screen of additives in BAM-catalyzed addition of bromonitromethane to <i>N</i> -Boc aldimines.....	59
Table 22. Substrate scope for BAM-catalyzed addition of bromonitromethane to <i>N</i> -Boc aldimines.....	60
Table 23. UmAS of alkyl β -amino α -bromonitroalkanes	61
Table 24. Evaluation of brominating reagents for the bromination of primary nitroalkanes	68
Table 25. Evaluation of halogenating reagents in the one-pot oxidative amidation of nitroalkanes	68
Table 26. Evaluation of a step-wise protocol for oxidative amidation of nitroalkanes	69
Table 27. Substrate scope for oxidative amidation of primary nitroalkanes.....	70
Table 28. Decapeptide formation.....	92
Table 29. Tridecapeptide formation	93
Table 30. Conditions for TSE deprotection	94
Table 31. Model substrate for TSE deprotection	95

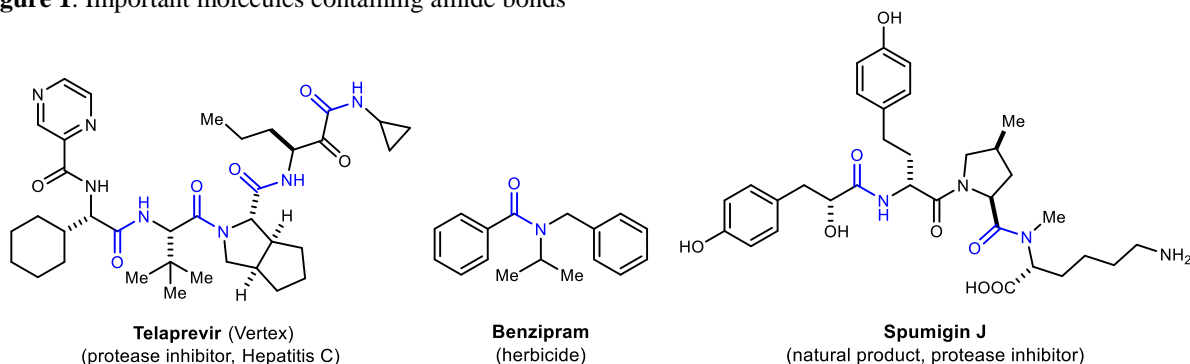
Chapter I

I. Development of Umpolung Amide Synthesis Substoichiometric in NIS¹

1.1 Importance and Synthesis of Amides

Amide bonds are arguably among the most prevalent bonds in chemistry and biology. They are essential to biological function as they are a core element of proteins and enzymes. Additionally, amide bonds are found in many small molecule therapeutics, agrochemicals, and natural products (Figure 1).² As of 2015, there are more than 60 peptide based drugs on the market in the United States with 140 more drug candidates in clinical trials.³ Of the top ten drugs sold globally in 2012, seven of them were peptides.⁴ Due to the importance of amide bonds, their synthesis has been an extensively researched area. The simplest and most straightforward strategy for amide bond synthesis, like nature, is the dehydrative coupling of a carboxylic acid and an amine. However, the direct condensation of an amine with a carboxylic acid requires very high temperatures to overcome the thermodynamic barrier caused by salt formation.⁵ For this reason, a number of innovative methods for amide bond synthesis have been developed.

Figure 1. Important molecules containing amide bonds



Coupling Reagents in Amide Bond Synthesis

Currently, the most common method for amide synthesis is the use of coupling reagents.⁶ Coupling reagents are used to generate an active ester intermediate from the carboxylic acid. The amine component then attacks the electrophilic active ester, providing the desired amide. One of the first reports of a coupling reagent was in 1955 when Sheehan described the use of a carbodiimide, dicyclohexyl carbodiimide (DCC, **2**), as an efficient reagent for peptide synthesis.⁷ The proposed mechanism of the coupling is shown in Figure 3. The carboxylic acid adds DCC to generate active ester **4**. The amine then adds to the carbonyl, releasing the DCC urea as a by-product and providing the amide product. While DCC and other carbodiimide coupling reagents work well in many cases there are a few problems. First, couplings with

¹ Schwieter, K. E.; Shen, B.; Shackelford, J. P.; Leighty, M. W.; Johnston, J. N. *Org. Lett.* **2014**, *16*, 4714-4717.

² International Pat., WO2007022459, Vertex Pharmaceuticals Inc., **2007**; Anas, A. R. J.; Kisugi, T.; Umezawa, T.; Matsuda, F.; Campitelli, M. R.; Quinn, R. J.; Okino, T. *J. Nat. Prod.* **2012**, *75*, 1546-1552.

³ Fosgerau, K.; Hoffmann, T. *Drug Discovery Today* **2015**, *20*, 122-128.

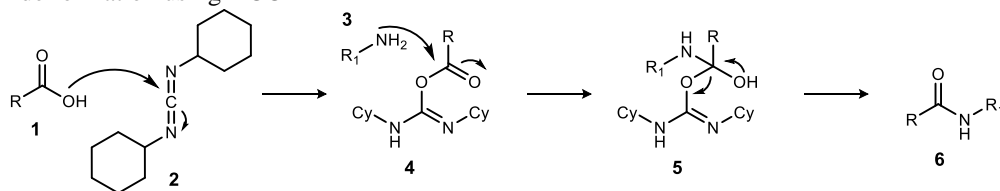
⁴ www.fiercepharma.com/special-reports/15-best-selling-drugs-2012

⁵ Ulijn, R. V.; Moore, B. D.; Janssen, A. E. M.; Halling, P. J. *Journal of the Chemical Society, Perkin Transactions 2* **2002**, 1024-1028.

⁶ Han, S.-Y.; Kim, Y.-A. *Tetrahedron* **2004**, *60*, 2447-2467. Valeur, E.; Bradley, M. *Chem. Soc. Rev.* **2009**, *38*, 606-631.

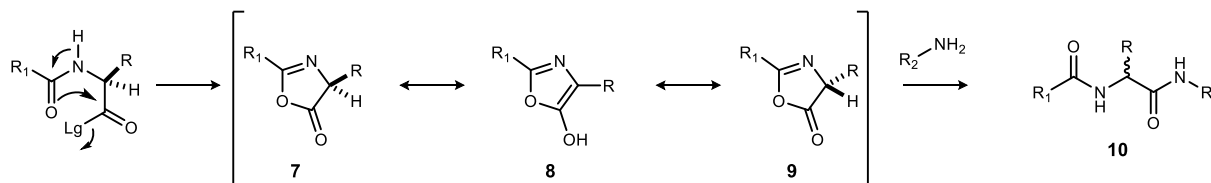
⁷ Sheehan, J. C.; Hess, G. P. *J. Am. Chem. Soc.* **1955**, *77*, 1067-1068.

Figure 3. Amide formation using DCC



complex substrates, including disubstituted amines and large peptides, proceed with low conversion. Secondly, is the possibility of epimerization of the α -carbon during peptide couplings especially with the electron rich arylglycines. Epimerization occurs through the formation of an oxazolone intermediate (Figure 2). The active ester intermediate is attacked by the neighboring amide carbonyl to form oxazolone **7**. At this point, the α -proton is sufficiently acidic to undergo base-catalyzed epimerization. The amine then opens up the oxazolone to provide the amide in reduced enantiopurity. In order to minimize epimerization, a number of additives have been developed to either increase the rate of coupling or slow the rate of epimerization (Figure 4). An early example, HOBt (**11**), was reported by Geiger and König in 1970. HOBt

Figure 2. Mechanism of epimerization during amide bond synthesis

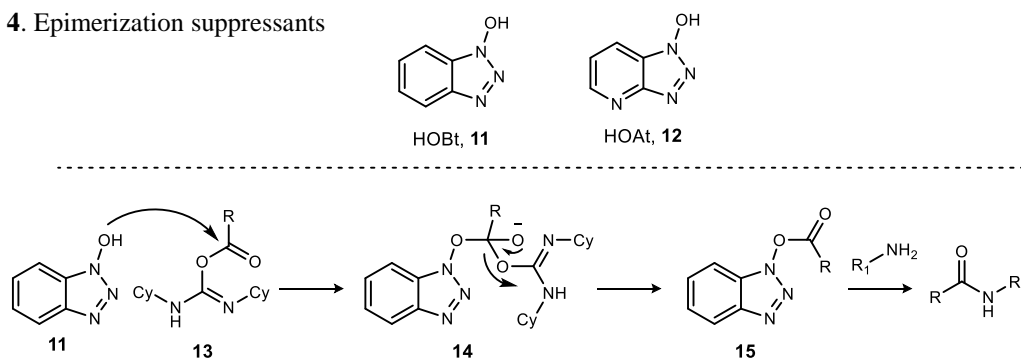


was shown to successfully reduce the epimerization levels from 35% to 1.5% when coupling Cbz-Gly-Phe-OH to H₂N-Val-OMe.⁸ HOBt adds to the active ester **13** to form the triazole active ester **15**. Active ester **15** provides hydrogen bond acceptors for the amine to increase its nucleophilicity and increase the rate of the desired coupling and minimize racemization.

Currently, the most common coupling reagents contain both the activator and the racemization suppressant. These include uronium/aminium, phosphonium, and immonium salts of benzotriazoles or other racemization suppressants (Figure 5). These function in a similar way to the DCC/HOBt combination depicted in Figure 4. The carboxylic acid adds to the uronium functionality, generating the active ester and releasing the benzotriazole as a racemization suppressant. The benzotriazole then adds to the active ester to generate intermediate **15** which undergoes amidation to provide the amide product.

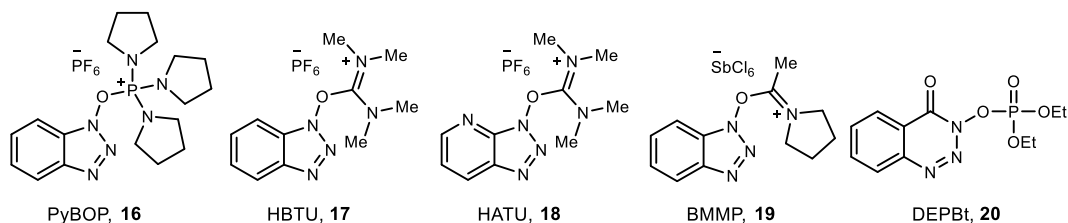
Compounds that generate the acid halide comprise another class of coupling reagents. This strategy is one of the oldest dating back to the use of thionyl chloride in 1902 to synthesize the glycine-glycine

Figure 4. Epimerization suppressants



⁸ König, W.; Geiger, R. *Chem. Ber.* **1970**, *103*, 788-798.

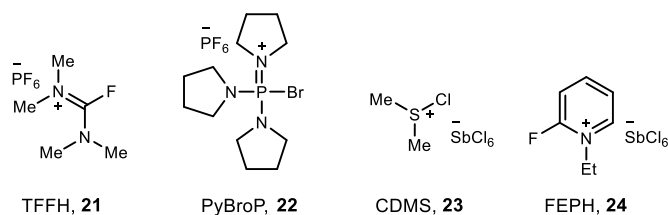
Figure 5. Coupling reagents based on benzotriazoles



dipeptide through an acid chloride intermediate.⁹ A number of reagents have been developed that circumvent the harsh conditions required when using thionyl chloride (Figure 6).

Despite the extensive research in the area of coupling reagents a few problems still remain. The reaction is not atom economical as stoichiometric byproducts are generated causing purification problems as well as resulting in a large excess of waste when performed on scale. Epimerization can still be an issue with complex substrates. Additionally, there are many choices of reagents to choose from, finding the optimal reagent is far from simple.

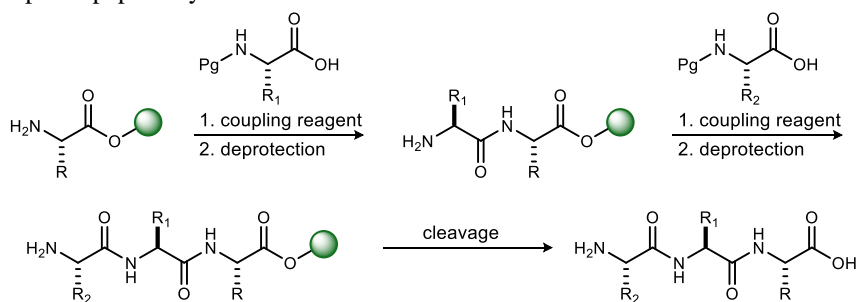
Figure 6. Coupling reagents that generate acid halides



Peptide Synthesis

The most widely used method for peptide synthesis is solid-phase peptide synthesis (SPPS). SPPS, pioneered by Merrifield,¹⁰ allows for the rapid synthesis of larger complex peptides as compared to traditional solution phase chemistry. The general scheme for SPPS is depicted in Scheme 1. The starting amino acid is affixed to an insoluble resin through an ester bond. The *N*-terminus of the amino acid is unprotected and ready to be coupled. The resin is treated with the excess amino acid to be coupled and a coupling reagent to provide the dipeptide. Deprotection of the *N*-terminus sets the stage for the cycle to be repeated. Upon completion of the synthesis, the peptide is cleaved from the resin. The entire process can take place in a single vessel as excess reagents from the previous step are simply washed away. The main advantages of SPPS are simplicity and speed of synthesis as well as efficiency in coupling. However, to

Scheme 1. Solid-phase peptide synthesis



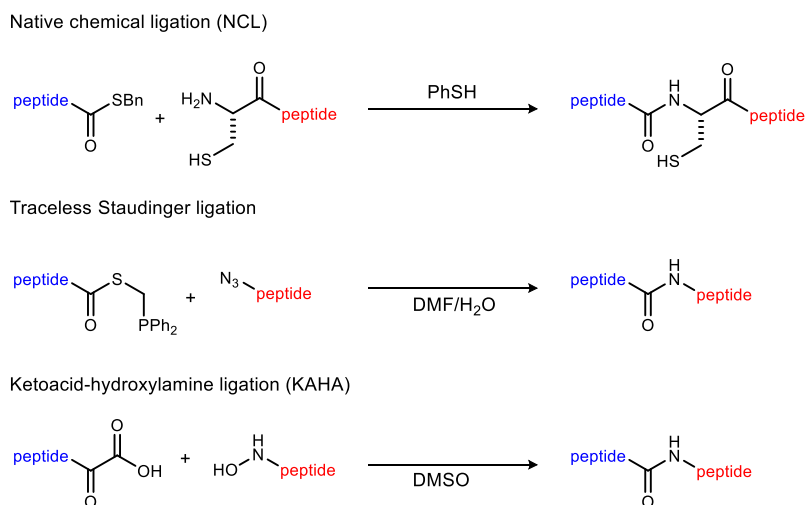
⁹ Fischer, E., Fourneau, E. *Ber. Dtsch. Chem. Ges.* **1901**, *34*, 2688

¹⁰ Merrifield, R. B. *J. Am. Chem. Soc.* **1963**, *85*, 2149-2154.

obtain these advantages, a large excess of reagents is necessary, making the process wasteful, which may be cost prohibitive in some cases. There are many variables including choice of nitrogen protecting group, choice of resin material, choice of linker, and choice of coupling reagents. Significant research has been conducted in this area to determine the optimal conditions for different syntheses.¹¹

One major limitation of SPPS is the length of peptide that can be synthesized. Peptides up to ~50 amino acid residues can be obtained in moderate yield and efficiency. However, as the size increases, yields and efficiency are decreased below synthetically useful levels. For this reason, a number of ligation methods have been developed to couple large peptides. The ideal ligation method would be able to provide the necessary amide linkage between two peptides while also being chemoselective and function in the presence of unprotected functional groups. Additionally, minimal byproducts should be formed. Three of the most impressive ligation methods are shown in Figure 7. Native chemical ligation (NCL), reported by Kent in 1994, couples a thioester at the C-terminus of one peptide to an N-terminal cysteine residue of another peptide.¹² The first step of the reaction is a reversible transthioesterification in which the cysteine thiol adds to the thioester. The final step is an irreversible *S,N*-acyl shift to provide the amide linkage. Due to the chemoselectivity of the reaction, unprotected functional groups in the peptides are unaffected during the transformation, providing the peptide in near quantitative yield. The major limitation is the necessity of having a cysteine residue at the N-terminus.

Figure 7. Peptide ligation methods



The traceless Staudinger ligation was first reported in 2000 as a novel method for peptide ligation.¹³ This method involves the coupling of a C-terminal phosphinothioester and an N-terminal azide. The reaction proceeds through nucleophilic attack of the phosphine on the azide releasing a molecule of nitrogen and forming an iminophosphorane intermediate, which breaks down to provide the amide linkage. The main limitations of the traceless Staudinger ligation are the necessity of a terminal azide as well as functional group tolerance, normally requiring a fully protected peptide.

In 2006 Bode reported α -ketoacid-hydroxylamine ligation (KAHA) as a reagent free novel amide forming reaction capable of coupling fully unprotected peptides.¹⁴ A C-terminal α -ketoacid is coupled to

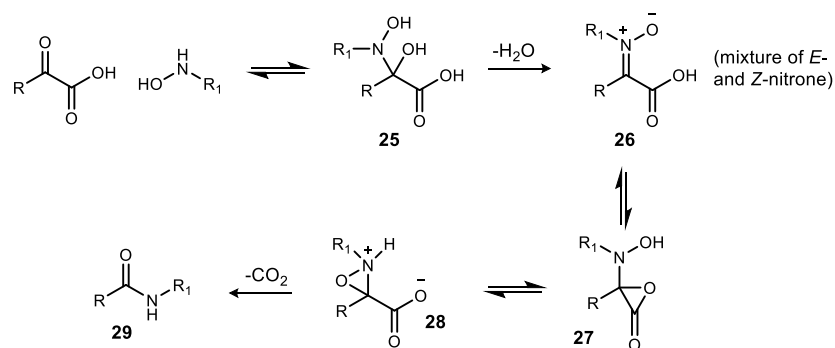
¹¹ Review: Palomo, J. M. *RSC Advances* **2014**, *4*, 32658-32672.

¹² Dawson, P.; Muir, T.; Clark-Lewis, I.; Kent, S. *Science* **1994**, *266*, 776-779.

¹³ Saxon, E.; Bertozzi, C. R. *Science* **2000**, *287*, 2007-2010; Saxon, E.; Armstrong, J. I.; Bertozzi, C. R. *Org. Lett.* **2000**, *2*, 2141-2143. Nilsson, B. L.; Kiessling, L. L.; Raines, R. T. *Org. Lett.*, 1939-1941.

¹⁴ Bode, J. W.; Fox, R. M.; Baucom, K. D. *Angew. Chem. Int. Ed.* **2006**, *45*, 1248-1252.

Scheme 2. Proposed mechanism for KAHA



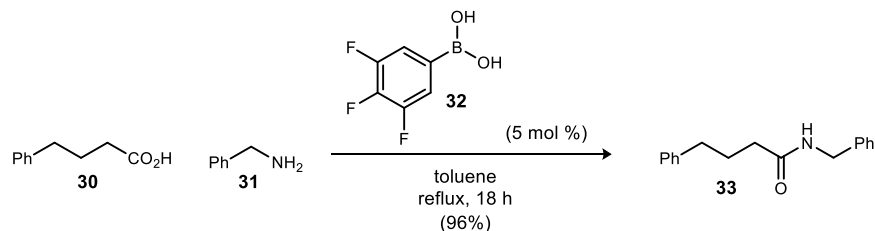
an *N*-terminal hydroxylamine to provide the desired amide. Carbon dioxide and water are generated as the only byproducts. Mechanistically, the reaction is believed to proceed through a nitronium intermediate (**26**), generated by the condensation of the hydroxylamine onto the α -keto acid (Scheme 2).¹⁵ The nitronium then undergoes a proton transfer and cyclization to form α -lactone **27**, which is opened up to provide oxaziridine **28**. Decarboxylation leads to the amide. KAHA is limited to coupling peptides containing less than 30 amino acid residues.

Tremendous strides have been made in the area of synthesis including the development of solid phase peptide synthesis and novel ligation methods. Nevertheless, there is significant room for improvement. Solid-phase peptide synthesis in particular is still limited by the need to use excess toxic reagents, the significant waste generation, and coupling efficiencies that limit broader use of unnatural amino acids. For these reasons and the ubiquity of amides in biologically active molecules, “amide formation avoiding poor atom economy reagents”¹⁶ has been hailed as a top challenge and need of critical importance.

Catalytic Amide Bond Formation

The use of stoichiometric boron-based reagents for the direct amidation of carboxylic acids with amines has been known for greater than half a century.¹⁷ Recently, efforts have been devoted to rendering this transformation catalytic in the boron reagent. In 1996, Yamamoto reported the direct amidation of unactivated carboxylic acids with amines using 3,4,5-trifluorobenzeneboronic acid (**32**) as an efficient catalyst (Scheme 3).¹⁸ They found that electron-deficient boronic acids were efficient catalysts for the direct amidation of aryl and aliphatic carboxylic acids with aryl and aliphatic amines. The electron withdrawing

Scheme 3. Yamamoto’s boronic acid catalyzed amidation



¹⁵ Pusterla, I.; Bode, J. W. *Angew. Chem. Int. Ed.* **2012**, *51*, 513-516.

¹⁶ Constable, D. J. C.; Dunn, P. J.; Hayler, J. D.; Humphrey, G. R.; Leazer, J. J. L.; Linderman, R. J.; Lorenz, K.; Manley, J.; Pearlman, B. A.; Wells, A.; Zaks, A.; Zhang, T. Y. *Green Chem.* **2007**, *9*, 411-420.

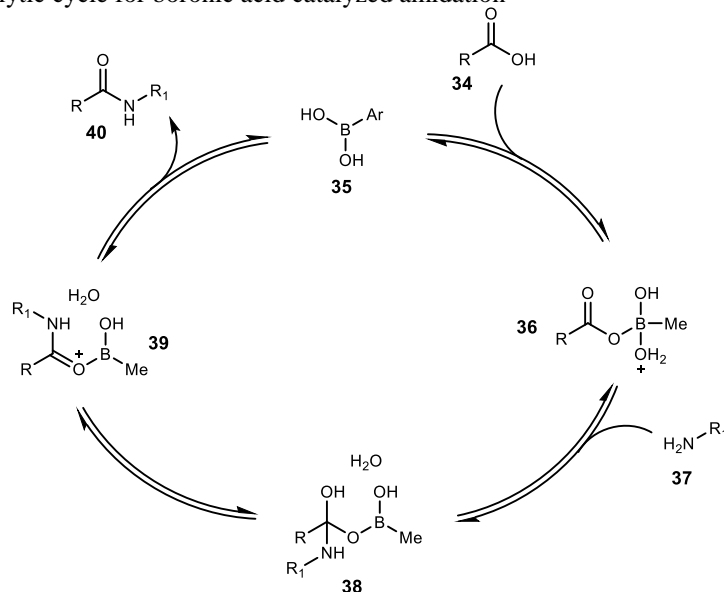
¹⁷ Nelson, P.; Pelter, A. *Journal of the Chemical Society (Resumed)* **1965**, 5142-5144.

¹⁸ Ishihara, K.; Ohara, S.; Yamamoto, H. *J. Org. Chem.* **1996**, *61*, 4196-4197.

nature of the boronic acids were necessary for catalyst turnover allowing catalyst loadings as low as 1 mol %.

The proposed catalytic cycle for boronic acid catalyzed amidation is shown in Figure 8 as reported by Marcelli following DFT calculations.¹⁹ The cycle begins with the reaction of carboxylic acid **34** with boronic acid catalyst **35** to form tetra-coordinate boronate **36** in a concerted process involving proton transfer and B-O bond formation. Subsequently, the amine adds to the activated acid to generate hemiaminal **38** concurrent with the expulsion of water. Hemiaminal **38** then undergoes a *cis*-selective water elimination to form amide complex **39**. Decomplexation provides the amide product as well as the catalyst.

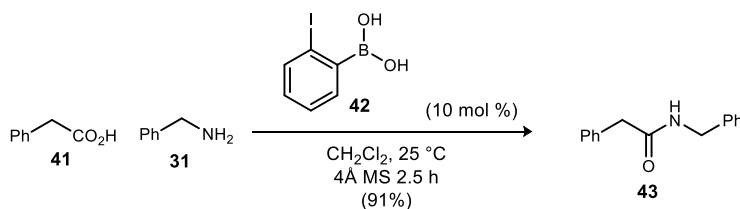
Figure 8. Proposed catalytic cycle for boronic acid catalyzed amidation



In 2008, Hall and coworkers reported a breakthrough in the boronic acid amidation field with the discovery of a more active boronic acid catalyst that functions efficiently at room temperature as opposed to the high temperatures previously used.²⁰ After a thorough screen of over 45 different boronic acids, *ortho*-iodophenylboronic acid (**42**) was found to be the optimal catalyst (Scheme 4). It was also found that molecular sieves as water scavengers were paramount to obtain high yield of amide. The catalyst can be successfully recovered, leaving water as the only waste.

Although there has been significant improvement in boronic acid catalyzed amidations, couplings between amino acids remain a challenge. Whiting reported that the coupling of a variety of amino acids and benzylamine uniformly requires 25 mol % of boronic acid catalyst (Scheme 5).²¹ When the amine

Scheme 4. Hall's boronic acid catalyzed amidation



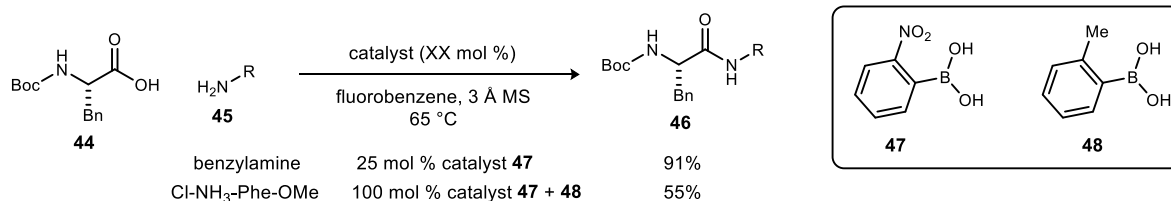
¹⁹ Marcelli, T. *Angew. Chem. Int. Ed.* **2010**, *49*, 6840-6843.

²⁰ Al-Zoubi, R. M.; Marion, O.; Hall, D. G. *Angew. Chem. Int. Ed.* **2008**, *47*, 2876-2879.

²¹ Liu, S.; Yang, Y.; Liu, X.; Ferdousi, F. K.; Batsanov, A. S.; Whiting, A. *Eur. J. Org. Chem.* **2013**, *2013*, 5692-5700.

coupling partner is also an amino acid, the boronic acid must be used in stoichiometric amounts to achieve high yields. The optimal conditions for dipeptide synthesis employ a 1:1 mixture of boronic acid catalysts at 50 mol % for each catalyst.

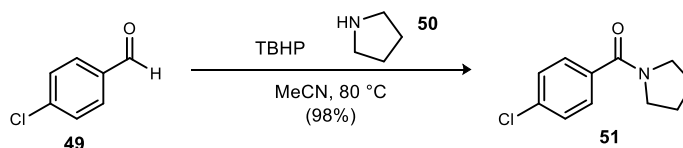
Scheme 5. Whiting's boronic acid catalyzed amidation with amino acids



Metal complexes have also been used as Lewis acid mediators in amide forming reactions dating back to 1970 when Weingarten used TiCl₄ as a stoichiometric promoter for amidation of carboxylic acids with amines.²² The first example of a catalytic intermolecular amidation was reported by Shteinberg in 1988 acylating aniline with a variety of carboxylic acids using Ti(OBu)₄ as a catalyst.²³ It was found that the addition of a Lewis acid significantly increased the rate of amidation above that of the thermal reaction rate. Since the initial report, many different metal complexes have been reported to catalyze the amidation of carboxylic acids with amines, including ZnCl₂²⁴, ZrCl₄²⁵, and FeCl₃•6H₂O.²⁶ Although these methods provide the amide in good yield with minimal by-products, they rely on high temperature and have limited substrate tolerance, making them unsuitable for peptide synthesis.

The most common strategy for amide bond synthesis is the coupling of a carboxylic acid and an amine. Recently, however, a number of methods have been developed utilizing other functional groups as amide precursors. Wolf reported the first metal-free oxidative amidation of aldehydes with TBHP and an amine (Scheme 6).²⁷ Mechanistically, the aldehyde and amine combine to generate an aminal which is subsequently oxidized to the amide product. This work was a significant improvement over other oxidative amidation methods that utilized expensive transition metal oxidants.²⁸

Scheme 6. Wolf's amidation of aldehydes



²² Wilson, J. D.; Weingarten, H. *Can. J. Chem.* **1970**, *48*, 983-986.

²³ Shteinberg, L. Y.; Kondratov, S. A.; Shein, S. M. *Zh. Org. Khim.* **1988**, *24*, 1968 – 1972

²⁴ Chandra Shekhar, A.; Ravi Kumar, A.; Sathaiyah, G.; Luke Paul, V.; Sridhar, M.; Shanthan Rao, P. *Tetrahedron Lett.* **2009**, *50*, 7099-7101.

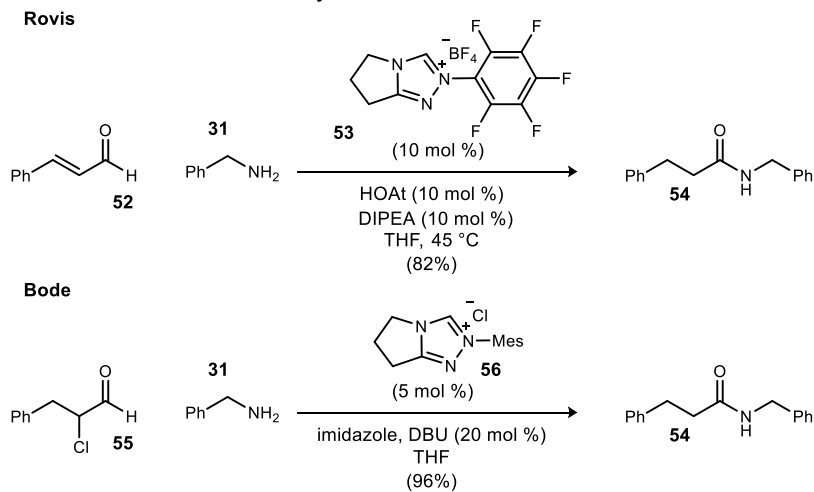
²⁵ Allen, C. L.; Chhatwal, A. R.; Williams, J. M. J. *Chem. Commun.* **2012**, *48*, 666-668; Lundberg, H.; Tinnis, F.; Adolfsson, H. *Chem. Eur. J.* **2012**, *18*, 3822-3826.

²⁶ Terada, Y.; Ieda, N.; Komura, K.; Sugi, Y. *Synthesis* **2008**, *2008*, 2318-2320.

²⁷ Ekoue-Kovi, K.; Wolf, C. *Org. Lett.* **2007**, *9*, 3429-3432.

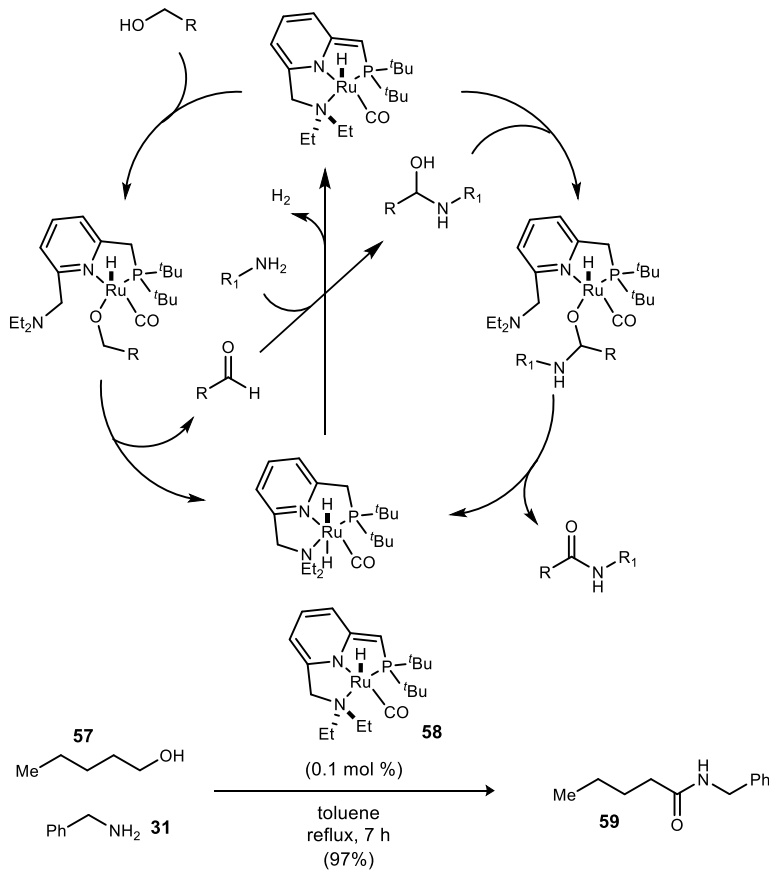
²⁸ Tamaru, Y.; Yamada, Y.; Yoshida, Z.-i. *Synthesis* **1983**, *1983*, 474-476; Tillack, A.; Rudloff, I.; Beller, M. *Eur. J. Org. Chem.* **2001**, *2001*, 523-528; Yoo, W.-J.; Li, C.-J. *J. Am. Chem. Soc.* **2006**, *128*, 13064-13065.

Scheme 7. Amidation of α -functionalized aldehydes



In 2007 Rovis and Bode simultaneously reported the use of *N*-heterocyclic carbenes (NHCs) as catalysts for the amidation of α -functionalized aldehydes (Scheme 7).²⁹ The reaction uses the principle of redox economy in which the aldehyde, in combination with the catalyst, generates an activated carbonyl as an intermediate to amide formation. A variety of functionalized substrates with internal oxidants, including

Scheme 8. Milstein's direct amidation of alcohols



²⁹ Vora, H. U.; Rovis, T. J. *Am. Chem. Soc.* **2007**, *129*, 13796-13797; Bode, J. W.; Sohn, S. S. *J. Am. Chem. Soc.* **2007**, *129*, 13798-13799.

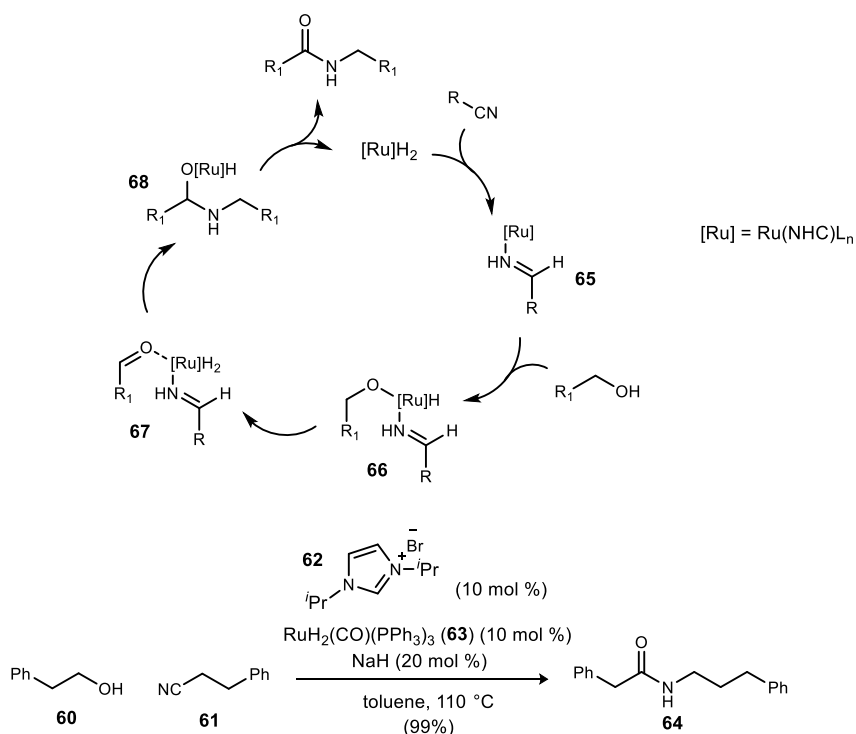
formylcyclopropanes, α,β -unsaturated aldehydes, α -halo aldehydes and epoxyaldehydes, were demonstrated to be competent amide precursors. The need for such functionalization limits its use in peptide synthesis.

In 2007 Milstein reported the first use of ruthenium catalysis for the coupling of alcohols and amines for amide synthesis through a dehydrogenation process (Scheme 8).³⁰ A ruthenium pincer complex is employed as the catalyst. Mechanistically, the catalyst promotes dehydrogenation of the alcohol to the aldehyde followed by formation of an amination intermediate with the amine. The amination intermediate is then oxidized by the ruthenium catalyst to generate the amide. This methodology sufficiently addressed the waste aspect of amide synthesis as H_2 is the only byproduct, but the reaction is limited to relatively simple substrates. Both Madsen³¹ and Hong³² subsequently reported the direct amide synthesis from alcohols and amines using ruthenium catalysis without significant improvement.

Hong and coworkers recently reported a redox-neutral amide synthesis from alcohols and nitriles (Scheme 9).³³ Ruthenium complex **63** was employed to oxidize the alcohol as well as reduce the nitrile in a completely atom economical process to obtain the desired amide. Mechanistically, the ruthenium hydride complex hydrogenates the nitrile to form imine complex **65**. Oxidative addition of the alcohol followed by dehydrogenation leads to aldehyde complex **67**. The imine then adds to the aldehyde followed by another dehydrogenation, providing the amide and regenerating the catalyst. The methodology tolerated a variety of simple alcohols and nitriles, but it is not amenable to peptide synthesis.

Scheme 9. Hong's amidation of alcohols and nitriles

Proposed mechanism:



³⁰ Gunanathan, C.; Ben-David, Y.; Milstein, D. *Science* **2007**, *317*, 790-792.

³¹ Nordström, L. U.; Vogt, H.; Madsen, R. *J. Am. Chem. Soc.* **2008**, *130*, 17672-17673.

³² Muthaiah, S.; Ghosh, S. C.; Jee, J.-E.; Chen, C.; Zhang, J.; Hong, S. H. *J. Org. Chem.* **2010**, *75*, 3002-3006.

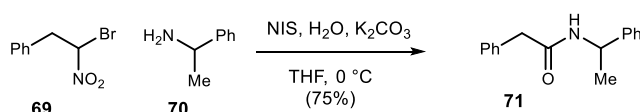
³³ Kang, B.; Fu, Z.; Hong, S. H. *J. Am. Chem. Soc.* **2013**, *135*, 11704-11707.

There has been tremendous growth and improvement in the area of catalytic amide synthesis. Many different systems have been developed with low catalyst loadings, mild conditions, broad substrate tolerance and low waste generation. However, these methods have yet to address the issue of catalytic amide formation with respect to peptide synthesis.

1.2 Umpolung Amide Synthesis

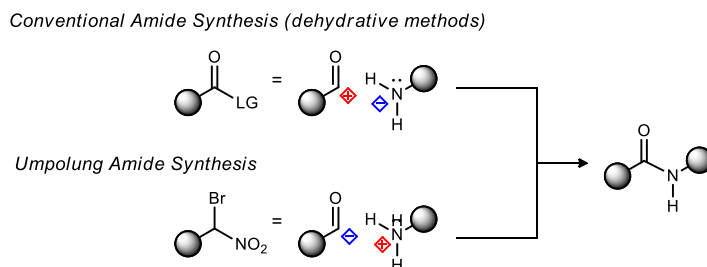
In 2010 our group reported a novel amide bond forming reaction coupling an α -bromonitroalkane and an amine (Scheme 10).³⁴ Preliminary studies suggested that the amine played the role of electrophile and the bromonitroalkane (carboxylate equivalent) played the role of nucleophile. In contrast, traditional amide bond forming reactions employ the opposite polarity for the two components (Figure 9). For that reason, the reaction was termed *umpolung*, meaning the polarities of the reactants are reversed to what is normally observed.³⁵

Scheme 10. Umpolung Amide Synthesis



The mechanism has been studied using a variety of direct and indirect methods leading to a working hypothesis. The amine is iodinated by electrophilic iodine provided by NIS. The bromonitroalkane is deprotonated by either K₂CO₃ or the amine forming the nitronate. Subsequent attack of the iodamine by the nitronate results in the tetrahedral intermediate. The tetrahedral intermediate breaks down to generate the amide.

Figure 9. Comparison of polarity in amide bond forming reactions



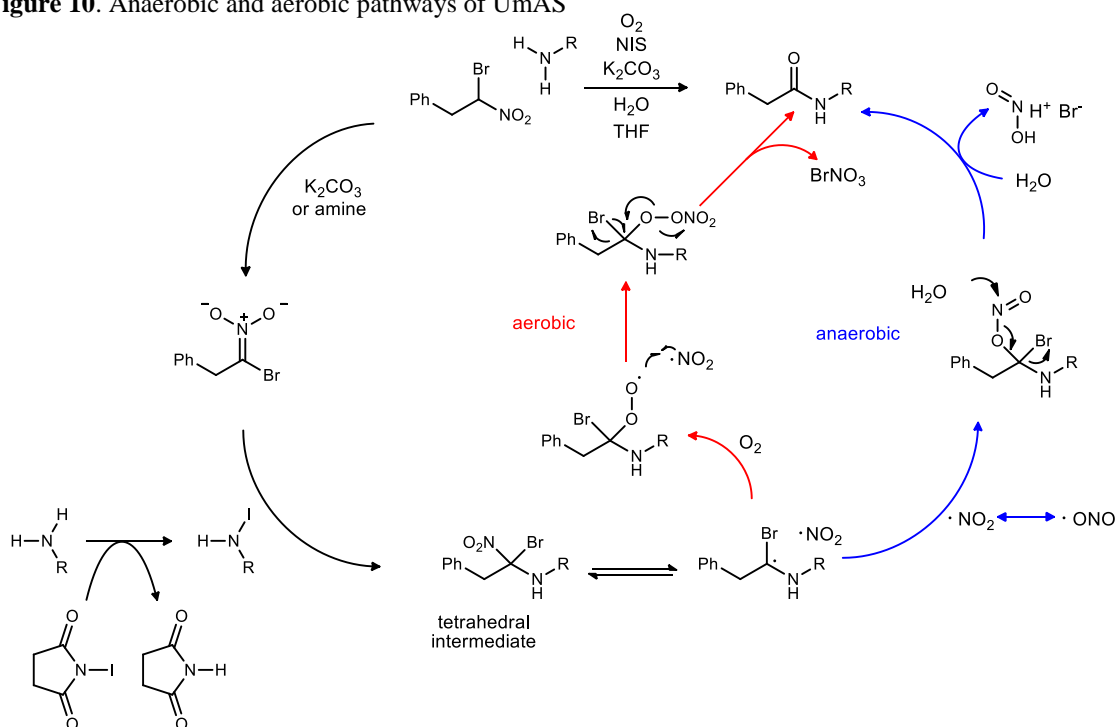
Additional mechanistic studies provided further insight into the nature of the breakdown of the tetrahedral intermediate.³⁶ Through a series of experiments, two pathways were proposed: anaerobic and aerobic (Figure 10). Using ¹⁸O-labeled oxygen, it was found that both routes follow the same mechanism as previously described up to the tetrahedral intermediate. The tetrahedral intermediate breaks down via homolytic bond cleavage forming the nitro radical. In the anaerobic pathway, the nitro radical recombines with the alkyl radical with attack of the oxygen centered radical, forming a carbon-oxygen bond. Subsequent attack by water and elimination of bromide furnishes the desired amide and nitrous acid as a byproduct. In the aerobic pathway, the alkyl radical traps triplet oxygen forming the peroxide radical. The resulting oxygen centered radical then combines with the nitro radical forming another tetrahedral

³⁴ Shen, B.; Makley, D. M.; Johnston, J. N. *Nature* **2010**, *465*, 1027-1032.

³⁵ Seebach, D.; Corey, E. J. *J. Org. Chem.* **1975**, *40*, 231-237.

³⁶ Shackelford, J. P.; Shen, B.; Johnston, J. N. *Proc. Natl. Acad. Sci. U. S. A.* **2012**, *109*, 44-46.

Figure 10. Anaerobic and aerobic pathways of UmAS



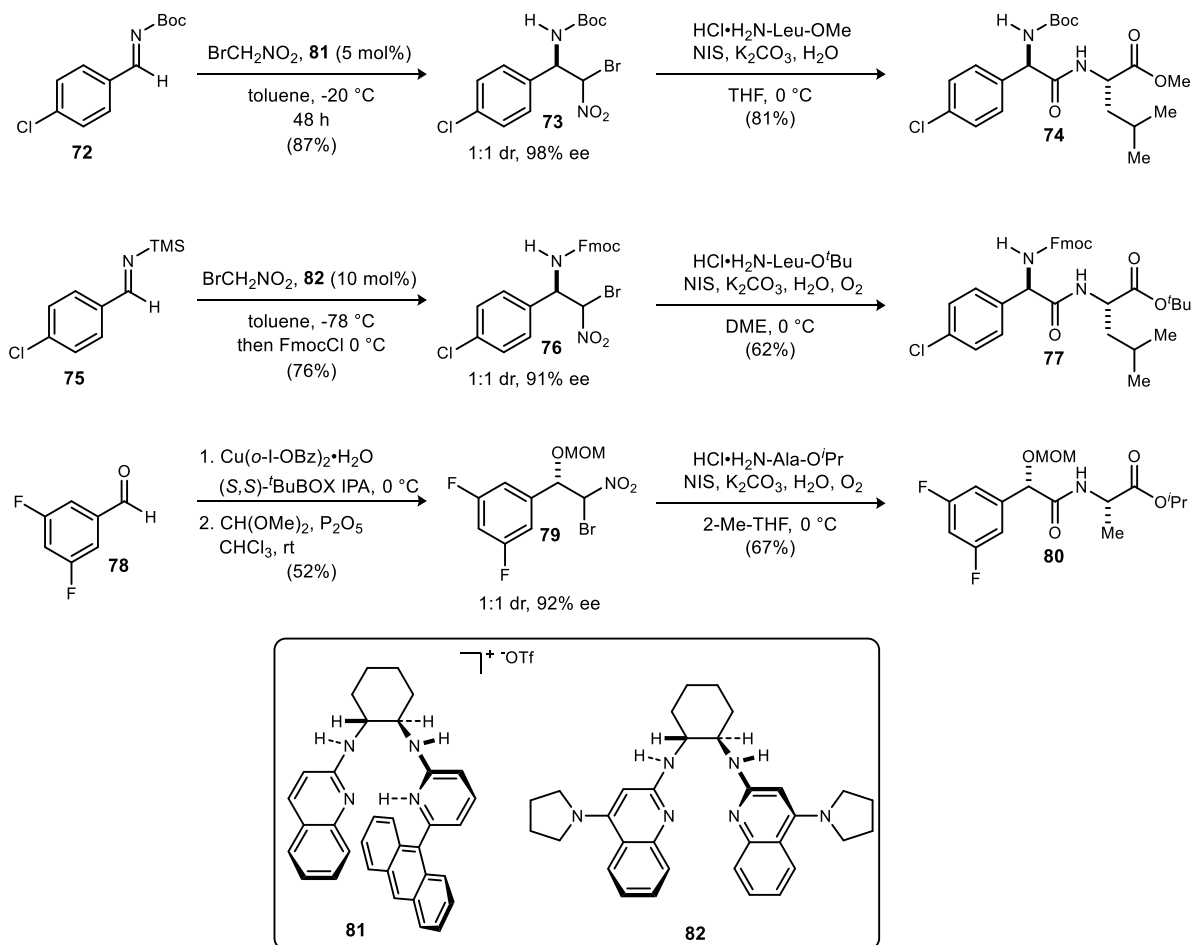
intermediate. Homolytic bond cleavage of the oxygen-oxygen bond and the bromine-carbon bond results in the desired amide.

The advantages of Umpolung Amide Synthesis (UmAS) as compared to traditional amide bond formation are twofold. In condensative peptide synthesis, the amide coupling proceeds through an active ester. Epimerization of the chiral carboxyl donors at the α -carbon is a common problem, especially with arylglycines. Since UmAS does not proceed through an active ester intermediate, epimerization cannot occur through that pathway. Secondly, a number of methods to synthesize chiral α -bromonitroalkanes have been developed allowing for peptide synthesis with unnatural amino acids (Scheme 11). Boc-protected arylglycine donors can be accessed through an enantioselective aza-Henry reaction with catalyst **81**.³⁴ The arylglycine donors can then be homologated with an amino acid to obtain a dipeptide. Another method has been developed to access arylglycine donors with a variety of protecting groups from the same starting substrate.³⁷ Aryl TMS-imines were employed in an aza-Henry reaction with bromonitromethane. The intermediate silyl-amine can be quenched with an electrophile to provide the desired protected arylglycine donor. Lastly, the synthesis of α -oxy amides was achieved using a copper bis(oxazoline) catalyzed Henry reaction coupled with UmAS.³⁸ These three methods give access to unnatural arylglycines as well as hydroxyamides that allow UmAS to be used in peptide and depsipeptide synthesis.

³⁷ Makley, D. M.; Johnston, J. N. *Org. Lett.* **2014**, *16*, 3146-3149.

³⁸ Leighty, M. W.; Shen, B.; Johnston, J. N. *J. Am. Chem. Soc.* **2012**, *134*, 15233-15236.

Scheme 11. Access to chiral bromonitroalkanes and their use in UmAS



1.3 Umpolung Amide Synthesis Substoichiometric in NIS

Our initial reports of UmAS required stoichiometric amounts of NIS, or other halonium sources, to achieve near complete conversion and high yield. Careful reasoning based on the proposed mechanism suggested that a pathway for halonium turnover may be present. As shown in Figure 11, under aerobic conditions, bromonium nitrate, or Br^+ and NO_3^- , is produced as a byproduct in amide formation. The formal formation of Br^+ should allow for the reaction to be substoichiometric in halonium promoter. Alternatively, under anaerobic conditions, the bromide/iodide produced should turnover, since bromonium is the byproduct.

Figure 11. UmAS: competing anaerobic and aerobic pathways to amide

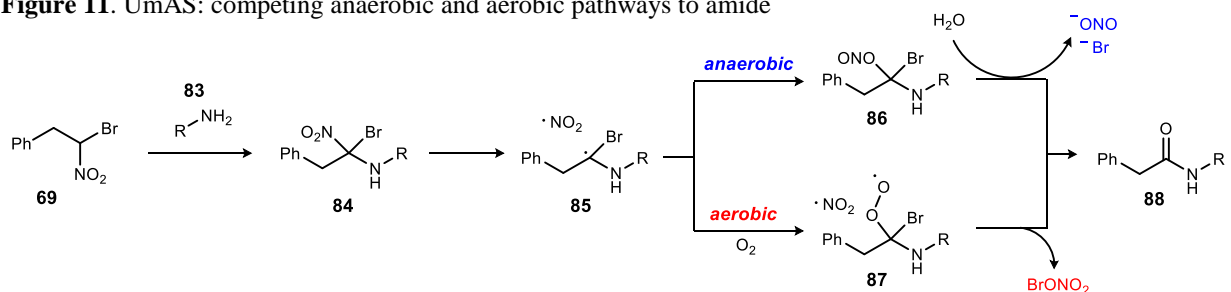
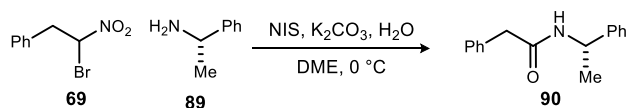


Table 1. Investigation of NIS reagent loading

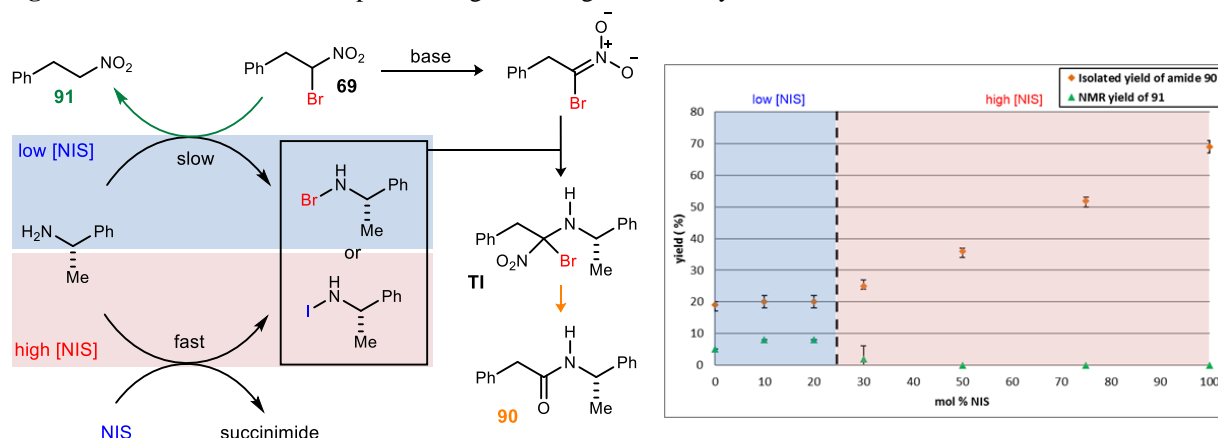
entry ^a	O ₂ ^b	NIS amount (mol %)	yield (%) ^c
1	yes	20	76
2	yes	10	73
3	yes	5	76
4	yes	1	55
5	yes	0	51
6	no	100	69
7	no	75	52
8	no	50	36
9	no	30	25
10	no	20	20
11	no	10	20
12	no	0	19

^aReactions are 0.2 M in nitroalkane and employ 1.2 equiv. amine and 5 equiv. H₂O. Under anaerobic conditions (entries 6-12), NIS was added once the nitroalkane was no longer visible by TLC, indicating that the nitronate predominated (see Experimental section). ^bAll solutions were first degassed (freeze-pump-thaw cycles), and entries not using oxygen were performed under an argon atmosphere (balloon), whereas entries using oxygen were performed under an oxygen atmosphere (balloon). ^cIsolated yield.

In order to test the hypothesis that the reaction should be capable of iodonium/bromonium turnover under aerobic conditions, bromonitroalkane **69** was coupled to (*S*)- α -methyl benzylamine (**89**) with substoichiometric amounts of NIS (20, 10, and 5 mol %) (Table 1). As was expected the reactions reached near full conversion and the desired amide was isolated in high yield (76%, 73%, 76% respectively). Further lowering of the NIS loading to 1 mol % resulted in diminished yield to 55%. Interestingly, when the reaction was run without NIS the amide product was obtained in 51% yield. Careful inspection of the crude NMR spectrum for this reaction elucidated the presence of de-brominated starting material. We hypothesized that the α -bromonitroalkane starting material donated bromonium to the amine to initiate the reaction which then proceeded normally. These results support the initial hypothesis that the reaction could be rendered substoichiometric in NIS.

To further support the hypothesis that halonium turnover only occurred under aerobic conditions, a series of reactions were conducted with a range of amounts of NIS (0-100 mol %) under anaerobic conditions (Table 1). Freeze-pump-thaw techniques were employed in order to rigorously ensure the exclusion of oxygen. Initial results were erratic and irreproducible as it appeared the debromination of the starting material played a significant role when all reagents were added at the beginning of the reaction. A new procedure was developed in an attempt to limit the bromonium donation of the substrate. Prior to the addition of NIS, the nitronate was fully formed (as judged by TLC, details in experimental section). The idea behind this procedure was that once the nitronate was formed, debromination would not occur. Fortunately, this procedural change allowed for reproducible results. At high NIS loadings (>30%), the yield tracked well with the amount of NIS as expected without the possibility of halonium turnover. At lower levels of NIS however, the yield of amide was higher than expected. For example, at 0 mol % NIS the amide product was obtained in 19% yield when we expected 0%. This suggests that substrate **69** acts as a competent halonium source, providing conversion to amide in the absence of NIS (Figure 12). At higher NIS loadings (≥ 30 mol %), debrominated nitroalkane **91** was not observed, signaling that the substrate contributes negligibly as a bromonium source. At these levels of NIS, a linear relationship is observed

Figure 12. Correlation of electrophilic halogen loading and amide yield under anaerobic conditions



between the yield and NIS loading. This behavior suggests that the substrate only acts as the bromonium source when the reaction is starved of NIS leading to two different pathways (iodonium- vs bromonium-mediated) to form the halamine.

The behavior outlined in Table 1 is consistent with the intermediates and pathways depicted in Scheme 12. Recombination of the nitrogen dioxide radical at oxygen to carbon radical **85** under anaerobic conditions leads to an alkyl nitrite that can hydrolyze to amide. The byproducts of this step are formally nitrite and bromide. Under aerobic conditions, however, dioxygen adds to carbon radical **85** to provide alkyl peroxy intermediate **87**. A straightforward equation balance of **87** and $\cdot\text{NO}_2$ with amide product leads to a difference of the elements of bromonium nitrate on the product side. Hence, aerobic conditions and NIS lead to the production of an equivalent of bromonium, in contrast to anaerobic conditions that lead to an equivalent each of bromide and iodide. It is unknown whether bromonium becomes the active halonium source for amine activation or rather bromonium oxidizes iodide to iodonium to regenerate the active halonium species.

The newly developed aerobic UmAS substoichiometric in NIS conditions (5 mol % NIS, O_2 atmosphere) were applied to a variety of different substrates and compared to the results using stoichiometric conditions (Table 2). In general, the yields using 5 mol % NIS were very similar to the stoichiometric protocol. Notably, the new protocol was efficient at coupling arylglycine precursors to provide peptide products (**74**, **103**, **106**).

Scheme 12. UmAS: halonium turnover

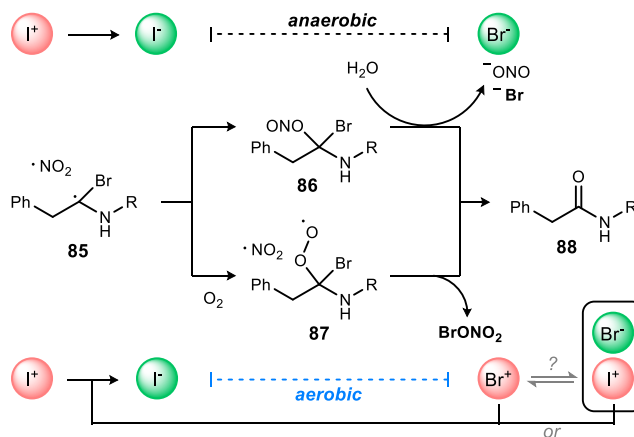
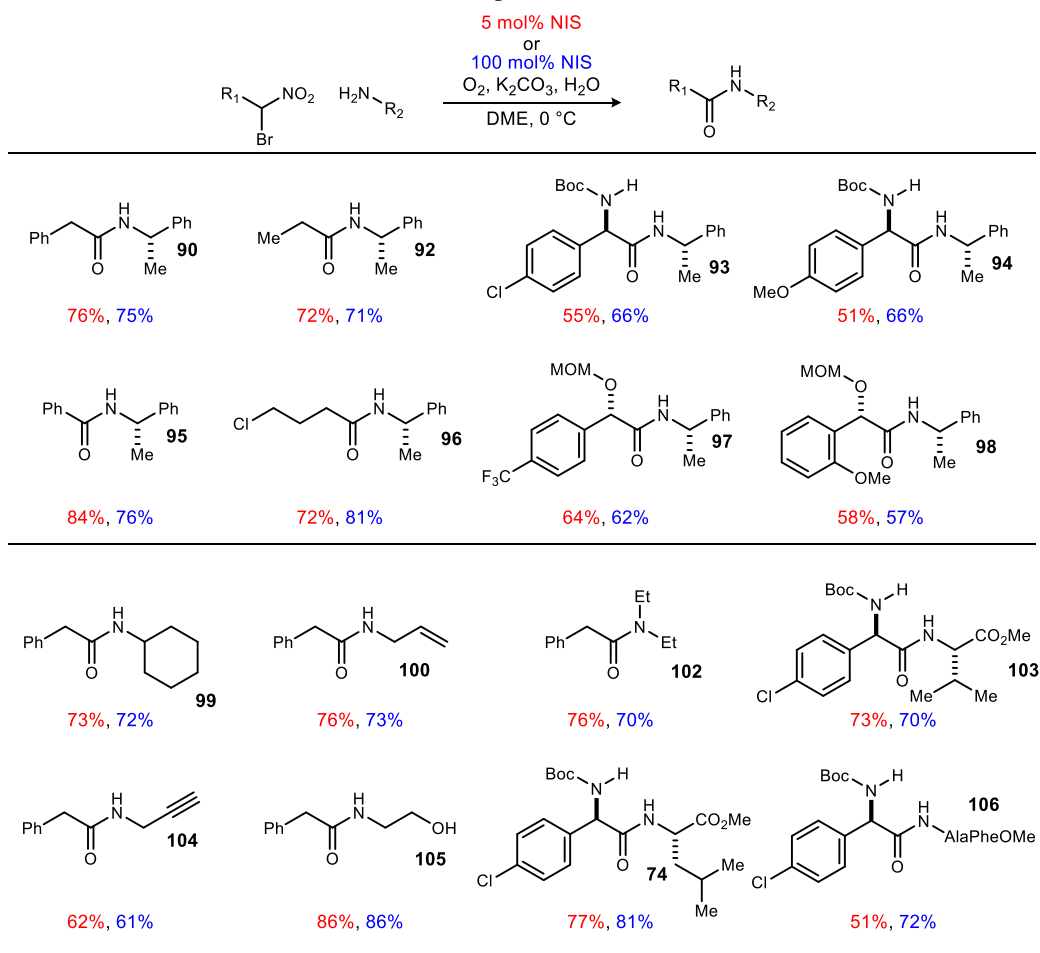


Table 2. UmAS substoichiometric in NIS substrate scope

Reactions are 0.2 M in nitroalkane and employ 1.2 equiv. amine, 5 equiv. H₂O and 5 or 100 mol % NIS. All reactions were run under O₂ atmosphere. Isolated yields reported.

In conclusion, after mechanistic consideration, it was proposed that Umpolung Amide Synthesis under aerobic conditions should provide a pathway to electrophilic halonium regeneration. This resulted in the development of a protocol for amide formation using substoichiometric NIS. The developed protocol does not require reagent excess and avoids the production of coproducts that present purification issues. In combination with methods previously developed for the synthesis of chiral nonracemic α -bromonitroalkanes, fully catalytic, enantioselective peptide synthesis is possible.

Chapter II

II. Organocatalyzed Enantioselective Synthesis of α -Alkyl Unnatural α -Amino Amides³⁹

The goal of this project is to develop a new platform to achieve the goals of on-demand peptide synthesis, for those α -amino amide residues that bear α -alkyl substituents. In order to be considered on-demand, the process must be affordable, efficient, timely, and allow the incorporation of a broad range of side chains for unnatural α -amino amide synthesis. Our approach features a two-step sequence: an organocatalyzed enantioselective aza-Henry reaction followed by Umpolung Amide Synthesis to provide homologated unnatural amino acids starting from aldehydes, an inexpensive feedstock (Figure 13). Previous work has begun to reach this goal for the inclusion of arylglycine amino acids, but the extension of the methodology to alkyl amino acids has proven difficult.

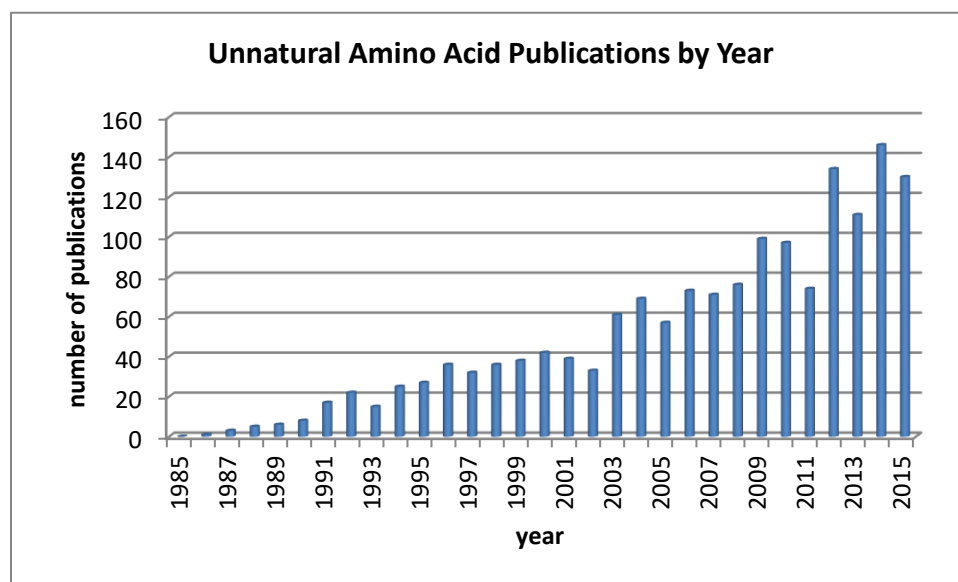
Figure 13. Proposed synthesis of alkyl unnatural amino amides



2.1 Importance and Synthesis of Unnatural Amino Acids

Unnatural α -amino acids, also referred to as nonnatural, nonproteinogenic, or noncanonical, encompass any α -amino acid residue with a side chain differing from the 20 canonical amino acids as well as those with differing stereochemistry. Although some unnatural amino acids are in fact found in nature, they are still referred to as unnatural. Incorporation of unnatural amino acids into peptides and proteins allows for further modulation of structure and function beyond what the canonical amino acids are capable

Figure 14. Unnatural amino acid publications by year



*SciFinder, 2016: search term “unnatural amino acids”

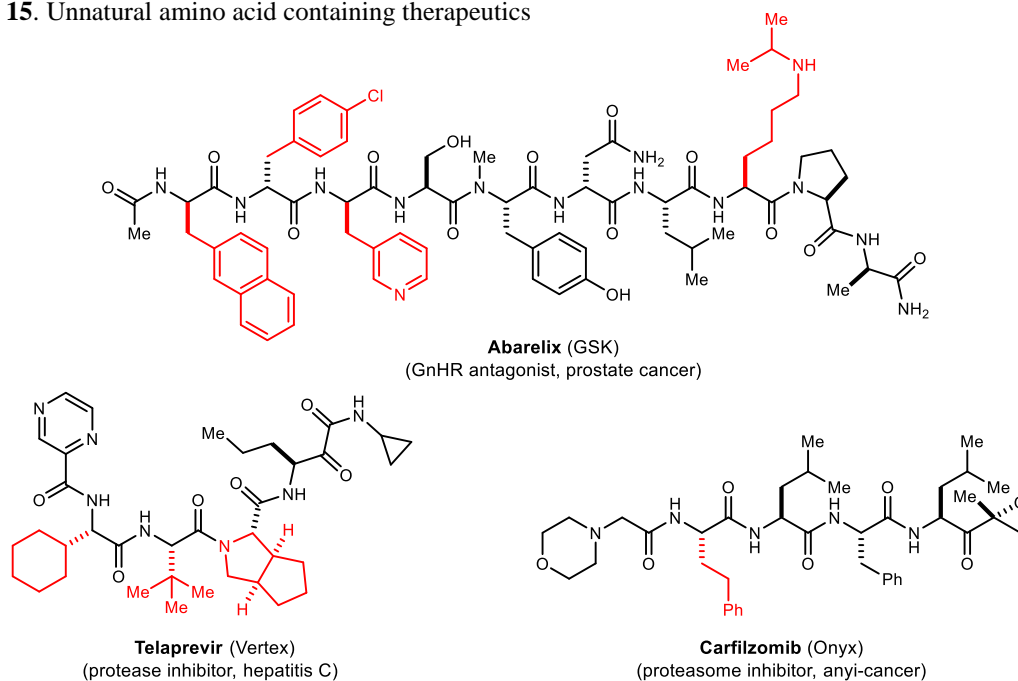
³⁹ Schwieter, K. E.; Johnston, J. N. *Chem. Sci.* **2015**, 6, 2590-2595; Schwieter, K. E.; Johnston, J. N. *ACS Catalysis* **2015**, 5, 6559-6562.

of doing. For this reason, unnatural amino acids have recently been extensively studied with regards to drug development, peptide stapling, and bioorthogonal labeling making them a fast growing field. Figure 14 shows the increased interest in unnatural amino acids over the last 30 years.

Although peptides containing only natural amino acids have found wide applications as drugs, there are a few major drawbacks, including rapid proteolytic metabolism and poorly selective interactions, which have limited their scope and effectiveness.⁴⁰ In an effort to circumvent these issues, peptidomimetics containing unnatural amino acids have been introduced to serve as surrogates, with the ability to maintain the same bioactivity and function, while offering several advantages, including improved in vivo stability, enhanced potency, better oral absorption, improved tissue distribution and increased selectivity.

A number of unnatural amino acid drugs are currently on the market, treating a variety of therapeutic areas (Figure 15). For example, Abarelix (trade name Plenaxis), developed by GSK, was approved in 2003 as a GnRH antagonist that was used as a treatment for prostate cancer.⁴¹ Structurally, Abarelix is a decapeptide containing four unnatural amino acid residues, three of which are D-phenylalanine derivatives while the other is an alkylated lysine residue. Another example, Telaprevir (trade names Incivek, Incivo), developed by Vertex and Johnson and Johnson, is a protease inhibitor used for the treatment of hepatitis C.² Telaprevir contains three unnatural amino acid residues as well as an amino α -ketoamide residue. In both of these examples, the unnatural amino acids were necessary to provide the desired activity as well as pharmacological properties.

Figure 15. Unnatural amino acid containing therapeutics



Peptide stapling serves as another application of unnatural amino acids.⁴² Stapled peptides are defined as peptides containing covalent linkages between amino acid side chains. The concept was introduced in an attempt to stabilize the α -helix structural motif in peptides that can be responsible for the observed activity. Peptides often lose their structure in solution and thus lose the desired activity. If the α -helix could be stabilized, it would be possible to maintain structure and activity in solution. The first all-

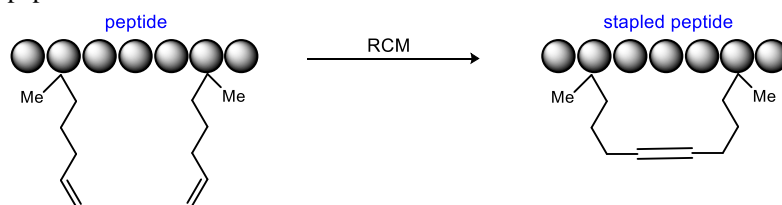
⁴⁰ Otvos, L.; Wade, J. D. *Front. Chem.* **2014**, *2*, 62

⁴¹ Mongiat-Artus, P.; Teillac, P. *Expert Opinion on Pharmacotherapy* **2004**, *5*, 2171-2179.

⁴² For a review: Walensky, L. D.; Bird, G. H. *J. Med. Chem.* **2014**, *57*, 6275-6288.

hydrocarbon stapled peptide was reported by Verdine in 2000 using unnatural α,α -disubstituted amino acids bearing olefin side chains as staple precursors.⁴³ Ring-closing olefin metathesis was used to generate the staple resulting in structural stabilization as well as observed protease resistance (Figure 16).

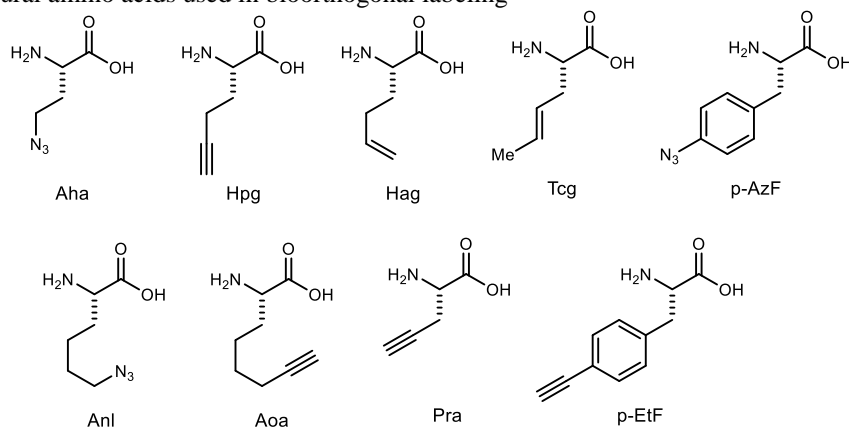
Figure 16. Stapled peptides



In 2004 Korsmeyer and coworkers utilized a similar all-hydrocarbon peptide staple to stabilize the α -helix of the BH3 domain from the BID protein.⁴⁴ BID is a pro-apoptotic protein that belongs to the BCL-2 protein family that contains only the BH3 domain. They found that by incorporating an all hydrocarbon chain into a protein mimicking the BH3 domain of BID, the α -helicity in solution dramatically increased from 16% up to 87%. Along with increased α -helicity came improved proteolytic stability, cell permeability, and in vitro and in vivo activity toward leukemia cells.

Peptide or protein labeling represents another important application of unnatural amino acids.⁴⁵ Bioorthogonal labeling entails unnatural amino acid incorporation into proteins in a living system followed by a chemoselective reaction to attach a probe with a specific functionality to the specific amino acid side chain. Probes are frequently imaging agents, such as fluorescent compounds, but they can also be spin labels and biomolecules, such as biotin. There are a number of developed biorthogonal reactions including the Staudinger ligation, alkyne-azide cycloaddition, alkene-azide cycloaddition, alkene-tetrazole cycloaddition, etc. In order to utilize one of these reactions, one of the necessary functional groups must be present in the unnatural amino acid incorporated in the protein. Common amino acid side chains for this purpose include azido, alkynyl, and alkenyl functionalities (Figure 17).⁴⁵

Figure 17. Unnatural amino acids used in bioorthogonal labeling



In 2005 Tirrell reported the incorporation of an alkyne bearing amino acid into a protein to allow for fluorescent labeling.⁴⁶ The model protein was synthesized in *E. coli* cells with the incorporation of alkynyl containing unnatural amino acid homopropargyl glycine (Hpg) replacing methionine residues. The

⁴³ Schafmeister, C. E.; Po, J.; Verdine, G. L. *J. Am. Chem. Soc.* **2000**, *122*, 5891-5892.

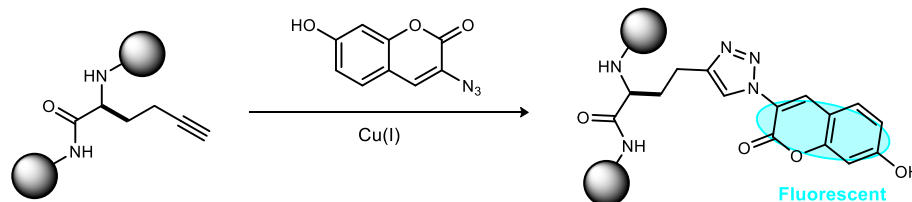
⁴⁴ Walensky, L. D.; Kung, A. L.; Escher, I.; Malia, T. J.; Barbuto, S.; Wright, R. D.; Wagner, G.; Verdine, G. L.; Korsmeyer, S. J. *Science* **2004**, *305*, 1466-1470.

⁴⁵ For a review: Lang, K.; Chin, J. W. *Chem. Rev.* **2014**, *114*, 4764-4806.

⁴⁶ Beatty, K. E.; Xie, F.; Wang, Q.; Tirrell, D. A. *J. Am. Chem. Soc.* **2005**, *127*, 14150-14151.

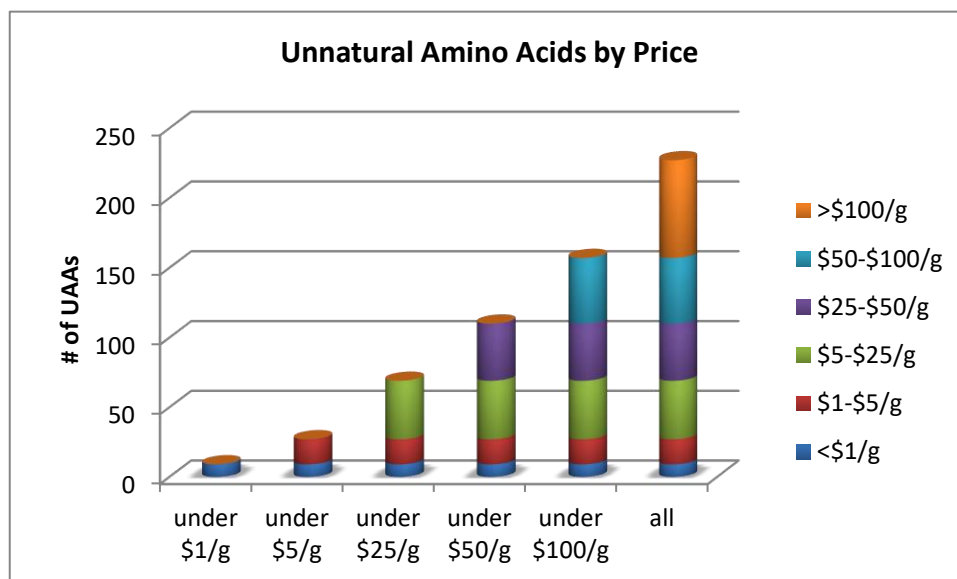
cells were then treated with CuBr and the azido fluorescent probe to successfully promote a [3+2] azide-alkyne cycloaddition resulting in an observed fluorescence (Figure 18). This work demonstrated the utility of the azide-alkyne cycloaddition for biorthogonal fluorescent labeling.

Figure 18. Fluorescent labeling of Hpg containing protein



Unlike the canonical amino acids that are obtained through extraction from natural sources, unnatural amino acids are predominantly obtained through chemical synthesis. For this reason, the commercial availability of unnatural amino acids varies dramatically based on synthetic access as well as demand. There are numerous vendors that supply a wide array of unnatural amino acids, either as the free amino acid or protected and ready for peptide synthesis, in a wide range of prices. In an effort to survey the current market, one vendor (Chem-Impex International) was selected to analyze the amino acids available for purchase. Only unprotected amino acids bearing unnatural side chains were included in the analysis. In total 227 amino acids were selected and organized based on \$/g in order to gain information about affordability (column graph). As shown in Figure 19, as the price increases, the number of available amino acids increases at a much greater rate. For example, only 27 are available for under \$5/g, while an additional 42 are available for under \$25/g. Significantly, 31% (70 amino acids) of the included unnatural amino acids are over \$100/g, making them prohibitively expensive. This data demonstrates the need for improvement in unnatural amino acid synthesis in order to lower the cost and increase the overall availability.

Figure 19. Commercial availability of unnatural amino acids



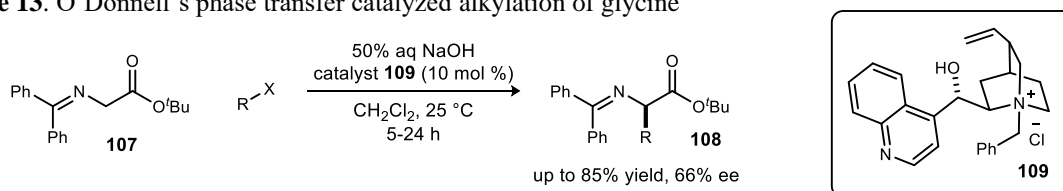
Catalytic Asymmetric Synthesis of Unnatural Alkyl Amino Acids

The asymmetric synthesis of α -amino acids has been extensively studied for many years resulting in the development of numerous strategies and methods. Many of these methods are limited by narrow

substrate scopes and thus are only suitable for the synthesis of a small subset of α -amino acids. For example, many methods focus solely on the synthesis of arylglycines.⁴⁷ Only a few asymmetric methods, namely the alkylation of a glycine, hydrogenation of either α,β -dehydro- α -amino acids or α -imino esters, and the Strecker reaction, are general enough to provide access to a wide array of alkyl α -amino acids.

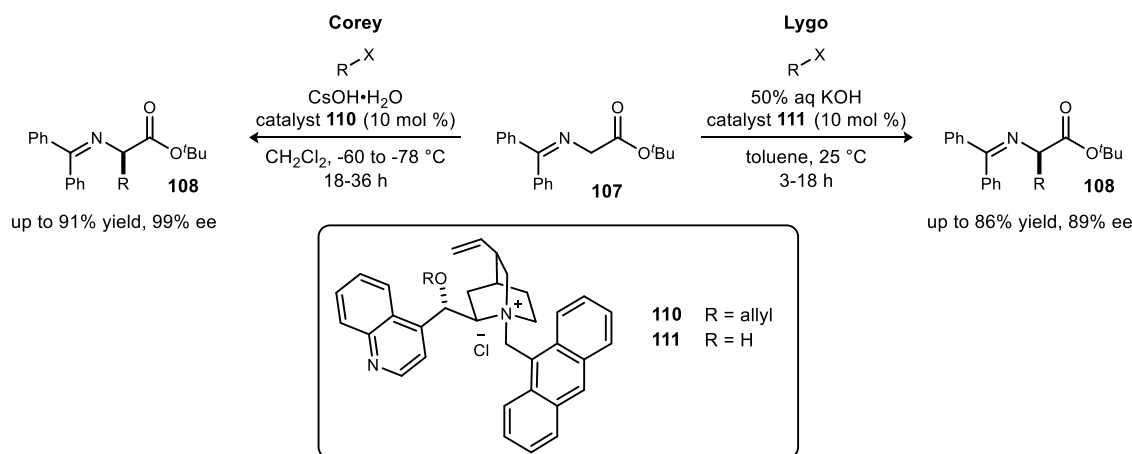
The asymmetric phase transfer catalyzed alkylation of glycine was first reported by O'Donnell in 1989.⁴⁸ Using cinchonine derived phase transfer catalyst **109** and aqueous NaOH, the benzophenone Schiff base of glycine was alkylated with a variety of alkyl and benzyl bromides to obtain α -amino acids upon deprotection in moderate enantiopurity (up to 66% ee) (Scheme 13). The ester protecting group was found to have a significant impact on enantioselectivity, as the benzyl ester provided the allylglycine product in 14% ee compared to 56% ee when the *tert*-butyl ester was employed. Other key findings included the observations that increasing the concentration of NaOH increased ee and using bromide as a leaving group provided higher enantioselectivity than chloride or iodide.

Scheme 13. O'Donnell's phase transfer catalyzed alkylation of glycine



In 1997 Lygo and Corey simultaneously reported a new modification of the phase transfer catalyst that drastically improved enantioselectivity.⁴⁹ Both groups discovered that by substituting the benzyl group on the quaternary ammonium with a 9-anthracenylmethyl group a higher degree of enantioselection can be achieved (Scheme 14). Corey's cinchona alkaloid catalyst differs from Lygo's in that the hydroxyl group is allylated in Corey's case while it remains a free hydroxyl group in Lygo's system. However, Lygo states

Scheme 14. Corey and Lygo's phase transfer catalyzed alkylations of glycine



⁴⁷ Reddy, K. L.; Sharpless, K. B. *J. Am. Chem. Soc.* **1998**, *120*, 1207-1217; Shang, G.; Yang, Q.; Zhang, X. *Angew. Chem. Int. Ed.* **2006**, *45*, 6360-6362; Beenen, M. A.; Weix, D. J.; Ellman, J. A. *J. Am. Chem. Soc.* **2006**, *128*, 6304-6305; Dai, H.; Yang, M.; Lu, X. *Adv. Synth. Catal.* **2008**, *350*, 249-253; Lee, E. C.; Fu, G. C. *J. Am. Chem. Soc.* **2007**, *129*, 12066-12067; Xu, B.; Zhu, S.-F.; Xie, X.-L.; Shen, J.-J.; Zhou, Q.-L. *Angew. Chem. Int. Ed.* **2011**, *50*, 11483-11486.

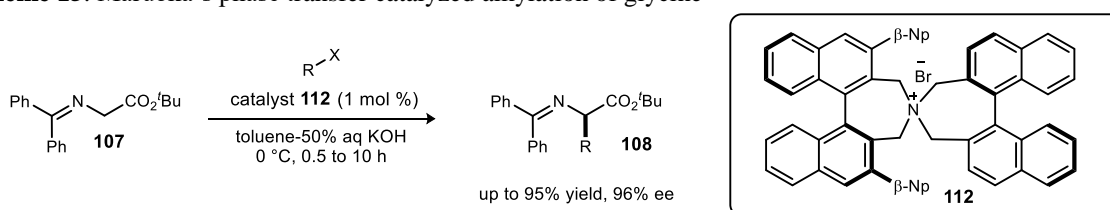
⁴⁸ O'Donnell, M. J.; Bennett, W. D.; Wu, S. *J. Am. Chem. Soc.* **1989**, *111*, 2353-2355.

⁴⁹ Corey, E. J.; Xu, F.; Noe, M. C. *J. Am. Chem. Soc.* **1997**, *119*, 12414-12415; Lygo, B.; Wainwright, P. G. *Tetrahedron Lett.* **1997**, *38*, 8595-8598.

that the hydroxyl group is alkylated in situ to generate the active catalyst. Corey demonstrated that by lowering the reaction temperature to $-78\text{ }^{\circ}\text{C}$, ee's up to 99.5% can be obtained. The development of this new catalyst was a significant step as the amino acid products were obtained in high enough enantiopurity for peptide synthesis.

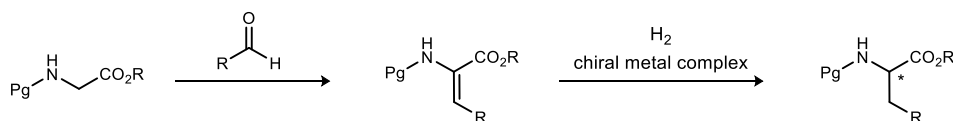
Maruoka contributed to this field in 1999 with the discovery of a new type of chiral phase transfer catalyst.⁵⁰ The C_2 -symmetric spiro quaternary ammonium salt catalyst **112** derived from (*S*)-BINOL was able promote the glycine alkylation in high yield and enantioselectivity (Scheme 15). The aryl-groups off of the naphthyl backbone proved to be key to stereinduction as the product was obtained in 79% ee without an aryl group while the optimal catalyst **112** provided the product in 96% ee. More recently, a number of new catalysts have been developed to foster the same asymmetric alkylation of glycine to gain access to a variety of α -amino acids.⁵¹

Scheme 15. Maruoka's phase transfer catalyzed alkylation of glycine



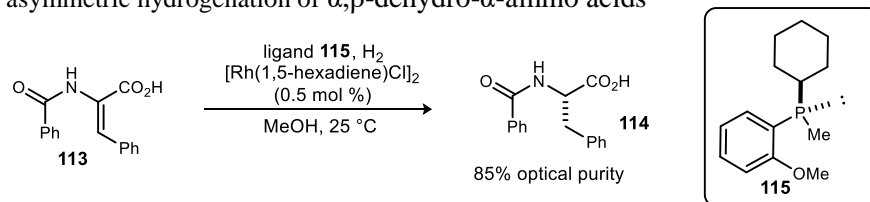
Asymmetric hydrogenation has emerged as one of the best methods for the synthesis of optically active α -amino acids. This approach features the enantioselective introduction of the α -hydrogen as opposed

Scheme 16. Strategy for synthesis of α -amino acids via asymmetric hydrogenation



to the enantioselective introduction of the α -side chain as is the case in the asymmetric glycine alkylations. α,β -Dehydro- α -amino acids (DAA), the necessary substrates, are prepared via a condensation reaction between protected glycine and an aldehyde. The subsequent transition metal catalyzed asymmetric hydrogenation provides the protected amino acid (Scheme 16). The pioneering work by Knowles, Horner, and Kagan set the stage for significant advances in this area.⁵² Knowles demonstrated that a chiral phosphine rhodium complex in the presence of H_2 was able to hydrogenate dehydro amino acid **113**, to provide protected phenylalanine in 85% optical purity (Scheme 17). Although the substrate scope was very

Scheme 17. First asymmetric hydrogenation of α,β -dehydro- α -amino acids



⁵⁰ Ooi, T.; Kameda, M.; Maruoka, K. *J. Am. Chem. Soc.* **1999**, *121*, 6519-6520.

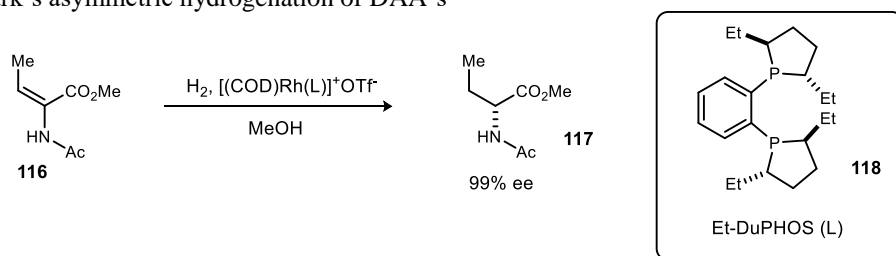
⁵¹ Shirakawa, S.; Maruoka, K. *Angew. Chem. Int. Ed.* **2013**, *52*, 4312-4348.

⁵² Knowles, W. S.; Sabacky, M. J. *Chem. Commun.* **1968**, 1445-1446; Horner, L.; Siegel, H.; Büthe, H. *Angew. Chem. Int. Ed.* **1968**, *7*, 942-942; Dang, T. P.; Kagan, H. B. *Journal of the Chemical Society D: Chemical Communications* **1971**, 481-481; Knowles, W. S.; Sabacky, M. J.; Vineyard, B. D. *J. Chem. Soc., Chem. Commun.* **1972**, *0*, 10-11.

minimal, allowing synthesis of only phenylalanine derivatives, this served as a proof of concept for further advancements.

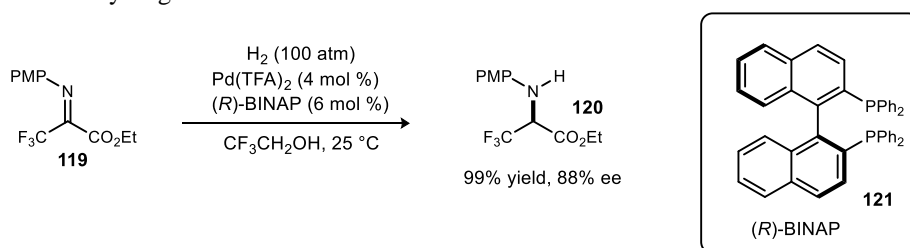
More recently, in 1993 Burk reported the first use of a rhodium phospholane complex in the asymmetric hydrogenation of DAAs resulting in the corresponding amino acids (Scheme 18).⁵³ The use of Et-DuPHOS (**118**) as the ligand allowed for high enantioselection (up to 99% ee) with a wide variety of alkyl substituents as well as substituted phenylalanine derivatives. The phospholane ligands provided improved selectivity, efficiency, and substrate scope as compared to phosphine ligands that were previously employed. Further discoveries leveraged phosphoramidites and phosphites as competent ligands for asymmetric hydrogenation.⁵⁴

Scheme 18. Burk's asymmetric hydrogenation of DAA's



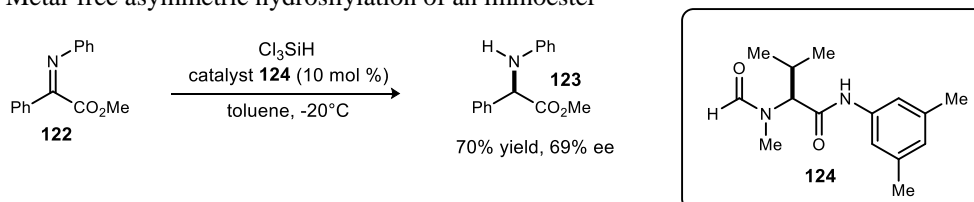
Iminoesters have also been utilized as competent precursors to α -amino acids through catalytic asymmetric hydrogenation. Uneyama and coworkers reported the palladium catalyzed hydrogenation of fluoro iminoesters employing (*R*)-BINAP (**121**) as the chiral ligand (Scheme 19).⁵⁵ This approach gives access to unnatural amino acids bearing fluorine side chains in high enantiopurity (up to 91% ee). Key to the discovery was the necessity of using a fluorinated solvent to obtain high enantioselectivity.

Scheme 19. Asymmetric hydrogenation of fluoro iminoesters



A metal-free approach was developed in 2006 by Malkov and coworkers. The hydrosilylation reaction utilized trichlorosilane as the reductant and valine organocatalyst **124** as the source of chirality (Scheme 20). Although this approach was initially developed for the reduction of ketimines, it was applied to phenyl iminoester to provide phenylglycine in moderate ee.

Scheme 20. Metal-free asymmetric hydrosilylation of an iminoester



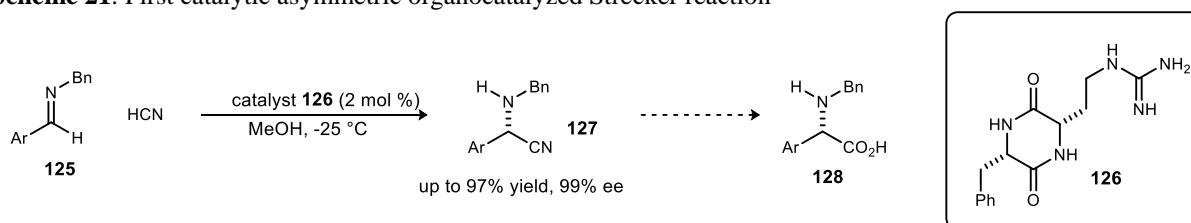
⁵³ Burk, M. J.; Feaster, J. E.; Nugent, W. A.; Harlow, R. L. *J. Am. Chem. Soc.* **1993**, *115*, 10125-10138.

⁵⁴ Nájera, C.; Sansano, J. M. *Chem. Rev.* **2007**, *107*, 4584-4671.

⁵⁵ Abe, H.; Amii, H.; Uneyama, K. *Org. Lett.* **2001**, *3*, 313-315.

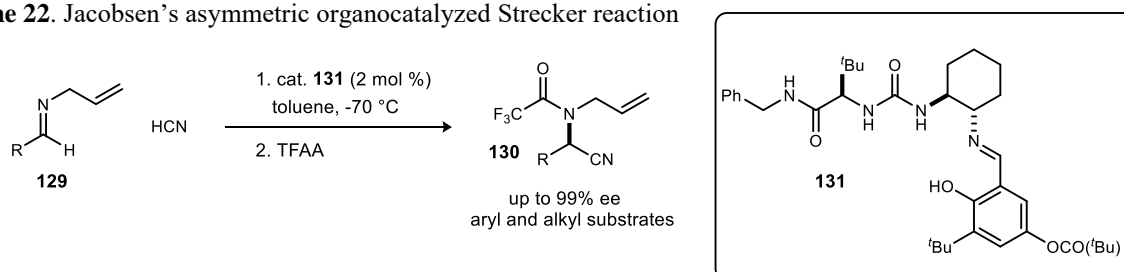
The Strecker reaction has emerged as a proficient method to gain access to unnatural α -amino acids.⁵⁶ Lipton was the first to report a catalytic asymmetric organocatalyzed version that allowed for the asymmetric introduction of the carboxy group in the form of a nitrile (Scheme 21).⁵⁷ Subsequent hydrolysis can provide phenylglycine derivatives in varying enantiopurity (10-99% ee). The catalyst employed was a cyclic dipeptide consisting of (*S*)-phenylalanine and an (*S*)-arginine homologue. Alkyl imines provided adducts in low enantiopurity, proving to be the main limitation of this work.

Scheme 21. First catalytic asymmetric organocatalyzed Strecker reaction



Jacobsen reported the development of a chiral urea catalyst capable of promoting the asymmetric Strecker reaction (Scheme 22).⁵⁸ This report significantly broadened the scope of the reaction as compared to Lipton's report, providing access to both aryl and aliphatic amino acids in high yield and stereoselectivity. From a catalyst design perspective, it was found that the two bulky *tert*-butyl groups were necessary for high enantioselectivity. The main limitation of this report is the harsh conditions needed to hydrolyze the nitrile to the carboxylic acid.

Scheme 22. Jacobsen's asymmetric organocatalyzed Strecker reaction



Currently, the asymmetric synthesis of unnatural amino acids is dominated by the three previously discussed methods: glycine alkylation, hydrogenation, and the Strecker reaction. Significant work has been done on these methods allowing for wide substrate tolerance giving access to a large array of unnatural amino acids. Nevertheless, there is still room for improvement as certain side chain functionalities prove difficult to synthesize using these methods. Additionally, many of the necessary protecting groups for these strategies are not compatible with peptide synthesis, adding synthetic steps to access the properly functionalized amino acids.

2.2 The aza-Henry Reaction

The aza-Henry, or nitro-Mannich, reaction is a carbon-carbon bond forming reaction in which a nitroalkane is added to an imine under either acidic or basic conditions to generate β -nitroamines.⁵⁹ The

⁵⁶ Wang, J.; Liu, X.; Feng, X. *Chem. Rev.* **2011**, *111*, 6947-6983.

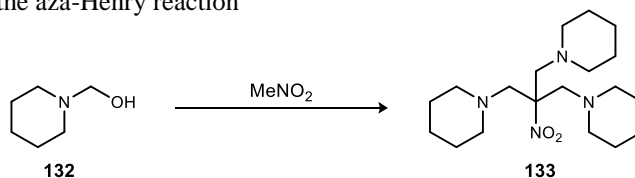
⁵⁷ Iyer, M. S.; Gigstad, K. M.; Namdev, N. D.; Lipton, M. *J. Am. Chem. Soc.* **1996**, *118*, 4910-4911.

⁵⁸ Sigman, M. S.; Vachal, P.; Jacobsen, E. N. *Angew. Chem. Int. Ed.* **2000**, *39*, 1279-1281.

⁵⁹ For a review: Noble, A.; Anderson, J. C. *Chem. Rev.* **2013**, *113*, 2887-2939.

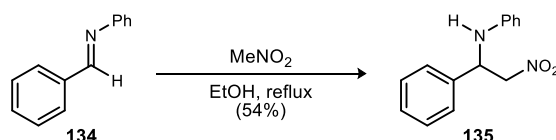
aza-Henry reaction was first reported in 1896 by Henry around the same time he reported the addition of nitroalkanes to aldehydes (Henry reaction).⁶⁰ He found that the hemiaminal derived from piperidine and formaldehyde reacted with nitromethane to form tri-adduct **133**. The reaction presumably proceeds through the formation of the piperidine iminium followed by nucleophilic attack of nitromethane (Scheme 23). No yields or procedures were initially reported. A number of other reports followed utilizing the hemiaminal approach.

Scheme 23. First report of the aza-Henry reaction



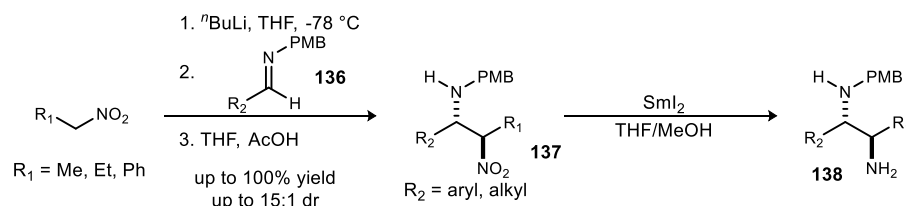
It was not until 1950 that a traditional preformed imine was employed in the aza-Henry reaction. Hurd and Strong reported adding nitromethane into *N*-phenyl benzaldimine in refluxing ethanol (Scheme 24).⁶¹ The aza-Henry adduct was obtained in 64% yield. Nitroethane was also discovered to be a competent nucleophile for the same transformation.

Scheme 24. First report of the aza-Henry reaction using preformed imines



The base-promoted aza-Henry reaction was reported in 1998 by Anderson and coworkers.⁶² The first acyclic diastereoselective aza-Henry reaction was attained through generation of the lithium nitronate followed by addition of the imine (Scheme 25). A variety of aryl and alkyl imines and alkyl nitroalkanes were employed to obtain the β-nitroamines in high yield and up to 15:1 dr. The nitroalkane products were then reduced with SmI₂ to provide 1,2-diamines, demonstrating the synthetic utility of the reaction. This report sparked significant interest in the field resulting in new reaction developments.

Scheme 25. Diastereoselective base-promoted aza-Henry reaction



In 1999, Shibasaki reported the first catalytic enantioselective aza-Henry reaction.⁶³ Nitromethane was successfully added into *N*-phosphinoyl imines providing the aza-Henry adducts in high yield and ee up to 91% (Scheme 26). A heterobimetallic complex generated from Yb(OⁱPr)₃, KOⁱBu, and (*R*)-BINOL was used in 20 mol %. This catalyst system was unable to catalyze the addition of nitroethane or other higher

⁶⁰ Henry, L. *Bull. Acad. Roy. Belg.* **1896**, 32, 33

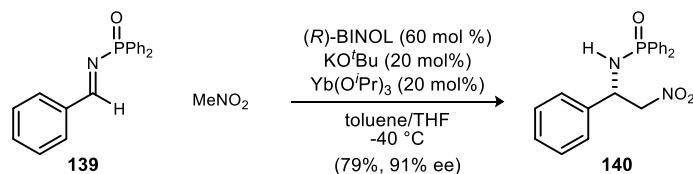
⁶¹ Hurd, C. D.; Strong, J. S. *J. Am. Chem. Soc.* **1950**, 72, 4813-4814.

⁶² Adams, H.; Anderson, J. C.; Peace, S.; Pennell, A. M. K. *J. Org. Chem.* **1998**, 63, 9932-9934.

⁶³ Yamada, K.-i.; Harwood, S. J.; Gröger, H.; Shibasaki, M. *Angew. Chem. Int. Ed.* **1999**, 38, 3504-3506.

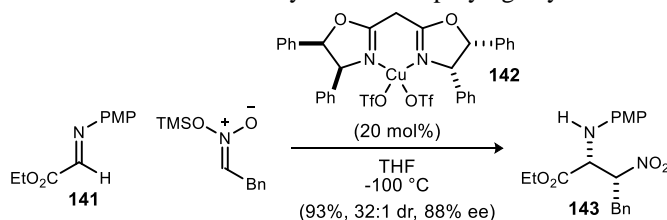
order nitroalkanes. A subsequent report detailed a new catalyst system that was able to effect that transformation.⁶⁴

Scheme 26. First enantioselective aza-Henry reaction



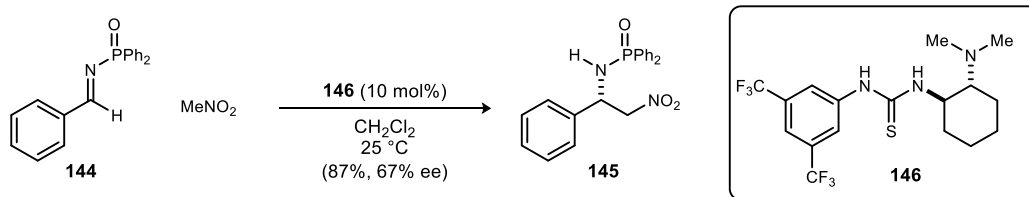
The first catalytic enantioselective addition of silyl nitronates was reported by Jørgensen in 2001.⁶⁵ The use of a silyl nitronate instead of a nitroalkane eliminated the need for basic conditions allowing the use of a chiral Lewis acid to obtain high stereoselectivity in the addition to α -imino esters (Scheme 27). Cu-BOX catalyst **142** was chosen as the optimal catalyst to provide the aza-Henry adducts in high yield, diastereoselectivity and enantioselectivity.

Scheme 27. Jørgensen's enantioselective aza-Henry reaction employing silyl nitronates



One of the first enantioselective organocatalyzed aza-Henry reaction was reported by Takemoto and coworkers in 2004 (the other being reported by our group discussed later in this section).⁶⁶ Thiourea catalyst **146** was employed to add nitromethane into a variety of *N*-phosphinoyl aryl imines (Scheme 28). The aza-Henry adducts were obtained in high yield with modest enantioselection (63-76% ee). Subsequent organocatalysts have been developed and employed in the aza-Henry reaction to obtain high reactivity and enantioselectivity.

Scheme 28. First enantioselective organocatalyzed aza-Henry reaction



Alkyl Imines as Electrophiles in the Enantioselective aza-Henry Reaction

The majority of aza-Henry reactions have been limited to employing solely aryl imines, or other non-enolizable imines, as electrophiles. Alkyl imines have been sparingly used due to their propensity to tautomerize to the more stable enamine. Recently, a number of examples have been reported employing alkyl imines as electrophiles. These reports can be divided into two categories: phase-transfer catalyzed

⁶⁴ Yamada, K.-i.; Moll, G.; Shibasaki, M. *Synlett* **2001**, 2001, 0980-0982.

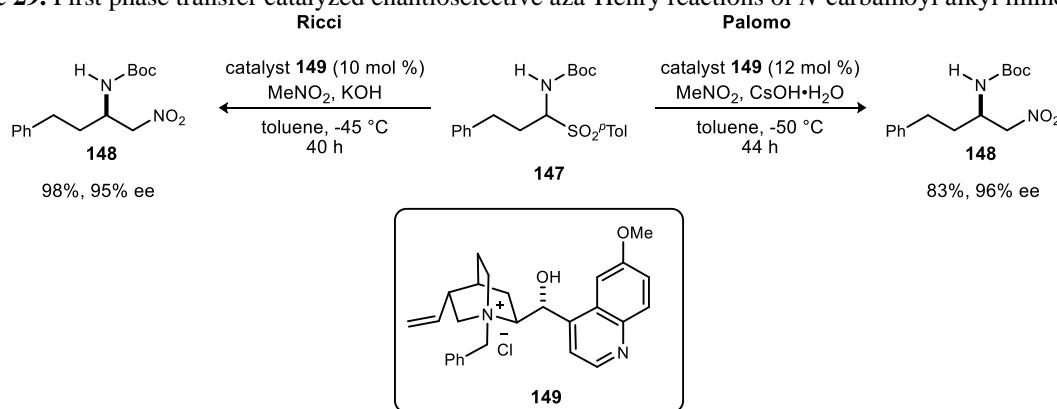
⁶⁵ Knudsen, K. R.; Risgaard, T.; Nishiwaki, N.; Gothelf, K. V.; Jørgensen, K. A. *J. Am. Chem. Soc.* **2001**, *123*, 5843-5844.

⁶⁶ Okino, T.; Nakamura, S.; Furukawa, T.; Takemoto, Y. *Org. Lett.* **2004**, *6*, 625-627.

additions where the imine is generated in situ from an α -amido sulfone and additions directly to a prepared and isolated imine.

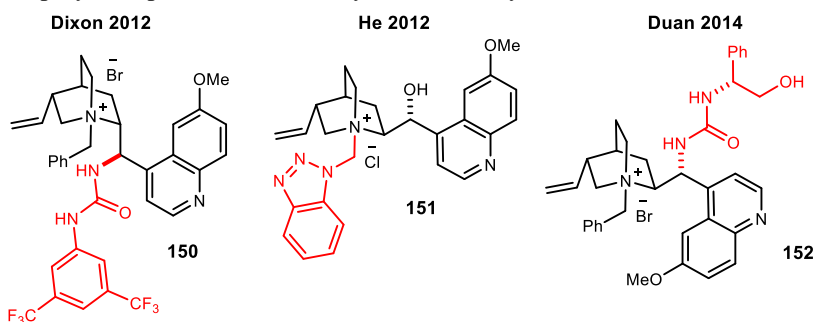
In 2005, Palomo and Ricci simultaneously reported the use of alkylated cinchona alkaloids as phase-transfer catalysts in the enantioselective addition of nitromethane and nitroethane to aryl and alkyl α -amido sulfones (Scheme 29).⁶⁷ These were the first reports providing *N*-carbamoyl alkyl imine derived aza-Henry adducts as the isolation of such imines was not reported at the time. Both groups generated alkyl imines in situ from α -amido sulfones utilizing a phase transfer catalyst and inorganic base. *N*-Benzyl quininium chloride (**147**) was chosen as the optimal catalyst in both instances to provide the desired β -amino α -nitroalkanes in high yield. Palomo chose CsOH•H₂O as the stoichiometric base, while Ricci employed KOH. Subsequently, Palomo extended the scope of the reaction to include additional nitroalkane pronucleophiles and proposed a mechanism for the transformation (discussed in section 2.5).⁶⁸

Scheme 29. First phase transfer catalyzed enantioselective aza-Henry reactions of *N*-carbamoyl alkyl imines



Following the two initial reports, three other groups reported the same transformation using slight modifications of the cinchona alkaloid derived phase transfer catalyst initially employed (Scheme 30).⁶⁹ Dixon and coworkers combined the concepts of chiral phase transfer catalysis and bifunctional Brønsted base/H-bond donor catalysis to come up with catalyst **150**, which proved to be a more reactive catalyst than previously reported as the reaction times were decreased from 44 h to 12 h. The He group employed quinine

Scheme 30. Catalysts employed in phase transfer catalyzed aza-Henry reactions



⁶⁷ Palomo, C.; Oiarbide, M.; Laso, A.; López, R. *J. Am. Chem. Soc.* **2005**, *127*, 17622-17623. Fini, F.; Sgarzani, V.; Pettersen, D.; Herrera, R. P.; Bernardi, L.; Ricci, A. *Angew. Chem. Int. Ed.* **2005**, *44*, 7975-7978.

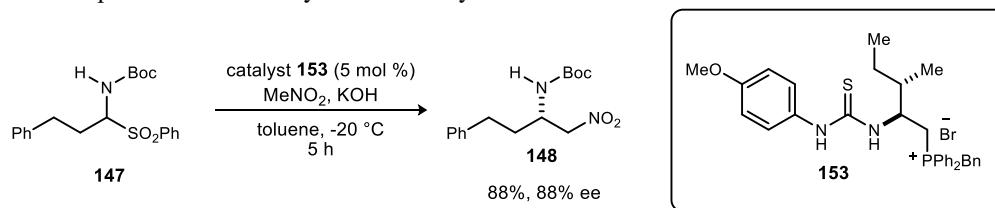
⁶⁸ Gomez-Bengoia, E.; Linden, A.; López, R.; Múgica-Mendiola, I.; Oiarbide, M.; Palomo, C. *J. Am. Chem. Soc.* **2008**, *130*, 7955-7966.

⁶⁹ Johnson, K. M.; Rattley, M. S.; Sladojevich, F.; Barber, D. M.; Nuñez, M. G.; Goldys, A. M.; Dixon, D. J. *Org. Lett.* **2012**, *14*, 2492-2495. Wei, Y.; He, W.; Liu, Y.; Liu, P.; Zhang, S. *Org. Lett.* **2012**, *14*, 704-707. Wang, B.; Liu, Y.; Sun, C.; Wei, Z.; Cao, J.; Liang, D.; Lin, Y.; Duan, H. *Org. Lett.* **2014**, *16*, 6432-6435.

derived benzotriazole catalyst **151** in the same aza-Henry reaction. Interestingly, they observed a complete reversal in enantioselectivity as compared to Palomo and Ricci even though each catalyst was prepared from the same chiral source. In 2014, Duan employed a multiple hydrogen-bonding strategy to achieve high enantioselectivity in the same aza-Henry reaction. Cinchona alkaloid derived catalyst **152** containing a chiral β -aminoalcohol allowed for excellent enantioselectivity. More importantly, both enantiomers of the product were obtained in high ee by switching to the pseudoenantiomeric catalysis, traditionally a problem in cinchona alkaloid catalysis.

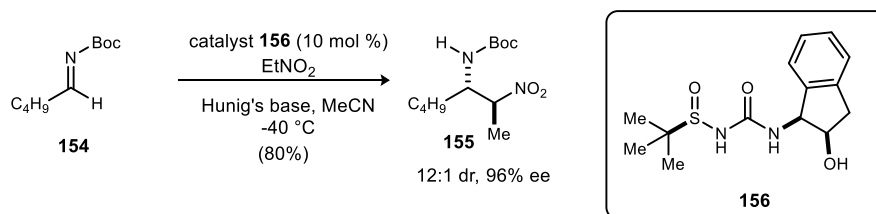
Zhao reported the use of chiral bifunctional thiourea-phosphonium salts as efficient catalysts for the phase transfer catalyzed addition of nitromethane to α -amido sulfones (Scheme 31).⁷⁰ A similar protocol to that of Ricci was employed using KOH as the stoichiometric base to obtain the aza-Henry adducts in high enantioselectivity. They provide evidence to support a bifunctional mode of action where both hydrogen bond donors of the thiourea and the phosphonium functionality are essential to selectivity. Removal of one of the hydrogen bond donors through *N*-methylation or removal of the phosphonium ion results in significant decrease in enantioselectivity.

Scheme 31. Zhao's phase transfer catalyzed aza-Henry reaction



In 2007 Ellman reported the first use of asymmetric H-bonding catalysis in the aza-Henry reaction with *N*-Boc alkyl imines.⁷¹ Sulfinyl urea catalyst **156** was employed to obtain the nitroethane aza-Henry adducts in high ee and dr (Scheme 32). Hunig's base was used to generate the nitronate while the sulfinyl functionality served as both an acidifying agent and the source of chirality.

Scheme 32. Ellman's nitroethane additions to *N*-Boc aldimines



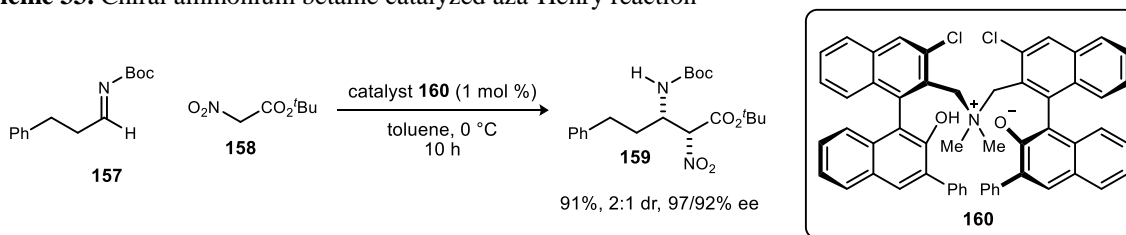
Ooi and coworkers developed a chiral ammonium betaine catalyst capable of facilitating the addition of nitroesters to *N*-Boc aldimines (Scheme 33).⁷² The phenoxide functionality provides the necessary basicity to generate the nitronate while the ammonium group is able to coordinate with the nitronate to provide high enantioselection. The methodology tolerates both aryl and alkyl aldimines as well as primary and secondary nitroalkanes.

⁷⁰ Cao, D.; Chai, Z.; Zhang, J.; Ye, Z.; Xiao, H.; Wang, H.; Chen, J.; Wu, X.; Zhao, G. *Chem. Commun.* **2013**, 49, 5972-5974.

⁷¹ Robak, M. T.; Trincado, M.; Ellman, J. A. *J. Am. Chem. Soc.* **2007**, 129, 15110-15111.

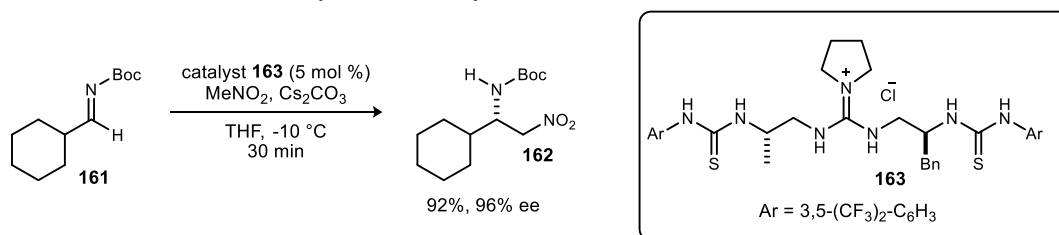
⁷² Uraguchi, D.; Koshimoto, K.; Ooi, T. *J. Am. Chem. Soc.* **2008**, 130, 10878-10879.

Scheme 33. Chiral ammonium betaine catalyzed aza-Henry reaction



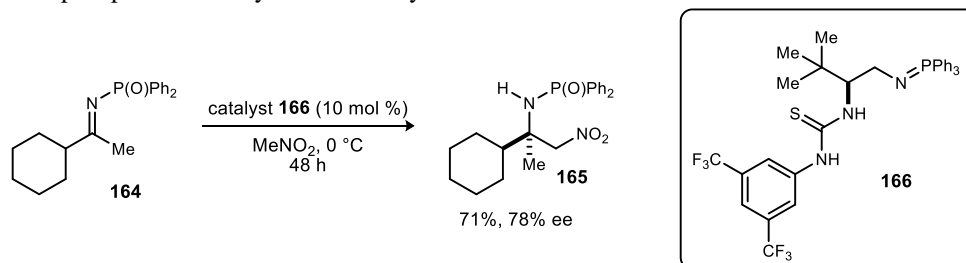
In 2009 Nagasawa reported the use of a bifunctional guanidine-thiourea organocatalyst in the enantioselective aza-Henry reaction (Scheme 34).⁷³ The solid-liquid biphasic reaction provided both aryl and aliphatic nitromethane aza-Henry adducts in high yield and ee. A number of bulkier nitroalkanes were successfully employed including nitroethane and nitropropane.

Scheme 34. Guanidine-thiourea catalyzed aza-Henry reaction



The first enantioselective organocatalytic aza-Henry reaction of nitromethane to unactivated ketimines was reported by Dixon and coworkers in 2013.⁷⁴ Bifunctional iminophosphorane catalyst **166** promoted the addition of nitromethane to *N*-phosphinoyl ketimines in high yield and ee. Notably, ketimine **164**, bearing two aliphatic substituents, was obtained in moderate yield and ee (Scheme 35).

Scheme 35. Iminophosphorane catalyzed aza-Henry addition of nitromethane to ketimines



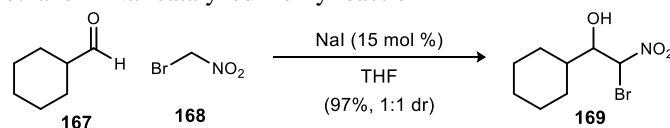
Bromonitromethane Additions

Recently, the Henry reaction employing bromonitromethane has been reported. In 2006, Concellon utilized sodium iodide as a catalyst to promote the addition of bromonitromethane into a variety of aldehydes (Scheme 36).⁷⁵ The racemic products were obtained in excellent yield and 1:1 dr.

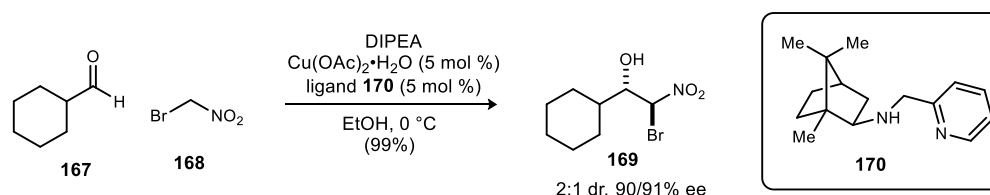
⁷³ Takada, K.; Nagasawa, K. *Adv. Synth. Catal.* **2009**, *351*, 345-347.

⁷⁴ Núñez, M. G.; Farley, A. J. M.; Dixon, D. J. *J. Am. Chem. Soc.* **2013**, *135*, 16348-16351.

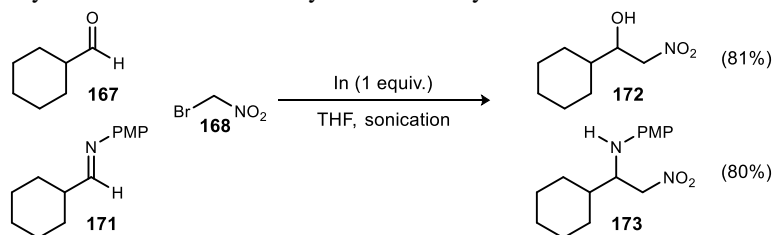
⁷⁵ Concellón, J. M.; Rodríguez-Solla, H.; Concellón, C.; García-Granda, S.; Díaz, M. R. *Org. Lett.* **2006**, *8*, 5979-5982.

Scheme 36. Bromonitromethane in NaI catalyzed Henry reaction

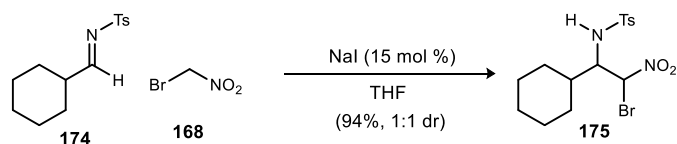
Blay reported the first enantioselective addition of bromonitromethane into aldehydes. Camphor derived ligand **170** along with copper (II) acetate was employed as the catalyst to provide enantioenriched alcohols (Scheme 37).⁷⁶ The methodology tolerates many different types of aldehydes (aliphatic, aromatic, heteroaromatic) in high enantioselection but poor dr.

Scheme 37. First enantioselective Henry reaction

In 2010, Soengas and coworkers developed a Barbier-type debrominative Henry reaction. Bromonitromethane undergoes oxidative addition with indium to generate an alkyl indium species, which then adds to the aldehyde yielding the desired alcohol (Scheme 38).⁷⁷ The reaction was later rendered catalytic in indium by utilizing Zn to reduce In⁺³ back to In⁰.⁷⁸ The same reaction conditions were later applied to PMP-protected imines in the aza-Henry reaction to provide β -nitroamines.⁷⁹

Scheme 38. Indium catalyzed debrominative Henry and aza-Henry reaction

Rodríguez-Solla also reported an aza-Henry reaction using bromonitromethane.⁸⁰ Similar conditions to those developed by Concellon were employed using sodium iodide as the catalyst to add

Scheme 39. Bromonitromethane in NaI catalyzed aza-Henry reaction

⁷⁶ Blay, G.; Hernandez-Olmos, V.; Pedro, J. R. *Chem. Commun.* **2008**, 4840-4842.

⁷⁷ Soengas, R. G.; Estévez, A. M. *Eur. J. Org. Chem.* **2010**, 2010, 5190-5196.

⁷⁸ Soengas, R. G.; Silva, A. M. S. *Synlett* **2012**, 23, 873-876.

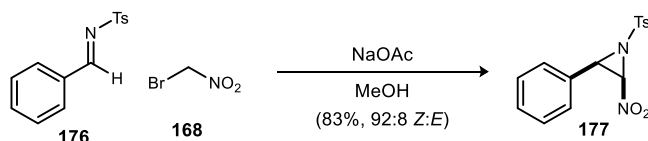
⁷⁹ Soengas, R. G.; Silva, S.; Estévez, A. M.; Estévez, J. C.; Estévez, R. J.; Rodríguez-Solla, H. *Eur. J. Org. Chem.* **2012**, 2012, 4339-4346.

⁸⁰ Rodríguez-Solla, H.; Concellón, C.; Alvaredo, N.; Soengas, R. G. *Tetrahedron.* **2012**, 68, 1736-1744.

bromonitromethane to a variety of imines (aliphatic and aromatic) with a variety of protecting groups (Ts, Boc, PMP) with moderate to high yield (Scheme 39).

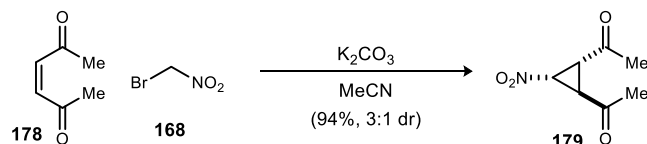
In 2009 Yadav and coworkers reported the use of bromonitromethane in a nitroaziridination reaction. Bromonitromethane was added into an *N*-tosyl imine in the presence of NaOAc (Scheme 40). Subsequently, the amine closes down releasing bromide and generating the nitroaziridine product. The reaction proceeds in high yield and good *Z*-selectivity.

Scheme 40. Bromonitromethane in nitroaziridination reaction



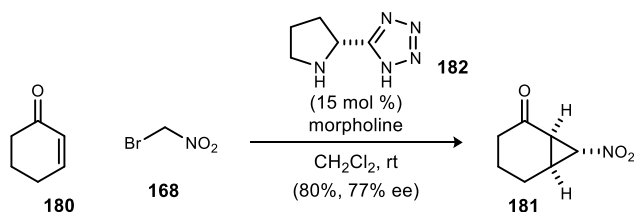
Bromonitromethane has also been used in nitrocyclopropanation reactions. Typically, bromonitromethane is added to a Michael acceptor followed by substitution of the bromide by the resulting enolate to generate a nitrocyclopropane. Ballini reported this transformation employing acyclic enone **178** and K_2CO_3 as base (Scheme 41).⁸¹ The nitrocyclopropane product was obtained in excellent yield and modest dr.

Scheme 41. Bromonitromethane in nitrocyclopropanation reaction



In 2006 Ley reported the first enantioselective nitrocyclopropanation reaction using bromonitromethane (Scheme 42).⁸² *D*-Proline derived tetrazole catalyst **182** was to affect the cyclopropanation of a variety of cyclic enones. The products were obtained in high yield and moderate selectivity. Since this initial report, many similar nitrocyclopropanation reactions have been developed utilizing a variety of chiral catalysts. A number of examples are shown in Figure 21 with a sample substrate employed for the transformation.⁸³

Scheme 42. First enantioselective nitrocyclopropanation reaction using bromonitromethane

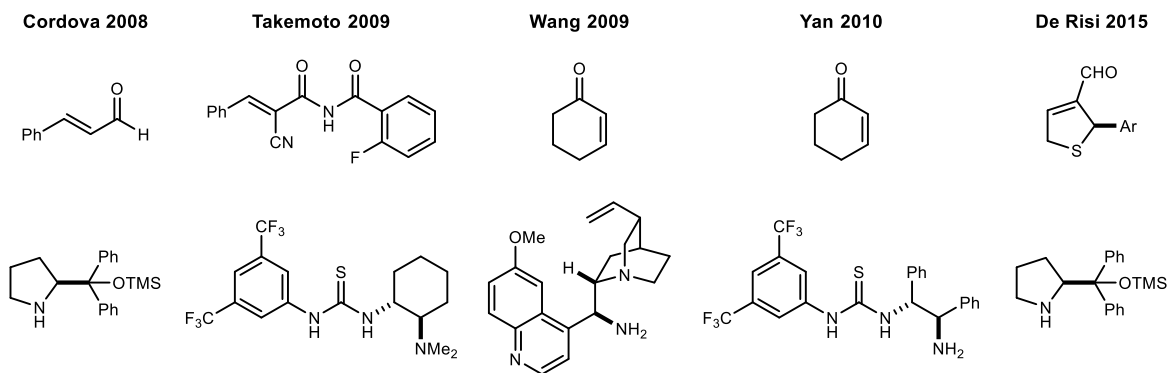


⁸¹ Ballini, R.; Fiorini, D.; Palmieri, A. *Synlett* **2003**, 2003, 1704-1706.

⁸² Hansen, H. M.; Longbottom, D. A.; Ley, S. V. *Chem. Commun.* **2006**, 4838-4840.

⁸³ Vesely, J.; Zhao, G.-L.; Bartoszewicz, A.; Córdova, A. *Tetrahedron Lett.* **2008**, 49, 4209-4212; Inokuma, T.; Sakamoto, S.; Takemoto, Y. *Synlett* **2009**, 2009, 1627-1630; Lv, J.; Zhang, J.; Lin, Z.; Wang, Y. *Chem. Eur. J.* **2009**, 15, 972-979; Dong, L.-t.; Du, Q.-s.; Lou, C.-l.; Zhang, J.-m.; Lu, R.-j.; Yan, M. *Synlett* **2010**, 2010, 266-270; Zaghi, A.; Bernardi, T.; Bertolasi, V.; Bortolini, O.; Massi, A.; De Risi, C. *J. Org. Chem.* **2015**, 80, 9176-9184.

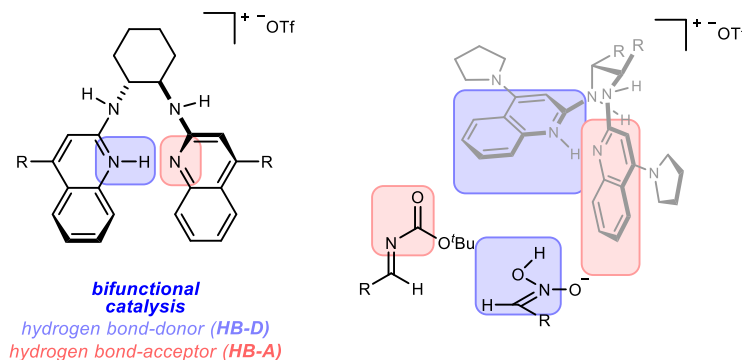
Figure 21. Enantioselective nitrocyclopropanation reactions using bromonitromethane



Chiral Proton Catalysis

Our group has reported many highly enantioselective aza-Henry reactions utilizing Bis(AMidine) (BAM) catalysis. The bifunctional catalysts feature both a Brønsted basic, or hydrogen bond acceptor, and a Brønsted acidic, or hydrogen bond donor, site allowing for binding to both the electrophile and the

Figure 20. Bis(Amidine) catalysis



nucleophile (Figure 20). The seminal report, one of the first organocatalyzed aza-Henry reactions, featured ⁴H₂QuinBAM **182** as the catalyst for the addition of nitroethane into aryl *N*-Boc imines.⁸⁴ Since that report, a variety of nitroalkanes with differing substituents have been employed with great success (Scheme 43).⁸⁵ A major advance was the introduction of the pyrrolidine group at the 4-position of the quinoline (PBAM, **82**), providing an increase in reactivity by a more Brønsted basic Brønsted acid catalyst system. Shorter reaction times and stoichiometric amounts of the nitroalkane as opposed to the large excess originally needed. Up to this point, only aryl imines have been successfully employed as electrophiles in the aza-Henry reaction with BAM catalysis.

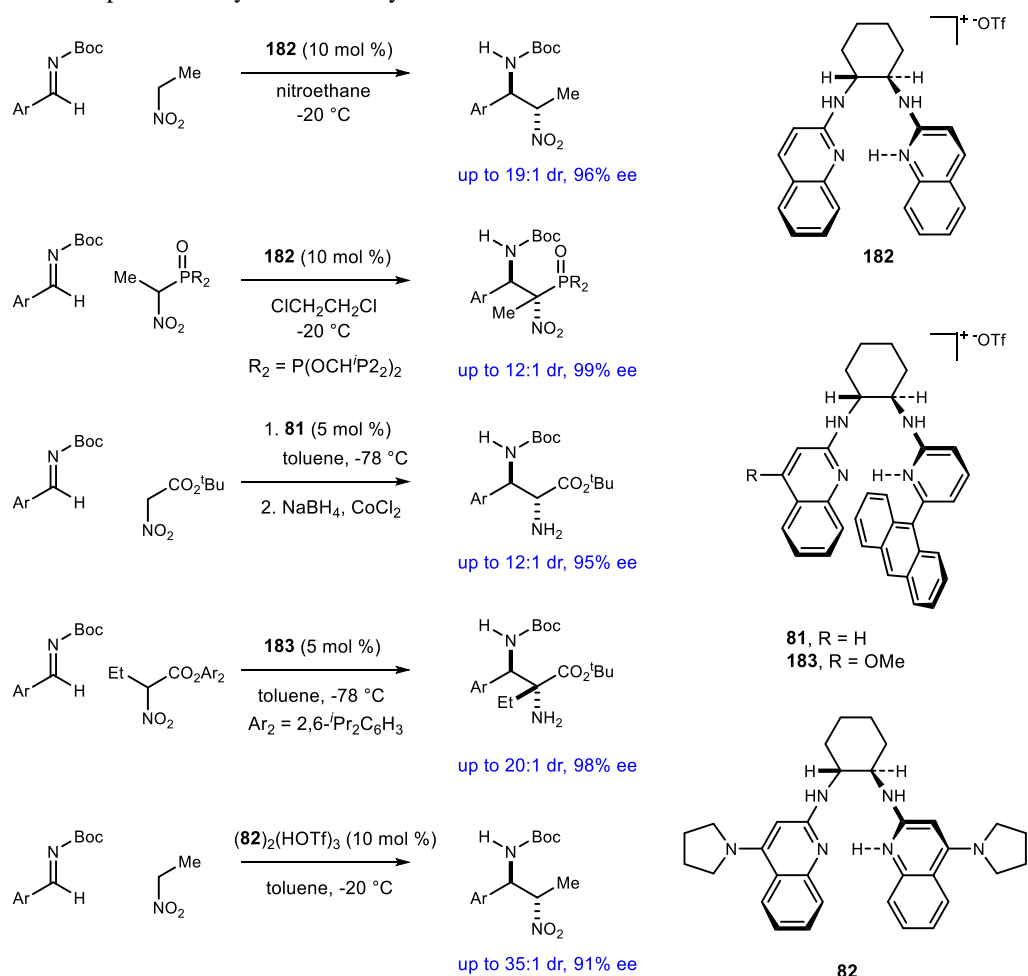
2.3 Bis(Amidine) Catalyzed Bromonitromethane Addition to Alkyl *N*-Tosyl-Imines

Alkyl imines, as compared to their aryl counterparts, are notoriously difficult substrates to work with due to their propensity to tautomerize under basic conditions to the more stable enamine tautomer

⁸⁴Nugent, B. M.; Yoder, R. A.; Johnston, J. N. *J. Am. Chem. Soc.* **2004**, *126*, 3418-3419.

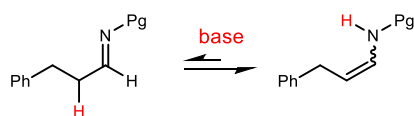
⁸⁵Wilt, J. C.; Pink, M.; Johnston, J. N. *Chem. Commun.* **2008**, 4177-4179. Singh, A.; Yoder, R. A.; Shen, B.; Johnston, J. N. *J. Am. Chem. Soc.* **2007**, *129*, 3466-3467. Singh, A.; Johnston, J. N. *J. Am. Chem. Soc.* **2008**, *130*, 5866-5867. Shen, B.; Johnston, J. N. *Org. Lett.* **2008**, *10*, 4397-4400. Davis, T. A.; Wilt, J. C.; Johnston, J. N. *J. Am. Chem. Soc.* **2010**, *132*, 2880-2882. Makley, D. M.; Johnston, J. N. *Org. Lett.* **2014**, *16*, 3146-3149.

Scheme 43. Chiral proton catalyzed aza-Henry additions



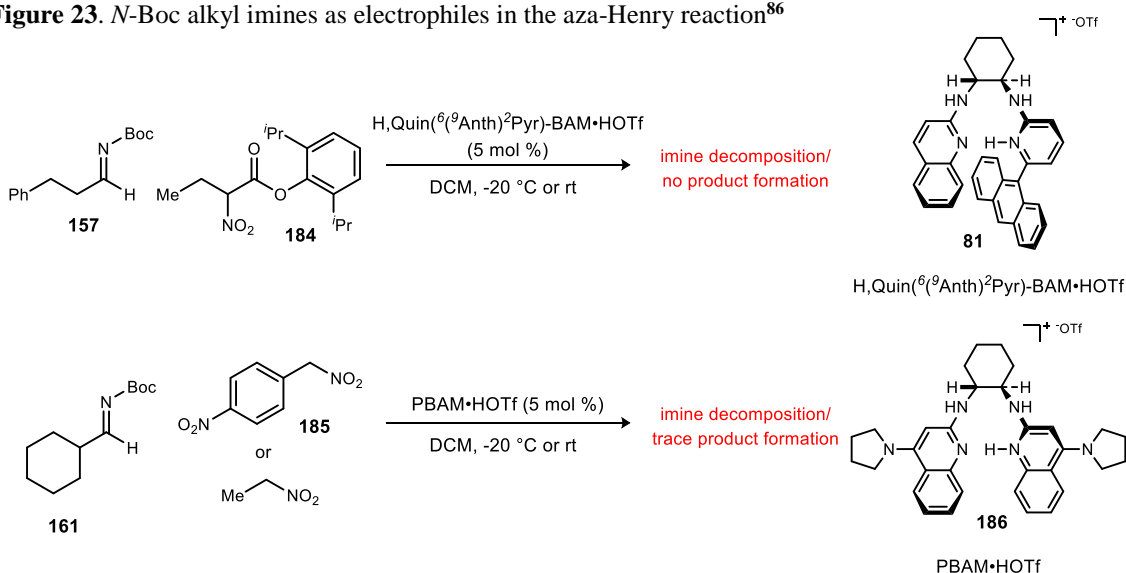
(Figure 22). The imine *N*-protecting group has a significant impact on the tautomerization. For example, *N*-tosyl imines are more stable and less prone to tautomerization than *N*-Boc imines.

Figure 22. Imine tautomerization



When choosing the imine protecting group for this study, two factors were considered: stability and potential for catalyst recognition. As previously discussed, the most effective imine protecting group for aryl substrates in the BAM-catalyzed aza-Henry reaction is the *N*-Boc group, hypothesized to be due to its two-point binding with the catalyst. However, initial results adding a variety of nitroalkanes into alkyl *N*-Boc aldimines proved fruitless resulting in enamine formation and imine decomposition (Figure 23). Imines bearing *N*-tosyl protecting groups are known to be more stable and are widely used in synthesis. Although they have never been used in BAM catalysis, there is potential for catalyst recognition similar to the *N*-Boc protecting group. The one of the oxygens of the sulfonyl group should be capable of hydrogen bonding to the catalyst in the same way that the carbonyl oxygen of the Boc group is able to providing the similar two-point binding mode.

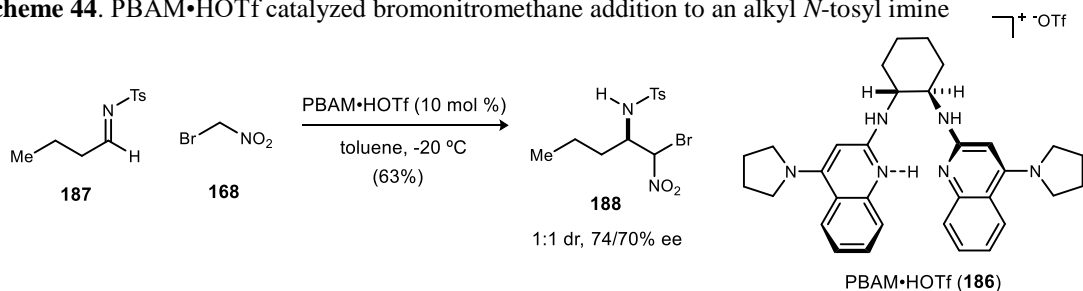
Figure 23. *N*-Boc alkyl imines as electrophiles in the aza-Henry reaction⁸⁶



Previous Efforts⁸⁶

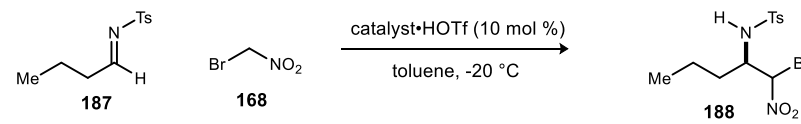
Due to the inability to obtain the desired product with the *N*-Boc protecting group, the use of the *N*-tosyl group was investigated. Initial efforts adding bromonitromethane (**168**) into imine **187** using PBAM•HOTf (**186**) as the catalyst at -20 °C gratifyingly provided the desired product as a 1:1 mixture of diastereomers with 74% and 70% ee, respectively (Scheme 44). Fortunately, both diastereomers showed similar enantiopurity, which will be required to obtain enantioenriched amides after submitting to the Umpolung Amide Synthesis as the two diastereomers will converge to a single enantiomer as the sp³ chiral center is transformed into an sp² carbon.

Scheme 44. PBAM•HOTf catalyzed bromonitromethane addition to an alkyl *N*-tosyl imine

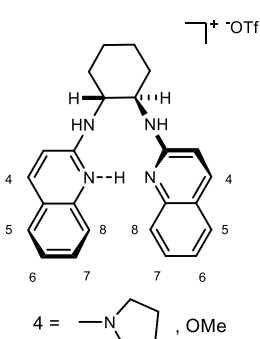


In an effort to increase the enantioselection, a variety of other BAM catalysts were used in the reaction (Table 3). Adding substituents at the 6, 7, and 8-positions of the quinoline ring systems failed to increase yield or enantioselection. Both steric and electronic effects were addressed without resulting in positive results. However, changing the pyrrolidine substituent at the 4-position to a methoxy group resulted in a more favorable catalyst that significantly increased the yield (63 to 82%) while maintaining the same level of enantioselection.

⁸⁶ Singh, A.; Dobish, M. C.; Johnston, J. N. *unpublished results*

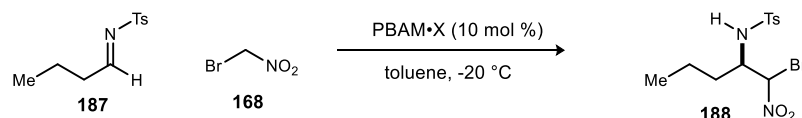
Table 3. Catalyst screen in bromonitromethane addition to alkyl *N*-tosyl imines


entry ^a	catalyst	d.r. ^b	yield ^c (%)	ee ^d (%)
1	PBAM	1:1	63	74/70
2	⁷ iPr-PBAM	1:3	55	60/60
3	⁷ tBu-PBAM	1:2	58	56/56
4	⁷ MeO-PBAM	1.1:1	51	54/54
5	^{6,7} Me-PBAM	1.1:1	53	58/58
6	⁸ MeO-PBAM	1:1	55	45/45
7	⁸ Me-PBAM	1:1	55	56/56
8	⁴ MeO-BAM	1:1	82	71/68

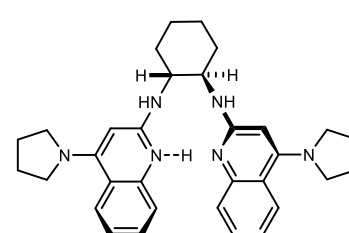


^aAll reactions are 0.5 M in imine and use 1.5 equivalents of the nitroalkane. ^bDiastereomer ratios were measured using ¹H NMR. ^cIsolated yield. ^dEnantiomer ratios were measured using HPLC and a chiral stationary phase.

Although the specific role the counterion plays in the reaction is not known, changing the achiral counterion has been shown to have a significant effect on both selectivity and yield in a few cases.⁸⁷ For this reason, a variety of counterions were screened using (Table 4). Even though ⁴MeO-BAM was the optimal catalyst at this point, PBAM (**82**) was chosen for this series of experiments due to higher availability. The results were expected to be analogous between the two catalysts. Although the screen did not provide improved results, it did show a significant trend. Enantioselectivity is directly related to the amount of dissociation between the counterion and the catalyst. The stronger the acid, the more dissociated the counterion is from the catalyst resulting in higher enantioselectivity. The strongest acids screened, triflic acid and triflimidic acid, gave the highest enantioselections.

Table 4. Counterion effects in the PBAM catalyzed additions of bromonitromethane to alkyl *N*-tosyl imines


entry ^a	X	d.r. ^b	yield ^c (%)	ee ^d (%)
1	none	1.4:1	30	35/38
2	HOTf	1:1	63	74/70
3	HNTf ₂	1.3:1	60	68/68
4	CH ₂ Tf ₂	1:1	61	60/67
5	CSA	1:1	49	39/42
6	FSO ₃ H	1:1	51	59/56
7	C ₄ H ₉ SO ₃ H	1.1:1	57	55/62

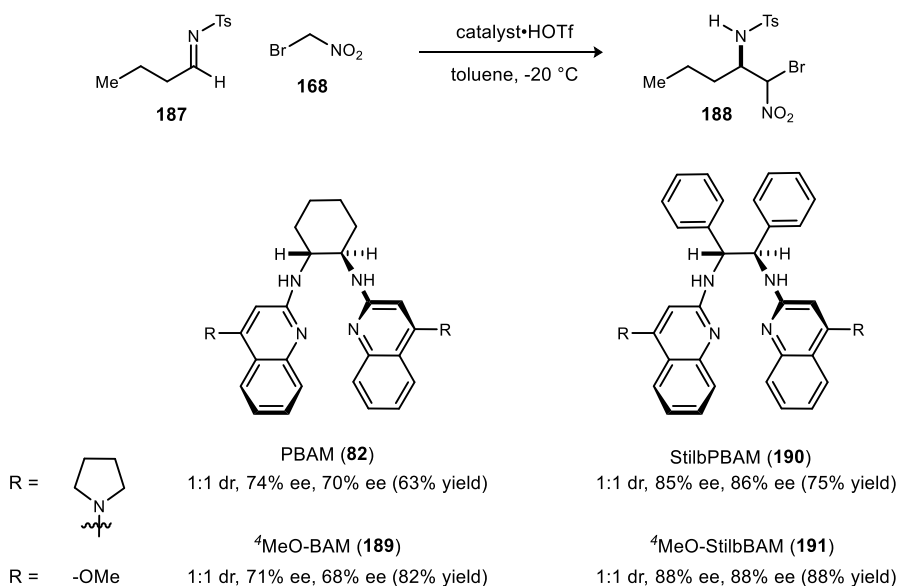


^aAll reactions are 0.5 M in imine and use 1.5 equivalents of the nitroalkane. ^bDiastereomer ratios were measured using ¹H NMR. ^cIsolated yield. ^dEnantiomer ratios were measured using HPLC and a chiral stationary phase.

⁸⁷ Dobish, M. C.; Johnston, J. N. *J. Am. Chem. Soc.* **2012**, *134*, 6068-6071.

After no considerable increase in enantioselection was observed by altering the substituents on the quinoline ring system as well as adjusting the counterion, efforts were focused on a previously unexplored portion of the catalyst: the diamine backbone (Scheme 45). The cyclohexyl diamine was replaced with stilbene diamine. The PBAM derivative of the stilbene diamine was synthesized and provided a significant increase in enantioselection up to 85% and 86% ee for each of the two diastereomers. One effect of changing the diamine backbone is modulation of the bite angle between the two quinoline rings. In a study conducted by Chin⁸⁸, stilbene diamine was found to provide a smaller bite angle than cyclohexane diamine. We propose that the smaller bite angle favorably modifies the catalyst pocket allowing for better binding to the imine resulting in higher enantioselection. By utilizing the stilbene diamine motif to increase enantioselection and installing the methoxy group at the 4-position of the quinoline rings to increase yield, a new optimal catalyst was developed, ⁴MeO-StilbBAM (**191**), which provided α -bromonitroalkane **188** in 88% yield, 1:1 dr, and 88/88% ee when using the triflate salt.

Scheme 45. Catalyst backbone modifications: additions of bromonitromethane to alkyl *N*-tosyl imines



Decreasing the temperature of the reaction from -20 °C to -78 °C using StilbPBAM resulted in a slight increase in enantioselection to 89% and 91% ee for the two diastereomers. The reactivity of the catalyst at low temperatures, however, was significantly decreased as expected resulting in a significantly lower yield of 32%. At this point the optimal conditions proved to be ⁴MeO-StilbBAM at -20 °C giving a 1:1 mixture of diastereomers at 88% and 88% ee with a yield of 88%.

Additions of Bromonitromethane to Alkyl *N*-Tosyl-Imines

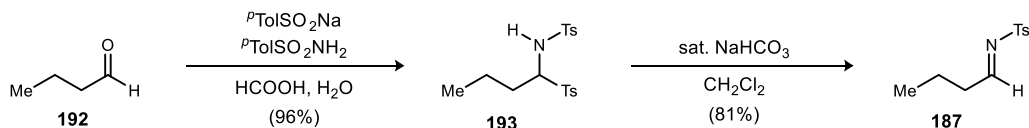
Prior to attempting to further optimize the bromonitromethane addition to alkyl imines, repeating the previous results was the focus. The imine was prepared from the aldehyde utilizing a high yielding two-step procedure (Scheme 46). The aldehyde is transformed into the α -amido sulfone upon reaction with *p*-toluenesulfonamide and *p*-toluenesulfinic acid sodium salt in the presence of formic acid.⁸⁹ The resulting

⁸⁸ Kim, H.; Yen, C.; Preston, P.; Chin, J. *Org. Lett.* **2006**, 8, 5239-5242.

⁸⁹ Chemla, F.; Hebbe, V.; Normant, J.-F. *Synthesis* **2000**, 1, 75-77.

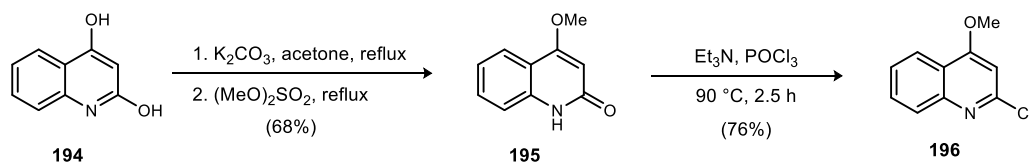
sulfone undergoes elimination to the desired imine with a simple washing with saturated sodium bicarbonate.⁹⁰

Scheme 46. Synthesis of *N*-tosyl protected alkyl imine



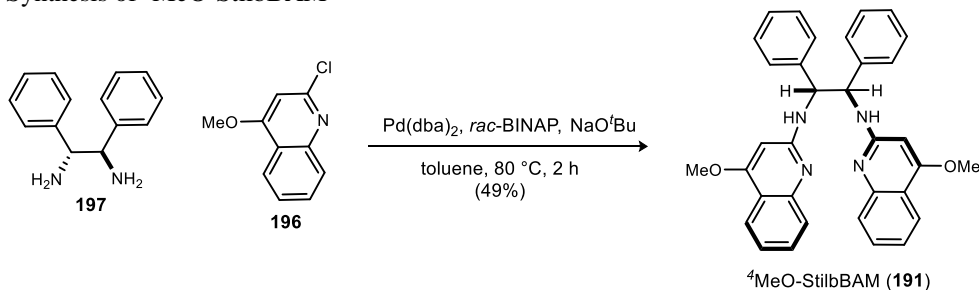
⁴MeO-StilbBAM (**191**) was synthesized from (*R,R*)-stilbene diamine and the necessary quinoline. The desired quinoline, 2-chloro-4-methoxyquinoline (**196**) was synthesized following a two-step procedure from 2,4-quinolinediol (Scheme 47). Treatment of the quinolinediol with base followed by dimethyl sulfate provided **195**. Upon refluxing in phosphorous oxychloride, intermediate **195** yielded the desired 2-chloro-

Scheme 47. Preparation of 2-chloro-4-methoxyquinoline



4-methoxyquinoline in 52% yield over two steps. Adapting from known procedures⁹¹, the quinoline ring was coupled to (*R,R*)-stilbene diamine through a Buchwald-Hartwig coupling to furnish the desired catalyst, ⁴MeO-StilbBAM in 49% yield (Scheme 48). Subsequent treatment with one equivalent of triflic acid gave the active catalyst.

Scheme 48. Synthesis of ⁴MeO-StilbBAM

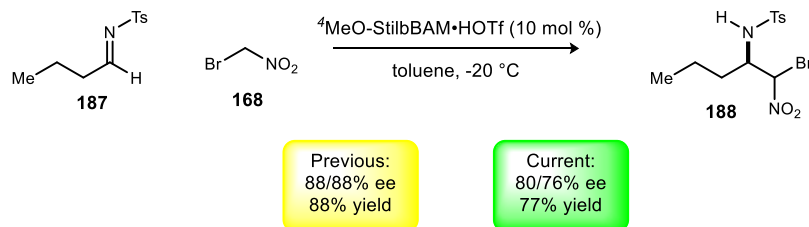


With the catalyst and imine in hand, the reaction was conducted under the previously developed optimal conditions. The expected results of 88% yield, 88/88% ee were not observed as the product was obtained in 77% yield and 80/76% ee (Scheme 49). Subsequent attempts to repeat the previous results while focusing on the purity of each reagent proved fruitless. Throughout the process, new batches of catalyst and imine were produced but did not provide the desired results. Additionally, multiple bottles of bromonitromethane were used as well as freshly distilled bromonitromethane to no avail. Unable to isolate the problematic variable, we addressed other elements of the reaction in hopes of reaching the ultimate goal of obtaining the aza-Henry adducts in greater than 90% ee and high yield.

⁹⁰ Cui, Z.; Yu, H.-J.; Yang, R.-F.; Gao, W.-Y.; Feng, C.-G.; Lin, G.-Q. *J. Am. Chem. Soc.* **2011**, *133*, 12394-12397.

⁹¹ Adapted from Wagaw, S.; Rennels, R. A.; Buchwald, S. L. *J. Am. Chem. Soc.* **1997**, *119*, 8451-8458.

Scheme 49. Efforts to repeat initial results



Previous experiences with chiral proton catalysis in the aza-Henry reaction have proven toluene to be the optimal solvent for high enantioselection. Nonetheless, in an attempt to gain an increase in enantioselection a moderate solvent screen was conducted (Table 5). All of the toluene derivatives (*o*-xylene, *m*-xylene, benzene, anisole, and trifluoro-toluene) showed similar enantioselection. As has been the case in the past, dichloroethane and cyclohexane gave low enantioselection. Surprisingly, *tert*-butyl methyl ether behaved similarly to the toluene family. Toluene was chosen as the optimal solvent due to its higher yield and similar enantioselectivity.

Table 5. Solvent screen of additions of bromonitromethane to alkyl *N*-tosyl imines

entry ^a	solvent	yield ^b (%)	ee ^c (%)
1	toluene	77	80/76
2	benzene	44	77/75
3	<i>o</i> -xylene	71	82/79
4	<i>m</i> -xylene	38	81/81
5	anisole	44	82/80
6	PhCF ₃	27	75/75
7	DCE	64	68/65
8	TBME	61	81/79
9	<i>c</i> -C ₆ H ₁₂	36	50/44

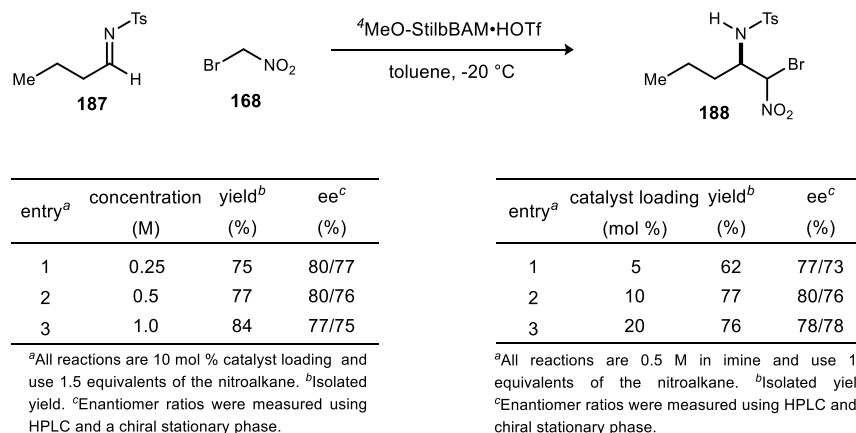
${}^4\text{MeO-StilbBAM}\cdot\text{HOTf}$ (**198**)

^aAll reactions are 0.5 M in imine and use 1.5 equivalents of the nitroalkane. ^bIsolated yield.

^cEnantiomer ratios were measured using HPLC and a chiral stationary phase.

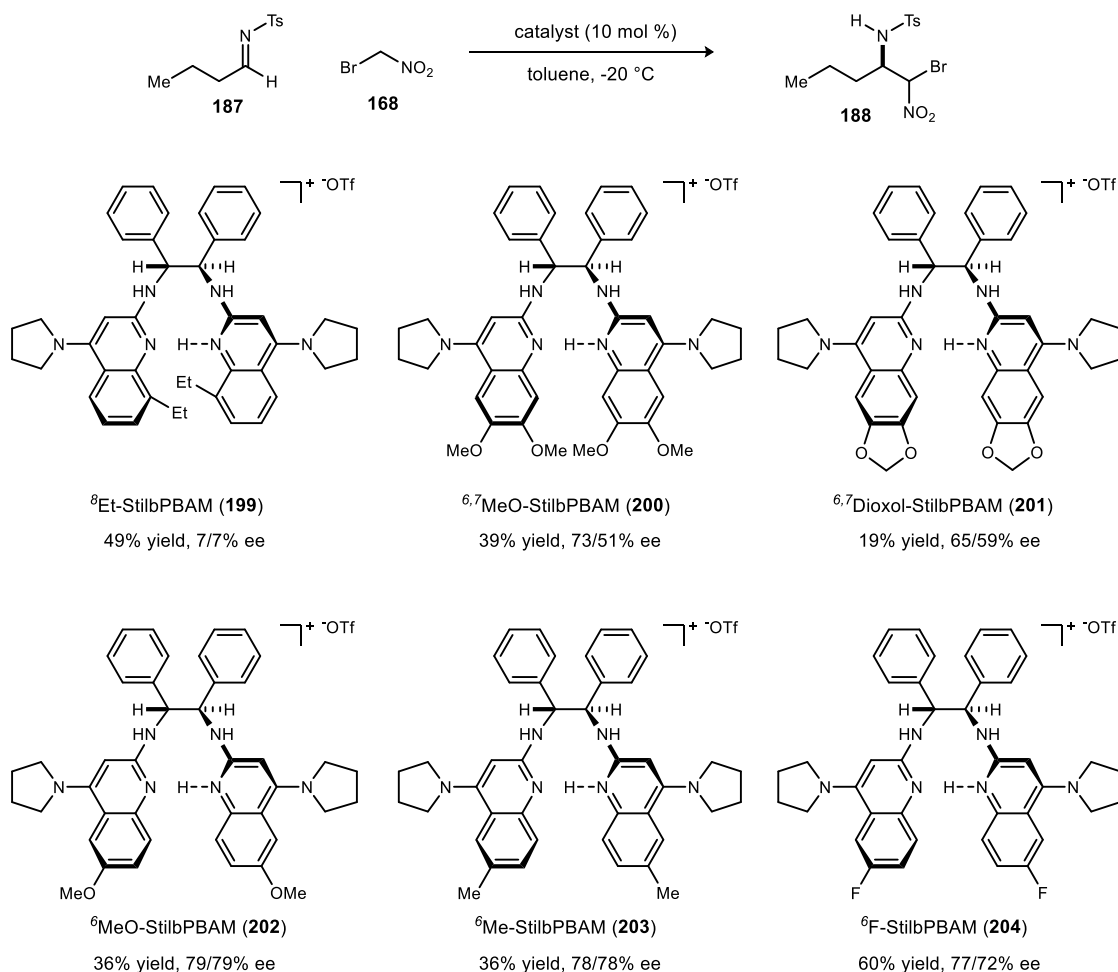
With toluene selected as the optimal solvent, the effect of changing the concentration was investigated (Table 6). Up to this point, all reactions have been run at 0.5 M with respect to imine. Unfortunately, running the reaction half as concentrated (entry 1) as well as twice as concentrated (entry 3) did not show a significant difference. Similar to concentration, catalyst loading had yet to be studied. Running reactions at 0.5 M, the catalyst loading was halved (entry 1) as well as doubled (entry 3). All three different loadings gave very similar results with 10 mol % still being slightly better (Table 6).

Table 6. Concentration and catalyst loading screen in addition of bromonitromethane to alkyl *N*-tosyl imines



Focus was again directed at catalyst modification in an attempt to tune the reactivity and enantioselectivity provided by the catalyst. To this point, no stilbene backbone catalyst derivatives had been examined except StilbPBAM (**190**) and ⁴MeO-StilbBAM (**191**). The electronic and steric effects provided by substituents at the 6-, 7-, and 8-positions were investigated (Scheme 50). Even though the yield was

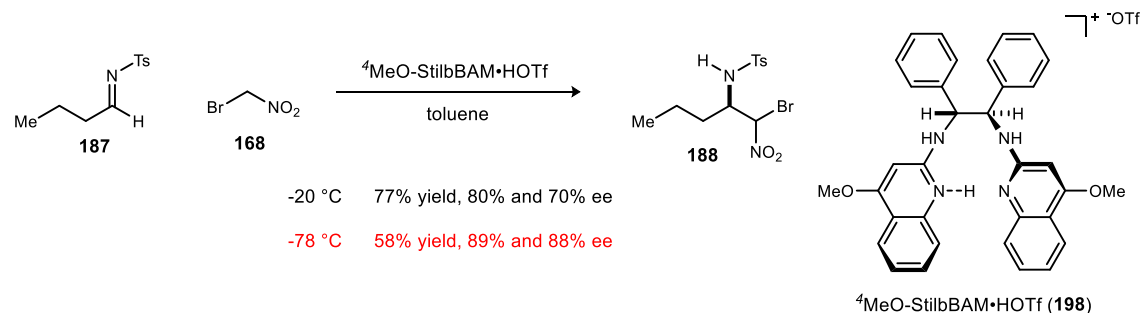
Scheme 50. Catalyst screen in additions of bromonitromethane to alkyl *N*-tosyl imines



better using ⁴MeO-StilbBAM (**191**) as compared to StilbPBAM (**190**), the StilbPBAM derivatives were synthesized due to 2,4-dichloroquinoline availability. If any improvement was observed, the 4-MeO derivatives would then be synthesized. Adding a bulky group at the 8-position (⁸Et-StilbPBAM **199**) significantly decreased enantioselection down to a near racemic level. Installation of electron donating groups at both the 6 and 7 positions also decreased the enantioselection of the catalyst (^{6,7}MeO-StilbPBAM (**200**) and ^{6,7}Dioxol-StilbPBAM (**201**)). The yields for the 7- and 8-substituted catalysts were significantly lower than their unsubstituted counterparts. We hypothesize that the steric bulk provided by these substituents blocks the active site of the catalyst hindering reactivity. Initial results when looking at the 6-position showed promise. An electron donating methoxy group at the 6-position (⁶MeO-StilbPBAM (**202**)) furnished diminished yield but similar enantioselection. Unfortunately, changing the electronic properties of the substituent to less electron donating (Me) and electron withdrawing (F) did not give the desired increase in enantioselection (⁶Me-StilbPBAM (**203**) and ⁶F-StilbPBAM (**204**)).

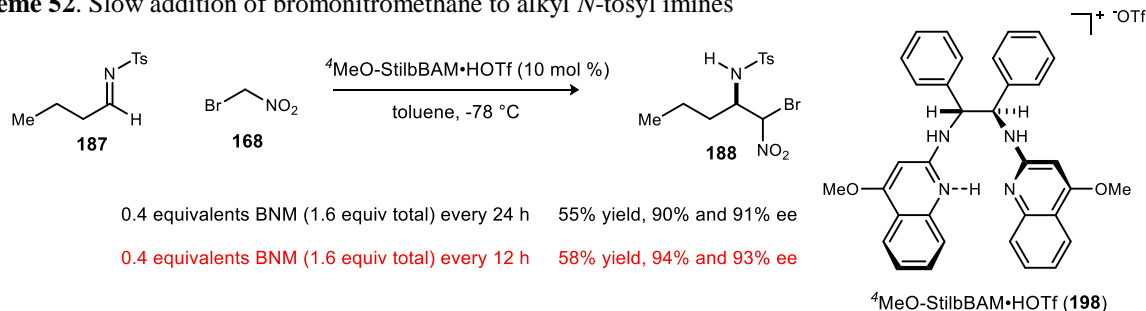
Up to this point many variables of the reaction including solvent, catalyst, catalyst loading, and concentration had been studied. Equivalence of bromonitromethane had not been addressed due to previous systems showing catalyst inhibition results from excess nitroalkane. We had yet to address the effect of temperature on the reaction with the other optimal conditions. Previously, StilbPBAM•HOTf was used as the catalyst at -78 °C to provide a small increase in enantioselection but a significant decrease in reactivity. The optimal catalyst, ⁴MeO-StilbBAM•HOTf, had not been tried at the lower temperature (Scheme 51). Under the standard conditions of 1.5 equivalents bromonitromethane, 0.5 M in toluene, and 10 mol % catalyst loading at the lower temperature of -78 °C the enantioselection, as expected, was increased to 88% and 89% ee with only slightly diminished yield of 55%.

Scheme 51. Effect of temperature on additions of bromonitromethane to alkyl *N*-tosyl imines



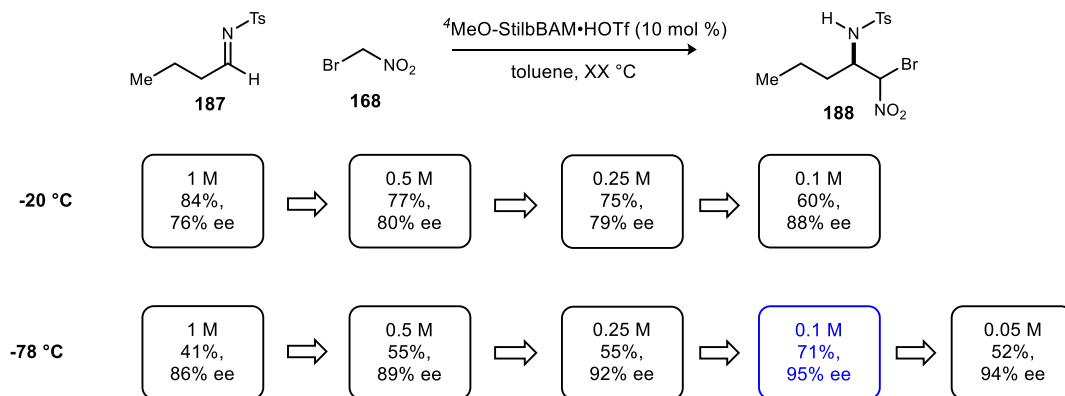
In a previous case³⁷, a slow addition of bromonitromethane was employed to increase the enantioselection in the BAM-catalyzed aza-Henry reaction into TMS-imines. In that instance, the slow addition served to ensure that at all times the ratio of nucleophile to catalyst was 1:1, diminishing the possibility of a substrate catalyzed background reaction. In this case, a background reaction was not a concern due to the lower basicity of the Ts-imine compared to the TMS-imine, but we were interested to see the effect a slow addition would have. The reaction was run at -78 °C adding 0.4 equivalents of bromonitromethane every 24 hours for a total of 1.6 equivalents with a reaction time of 96 hours (Scheme 52). The yield of the reaction did not improve upon the standard addition, but the enantioselection increased to 90% and 91% ee. Altering the time between additions to only 12 hours giving a total reaction time of 48 hours further raised the ee to 94% and 93% while maintaining the yield. One hypothesis as to why the slow addition increased the enantioselection was that the concentration of the reaction with respect to bromonitromethane is lower throughout the reaction during the slow addition as opposed to the standard addition. Performing the standard addition reaction at a lower concentration would create a similar scenario.

Scheme 52. Slow addition of bromonitromethane to alkyl *N*-tosyl imines

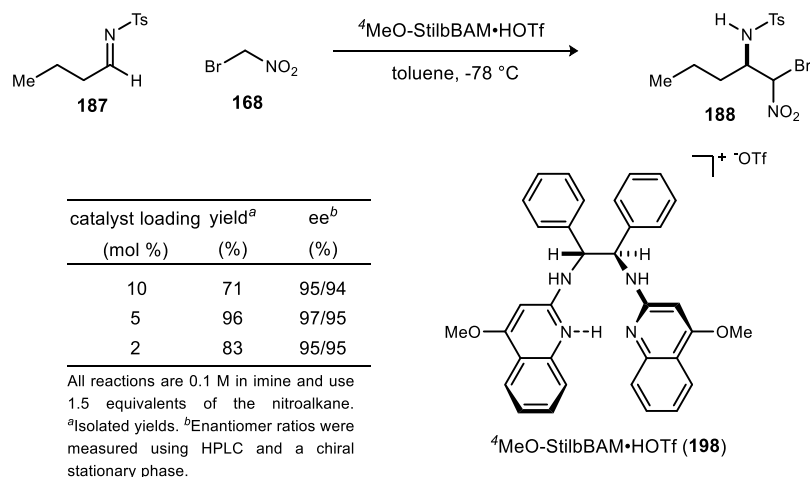


The standard addition reaction was run at concentrations ranging from 0.05 M to 1.0 M at -78 °C (Scheme 53). The enantioselection increased as the concentration decreased from 1.0 M to 0.1 M. The increasing effect leveled off at 0.1 M as 0.05 M gave essentially the same enantioselectivity. The yield peaked at 0.1 M giving optimal results of 71% yield and 95% and 94% ee. We hypothesize that the increase in enantioselection pertains to the solubility of the imine in toluene. As the concentration decreases, the imine is more soluble giving the desired 10:1 ratio of imine to catalyst in solution. To further verify the trend in concentration, the reactions were run under the same conditions at -20 °C, as opposed to -78 °C. Although there was little increase in enantioselection between 1.0 M and 0.5 M, the enantioselection increased significantly from 0.5 M to 0.1 M, suggesting a real trend.

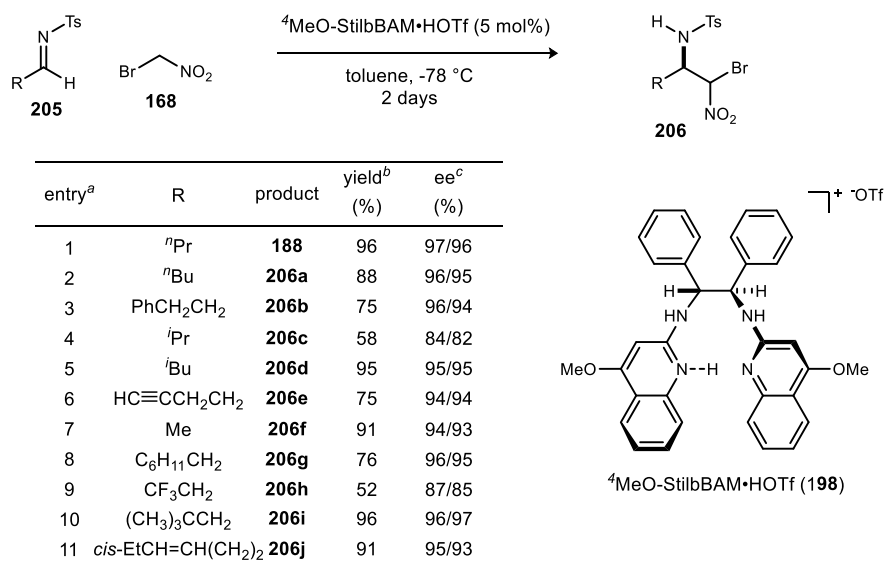
Scheme 53. Concentration effects on additions of bromonitromethane to alkyl *N*-tosyl imines



With the enantioselection at an exceptional level, focus shifted to increase the yield. The catalyst loading was again addressed at the optimal concentration of 0.1 M. Catalyst loadings of 10 mol %, 5 mol % and 2 mol % were tried (Table 7). Counterintuitively, decreasing the catalyst loading increased the yield. Typically, lower catalyst loading slows down the reaction, consequently decreasing the yield over the same time frame. In this case the yield was improved from 71% at 10 mol % catalyst loading up to 96% at 5 mol % catalyst loading. We propose that the catalyst may be promoting decomposition of the imine through an unselective pathway resulting in a lower yield.

Table 7. Catalyst loading in additions of bromonitromethane to alkyl *N*-tosyl imines

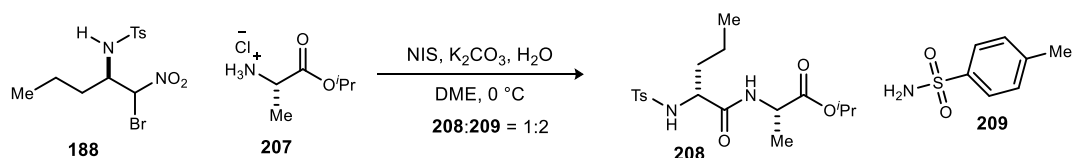
The optimized reaction conditions were applied to a number of substrates with differing functionality on the side chain (Table 8). Ideally, the methodology should be applicable to any alkyl aldehyde. As all of the optimization was performed with R = ⁿPr (entry 1), similar substrates where R = ⁿBu and Me (entries 2 and 7) also provided high yield and enantioselection. While lower than desired, the isopropyl substrate (entry 4) gave moderate yield at 58% and good ee of 84% and 82%. When the branching was placed one carbon further in the cases of the isobutyl, R = C₆H₁₁CH₂, and R = (CH₃)₃CCH₂ (entries 5, 8, 10), the yield and enantioselectivity returned to the desired high levels. The methodology also tolerates a phenyl ring (entry 3) as well as an alkyne (entry 6) and an alkene (entry 11) as the products were obtained in high enantioselection. Additionally, a trifluoromethyl motif (entry 9) on the carbon side chain provides moderate yield and good ee at 87% and 85%.

Table 8. Substrate scope of additions of bromonitromethane to alkyl *N*-tosyl imines

Umpolung Amide Synthesis with *N*-Tosyl Bromonitroalkanes

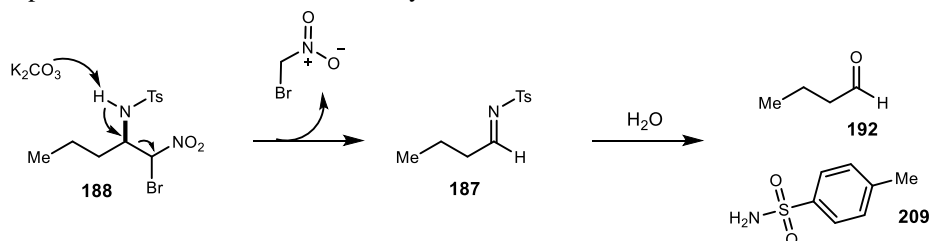
With the successful optimization of the aza-Henry reaction, the next step was to couple the α -bromonitroalkanes to amino acids utilizing Umpolung Amide Synthesis (UmAS). Initial attempts at synthesizing dipeptide **208** employing traditional UmAS conditions³⁴ using stoichiometric NIS provided a 2:1 ratio of toluenesulfonamide and the desired amide (Scheme 54). We propose the toluenesulfonamide side product is a result of a retro aza-Henry in which a base, presumably potassium carbonate, deprotonates

Scheme 54. Initial attempt at Umpolung Amide Synthesis using alkyl *N*-tosyl α -bromonitroalkanes



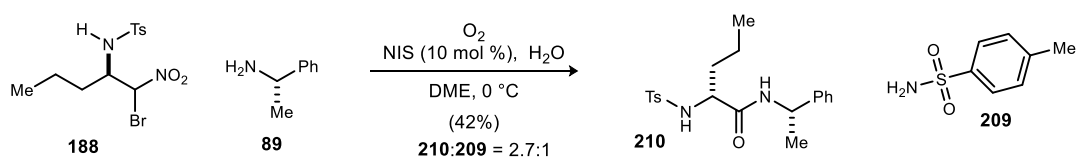
the *N*-tosyl amine eliminating bromonitromethane (Scheme 55). The resulting imine is then hydrolyzed resulting in the formation of toluenesulfonamide and butyraldehyde. Due to volatility, butyraldehyde was not isolated and only trace amounts were occasionally observed. It is important to note that this is the only system in which the retro aza-Henry process has been observed in any appreciable rate under UmAS conditions.

Scheme 55. Proposed mechanism of retro aza-Henry

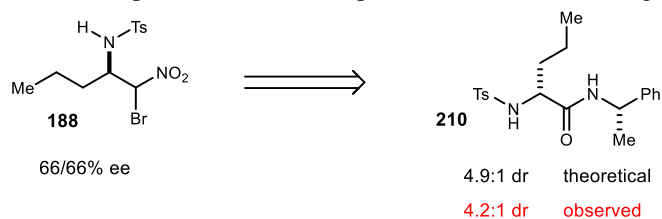


The reaction was also run using catalytic amounts of NIS (10 mol %) under aerobic conditions (O_2 balloon) with similar results. Due to the similar results with a slightly faster reaction rate, aerobic and catalytic conditions were used for all subsequent studies. In an effort to reduce the amount of retro aza-Henry observed, the potassium carbonate was removed from the reaction and replaced with four additional equivalents of the amine to be coupled. The HCl salt of alanine was also replaced with (*S*)- α -methylbenzylamine to allow the free amine to not only function as the coupling partner but also the base. (Scheme 56). With those substitutions, the retro reaction was reduced yielding a ratio of 2.7 to 1 of the desired amide to toluenesulfonamide and an isolated yield of 42%. At this point, the diastereomeric ratio of products was examined to ensure that the α -bromonitroalkane diastereomers were formed with the same sense of enantioselection (Scheme 57). The aza-Henry adduct used in the reaction had an ee of 66% for each diastereomer which correlates to 4.9:1 dr. Since the observed 4.2:1 dr was very close to the theoretical

Scheme 56. UmAS reaction using free amine as coupling partner and base



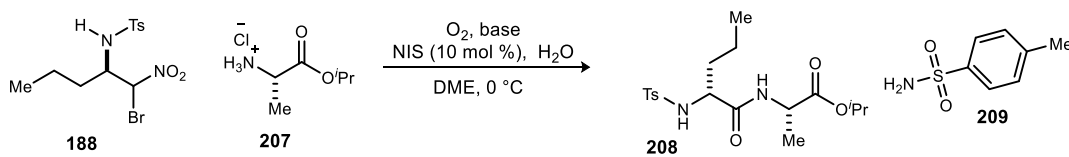
Scheme 57. Correlation between expected and observed product dr based on starting material ee



value, we concluded that the enantioenriched stereocenters of bromonitroalkane diastereomers were formed with the same sense of enantioselection.

Although using the free amine provided better results than the inorganic base and amine salt, we hoped to improve the method to allow for the use of amine salts. A number of inorganic and organic bases were screened using alanine isopropyl ester hydrochloride as the amine (Table 9). Sodium bicarbonate and cesium hydroxide did not promote the reaction resulting in mostly starting material. Cesium carbonate,

Table 9. Screen of bases in UmAS reaction



entry ^a	base	208	:	209
1	K ₂ CO ₃	1		1.7
2	NaHCO ₃	0		trace
3	Cs ₂ CO ₃	trace		99
4	CsOH	0		trace
5	DMAP	trace		99
6	Hunig's	trace		99
7	Et ₂ NH	trace		99

^aAll reactions are 0.2 M in bromonitro alkane and use 0.1 equivalents of NIS and 5 equivalents of H₂O. Ratios are of crude reaction mixture and were determined using ¹H NMR.

DMAP, Hunig's base, and diethyl amine resulted in complete consumption of starting material but toluenesulfonamide was observed with only trace amounts of the amide.

Due to our inability to improve the results using the amine salt, we chose to optimize the reaction using the free amine as the base. A cursory solvent screen using THF, 2-methyl-THF, and TBME did not improve upon the reaction outcome (Table 10). All three solvents provided more retro aza-Henry than was seen when using DME as the solvent. The ratio dropped from 2.7:1 amide to toluenesulfonamide down to almost equal amounts of desired amide and toluenesulfonamide.

Scheme 58. UmAS reaction temperature study

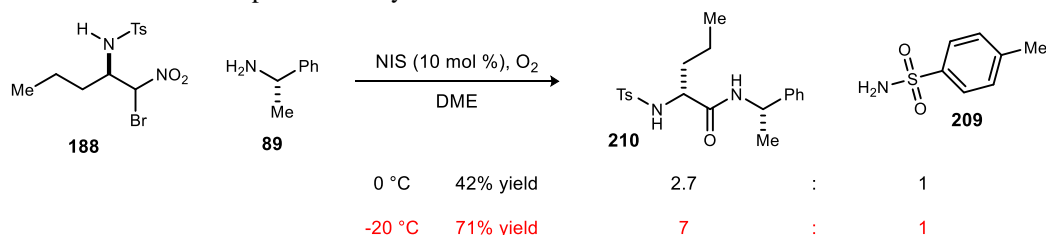
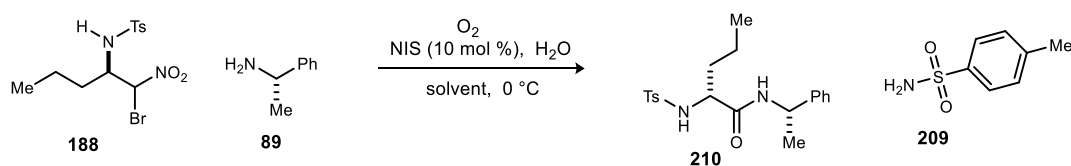


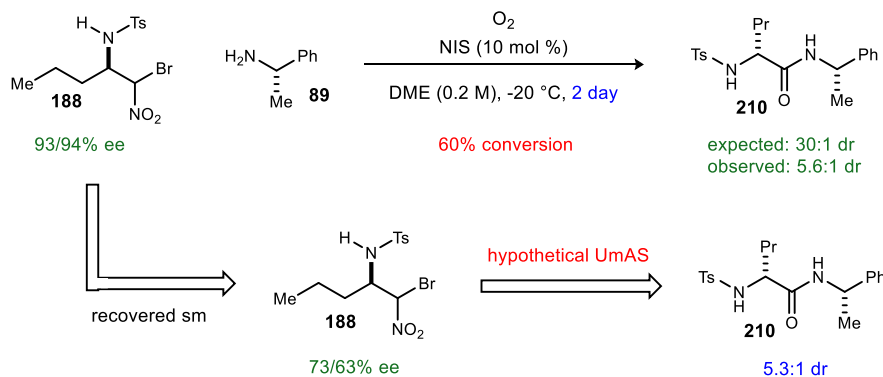
Table 10. Solvent screen for UmAS reaction

entry ^a	solvent	210	:	209
1	DME	2.7		1
2	THF	1		1
3	2-Me-THF	1		1
4	TBME	1		1

^aAll reactions are 0.2 M in bromonitro alkane and use 0.1 equivalents of NIS and 5 equivalents of H₂O and amine. Ratios are of crude reaction mixture and were determined using ¹H NMR.

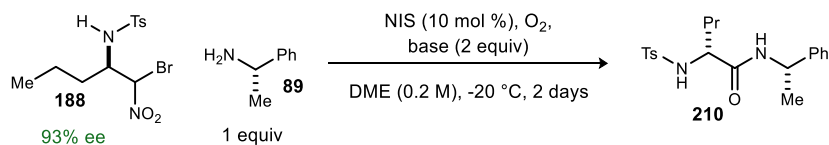
The only two variables yet to be addressed in the reaction were the temperature and the inclusion of water. It is known that under aerobic conditions water is not necessary for completion of the reaction.³⁶ This proved to be true as the exclusion of water did not change the outcome of the reaction. In an effort to slow down the retro aza-Henry reaction, the UmAS reaction was run at -20 °C (Scheme 58). Gratifyingly, the crude reaction mixture showed a significantly increased ratio of product to toluenesulfonamide up to 7:1 compared to the 2.7:1 ratio observed at 0 °C. The isolated yield increased from 42% to 71% and the reaction time also increased from 48 hours to 96 hours. Unfortunately, the dr of the amide was found to be 5:1 as opposed to the expected >20:1 based on the enantiopurity of the bromonitroalkane. We hypothesized that after the retro aza-Henry occurred, the two components underwent an aza-Henry reaction to recombine forming a racemic mixture. In order to test this hypothesis, an UmAS reaction was run with 93/94% ee material and stopped at 60% conversion. The amide product and the remaining starting material were isolated separately. The expected dr of the amide based on the enantiopurity of the starting material was 30:1. The isolated amide was determined to be 5.6:1 dr. The recovered starting material was assayed to be 73/63% ee, a significant drop from 93/94% ee (Figure 24). A theoretical UmAS reaction using the recovered starting material should provide the amide in 5.3:1 dr, close to what was observed, further supporting the retro/recombination hypothesis.

In order to solve the retro/recombination dilemma, a base screen was undertaken. Ideally, there would be a base that would promote the desired UmAS pathway by forming the nitronate but would be

Figure 24. Difference between expected and observed product dr based on partially racemized unreacted starting material, and evidence for racemization prior to, and competitive with UmAS

unable to deprotonate the N-H and promote the retro process. A variety of nitrogen bases as well as inorganic bases were screened with the dr of the product recorded (Table 11). Unfortunately, none of the screened bases provided the amide product in the expected dr of >20:1. Other variables in the reaction were screened such as equivalents of water (0-50 equiv.), equivalence of amine (1-5 equiv.), solvents (4 solvents) and time (24-120 h). Additionally, the procedure was altered to ensure the halamine was formed prior to the addition of the base and bromonitroalkane. All of these screens did not provide any improved results.

Table 11. Base screen for UmAS reaction

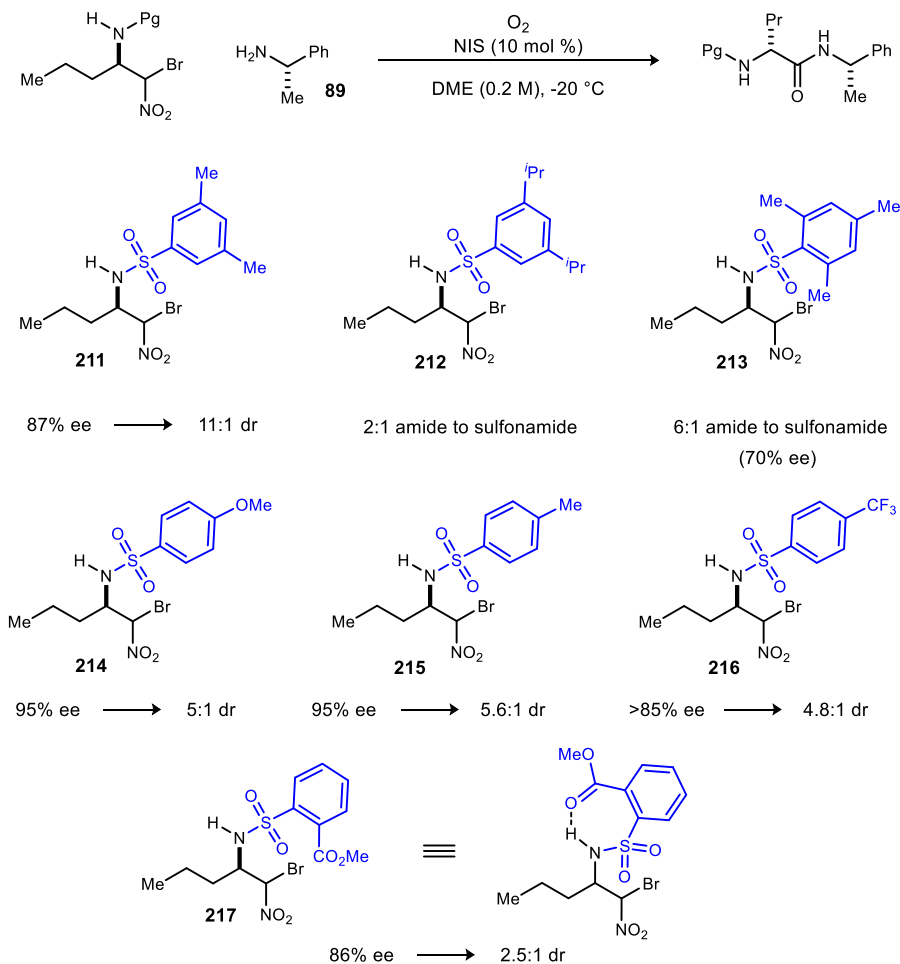


entry ^a	base	dr ^b
1	Hunig's	5.1:1
2	Et ₃ N	5:1
3	Et ₂ NH	6.3:1
4	piperidine	4.5:1
5	pyridine	9.9:1
6	DMAP	6.8:1
7	imidazole	5.7:1
8	TMG	-
9	urea	9.9:1
10	H.Quin-BAM	5.7:1
11	Cs ₂ CO ₃	5.5:1
12	Na ₂ CO ₃	8.6:1
13	Ba(OH) ₂	7.1:1
14	NaOH	9.2:1
15	LiOH	5.8:1

^aAll reactions are 0.2 M in bromonitroalkane and use 10 mol % NIS and 5 equivalents of H₂O and 1 equiv. amine. ^bRatios are of crude reaction mixture and were determined using ¹H NMR.

Next, other sulfonyl protecting groups were tested in the UmAS reaction (Figure 25). The steric effects of the protecting group were first investigated. Installing methyl groups at the two meta positions of the aryl sulfonyl group improved the results slightly as the dr of the amide product was observed to be 11:1. Unfortunately, the different protecting group hindered the aza-Henry reaction as the product was obtained in 87% ee instead of 97% ee. Changing the methyl groups to bulkier isopropyl groups resulted in significant retro aza-Henry as the amide was obtained in a 2:1 ratio with the sulfonamide. Installing methyl groups at the ortho and para positions significantly reduced the enantiopurity of the product obtained from the aza-Henry reaction and did not stop the retro reaction. The electronics of the protecting group were addressed next. The para-methoxy and para-CF₃ derivatives were synthesized and tried in the UmAS reaction in an effort to make the N-H proton less acidic and prevent the retro reaction. Presumably, the methoxy group should lower the acidity while the trifluoromethyl group should raise the acidity. Neither of the groups made a difference in the reaction as both products were obtained in about 5:1 dr. Finally, an ortho-ester derivative was tried in an effort to create an intramolecular hydrogen bond that may prevent the deprotonation of the N-H proton. Unfortunately, the amide was obtained in 2.5:1 dr.

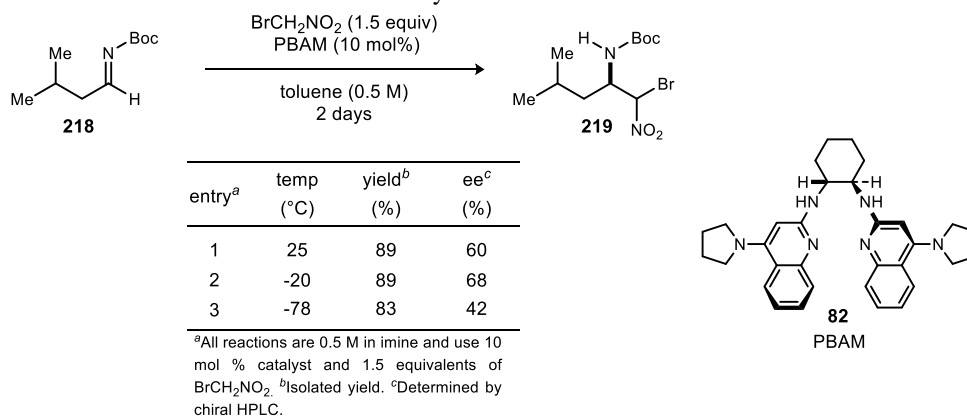
Figure 25. UmAS: sulfonyl protecting group screen



With the unsuccessful attempts at suppressing the retro aza-Henry reaction occurring during the UmAS transformation, a new substrate was needed. We next moved to explore Boc-imines as they are known to perform well in UmAS.

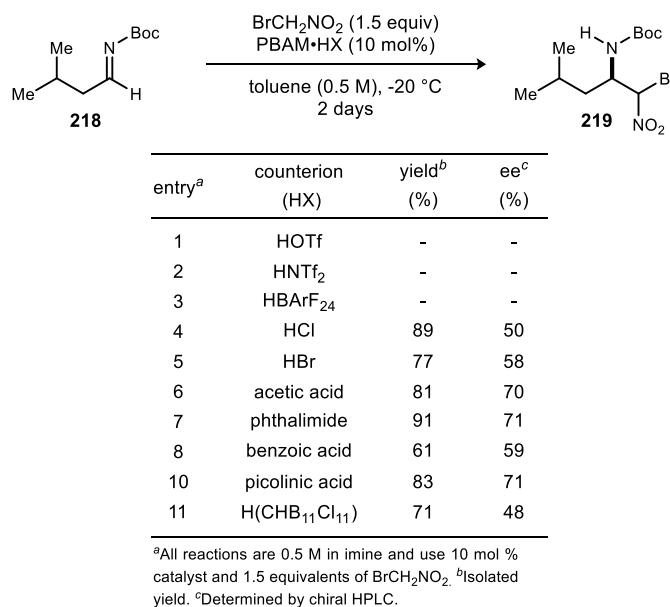
2.4 Bis(Amidine)-Catalyzed Bromonitromethane Additions to Alkyl *N*-Boc Imines

The high enantioselectivity obtained in the aza-Henry addition of bromonitromethane to *N*-sulfonyl aliphatic imines could not be entirely translated to their product amide as the enantiomeric enrichment was eroded via a retro aza-Henry mechanism followed by racemic recombination in the subsequent UmAS reaction. The suspected cause of the retro process is the relatively high acidity of the amine hydrogen caused by the electron withdrawing sulfonyl protecting group. Other protecting groups with less electron withdrawing properties such as Boc, Cbz, and Fmoc, have been employed successfully in the UmAS reaction. Therefore, focus shifted toward developing the enantioselective aza-Henry reaction utilizing a different imine protecting group that would tolerate the UmAS reaction.

Table 12. Bromonitromethane addition to *N*-Boc alkyl imines

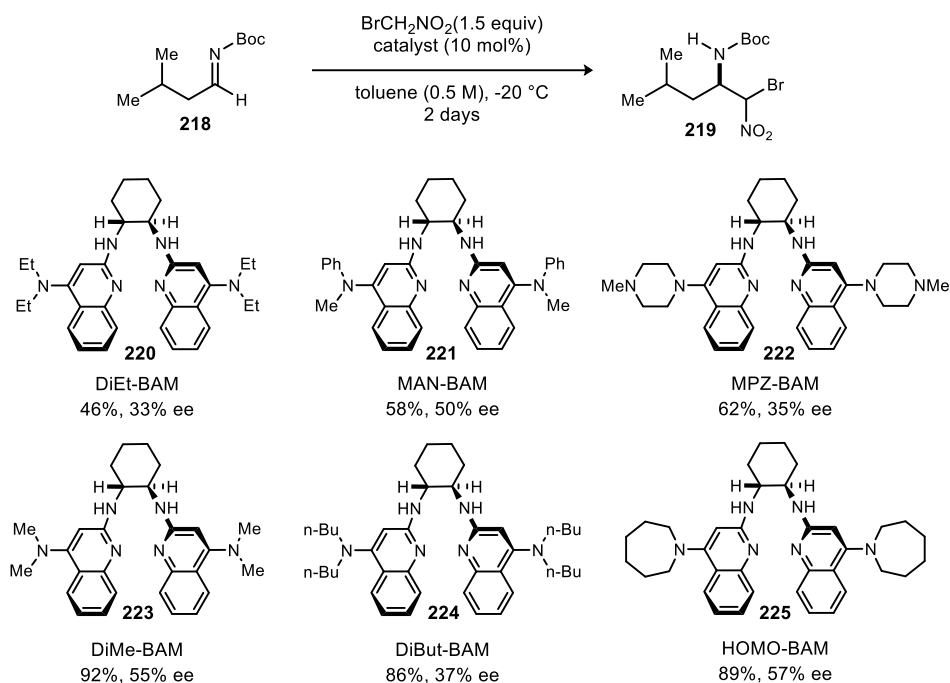
As previously discussed, the use of the *N*-Boc alkyl imines as effective electrophiles in the BAM catalyzed aza-Henry reaction had been explored with decisively negative results (Figure 23, page 33). With the emergence of new useful catalysts as well as counter-ions, efforts were again focused on the aza-Henry addition utilizing the *N*-Boc alkyl imines. As was previously observed, employing PBAM•HOTf as the catalyst only resulted in imine decomposition. However, it was observed that PBAM (**82**) free base furnished the desired product in 89% yield, 1:1 dr and 60% ee (average of two diastereomers) at ambient temperature (Table 12). Lowering the temperature to -20 °C increased the enantioselectivity up to 68% ee while maintaining high yield. Subsequent decrease in temperature did not increase the enantioselection. Even though using triflate as a counter-ion resulted in decomposition, it was thought that other acids may successfully provide the desired adduct in higher levels of enantioselectivity (Table 13). HNTf₂ and HBArF₂₄ behaved similarly to HOTf in that they solely provided imine decomposition. Moving to weaker acids allowed for product formation. Acetic acid, phthalimide and picolinic acid provided a slight increase in enantioselection up to 70%, 71%, and 71% ee, respectively.

Other catalysts were also screened in an effort to increase the enantioselection. Steric and electronic alterations on the quinoline rings of PBAM were tested in the reaction without success. Further modification

Table 13. Counter-ion screen

of the catalyst focused on the four position. Replacing the pyrrolidine substituents with a variety of amines only resulted in lower enantioselection (Figure 26). Changing the catalyst backbone from cyclohexyl diamine to stilbene diamine only further decreased the enantioselection below 40% ee. Additional alterations of the catalyst loading (5%-20%), concentration (0.1 M-1 M), and equivalence of bromonitromethane (1.5-50) did not result in any increase in enantioselection. A small solvent screen provided a slight increase in enantioselection up to 75% ee using *o*-xylene instead of toluene.

Figure 26. Catalyst screen: quinoline 4-position

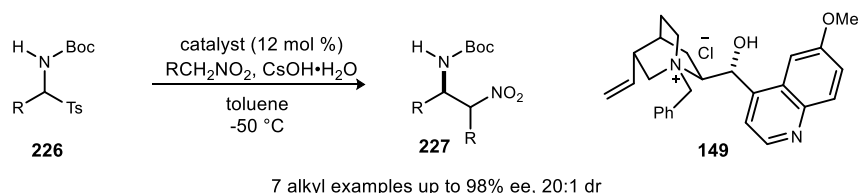


2.5 Catalytic Enantioselective Synthesis of D-Amino Amides using a Phase Transfer Catalyzed aza-Henry Addition and Umpolung Amide Synthesis³⁹

Background: Palomo's Phase Transfer Catalyzed aza-Henry Reaction

With the BAM-catalyzed route to the desired α -bromonitroalkanes proving unsuccessful, we chose to take a different approach. In 2005 Palomo and coworkers reported an enantioselective phase transfer catalyzed aza-Henry reaction in which a variety of nitroalkanes were added into aliphatic and aryl *N*-Boc α -amidossulfones.⁶⁸ The reaction was conducted in toluene at $-50\text{ }^\circ\text{C}$ employing *N*-benzylquininium chloride (**149**) as the catalyst and $\text{CsOH}\cdot\text{H}_2\text{O}$ as the stoichiometric base. Using nitroethane as the pronucleophile, the aza-Henry adducts were obtained in good yield with dr up to 20:1 and ee up to 98% (Scheme 59). The reaction tolerates electron-rich and electron-poor aryl sulfones as well as alkyl sulfones. The primary nitroalkane can be modified to contain alkenes, acetals and esters while maintaining high stereoselectivity.

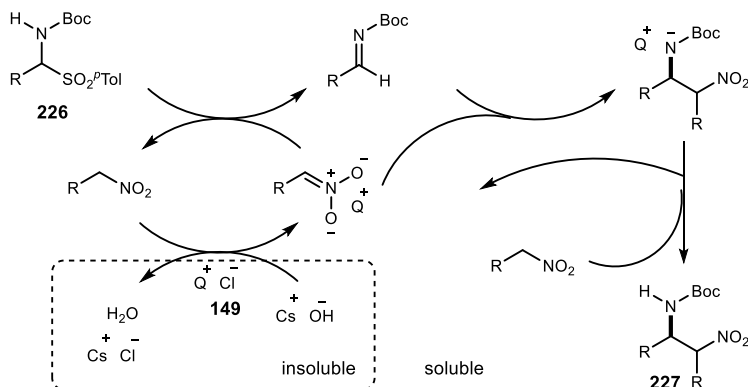
Scheme 59. Palomo's phase transfer catalyzed aza-Henry reaction



While secondary nitroalkanes participate in the reaction, the enantioselection is diminished down to 20% ee.

Palomo's proposed mechanism for the phase transfer catalyzed aza-Henry reaction is depicted in Figure 27. Initially, quininium chloride catalyst **149** exchanges chloride for hydroxide generating *N*-benzylquininium hydroxide and CsCl. Deprotonation of the nitroalkane leads to the quininium nitronate which fosters elimination of the sulfone to the imine. Subsequently, another ion-pair of the quininium nitronate adds into the imine, forming the product. They believe the elimination is much slower than the addition based on NMR experiments which showed no appreciable amount of the imine during the reaction. When using a more acidic nitroalkane, methyl 2-nitroacetate, the reaction slowed significantly, lending further evidence that the basicity of the nitronate plays a key role in the elimination.

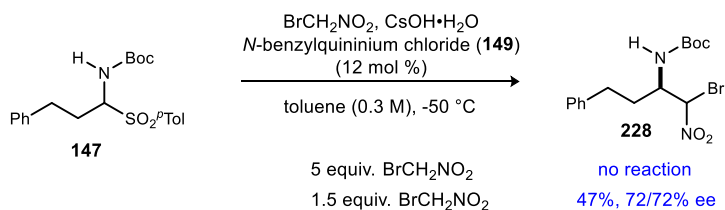
Figure 27. Proposed mechanism of Palomo's phase transfer catalyzed aza-Henry reaction



Phase Transfer Catalyzed aza-Henry with Bromonitromethane

We proposed to adapt this procedure to tolerate bromonitromethane to yield the desired α -bromonitroalkane donors necessary for UmAS. Based on the proposed mechanism, the more acidic nature of bromonitromethane relative to nitromethane may cause the initial elimination of the sulfone to imine to be difficult. Nonetheless we pushed forward in our attempts to adapt the reaction to tolerate bromonitromethane. Our first attempt was to simply substitute bromonitromethane into the reaction in place of nitroethane and keep the other conditions the same. The reaction was run with 5 equivalents of bromonitromethane, 1.3 equivalents CsOH•H₂O, and 12 mol % of catalyst, *N*-benzylquininium chloride (**149**) in toluene. Upon addition of CsOH•H₂O at -40 °C to the reaction, an exotherm was observed as well as a slight outgas from the reaction. The CsOH•H₂O, which should be a free-flowing white solid became a sticky orange-brown gel. The reaction resulted in no conversion with full recovery of starting material (Scheme 60). The viability of the catalyst was verified as the reaction was also run with nitromethane, providing the desired adduct in 60% yield and 94% ee. It appeared that the exotherm and outgassing that was preventing the desired reaction was a result of the interaction between bromonitromethane and

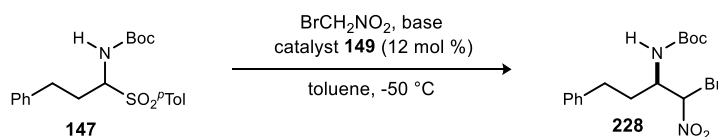
Scheme 60. Initial attempts at phase transfer catalyzed addition of bromonitromethane to *N*-Boc aldimines



CsOH•H₂O. Reducing the equivalents of bromonitromethane down to 1.5 lessened the negative reaction and furnished the desired bromonitroalkane in 47% yield and 72/72% ee.

Although the reaction provided the desired product, the subpar enantioselection and yield as well as the presences of the exotherm led us to screen a variety of inorganic bases (Table 14). Using K₂CO₃ resulted in decreased conversion and enantioselection (20%, 59/43% ee). Although there was no exothermic reaction and formation of the orange-brown substance, the other carbonate bases (Na₂CO₃, CaCO₃, Cs₂CO₃) further reduced the conversion down to <10%. KOH gave similar results to CsOH•H₂O but no better (63%, 62/68% ee). Without further improvement CsOH•H₂O was chosen as the optimal base.

Table 14. Base screen in phase transfer catalyzed addition of bromonitromethane to *N*-Boc aldimines

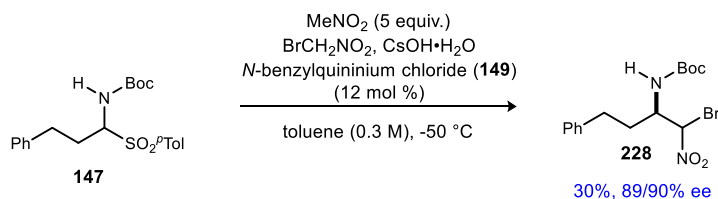


entry ^a	base	BrCH ₂ NO ₂ (equiv.)	conversion ^b	ee ^c (%)
1	CsOH•H ₂ O	5	0	-
2	CsOH•H ₂ O	1.5	68	72/72
3	K ₂ CO ₃	1.5	20	59/43
4	Na ₂ CO ₃	1.5	<10	-
5	CaCO ₃	1.5	<10	-
6	KOH	1.5	63	62/68
7	Cs ₂ CO ₃	1.5	<10	-

^aAll reactions were conducted using sulfone (1 equiv), 12 mol % catalyst, base (1.3 equiv) and bromonitromethane (1.5 equiv) in toluene (0.3 M). ^bBased on ¹H NMR. ^cEnantiomeric excesses determined by chiral HPLC using an OD-H column (Chiral Technologies)

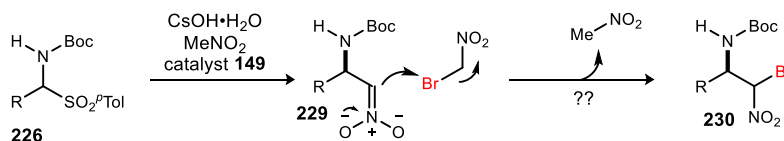
We hypothesized that the exothermic negative reaction observed was due to the more acidic nature of bromonitromethane as compared to nitromethane. We thought we may be able to temper the negative reaction by adding both nitromethane and bromonitromethane to the reaction. The presence of nitromethane may interact with the CsOH•H₂O and prevent the negative reaction, but the bromonitromethane, being more acidic, should add into the imine preferentially over nitromethane. The reaction was run with 5 equivalents of nitromethane and 1.5 equivalents of bromonitromethane. The negative exothermic reaction did not occur and near full conversion was observed (~85%). The desired product was isolated in 30% yield and 89/90% ee (Scheme 61). The balance of the mass was the nitromethane adduct. The conversion and enantioselection were significantly improved, however the isolated yield suffered due to nitromethane addition.

Scheme 61. Nitromethane as an additive in the phase transfer catalyzed addition of bromonitromethane to *N*-Boc aldimines



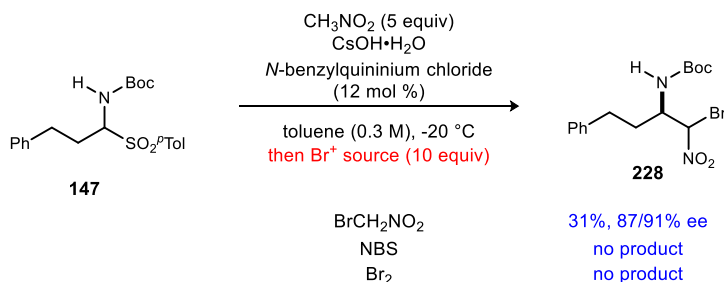
The significant increase in enantioselection (72 to 90% ee) was a puzzling discovery. We did not expect to see a jump in enantioselection by simply adding nitromethane to the reaction mixture. A possible explanation for this occurrence is an electrophilic bromine transfer from bromonitromethane to the nitromethane aza-Henry adduct (Figure 28). The nitromethane adduct does form in high enantioselection

Figure 28. Proposed bromine transfer from bromonitromethane to nitromethane aza-Henry adduct

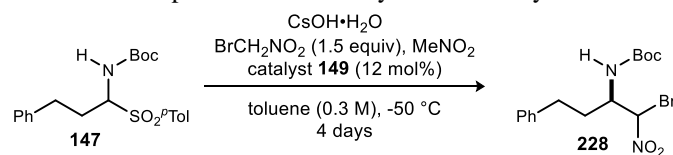


(<90% ee) which upon bromine transfer would result in high enantiopurity of the bromonitroalkane. In order to probe this possibility, we ran the reaction using nitromethane at $-20\text{ }^{\circ}\text{C}$ and after two days added bromonitromethane and allowed the reaction to stir for another 24 hours. The same reaction was run using NBS and Br_2 as the electrophilic source of bromine (Figure 29). The bromonitromethane reaction furnished the bromonitroalkane in 31% yield and 87/91% ee. The reactions with NBS and Br_2 resulted in only the nitromethane adduct, providing evidence against the possible bromine transfer mechanism. Most likely, the reaction is in constant equilibrium and upon addition of bromonitromethane, the forward reaction takes place with bromonitromethane as opposed to nitromethane to afford the bromonitroalkane product.

Figure 29. Screen of bromonium sources in proposed bromine transfer reaction

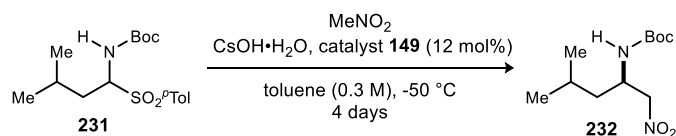


In an effort to further increase the observed enantioselection of the reaction, the equivalents of the nitromethane additive were varied. As the equivalents of nitromethane were increased from zero to ten the enantioselectivity also increased from 72/72% ee to 95/94% ee (Table 15). As expected the yield decreased as the equivalents of nitromethane increased due to increasing competition to form the nitromethane adduct. Although not reported by Palomo, the trend of increasing enantiopurity with respect to increasing equivalents of nitromethane holds for the nitromethane addition reaction as well. The enantiopurity increased from 75% ee up to 93% ee as the equivalence of nitromethane increased from one to five. Further increase in equivalents of nitromethane did not result in an increase in enantiopurity.

Table 15. Nitromethane additive in the phase transfer catalyzed aza-Henry reaction

entry ^a	MeNO_2 (equiv)	yield ^b (%)	ee ^c (%)
1	0	47	72/72
2	1.5	62	81/78
3	3	56	88/88
4	5	30	89/90
5	10	27	95/94

^aAll reactions were conducted using sulfone (1 equiv), 12 mol % catalyst **149**, $\text{CsOH}\cdot\text{H}_2\text{O}$ (1.3 equiv) and bromonitromethane (1.5 equiv) in toluene (0.3 M). ^bIsolated yield. ^cEnantiomeric excesses determined by chiral HPLC.

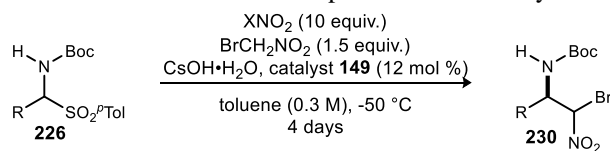


entry ^a	MeNO_2 (equiv)	yield ^b (%)	ee ^c (%)
1	1	20	75
2	3	73	85
3	5	76	93
4	10	82	92

^aAll reactions were conducted using sulfone (1 equiv), 12 mol % catalyst **149**, and $\text{CsOH}\cdot\text{H}_2\text{O}$ (1.3 equiv) in toluene (0.3 M). ^bIsolated yield. ^cEnantiomeric excesses determined by chiral HPLC.

Although the inclusion of nitromethane as an additive increased the enantioselection of the reaction, the yield suffered due to competitive nitromethane addition. In an effort to increase the yield, nitromethane was replaced with nitroethane and 2-nitropropane. The additional steric bulk provided by these two different nitroalkanes should slow down their addition to the imine relative to nitromethane and allow for greater conversion to the desired product. The additives were tested in the reaction across seven different substrates with varying results (Table 16). Relative to nitromethane, nitroethane provided an increased yield for most substrates. The enantiopurity slightly dropped in most cases but not by a significant amount. Using 2-nitropropane as an additive further increased the yield in most cases. However, the enantiopurity suffered drastically in most cases dropping by as much as 20%.

Table 16. Effect of different nitroalkane additives on the phase transfer catalyzed addition of bromonitromethane to *N*-Boc aldimines

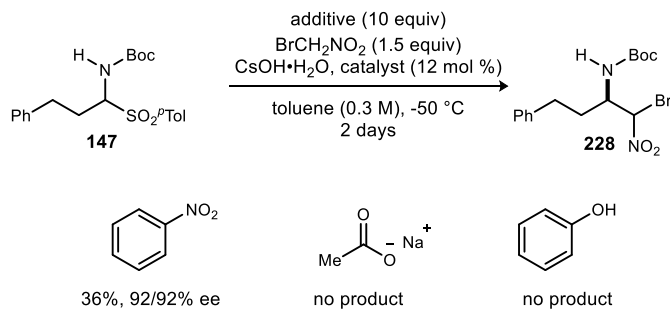


entry ^a	R	X	yield ^b (%)	ee ^c (%)
1	CH ₂ CH ₂ Ph	Me	45	93/88
2	ⁱ Bu	Me	58	90/91
3	(CH ₃) ₃ CCH ₂	Me	60	94/94
4	Cy	Me	51	82/82
5	ⁱ Pr	Me	40	75/78
6	C ₁₀ H ₂₁	Me	39	91/90
7	HC≡CCH ₂ CH ₂	Me	47	84/83
8	CH ₂ CH ₂ Ph	Et	57	96/97
9	ⁱ Bu	Et	57	87/90
10	(CH ₃) ₃ CCH ₂	Et	65	92/93
11	Cy	Et	27	86/87
12	ⁱ Pr	Et	44	72/75
13	C ₁₀ H ₂₁	Et	51	91/91
14	HC≡CCH ₂ CH ₂	Et	42	87/87
15	CH ₂ CH ₂ Ph	ⁱ Pr	53	87/86
16	ⁱ Bu	ⁱ Pr	72	81/84
17	(CH ₃) ₃ CCH ₂	ⁱ Pr	79	89/90
18	Cy	ⁱ Pr	51	57/65
19	ⁱ Pr	ⁱ Pr	50	65/57
20	C ₁₀ H ₂₁	ⁱ Pr	71	91/87
21	HC≡CCH ₂ CH ₂	ⁱ Pr	41	83/66

^aAll reactions were conducted using sulfone (1 equiv.), 12 mol % catalyst **149**, BrCH₂NO₂ (1.5 equiv.), nitroalkane additive (10 equiv.) and CsOH·H₂O (1.3 equiv.) in toluene (0.3 M). ^bIsolated yield. ^cEnantiomeric excesses for each diastereomer (1:1 dr) were determined by chiral HPLC.

At this point we decided to look further into the function of the nitroalkane additive. Three different additives were tried in its place to probe its function (Scheme 62). When nitrobenzene was used as the additive, the desired product was obtained in 36% yield and 92/92% ee. However, the exothermic reaction concurrent with the apparent decomposition of bromonitromethane occurred. These observations favor the idea that the acidic nature of the nitroalkane is not necessary for high enantioselection but is required to mitigate the “negative” reaction observed. The lower yield could be a result of less nitronate present to perform the elimination. Sodium acetate was chosen as an additive due to the similarity in structure of acetate and the nitro group. The reaction resulted in decomposition of the starting material. Phenol was also chosen as an additive to provide similar acidity to that of nitromethane and nitroethane. This reaction also

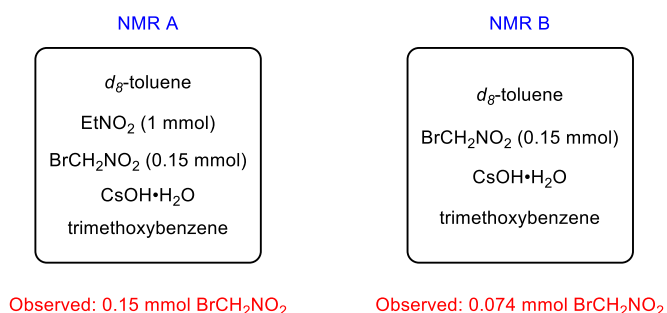
Scheme 62. Probing effect of additive on addition of bromonitromethane to *N*-Boc aldimines



resulted in decomposition of starting material. Although no clear conclusions can be drawn, it appears that the solubilizing ability of the nitroalkane is the important factor in contributing to the high enantioselection, while the acidity of the nitroalkane is required for bromonitromethane decomposition prevention.

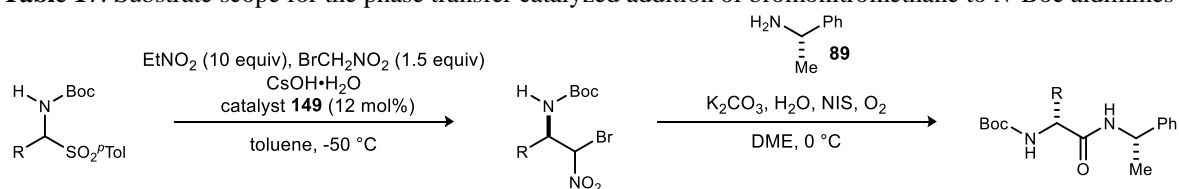
We also wanted to probe the potential decomposition of bromonitromethane in the presence of CsOH•H₂O. Two simple ¹H NMR experiments were run in an attempt to observe the decomposition products (Figure 30). One experiment contained *d*₈-toluene, EtNO₂, BrCH₂NO₂ (.15 mmol), CsOH•H₂O, and trimethoxybenzene as an internal standard (NMR A). When CsOH•H₂O was added to the NMR tube no visible reaction was observed as expected. The spectrum showed 0.15 mmol of BrCH₂NO₂. The second experiment contained *d*₈-toluene, BrCH₂NO₂ (.15 mmol), CsOH•H₂O, and trimethoxybenzene as an internal standard (NMR B). This experiment was run in a sealed NMR tube and was sealed immediately following the addition of CsOH•H₂O. The spectrum showed 0.074 mmol BrCH₂NO₂. It was evident that some of the BrCH₂NO₂ was decomposed. Bromonitromethane is reported to react with aqueous base to generate formic acid and methanol,⁹² however these products were not observed in the NMR spectrum. It is evident that the nitroalkane additive is necessary to prevent the decomposition of bromonitromethane, allowing the reaction to proceed.

Figure 30. NMR experiments probing bromonitromethane decomposition



A combination of 10 equivalents of nitroethane and 1.5 equivalents of bromonitromethane using *N*-benzylquininium chloride **149** and CsOH•H₂O as the base were chosen as optimal conditions to examine a variety of α-amido sulfones (Table 17). Straight carbon chain substrates provided the corresponding α-bromonitroalkanes (Table 17, entries 6, 7, 8) in 96%, 87%, and 91% ee, respectively with moderate yields. Substrates with branching β to the imine carbon (Table 17, entries 2, 3, 9, 11) furnished the corresponding products in 89%, 93%, 96% and 86% ee, respectively, all with moderate yields with one exception (Table 17, entry 11, 38%). Unfortunately, branching α to the imine resulted in diminished yield and enantioselection. The isopropyl side chain (Table 17, entry 4) and cyclopropyl side chain (Table 17, entry 15) gave diminished enantioselection down to 74% and 78% ee, respectively. The cyclohexyl side chain (Table 17, entry 5) resulted in 89% ee but with poor yield (36%). The methodology tolerated unsaturation on the side chains while maintaining moderate yields and high enantioselection. Alkenyl side chains (Table 17, entries 12, 14) provided the desired α-bromonitroalkanes in 86% and 88% ee, respectively. The terminal alkyne substrate (Table 17, entry 10) was provided in 42% yield with 87% ee. The inclusion of an electron-poor trifluoromethyl side chain (Table 17, entry 13) resulted in 91% ee while an electron-rich side chain (Table 17, entry 16) resulted in diminished enantioselectivity at 75% ee.

⁹² Challis, B. C.; Yousaf, T. I. *Journal of the Chemical Society, Perkin Transactions 2* **1991**, 283-286.

Table 17. Substrate scope for the phase transfer catalyzed addition of bromonitromethane to *N*-Boc aldimines

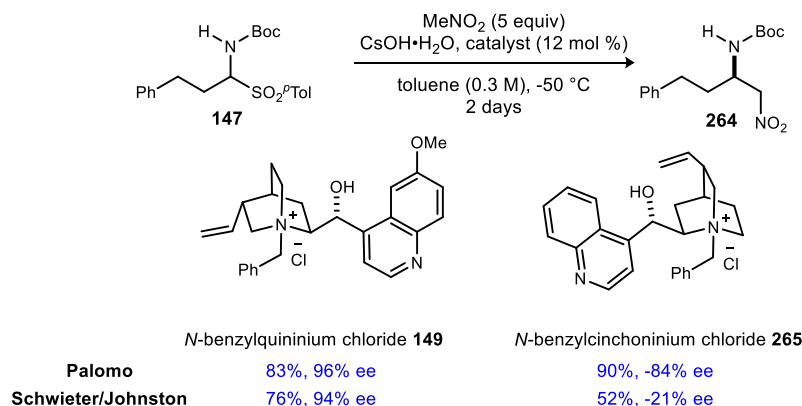
entry	R	name	XX	yield ^b (%)	ee ^c (%)	er	dr ^e	XX	yield ^b (%)
1	CH ₂ CH ₂ Ph	homophenylalanine (Hph)	228	59	96/96	49:1	64:1	248	61
2	^t Bu	leucine (Leu)	233	57	87/90	15:1	16:1	249	58
3	(CH ₃) ₃ CCH ₂	neopentylglycine (Npg)	234	60	92/93	37:1	35:1	250	58
4	ⁱ Pr	valine (Val)	235	44	72/75	5:1	5:1	251	73
5	Cy	cyclohexylglycine (Chg)	236	36	88/89	16:1	14:1	252	56
6	ⁿ Bu	norleucine (Nle)	237	54	96 ^f	49:1	41:1	253	52
7	ⁿ Pr	norvaline (Nva)	238	52	87 ^f	14:1	25:1	254	69
8	C ₁₀ H ₂₁	2-amino-dodecanoic acid (Adod)	239	51	91/91	22:1	29:1	255	65
9	(C ₆ H ₁₁)CH ₂	cyclohexylalanine (Cha)	240	53	96 ^f	46:1	71:1	256	53
10	HC≡CCH ₂ CH ₂	homopropargylglycine (Hpg)	241	42	87/87	15:1	45:1	257	48
11	PhCH ₂	phenylalanine (Phe)	242	38	86 ^f	14:1	14:1	258	69
12	H ₂ C=CHCH ₂ CH ₂	homoallylglycine (Hag)	243	57	86 ^f	13:1	20:1	259	42
13	CF ₃ CH ₂	trifluoromethylalanine (CF ₃ -Ala)	244	46	91 ^f	20:1	35:1	260	38
14	<i>cis</i> -CH ₃ CH ₂ CH=CH(CH ₂) ₂	-	245	57	88 ^f	16:1	17:1	261	38
15	<i>c</i> -C ₃ H ₅	cyclopropylglycine	246	50	78/77	8:1	8:1	262	49
16	EtOCH ₂ CH ₂	ethyl homoserine (Et-Hse)	247	37	75 ^f	7:1	8:1	263	61

^aAll reactions were conducted using sulfone (1 equiv, 0.3 M in toluene), 12 mol % catalyst, CsOH·H₂O (1.3 equiv), nitroethane (10 equiv) and bromonitromethane (1.5 equiv) at -50 °C. ^bIsolated yield. ^cDetermined by chiral HPLC using chiral stationary phase. ^dAll reactions were conducted using bromonitroalkane (1 equiv), H₂O (5 equiv), (*S*)- α -Me-benzylamine (1.2 equiv), K₂CO₃ (3 equiv) and NIS (0.1 equiv) in DME (0.2 M) under an O₂ atmosphere at 0 °C. ^eDetermined by HPLC using AD-H column (Chiral Technologies). ^fEnantiomeric excess of debrominated adduct.

The resulting α -bromonitroalkanes were submitted to UmAS using the previously developed aerobic conditions substoichiometric in NIS. The reactions were run in DME with 1.2 equivalents of (*S*)- α -methylbenzylamine, 3 equivalents of K₂CO₃, 0.1 equivalents NIS, and an O₂ balloon. The amino amides were formed in moderate to good yields ranging from 38% to 73%. The amino amides were formed in diastereomeric ratios equal or greater to those expected based on the % ee of the starting α -bromonitroalkane.

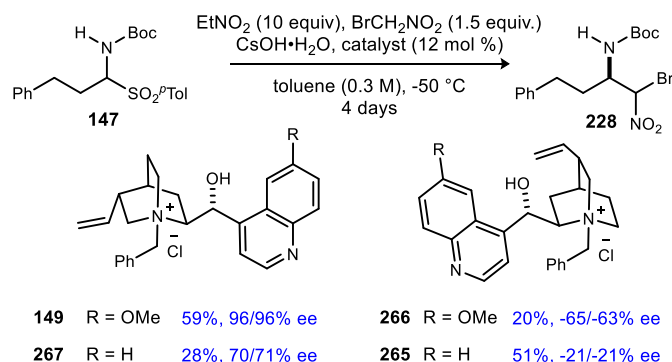
At this point we had developed a method to access the *R*-enantiomer in high enantiopurity of the β -amino- α -bromonitroalkanes which can be transformed into the corresponding α -D-amino amides. The

Scheme 63. Cinchona alkaloid derived catalysts in nitromethane addition to *N*-Boc aldimines



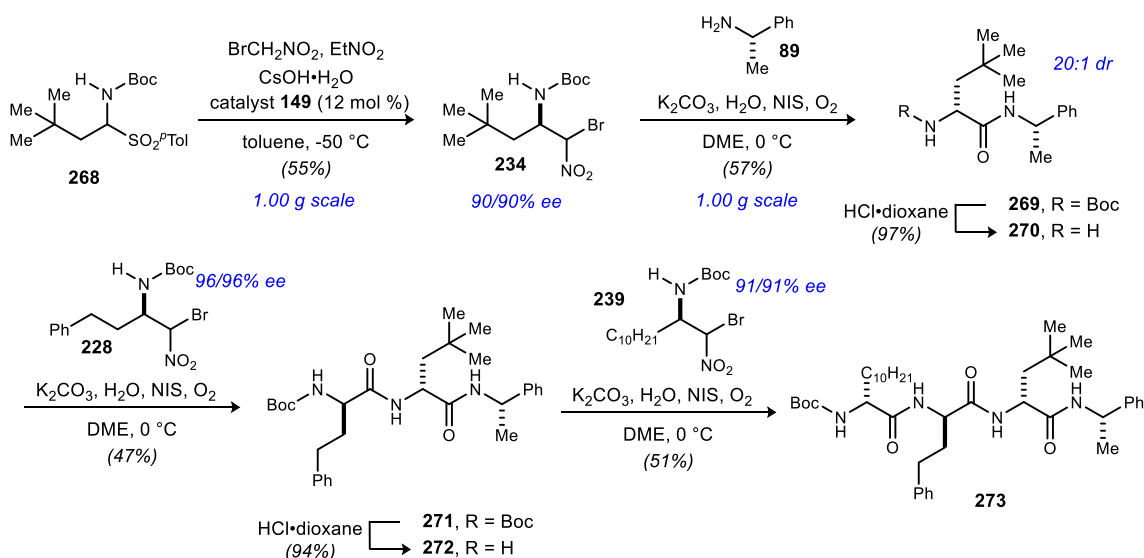
next step was to change the catalyst and obtain access to the *S*-enantiomer of the same β -amino- α -bromonitroalkanes (L-amino acid donors). Palomo reported obtaining the *S*-enantiomer of the nitromethane adduct in similarly high enantiopurity as the *R*-enantiomer by simply replacing *N*-benzylquininium chloride **149** with *N*-benzylcinchoninium chloride **265**. However, we were unable to achieve the same high enantioselection when performing the same reaction (Scheme 63). When applied to the bromonitromethane addition, *N*-benzylcinchoninium chloride **265** performed poorly providing the desired product in 51% yield and 21/21% ee (Scheme 64). We also tested *N*-benzylquinidinium chloride **266**, the psuedoenantiomer of our preferred catalyst, without success as the product was obtained in 20% yield and 65/63% ee.

Scheme 64. Other cinchona alkaloid derived catalyst in phase transfer catalyzed addition of bromonitromethane to *N*-Boc aldimines



In order to demonstrate the scalability and utility of the methodology we synthesized a tripeptide containing three different unnatural amino acids. We performed the aza-Henry reaction using 1.00 g of α -amido sulfone **268**. The resulting adduct was obtained in 55% yield and 90/90% ee. The subsequent UmAS coupling was undertaken on 1.00 g of the α -bromonitroalkane to provide the desired amide in 57% yield and 20:1 dr. Boc-deprotection and subsequent UmAS coupling with **228** gave dipeptide **271** in 47% yield. Another Boc-deprotection followed by UmAS coupling with **239** provided tripeptide **273** in 51% yield (Scheme 65).

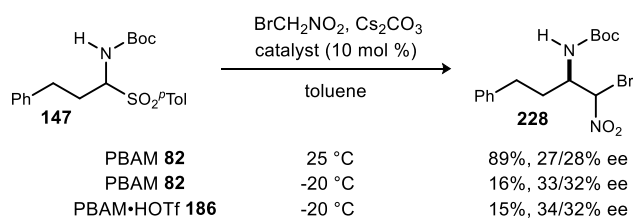
Scheme 65. Iterative synthesis of a tripeptide containing unnatural amino acids



2.6 Enantioselective Addition of Bromonitromethane to Aliphatic *N*-Boc Aldimines Using a Homogeneous Bifunctional Chiral Organocatalyst

In an effort to gain access to the *S*-enantiomer of the desired α -bromonitroalkanes, we again turned towards our BAM catalysis. If we are able to develop a procedure that would provide the desired adducts in high enantiopurity using BAM catalysis, we would be able to provide both enantiomers by simply using the other enantiomer of the catalyst, thus solving the main problem encountered with the phase transfer catalysis procedure. Previous efforts using BAM catalysis resulted in lower than desired enantiopurity or decomposition of the imine when using the triflic acid salt. With the success of the one-pot elimination/addition phase transfer reaction, we sought to map that strategy onto our catalysis where the imine would be generated from the α -amidosulfone *in situ*. The simplest embodiment was attempted by combining sulfone **147**, PBAM (**82**), bromonitromethane, and Cs₂CO₃ as a stoichiometric base to effect elimination of the sulfone to the imine (Scheme 66). The reaction, run at room temperature, provided the α -bromonitroalkane in 89% yield and 27/28% ee. The observed reactivity was promising, however the enantioselectivity was poor. Lowering the temperature of the reaction down to -20 °C resulted in poor conversion as the product was isolated in 16% yield with a modest increase in ee. When the catalyst was changed to the triflic acid salt (**186**), the results remained the same as the product was obtained in 15% yield and 34/32% ee. The similar level of enantioselection observed from the two catalysts show that the triflic acid salt was likely converted to the free base under the reaction conditions. These experiments highlighted two challenges that would need to be addressed: balancing the warmer temperature needed for sulfone elimination with the cryogenic temperature necessary to enhance enantioselection and solving the problem of the catalyst salt being converted to the free base.

Scheme 66. One-pot procedure for BAM-catalyzed addition of bromonitromethane to *N*-Boc aldimines



A new two-pot procedure was developed to address the two challenges. The sulfone was dissolved in toluene and stirred with five equivalents of Cs₂CO₃ until the elimination was complete as judged by ¹H NMR (~3h). The reaction mixture was then filtered through a plug of Celite, washing with toluene, to remove the Cs₂CO₃. PBAM•HOTf was added to the mixture and it was cooled to -20 °C. Bromonitromethane was then added and the reaction was allowed to stir for 24 h. The desired product was obtained in 72% yield and 83/83% ee with only minor decomposition (Scheme 67). Using PBAM free base as the catalyst provided the same enantioselection as the one-pot procedure with increased yield. This new two-pot procedure allowed for the use of the triflic acid salt without imine decomposition.

Scheme 67. Two-pot procedure for BAM-catalyzed addition of bromonitromethane to *N*-Boc aldimines

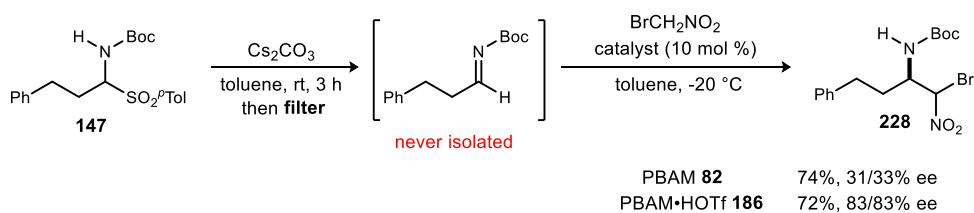


Table 18. Catalyst screen for BAM-catalyzed addition of bromonitromethane to *N*-Boc aldimines

entry ^a	catalyst	yield ^b (%)	ee ^c (%)
1	PBAM (82)	74	42/40
2	PBAM•HOTf 186	68	91/91
3	StilbPBAM•HOTf 190	71	53/47
4	⁴ MeO-StilbBAM•HOTf 198	50	25/22
5	⁶ MeO-PBAM•HOTf 274	79	86/85
6	⁸ MeO-PBAM•HOTf 275	74	57/61

PBAM 82 R¹,R²=H
186 PBAM•HOTf
274 R¹= OMe, R²=H
275 R¹= H, R²=OMe

190 R=

198 R=OMe

^aReaction filtered through Celite after 3h to remove Cs₂CO₃ prior to the second step. ^bIsolated yields. ^cAdducts isolated as mixture of diastereomers (1:1), ee's reported for each diastereomer.

To further increase the enantioselection, the aza-Henry portion of the procedure was cooled down to -78 °C. PBAM•HOTf provided α -bromonitroalkane **228** in 68% yield and 91/91% ee. A number of modified catalysts were then tested in the reaction (Table 18). Changing the catalyst backbone from cyclohexyl diamine to stilbene diamine resulted in diminished ee (entry 3). Electronic modification of the quinoline rings by adding electron-rich methoxy groups at either the 6-position or the 8-position did not improve results (entries 5 and 6). PBAM•HOTf (**186**) was taken on as the optimal catalyst.

The next focus was to alter the counterion of the catalyst. At this point, only fluorinated sulfonic acids were screened because a variety of weaker acids were previously screened without positive results. Substituting triflimidic acid in place of triflic acid provided lower enantioselection at 81/81% ee (Table 19). Using fluorosulfonic acid as the counterion provided a slight drop in enantioselection (entry 3). Lastly, cyclic triflimide **276** resulted in a significant decrease in enantioselection (entry 4). PBAM•HOTf was chosen as the optimal catalyst-counterion pair to further optimize the reaction.

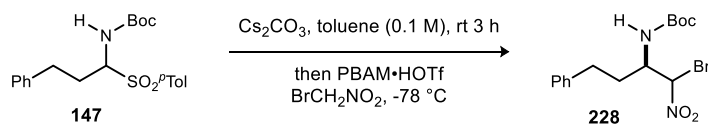
Table 19. Counterion screen for BAM-catalyzed addition of bromonitromethane to *N*-Boc aldimines

entry ^a	counterion	yield ^b (%)	ee ^c (%)
1	HOTf	68	91/91
2	HNTf ₂	76	81/81
3	FSO ₃ H	62	86/86
4	276	61	66/65

276

^aReaction filtered through Celite after 3h to remove Cs₂CO₃ prior to the second step. ^bIsolated yields. ^cAdducts isolated as mixture of diastereomers (1:1), ee's reported for each diastereomer.

All reactions up to this point utilized 10 mol % catalyst loadings. Decreasing the catalyst loading down to as low as 2 mol % did not affect the yield or enantioselection (Table 20). A handful of additives were screened in hopes of finding a small increase in enantioselection. Unfortunately, many of the additives had no effect on the outcome of the reaction while a few (imidazole, phenol, succinimide) had detrimental

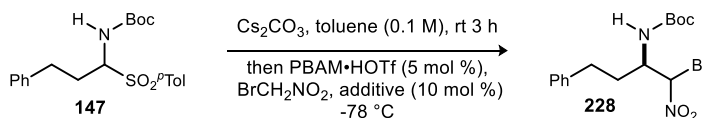
Table 20. Catalyst loading in BAM-catalyzed addition of bromonitromethane to *N*-Boc aldimines

entry ^a	cat. loading (mol %)	yield ^b (%)	ee ^c (%)
1	10	68	91/91
2	5	74	91/90
3	2	70	93/93

^aReaction filtered through Celite after 3h to remove Cs_2CO_3 prior to the second step. ^bIsolated yields.

^cAdducts isolated as mixture of diastereomers (1:1), ee's reported for each diastereomer.

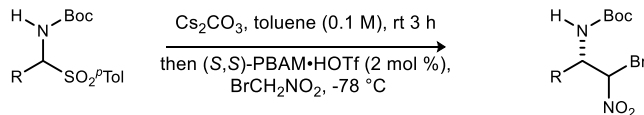
effects on the reaction (Table 21). The additions of phenol and succinimide to the reaction resulted in a complete shutdown of the reaction while imidazole reduced the enantiopurity of the product down to 23/27% ee.

Table 21. Screen of additives in BAM-catalyzed addition of bromonitromethane to *N*-Boc aldimines

entry ^a	additive	yield ^b (%)	ee ^c (%)
1	nitrobenzene	76	88/90
2	EtOAc	70	90/89
3	benzamide	62	90/90
4	imidazole	49	23/27
5	2,3-dihydropyran	78	90/90
6	thiophene	68	89/90
7	phenol	-	-
8	IPA	22	87/85
9	succinimide	-	-
10	2-nitropropane	81	90/90

^aReaction filtered through Celite after 3h to remove Cs_2CO_3 prior to the second step. ^bIsolated yields. ^cAdducts isolated as mixture of diastereomers (1:1), ee's reported for each diastereomer.

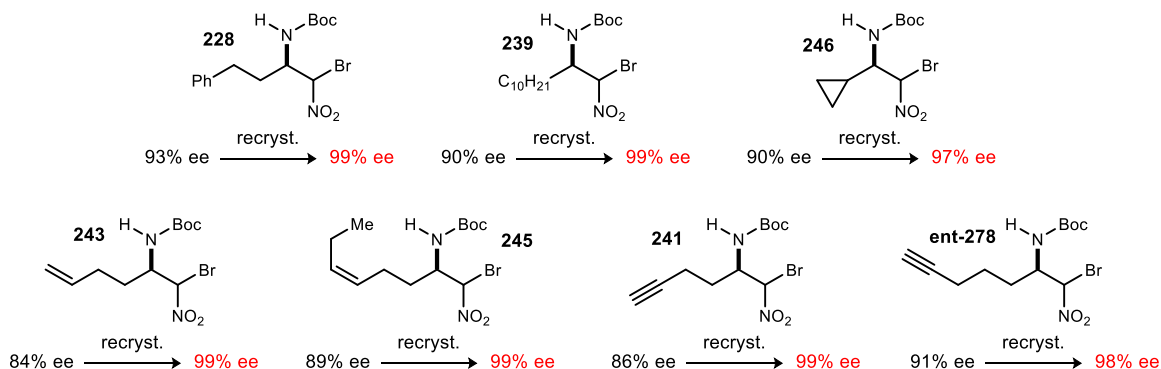
The optimal conditions were applied to a variety of α -amido sulfones (Table 22). (*S,S*)-PBAM•HOTf was used as the catalyst to demonstrate the ability to provide both the *R*-enantiomer (*D*-amino acid donor) and *S*-enantiomer (*L*-amino amide donor) of the α -bromonitroalkanes. Straight chain aliphatic imines are tolerated in the reaction with high yields and 81-90% ee (entries 2-5). Branching beta to the imine center is also tolerated well in the reaction giving high yield and 85-92% ee (entries 6-9). Branching alpha to the imine center gave mixed results. Cyclohexyl imine (entry 12) works well at 92% ee, while isopropyl imine (entry 10) provided the product in 79% ee. Cyclopropyl imine (entry 11) found itself in the middle of the previous two at 84% ee. The methodology also tolerates unsaturation in the form of alkenes and alkynes with enantioselections ranging from 84-91% ee (entries 13-16). Electron donating (entries 18 and 19) and electron withdrawing (entry 17) side chains are also tolerated.

Table 22. Substrate scope for BAM-catalyzed addition of bromonitromethane to *N*-Boc aldimines

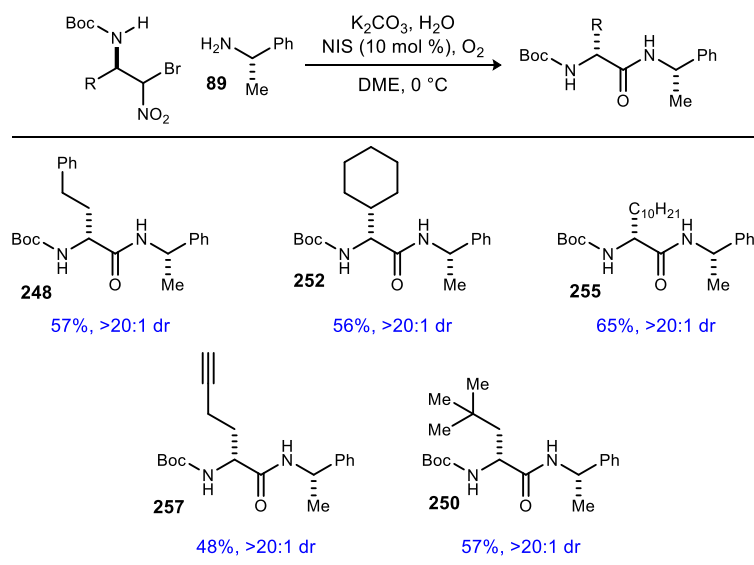
entry ^a	R	XX	yield ^b (%)	ee ^c (%)
1	PhCH ₂ CH ₂	ent-228	70	93
2	Et	277	90	81
3	ⁿ Pr	ent-238	87	90
4	ⁿ Bu	ent-237	94	88
5	C ₁₀ H ₂₁	ent-239	88	90
6	(CH ₃) ₃ CCH ₂	ent-234	88	90
7	ⁱ Bu	ent-233	83	92
8	(C ₆ H ₁₁)CH ₂	ent-240	82	85
9	PhCH ₂	ent-242	39	89
10	ⁱ Pr	ent-235	59	79
11	<i>cyclo</i> -C ₃ H ₅	ent-246	61	90
12	Cy	ent-236	61	92
13	H ₂ C=CHCH ₂ CH ₂	ent-243	77	84
14	<i>cis</i> -CH ₃ CH ₂ CH=CH(CH ₂) ₂	ent-245	80	89
15	HC≡CCH ₂ CH ₂	ent-241	63	86
16	HC≡CCH ₂ CH ₂ CH ₂	278	73	91
17	CF ₃ CH ₂	ent-244	57	85
18	^p (MeO)PhCH ₂ CH ₂	279	68	90
19	EtOCH ₂ CH ₂	ent-247	68	76

^aReaction filtered through Celite after 3h to remove Cs₂CO₃ prior to the second step. The reaction time for the second step was 24h. ^bIsolated yields. ^cAdducts isolated as mixture of diastereomers (1:1), ee's reported as an average of diastereomer ee's.

Although many of the α -bromonitroalkanes are obtained in high enantiopurity, they are not of the necessary levels for peptide synthesis. Fortunately, the majority of them are crystalline solids and are able to be recrystallized to provide product in higher enantiopurity. Seven examples are shown in Figure 31.

Figure 31. Recrystallized β -amino α -bromonitroalkanes

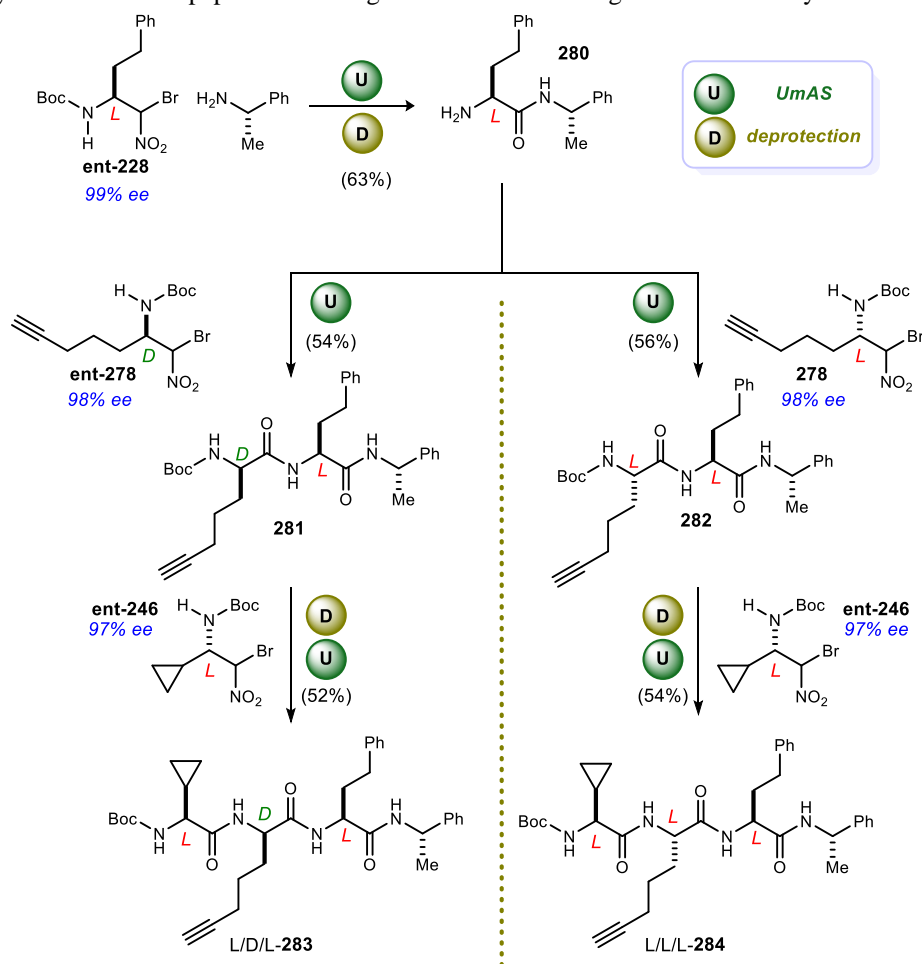
Select substrates were submitted to UmAS employing aerobic conditions substoichiometric in NIS (Table 23). The α -bromonitroalkanes were coupled to enantiopure (*S*)- α -methylbenzylamine to verify that their β -homochirality would translate to high diastereomeric ratio of the resulting *D*- α -amino amides. All substrates were obtained in moderate yield and high dr, as expected.

Table 23. UmAS of alkyl β -amino α -bromonitroalkanes

Reactions are 0.2 M in nitroalkane and employ 1.2 equiv. amine, 5 equiv. H_2O and 10 mol % NIS. All reactions were run under O_2 atmosphere. Isolated yields reported. Dr's are determined by 1H NMR

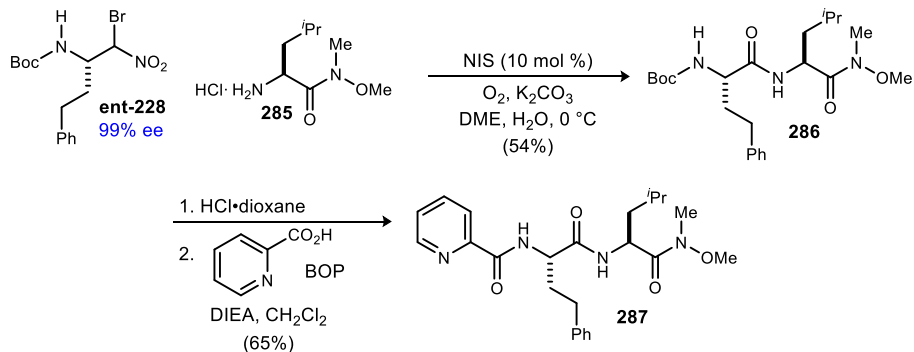
Our two reaction protocol, aza-Henry addition followed by UmAS, ideally allows for the inclusion of any amino acid side chain with either D or L configuration into a peptide. To further demonstrate the configurational and substituent diversity provided by this methodology, two tripeptides were synthesized (Scheme 68). Previously we showed the iterative synthesis of a tripeptide containing three consecutive D-amino acid residues. Following a similar approach, we synthesized a tripeptide containing only L-amino acid residues and one featuring alternating L and D-amino acid residues. The syntheses began with the coupling of L-homophenylalanine (L-Hph) donor **ent-228** with (*S*)- α -methylbenzylamine to cap the C-termini. All L peptide **284** was completed by two subsequent UmAS couplings with L-alkynyl amino acid donor **278** and L-cyclopropylglycine (L- Δ pg) donor **ent-246**. Alternating peptide **283** was completed in the same manner using D-alkynyl amino acid donor **ent-278** and L- Δ pg donor **ent-246**.

Scheme 68. Synthesis of two tripeptides featuring substituent and configurational diversity



To further support our overarching goal of providing rapid access to peptides derived from unnatural α -amino acids, the developed method was applied to the straightforward preparation of short peptide **287**, a small molecule effective in the reversal of P-glycoprotein-mediated resistance to carfilzomib (Scheme 69).⁹³ Donor **ent-228** was prepared as previously described, recrystallized (to 99% ee), and then coupled to amine **285** using UmAS in 54% isolated yield. Immediate Boc-deprotection and conventional amide synthesis from pyridyl-2-carboxylic acid delivered the product in 65% yield.

Scheme 69. Synthesis of a peptide effective in reversal of P-glycoprotein-mediated resistance to carfilzomib



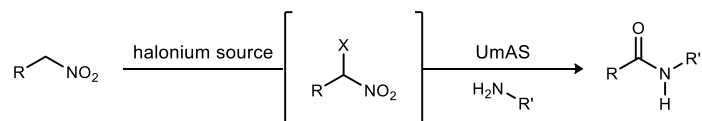
⁹³ Ao, L.; Wu, Y.; Kim, D.; Jang, E. R.; Kim, K.; Lee, D.-m.; Kim, K. B.; Lee, W. *Mol. Pharm.* **2012**, *9*, 2197-2205.

Chapter III

III. Oxidative Amidation of Primary Nitroalkanes⁹⁴

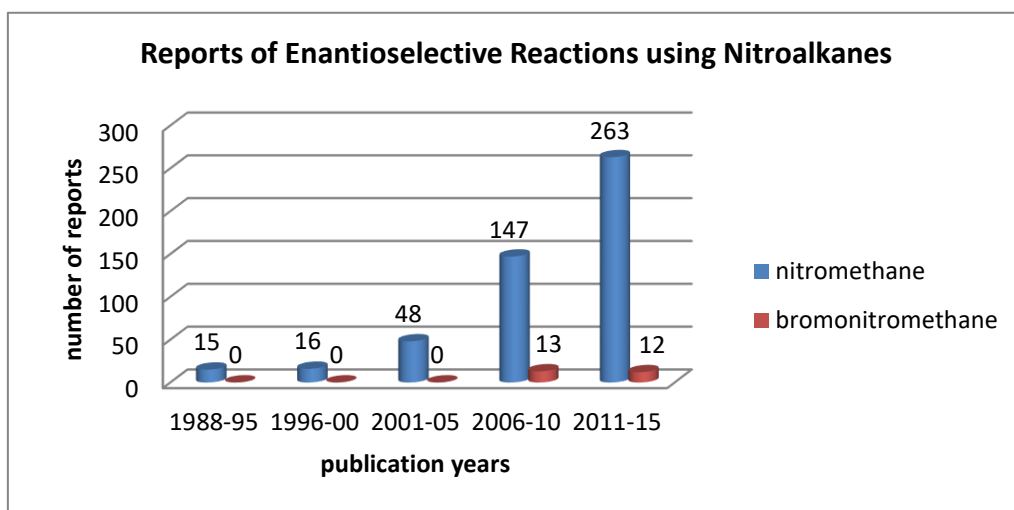
The goal of this project is to adapt the Umpolung Amide Synthesis (UmAS) protocol, which combines α -bromonitroalkanes with amines to produce amides, to be able to amidate primary nitroalkanes. We envision a one-pot sequential halogenation amide transformation sequence described in Figure 32. Key to this reaction development will be the identification of a compatible halonium source base combination capable of generating the α -halonitroalkane under UmAS conditions.

Figure 32. Strategy for oxidative amidation of primary nitroalkanes



Recently, a number of oxidative amidation methods have been developed providing alternative pathways to amides, apart from the traditional amine-carboxylic acid coupling (described in section 1.1). These methods draw from alcohols, aldehydes, and alkyl halide feedstock to access amides. However, primary (terminal) nitroalkanes have yet to be used as competent substrates in an amide bond forming reaction. In addition to adding nitroalkanes to the list of amide feedstock, the extension of UmAS to primary nitroalkanes would significantly broaden the scope of the reaction giving efficient access to a number of interesting chiral amides, due to the substantially larger number of reported enantioselective transformations utilizing nitromethane as compared to bromonitromethane (Figure 33).

Figure 33. Nitromethane vs. bromonitromethane in enantioselective transformations



3.1 Nitroalkane to Carbonyl Transformation

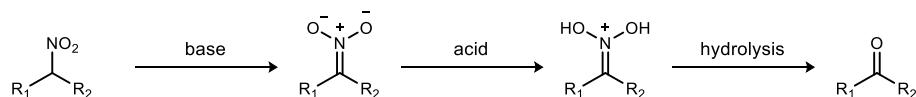
Nef Reaction

Nitroalkanes are synthetically important functional groups due to their wide range of reactivity. The electron-withdrawing character of the nitro group increases the acidity of the α -hydrogen allowing for

⁹⁴ Schwieter, K. E.; Johnston, J. N. *Chem. Commun.* **2016**, 52, 152

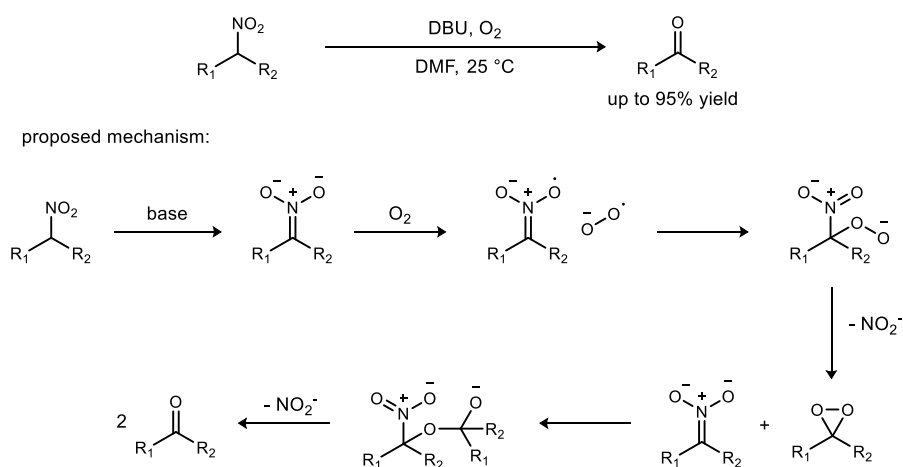
the generation of the nitronate that acts as a carbon nucleophile. Nitroalkanes also act as masked amines as a simple reduction reveals the free amine. The most exploited synthetic transformation, however, is the conversion of the nitroalkane to a carbonyl, likely due to the switch in polarity of the carbon atom from nucleophilic to electrophilic. This transformation was discovered in 1894 by Nef and was subsequently named the Nef reaction.⁹⁵ Secondary nitroalkanes are converted to ketones while primary nitroalkanes can be converted to either aldehydes or carboxylic acids. The traditional reaction as described by Nef is essentially the hydrolysis of the nitronate salt (Scheme 70). The nitroalkane is first treated with strong base to generate the nitronate salt. Subsequent treatment with strong acid generates the protonated nitronic acid, which is hydrolyzed to the carbonyl product.

Scheme 70. Mechanism of traditional Nef reaction



The harsh conditions required for this transformation have led researchers to develop alternative methods for the nitro to carbonyl conversion. The most common of these methods is the oxidative cleavage of the carbon-nitrogen double bond of the nitronate.⁹⁶ A number of reagents have demonstrated the ability to perform this transformation including potassium permanganate, hydrogen peroxide, DMDO, sodium perborate, sodium percarbonate, ozone, and molecular oxygen. All of these oxidants are capable of selectively converting a primary nitroalkane to an aldehyde without over oxidation to the carboxylic acid. In a recent example, Hayashi and coworkers reported a base promoted Nef reaction employing molecular oxygen as the oxidant in the transformation of nitroalkenes to enones and secondary nitroalkanes to ketones (Scheme 71).⁹⁷ Mechanistically, they propose the nitronate undergoes a single-electron transfer with O₂ to generate a nitroalkyl radical and a superoxide ion. The nitroalkyl radical then couples with the superoxide ion forming a peroxide intermediate, which subsequently generates a dioxirane species, releasing nitrite. Another molecule of the nitronate is oxidized by the dioxirane to afford the carbonyl product.

Scheme 71. Base promoted Nef reaction with molecular oxygen as proposed by Hayashi



⁹⁵ Nef, J. U. *Justus Liebigs Ann. Chem.* **1894**, 280, 263-291.

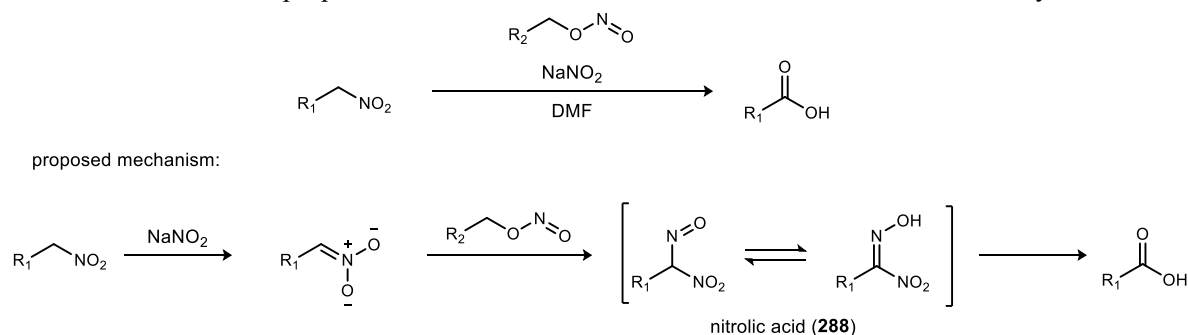
⁹⁶ For a review: Ballini, R.; Petrini, M. *Adv. Synth. Catal.* **2015**, 357, 2371-2402; Ballini, R.; Petrini, M. *Tetrahedron* **2004**, 60, 1017-1047.

⁹⁷ Umemiya, S.; Nishino, K.; Sato, I.; Hayashi, Y. *Chem. Eur. J.* **2014**, 20, 15753-15759.

Kornblum Chemistry

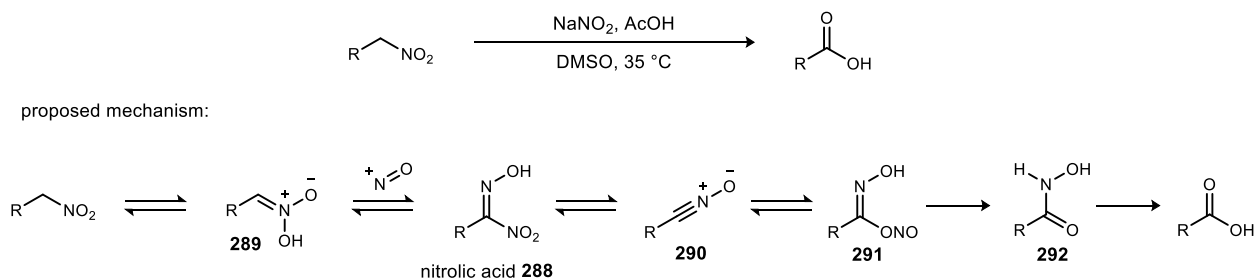
In 1956 Kornblum and coworkers reported the conversion of primary nitroalkanes to carboxylic acids under surprisingly mild conditions compared to those employed in the traditional Nef reaction.⁹⁸ It was found that the combination of sodium nitrite and a nitrite ester effected the transformation, providing the carboxylic acid in up to 52% yield. Sodium nitrite was proposed to function solely as a base while the nitrite ester was a nitrosonium source. Kornblum postulated that the reaction proceeded through a nitrolic acid intermediate (**288**) generated through nitrosation of the nitronate by the nitrite ester (Scheme 72). The ‘unstable’ nitrolic acid then readily decomposes to the carboxylic acid. Although the reaction suffered from poor yield (ranging from 9% to 52%) and long reaction times, it provided a mild alternative to the traditional Nef reaction.

Scheme 72. Kornblum’s proposed mechanism for the conversion of nitroalkanes to carboxylic acids



Mioskowski further investigated the same primary nitroalkane to carboxylic acid transformation.⁹⁹ He reported that treating the primary nitroalkane with sodium nitrite and acetic acid at 35 °C resulted in the formation of the carboxylic acid. A similar mechanism to that of Kornblum’s was proposed featuring a nitrolic acid intermediate (Scheme 73). The combination of nitrite and acetic acid generates a nitrosonium ion, which is attacked by the *aci*-nitronate (**289**) providing the nitrolic acid. The nitro group of the nitrolic acid undergoes an isomerization reaction to the nitrite through nitrile oxide intermediate (**290**) eventually providing hydroxamic acid (**292**) that readily converts to the carboxylic acid. In order to provide evidence for the proposed mechanism, they prepared and isolated the nitrolic acid intermediate. The nitrolic acid was isolated from the same reaction conditions at reduced temperature (18 °C). The stable nitrolic acid was converted to the carboxylic acid when submitted to the initial reaction conditions of sodium nitrite and acetic acid at 35 °C. Next, they demonstrated that the nitrolic acid converts to a nitrile oxide intermediate by trapping the nitrile oxide with an alkene generating an isoxazole through a dipolar cycloaddition. Control

Scheme 73. Mioskowski’s proposed mechanism for the conversion of nitroalkanes to carboxylic acids



⁹⁸ Kornblum, N.; Blackwood, R. K.; Mooberry, D. D. *J. Am. Chem. Soc.* **1956**, 78, 1501-1504.

⁹⁹ Matt, C.; Wagner, A.; Mioskowski, C. *J. Org. Chem.* **1997**, 62, 234-235; Matt, C.; Gissot, A.; Wagner, A.; Mioskowski, C. *Tetrahedron Lett.* **2000**, 41, 1191-1194.

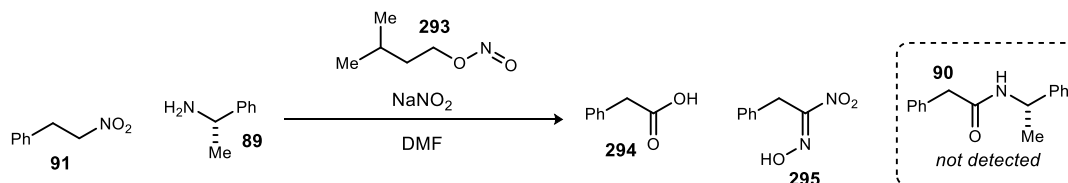
experiments showed that both acetic acid and sodium nitrite were required for carboxylic acid formation. Finally, the reaction was conducted with nitrosonium tetrafluoroborate in the absence of acetic acid demonstrating the necessity of a nitrosonium species in the mechanism.

3.2 One-pot Oxidative Amidation of Primary Nitroalkanes

Investigation of Nitrolic Acid Intermediate

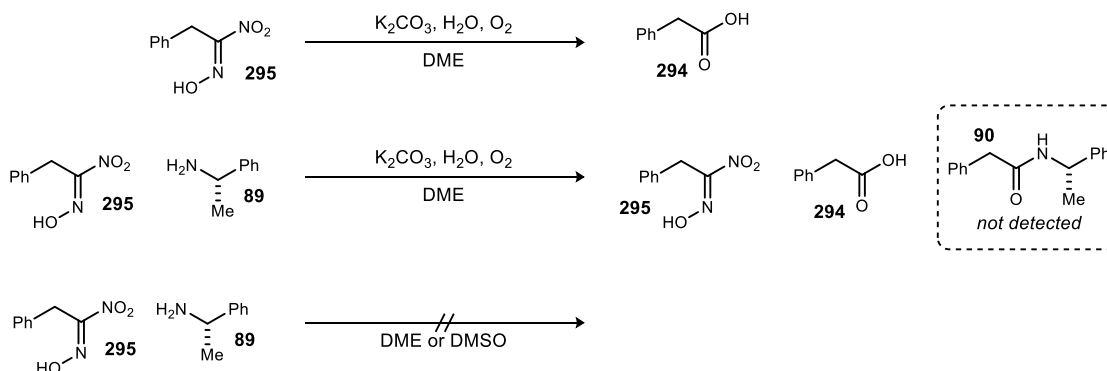
After the examination of the Kornblum and Mioskowski work, we were intrigued by the nitrolic acid intermediate and its potential as an amide precursor. Despite its active ester nature and two carbon nitrogen bonds, the nitrolic acid has only been demonstrated as a precursor to carboxylic acids and not amides. Our investigation into amide formation through a nitrolic acid intermediate began with the most straightforward embodiment in which an amine was added to Kornblum's conditions for the transformation of a nitroalkane to carboxylic acid (Scheme 74). The reaction resulted in full conversion of the nitroalkane and formation of the carboxylic acid and nitrolic acid without detection of the desired amide product.

Scheme 74. Investigation of Kornblum's conditions for amide synthesis



The next step was to prepare the nitrolic acid and assess its reactivity in a variety of conditions (Scheme 75). The nitrolic acid was prepared following Mioskowski's procedure and purified prior to its use. When treated with aqueous base in the presence of oxygen in DME, the nitrolic acid fully converted to carboxylic acid. Under the same conditions with the addition of an amine, amide product was not observed while carboxylic acid and unreacted nitrolic acid were observed. Additionally, the simple combination of the nitrolic acid and amine resulted in no reaction. Although these experiments are far from exhaustive, they demonstrate that the nitrolic acid is not a competent precursor to amide as only carboxylic acid was observed under a variety of conditions in the presence of a nucleophilic amine.

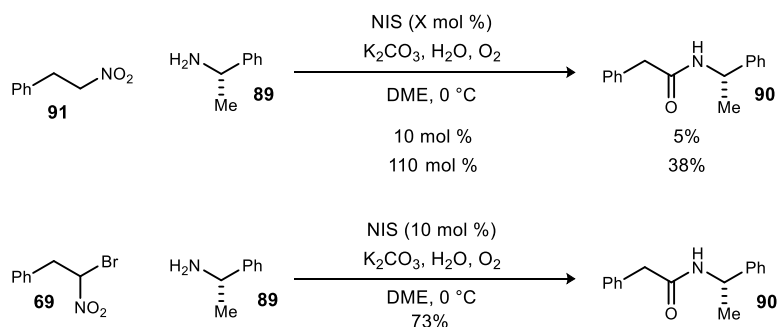
Scheme 75. Investigation of nitrolic acid as amide precursor



Discovery of a One-pot Oxidative Amidation of Primary Nitroalkanes

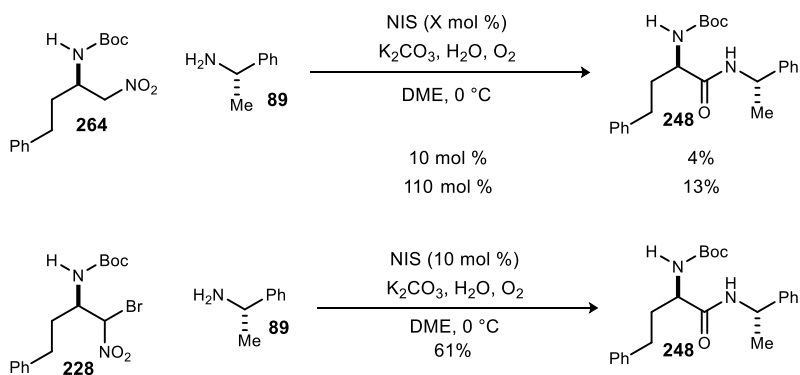
Our attempts to effect the desired amidation of primary nitroalkanes began with the most straightforward embodiment in which the traditional UmAS conditions were directly applied to nitroalkane **91**: 2 equiv. K_2CO_3 , 5 equiv. H_2O , and NIS in DME under an O_2 atmosphere at $0\text{ }^\circ\text{C}$ (Scheme 76). Although it was expected that one full equivalent of NIS would be necessary for full halogenation and as little as 5

Scheme 76. Comparison of nitroalkane and α -bromonitroalkane under standard UmAS conditions



mol % for the subsequent amide forming step, the reaction was also run with 10 mol % as well as 110 mol % NIS. For the reaction with 110 mol % NIS, the amide was obtained in 38% yield, with the yield significantly lower when only 10 mol % NIS was used. These conditions showed promise, but comparatively, the α -bromonitroalkane under the same reaction conditions provided the amide in 73% yield. The discrepancy in yield between the nitroalkane and bromonitroalkane was further amplified when the slightly more complex homophenylalanine donors (**264**, **228**) were employed as the amide was obtained in 13% and 61% yield from the nitroalkane and α -bromonitroalkane, respectively (Scheme 77). Although suboptimal, these results served as a starting point as they validated the feasibility of a one-pot amidation approach.

Scheme 77. Comparison of nitroalkane and α -bromonitroalkane under standard UmAS conditions



Based on these initial results, it was unclear whether the conditions were suboptimal for the nitronate halogenation step or for the subsequent amide bond forming step. We chose to first focus on the nitroalkane halogenation aspect of the reaction. During the initial optimization of UmAS it was found that α -bromonitroalkanes performed the best in the reaction relative to their iodo, chloro, and fluoro counterparts. For this reason, α -bromination was chosen as the focus of the study. The typical procedure for α -bromination of nitroalkanes involves complete formation of the nitronate with aqueous potassium hydroxide followed by the addition of elemental bromine in organic solvent. UmAS, however, is traditionally performed using a combination of an amine base with potassium carbonate in predominantly organic solvent. Therefore, the nitronate α -bromination was examined employing two different protocols:

aqueous base (Method A) and amine base (Method B) (Table 24). Each method was performed with five different bromonium sources. The traditional bromination procedure (Method A) provided the desired product in each case with elemental bromine and NBS being superior to the other bromonium sources (74% and 78% yield). When method B was employed, using triethyl amine as the base in DME to closely mimic standard UmAS conditions, the desired α -bromonitroalkane was only obtained in appreciable yield when dibromotetrachloroethane (DBTCE) was the bromonium source (57% yield). All other bromonium sources provided only trace product in less than 5% yield. This observed behavior may reflect both the compatibility of DBTCE with the amine base, as well as an alignment of reactivity between the nitronate and brominating agent.

Table 24. Evaluation of brominating reagents for the bromination of primary nitroalkanes

Method A

KOH, MeOH/H₂O, 25 °C
then Br⁺ source, DCM, -78 °C

c1ccc(cc1)CC[N+](=O)[O-] **91**

$\xrightarrow{\hspace{10em}}$

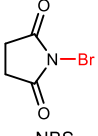
Method B

Et₃N, Br⁺ source
DME, 25 °C

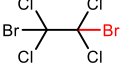
c1ccc(cc1)C(Br)C[N+](=O)[O-] **69**

entry	Br ⁺ source	Method A ^a yield ^c (%)	Method B ^b yield ^c (%)
1	NBS	78	<5
2	DBTCE	27	57
3	Br ₂	74	<5
4	DBDMH	57	<5
5	TBCO	14	<5

Br⁺ sources

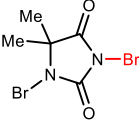


NBS

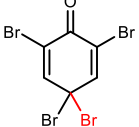


DBTCE

Br-Br



DBDMH



TBCO

^aReactions are 0.4 M (3:1 H₂O/MeOH) in nitroalkane and employ 1 equiv. of Br⁺ source. ^bReactions are 0.2 M in nitroalkane and employ 3 equiv. Et₃N and 1 equiv. Br⁺ source and were run for 24 h. ^cIsolated yield.

The development of a mix-and-stir protocol for the one-pot amidation of primary nitroalkanes was attempted next (Table 25). The nitroalkane was submitted to standard UmAS conditions with the addition of 1 equivalent of a bromonium source. The UmAS step requires an electrophilic halogen, and this protocol employs 10 mol % NIS, but we have shown that a bromonium source (including the α -bromonitroalkane itself) is sufficient to produce some amide product. In the event, significant formation of amide product was observed in each case. The superiority of DBTCE appeared to carry through in this protocol, providing the desired amide in 71% yield, while all other sources provided the amide in less than 43% yield. NIS and

Table 25. Evaluation of halogenating reagents in the one-pot oxidative amidation of nitroalkanes

c1ccc(cc1)CC[N+](=O)[O-] **91**

$\xrightarrow{\hspace{10em}}$

X⁺ source (100 mol %)
K₂CO₃, H₂O, O₂, NIS (10 mol %)
DME, 25 °C
24 h

c1ccc(cc1)C(=O)N(C)Cc2ccccc2 **90**

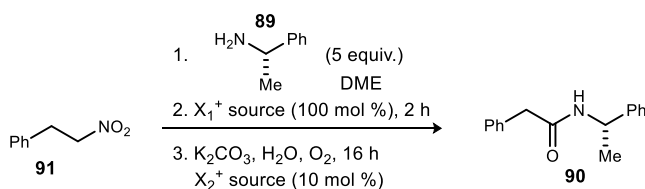
entry ^a	halonium source	yield ^b (%)
1	NBS	43
2	DBTCE	71
3	Br ₂	25
4	DBDMH	26
5	TBCO	29
6	NCS	33
7	NIS	38

^aReactions are 0.2 M in nitroalkane and employ 2 equiv. amine, 2 equiv. K₂CO₃, 10 mol % NIS, and 5 equiv. H₂O. ^bIsolated yield.

NCS were also screened under the reaction conditions to further verify that bromonium is the optimal halonium. An important aspect of these results is the dual role that halogens play, and it is the parallel optimization of these roles that leads to the highest yield of amide.

Whether the amide is produced through an iodonium-only, bromonium-only or mixed-halonium pathway is less important, and ultimately determined by equilibria at play under specific conditions. It is of interest, however, to know the extent to which a specific halonium combination and order might affect the yield of amide. The results described in Table 24 highlighted the need to avoid ineffective combinations of base and halonium source. This was probed further using the step-wise sequence outlined in Table 26. This protocol employed the amine to be used in the subsequent amide synthesis step as a base for the first step, as a variation on Method B from the nitroalkane bromination. The nitroalkane and amine were stirred for 5 hours, and then treated with a stoichiometric amount of halogenating agent and allowed to stir for 2 hours. At this point, potassium carbonate, water, and 10 mol % of a second halonium source were added to the mixture, which was placed under an oxygen atmosphere. Use of NIS for each step resulted in a 29% yield of amide, in close parallel to the analogous, non-stepwise addition protocol utilized earlier (Table 25, 38% yield). With this protocol, NBS was similarly ineffective when used for both steps as the amide was obtained in 27% yield. When an NBS/NIS sequence was employed, a significant, but still low yield of the amide was produced (33% yield). Collectively, results to this point seemed to emphasize two features: (1) the yield of amide is directly related to the efficiency of nitronate bromination, and the specific combination of α -halo nitroalkane and halamine created for amidation, and (2) the various halogenated species may be in equilibrium despite the physical sequencing characteristic of the protocol. This reasoning led to further examination of DBTCE, since it proved more effective in the nitronate bromination using an amine base (Method B), and was somewhat tolerant of aqueous base (Method A) (Table 24). In the event, the yield of amide increased dramatically (70%) when employed with NIS as the second halonium source, in line with the yield of amide when beginning from α -bromonitroalkane **69**. When the roles of NIS and DBTCE were reversed, the yield suffered and returned to 29% as seen when the NIS/NBS combinations were used. The benefit of iodonium in the UmAS step was reaffirmed when it was not added and the amide was provided in 37% yield. This set of experiments suggests that a dual halonium combination is necessary to provide high yield of amide with bromonium being optimal for the halogenation step and iodonium being optimal for the subsequent UmAS step.

Table 26. Evaluation of a step-wise protocol for oxidative amidation of nitroalkanes

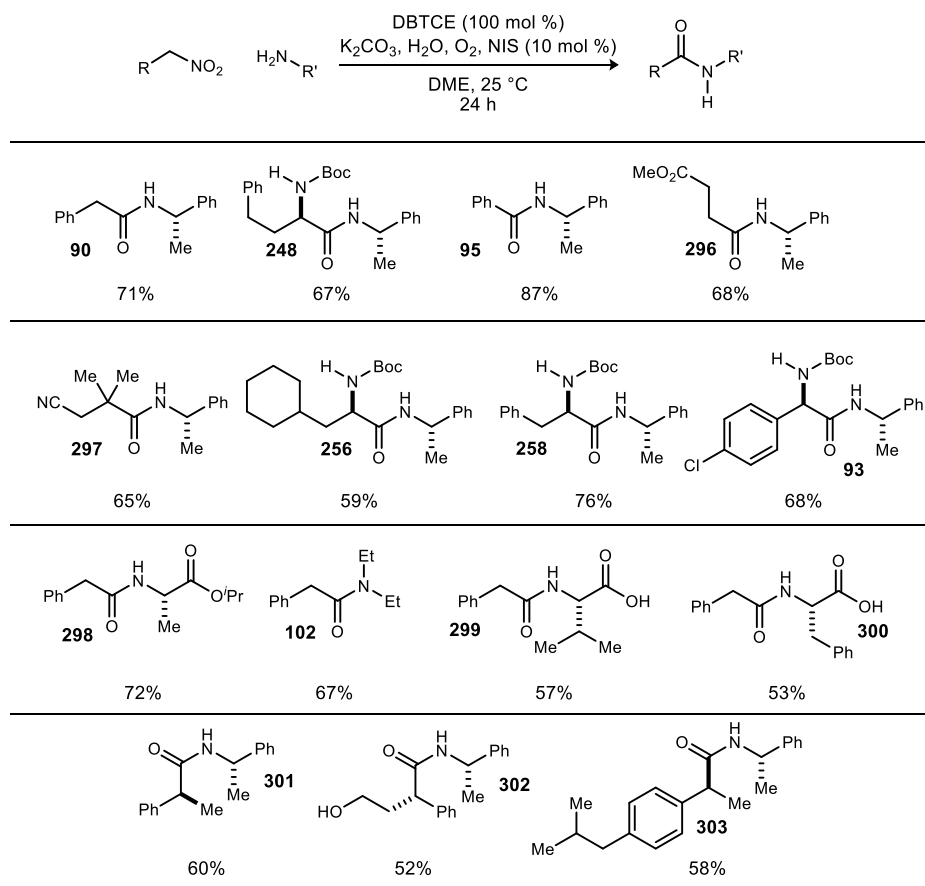


entry ^a	X ₁ ⁺ source	X ₂ ⁺ source	yield ^b (%)
1	NIS	NIS	29
2	NBS	NBS	27
3	NBS	NIS	33
4	DBTCE	NIS	70
5	NIS	DBTCE	29
6	DBTCE	none	37

^aReactions are 0.2 M in nitroalkane and employ 5 equiv. of amine, 2 equiv. K₂CO₃, and 5 equiv. H₂O at 25 °C. ^bIsolated yield.

Based on these studies, a one-pot mix-and-stir protocol was developed for the amidation of primary nitroalkanes. An aqueous DME solution of nitroalkane and amine is treated with potassium carbonate, DBTCE (100 mol %) and NIS (10 mol %) under an oxygen atmosphere (balloon). This procedure resulted in significant improvement in yield for amides **90** and **248** as compared to the initial conditions employed (Scheme 76, Scheme 77, vs Table 27) and was applied to a range of primary nitroalkanes resulting in moderate to good yields of the derived amides (Table 27). Notable examples include the use of a γ -nitro ester to prepare succinate **296** and amidation of a hindered nitroalkane to give β -cyano amide **297**. To illustrate the value and complementarity of the approach, several terminal nitroalkanes were prepared using enantioselective catalysis, thereby providing a more direct entry to enantioenriched amides. α -Amino amides **93**, **248**, **256**, and **258** were derived from the respective nitromethane aza-Henry adducts. The use of an enantioselective conjugate reduction provided the nitroalkane precursor to **301**. Furthermore, γ -hydroxy amide **52** was prepared without lactone formation that would otherwise compete with active ester-based amide synthesis. Unprotected valine (**299**) and phenylalanine (**300**) were successfully coupled demonstrating the orthogonality of the current method with condensative peptide couplings. The method was also leveraged to prepare an ibuprofen amide derivative, **303**, through an enantioselective conjugate reduction followed by oxidative amidation.

Table 27. Substrate scope for oxidative amidation of primary nitroalkanes



Reactions are 0.2 M in nitroalkane and employ 2 equiv. amine, 2 equiv. K_2CO_3 , and 5 equiv. H_2O . Isolated yields reported.

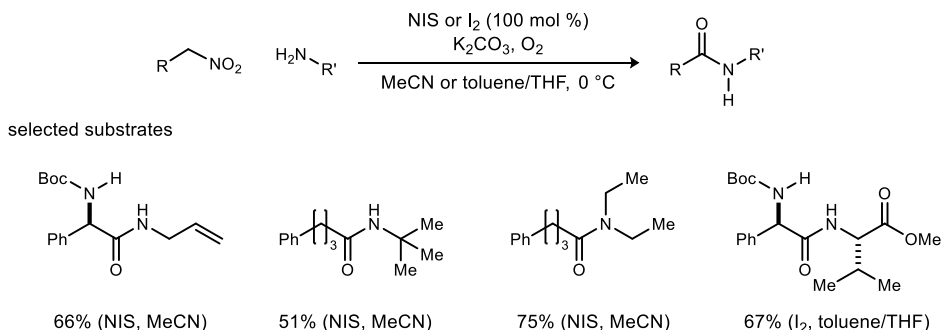
In summary, a detailed evaluation of nitronate bromination and the subsequent UmAS step leading to amide, has resulted in a convenient one-pot, mix-and-stir protocol to convert primary nitroalkanes to amides. Select examples of enantioenriched nitroalkanes were converted to their amide products in

moderate to good yield. In principle, the advances in nitromethane-based enantioselective synthesis can now be generally leveraged to prepare a broad selection of amides, for which nitroalkanes serve as an alternative to carboxylic acids and their precursors, particularly terminal alcohols.

Comparison with Hayashi Protocol

While we were in the final stages of completing this investigation, Hayashi and Lear reported an ostensibly similar method for the amidation of primary nitroalkanes.¹⁰⁰ Hayashi and Lear demonstrated that the desired amidation could be effected with 1 equivalent NIS or I₂ as halonium source in the presence of potassium carbonate and oxygen in either acetonitrile or toluene/THF as the solvent (Scheme 78). The protocol was leveraged to access a variety of amides including dipeptides from aza-Henry adducts. They also discuss the possibility of different mechanism for UmAS, one that contradicts the proposal discussed in Chapter 1 of this document, which will be addressed in Chapter 5 of this document.

Scheme 78. Hayashi-Lear oxidative amidation of nitroalkanes



There are two practical differences between our amidation protocol and that reported by Hayashi-Lear: halonium source and solvent. DBTCE/NIS and DME were employed in our protocol while Hayashi-Lear utilized NIS and MeCN in their protocol. We chose to do a direct comparison of the two methods as well as solvent ‘crossover’ experiments (Figure 34 and Figure 36). Two representative nitroalkanes (**91** and **304**) were chosen to perform the experiments. When performing the amidation of nitroalkane **91** under our conditions, the amide was isolated in 70% yield compared to 59% yield when employing the Hayashi-Lear conditions. In order to probe the effect of solvent on the reaction, two ‘crossover’ experiments were conducted in which our conditions were run in MeCN and the Hayashi-Lear protocol was run in DME. Interestingly, our protocol was tolerant of MeCN as the amide was obtained in 67% yield while Hayashi-Lear’s conditions in DME provided the amide in diminished yield at 38%. The crude ¹H NMR spectra are provided to analyze the formation of by-products as well as the general ‘cleanliness’ of each reaction. The same set of experiments run with nitroalkane **304** gave similar results. The comparisons provided suggest that the solvent change makes little difference as our method works equally well in acetonitrile. Preliminarily, our protocol appears to provide the amide products in slightly higher isolated yields with a ‘cleaner’ crude reaction mixture as analyzed by ¹H NMR. However, a more careful comparison is needed to validate these conclusions.

¹⁰⁰ Li, J.; Lear, M. J.; Kawamoto, Y.; Umemiya, S.; Wong, A. R.; Kwon, E.; Sato, I.; Hayashi, Y. *Angew. Chem. Int. Ed.* **2015**, *54*, 12986-12990.

Figure 34. Comparison of Hayashi-Lear and Schwieter-Johnston Protocols Across Platforms (NIS/acetonitrile vs. DBTCE/NIS/dimethoxyethane) using Nitroalkane **91**.

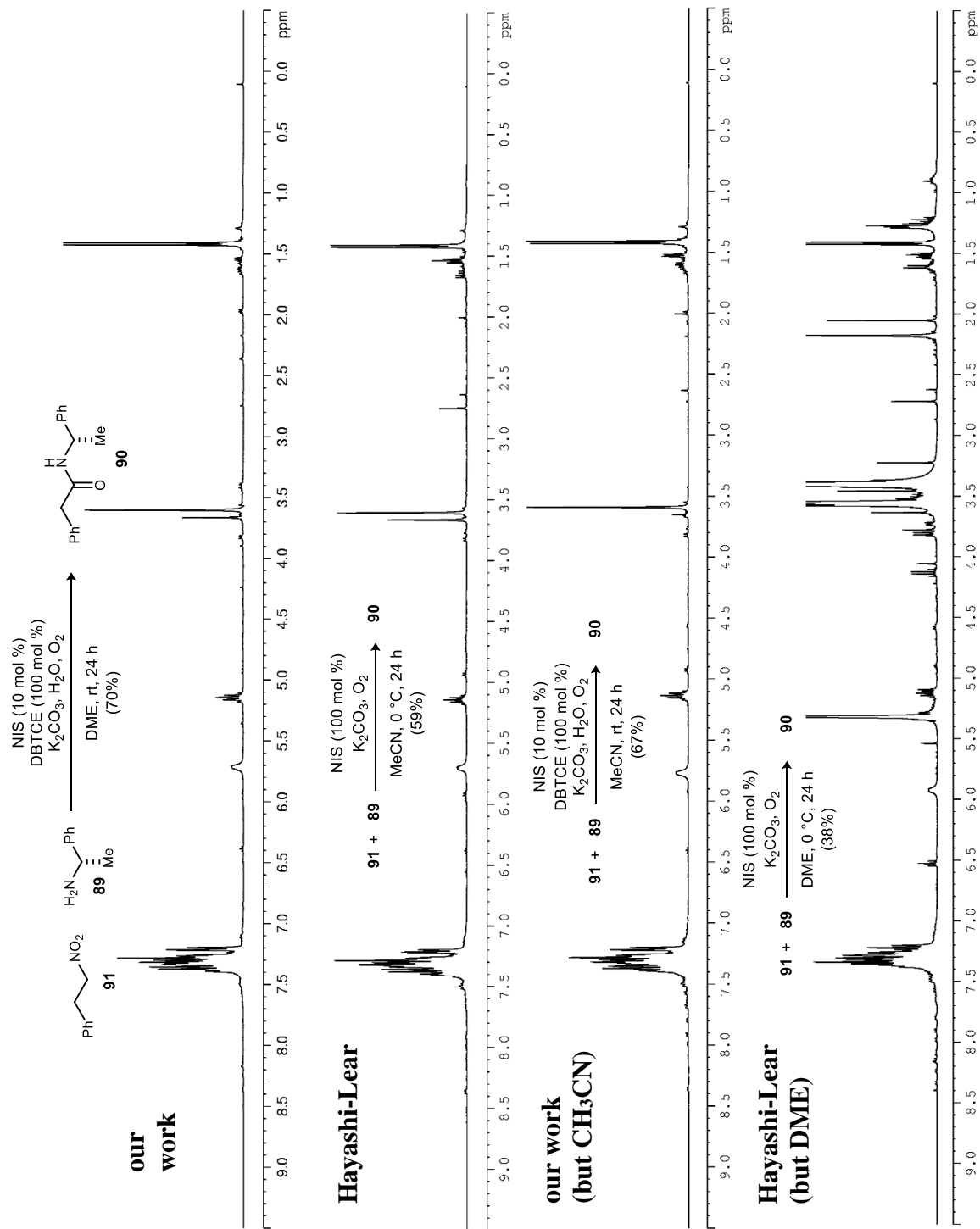


Figure 35. ^1H NMR (CDCl_3) of **90**.

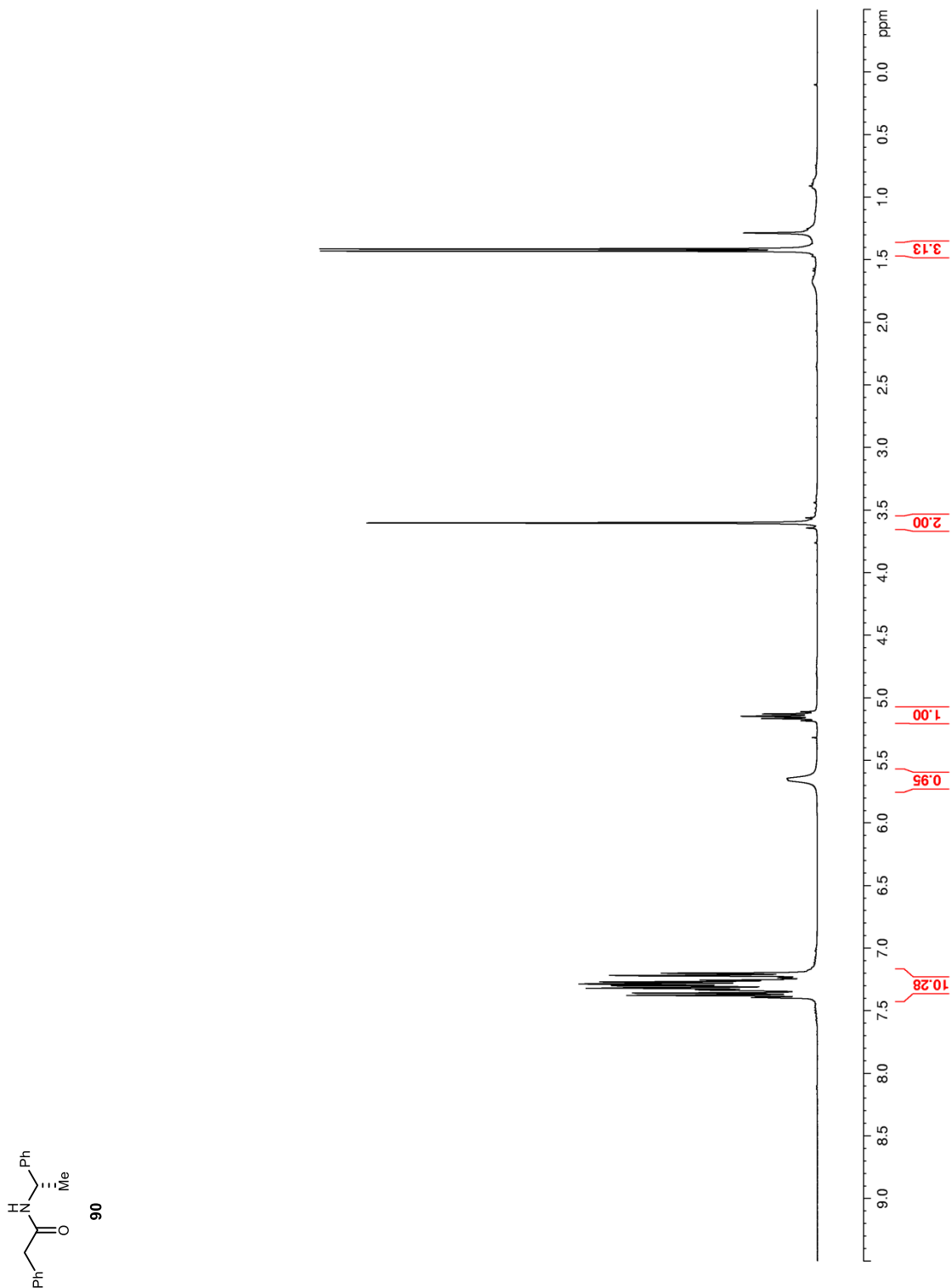


Figure 36. Comparison of Hayashi-Lear and Schwieter-Johnston Protocols Across Platforms (NIS/acetonitrile vs. DBTCE/NIS/dimethoxy ethane) using Nitroalkane **304**.

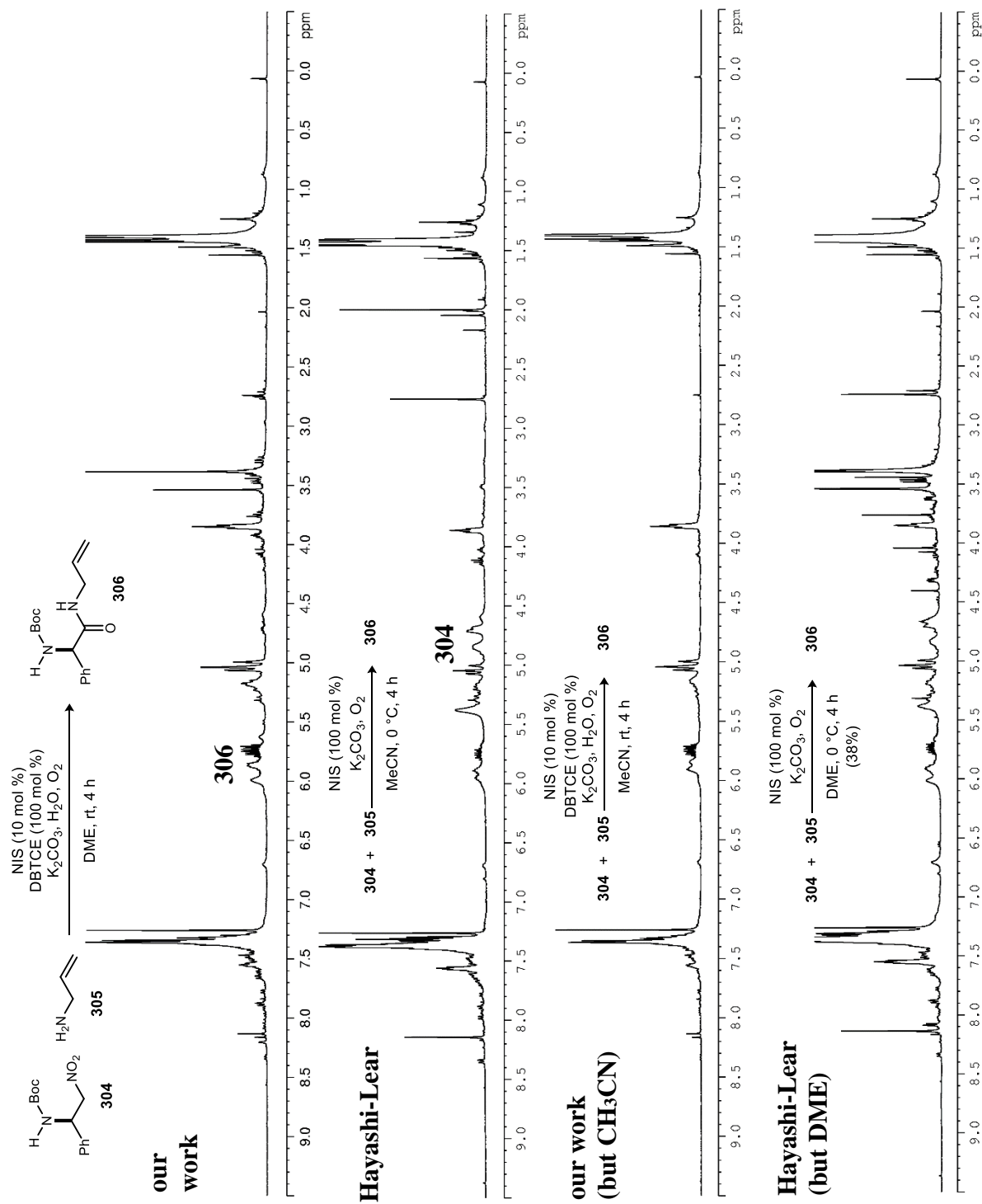
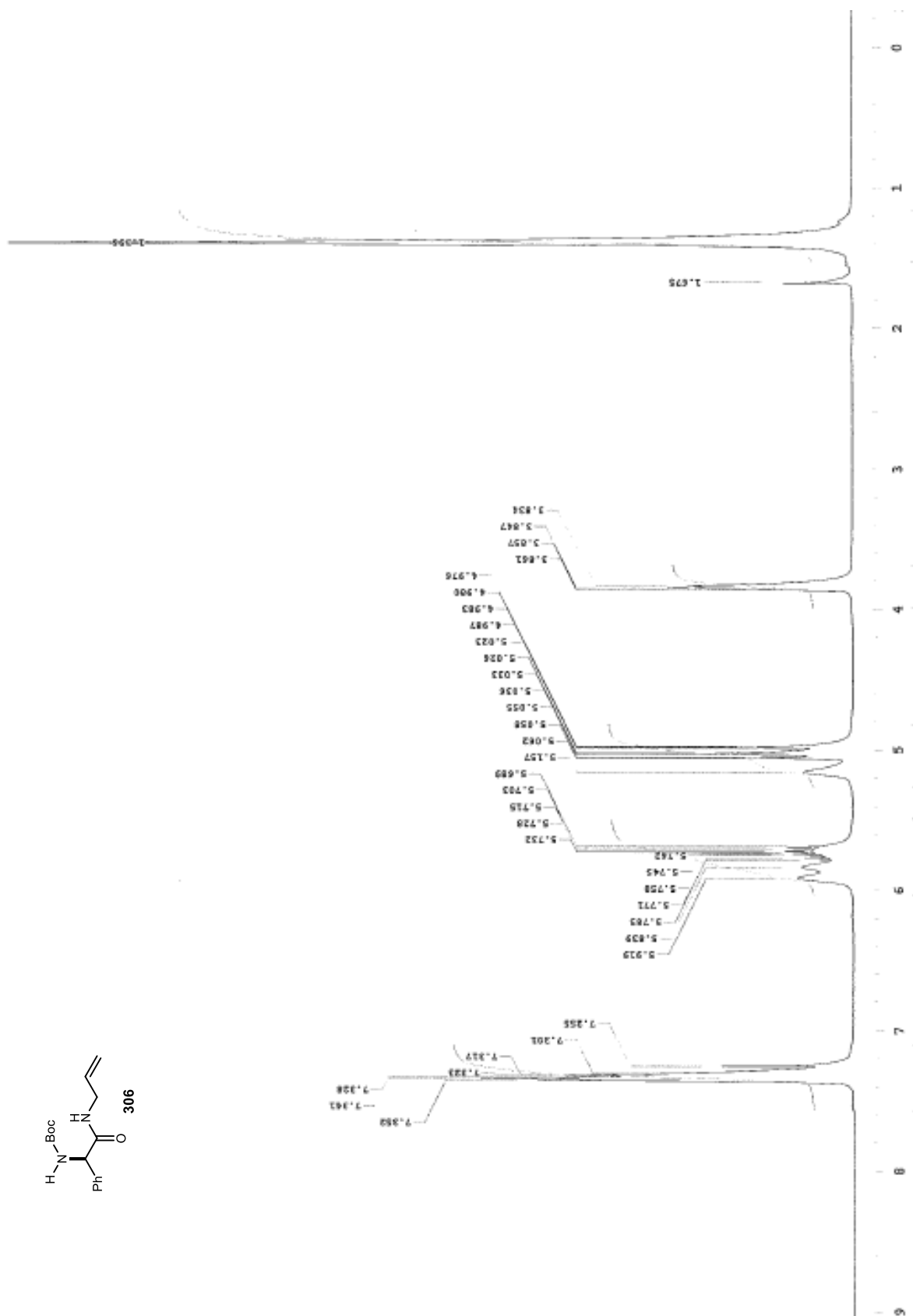


Figure 37. ^1H NMR (CDCl_3) of **306** (from Hayashi-Lear work).¹⁰⁰



Chapter IV

IV. Synthesis of a Fluorinated Feglymycin Derivative, Ffeglymycin

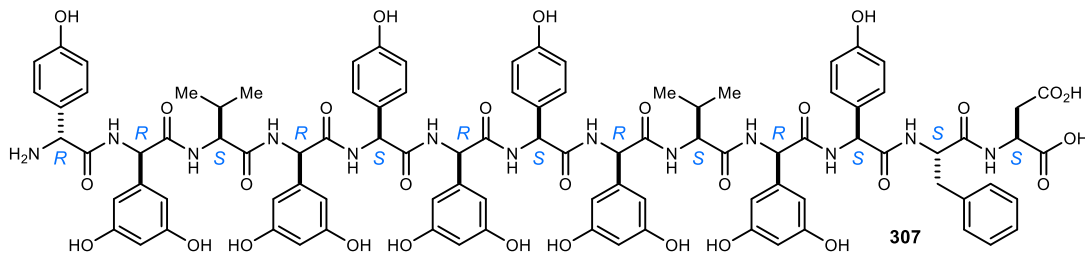
The combination of the enantioselective aza-Henry reaction and UmAS provide a powerful new method for the synthesis of unnatural amino acid containing peptides. In only three or four steps from the requisite aldehyde, unnatural amino acid residues can be synthesized and incorporated into peptides with a high degree of stereocontrol. In order to demonstrate the utility of this methodology, we sought to apply it to the synthesis of an unnatural amino acid-rich peptide. Feglymycin (**307**) was chosen due to its large number of unnatural amino acid residues as well as interesting biological activity.

4.1 Feglymycin: Isolation and Background

Isolation and Structure Determination

Feglymycin (**307**) was isolated in 1999 from a fermentation culture of *Streptomyces* sp. DSM 11171 using solid phase extraction, size exclusion chromatography and reverse-phase chromatography.¹⁰¹ Mass spectrometry provided an *m/z* of 1900.60 corresponding to the molecular formula C₉₅H₉₇N₁₃O₃₀. ¹H and ¹³C NMR analysis revealed that feglymycin contained 13 amino acid residues. Of the 13 residues, four of them are 4-hydroxyphenylglycine (Hpg) residues and five are 3,5-dihydroxyphenylglycine (Dpg) residues. The remaining four amino acid residues were determined to be two L-valine residues and one each of L-phenylalanine and L-aspartic acid through analysis after hydrolysis in boiling HCl. The linear structure of

Figure 38. Structure of feglymycin



feglymycin was determined by 2D NMR analysis (HSQC, HMBC, COSY, TOCSY and NOESY) and confirmed by MS-MS analysis. The relative and absolute stereochemistry of each amino acid residue was not assigned until 2005, when a crystal structure of feglymycin was obtained.¹⁰² The crystal structure directly provided the relative stereochemistry of each residue in the feglymycin structure, and since the stereochemistry of the natural amino acids had previously been determined, the absolute stereochemistry was also assigned.

Structurally, there are several interesting aspects to feglymycin apart from the large percentage of unnatural amino acids. First, the absolute stereochemistry of the phenylglycine residues is not conserved throughout the molecule. There are three L-Hpg residues, while the *N*-terminal residue has the opposite configuration, D-Hpg. All five of the Dpg residues were determined to be D-Dpg. Another interesting structural aspect is the stereochemical arrangement of the amino acid residues. With the exception of two terminal residues (*C*-terminal L-Asp and *N*-terminal D-Hpg), all other residues alternate between L and D.

¹⁰¹ Vertesy L.; Aretz, W.; Knauf, M.; Markus, A; Vogel, M.; Wink, J. J. *Antibiot.* **1999**, *52*, 374 – 382

¹⁰² Bunkoczi, G.; Vertesy, L.; Sheldrick, G. M. *Angew. Chem. Int. Ed.* **2005**, *44*, 1340.

As observed with other alternating D,L-peptides,¹⁰³ the crystal structure of feglymycin features a double-helical dimer. When lined up end to end, the feglymycin dimers form an infinite helical structure which can be described as a right-handed, wide, antiparallel, double-stranded β -helix.¹⁰²

Biological Activity

Feglymycin (**307**) was initially reported to have weak antibacterial activity against Gram positive bacteria (IC₅₀ = 32-64 μ g/mL against several strains of *Staphylococcus aureus*) as well as the ability to inhibit the formation of HIV syncytia in vitro (IC₅₀ = ~5 μ M).¹⁰¹ Later biological studies performed by Süssmuth revealed that feglymycin was active against methicillin-resistant *Staphylococcus aureus* (MRSA) with an IC₈₀ value of 2 μ g/mL.¹⁰⁴ This stronger antibacterial activity prompted further studies into the mechanism of action of feglymycin. Other arylglycine containing antibacterial peptides, such as vancomycin and ramoplanin, are known to interfere in cell wall biosynthesis by inhibiting the last two stages of peptidoglycan production.¹⁰⁵ Initial studies by Süssmuth and coworkers indicated that feglymycin had no effect on the last two stages of peptidoglycan biosynthesis, but instead was inhibiting earlier biosynthetic steps. Based on this observation, feglymycin's effect on enzymes MurA-F, which are involved in the early stages of peptidoglycan synthesis, was examined. It was found that feglymycin noncompetitively inhibited the enzymes Mur A (IC₅₀ = 3 μ M) and Mur C (IC₅₀ = 1 μ M) while showing no effect on the other enzymes, making it the first known natural inhibitor of these enzymes. This unique mechanism of action gives feglymycin the potential to be a useful antibiotic against resistant bacterial strains.

As previously mentioned, feglymycin was also reported to strongly inhibit the formation of HIV syncytia. Syncytia are multinucleate cells which are formed by the joining of two or more single nucleate cells.¹⁰⁶ A trademark of HIV infection, syncytia are formed through the joining of multiple CD⁴⁺ T-cells and can often be seen in the infected patient's blood stream. The mechanism of syncytia formation in HIV infected cells involves the viral membrane fusion glycoprotein gp41. This membrane fusion glycoprotein, a subunit of the envelope protein complex of the HIV retrovirus, is responsible for the second step of white blood cell HIV infection. After the virus is bound by the CD⁴⁺ T-cell, gp41 acts to fuse the HIV to the cell membrane of the T-cell, allowing it to enter into the cell.¹⁰⁷

Once HIV infects a healthy CD⁴⁺ T-cell, it induces production of viral proteins, including gp41, which are then displayed on the cell membrane. These membrane proteins then allow the infected cell to fuse to other nearby CD⁴⁺ helper T-cells using the same mechanism with which HIV used to enter a cell. Once the cells are fused, the cell membrane of these cells join together, forming a large, non-functional syncytium.¹⁰⁸ By this process, a single HIV virion is able to infect and kill many CD⁴⁺ T-cells. Monitoring syncytia formation is a common way to assay a compound's efficacy at inhibiting the binding of the viral membrane fusion protein gp41 to a cell membrane. Due to the vital role in which gp41 plays in both HIV infection and syncytia formation, a compound that successfully inhibits syncytia formation will likely also inhibit HIV infection.

¹⁰³ Langs, D. A. *Science* **1988**, *241*, 188.

¹⁰⁴ Rausch, S.; Hanchen, A.; Denisiuk, A.; Lohken, M.; Schneider, T.; Süssmuth, R. D. *Chem. Bio. Chem.* **2011**, *12*, 1171.

¹⁰⁵ Nieto, M.; Perkins, H. R. *Biochem. J.* **1971**, *123*, 789.; Farver D. K.; Hedge D. D.; Lee S. C. *Ann. Pharmacother.* **2005**, *39*, 863

¹⁰⁶ Daubenmire, R. F. *Science* **1936**, *84*, 533.

¹⁰⁷ Kim P. S.; Malashkevich V. N.; Chan D. C.; Chutkowski C. T. *Proc. Natl. Acad. Sci. U.S.A.* **1998**, *95*, 9134.

¹⁰⁸ Huerta, L.; López-Balderas, N.; Rivera-Toledo, E.; Sandoval, G.; Grómez-Icazbalceta, G.; Villarreal, C.; Lamoyi, E.; Larralde, C. *The Scientific World Journal* **2009**, *9*, 746.

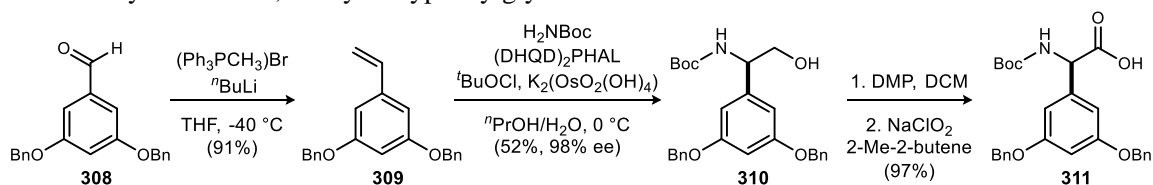
In 2012, Schols and coworkers reported a comprehensive study of feglymycin's antiretroviral properties.¹⁰⁹ When tested against various HIV-1 clinical isolates, feglymycin showed a consistent and potent broad-spectrum antiretroviral activity profile. It was also determined that feglymycin acts as an early viral/binding adsorption inhibitor, meaning it inhibits viral entry into the cell. Confirming the initial reports, feglymycin was also found to inhibit syncytia formation, preventing infected cell to healthy cell HIV transmission. Feglymycin was found to have a unique mechanism of action in that it inhibits the gp120/CD4 interaction (part of the viral entry process), unlike any other peptide inhibitors. The unique mechanism of action makes feglymycin an interesting lead structure for further drug development.

4.2 Süßmuth's Synthesis of Feglymycin

In 2009 Süßmuth and coworkers reported the first and, to date, only total synthesis of the peptide natural product feglymycin.¹¹⁰ They employed a convergent fragment condensation approach as opposed to an iterative amino acid coupling strategy to avoid activating the acid of the epimerization-prone 3,5-Dpg residues. Retrosynthetically, feglymycin was broken in half to provide heptapeptide **312** and hexapeptide **313** (Scheme 80). These peptide fragments would be prepared from tripeptide **314** and dipeptides **315-318** with careful consideration to only activate Val, Phe, and Hpg residues during fragment couplings to minimize the risk of epimerization. Further breakdown of the peptide fragments gives five commercially available amino acids (L-Val, L-Phe, L-Asp, L-Hpg, and D-Hpg) and D-Dpg, which would be synthesized by Sharpless aminohydroxylation of the requisite styrene.

The synthesis began with the preparation of D-Dpg (**311**) in four steps from aldehyde **308** (Scheme 79). Aldehyde **308** was subjected to a Wittig olefination to provide styrene **309** in 91% yield. Sharpless aminohydroxylation conditions were employed to obtain Boc-protected α -amino alcohol **310** in 52% yield and 98% ee. Oxidation of alcohol **310** to the aldehyde with Dess-Martin periodinane followed by a Pinnick oxidation provided Boc-D-Dpg (**311**) in 97% yield over two steps.

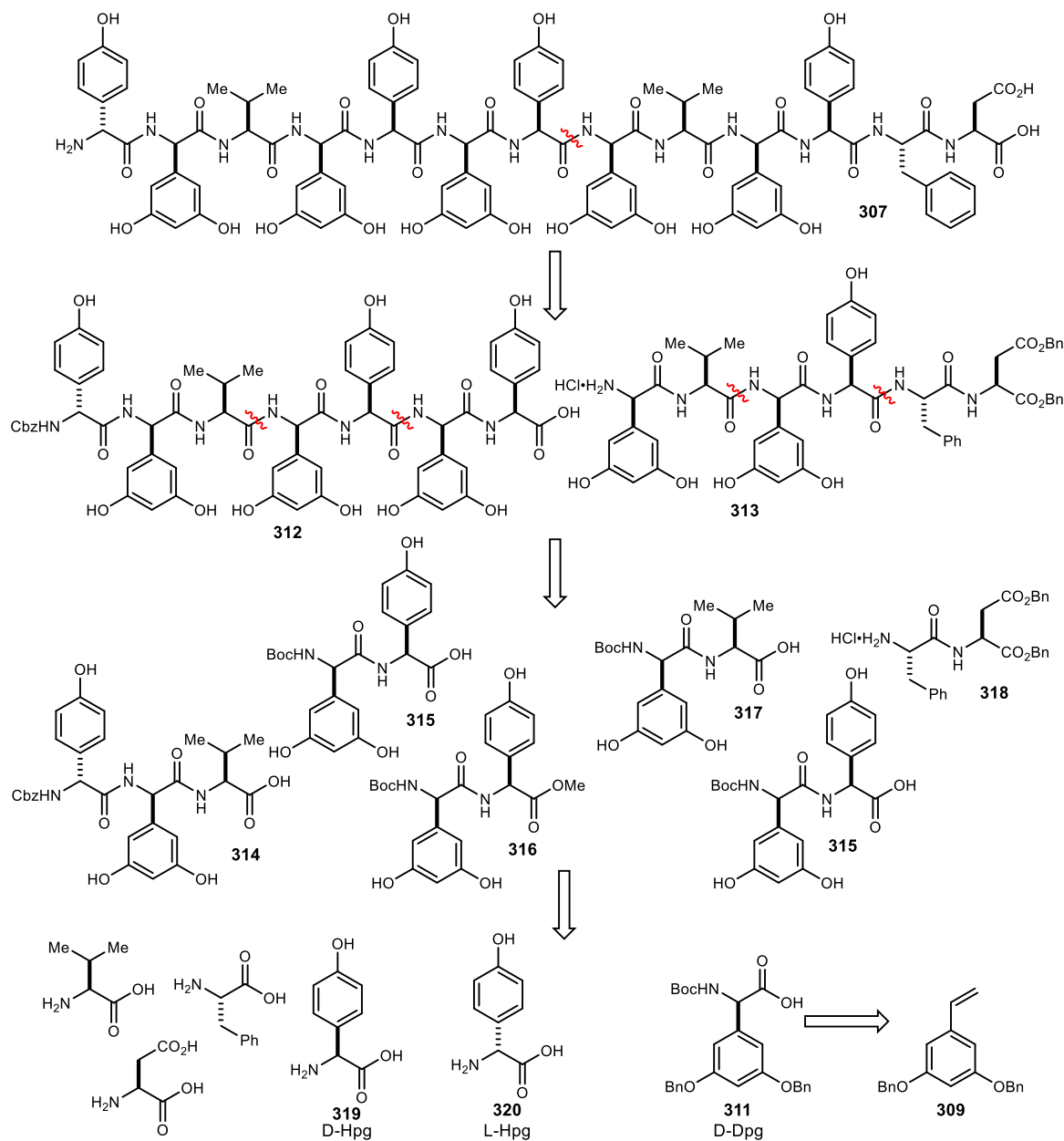
Scheme 79. Synthesis of 3,5-dihydroxyphenylglycine



¹⁰⁹ Férir, G.; Hänchen, A.; François, K. O.; Hoorelbeke, B.; Huskens, D.; Dettner, F.; Süßmuth, R. D.; Schols, D. *Virology* **2012**, *433*, 308-319.

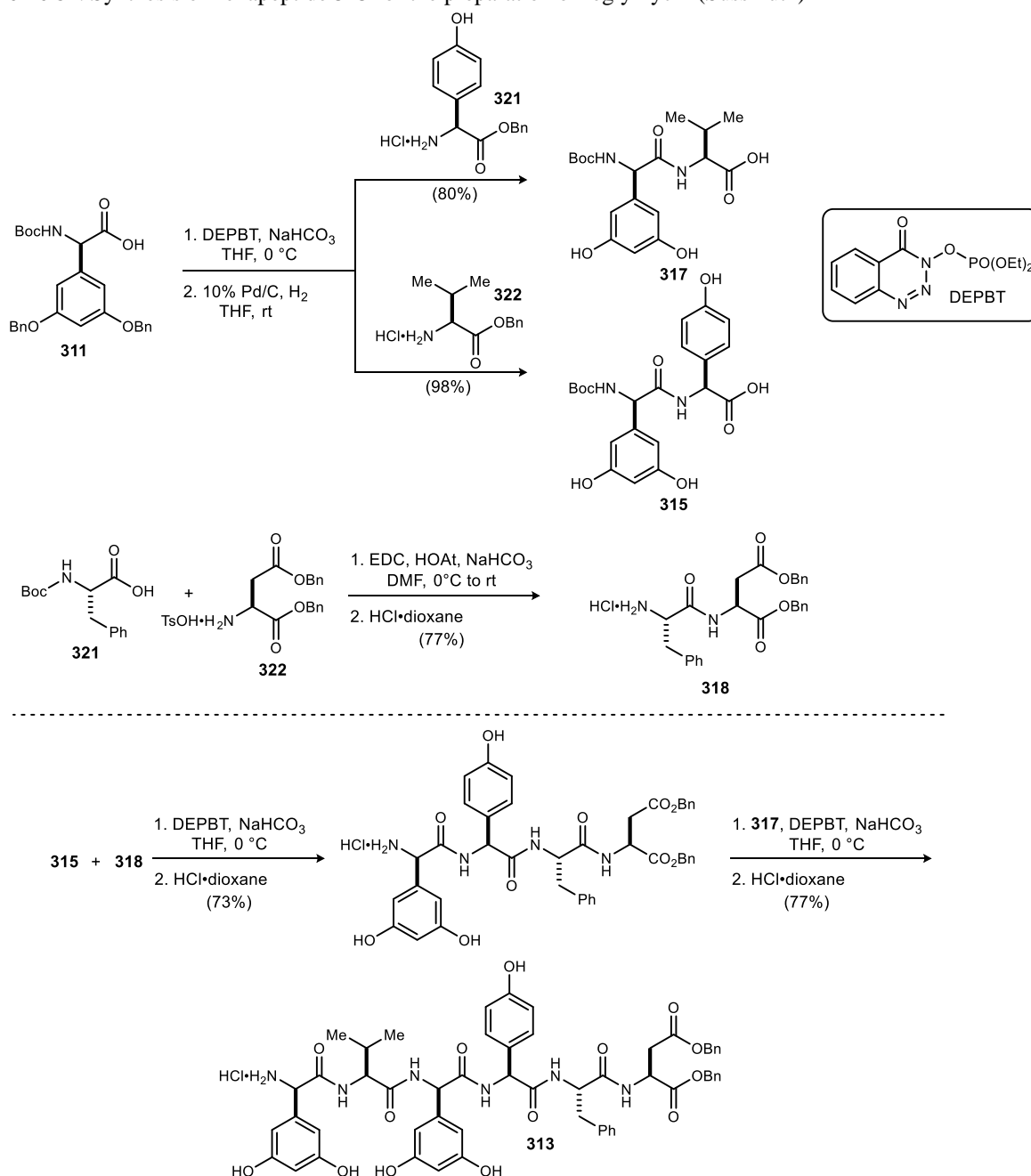
¹¹⁰ Dettner, F.; Hänchen, A.; Schols, D.; Toti, L.; Nußer, A.; Süßmuth, R. D. *Angew. Chem. Int. Ed.* **2009**, *48*, 1856-1861.

Scheme 80. Süßmuth's retrosynthetic analysis of feglymycin



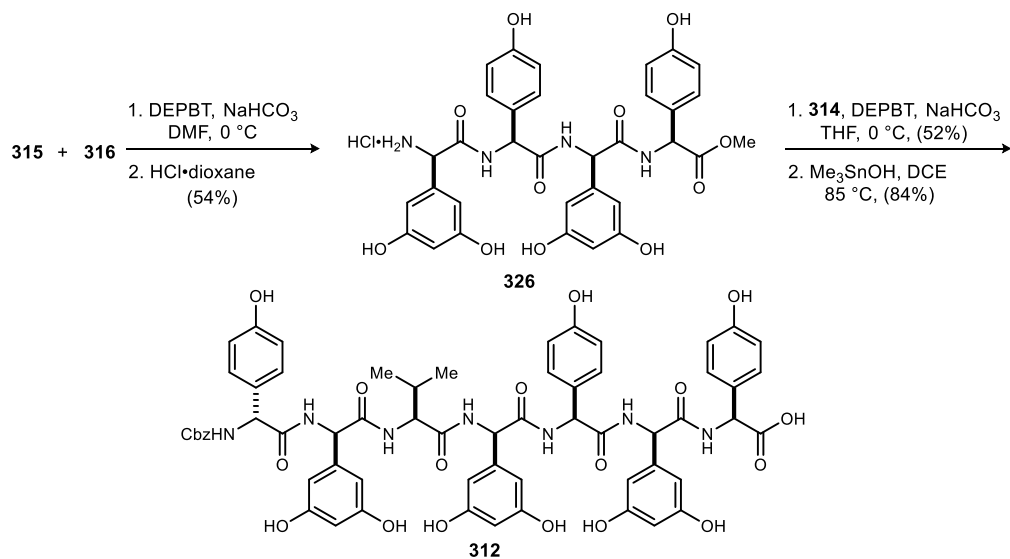
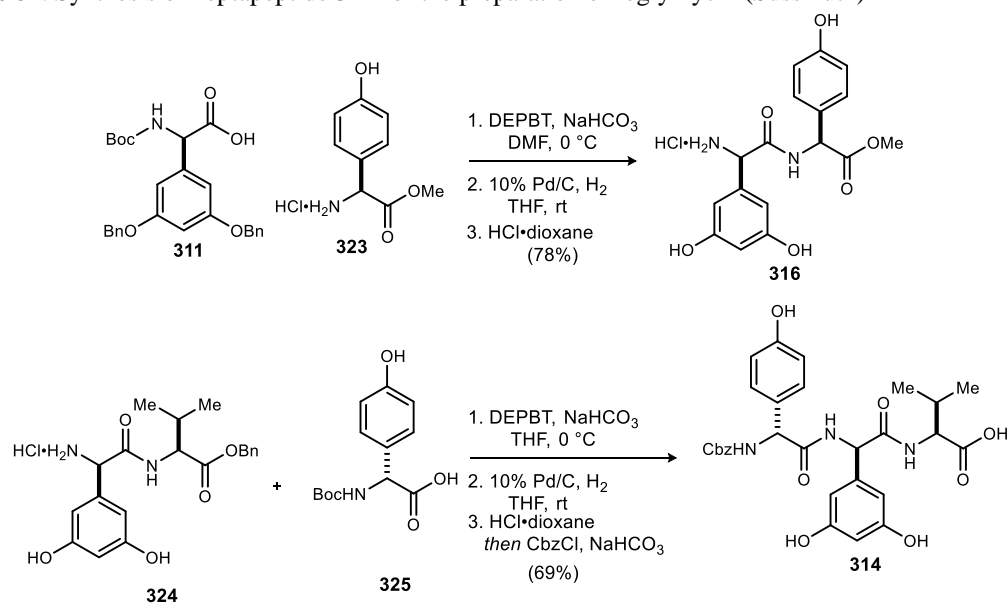
The synthesis of the necessary fragments began with the preparation of hexapeptide **313** (Scheme 81). All peptide couplings with the arylglycines (Hpg and Dpg) employed 3-(diethoxyphosphoryloxy)-1,2,3-benzotriazin-4(3*H*)-one (DEPBT) and NaHCO₃ as these conditions were found to significantly minimize epimerization compared to other coupling reagents. Dipeptide **317** was therefore obtained from the DEPBT coupling of Dpg acid and Hpg amine **321** in 80% yield followed by quantitative benzyl removal with H₂ and Pd/C. Dipeptide **315** was synthesized in a similar manner coupling Dpg acid and valine amine **322** followed by benzyl deprotection. The final dipeptide (**318**) needed for the synthesis of hexapeptide **313** was prepared from the EDC/HOAt promoted coupling of Phe-OH and TsOH•H₂N-Asp (77% yield) followed by Boc-deprotection with HCl in dioxane. The tetrapeptide was obtained from the DEPBT promoted fragment coupling of dipeptides **315** and **318**. Subsequent Boc-deprotection with HCl in dioxane and DEPBT coupling with dipeptide **317** followed by Boc deprotection provided hexapeptide **313** in 77% yield.

Scheme 81. Synthesis of hexapeptide **313** for the preparation of feglymycin (Süssmuth)



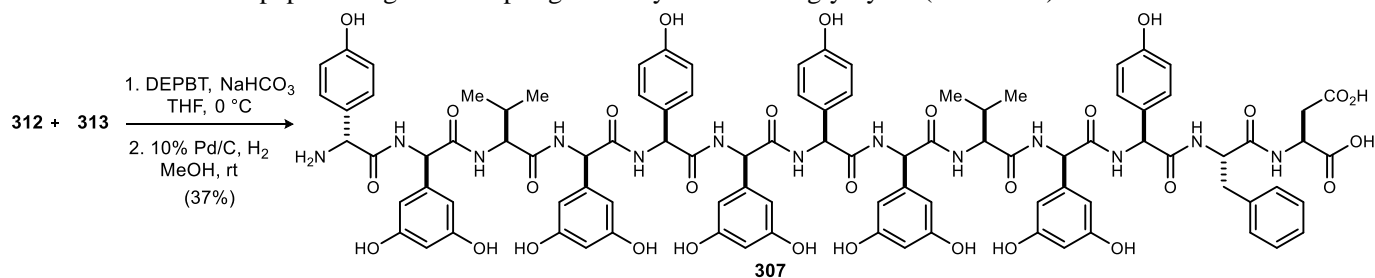
Heptapeptide **312** was prepared following a similar approach. DEPBT promoted coupling of Dpg acid **311** and methyl ester Hpg amine **323** followed by benzyl and Boc deprotection provided dipeptide **316** in 78% yield (Scheme 82). Tripeptide **314** was synthesized through an amide coupling reaction between previously prepared dipeptide **324** (after Boc-deprotection) and D-Hpg **325** in 79% yield. Benzyl deprotection and *N*-terminal protecting group swap from Boc to Cbz provided the tripeptide ready for fragment coupling. Dipeptide **315** was coupled with previously prepared dipeptide **316** to afford tetrapeptide **326** in 54% yield. Deprotection with HCl in dioxane and subsequent peptide coupling with tripeptide **314** provided the protected heptapeptide. Mild saponification with trimethyltin hydroxide provided heptapeptide free acid **312** ready for the final fragment coupling in 84% yield.

Scheme 82. Synthesis of heptapeptide **312** for the preparation of feglymycin (Süssmuth)



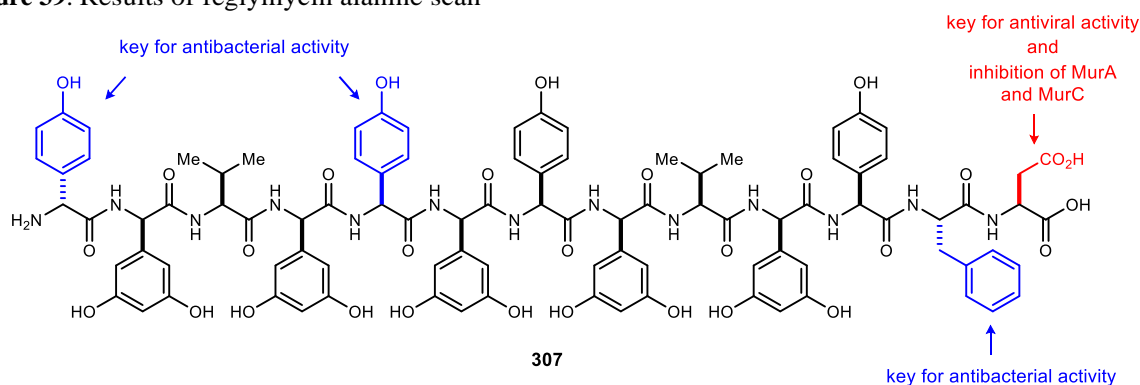
Peptide fragments hexapeptide **313** and heptapeptide **312** were condensed employing DEPBT as the coupling reagent to provide protected tridecapeptide in 42% yield (Scheme 83). All that remained to complete the total synthesis was global deprotection. The *N*-terminal Cbz group and the two *C*-terminal benzyl esters were removed in one step through hydrogenolysis to reveal feglymycin (**307**) in 89% yield. Overall, the synthesis was accomplished in 14 longest linear steps (31 total) with a 4% overall yield.

Scheme 83. Final peptide fragment coupling in the synthesis of feglymycin (Süssmuth)



With the successful synthesis of feglymycin, Süßmuth and coworkers performed an alanine scan to determine the importance of each residue on the antibacterial activity.¹¹¹ Thirteen feglymycin analogues were synthesized each with one amino acid substituted by alanine (L or D depending on the stereochemistry of the replaced residue) following the same strategy described for the preparation of feglymycin. All thirteen derivatives' antibacterial activity were tested against *S. aureus* and compared to parent feglymycin. A moderate decrease was observed in activity when any of the Dpg residues were replaced with alanine. However, when D-Hpg1, L-Hpg5, or L-Phe12 were replaced, a significant decrease in activity was observed. In another assay testing for inhibitory activity against enzymes MurA and MurC, part of peptidoglycan biosynthesis, only L-Asp13 was found to play a key factor in inhibition. The same residue was also found to be important for antiviral activity in an HIV assay.¹⁰⁹

Figure 39. Results of feglymycin alanine scan



4.3 Previous Efforts Towards the Synthesis of Feglymycin¹¹²

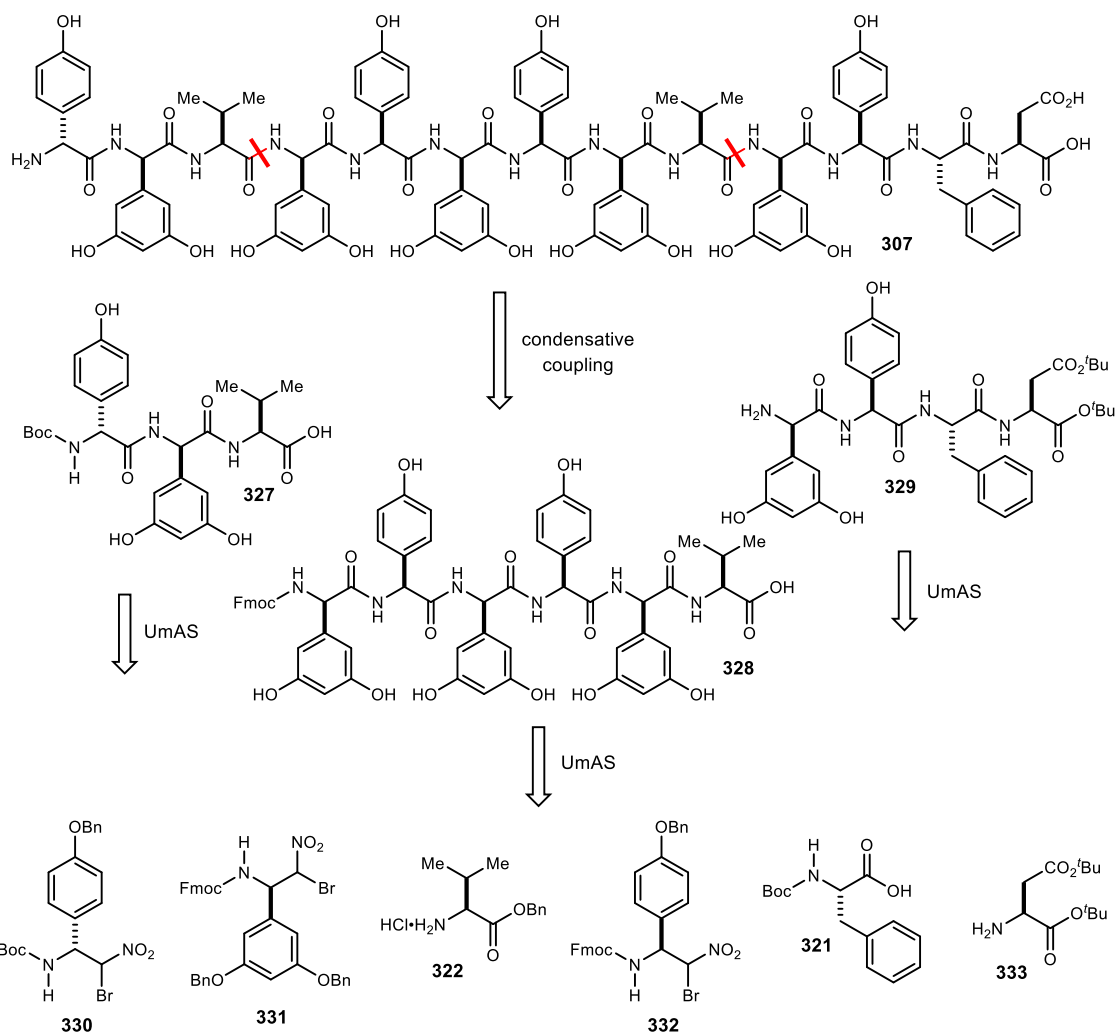
UmAS in conjunction with standard condensative peptide coupling methods provides a powerful method for peptide synthesis. The iterative nature of UmAS allows for the synthesis of peptide fragments containing unnatural amino acids, while traditional peptide coupling methods can be employed to connect the fragments generating a larger peptide. Our group envisioned applying this strategy to the synthesis of feglymycin. Retrosynthetically, the tridecapeptide was broken down into three smaller peptide fragments (**327**, **328** and **329**) at the *C*-terminal side of the two valine residues (Scheme 84). These disconnections provided a *C*-terminal natural amino acid from which UmAS homologation could be used to iteratively prepare each peptide fragment. The necessary α -bromonitroalkane donors would be prepared via enantioselective aza-Henry reactions. An Fmoc protecting group strategy was initially selected to showcase the newly developed aza-Henry chemistry with TMS-imines as well as to provide protecting group orthogonality between the growing chain *N*-termini and the benzyl protected sidechains. The *C*-terminus would be protected as the di-*tert*-butyl ester while the *N*-terminus would be protected with a Boc group to allow for concurrent deprotection.

The necessary bromonitroalkane building blocks were synthesized from the requisite imines using PBAM (Scheme 85). Fmoc-benzyloxyphenylglycine donor **332** was prepared in 74% yield and 76/74% ee for each diastereomer (1:1 dr). The enantiopurity was increased up to 98/99% ee after recrystallization. In the same manner, dibenzyloxy donor **331** was obtained in 61% yield and 97/98% yield after recrystallization. *N*-Terminal Boc-benzyloxy donor **330** was prepared from the imine in 90% yield and 92/92% ee.

¹¹¹ Hänchen, A.; Rausch, S.; Landmann, B.; Toti, L.; Nusser, A.; Süßmuth, R. D. *ChemBioChem* **2013**, *14*, 625-632.

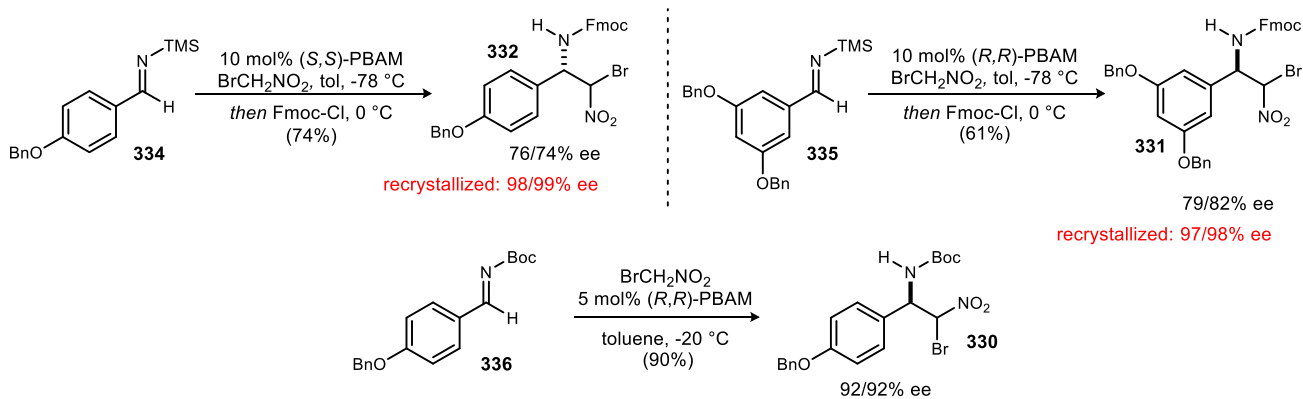
¹¹² Tsukanov, Doody, Makley *unpublished results*.

Scheme 84. Retrosynthetic analysis of feglymycin

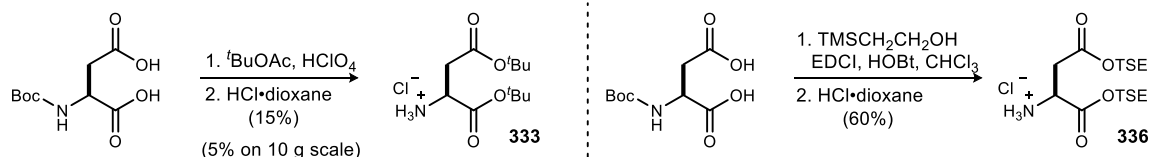


The synthesis of tetrapeptide **329** began with the double protection of aspartic acid as the *tert*-butyl ester (Scheme 86). Following a known literature procedure, free amine aspartic acid was treated with perchloric acid and *tert*-butyl acetate. Isolation of the product proved difficult due to volatility. It was found that the ammonium salt could be isolated in 34% yield upon treatment with HCl in dioxane, however partial ester deprotection was observed under these conditions. When the reaction was scaled up, the yield decreased to 10%. Dipeptide **337** was obtained from an uneventful amide coupling with Fmoc-Phe followed

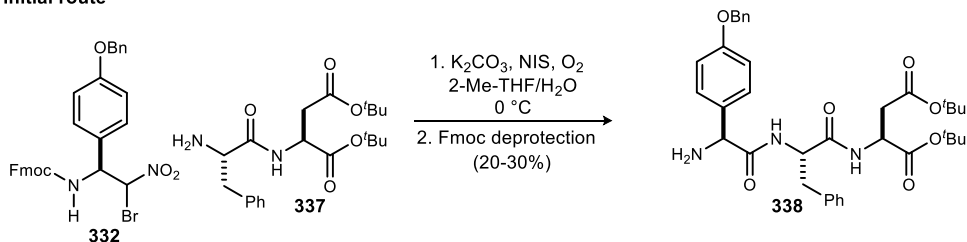
Scheme 85. Preparation of building blocks for synthesis of feglymycin¹¹²



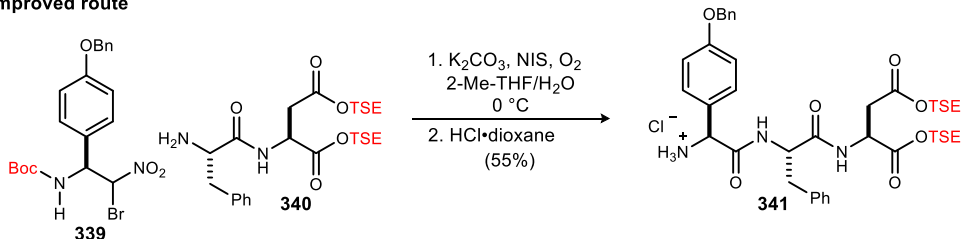
Scheme 86. Challenges in preparation of tetrapeptide **329**¹¹²



initial route

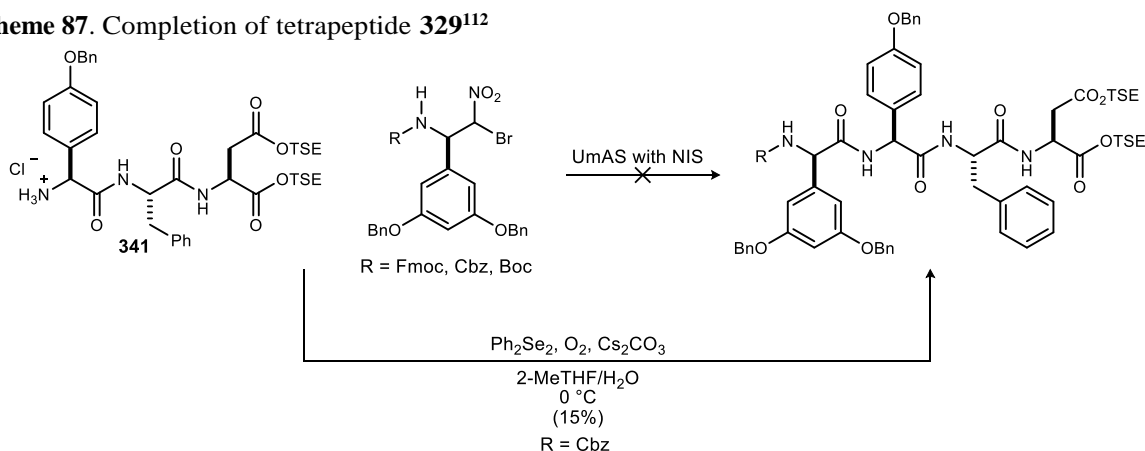


improved route



by deprotection. The following UmAS homologation step with Fmoc-donor **332** presented further challenges as purification of the Fmoc-protected peptide or deprotected tripeptide **338** proved difficult as the product was obtained in 20-30% yield. In order to increase material throughput, two changes were made to the synthesis of this fragment. The C-terminus was protected as two trimethylsilylethyl esters allowing for protected Asp **336** to be prepared in 60% yield on scale. Additionally, Fmoc donor **332** was replaced with Boc-donor **339** doubling the yield for tripeptide **341**. The stage was set for the final UmAS homologation step for this fragment, the first with Fmoc-dibenzyloxy donor **331**. Unfortunately, the desired product was unable to be obtained under various UmAS conditions. Altering the donor protecting group to Cbz or Boc also resulted in no product formation. After a thorough screen of reaction conditions, the Cbz-tetrapeptide could be obtained in low yield (15%) when NIS was replaced with Ph_2Se_2 (Scheme 87).

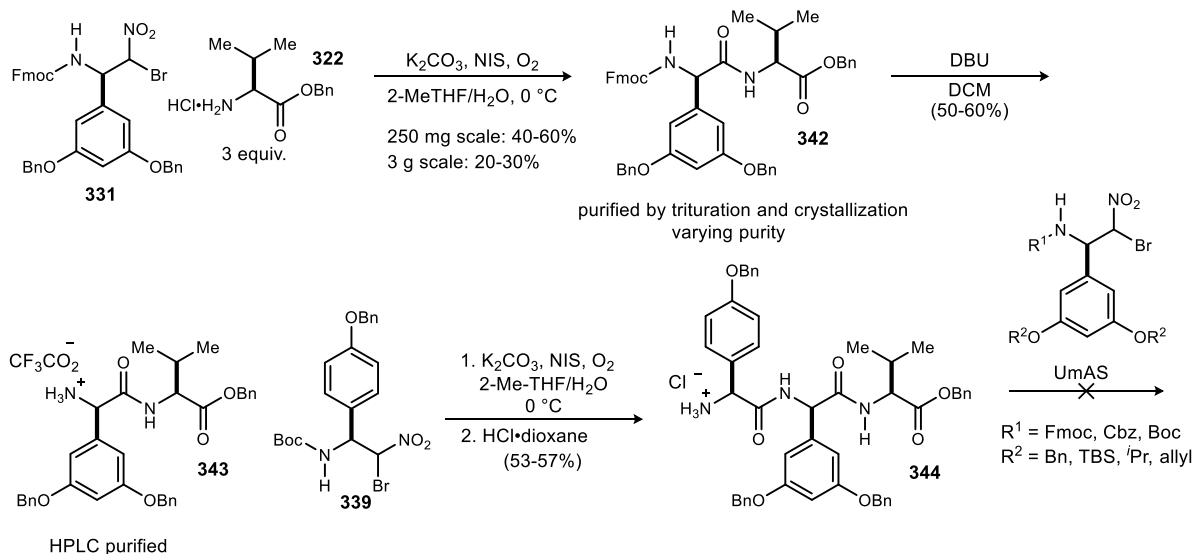
Scheme 87. Completion of tetrapeptide **329**¹¹²



In parallel to the discovery of the challenges associated with the synthesis of tetrapeptide **329**, the synthesis of hexapeptide **328** faced similar difficulties (Scheme 88). Dipeptide **342** was obtained in variable yield and purity from the coupling of valine benzyl ester **322** and Fmoc-dibenzyloxy donor **331**. On smaller

scale (250 mg of donor **331**) the dipeptide was obtained in 40-60% yield after trituration and crystallization. Upon scale up, (3 g of **331**) the yield decreased to 20-30%. Fmoc deprotection and subsequent purification resulted in dipeptide TFA salt **343** in 50-60% yield. Coupling with Boc Hpg donor **339** under UmAS conditions followed by deprotection provided tripeptide **344** in 53-57% yield. Similar to the synthesis of tetrapeptide **329**, homologation with donor **331** to generate the tetrapeptide was unsuccessful under many different UmAS conditions employed. A variety of amine and phenol protecting groups were tried in the reaction without success. The viability of the amine was verified as it was successfully coupled to a few more simple bromonitroalkanes (such as **69**), demonstrating that the issue resided with donor **331**.

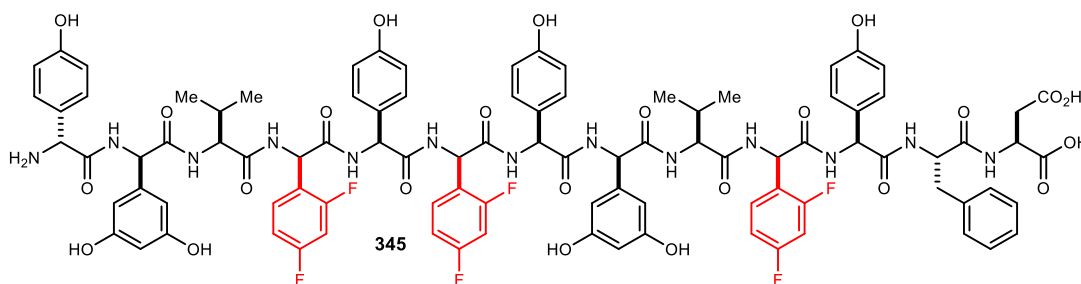
Scheme 88. Efforts toward the synthesis of hexapeptide **328**¹¹²



In order to circumvent the many issues surrounding donor **331** and investigate the later stages of the synthesis, a model peptide was targeted. Feglymycin derivative **345** was selected with 2,4-difluorophenylglycine residues replacing three of the five 3,5-Dpg residues (Figure 40). Two Dpg residues remained as those pieces were able to be prepared, albeit in low yield. The fluorinated residues were selected for their electron-withdrawing character, which typically leads to higher efficiency in UmAS couplings.

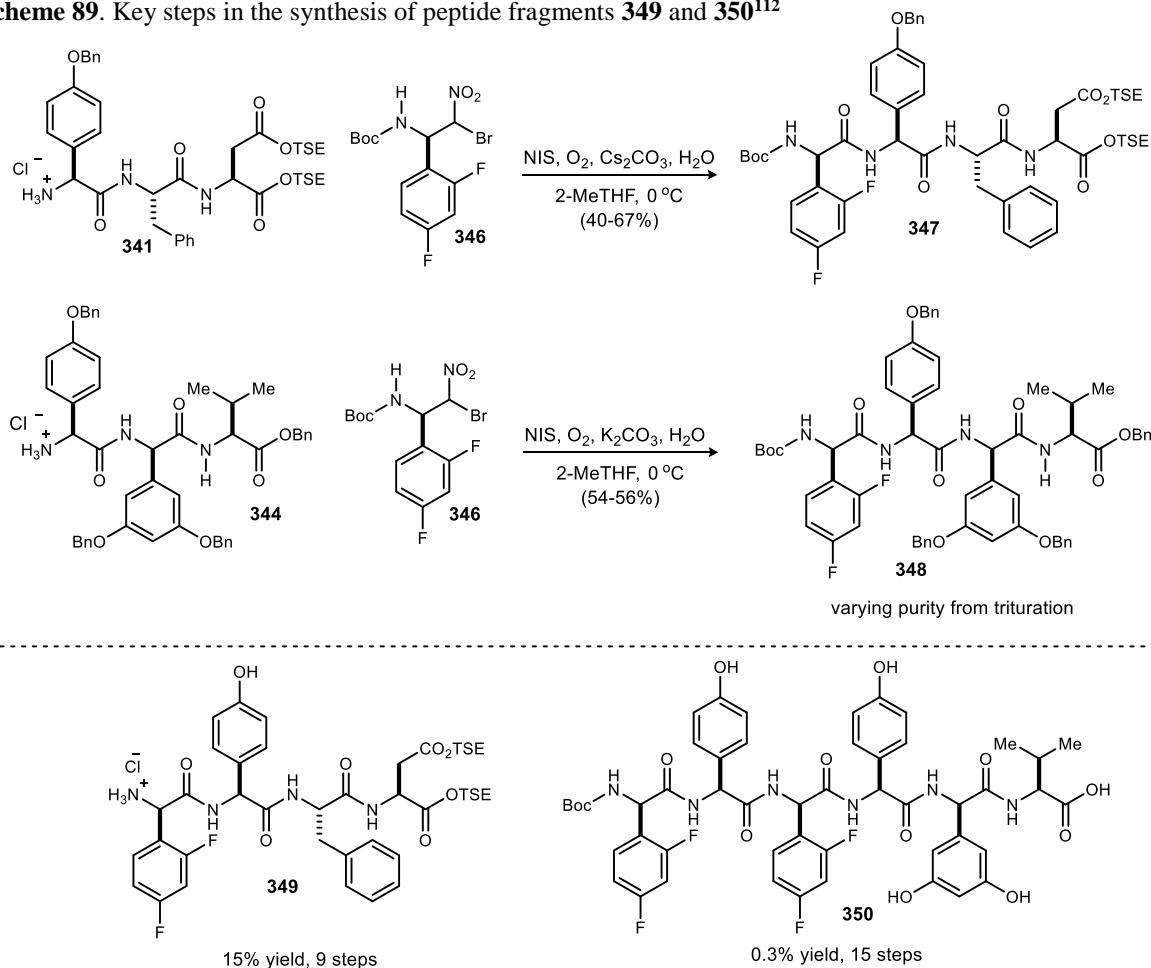
The residue substitution significantly improved the synthesis of the tetrapeptide fragment (Scheme 89). Tetrapeptide **347** was obtained from coupling of tripeptide **341** and difluoro donor **346** in 40-67% yield, as compared to 15% yield when employing the Cbz donor. A similar improvement was observed in the synthesis of the hexapeptide fragment with the residue substitutions. Previously, the Fmoc-tetrapeptide containing an *N*-terminal Dpg residue was unable to be synthesized. When replaced with donor **346**, tetrapeptide **348** was prepared in 54-56% yield, albeit in varying purity as the peptide was only purified by trituration due to solubility difficulties during column chromatography. The subsequent homologations

Figure 40. Feglymycin model target peptide with 2,4-difluorophenylglycine residues



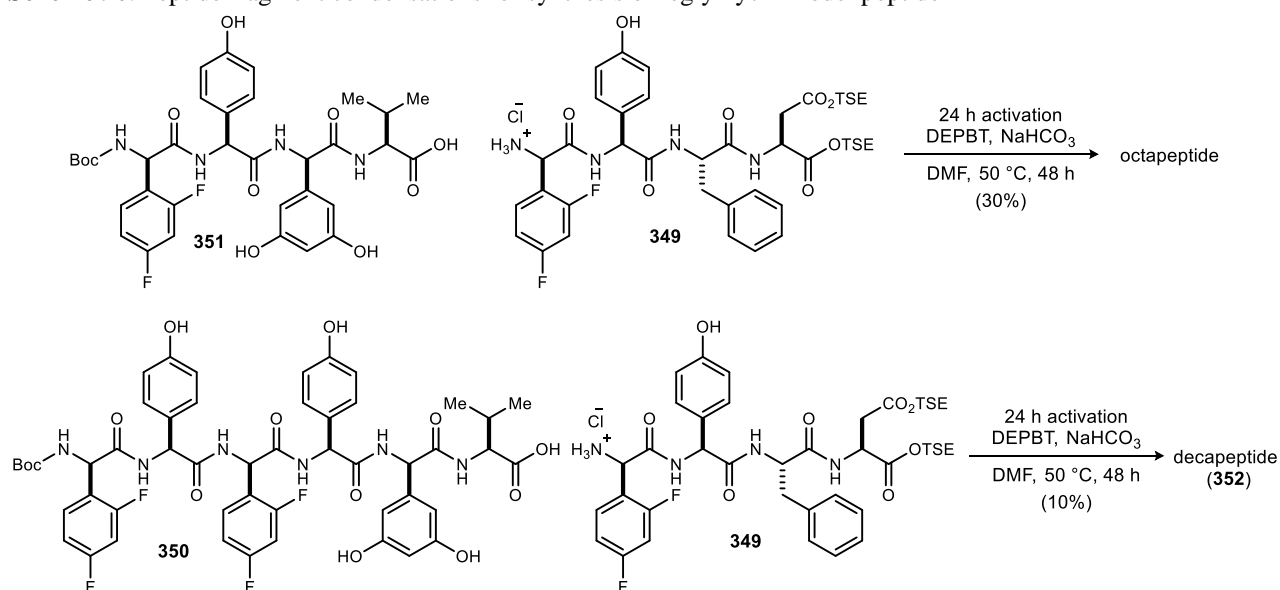
proceeded in moderate to low yield. HPLC purification prior to the final coupling gave analytically pure material with a significant loss of mass due to impurities. Tetrapeptide **349** was prepared in 15% yield over nine linear steps, while hexapeptide **350** was prepared in 0.3% yield over 15 linear steps. When starting with 10 g of aldehyde, a total of 36 reactions were performed to prepared 20-30 mg of hexapeptide **350**.

Scheme 89. Key steps in the synthesis of peptide fragments **349** and **350**¹¹²



With the preparation of tetrapeptide **349** and hexapeptide **350** complete, the next step was the fragment coupling to generate decapeptide **352**. Due to lack of material and relative value of hexapeptide **350**, a model system employing tetrapeptide **351** featuring the same four C-terminal residues was used to optimize the coupling conditions. A number of different coupling reagents including EDC/HOBt, PyBOP, PyCIU, PyBrOP, and TFFH were used in the coupling without product formation. Ultimately, DEBPT was found to be the only viable coupling reagent for this system as the octapeptide was obtained in 30% yield (Scheme 90). When the optimized conditions were applied to the six plus four coupling, decapeptide **352** was isolated in only 10% yield with impurities. Throughout the life of the project, over 70 g of starting aldehyde were consumed to provide ~20 mg of decapeptide. Tridecapeptide formation was attempted but the product was never detected. With insufficient material throughput due to low yields caused by the Dpg residue, this route was abandoned.

Scheme 90. Peptide fragment condensations for synthesis of feglymycin model peptide¹¹²



4.4 Synthesis of Ffeglymycin and other Derivatives

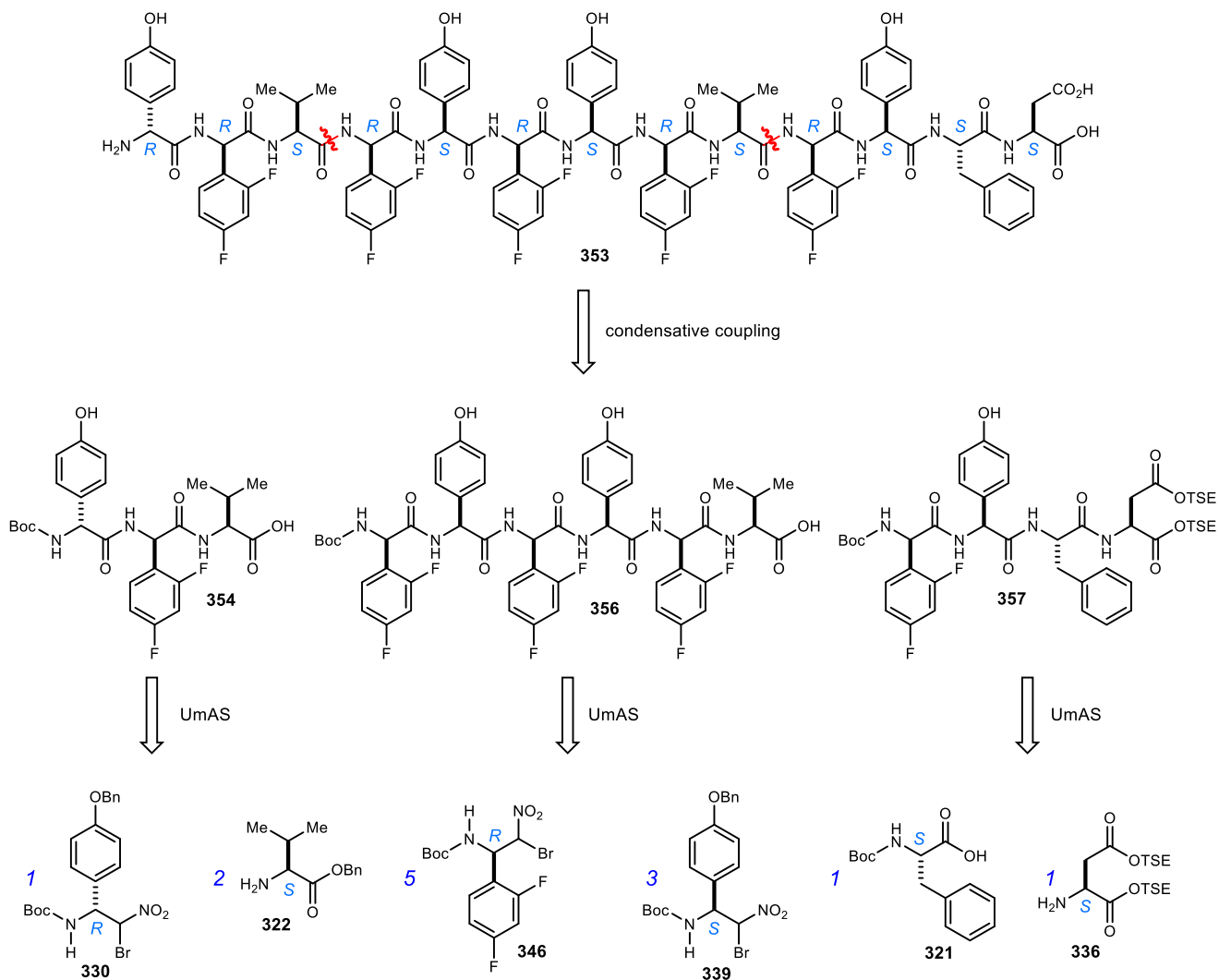
Synthesis of Ffeglymycin

The initial impetus for this project was to showcase the ability of the aza-Henry/UmAS reaction sequence to synthesize a complex peptide target containing unnatural α -amino acid residues that are difficult to couple under traditional peptide synthesis conditions. The previously discussed challenges in the synthesis of feglymycin limited our ability to fully demonstrate the power of the aza-Henry/UmAS reaction sequence for peptide synthesis. Although, the problems surrounding coupling with the Dpg residue highlight a limitation of the current methodology, the ultimate goal of the project could still be realized through the synthesis of a derivative by replacing the troublesome Dpg residue with a different arylglycine residue. This approach would accomplish two things: 1) benchmark the aza-Henry/UmAS reaction sequence in peptide synthesis as compared to standard peptide synthesis and 2) demonstrate the ability of UmAS to incorporate any arylglycine, including those not found in nature. We chose to target feglymycin derivative **353** (Ffeglymycin) featuring D-2,4-difluorophenylglycine (D-2,4-F-Phg) in place of the Dpg residues. This particular residue was chosen for three reasons: 1) fluorinated compounds have attracted interest in the medicinal community, 2) the fluorines allow for the use of ¹⁸F NMR as a diagnostic analytical tool and 3) previous work with UmAS showed that electron deficient arylglycine donors worked the best in the coupling reaction. Ideally, we would be able to synthesize fluorinated derivative **353** while optimizing the conditions for each coupling, and then apply the new optimized conditions to feglymycin itself or other derivatives.

Retrosynthetically, we adopted the same strategy as was previously applied to feglymycin by breaking the tridecapeptide into three smaller peptide fragments (**354**, **356**, **357**) to maximize convergency (Scheme 91). Tetrapeptide **357** and hexapeptide **356** will be coupled followed by coupling with tripeptide **354**, each employing traditional peptide coupling methods. The scissions were strategically placed with a valine residue at the C-termini of tripeptide **354** and hexapeptide **356** to avoid epimerization of the epimerization-prone arylglycine residues during the condensative peptide couplings. Each peptide fragment would then be prepared using the iterative UmAS methodology, except for the standard peptide coupling of aspartic acid and phenylalanine in tetrapeptide **357**. This breakdown leads to five R-2,4-difluorophenyl

bromonitroalkanes (**346**), three *S*-hydroxyphenyl bromonitroalkanes (**339**), one *R*-hydroxyphenyl bromonitroalkane (**330**), two L-valine residues, one L-aspartic acid, and one L-phenylalanine residue.

Scheme 91. Retrosynthetic analysis of Ffeglymycin

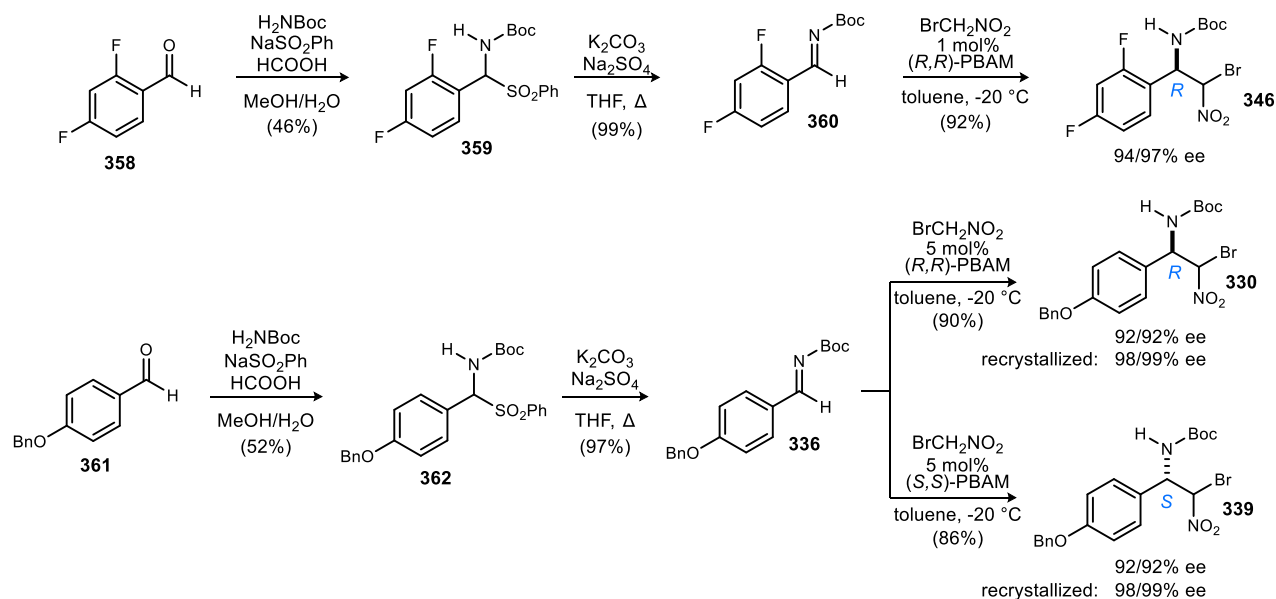


Efforts began with the synthesis of the necessary α -bromonitroalkane building blocks (Scheme 92). *N*-Boc α -amidossulfones **359** and **362** were prepared from the requisite aldehydes following the standard protocol. Subsequent elimination of the sulfinate provided *N*-Boc imines **360** and **336**. The imines were then subjected to an enantioselective bromonitromethane addition with organocatalyst PBAM (**82**). Using (*R,R*)-PBAM, 2,4-difluorophenylglycine donor **346** was obtained in 92% yield and 94/97% ee for each diastereomer. Both enantiomers of the benzyl-protected hydroxyphenylglycine donors (**330** and **339**) were obtained in high yield and 92/92% ee for each diastereomer from the respective enantiomers of the catalyst. Recrystallization of both benzyloxy bromonitroalkanes increased the ee up to 98/99%. Benzyl valine **322** was prepared through an alkylation of the free acid with benzyl bromide followed by Boc-deprotection to afford the HCl salt. Starting from Boc-aspartic acid, bis-esterification with 2-trimethylsilylethanol provided protected aspartic acid **336**. The last amino acid residue, Boc-Phe, was used as purchased.

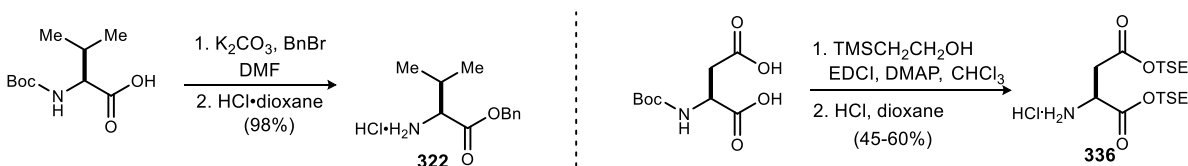
With all the necessary building blocks prepared, focus shifted to synthesizing the three peptide fragments. The preparation of tetrapeptide **349** began with the coupling of aspartic acid ester **336** to Boc-Phe using EDC/HOBt to provide dipeptide **363** in up to 90% yield (Scheme 94). The crude dipeptide was

Scheme 92. Synthesis of building blocks for the synthesis of Ffeglymycin

synthesis of arylglycine donors



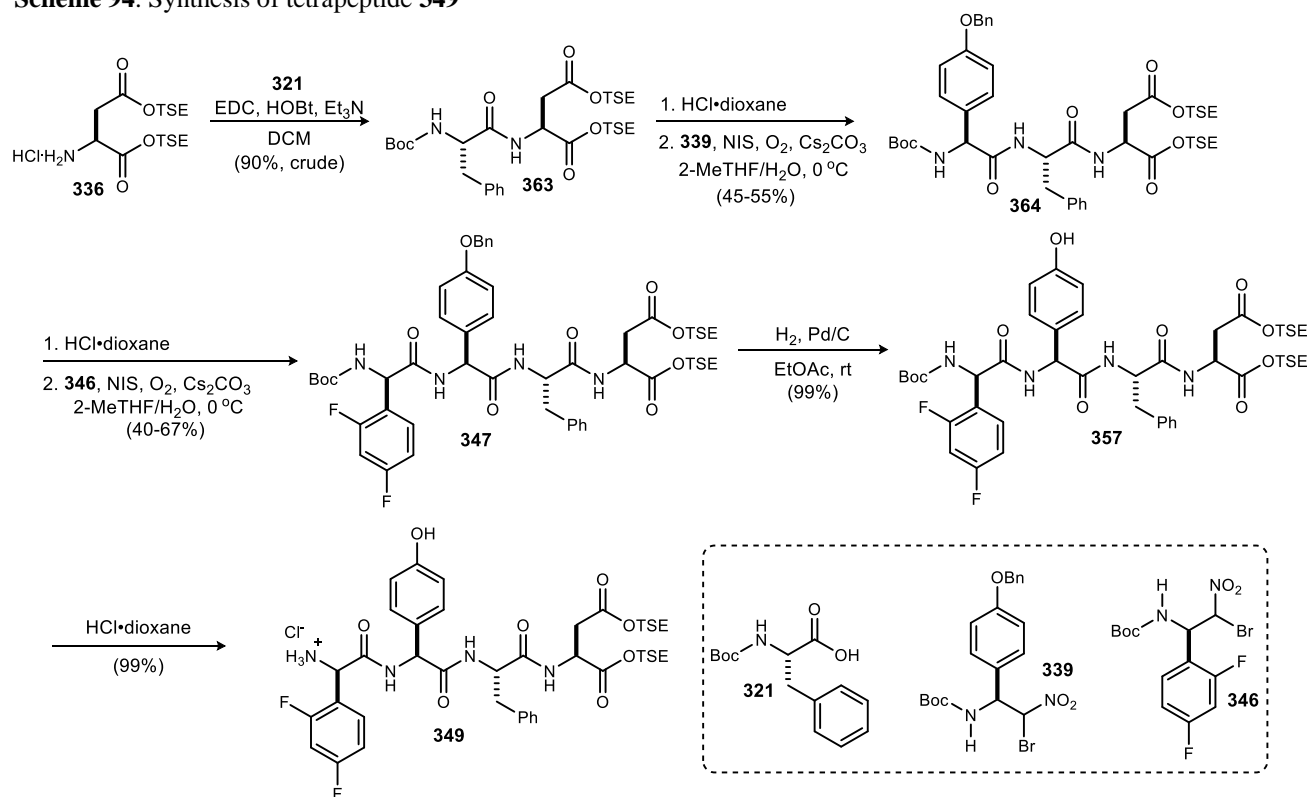
preparation of amino acids



submitted to HCl in dioxane to afford the deprotected amine salt. UmAS coupling using 100 mol % NIS between the dipeptide amine salt and benzyloxyphenylglycine donor **339** gave tripeptide **364** in moderate yield (45-55%). Subsequent Boc-deprotection and UmAS coupling with 2,4-difluorophenylglycine donor **346** provided protected tetrapeptide **347** in 40-67% yield. A two-step deprotection sequence was then employed to obtain the desired peptide fragment. Hydrogenolysis of the benzyl protecting group proceeded in excellent yield followed by Boc-deprotection to give tetrapeptide **349**. Tetrapeptide **349** was prepared in 15% yield over nine steps from Boc-aspartic acid.

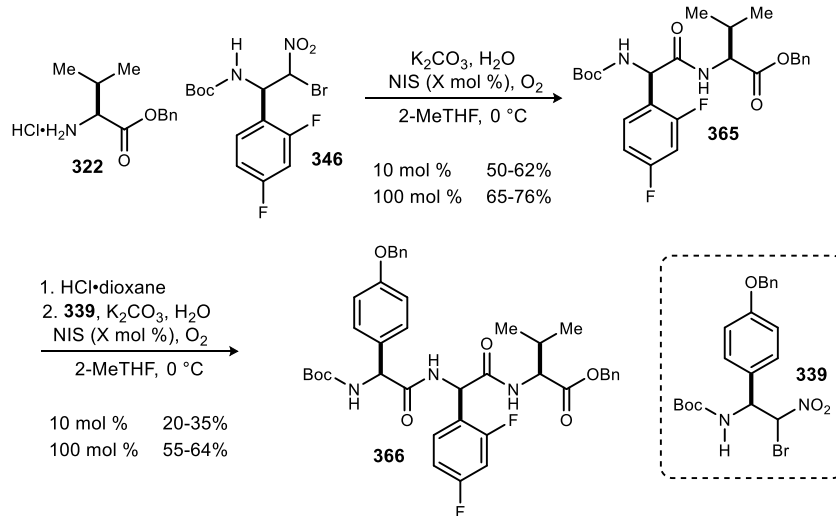
The synthesis of hexapeptide **356** featured five consecutive deprotection/UmAS sequences starting from valine benzyl ester. Dipeptide **365** was prepared through the coupling of valine benzyl ester hydrochloride and 2,4-difluorophenylglycine donor **346** (Scheme 93). We envisioned employing the optimized conditions for the use of catalytic NIS (10 mol % NIS and O₂) as this would minimize waste and provide an overall better synthesis. When these conditions were applied to the coupling, dipeptide **365** was isolated in only moderate yield (50-62%). Boc-deprotection and subsequent coupling with benzyloxyphenylglycine donor **339** under catalytic NIS conditions yielded tripeptide **366** in poor yield (20-35%). In an effort to improve the yield of these two couplings, both reactions were run with stoichiometric NIS. Significant improvement was observed as the yield for dipeptide **365** formation was increased up to 76%, while tripeptide **366** formation was increased up to 64%.

Scheme 94. Synthesis of tetrapeptide **349**



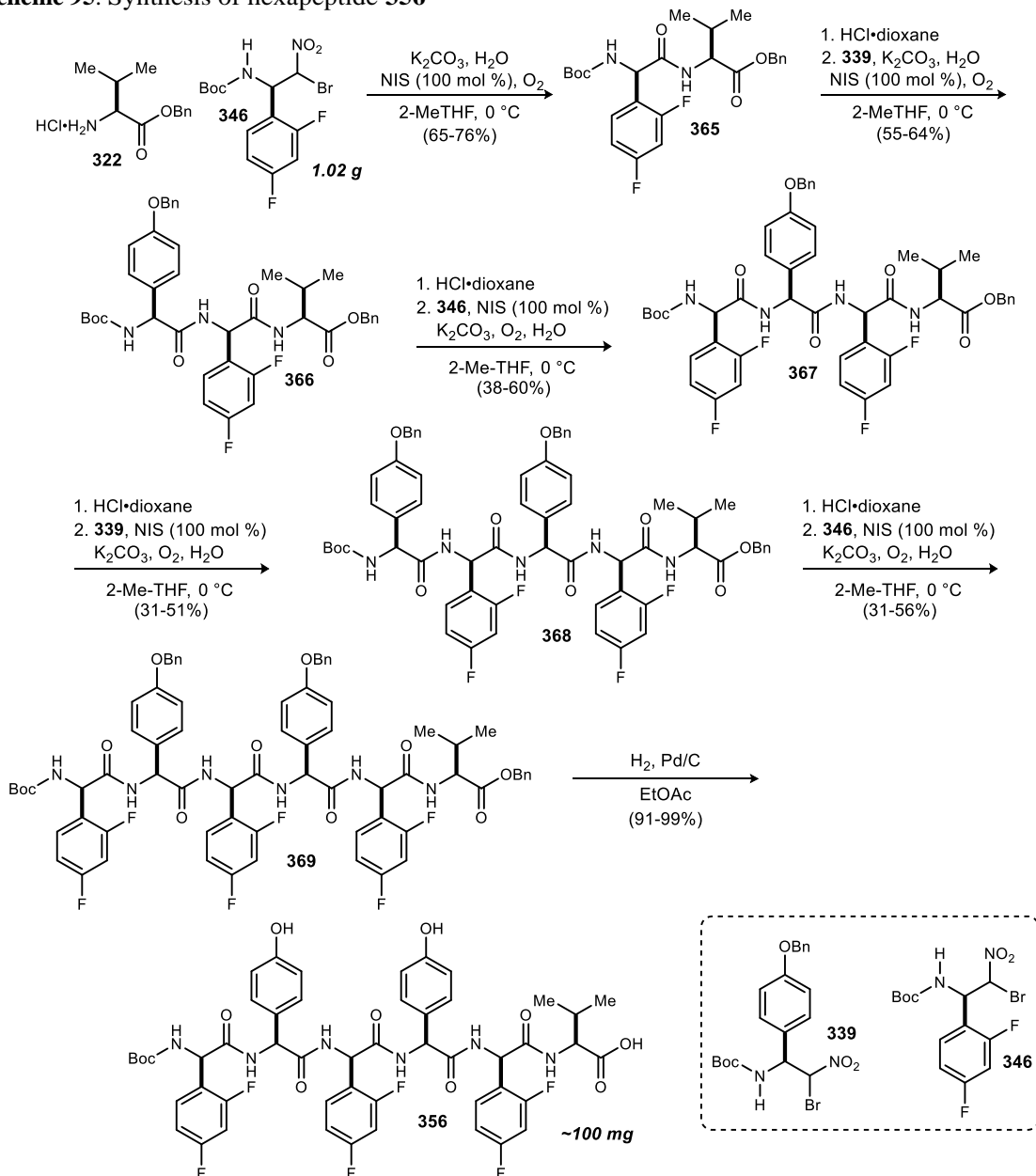
The same UmAS conditions employing one equivalent of NIS were applied to the subsequent three couplings to arrive at hexapeptide fragment **369** (Scheme 95). Tripeptide **366** was submitted to Boc-deprotection conditions followed by UmAS coupling with 2,4-difluorophenylglycine donor **346** to afford tetrapeptide **367** in 38–60% yield. Deprotection followed by UmAS coupling with benzyloxyphenylglycine donor **339** provided pentapeptide **368** in 31–51% yield. The final homologation was achieved through the coupling of 2,4-difluorophenylglycine donor **346** and the hydrochloride salt of deprotected pentapeptide **368** to give protected hexapeptide **369** in 31–56% yield. To date, this is the longest peptide fragment prepared exclusively through UmAS coupling reactions. Benzyl deprotection via hydrogenolysis provided

Scheme 93. Comparison of catalytic and stoichiometric NIS in UmAS couplings in the synthesis of Ffeglymycin



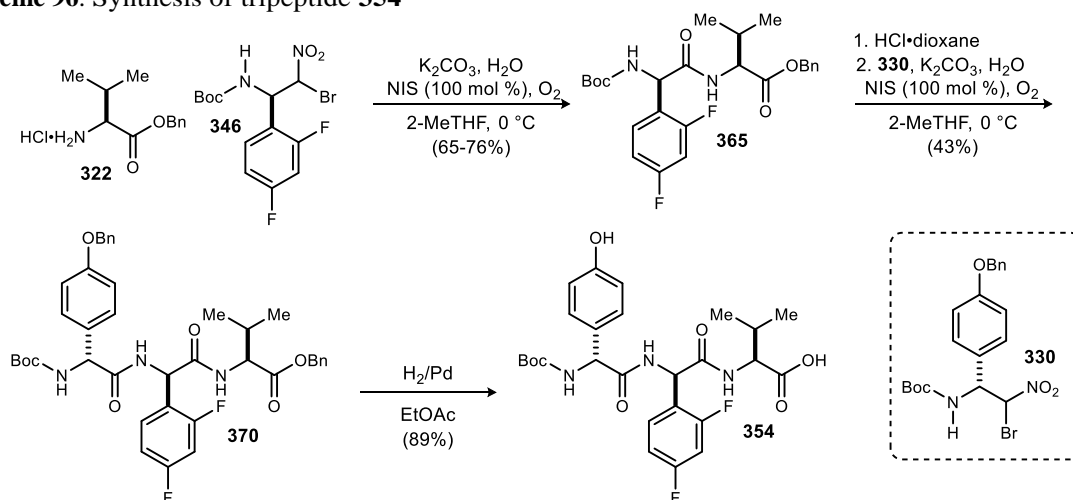
hexapeptide **356** ready for the fragment coupling step. The hexapeptide was prepared in 4% overall yield (using average yield) in 10 steps starting from valine benzyl ester hydrochloride salt and 2,4-difluorophenylglycine donor **346**. Starting from 1.02 g of α -bromonitroalkane **346**, about 100 mg of hexapeptide **356** could be prepared.

Scheme 95. Synthesis of hexapeptide **356**



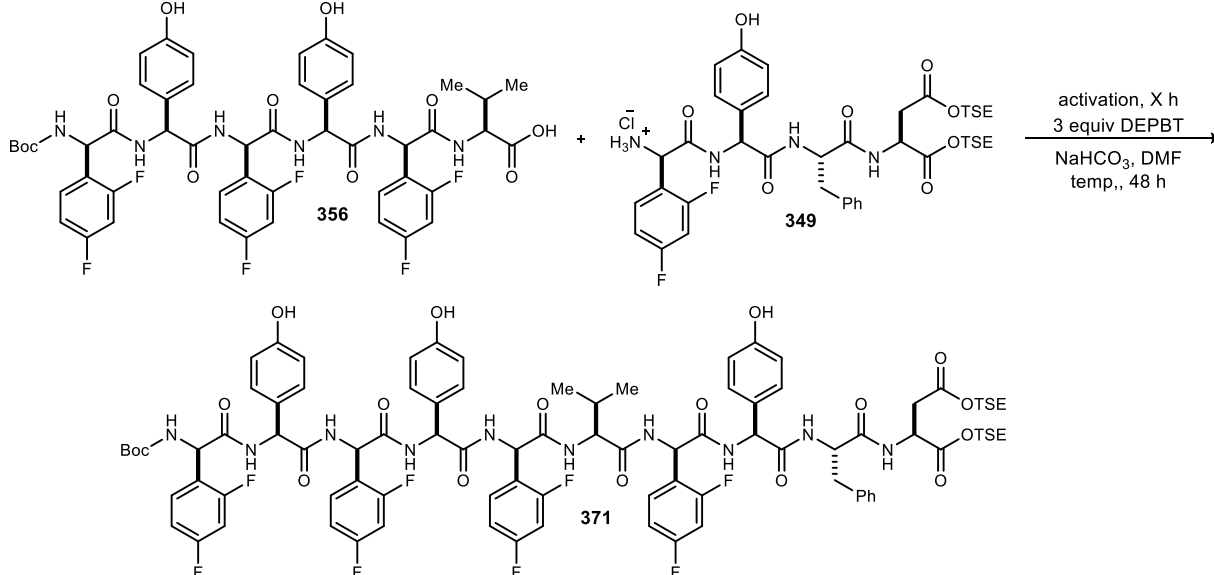
Tripeptide **354**, the final peptide fragment, is almost identical to tripeptide **366** that was synthesized on the route to hexapeptide **356**. The two tripeptides differ only in the stereochemistry of the Hpg residue where previously prepared tripeptide **366** contains (*S*)-Hpg, tripeptide **354** contains (*R*)-Hpg. Thus, dipeptide **365** was synthesized in the same manner as previously disclosed followed by UmAS coupling with the *R*-enantiomer of the benzyloxyphenylglycine donor (**330**) (Scheme 96). Protected tripeptide was obtained in 43% yield from the coupling reaction. Hydrogenolysis provided the side-chain deprotected, free acid tripeptide **354**, which was ready for fragment coupling.

Scheme 96. Synthesis of tripeptide 354



With all three peptide fragments in hand, focus shifted to the condensative peptide couplings. The first coupling would be between the *C*-terminus of hexapeptide **356** and the *N*-terminus of tetrapeptide **349**

Table 28. Decapeptide formation



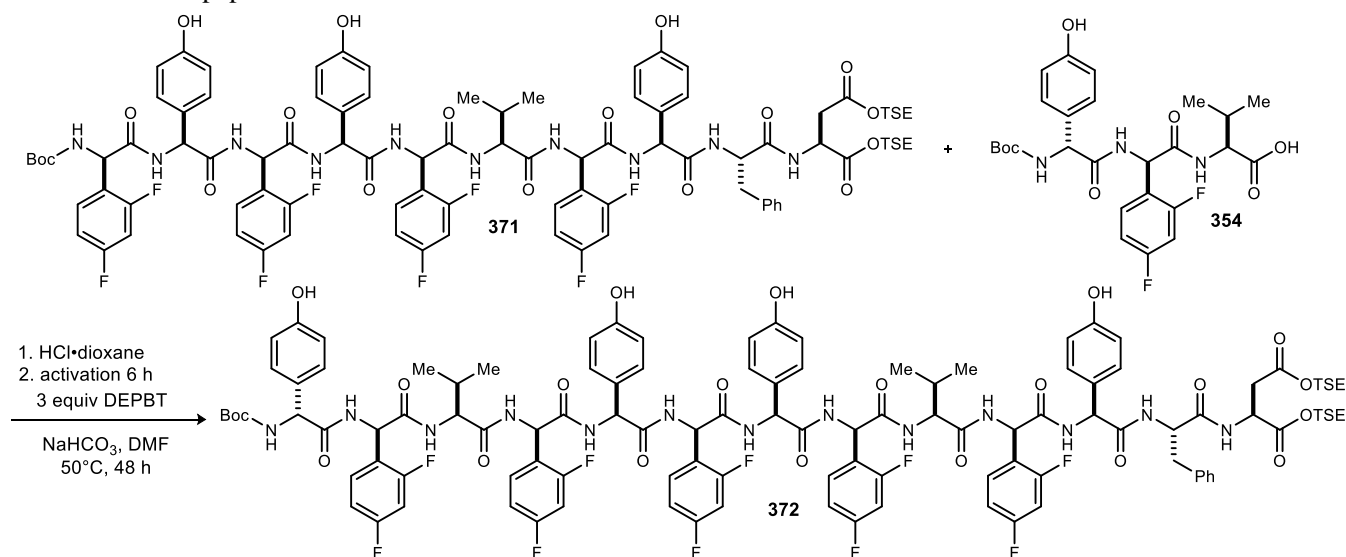
entry ^a	scale ^b	activation time ^c (h)	temperature (°C)	yield ^d (%)
1	10 mg	24	50	60
2	22 mg	3	50	56
3	40 mg	3	50	58
4	55 mg	3	50	62
5	64 mg	3	50	65
6	20 mg	0.33	50	33
7 ^e	12 mg	24	75	62
8	12 mg	24	25	trace

^aReactions are 0.3 M in hexapeptide and employ 1.5 equiv. tetrapeptide, 3 equiv. DEPBT, and 4 equiv. NaHCO₃. ^bMass of hexapeptide. ^cHexapeptide, DEPBT, and NaHCO₃ were stirred at room temp. prior to addition of tetrapeptide. ^dIsolated yield. ^eReaction was run for 8 h.

to provide decapeptide **371**. As a starting point, we chose the optimal conditions employed by Süssmuth in the large fragment couplings in the synthesis of feglymycin.¹¹⁰ These conditions also had proven optimal during our previous attempts at synthesizing a different feglymycin derivative (see section 4.3). In the event, hexapeptide **356** was combined in DMF with DEPBT (3 equiv.) and NaHCO₃ (4 equiv.) and stirred at room temperature for 24 hours. After the activation time, tetrapeptide **349** was added and the reaction was heated to 50 °C and allowed to stir for 48 hours. Upon completion of the reaction, the DMF was removed by vacuum and the residue was directly submitted to reverse-phase preparative HPLC for analysis. Interestingly, two different compounds were isolated that appeared to be consistent with the desired decapeptide by HRMS as well as ¹H NMR and ¹⁸F NMR. It was later determined that one of the compounds was the desired decapeptide **371**, while the other was the Boc-protected decapeptide, as the former was converted to the latter upon treatment with HCl in dioxane. We initially suspected that the deprotection was occurring during HPLC purification in the presence of TFA, but when Boc-decapeptide **371** was resubmitted to HPLC purification, the deprotected product was not observed. Nevertheless, the desired decapeptide was obtained in 60% yield (combined yield) from these initial reaction conditions.

Although the initial conditions provided the desired coupling product in moderate yield and was comparable to that reported with similar substrates by Süssmuth, we sought to improve the result through minor optimization of the reaction conditions (Table 28). When the activation time was shortened from 24 h to 3 h, the decapeptide was obtained in similar yield (56-65%). The activation period proved to be essential

Table 29. Tridecapeptide formation



entry ^a	scale ^b	concentration (M)	yield ^d (%)
1	33 mg	0.1	23
2	30 mg	0.1	25
3	23 mg	0.2	30
4	30 mg	0.3	40
5	50 mg	0.3	32
6	50 mg	0.3	38
7	57 mg	0.3	37
8	73 mg	0.3	38

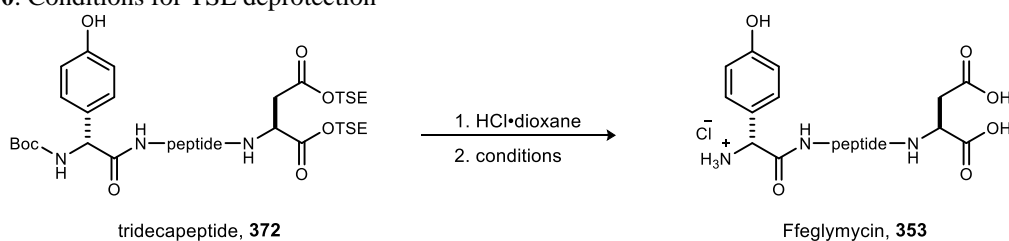
^aReactions employ 1.5 equiv. tripeptide, 3 equiv. DEPBT, and 4 equiv. NaHCO₃. ^bMass of decapeptide. ^cTripeptide, DEPBT, and NaHCO₃ were stirred at room temp. prior to addition of tetrapeptide. ^dIsolated yield.

as the product was obtained in 33% yield when the activation time was reduced to 20 minutes. When the reaction temperature was increased from 50 °C to 75 °C, the product was obtained in a similar yield of 62%, however, the crude reaction mixture appeared messier. Reactivity was halted when the reaction was run at room temperature as only trace product was observed. The three hour activation time and a reaction temperature of 50 °C was chosen as optimal as the product could be obtained in up to 65% yield on the largest scale run.

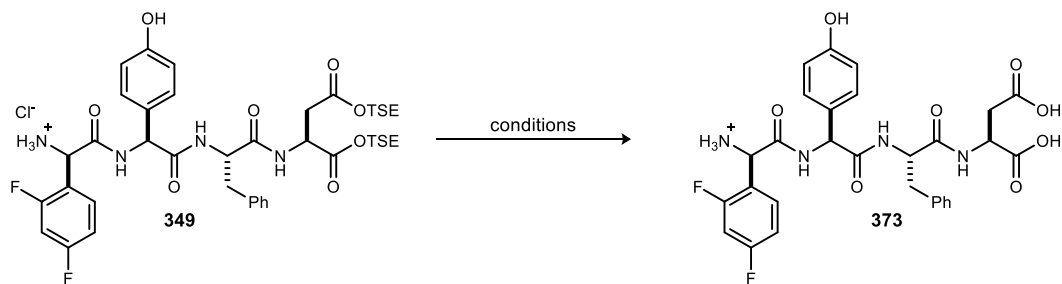
The final fragment coupling between the *C*-terminus of tripeptide **354** and *N*-terminus of decapeptide **371** was all that remained. After Boc-deprotection of the decapeptide, the same coupling conditions that were used for decapeptide formation were applied for the formation of protected tridecapeptide **372** employing an activation time of 6 hours. Starting with 33 mg of decapeptide **371**, deprotection and subsequent peptide coupling with activated tripeptide **354** yielded 9 mg of tridecapeptide **372** (determined by HRMS) after HPLC purification (23% yield) (Table 29). The yield was increased up to 40% as the concentration of the reaction was increased as well as the scale. The coupling reaction was run numerous times with yields ranging from 30-40% under the optimal conditions providing over 150 mg of protected tridecapeptide **372**.

With the framework of Ffeglymycin in place, all that remained was deprotection. The Boc-group was simply removed with HCl in dioxane, leaving the two trimethylsilylethyl esters as the only remaining protecting groups. TBAF was initially employed in an attempt to affect the desired transformation (Table 30). The tridecapeptide hydrochloride salt (9 mg) was treated with 4 equiv. of TBAF and allowed to stir at room temperature. The reaction was monitored by ¹H NMR looking for the disappearance of the diagnostic TMS signal. After 2 hours, minimal conversion was observed. Subsequent addition of more TBAF and exposure to an additional 5 hours did not result in any additional conversion. The unreacted starting material was recovered in 90% yield. The material was again submitted to TBAF and heated to 85 °C in DMF for 16 hours resulting in no conversion. In an attempt to saponify the two esters, the tridecapeptide was treated with ammonium hydroxide. No conversion was observed and 5 mg of starting material was recovered. The tridecapeptide was then submitted to lithium hydroxide and hydrogen peroxide in THF at 0 °C and allowed to warm to room temperature for 6 h. Partial conversion was observed by ¹H NMR and the material was resubmitted to the same conditions and allowed to stir for 16 h. Full conversion was observed, however, no desired product was isolated after HPLC purification.

Table 30. Conditions for TSE deprotection



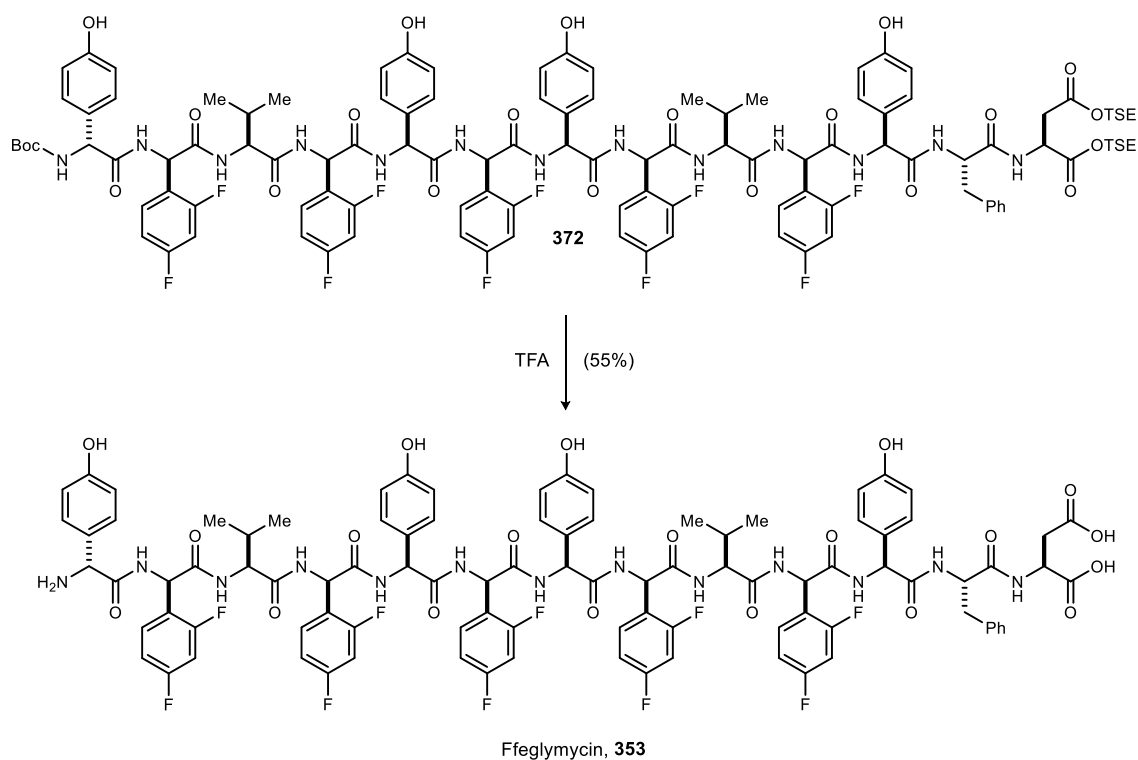
entry	conditions	result
1	TBAF (4 equiv.), THF, rt, 2 h	minimal conversion
2	TBAF (8 equiv.), THF, rt, 5 h	minimal conversion
3	TBAF (16 equiv.), DMF, 85 °C, 16 h	minimal conversion
4	NH ₄ OH, MeOH, rt, 4 h	no conversion
5	LiOH (2 equiv.), H ₂ O ₂ (4 equiv.), THF, 0 °C to rt, 4 h	no conversion
6	LiOH (100 equiv.), H ₂ O ₂ (200 equiv.), THF, 0 °C to rt, 3 h	partial conversion, decomposition
7	LiOH (100 equiv.), H ₂ O ₂ (200 equiv.), THF, 0 °C to rt, 16 h	full conversion, decomposition

Table 31. Model substrate for TSE deprotection

entry	conditions	result
1	TBAF (16 equiv.), DMF, 85 °C, 16 h	no conversion
2	LiOH (100 equiv.), H ₂ O ₂ (200 equiv.), THF, 0 °C to rt, 16 h	full conversion, decomposition
3	TFA, rt, 2 h, EtOH in work-up	full conversion to diethyl ester
4	TFA, rt, 2 h	full conversion to product
5	TFA, rt, 18 h	full conversion to product

At this point we chose to employ a model system to focus on the ester deprotection. Tetrapeptide **349** was chosen as the model substrate as it contains the same 4 amino acid residues at the C-terminus as the tridecapeptide does. The tetrapeptide was submitted to TBAF and LiOH/H₂O₂, the same conditions previously tried on the tridecapeptide (Table 31). The results were the same as TBAF provided no reaction, while LiOH/H₂O₂ resulted in full conversion but no desired product. We next tried TFA for the ester deprotection. In the event, full deprotection was observed as the diethyl ester was obtained after work-up with ethanol. When the tetrapeptide deprotection was run neat in TFA for 2 hours at room temperature the deprotected diacid was obtained after removal of TFA by vacuum. These conditions were then applied to

Scheme 97. Final deprotection to provide Ffeglymycin



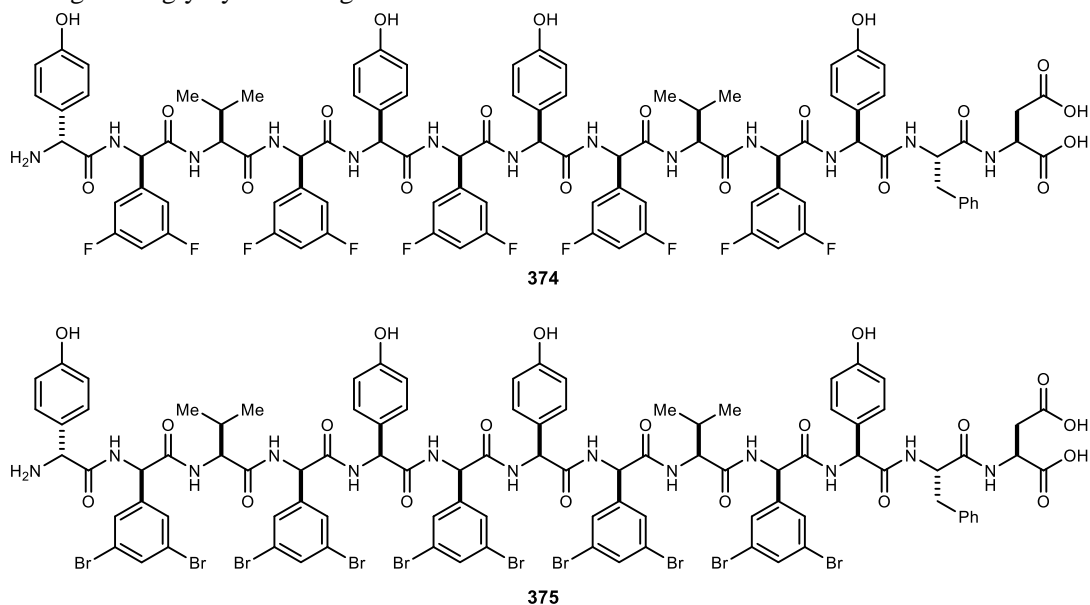
tridecapeptide **372** resulting in both Boc and TSE deprotection affording Ffeglymycin in 42-55% yield after HPLC purification (Scheme 97).

The synthesis of the feglymycin derivative Ffeglymycin, containing 2,4-difluorophenylglycine residues as substitutions for the 3,5-dihydroxyphenylglycine residues, was synthesized in an 18-step longest linear sequence (35 steps overall) in 0.4% overall yield featuring 3 enantioselective aza-Henry reactions, 8 UmAS couplings, and 2 condensative peptide fragment couplings. Although the overall yield was poor, the synthesis demonstrated the ability of UmAS to function as a synthetically useful reaction in peptide synthesis, particularly for the inclusion of unnatural amino acids.

Efforts Towards the Synthesis of other Feglymycin Analogues

With the synthesis of Ffeglymycin completed, we sought to apply the same reaction sequence towards other feglymycin analogues containing different arylglycine residues in place of the Dpg residues (Figure 41). Two analogues were selected, each containing 3,5-disubstituted phenylglycine residues. The first analogue, **374**, is a regioisomer of Ffeglymycin with 3,5-difluorophenylglycine residues. This was chosen as the reactivity of the residues was expected to be similar to that of the 2,4-difluoro residues of Ffeglymycin, while having the same substitution pattern as feglymycin. The second analogue, **375**, contains 3,5-dibromophenylglycine residues in place of the Dpg residues. This derivative was chosen due to its potential to act as a feglymycin precursor through a metal-catalyzed etherification in which the arylbromides could be substituted with an alcohol, providing protected Dpg residues.¹¹³

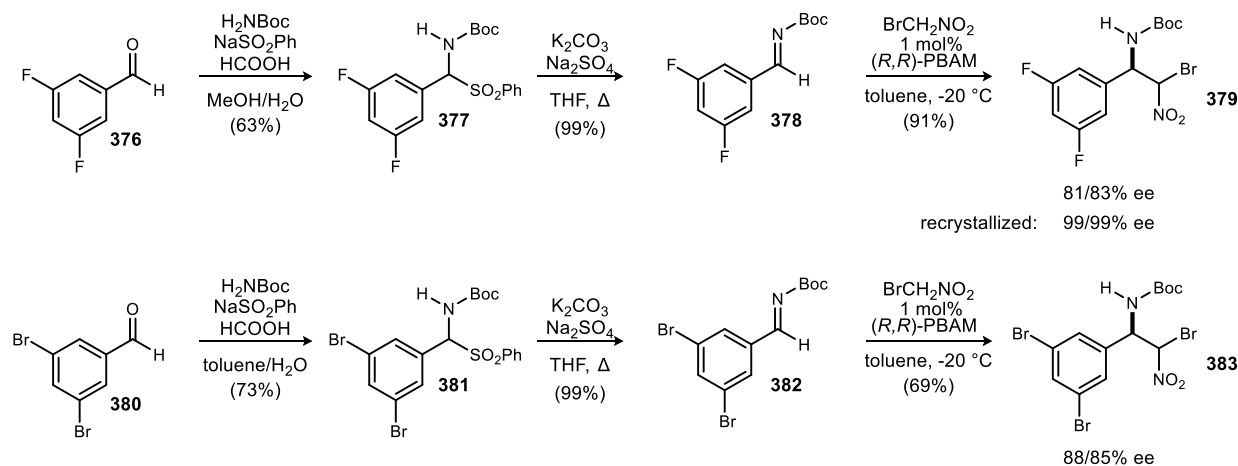
Figure 41. Targeted feglymycin analogues



We envision employing the same synthetic strategy as was used for the synthesis of Ffeglymycin to access analogues **374** and **375**. First, the α -bromonitroalkanes were prepared in three steps from the respective aldehydes (Scheme 98). PBAM catalyzed bromonitromethane additions provided difluoro bromonitroalkane **379** in 91% yield and 81/83% ee and dibromo bromonitroalkane **383** in 69% yield and 88/85% ee. Difluoro bromonitroalkane **379** was recrystallized up to 99/99% ee prior to use in the synthesis.

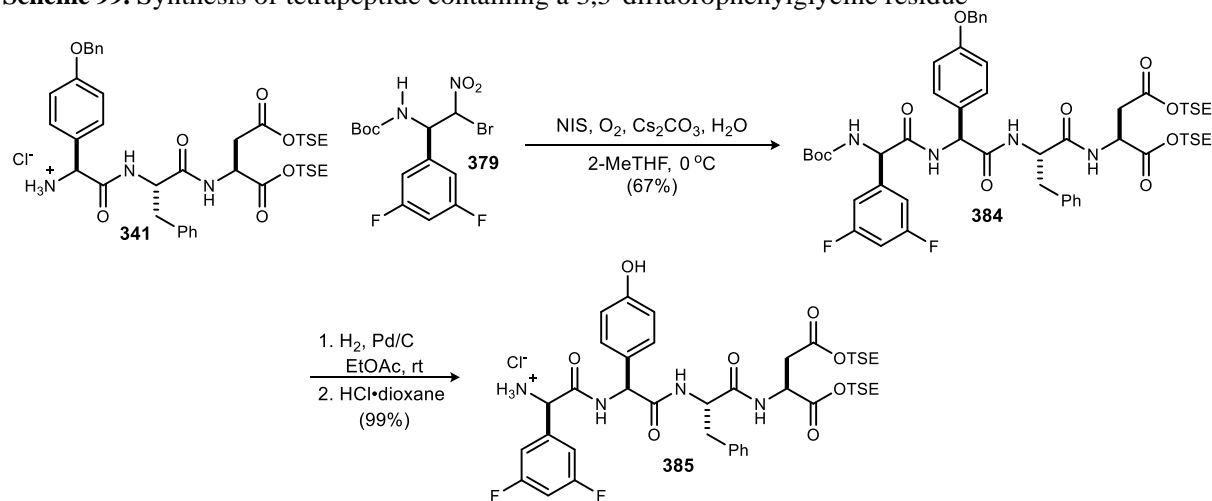
¹¹³ Vorogushin, A. V.; Huang X.; Buchwald, S. L. *J. Am. Chem. Soc.*, **2005**, *127*, 8146

Scheme 98. Synthesis of α -bromonitroalkanes for feglymycin analogues



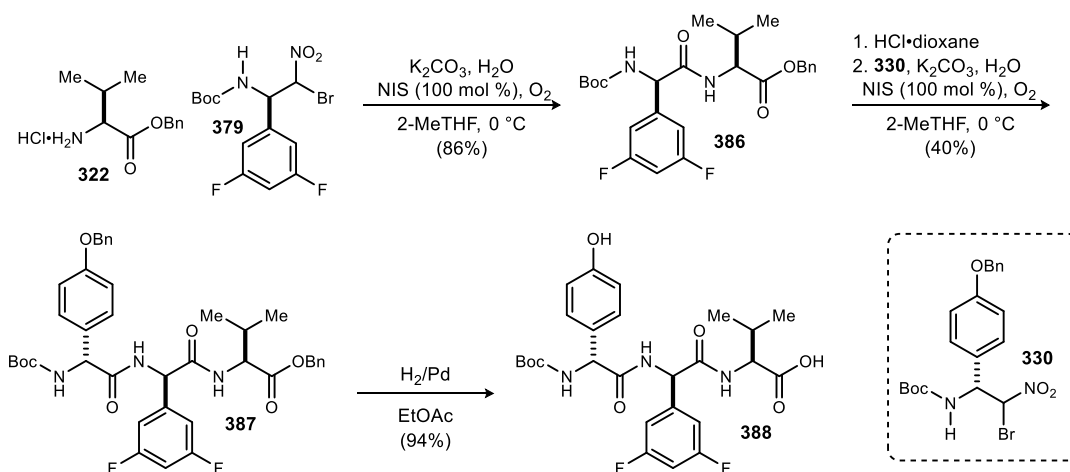
We selected the fluoro analog as the first target for synthesis to then be followed by the preparation of the bromo derivative. The first peptide fragment prepared towards that goal was tetrapeptide **385** containing one 3,5-difluorophenylglycine residue (Scheme 99). Tripeptide **341** was prepared as previously disclosed in the synthesis of Ffeglymycin. Homologation with 3,5-difluoro bromonitroalkane **379** proceeded in good yield (67%) to provide protected tetrapeptide **384**. Benzyl deprotecton followed by Boc deprotection afforded tetrapeptide hydrochloride salt **385** without event.

Scheme 99. Synthesis of tetrapeptide containing a 3,5-difluorophenylglycine residue



Next, 3,5-difluorophenylglycine-containing tripeptide **388** was synthesized (Scheme 100). Dipeptide formation proceeded in excellent yield as the coupling between valine benzyl ester **322** and 3,5-difluorophenylglycine donor **379** provided dipeptide **386** in 86% yield. Boc deprotection and subsequent homologation with benzyloxyphenylglycine donor **330** afforded protected tripeptide **387** in 40% yield. Hydrogenolysis of the phenol and the acid's benzyl protecting groups provided tripeptide **388** in 94% yield.

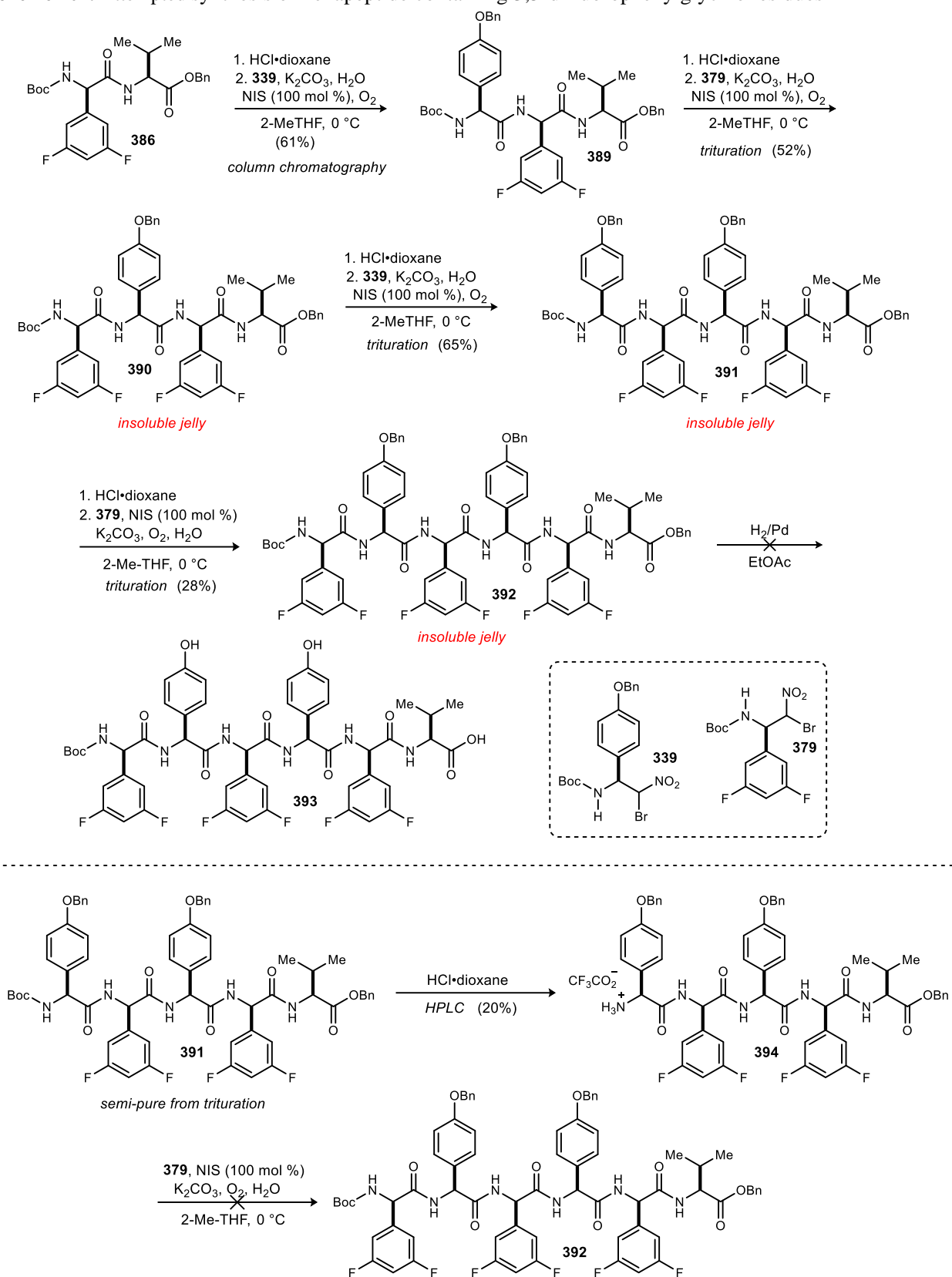
Scheme 100. Synthesis of tripeptide containing a 3,5-difluorophenylglycine residue



With both the tetrapeptide and tripeptide in hand, all that remained was the preparation of the central fragment, hexapeptide **393**. Starting from dipeptide **386**, as prepared in the previous tripeptide synthesis, coupling with benzyloxyphenylglycine donor **338** provided tripeptide **389** in 61% yield (Scheme 101). Subsequent homologation with 3,5-difluorophenylglycine donor **379** afforded tetrapeptide **390** as a relatively insoluble jelly-like compound. Standard column chromatography proved ineffective due to solubility, and trituration with a DCM/hexanes mixture was employed to obtain semi-pure material in 52% yield. Pentapeptide **391** exhibited the same solubility properties and was obtained after the UmAS coupling and trituration in 65% yield. The final homologation step was performed adding the final 3,5-difluorophenylglycine residue with a similar result. Chromatography was not possible and trituration provided semi-pure material that was consistent with the desired hexapeptide. We hoped that after hydrogenolysis the resulting deprotected peptide would be able to be purified by reverse-phase preparative HPLC. However, no desired product was obtained from attempts at purification.

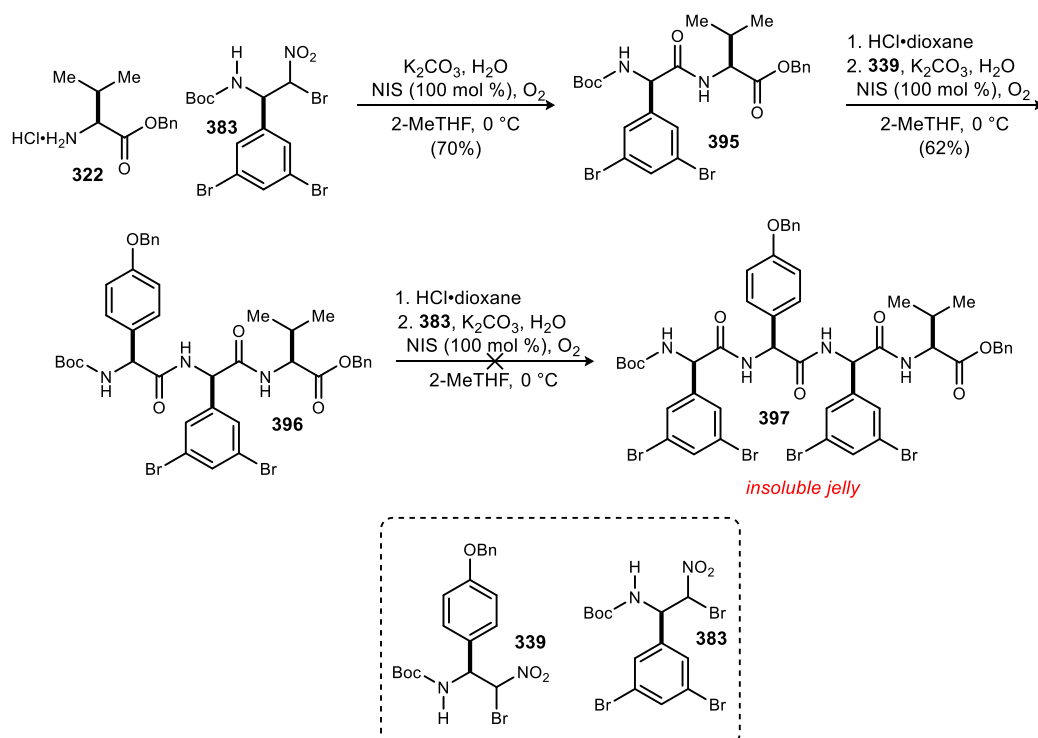
As we were unsure if hexapeptide **392** had even been formed from the previous reaction sequence due to difficulties with purification, we sought a better solution for purification of an earlier intermediate. We have had previous success in purifying the peptide amine salts using HPLC so we targeted deprotected pentapeptide **394** as the desired point of purification. Pentapeptide **391** was submitted to HCl in dioxane to remove the Boc protecting group and then submitted to HPLC purification (Scheme 101). An amount of 500 mg of semi-pure pentapeptide **391** provided 100 mg (20% yield) of the pure deprotected pentapeptide TFA salt. The pure material was submitted to the final UmAS coupling with 3,5-fluorophenylglycine donor **379** resulting in a complex mixture with no sign of the desired product. At this point, the synthesis of this derivative was abandoned due to solubility and purification issues.

Scheme 101. Attempted synthesis of hexapeptide containing 3,5-difluorophenylglycine residues



We next moved on to the synthesis of bromo feglymycin analogue **375**. We hypothesized that the solubility issues observed with the previous fluoro analogue may appear in this synthesis as well due to the same 3,5-substitution of the arylglycine residues. For that reason, we started with the synthesis of the hexapeptide fragment (Scheme 101). In the event, dipeptide **395** was prepared from the coupling of valine benzyl ester **322** and 3,5-dibromophenylglycine donor **383** in 70% yield. Further homologation with benzyloxyphenylglycine donor **339** provided tripeptide **396** in 62% yield. Boc deprotection with HCl in dioxane and attempted coupling with 3,5-dibromophenylglycine donor **383** resulted in the generation of an insoluble jelly-like compound similar to that observed with the 3,5-difluoro analog. This result further supported our hypothesis that the 3,5-substitution was the cause of the solubility and thus purification issues encountered. For that reason, synthesis of this derivative was also abandoned.

Scheme 102. Attempted synthesis of hexapeptide containing 3,5-dibromophenylglycine residues



The original goal of this study was to demonstrate the utility of the aza-Henry/UmAS reaction combination in peptide synthesis with unnatural amino acids. The successful synthesis of Ffeglymycin spotlighted the impact UmAS can have on iterative peptide synthesis as difluorophenylglycine was seamlessly incorporated within the feglymycin peptide framework. Although the unsuccessful syntheses highlighted limitations of UmAS, they also highlighted general limitations of arylglycine-rich peptide synthesis. The struggles associated with the synthesis of the other derivatives and feglymycin itself were mostly based on the poor solubility of arylglycine-rich, a challenge acknowledged by Süßmuth.¹¹⁰ This fact further demonstrates the need for new methods for peptide synthesis incorporating unnatural amino acid residues.

Chapter 5

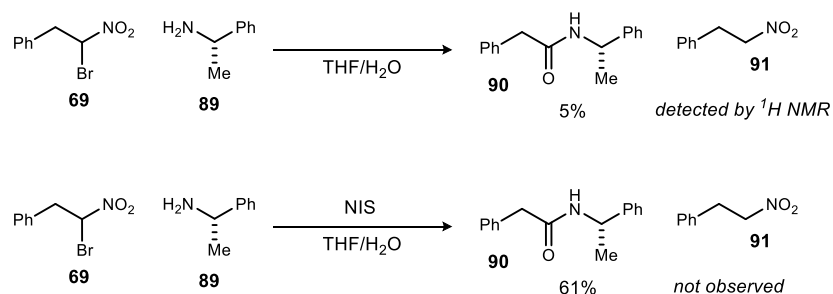
V. Umpolung Amide Synthesis: Mechanistic Investigation

5.1 UmAS: Current Mechanistic Understanding

The reaction of α -halonitroalkanes and amines promoted by a halonium source under basic conditions, termed Umpolung Amide Synthesis (UmAS), has proven to be a powerful reaction. Combined with the enantioselective aza-Henry reaction, UmAS allows for the goal of peptide synthesis using solely enantioselective and catalytic methods to be achieved. Understanding the mechanism of this novel transformation will facilitate further improvements (as discussed in section 1.3) to the reaction as well as potentially reveal opportunities for new reaction development.

Our current understanding of the UmAS mechanism, as described in section 1.2, features umpolung reactivity in the key C-N bond forming step. The bromonitroalkane, a carbonyl surrogate, is the nucleophilic partner while the amine, activated by NIS, is electrophilic. This C-N bond forming step produces the putative tetrahedral intermediate which ultimately provides amide through one of two potential pathways, anaerobic or aerobic. This mechanistic picture is based on a number of key observations and experiments. When bromonitroalkane **69** was combined with amine **89** and allowed to stir open to air, the amide product was observed in conjunction with debrominated nitroalkane **91**, suggesting bromonium transfer from the bromonitroalkane to the amine (Scheme 103). The same reaction with addition of NIS provided amide in increased yield without detection of nitroalkane **91**. These experiments as well as ^1H NMR characterization of *N*-iodamines (or NIS-amine complex) support the described C-N bond forming step.¹¹⁴

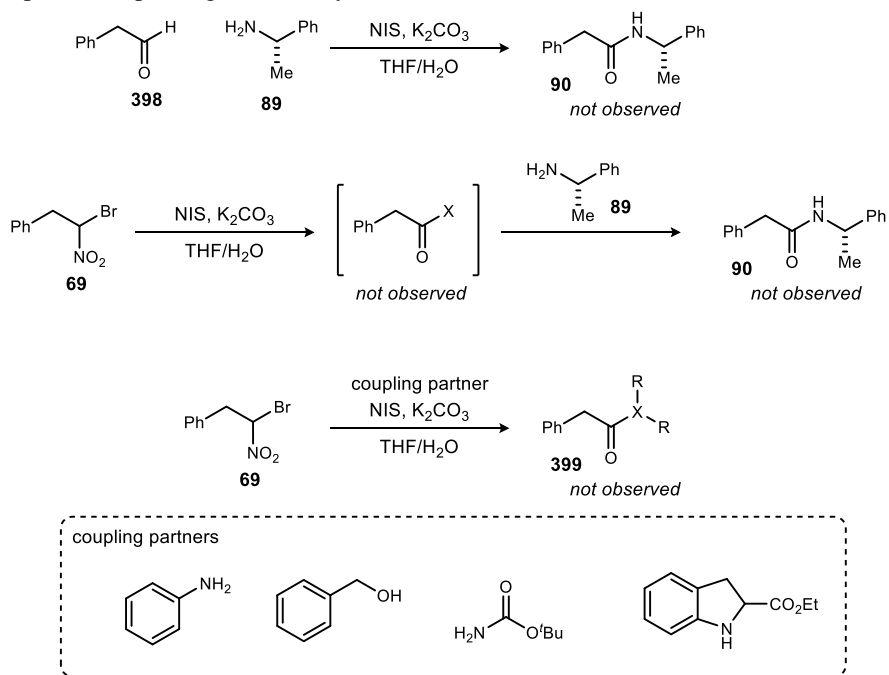
Scheme 103. Early UmAS experiments probing halamine intermediacy



Another possible pathway considered was the generation of an electrophilic carbonyl intermediate from the bromonitroalkane followed by nucleophilic amine addition. An oxidative Nef reaction promoted by NIS could provide an acyl halide or an aldehyde intermediate. In order to probe these possibilities, three key experiments were conducted (Scheme 104).³⁴ First, phenylacetaldehyde was subjected to the reaction conditions to probe it as a potential intermediate. Amide product was not observed suggesting an aldehyde intermediate is unlikely. Next, bromonitroalkane **69** was submitted to standard reaction conditions without the amine coupling partner in order to probe the intermediacy of an acyl halide. Upon full conversion of the bromonitroalkane to a complex mixture (^1H NMR), the amine was added. Amide product was not observed. To further probe the potential for an acyl halide intermediate, the coupling reaction was attempted with a variety of nucleophiles that are readily acylated under standard acylation conditions. Aniline, benzyl alcohol, indolino ester, and Boc-carbamate were all found to be incompetent coupling partners as no

¹¹⁴ Shen, B. *dissertation*, Vanderbilt University, 2010.

Scheme 104. Experiments probing for carbonyl intermediates in UmAS



acylated products were observed. These experiments suggest that an acyl halide intermediate is not operative under UmAS conditions.

In order to probe the potential pathway to amide from the putative tetrahedral intermediate, ¹⁸O isotopic labeling experiments were conducted (Scheme 105).³⁶ Under anaerobic conditions (or open to air), ¹⁸O incorporation was not observed when H₂¹⁸O was used ruling out a possible hydrolysis of the tetrahedral intermediate. When the nitro group was ¹⁸O labeled, significant ¹⁸O incorporation in the amide product was observed. Under aerobic conditions using ¹⁸O₂, the amide product was obtained with high ¹⁸O incorporation. These experiments call for two distinct pathways to amide, one featuring oxygen incorporation from the nitro group with the other having oxygen incorporation from O₂. Figure 42 outlines our current mechanistic understanding based on these and other experiments and observations.

Scheme 105. Isotopic labeling experiments probing UmAS mechanism

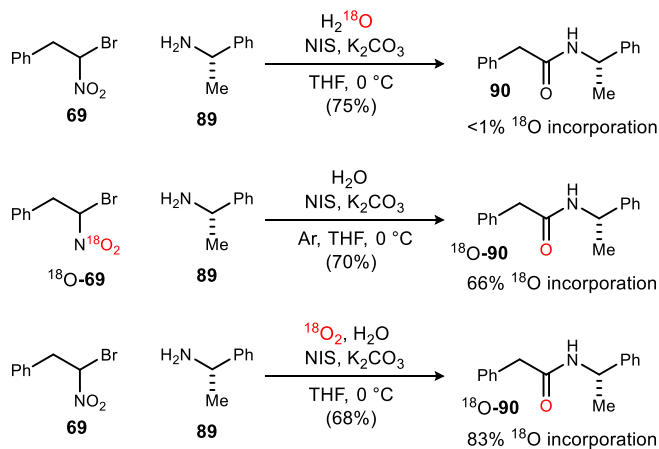
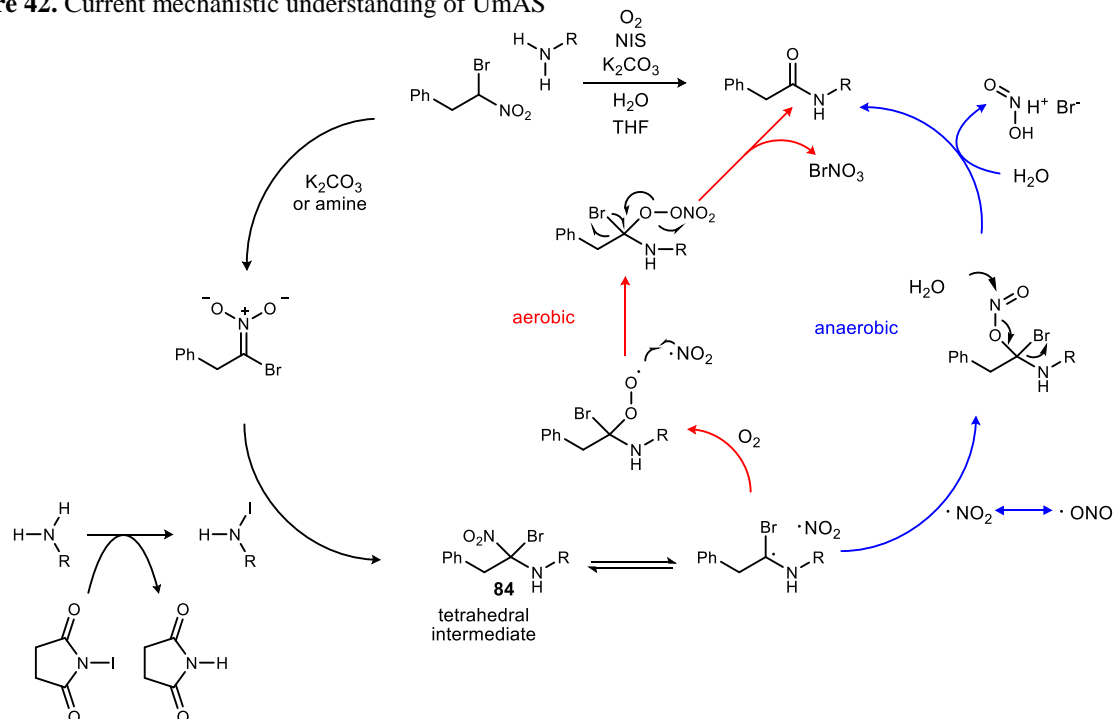


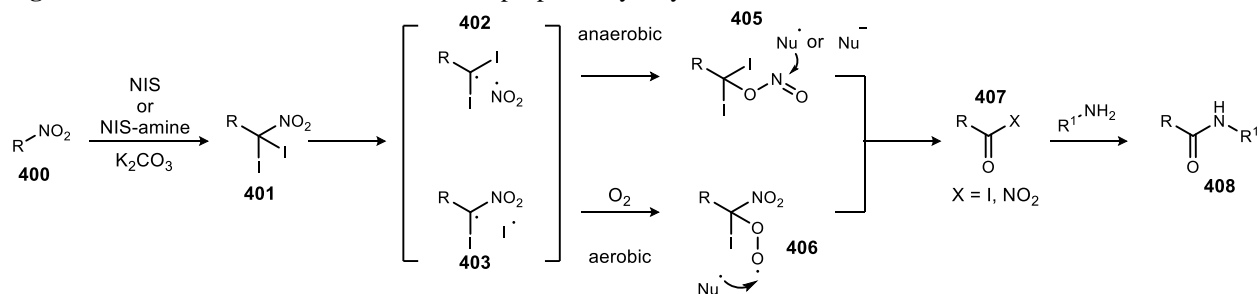
Figure 42. Current mechanistic understanding of UmAS



Hayashi-Lear: Nitroalkane Amidation Mechanism

Recently, Hayashi and coworkers proposed an alternative mechanistic pathway for ostensibly the same amide forming reaction (Figure 43).¹¹⁵ Starting from nitroalkane **400**, they propose diiodination with NIS or an NIS-amine complex to provide diiodonitroalkane **401** as the entry point to the amide bond forming pathway. Homolysis of either the C-NO₂ bond or a C-I bond generates a radical intermediate. Under anaerobic conditions, the diiodo radical combines with the nitrite radical followed by nitrosyl transfer to form key acyl halide intermediate **407**. Under aerobic conditions, the alkyl radical is trapped with O₂ followed by combination with a nucleophile and subsequent breakdown to form the same active ester intermediate **407**. Nucleophilic acyl substitution with the amine yields the amide product.

Figure 43. Alternative mechanism for UmAS proposed by Hayashi

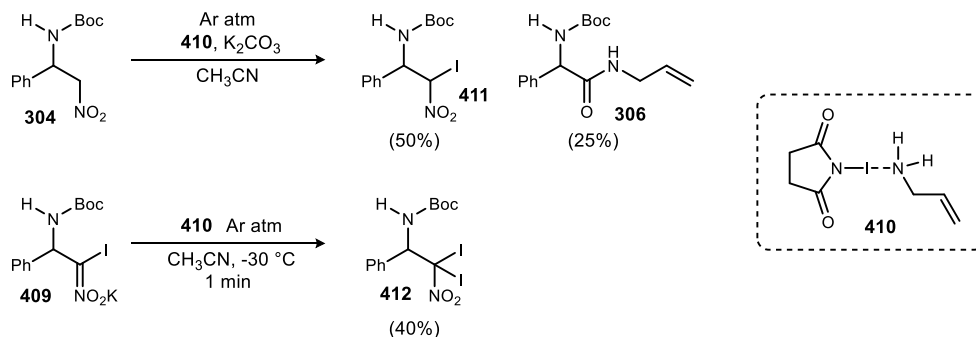


Hayashi and coworkers came to this rationale through a series of key experiments and observations. First, in attempts to generate an *N*-halamine with NIS and allyl amine, NIS-amine complex **410** (structure confirmed by X-ray analysis) was isolated instead of an *N*-iodamine. Combining NIS-amine complex **410** with either nitroalkane **304** or iodonitronate **409** did not result in observation of an aminonitroalkane species (our tetrahedral intermediate) but instead observed monoiodonitroalkane **411** and diiodonitroalkane **412**,

¹¹⁵ Li, J.; Lear, M. J.; Kwon, E.; Hayashi, Y. *Chem. Eur. J.* **2016**, *22*, 5538-5542.

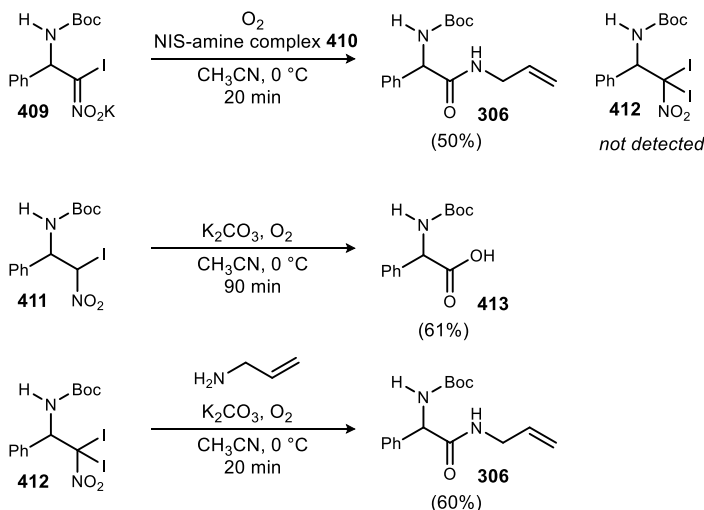
respectively (Scheme 106). Two conclusions were drawn (by Hayashi and co-authors) from these experiments: 1) an *N*-iodamine is not generated in the reaction and 2) NIS-amine complex acts as an iodonium source and not an electrophilic amine source.

Scheme 106. Hayashi's key experiments: NIS-amine complex



The observation of diiodonitroalkane **412** and not tetrahedral intermediate **84** led Hayashi to investigate if diiodonitroalkane **412** is a precursor to amide (Scheme 107). When nitronate **409** was treated with NIS-amine complex **410** under aerobic conditions, amide product was obtained without detection of diiodonitroalkane **412**. Additionally, when iodonitroalkane **411** was treated with base and O₂ in the absence of amine, carboxylic acid was obtained presumably through disproportionation of **411** to form **304** and **412** followed by reaction of **412** with O₂. These experiments led to them to conclude that diiodonitroalkane **412** is capable of reacting directly with O₂ to form either amide or acid depending on the presence or absence of amine. When diiodonitroalkane **412** was isolated and submitted to the amide forming conditions, the amide product was indeed isolated in 60% yield.

Scheme 107. Hayashi's key experiments: diiodonitroalkane



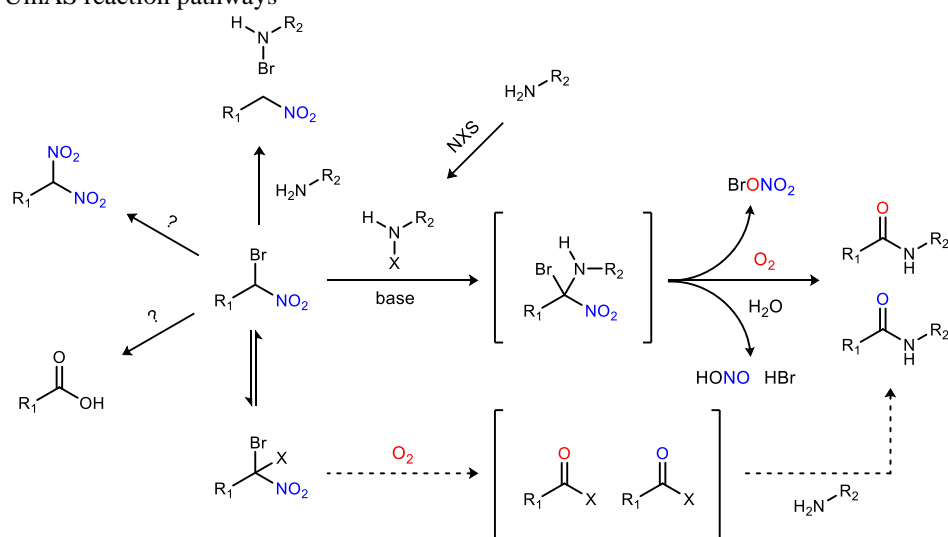
Isotopic labelling experiments were also conducted with ¹⁸O₂ similar to those reported by our group. The results were identical in that a large percentage of incorporation was observed in the amide product which is consistent with both proposed mechanisms. Based on these experiments Hayashi proposed the mechanism described in Figure 43. The key differences between the two reported mechanisms are 1) the intermediacy of an acyl halide species vs. tetrahedral intermediate **84**, 2) NIS-amine complex acting as iodonium-only source vs. electrophilic amine, and 3) diiodonitroalkane as entry to the amide forming

process vs. monohalogenoalkane. Together these differences result in fundamentally different mechanisms where the polarity of the components in the C-N bond forming step are switched, one with traditional polarity (Hayashi-Lear) and one with umpolung polarity (Johnston).

5.2 UmAS: Mechanistic Investigation

After careful review of Hayashi's proposed alternative mechanism, we sought to further elucidate the mechanism of amide formation from α -halonitroalkanes. Scheme 108 diagrams all known pathways and side reactions present in UmAS as determined from experiments in our lab as well as those reported by Hayashi. The goal of this investigation is to study and characterize every transformation and interaction in order to differentiate between the two proposed mechanisms and ultimately provide strong evidence for a particular mechanism.

Scheme 108. UmAS reaction pathways

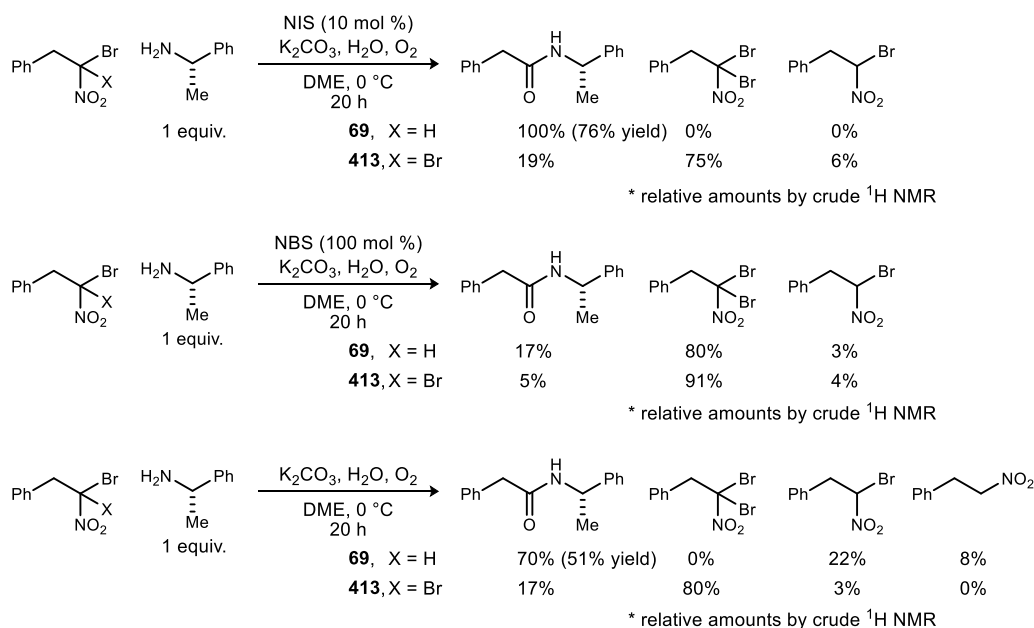


Dihalonitroalkane vs. Monohalonitroalkane

As a starting point, we chose to analyze the relationship between monohalonitroalkanes and dihalonitroalkanes. This is a key difference in the two mechanistic proposals as Hayashi suggests that a dihalonitroalkane enters the amide forming pathway while we believe that the monohalonitroalkane is the starting point for amide formation. In the past, we have observed dihalonitroalkanes in the UmAS reaction mixture, especially when using NBS as the halonium source, and have shown them to be competent precursors to amide, albeit at a much slower rate compared to the monohalonitroalkane counterpart. We hypothesized that the dihalonitroalkane is generated in the reaction mixture as a resting state and is in equilibrium with the monohalonitroalkane. In order to test this hypothesis, we first chose to benchmark the reactivity of bromonitroalkane **69** and dibromonitroalkane **413** across three different sets of reaction conditions (Scheme 109). When bromonitroalkane **69** was submitted to standard UmAS conditions with 10 mol % NIS, full conversion was observed with the amide as the only product (76% isolated yield). In contrast, under the same conditions, dibromonitroalkane **413** provided poor conversion to amide as a significant amount of starting material remained. The formation of amide and monobromo nitroalkane in this experiment, while leaving much dibromonitroalkane unreacted, might indicate the slow action of amine to form *N*-bromo amine and α -bromonitronate. This pair may lead to amide (via either *N*-bromo or *N*-iodo amine) or monobromo nitroalkane (via protonation). In a second set of experiments, halonitroalkanes **69** and **413** were submitted to UmAS conditions with 100 mol % NBS. After 20 h, each reaction mixture

contained predominantly dibromonitroalkane **413** with low yield of amide. One would expect the types of products in this reaction and the NIS reaction (*vide supra*) to be identical, but their relative amounts should reflect a difference in reactivity based on electrophilic iodine vs. bromine intermediates. However, the use of stoichiometric NBS, which can limit the amount of nucleophilic amine available to debrominate **413**, may also be the cause of low conversion. The third set of reactions removed the halonium reagent (NIS/NBS) source from the reaction conditions. Under these conditions, bromonitroalkane **69** provided amide in 51% yield while minimal conversion was observed in the case of dibromonitroalkane **413** as the yield for the amide was <20%. These experiments seem to favor bromonitroalkane as opposed to dibromonitroalkane as entry to the amide forming pathway due to the higher conversion and higher yield of amide observed over a set of different conditions when starting with bromonitroalkane. However, the potential for an equilibrium between monohalogenitroalkane and dihalogenitroalkane is not directly addressed by these examples.

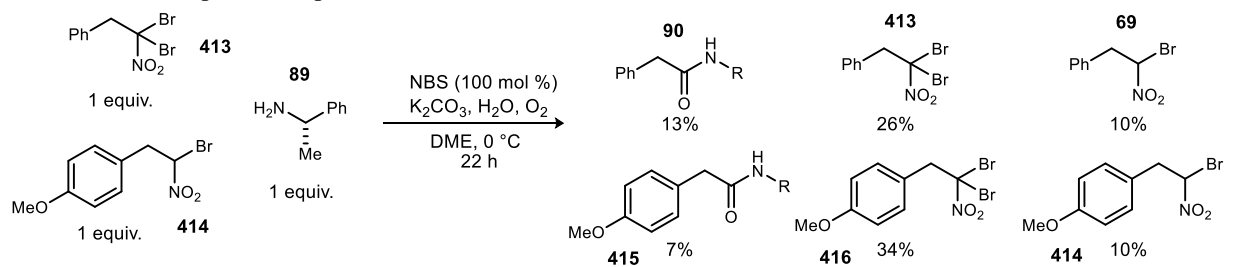
Scheme 109. Comparison of bromonitroalkane and dibromonitroalkane in UmAS



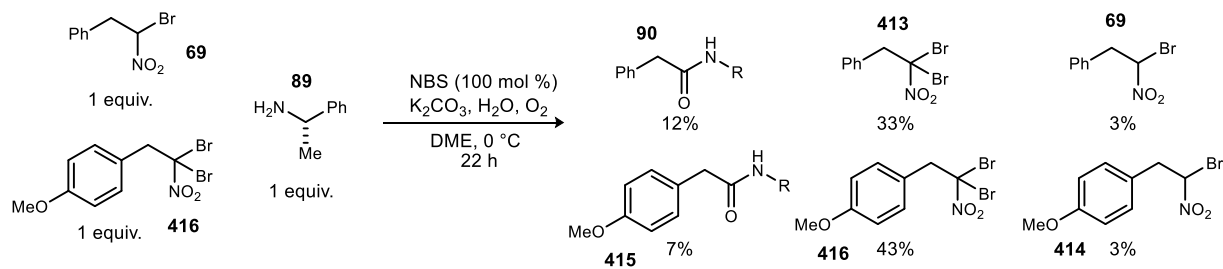
In order to further probe the behavior of monohalogenitroalkanes and dihalogenitroalkanes, a set of competition experiments were conducted. In the first experiment, dibromonitroalkane **413** and methoxy-bromonitroalkane **414** were combined in equal amounts (1 equiv. each) and submitted to UmAS conditions with 100 mol % NBS and 1 equiv. amine. Analysis of the crude reaction mixture by ¹H NMR revealed the presence of six different compounds: amide, bromonitroalkane, and dibromonitroalkane derived from each starting material (Scheme 110), making it immediately evident that amine-mediated (as a base and/or nucleophile – *vide infra*) bromine transfer is operative. Amide **90** from dibromonitroalkane **413** was almost twice as prevalent as amide **415** from methoxy-bromonitroalkane **414**. Dibromonitroalkanes **413** and **416** constituted a majority of the reaction mixture. The ratio of amide products seems to favor amide formation from dibromonitroalkane vs. bromonitroalkane, however the significant amount of each dibromonitroalkane refutes that theory. The same experiment was run in which methoxy-dibromonitroalkane **416** and bromonitroalkane **69** were employed to look for substrate bias in amide formation. The results of the second experiment mimicked that of the first where phenyl amide **90** was obtained in approximately twice the yield of methoxy amide **415**. The combined results of these two experiments in which almost identical ratios of products were observed regardless of which substrate began

as the dibromonitroalkane strongly support halonium transfer amongst the nitroalkanes on the reaction time scale.

Scheme 110. Competition experiments between bromonitroalkanes and dibromonitroalkanes in UmAS



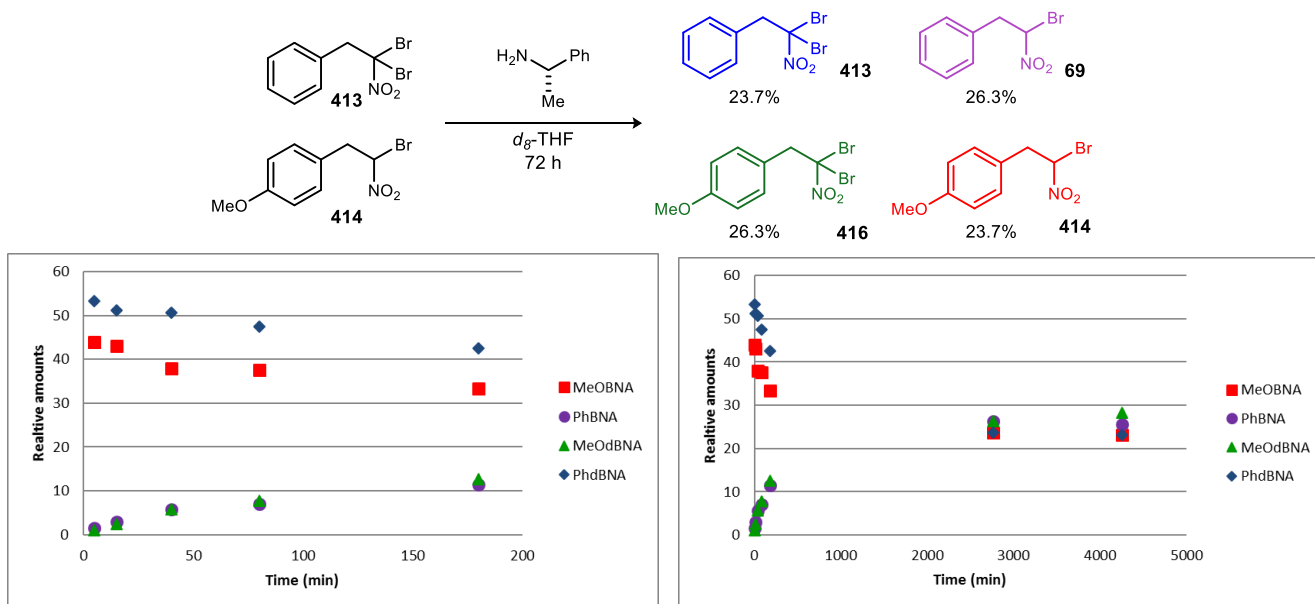
* relative amounts by crude ^1H NMR



* relative amounts by crude ^1H NMR

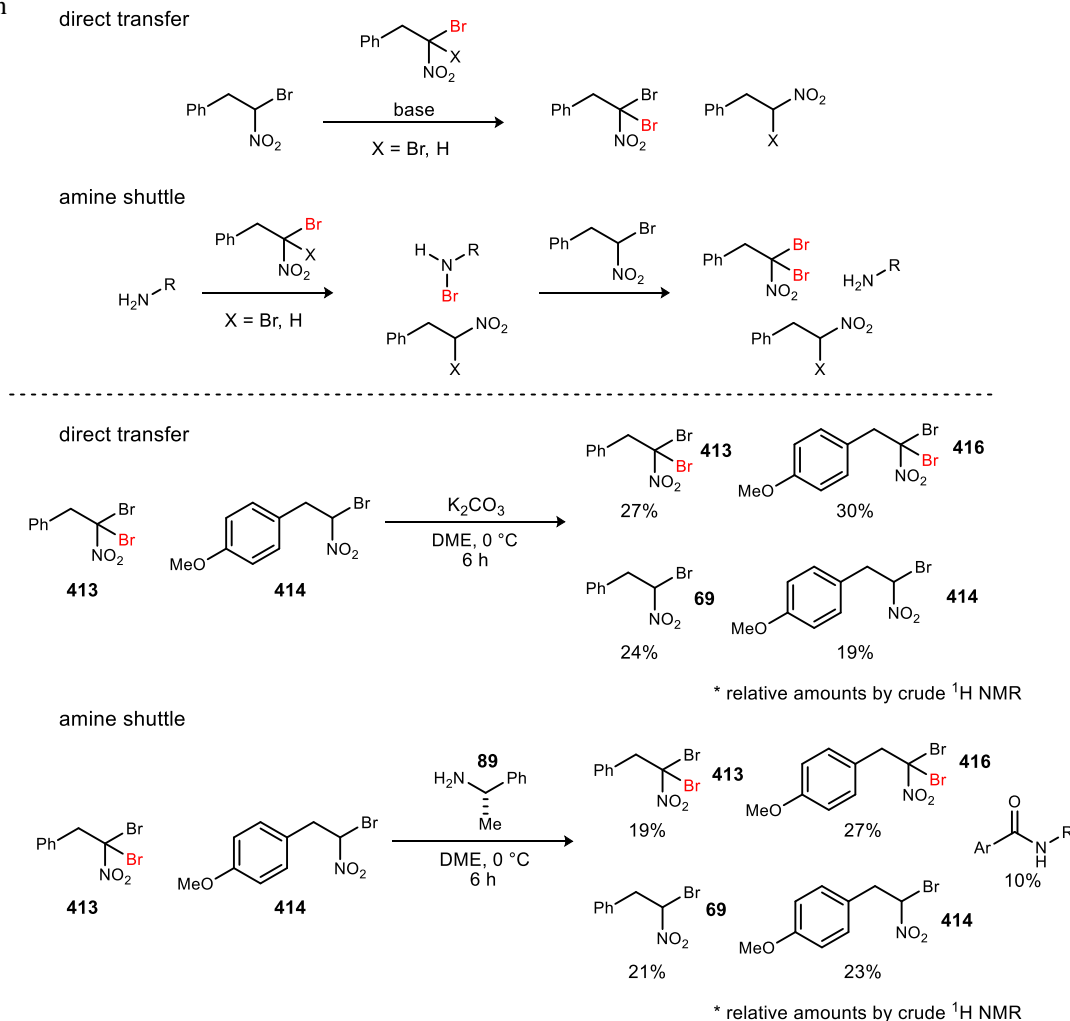
A ^1H NMR experiment was conducted to further characterize the equilibrium between dibromonitroalkane and bromonitroalkane (Figure 44). Phenyl dibromonitroalkane **413** was combined with methoxy bromonitroalkane **414** and 1 equivalent amine in d_8 -THF. ^1H NMR spectra were obtained at 5, 15, 40, 80, 180, 2760, and 4260 minutes after addition of the amine. Immediate formation of phenyl bromonitroalkane **69** and methoxy dibromonitroalkane **414** was observed as shown in Figure 44. After 46 hours (2760 min), the reaction appeared to have reached equilibrium with almost a statistical mixture of compounds as no significant change was observed between that time point and 71 hours (4260 min). Based on the initial observed rate, equilibrium should have been reached after approximately 400 min. This

Figure 44. Bromonium transfer between dibromonitroalkane and bromonitroalkane



experiment verifies the that the bromonitroalkane and dibromonitroalkane are in fact in equilibrium and that halonium transfer occurs on the reaction time scale.

Scheme 111. Possible mechanisms of halonium transfer and experiments to probe them during bromonitroalkane amidation

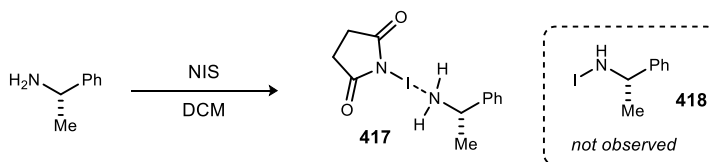


We next investigated the mechanism of halonium transfer. There are two possible mechanisms: direct nitroalkane to nitroalkane transfer and amine shuttle (Scheme 111). In the former, the nitronate of one bromonitroalkane is directly brominated by another equivalent of bromonitroalkane. In the amine shuttle mechanism, the amine is first brominated and acts as a bromonium source for the nitronate. Two different experiments were conducted to probe the mechanism (Scheme 111). In the first, dibromonitroalkane **413** and bromonitroalkane **414** were combined and treated with K_2CO_3 . Bromonium transfer occurred as dibromonitroalkane **416** was observed, providing evidence for the direct transfer mechanism. Similarly, dibromonitroalkane **413** and bromonitroalkane **414** were combined with amine **89** and allowed to stir for 6 hours. All four possible halonitroalkanes were observed in addition to a small amount of each amide product. This result provides evidence for an amine shuttle mechanism, although the direct transfer mechanism could also be operable under these conditions. The formation of amide would seem to support an amine shuttle mechanism as the bromamine intermediate could lead to amide. However, under the mechanism proposed by Hayashi, amide is formed from the dibromonitroalkane and does not need a haloamine intermediate. Overall, these experiments suggest that halonium transfer can occur via either mechanism, and at a rate competitive with amide formation.

N-Iodamine and other Electrophilic Amine Sources

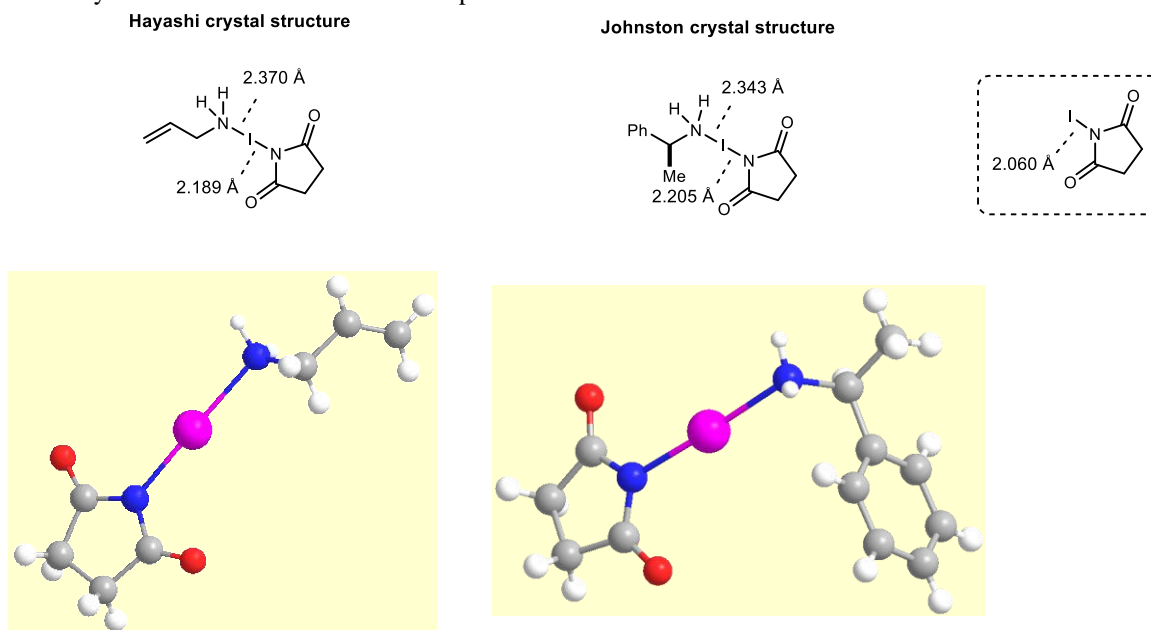
The crux of our proposed mechanism is the combination of the nucleophilic nitronate and the electrophilic *N*-iodamine. Although *N*-iodamines (and other haloamines) have been proposed as electrophilic amine sources numerous times,¹¹⁶ their isolation and characterization have received significantly less attention.¹¹⁷ We sought to prepare and characterize an alkyl *N*-iodamine to provide evidence for their existence and reactivity as an electrophilic amine.

Scheme 112. Attempted preparation of *N*-iodamine with α -methyl benzylamine



Our preferred iodamine target was *N*-iodo α -methyl benzylamine **418**, ideally prepared using NIS as the iodonium source to be as similar as possible to UmAS conditions. The combination of NIS and α -methyl benzylamine in DCM resulted in the formation of a precipitate that was consistent with the putative *N*-iodamine previously observed by ¹H NMR (Scheme 112) and further characterized by HRMS (ESI). In order to definitively assign the structure of the precipitate, we grew a single crystal for X-ray analysis in MeOH. X-ray analysis revealed that the precipitate was NIS-amine complex **417** similar to the complex observed by Hayashi (**410**) with allyl amine. Analysis of the N-I bond lengths in both NIS-amine complex crystal structures revealed a lengthening of the N_{suc}-I bond compared to that of NIS (Figure 45). This bond

Figure 45. Crystal structures of NIS-amine complexes



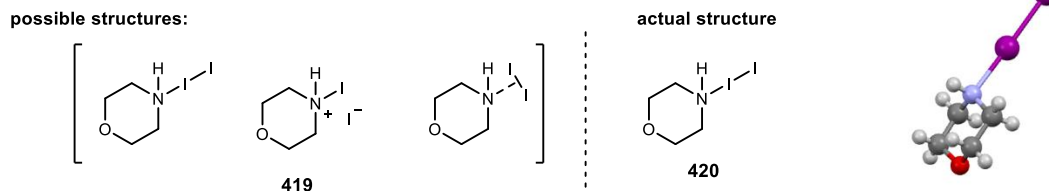
¹¹⁶ Erdik, E.; Ay, M. *Chem. Rev.* **1989**, 89, 1947-1980; Kovacic, P.; Lowery, M. K.; Field, K. W. *Chem. Rev.* **1970**, 70, 639-665; Sinha, P.; Knochel, P. *Synlett* **2006**, 2006, 3304-3308.

¹¹⁷ Wille, U., In *Science of Synthesis*, Enders, D; Schaumann, E., Eds.; Thieme: Stuttgart, (2009); Vol. 40b, 893

lengthening signifies that the iodonium transfer process has begun. We hypothesized that the transfer process may need an additional impetus to go to completion. The addition of base may facilitate the necessary proton transfer from the amine to succinimide. Both an amine base (Et_3N) and an inorganic base (Na_2CO_3) were added to NIS-amine complex **417** in DCM without observation of anything resembling the desired iodamine by ^1H NMR.

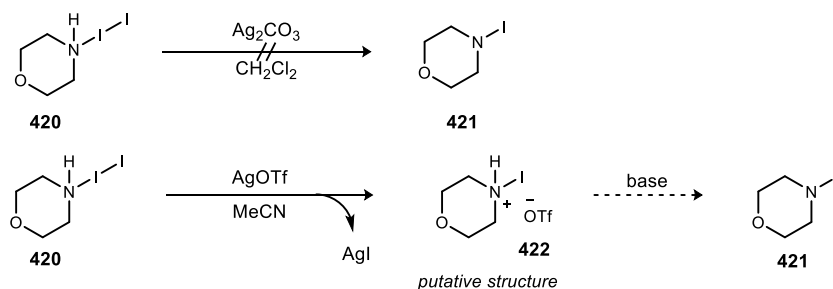
As we were unable to confirm the formation of the desired iodamine, our interest shifted to *N*-iodomorpholine hydroiodide (**419**). *N*-Iodomorpholine hydroiodide was first prepared and reported in 1943 and is now commercially available.^{118,119} It has been described as both an amine-iodine complex as well as the hydroiodide salt of *N*-iodomorpholine and shown to act as an iodonium source. Furthermore, it was used to postulate an *N*-iodamine as a reactive intermediate in an amination reaction.¹²⁰ Although this compound has been known for over half a century, to our knowledge the exact structure has yet to be determined. In order to determine the structure, *N*-iodomorpholine hydroiodide crystals were grown from MeOH for X-ray analysis. The crystal structure is consistent with an amine-iodine complex, similar to the amine-NIS complexes previously described (Figure 46).

Figure 46. Crystal structure of morpholine-iodine complex



As the goal remained the preparation and characterization of a bona fide iodamine, we sought to convert the amine-iodine complex to the desired *N*-iodomorpholine. Treatment with silver (I) could remove iodide through precipitation of silver iodide while exposure to base could remove the ammonium proton allowing conversion to the iodamine. In the event, iodomorpholine complex **420** was treated with AgCO_3 in DCM (Scheme 113). No precipitation was observed and ^1H NMR revealed no changes. The same transformation was then attempted in two separate steps. First, iodomorpholine complex **420** was treated with silver triflate to remove iodide. Morpholine-iodine complex **420** was dissolved in acetonitrile followed by the addition of AgOTf . Immediate precipitation (presumably AgI) was observed. Filtration and concentration provided a sticky amorphous solid thought to be iodomorpholine triflate **422**. ^1H NMR showed a shift in morpholine peaks while a peak in ^{19}F NMR provided evidence supporting the putative

Scheme 113. Attempts at preparing *N*-iodomorpholine



¹¹⁸ Rice, V. R.; Beal, G. D. US2290710 A, **1943**.

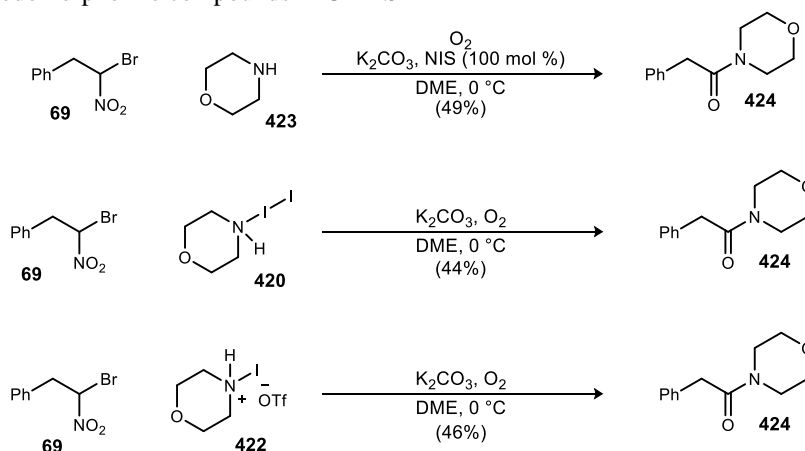
¹¹⁹ Sigma Aldrich, item number: 730556

¹²⁰ Southwick, P. L.; Christman, D. R. *J. Am. Chem. Soc.* **1952**, *74*, 1886-1891; Froehr, T.; Sindlinger, C. P.; Kloeckner, U.; Finkbeiner, P.; Nachtsheim, B. J. *Org. Lett.* **2011**, *13*, 3754-3757.

structure. In order to verify the structure, a crystal structure must be obtained. Efforts to grow a crystal have proven difficult and are ongoing. When the putative iodomorpholine triflate was treated with base a slight shift in peaks by ^1H NMR was observed, but ^{19}F NMR still showed the presence of fluorine.

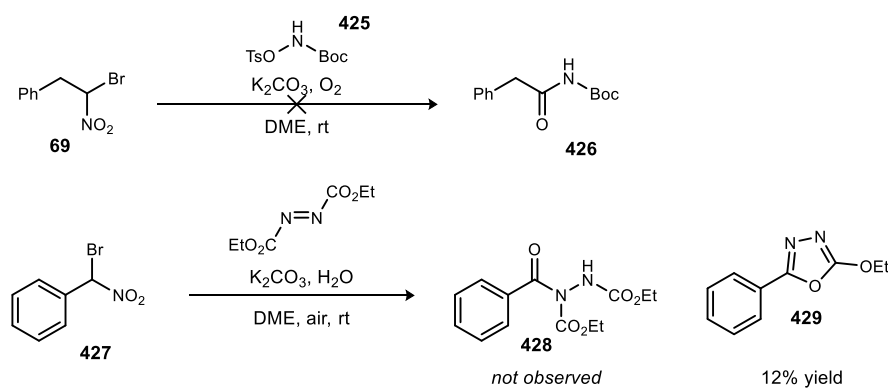
The other aspect of this investigation is to demonstrate that the iodamine or iodamine complexes are competent in UmAS. As a benchmark, morpholine was coupled with bromonitroalkane **69** under standard UmAS conditions to provide amide **424** in 49% yield (Scheme 114). Both morpholine-iodine complex **420** and iodomorpholine triflate **422** provided amide in similar yield under UmAS conditions without NIS (44% and 46%). These results support our hypothesis that an *N*-iodamine is the active intermediate in UmAS, however, both compounds can conceivably act as iodonium sources allowing for the alternative mechanism of amide formation to be functional.

Scheme 114. Iodomorpholine compounds in UmAS



In addition to the preparation and characterization of an *N*-iodamine to support the proposal of an electrophilic amine in UmAS, the use of other electrophilic amine sources could serve the same purpose. If a different electrophilic amine was a capable coupling partner with a bromonitroalkane under NIS-less UmAS conditions, it would strongly support the umpolung aspect of the mechanism. To date, two different electrophilic amines have been investigated for the utility in UmAS (Scheme 115). Tosyl-protected hydroxyl Boc-amine **425** was found to be unreactive under UmAS conditions. The other electrophilic amine source, DEAD, did not provide the desired amide as the reaction resulted in a complex mixture. Analysis of the reaction mixture revealed the formation of oxadiazole **429**.¹²¹ The formation of the oxadiazole was

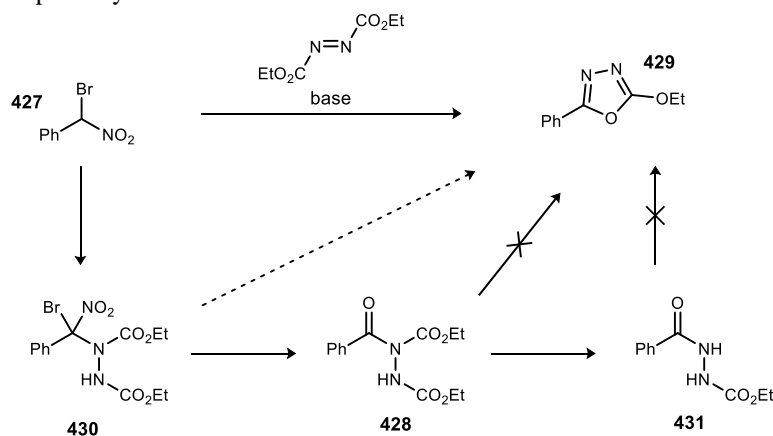
Scheme 115. UmAS with other electrophilic amine sources



¹²¹ Tokumaru, K; Johnston, J. N. *unpublished*.

of interest as the mechanistic pathway could be similar to that of UmAS. Scheme 116 shows possible mechanistic pathways for oxadiazole formation from bromonitroalkane **427** and DEAD. Starting with the assumption that the bromonitroalkane combines with DEAD to form tetrahedral intermediate **430**, there are two straightforward pathways to oxadiazole. Intermediate **430** could proceed to amide formation followed by dehydrative cyclization and decarboxylation. Alternatively, the amide could undergo decarboxylation first followed by cyclization. Both of these pathways were ruled out as authentic samples of **428** and **431** were prepared and submitted to reaction conditions without oxadiazole formation. A third pathway, presumably from tetrahedral intermediate **430** is likely operative.

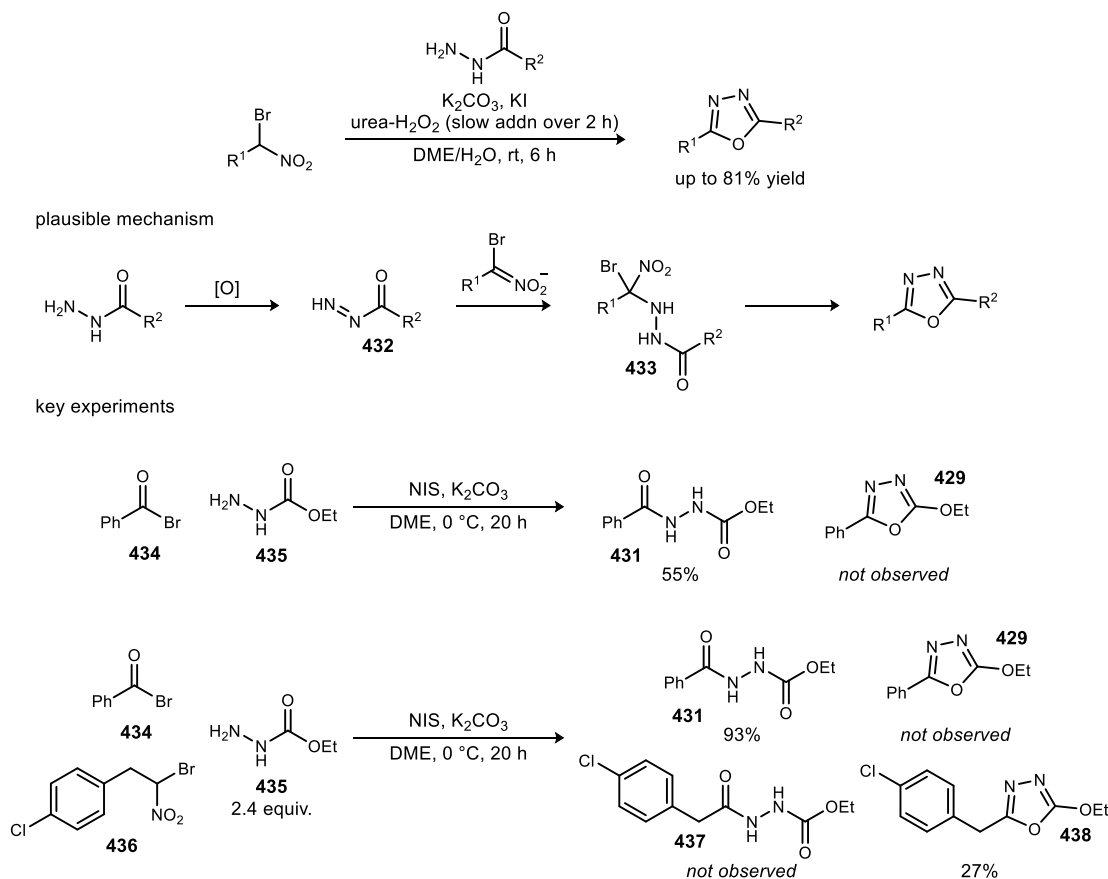
Scheme 116. Possible pathways of oxadiazole formation¹²¹



Optimization of the oxadiazole formation from bromonitroalkanes led to the conditions described in Scheme 117.¹²² It was found that improved yields (up to 81%) were obtained when the azodicarboxylate was replaced with the combination of an oxidant and an acyl hydrazine. More pertinent to this discussion is the mechanistic pathway for oxadiazole formation and how it relates to the UmAS mechanism. The two most likely pathways are similar to the two proposed pathways for amide formation. One involves nitronate attack on an electrophilic amine while the other is a nucleophilic acyl substitution reaction. Two key experiments were conducted that collectively ruled out the formation of an acyl halide (or other active acyl species) (Scheme 117). First, acyl bromide **434** was reacted with acyl hydrazine **435** under oxadiazole-forming conditions. Diacyl hydrazine **431** was obtained in moderate yield while the oxadiazole product was not observed. This experiment shows that the hydrazine can react with an acyl halide if present under the reaction conditions. In the second experiment, acyl bromide **434** and bromonitroalkane **436** were combined with acyl hydrazine **435** under the same conditions. Of the four possible products, only the acylation product from the acyl halide and the oxadiazole from the bromonitroalkane were observed supporting the hypothesis that an acyl halide is not formed from bromonitroalkane **436**. These experiments strongly refute the possibility of an acyl halide intermediate.

¹²² Tokumaru, K.; Johnston, J. N. *manuscript in preparation*.

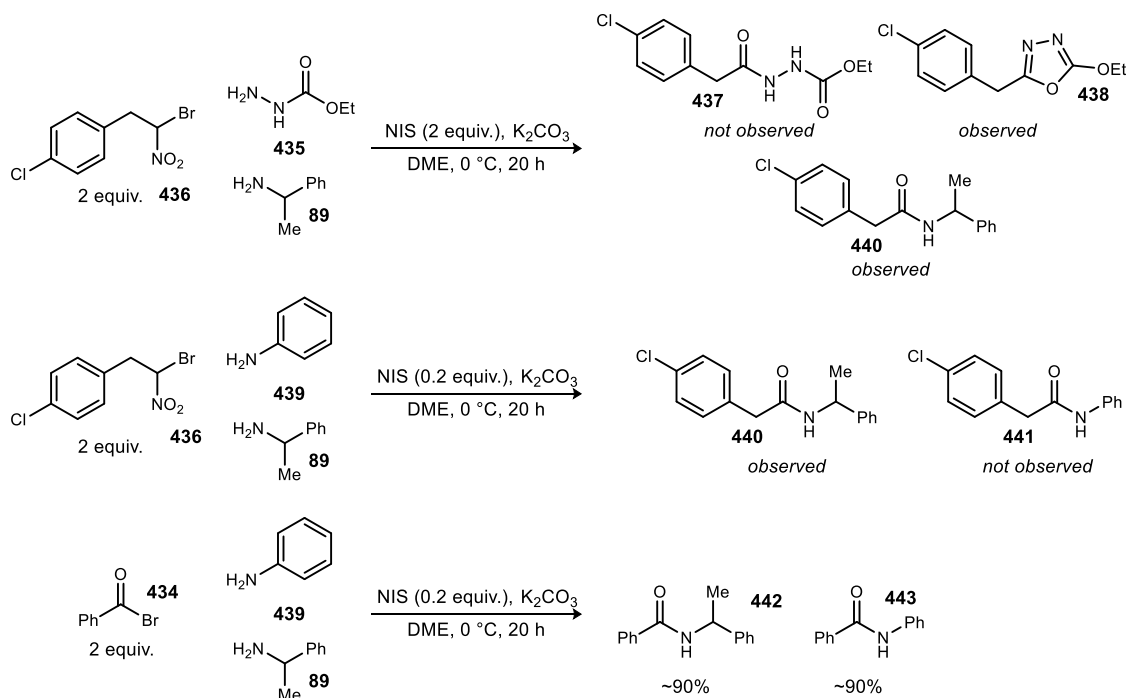
Scheme 117. Oxadiazole formation: optimal conditions and mechanistic investigation¹²²



The mechanistic insight gained from the oxadiazole formation experiments can assist in the investigation of the UmAS mechanism as we now have a simple way to check for an acyl halide intermediate in the reaction. In an experiment designed to probe the potential of an acyl halide intermediate in UmAS, bromonitroalkane **436** was combined with both acyl hydrazine **435** and aliphatic amine **89** resulting in the formation of oxadiazole **438** and amide **440** derived from the amine (Scheme 118). The formation of the oxadiazole product and the absence of diacyl hydrazine **437** was expected based on the previous experiment indicating the absence of an acyl halide intermediate. The presence of the alkyl amine derived amide indicates that amide formation must go through a pathway that does not contain an acyl halide. Two additional experiments were conducted to support these findings taking advantage of the difference of reactivity observed between alkyl amines and aniline in UmAS (Scheme 118). In separate setups, bromonitroalkane **436** and acyl bromide **434** were each combined with aliphatic amine **89** and aniline under UmAS conditions. The reaction with the bromonitroalkane gave amide **440** from the aliphatic amine without formation of aryl amide **441**. Acyl bromide **434** coupled with both amines providing the amides in a 1:1 ratio. These two experiments provide further evidence against an acyl halide intermediate.

The quest to find alternative electrophilic amine sources that were competent in UmAS did not provide conclusive results. However, a novel oxadiazole synthesis was discovered through which mechanistic insight into UmAS was gained. Namely, the existence of an acyl halide reactive intermediate was further contraindicated supporting the umpolung aspect of the amide forming reaction.

Scheme 118. UmAS: probing formation of acyl halide intermediate



Kinetic Studies

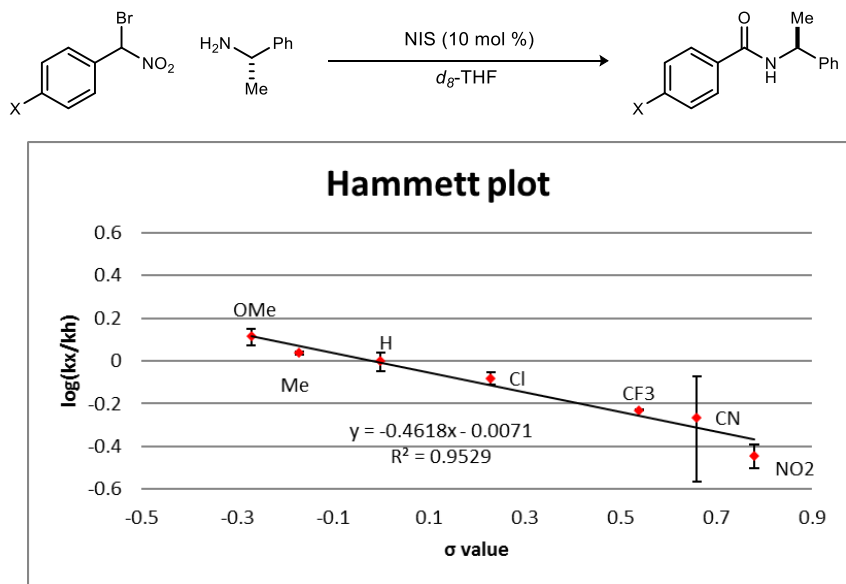
Studying the kinetics of a reaction can provide mechanistic insight. As a start for the analysis of the UmAS mechanism, we chose to construct a Hammett plot to gain information about the rate-determining step. Under our proposed mechanism featuring an electrophilic amine and nucleophilic nitronate, we suspect the rate-determining step is the C-N bond-forming reaction with bromonitroalkane deprotonation as another possibility. Predicting the rate-determining step in Hayashi's alternative mechanism is a little more difficult. Nevertheless, the construction of a Hammett plot can provide evidence for the polarity of the reactants in the rate-determining step and continue to elucidate the mechanism of amide formation.

Seven aryl bromonitroalkanes were selected with varying *para*-substituents as amide precursors to collect kinetic data for the Hammett plot. Modified reaction conditions were employed to allow reproducible data collection. The reactions combined the bromonitroalkane with two equivalents of amine and 10 mol % NIS in *d*₈-THF and were run in an NMR tube at 25 °C. Product formation was tracked by ¹H NMR for the first 60 min of the reaction. Plotting the product formation versus time allowed for the calculation of the initial rate (*k*) of each reaction. Each substrate was run in duplicate and the average of the initial rates was used to construct a Hammett plot (Figure 47).

The Hammett plot provided a good substituent correlation with an R² value of 0.95. The observed ρ value (slope) of -0.46 signifies a moderate substituent effect in which positive charge is built up (or negative charge is lost) in the rate-determining step. In this case it is more straightforward to view the reaction as losing negative charge in the rate-determining step, meaning the bromonitroalkane is nucleophilic in the rate-determining step. To put it another way, electron donating substituents increase the rate of the reaction while electron withdrawing substrates decreased the rate of the reaction signifying nucleophilic reactivity. These results support the hypothesis that the rate-determining step is the C-N bond forming step with a nucleophilic nitronate and an electrophilic amine and preclude the deprotonation of the nitronate as the rate-determining step. How these results factor in to differentiating the two proposed mechanisms is a much more difficult question. The rate-determining step of Hayashi's proposed mechanism

is likely either the homolysis of the C-I (or C-NO₂) bond or the addition of the resulting radical with O₂ (or NO₂ radical under anaerobic conditions). The rate-determining step could also be the nucleophilic addition of the amine to an acyl halide, which seems to be excluded based on previous experiments as well as this Hammett correlation. Determining the polarity of the other two options is not so straightforward. Although clear differentiation between the mechanisms was not obtained, this study does support our proposed mechanism and more importantly shows that in the rate-determining step the carbonyl synthon (bromonitroalkane) displays umpolung reactivity as it is negatively polarized as opposed to positively polarized.

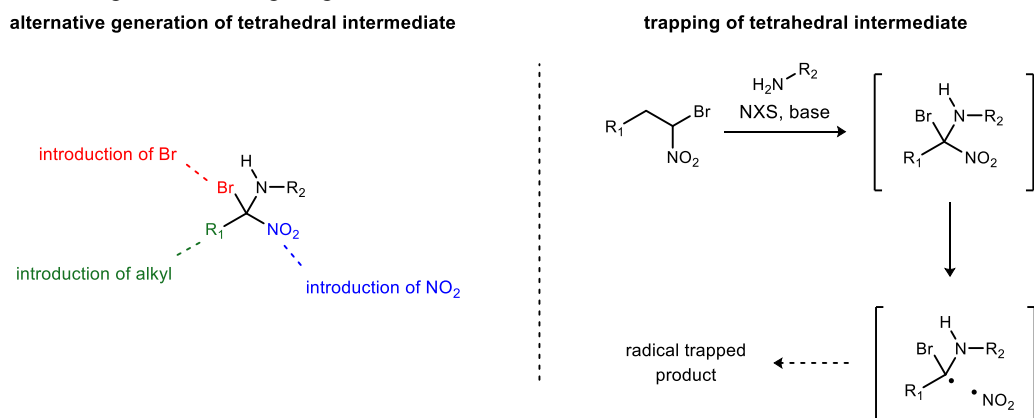
Figure 47. Hammett plot for UmAS



Investigating the Tetrahedral Intermediate: Preliminary and Future Work

The next step of the mechanistic investigation was a synthesis of the proposed tetrahedral intermediate via alternative pathways. This is the most important aspect of the investigation as the tetrahedral intermediate is the first species along the proposed mechanism that we have not yet observed directly. However, this is also the most difficult task of the mechanistic investigation. To date, there has been no observation, circumstantial or otherwise, of the tetrahedral intermediate, although all outcomes (e.g. ¹⁸O-labeling experiments) are consistent with its intermediacy. We have always rationalized this by the belief that the intermediate is extremely reactive and upon its formation it immediately converts to other compounds, mainly the amide. The ‘holy grail’ of this investigation would be to isolate and characterize the tetrahedral intermediate with X-ray crystallography and subsequently convert it to the amide. Currently, there has not been any indication of a promising pathway pursue this goal. In the absence of the ability to directly observe the tetrahedral intermediate, two different strategies have been devised to probe the existence of the tetrahedral intermediate (Figure 48). The first is to produce amide via access to the tetrahedral intermediate in a different way. In UmAS, the C-N bond is the last bond formed generating the tetrahedral intermediate. If we can form any of the other bonds (C-Br, C-NO₂, or C-C) last and observe amide formation that would provide evidence that the tetrahedral intermediate is a competent precursor to amide. The second approach is to develop a radical trap that upon formation of the carbon radical from the tetrahedral intermediate the radical can react with a different functional group. This strategy could allow

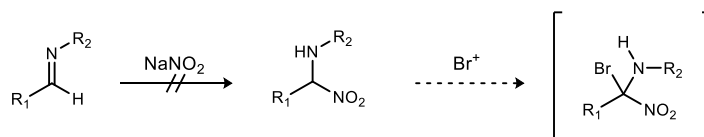
Figure 48. Strategies for investigating the existence of the tetrahedral intermediate



isolation of the radical trapped product giving insight into what covalent bonds are present when the radical is generated.

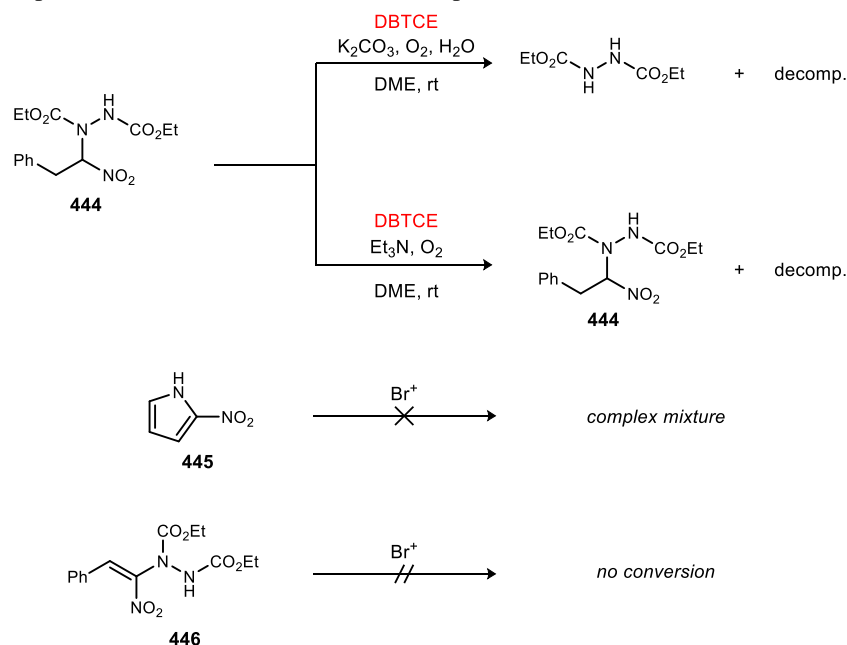
To begin with the first strategy of changing which bond is formed last in accessing the tetrahedral intermediate, we first investigated introducing bromine last. The required substrates to pursue this pathway, α -amine nitroalkanes, have been only minimally researched and are difficult to synthesize. Our first approach was to add nitrite into an imine (Scheme 119). The resulting amino nitroalkane would then be treated with base and a bromonium source to access the tetrahedral intermediate and ultimately form amide. Efforts to synthesize α -amino nitroalkanes via this method proved difficult as a screen of imine protecting groups (Boc and Bn), solvents (DCM, MeCN, DMSO), and acid additives (benzoic acid, HNTf₂, PBAM•HOTf) resulted in no formation of the desired product. With the inability to add nitrite into imines, a different approach was tried to gain access to the necessary substrates.

Scheme 119. Attempted synthesis of α -amino nitroalkanes



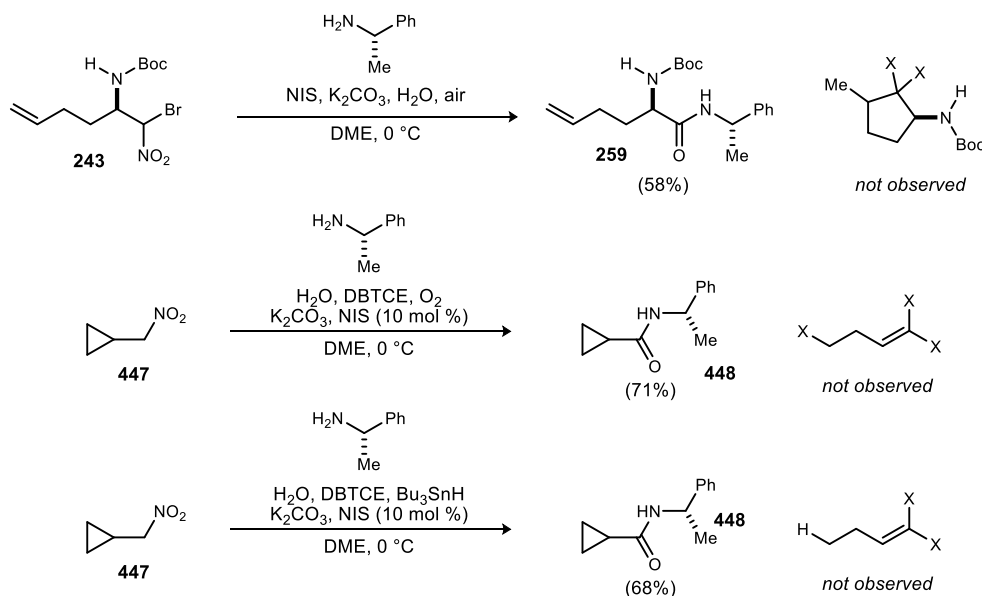
As the introduction of the nitro group to the imine proved fruitless, we adjusted the strategy and chose to attempt amination of the nitroalkane using electrophilic nitrogen. DEAD proved to be a viable electrophilic amine as α -amino nitroalkane **444** was accessed from the combination of nitroalkane **91** and DEAD with PBAM as the base (Scheme 120). Attempts to brominate with DBCTE and either inorganic or organic base only resulted in decomposition of amino nitroalkane **444** and recovery of starting material in the case of the organic base. Two other α -amino nitro compounds were synthesized followed by attempted bromination. 2-Nitropyrrole was prepared through the nitration of pyrrole while amino nitroolefin **446** was prepared from nitrostyrene via a Morita Baylis Hillman reaction. When 2-nitropyrrole was submitted to a variety of brominating conditions a complex mixture resulted in which nothing discernible was isolated. Nitroolefin **446** was resistant to bromination as only starting material was observed when it was submitted to brominating conditions. Although current efforts to access the tetrahedral intermediate through this method have been unsuccessful, there is room for further exploration. Additionally, the introduction of the alkyl chain (forming C-C bond last) and introduction of the nitro group (forming C-NO₂) bond last have yet to be addressed and may hold the key to accessing the tetrahedral intermediate.

Scheme 120. Attempted bromination of α -amino nitro compounds



The second strategy of developing a radical trap has been very briefly investigated. Two different potential radical traps have been synthesized and submitted to UmAS conditions (Scheme 121). The first was bromonitroalkane **243** bearing a terminal olefin. The radical intermediate could undergo a 5-exo-trig cyclization. When bromonitroalkane **243** was submitted to UmAS conditions, nothing resembling cyclized product was observed and the amide product was isolated in 58% yield. The second potential radical trap synthesized was cyclopropylmethyl nitroalkane **447**. When nitroalkane **447** was submitted to oxidative amidation conditions with DBTCE, only the amide product was observed without sign of any ring-opened product. The same reaction was run with the addition of Bu_3SnH in an attempt to trap the ring-opened

Scheme 121. Preliminary results with radical traps in UmAS



product, however, only amide was observed. Design and testing of additional radical traps should be undertaken as this remains a promising strategy to investigate the existence of the tetrahedral intermediate.

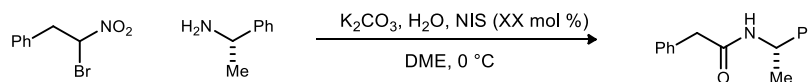
Future research is necessary to sufficiently differentiate between the two proposed mechanisms or propose a new alternative. The results described in this chapter serve as a starting point to fully understand the mechanism of amide formation from α -halonitroalkanes. There are three main takeaways from these results. First, monohalonitroalkane and dihalonitroalkane are in equilibrium under UmAS reaction conditions and the halonium transfer occurs on the time scale of the amide forming reaction. Second, it is unlikely that an acyl halide or other electrophilic acyl equivalent is generated in the amide-forming process from α -bromo nitroalkanes. And finally, in the rate-determining step of amide formation the bromonitroalkane (acyl equivalent) is nucleophilic, affirming the umpolung nature of the reaction.

Chapter 6

VI. Experimentals

All reagents and solvents were commercial grade and purified prior to use when necessary. Bromonitroalkanes were prepared according to the literature procedures.^{34,123} Amides prepared using stoichiometric conditions were prepared following literature procedure.^{34,38} NIS was recrystallized from dioxane/ CCl_4 . Toluene was dried by passage through a column of activated alumina as described by Grubbs.¹²⁴ *N*-Tosyl aldimines were prepared as reported in the literature.^{89,90,125} Catalyst *N*-benzylquininium chloride **147** is commercially available and was used as received. *N*-Boc- α -amido sulfones were prepared following literature procedure.⁶⁷ BAM-catalysts were prepared according to literature procedures.¹²⁶ Nitroalkanes were prepared according to literature procedures.^{34,123,127,128} Flash column chromatography was performed using Sorbent Technologies 40-63 mm, pore size 60 Å silica gel with solvent systems indicated. Analytical thin layer column chromatography was performed using Sorbent Technologies 250 mm glass-backed UV254 silica gel plates, and were visualized by fluorescence upon 250 nm radiation and/or the by use of ceric ammonium molybdate, ninhydrin, or potassium permanganate. Solvent removal was effected by rotary evaporation under vacuum (~ 25-40 mm Hg). All extracts were dried with MgSO_4 unless otherwise noted.

Nuclear magnetic resonance spectra (NMR) were acquired on a Bruker AV-400 (400 MHz), Bruker DRX-500 (500 MHz), or Bruker AV II-600 (600 MHz) instrument. Chemical shifts are measured relative to residual solvent peaks as an internal standard set to δ 7.26 and δ 77.16 (CDCl_3), unless otherwise specified. Mass spectra were recorded on a Thermo Electron Corporation MAT 95XP-Trap mass spectrometer by use of the ionization method noted by the Indiana University Mass Spectrometry Facility. IR spectra were recorded on a Nicolet Avatar 360 spectrophotometer and are reported in wavenumbers (cm^{-1}) as neat films on a NaCl plate (transmission). Melting points were measured on a Meltemp melting point apparatus and are not corrected. Optical rotations were measured on a Perkin Elmer-341 polarimeter.



Anaerobic Umpolung Amide Synthesis with freeze-pump-thaw: To a 2-necked 10 mL round-bottom flask containing (2-bromo-2-nitroethyl)benzene (115 mg, 500 μmol), DME (2.5 mL), and water (45 μL , 2.5 mmol) was added (*S*)- α -methylbenzyl amine (77 μL , 600 μmol). One neck of the flask was fitted with a vacuum adapter and connected to a dual manifold. K_2CO_3 (138 mg, 1.00 mmol) was added and the other

¹²³Erickson, A. S.; Kornblum, N. *J. Org. Chem.* **1977**, *42*, 3764-3765.

¹²⁴Pangborn, A. B.; Giardello, M. A.; Grubbs, R. H.; Rosen, R. K.; Timmers, F. J. *Organometallics* **1996**, *15*, 1518-1520.

¹²⁵Fukuda, Y.; Maeda, Y.; Kondo, K.; Aoyama, T. *Synthesis* **2006**, *2006*, 1937-1939.

¹²⁶Davis, T. A.; Dobish, M. C.; Schwieter, K. E.; Chun, A. C.; Johnston, J. N. *Org. Synth.* **2012**, *89*, 380; Dobish, M. C.; Johnston, J. N. *J. Am. Chem. Soc.* **2012**, *134*, 6068

¹²⁷Martin, N. J. A.; Ozores, L.; List, B. *J. Am. Chem. Soc.* **2007**, *129*, 8976-8977.

¹²⁸Palomo, C.; Landa, A.; Mielgo, A.; Oiarbide, M.; Puente, Á.; Vera, S. *Angew. Chem. Int. Ed.* **2007**, *46*, 8431-8435.

neck was fitted with a septum.³ The flask was immediately degassed using freeze-pump-thaw techniques (30 min. pump stage), backfilling with argon (3 cycles). The flask was warmed to 0 °C and allowed to stir until the bromonitroalkane disappeared by TLC (~ 5 h).¹²⁹ The flask was frozen with N₂ (*l*) and NIS (0-500 μmol) was added by quickly removing and refitting the septum. The flask was subjected to an additional freeze-pump-thaw cycle and then warmed to 0 °C and stirred for 24 h. The reaction was quenched with 1 M aq HCl at 0 °C and diluted with CH₂Cl₂. The layers were separated and the aqueous layer was extracted with CH₂Cl₂. The combined organic layers were washed with satd aq Na₂S₂O₃, the layers were separated, and the aqueous layer was extracted with CH₂Cl₂. The combined organic extracts were dried and concentrated without heating. The entire crude reaction mixture was transferred to an NMR tube with CDCl₃. Toluene (20 μL, 0.19 mmol) was added to the tube as an internal standard to estimate the amount of nitroalkane present. The crude mixture was purified by flash column chromatography (SiO₂, 15-20-30-40% ethyl acetate in hexanes).

Run	NIS (mol %)	NIS (mg)	Amide (mg)	Amide (% yield)	Nitroalkane (NMR % yield)
1	0	0	20	17	5
2	0	0	24	20	5
3	0	0	23	19	5
avg.	0			19	5
1	10	11.3	25	21	8
2	10	11.3	26	22	8
3	10	11.3	22	18	8
avg.	10			20	8
1	20	22.5	26	22	7
2	20	22.5	23	19	8
3	20	22.5	22	18	8
avg.	20			20	8
1	30	33.8	32	27	5
2	30	33.8	28	24	1
3	30	33.8	29	24	<1
avg.	30			25	2
1	50	56.3	43	36	<1
2	50	56.3	42	35	<1
3	50	56.3	45	38	<1
avg.	50			36	<1
1	75	84.4	59	50	<1
2	75	84.4	62	52	<1
3	75	84.4	63	53	<1
avg.	75			52	<1
1	100	112.5	84	71	<1
2	100	112.5	80	67	<1
3	100	112.5	81	68	<1
avg.	100			69	<1

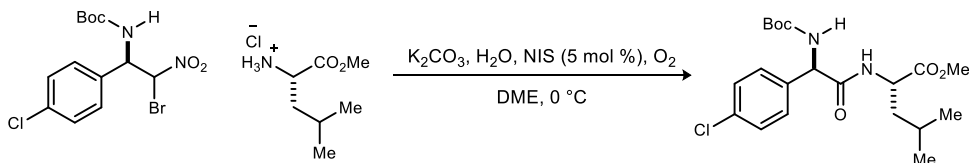
¹²⁹ We have determined that the nitronate will not reprotonate in the timeframe of standard TLC procedures, so the absence of bromonitroalkane suggests that the nitronate is fully formed. The reaction was not exposed to oxygen during this process.

Aerobic Umpolung Amide Synthesis with freeze-pump-thaw: To a 2-necked 5 mL round-bottom flask containing (2-bromo-2-nitroethyl)benzene (28.0 mg, 122 μmol), DME (600 μL), and water (11 μL , 610 μmol) was added (*S*)- α -methylbenzyl amine (19.0 μL , 146 μmol). One neck of the flask was fitted with a septum while the other was fitted with a vacuum adapter and connected to a dual manifold. The flask was immediately degassed using freeze-pump-thaw techniques (30 min. pump stage), backfilling with nitrogen (3 cycles). The flask was frozen with $\text{N}_2(l)$ and NIS (0-24 μmol) and K_2CO_3 (33.6 mg, 243 μmol) were added by quickly removing and refitting the septum.¹²⁹ The flask was subjected to an additional freeze-pump-thaw cycle, backfilled with O_2 , and then allowed to stir at 0 °C for 24 h. The reaction was quenched with 1 M aq HCl at 0 °C and diluted with CH_2Cl_2 . The layers were separated and the aqueous layer was extracted with CH_2Cl_2 . The combined organic layers were washed with satd. aq $\text{Na}_2\text{S}_2\text{O}_3$, the layers were separated, and the aqueous layer was extracted with CH_2Cl_2 . The combined organic extracts were dried and concentrated. The crude mixture was purified by flash column chromatography (SiO_2 , 15-20-30-40% ethyl acetate in hexanes).

NIS (mol %)	NIS (mg)	Amide (mg)	Amide (% yield)
20	5.5	22	76
10	2.7	21	73
5	1.4	22	76
1	0.3	16	55
0	0	15	51

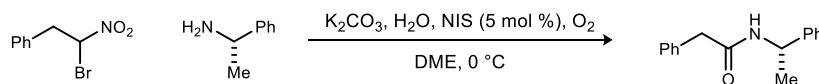
General procedure for UmAS using substoichiometric NIS under an O_2 atmosphere: K_2CO_3 (2.0 equiv) was added to a solution of α -bromo nitroalkane (1.0 equiv, 0.2 M) and NIS (5 mol%) in DME and H_2O (5.0 equiv) in a round-bottom flask at 0 °C. The flask was equipped with an O_2 balloon. The amine (1.2 equiv) was then added. The reaction mixture was stirred at 0 °C for 24 h. The reaction was quenched with 1 M aq HCl at 0 °C and diluted with CH_2Cl_2 . The layers were separated and the aqueous layer was extracted with CH_2Cl_2 . The combined organic layers were washed with satd aq $\text{Na}_2\text{S}_2\text{O}_3$, the layers were separated, and the aqueous layer was extracted with CH_2Cl_2 . The combined organic extracts were dried, the filtrate was concentrated, and the residue was subjected to purification by flash column chromatography on silica gel.

General procedure for one-pot amidation: To a round-bottomed flask equipped with a stir bar was added nitroalkane (1 equiv.), amine (2 equiv.), H_2O (5 equiv.) and DME (0.2 M). DBTCE (1 equiv.), K_2CO_3 (2 equiv.), and NIS (0.1 equiv.) were added. The reaction setup was equipped with an O_2 balloon and stirred at 25 °C for 24 h. The mixture was treated with 1 M HCl and extracted with DCM. The organics were washed with satd aq $\text{Na}_2\text{S}_2\text{O}_3$, dried and concentrated. The resulting residue was purified by flash column chromatography.

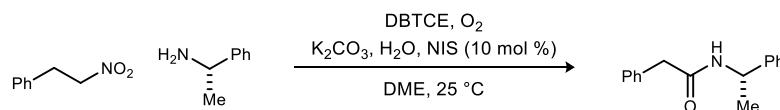


Methyl 2-((*R*)-2-((*tert*-butoxycarbonyl)amino)-2-(4-chlorophenyl)acetamido)-4-methylpentanoate (74). Following the General Procedure, the α -bromo nitroalkane (29.7 mg, 78.0 μmol) and amine (17.0 mg,

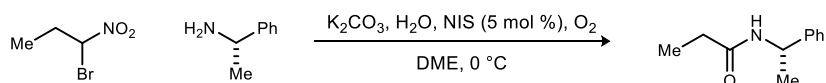
94.0 μmol) provided the amide after flash column chromatography (20-35% ethyl acetate in hexanes) as a white solid (25 mg, 77%). Characterization data matched the literature.³⁴



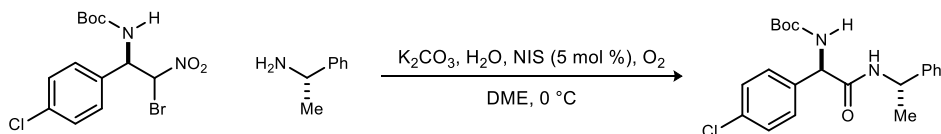
2-Phenyl-*N*-(1-phenylethyl)acetamide (90). Following the General Procedure (cat-NIS), the α -bromo nitroalkane (24.0 mg, 104 μmol) and amine (15.1 mg, 125 μmol) provided the amide after flash column chromatography (25-35% ethyl acetate in hexanes) as a white solid (18 mg, 73%). Characterization data matched the literature.³⁷



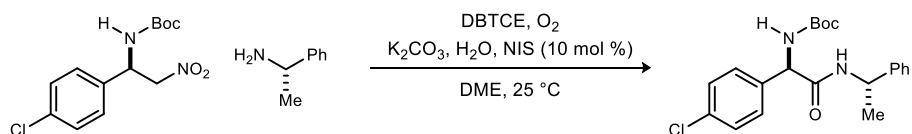
2-Phenyl-*N*-(1-phenylethyl)acetamide (90). Prepared according to the general procedure for nitroalkane amidation using (2-nitroethyl)benzene (30.2 mg, 200 μmol) and (*S*)-1-phenylethylamine (51 μL , 400 μmol). Flash column chromatography (SiO₂, 20-30% ethyl acetate in hexanes) yielded the amide as a white solid (34 mg, 70%). Characterization data matched the literature.³⁴



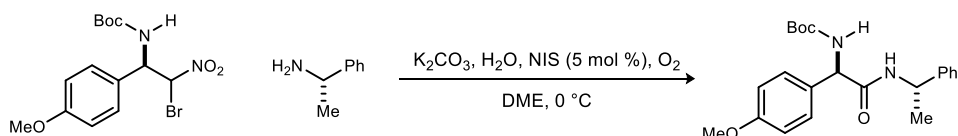
***N*-(1-Phenylethyl)propionamide (92).** Following the General Procedure (cat-NIS), the α -bromo nitroalkane (26.8 mg, 160 μmol) and amine (23.1 mg, 191 μmol) provided the amide after flash column chromatography (20-35% ethyl acetate in hexanes) as a white solid (20 mg, 72%). Characterization data matched the literature.³⁴



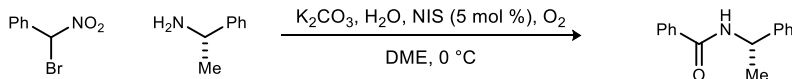
***tert*-Butyl ((1*R*)-1-(4-chlorophenyl)-2-oxo-2-((1-phenylethyl)amino)ethyl)carbamate (93).** Following the General Procedure (cat-NIS), the α -bromo nitroalkane (30.3 mg, 80.0 μmol) and amine (11.6 mg, 96.0 μmol) provided the amide after flash column chromatography (15-25% ethyl acetate in hexanes) as a white solid (19 mg, 55%). Characterization data matched the literature.³⁴



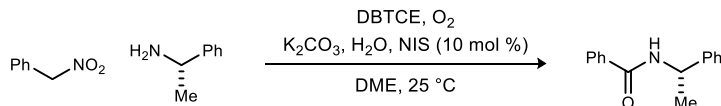
tert-Butyl ((R)-1-(4-chlorophenyl)-2-oxo-2-(((S)-1-phenylethyl)amino)ethyl)carbamate (93). Prepared according to the general procedure for nitroalkane amidation using *tert*-butyl (*R*)-1-(4-chlorophenyl)-2-nitroethylcarbamate (60.1 mg, 200 μ mol) and (*S*)-1-phenylethylamine (51 μ L, 400 μ mol). Flash column chromatography (SiO₂, 10-30% ethyl acetate in hexanes) yielded the amide as a white solid (52 mg, 67%) in >20:1 dr (¹H NMR). Characterization data matched the literature.³⁴



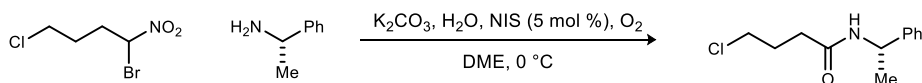
tert-Butyl ((1R)-1-(4-methoxyphenyl)-2-oxo-2-(((S)-1-phenylethyl)amino)ethyl)carbamate (94). Following the General Procedure (cat-NIS), the α -bromo nitroalkane (30.9 mg, 82.0 μ mol) and amine (12.0 mg, 99.0 μ mol) provided the amide after flash column chromatography (15-25% ethyl acetate in hexanes) as a white solid (16 mg, 51%). Characterization data matched the literature.³⁴



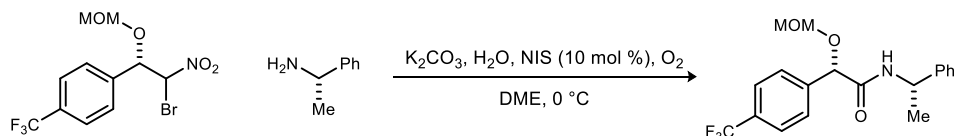
N-(1-Phenylethyl)benzamide (95). Following the General Procedure (cat-NIS), the α -bromo nitroalkane (23.5 mg, 109 μ mol) and amine (15.9 mg, 131 μ mol) provided the amide after flash column chromatography (15-25% ethyl acetate in hexanes) as a white solid (21 mg, 84%). Characterization data matched the literature.³⁴



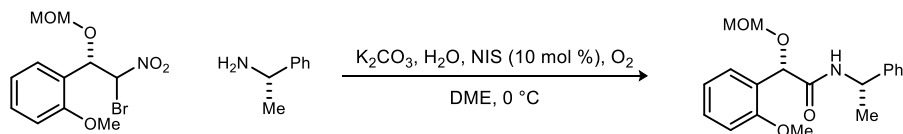
N-(1-Phenylethyl)benzamide (95). Prepared according to the general procedure for nitroalkane amidation using nitromethylbenzene (13.7 mg, 100 μ mol) and (*S*)-1-phenylethylamine (26 μ L, 200 μ mol). Flash column chromatography (SiO₂, 10-30% ethyl acetate in hexanes) yielded the amide as a white solid (20 mg, 87%). Characterization data matched the literature.³⁴



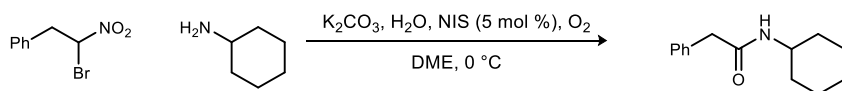
4-Chloro-*N*-(1-phenylethyl)butanamide (96). Following the General Procedure (cat-NIS), the α -bromo nitroalkane (28.8 mg, 133 μ mol) and amine (19.2 mg, 159 μ mol) provided the amide after flash column chromatography (15-25% ethyl acetate in hexanes) as a white solid (22 mg, 72%). Characterization data matched the literature.³⁴



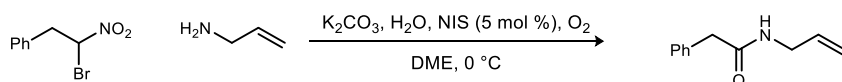
(2*S*)-2-(Methoxymethoxy)-*N*-(1-phenylethyl)-2-(4-(trifluoromethyl)phenyl)acetamide (97). Following the General Procedure (cat-NIS), the α -bromo nitroalkane (41.1 mg, 110 μ mol) and amine (16.9 mg, 140 μ mol) provided the amide after flash column chromatography (10-30% ethyl acetate in hexanes) as a white solid (27 mg, 64%). Characterization data matched the literature.³⁸



(2*S*)-2-(Methoxymethoxy)-2-(2-methoxyphenyl)-*N*-(1-phenylethyl)acetamide (98). Following the General Procedure (cat-NIS), the α -bromo nitroalkane (55.1 mg, 170 μ mol) and amine (25.4 mg, 210 μ mol) provided the amide after flash column chromatography (5-25% ethyl acetate in hexanes) as a white solid (33 mg, 58%). Characterization data matched the literature.³⁸

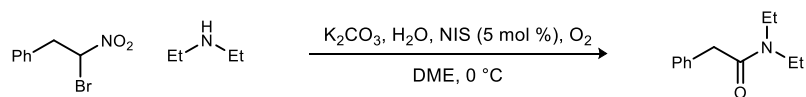


***N*-Cyclohexyl-2-phenylacetamide (99).** Following the General Procedure (cat-NIS), the α -bromo nitroalkane (23.5 mg, 102 μ mol) and amine (14.8 mg, 122 μ mol) provided the amide after flash column chromatography (20-30% ethyl acetate in hexanes) as a white solid (16 mg, 73%). Characterization data matched the literature.³⁴

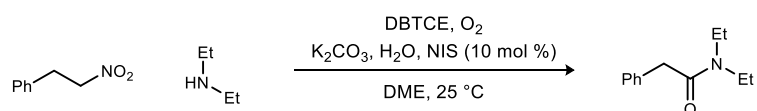


***N*-Allyl-2-phenylacetamide (100).** Following the General Procedure (cat-NIS), the α -bromo nitroalkane (28.3 mg, 123 μ mol) and amine (17.9 mg, 148 μ mol) provided the amide after flash column

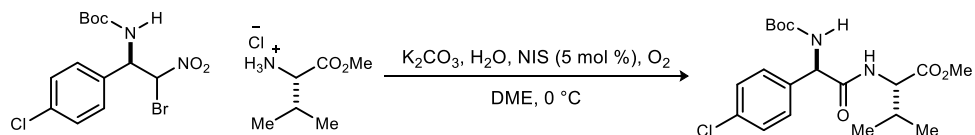
chromatography (30-40% ethyl acetate in hexanes) as a white solid (16 mg, 76%). Characterization data matched the literature.³⁴



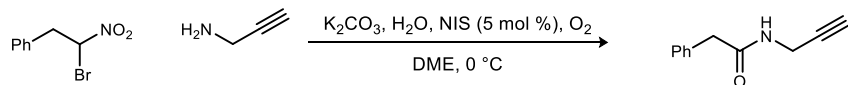
***N,N*-Diethyl-2-phenylacetamide (102).** Following the General Procedure (cat-NIS), the α -bromo nitroalkane (30.0 mg, 130 μ mol) and amine (18.9 mg, 156 μ mol) provided the amide after flash column chromatography (25-35% ethyl acetate in hexanes) as a white solid (15 mg, 76%). Characterization data matched the literature.³⁴



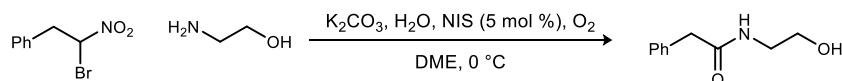
***N,N*-Diethyl-2-phenylacetamide (102).** Prepared according to the general procedure for nitroalkane amidation using (2-nitroethyl)benzene (15.1 mg, 100 μ mol) and diethylamine (21 μ L, 200 μ mol). Flash column chromatography (SiO₂, 20-30% ethyl acetate in hexanes) yielded the amide as a clear oil (12 mg, 63%). Characterization data matched the literature.³⁴



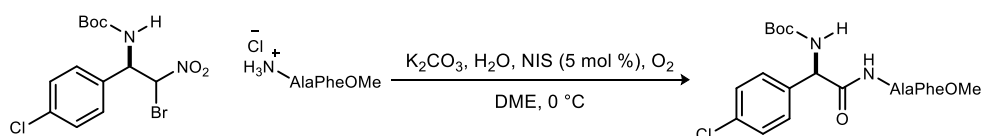
Methyl 2-((*R*)-2-((*tert*-butoxycarbonyl)amino)-2-(4-chlorophenyl)acetamido)-3-methylbutanoate (103). Following the General Procedure (cat-NIS), the α -bromo nitroalkane (31.5 mg, 83.0 μ mol) and amine (16.7 mg, 100 μ mol) provided the amide after flash column chromatography (20-35% ethyl acetate in hexanes) as a white solid (24 mg, 73%). Characterization data matched the literature.³⁴



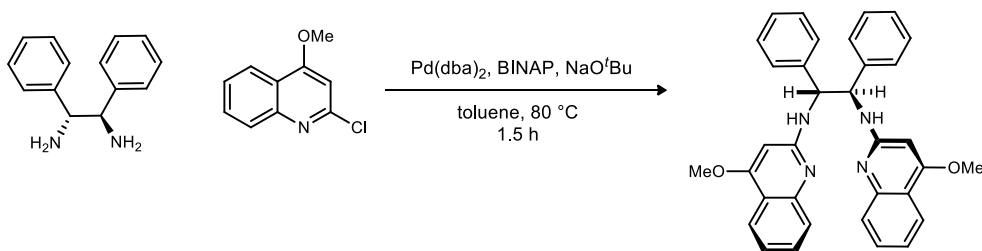
2-Phenyl-*N*-(prop-2-yn-1-yl)acetamide (104). Following the General Procedure (cat-NIS), the α -bromo nitroalkane (30.0 mg, 130 μ mol) and amine (18.9 mg, 156 μ mol) provided the amide after flash column chromatography (25-35% ethyl acetate in hexanes) as a white solid (14 mg, 62%). Characterization data matched the literature.³⁴



***N*-(2-Hydroxybutyl)-2-phenylacetamide (105).** Following the General Procedure (cat-NIS), the α -bromo nitroalkane (30.8 mg, 134 μ mol) and amine (9.7 μ l, 161 μ mol) provided the amide after flash column chromatography (4% methanol in dichloromethane) as an off-white solid (21 mg, 86%). $R_f = 0.37$ (5% MeOH/CH₂Cl₂); mp 52-56 °C; IR (neat) 3290, 3063, 3029, 2920, 2850, 1645, 1604, 1583, 1495 cm⁻¹; ¹H NMR (600 MHz, CDCl₃) δ 7.28-7.26 (m, 2H), 7.22-7.21 (m, 1H), 7.19-7.17 (m, 2H), 6.02 (br s, 1H), 3.56 (t, $J = 6.0$ Hz, 2H), 3.49 (s, 2H), 3.27 (dt, $J = 6.0, 6.0$ Hz, 2H); ¹³C NMR (150 MHz, CDCl₃) ppm 172.5, 134.6, 129.4, 129.0, 127.4, 62.1, 43.5, 42.6, 29.7; HRMS (ESI): Exact mass calcd for C₁₀H₁₄NO₂ [M+H]⁺ 180.1019, found 180.1014.

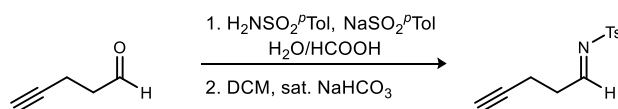


(6*R*,9*S*,12*S*)-Methyl 12-benzyl-6-(4-chlorophenyl)-2,2,9-trimethyl-4,7,10-trioxo-3-oxa-5,8,11-triazatridecan-13-oatemethylpentanoate (106). Following the General Procedure (cat-NIS), the α -bromo nitroalkane (25.5 mg, 67.0 μ mol) and amine (23.1 mg, 81.0 μ mol) provided the amide after flash column chromatography (30-40% ethyl acetate in hexanes) as a white solid (18 mg, 51%). Characterization data matched the literature.³⁴

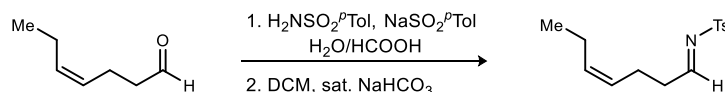


⁴MeO-StilbBAM ((1*R*,2*R*)-*N*1,*N*2-bis(4-methoxyquinolin-2-yl)-1,2-diphenylethane-1,2-diamine) (191) Pd(dba)₂ (54 mg, 94 μ mol), *rac*-BINAP (117 mg, 188 μ mol) and sodium *tert*-butoxide (1.35 g, 14.1 mmol) were loaded into a vial in a glove box. (1*R*,2*R*)-1,2-diphenylethane-1,2-diamine (1.00 g, 4.7 mmol) and 2-chloro-4-methoxyquinoline (1.81 g, 9.4 mmol) were loaded into a round bottomed flask. The contents of the vial were transferred into the flask and toluene (45 mL) was added. The reaction was allowed to stir at 80 °C under argon for 1.5 h. Upon completion as judged by TLC, the reaction mixture was cooled to room temperature, diluted with ethyl acetate and filtered through Celite. Flash column chromatography (SiO₂, 1-3-5-10% methanol in dichloromethane) yielded yellow foamy solid (1.21 g, 49%). $R_f = 0.45$ (5% MeOH/CH₂Cl₂); $[\alpha]_D^{20} +80.0$ (*c* .45, CHCl₃); IR (film) 3238, 2985, 2871, 1620 cm⁻¹; ¹H NMR (600 MHz, DMSO) δ 7.77 (d, $J = 8.0$ Hz, 2H), 7.71 (d, $J = 4.9$ Hz, 2H), 7.44-7.41 (m, 4H), 7.39 (d, $J = 7.6$ Hz, 4H), 7.17 (t, $J = 7.7$ Hz, 4H), 7.10-7.06 (m, 4H), 6.23 (s, 2H), 5.69 (bs, 2H), 3.85 (s, 6H); ¹³C NMR (150 MHz, DMSO) ppm 161.7, 158.3, 148.8, 142.7, 129.9, 128.17, 128.15, 126.9, 126.0, 121.6, 121.1, 117.5, 59.9, 55.8; HRMS (ESI): Exact mass calcd for C₃₄H₃₁N₄O₂ [M+H]⁺ 527.2447, found 527.2435.

General procedure for imine preparation: To a round-bottomed flask equipped with a stir bar was added aldehyde (1 equiv.), *p*-toluenesulfonamide (1 equiv.), *p*-toluenesulfonic acid sodium salt (1.1 equiv.), formic acid, and H₂O. The reaction was stirred for 24 h. The resulting white precipitate is filtered and washed with H₂O and hexanes to yield the α -amido sulfone. The α -amide sulfone was dissolved in CH₂Cl₂ and washed with sat. NaHCO₃ for 45 s in a separatory funnel. The organic phase was dried and concentrated provide the imine.

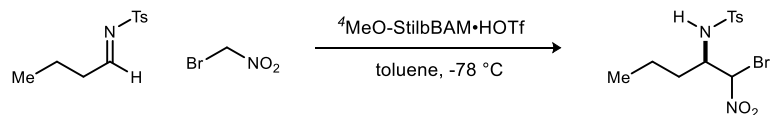


(E)-4-Methyl-N-(pent-4-yn-1-ylidene)benzenesulfonamide (205e). Prepared according to the general procedure using pent-4-ynal (0.82 g, 10.00 mmol), *p*-toluenesulfonamide (1.71 g, 10.00 mmol), *p*-toluenesulfonic acid sodium salt (2.15 g, 11.00 mmol), formic acid (15 mL), and H₂O (15 mL). The imine was obtained as a clear oil (1.22 g, 52%); IR (film) 3282, 1631 cm⁻¹; ¹H NMR (600 MHz, CDCl₃) δ 8.66 (t, *J* = 3.8 Hz, 1H), 7.82 (d, *J* = 8.3 Hz, 2H), 7.34 (d, *J* = 8.0 Hz, 2H), 2.76 (td, *J* = 7.0, 3.8 Hz, 2H), 2.53 (td, *J* = 7.4, 2.6 Hz, 2H), 2.45 (s, 3H), 1.96 (t, *J* = 2.7 Hz, 1H); ¹³C NMR (150 MHz, CDCl₃) ppm 175.8, 144.8, 134.3, 129.8, 128.2, 81.5, 69.9, 34.5, 21.6, 14.0; HRMS (CI): Exact mass calcd for C₁₂H₁₄NO₂S [M+H]⁺ 236.0740, found 236.0735.

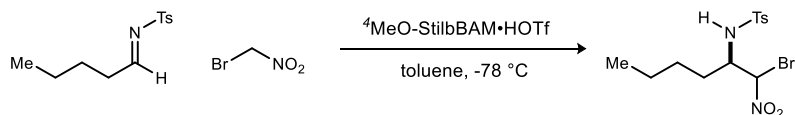


(N-((1E,4Z)-Hept-4-en-1-ylidene)-4-methylbenzenesulfonamide (205j). Prepared according to the general procedure using (*Z*)-hept-4-enal (1.12 g, 10.00 mmol), *p*-toluenesulfonamide (1.71 g, 10.00 mmol), *p*-toluenesulfonic acid sodium salt (2.15 g, 11.00 mmol), formic acid (15 mL), and H₂O (15 mL). The imine was obtained as a clear oil (2.05 g, 77%); IR (film) 3279, 3005, 2961, 2929, 2872, 1628 cm⁻¹; ¹H NMR (400 MHz, CDCl₃) δ 8.57 (t, *J* = 4.4 Hz, 1H), 7.80 (d, *J* = 8.3 Hz, 2H), 7.32 (d, *J* = 8.1 Hz, 2H), 5.44-5.37 (m, 1H), 5.28-5.21 (m, 1H), 2.55 (td, *J* = 7.3, 4.4 Hz, 2H), 2.43 (s, 3H), 2.34 (td, *J* = 7.2, 7.2 Hz, 2H), 1.99 (dq, *J* = 7.9, 7.5 Hz, 2H), 0.93 (t, *J* = 7.5 Hz, 1H); ¹³C NMR (1050 MHz, CDCl₃) ppm 177.9, 144.7, 134.5, 133.8, 129.7, 128.1, 125.7, 35.8, 22.3, 21.6, 20.4, 14.0; HRMS (CI): Exact mass calcd for C₁₄H₂₀NO₂S [M+H]⁺ 266.1215, found 266.1204.

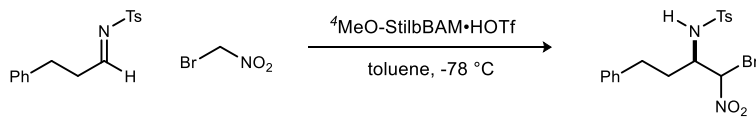
General procedure A for bromonitromethane additions: To a flame dried vial equipped with a stir bar was added ⁴MeO-StilbBAM•HOTf (3.4 mg, 5 μ mol), *N*-tosyl imine (100 μ mol), and toluene (1 mL), and the reaction was cooled to -78 °C. Bromonitromethane (11 μ L, 150 μ mol) was added and the reaction was stirred for 48 h. The mixture was loaded directly onto silica gel for flash column chromatography.



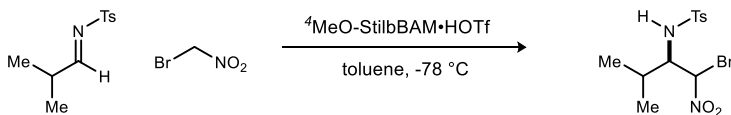
***N*-((*2R*)-1-Bromo-1-nitropentan-2-yl)-4-methylbenzenesulfonamide (188).** Prepared according to general procedure A using $^4\text{MeO-StilbBAM}\cdot\text{HOTf}$ (3.4 mg, 5.0 μmol), (*E*)-*N*-butylidene-4-methylbenzenesulfonamide (22.5 mg, 100 μmol), and bromonitromethane (11 μL , 150 μmol). Flash column chromatography (SiO₂ 5-10-20% ethyl acetate in hexanes) yielded the α -bromo nitroalkane (1:1 dr (¹H NMR)) as a yellow oil (35 mg, 96%). The diastereomers were determined to be 97 and 96% ee by chiral HPLC analysis (Chiralcel IC, 7% ⁱPrOH/hexanes, 1 mL/min, $t_r(d_1, \text{major}) = 16.3$ min, $t_r(d_1, \text{minor}) = 18.6$ min, $t_r(d_2, \text{minor}) = 31.7$ min, $t_r(d_2, \text{major}) = 37.5$ min); $R_f = 0.32$ (20% EtOAc/hexanes); IR (film) 3271, 2962, 2926, 2875, 2850, 1566 cm^{-1} ; ¹H NMR (600 MHz, CDCl₃, 1:1 mixture of diastereomers) δ 7.79 (d, $J = 8.3$ Hz, 2H), 7.73 (d, $J = 8.3$ Hz, 2H), 7.34 (d, $J = 8.4$ Hz, 2H), 7.32 (d, $J = 8.4$ Hz, 2H), 6.15 (d, $J = 4.0$ Hz, 1H), 6.05 (d, $J = 2.5$ Hz, 1H), 4.83 (d, $J = 9.4$ Hz, 1H), 4.71 (d, $J = 9.4$ Hz, 1H), 4.04-3.95 (m, 2H), 2.45 (s, 3H), 2.44 (s, 3H), 1.73 (m, 1H), 1.51 (m, 2H), 1.40 (m, 1H), 1.35 (m, 1H), 1.19 (m, 1H), 1.09 (m, 1H) 0.98 (m, 1H), 0.85 (t, $J = 7.3$, 3H), 0.76 (t, $J = 7.3$, 3H); ¹³C NMR (150 MHz, CDCl₃) ppm 144.5, 144.4, 137.1, 136.8, 130.3, 129.95, 127.3, 127.2, 85.3, 84.2, 57.9, 56.5, 33.7, 32.6, 29.8, 21.7, 18.9, 18.2, 13.4, 13.3; HRMS (ESI): Exact mass calcd for C₁₂H₁₇BrN₂NaO₄S [M+Na]⁺ 386.9990, found 387.0009.



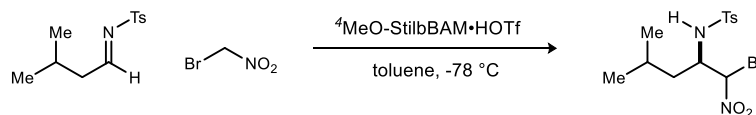
***N*-((*2R*)-1-Bromo-1-nitrohexan-2-yl)-4-methylbenzenesulfonamide (206a).** Prepared according to general procedure A using $^4\text{MeO-StilbBAM}\cdot\text{HOTf}$ (3.4 mg, 5.0 μmol), (*E*)-4-methyl-*N*-pentylidenebenzenesulfonamide (23.9 mg, 100 μmol), and bromonitromethane (11 μL , 150 μmol). Flash column chromatography (SiO₂ 5-10-20% ethyl acetate in hexanes) yielded the α -bromo nitroalkane (1:1 dr (¹H NMR)) as a yellow oil (33 mg, 88%). The diastereomers were determined to be 96 and 95% ee by chiral HPLC analysis (Chiralcel IC, 7% ⁱPrOH/hexanes, 1 mL/min, $t_r(d_1, \text{major}) = 18.5$ min, $t_r(d_1, \text{minor}) = 20.9$ min, $t_r(d_2, \text{minor}) = 34.9$ min, $t_r(d_2, \text{major}) = 45.1$ min); $R_f = 0.32$ (20% EtOAc/hexanes); IR (film) 3271, 2958, 2927, 2867, 2361, 1567 cm^{-1} ; ¹H NMR (600 MHz, CDCl₃, 1:1 mixture of diastereomers) δ 7.79 (d, $J = 8.3$ Hz, 2H), 7.73 (d, $J = 8.3$ Hz, 2H), 7.34 (d, $J = 8.0$ Hz, 2H), 7.32 (d, $J = 8.0$ Hz, 2H), 6.15 (d, $J = 4.0$ Hz, 1H), 6.07 (d, $J = 2.8$ Hz, 1H), 5.03 (d, $J = 9.3$ Hz, 1H), 4.94 (d, $J = 8.9$ Hz, 1H), 3.98-3.93 (m, 2H), 2.444 (s, 3H), 2.438 (s, 3H), 1.51-1.46 (m, 2H), 1.47-1.42 (m, 2H), 1.25-1.15 (m, 4H), 1.13-1.06 (m, 4H), 0.74 (t, $J = 7.2$ Hz, 3H), 0.73 (t, $J = 7.2$ Hz, 3H); ¹³C NMR (150 MHz, CDCl₃) ppm 144.4, 144.3, 137.0, 136.7, 129.92, 129.85, 127.2, 127.1, 85.3, 84.1, 58.0, 56.6, 31.2, 30.1, 27.5, 26.8, 21.9, 21.6, 13.63, 13.60; HRMS (APCI): Exact mass calcd for C₁₃H₂₀BrN₂O₄S [M+H]⁺ 379.0327, found 379.0328.



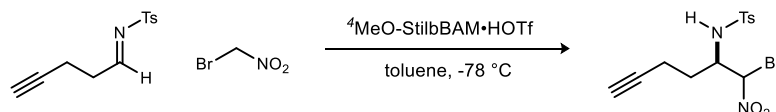
***N*-((2*R*)-1-Bromo-1-nitro-4-phenylbutan-2-yl)-4-methylbenzenesulfonamide (206b).** Prepared according to general procedure A using ⁴MeO-StilbBAM•HOTf (3.4 mg, 5.0 μmol), (*E*)-4-methyl-*N*-(3-phenylpropylidene)benzenesulfonamide (28.7 mg, 100 μmol), and bromonitromethane (11 μL, 150 μmol). Flash column chromatography (SiO₂ 5-10-20% ethyl acetate in hexanes) yielded the α-bromo nitroalkane (1:1 dr (¹H NMR)) as a yellow oil (31 mg, 75%). The diastereomers were determined to be 96 and 94% ee by chiral HPLC analysis (Chiralcel IC, 7% ⁱPrOH/hexanes, 1 mL/min, *t_r*(*d*₁, major) = 19.1 min, *t_r*(*d*₁, minor) = 21.7 min, *t_r*(*d*₂, minor) = 38.8 min, *t_r*(*d*₂, major) = 42.1 min); *R_f* = 0.29 (20% EtOAc/hexanes); IR (film) 3265, 2925, 2361, 1565 cm⁻¹; ¹H NMR (600 MHz, CDCl₃, 1:1 mixture of diastereomers) δ 7.80 (d, *J* = 8.3 Hz, 2H), 7.74 (d, *J* = 8.3 Hz, 2H), 7.35 (d, *J* = 8.0 Hz, 2H), 7.33 (d, *J* = 8.0 Hz, 2H), 7.27-7.18 (m, 6H), 7.01 (d, *J* = 7.1 Hz, 2H), 6.93 (d, *J* = 7.1 Hz, 2H), 6.16 (d, *J* = 3.9 Hz, 1H), 6.08 (d, *J* = 2.8 Hz, 1H), 5.22 (d, *J* = 9.5 Hz, 1H), 5.12 (d, *J* = 9.2 Hz, 1H), 4.02-3.96 (m, 2H), 2.67-2.57 (m, 2H), 2.46 (s, 3H), 2.45 (s, 3H), 2.38 (m, 1H), 2.14 (m, 1H), 1.90-1.77 (m, 4H); ¹³C NMR (150 MHz, CDCl₃) ppm 144.5, 144.4, 139.4, 136.8, 136.7, 130.0, 129.9, 128.62, 126.60, 128.4, 128.2, 128.1, 127.2, 127.1, 126.52, 126.48, 84.9, 83.7, 57.6, 56.3, 32.9, 32.2, 31.6, 31.0, 21.6; HRMS (ESI): Exact mass calcd for C₁₇H₁₉BrN₂NaO₄S [M+Na]⁺ 449.0147, found 449.0136.



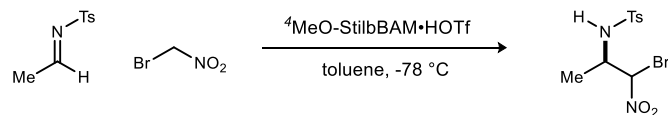
***N*-((2*R*)-1-Bromo-3-methyl-1-nitrobutan-2-yl)-4-methylbenzenesulfonamide (206c).** Prepared according to general procedure A using ⁴MeO-StilbBAM•HOTf (3.4 mg, 5.0 μmol), (*E*)-4-methyl-*N*-(2-methylpropylidene)benzenesulfonamide (22.5 mg, 100 μmol), and bromonitromethane (11 μL, 150 μmol). Flash column chromatography (SiO₂ 5-10-20% ethyl acetate in hexanes) yielded the α-bromo nitroalkane (1:1 dr (¹H NMR)) as a clear oil (20 mg, 58%). The diastereomers were determined to be 84 and 82% ee by chiral HPLC analysis (Chiralcel IC, 10% ⁱPrOH/hexanes, 1 mL/min, *t_r*(*d*₁, major) = 14.7 min, *t_r*(*d*₂, minor) = 20.4 min, *t_r*(*d*₁, minor) = 30.0 min, *t_r*(*d*₂, major) = 34.7 min); *R_f* = 0.21 (20% EtOAc/hexanes); IR (film) 3281, 2968, 2923, 1568 cm⁻¹; ¹H NMR (600 MHz, CDCl₃, 1:1 mixture of diastereomers) δ 7.75 (d, *J* = 8.3 Hz, 2H), 7.69 (d, *J* = 8.3 Hz, 2H), 7.31 (d, *J* = 8.0 Hz, 2H), 7.29 (d, *J* = 8.0 Hz, 2H), 6.09 (d, *J* = 2.9 Hz, 1H), 5.96 (d, *J* = 6.0 Hz, 1H), 5.03 (d, *J* = 9.7 Hz, 1H), 4.90 (d, *J* = 9.9 Hz, 1H), 4.06 (ddd, *J* = 10.1, 8.3, 2.8 Hz, 1H), 4.00 (ddd, *J* = 9.7, 6.0, 6.0 Hz, 1H), 2.433 (s, 3H), 2.427 (s, 3H), 2.09 (tt, *J* = 6.4, 6.4, 2.6 Hz, 1H), 1.85 (tt, *J* = 8.2, 8.2, 1.4 Hz, 1H), 1.01 (d, *J* = 2.6, 3H), 0.99 (d, *J* = 2.4, 3H), 0.93 (d, *J* = 6.8, 3H), 0.88 (d, *J* = 6.8, 3H); ¹³C NMR (150 MHz, CDCl₃) ppm 144.0, 143.9, 137.8, 137.4, 129.7, 129.6, 127.1, 126.9, 85.3, 81.8, 63.3, 62.3, 32.5, 30.3, 21.6, 19.7, 19.6, 18.9, 17.5; HRMS (APCI): Exact mass calcd for C₁₂H₁₈BrN₂O₄S [M+H]⁺ 365.0171, found 365.0177.



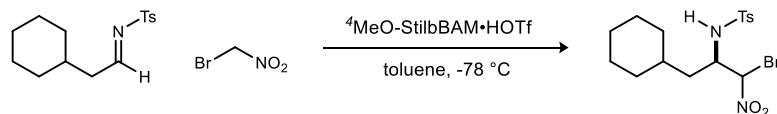
***N*-((*2R*)-1-Bromo-4-methyl-1-nitropentan-2-yl)-4-methylbenzenesulfonamide (206d).** Prepared according to general procedure A using $^4\text{MeO-StilbBAM}\cdot\text{HOTf}$ (3.4 mg, 5.0 μmol), (*E*)-4-methyl-*N*-(3-methylbutylidene)benzenesulfonamide (23.9 mg, 100 μmol), and bromonitromethane (11 μL , 150 μmol). Flash column chromatography (SiO_2 5-10-20% ethyl acetate in hexanes) yielded the α -bromo nitroalkane (1:1 dr ($^1\text{H NMR}$)) as a clear oil (36 mg, 95%). The diastereomers were determined to be 95 and 95% ee by chiral HPLC analysis (Chiralcel OZ-H, 3% $^i\text{PrOH}$ /hexanes, 1 mL/min, $t_r(d_1, \text{major}) = 41.2$ min, $t_r(d_1, \text{minor}) = 44.9$ min, $t_r(d_2, \text{minor}) = 60.2$ min, $t_r(d_2, \text{major}) = 75.9$ min); $R_f = 0.32$ (20% EtOAc/hexanes); IR (film) 3271, 2960, 2871, 1566 cm^{-1} ; $^1\text{H NMR}$ (600 MHz, CDCl_3 , 1:1 mixture of diastereomers) δ 7.81 (d, $J = 8.3$ Hz, 2H), 7.75 (d, $J = 8.3$ Hz, 2H), 7.35 (d, $J = 8.0$ Hz, 2H), 7.33 (d, $J = 8.0$ Hz, 2H), 6.21 (d, $J = 3.6$ Hz, 1H), 6.08 (d, $J = 2.7$ Hz, 1H), 5.12 (d, $J = 9.2$ Hz, 1H), 4.98 (d, $J = 8.8$ Hz, 1H), 4.03-3.98 (m, 2H), 2.45 (s, 3H), 2.44 (s, 3H), 1.59-1.54 (m, 1H), 1.52-1.42 (m, 3H), 1.38-1.33 (m, 1H), 1.11 (ddd, $J = 13.9, 10.1, 3.1$ Hz, 1H), 0.88 (d, $J = 6.6$ Hz, 3H), 0.82 (d, $J = 6.7$ Hz, 3H), 0.72 (d, $J = 6.4$ Hz, 3H), 0.56 (d, $J = 6.4$ Hz, 3H); $^{13}\text{C NMR}$ (150 MHz, CDCl_3) ppm 144.4, 144.3, 136.9, 136.6, 130.0, 129.9, 127.2, 127.1, 86.1, 84.1, 56.4, 54.8, 40.0, 39.2, 24.2, 23.7, 23.2, 22.7, 21.2, 20.8; HRMS (APCI): Exact mass calcd for $\text{C}_{13}\text{H}_{20}\text{BrN}_2\text{O}_4\text{S}$ $[\text{M}+\text{H}]^+$ 379.0327, found 379.0338.



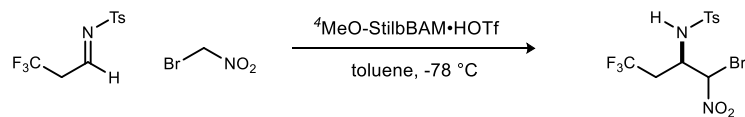
***N*-((*2R*)-1-Bromo-1-nitrohex-5-yn-2-yl)-4-methylbenzenesulfonamide (206e).** Prepared according to general procedure A using $^4\text{MeO-StilbBAM}\cdot\text{HOTf}$ (3.4 mg, 5.0 μmol), (*E*)-4-methyl-*N*-(pent-4-yn-1-ylidene)benzenesulfonamide (23.5 mg, 100 μmol), and bromonitromethane (11 μL , 150 μmol). Flash column chromatography (SiO_2 5-10-20% ethyl acetate in hexanes) yielded the α -bromo nitroalkane (1:1 dr ($^1\text{H NMR}$)) as a yellow oil (30 mg, 80%). The diastereomers were determined to be 94 and 94% ee by chiral HPLC analysis (Chiralcel IC, 7% $^i\text{PrOH}$ /hexanes, 1 mL/min, $t_r(d_1, \text{minor}) = 37.0$ min, $t_r(d_1, \text{major}) = 49.6$ min; Chiralcel AD-H, 7% $^i\text{PrOH}$ /hexanes, 1 mL/min, $t_r(d_2, \text{major}) = 22.0$ min, $t_r(d_2, \text{minor}) = 25.0$ min); $R_f = 0.41$ (20% EtOAc/hexanes); IR (film) 3292, 2924, 2855, 1567 cm^{-1} ; $^1\text{H NMR}$ (600 MHz, CDCl_3 , 1:1 mixture of diastereomers) δ 7.81 (d, $J = 8.3$ Hz, 2H), 7.75 (d, $J = 8.3$ Hz, 2H), 7.35 (d, $J = 8.0$ Hz, 2H), 7.33 (d, $J = 8.1$ Hz, 2H), 6.24 (d, $J = 4.1$ Hz, 1H), 6.20 (d, $J = 2.8$ Hz, 1H), 5.10 (d, $J = 8.7$ Hz, 1H), 5.08 (d, $J = 9.5$ Hz, 1H), 4.19-4.13 (m, 2H), 2.452 (s, 3H), 2.447 (s, 3H), 2.23-2.02 (m, 5H), 1.98 (t, $J = 2.6$ Hz, 1H), 1.94 (t, $J = 2.6$ Hz, 1H), 1.82-1.69 (m, 3H); $^{13}\text{C NMR}$ (150 MHz, CDCl_3) ppm 144.4, 144.3, 136.6, 136.4, 129.9, 129.8, 127.2, 127.1, 84.4, 83.3, 81.4, 81.2, 70.5, 57.0, 55.9, 29.9, 29.6, 29.2, 21.5, 14.9, 14.4; HRMS (CI): Exact mass calcd for $\text{C}_{13}\text{H}_{16}\text{BrN}_2\text{O}_4\text{S}$ $[\text{M}+\text{H}]^+$ 375.0009, found 375.0019.



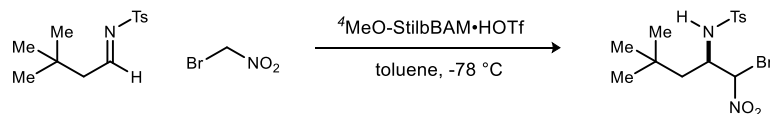
***N*-((2*R*)-1-Bromo-1-nitropropan-2-yl)-4-methylbenzenesulfonamide (206f).** Prepared according to general procedure A using ⁴MeO-StilbBAM•HOTf (3.4 mg, 5.0 μmol), (*E*)-*N*-ethylidene-4-methylbenzenesulfonamide (19.7 mg, 100 μmol), and bromonitromethane (11 μL, 150 μmol). Flash column chromatography (SiO₂ 5-10-20% ethyl acetate in hexanes) yielded the α-bromo nitroalkane (1:1 dr (¹H NMR)) as a clear oil (31 mg, 91%). The diastereomers were determined to be 94 and 93% ee by chiral HPLC analysis (Chiralcel AD-H, 10% ⁱPrOH/hexanes, 1 mL/min, *t*_r(*d*₁, minor) = 20.7 min, *t*_r(*d*₂, minor) = 26.6 min, *t*_r(*d*₁, major) = 32.6 min, *t*_r(*d*₂, major) = 54.4 min); *R*_f = 0.38 (20% EtOAc/hexanes); IR (film) 3263, 2923, 1568 cm⁻¹; ¹H NMR (600 MHz, CDCl₃, 1:1 mixture of diastereomers) δ 7.78 (d, *J* = 8.3 Hz, 2H), 7.74 (d, *J* = 8.3 Hz, 2H), 7.34 (d, *J* = 8.5 Hz, 2H), 7.33 (d, *J* = 8.6 Hz, 2H), 6.07 (d, *J* = 4.6 Hz, 1H), 6.02 (d, *J* = 3.2 Hz, 1H), 5.05 (d, *J* = 9.3 Hz, 1H), 4.98 (d, *J* = 9.1 Hz, 1H), 4.15-4.09 (m, 2H), 2.45 (s, 3H), 2.44 (s, 3H), 1.31 (d, *J* = 6.8 Hz, 3H), 1.20 (d, *J* = 6.7 Hz, 3H); ¹³C NMR (150 MHz, CDCl₃) ppm 144.4, 144.3, 136.8, 136.7, 130.02, 129.96, 127.2, 127.1, 85.0, 84.1, 53.7, 52.5, 21.59, 17.6, 16.9; HRMS (EI): Exact mass calcd for C₁₀H₁₃BrN₂O₄S [M]⁺ 335.9774, found 335.9780.



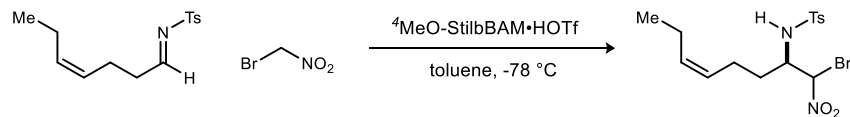
***N*-((2*R*)-1-Bromo-3-cyclohexyl-1-nitropropan-2-yl)-4-methylbenzenesulfonamide (206g).** Prepared according to general procedure A using ⁴MeO-StilbBAM•HOTf (3.4 mg, 5.0 μmol), (*E*)-*N*-(2-cyclohexylethylidene)-4-methylbenzenesulfonamide (27.9 mg, 100 μmol), and bromonitromethane (11 μL, 150 μmol). Flash column chromatography (SiO₂ 5-10-20% ethyl acetate in hexanes) yielded the α-bromo nitroalkane (1:1 dr (¹H NMR)) as a yellow oil (32 mg, 76%). The diastereomers were determined to be 96 and 93% ee by chiral HPLC analysis (Chiralcel IC, 5% ⁱPrOH/hexanes, 1 mL/min, *t*_r(*d*₁, major) = 19.6 min, *t*_r(*d*₁, minor) = 21.4 min, *t*_r(*d*₂, minor) = 47.4 min, *t*_r(*d*₂, major) = 59.2 min); *R*_f = 0.59 (20% EtOAc/hexanes); IR (film) 3271, 2925, 2852, 1565 cm⁻¹; ¹H NMR (600 MHz, CDCl₃, 1:1 mixture of diastereomers) δ 7.81 (d, *J* = 8.3 Hz, 2H), 7.75 (d, *J* = 8.3 Hz, 2H), 7.36 (d, *J* = 8.0 Hz, 2H), 7.33 (d, *J* = 8.0 Hz, 2H), 6.30 (d, *J* = 3.3 Hz, 1H), 6.15 (d, *J* = 2.7 Hz, 1H), 5.03 (d, *J* = 9.0 Hz, 1H), 4.87 (d, *J* = 8.6 Hz, 1H), 4.02-3.94 (m, 2H), 2.45 (s, 3H), 2.44 (s, 3H), 1.70-0.67 (m, 25H), 0.54 (dddd, *J* = 11.2, 3.5, 3.5, 3.5 Hz, 1H); ¹³C NMR (150 MHz, CDCl₃) ppm 144.4, 144.3, 136.8, 136.5, 130.0, 129.9, 127.2, 127.1, 86.6, 84.1, 55.7, 53.9, 38.3, 37.7, 33.8, 33.4, 33.3, 32.8, 32.0, 31.7, 29.7, 26.1, 25.5, 21.53, 21.48; HRMS (EI): Exact mass calcd for C₁₆H₂₁BrNO₂S [M-NO₂H₂]⁺ 370.0471, found 370.0458.



***N*-((*2R*)-1-Bromo-4,4,4-trifluoro-1-nitrobutan-2-yl)-4-methylbenzenesulfonamide (206h)** Prepared according to general procedure A using ⁴MeO-StilbBAM•HOTf (3.4 mg, 5.0 μmol), (*E*)-4-methyl-*N*-(3,3,3-trifluoropropylidene)benzenesulfonamide (26.5 mg, 100 μmol), and bromonitromethane (11 μL, 150 μmol). Flash column chromatography (SiO₂ 5-10-20% ethyl acetate in hexanes) yielded the α-bromo nitroalkane (1:1 dr (¹H NMR)) as a yellow oil (21 mg, 52%). The diastereomers were determined to be 87 and 85% ee by chiral HPLC analysis (Chiralcel AD-H, 5% EtOH/hexanes, 1 mL/min, *t*_r(*d*₁, minor) = 22.1 min, *t*_r(*d*₂, major) = 23.5 min, *t*_r(*d*₂, minor) = 25.0 min, *t*_r(*d*₁, major) = 30.0 min); *R*_f = 0.44 (20% EtOAc/hexanes); IR (film) 3271, 2923, 1571 cm⁻¹; ¹H NMR (600 MHz, CDCl₃, 1:1 mixture of diastereomers) δ 7.77 (d, *J* = 8.3 Hz, 2H), 7.72 (d, *J* = 8.2 Hz, 2H), 7.35 (d, *J* = 8.7 Hz, 2H), 7.34 (d, *J* = 8.6 Hz, 2H), 6.34 (d, *J* = 4.6 Hz, 1H), 6.29 (d, *J* = 3.1 Hz, 1H), 5.41 (d, *J* = 8.8 Hz, 1H), 5.35 (d, *J* = 8.8 Hz, 1H), 4.31 (ddt, *J* = 4.7, 4.7, 4.7 Hz, 1H), 4.24-4.22 (m, 1H), 2.95-2.89 (m, 1H), 2.84-2.78 (m, 1H), 2.63-2.52 (m, 2H), 2.45 (s, 3H), 2.44 (s, 3H); ¹³C NMR (150 MHz, CDCl₃) ppm 144.9, 144.8, 135.6(2), 130.0, 129.5, 127.4, 127.3, 125.5, 123.7, 82.8, 81.4, 52.6, 51.7, 35.6, 35.1, 21.62, 21.60; HRMS (CI): Exact mass calcd for C₁₁H₁₂BrF₃N₂O₄S [M-H]⁺ 403.9648, found 403.9659.



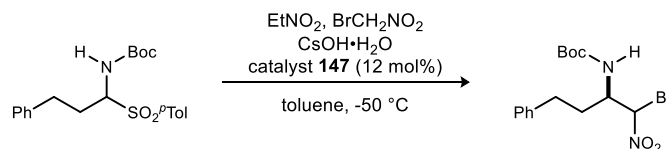
***N*-((*2R*)-1-Bromo-4,4-dimethyl-1-nitropentan-2-yl)-4-methylbenzenesulfonamide (206i)**. Prepared according to general procedure A using ⁴MeO-StilbBAM•HOTf (3.4 mg, 5.0 μmol), (*E*)-*N*-(3,3-dimethylbutylidene)-4-methylbenzenesulfonamide (25.3 mg, 100 μmol), and bromonitromethane (11 μL, 150 μmol). Flash column chromatography (SiO₂ 5-10-20% ethyl acetate in hexanes) yielded the α-bromo nitroalkane (1:1 dr (¹H NMR)) as a colorless oil (38 mg, 96%). The diastereomers were determined to be 96 and 97% ee by chiral HPLC analysis (Chiralcel AD-H, 7% EtOH/hexanes, 1 mL/min, *t*_r(*d*₁, major) = 9.4 min, *t*_r(*d*₁, minor) = 10.5 min, *t*_r(*d*₂, major) = 11.3 min, *t*_r(*d*₂, minor) = 16.5 min); *R*_f = 0.56 (20% EtOAc/hexanes); IR (film) 3279, 2957, 1565 cm⁻¹; ¹H NMR (600 MHz, CDCl₃, 1:1 mixture of diastereomers) δ 7.82 (d, *J* = 8.3 Hz, 2H), 7.77 (d, *J* = 8.3 Hz, 2H), 7.37 (d, *J* = 8.0 Hz, 2H), 7.34 (d, *J* = 8.0 Hz, 2H), 6.24 (d, *J* = 3.1 Hz, 1H), 6.09 (d, *J* = 2.4 Hz, 1H), 5.04 (d, *J* = 9.2 Hz, 1H), 4.77 (d, *J* = 8.7 Hz, 1H), 4.14 (ddt, *J* = 8.8, 3.0, 1.8 Hz, 1H), 4.05 (ddt, *J* = 8.9, 3.1, 2.6 Hz, 1H), 2.46 (s, 3H), 2.45 (s, 3H), 1.80 (dd, *J* = 14.8, 2.8 Hz, 1H), 1.38 (dd, *J* = 15.4, 8.9 Hz, 1H), 1.32-1.26 (m, 2H), 0.86 (s, 9H), 0.74 (s, 9H); ¹³C NMR (150 MHz, CDCl₃) ppm 144.6, 144.5, 137.1, 136.7, 130.1, 130.0, 127.3, 127.1, 87.5, 84.0, 56.0, 53.0, 44.0, 43.2, 30.1, 29.8, 29.4, 29.3, 21.6; HRMS (CI): Exact mass calcd for C₁₄H₂₂BrN₂O₄S [M+H]⁺ 393.0478, found 393.0463.



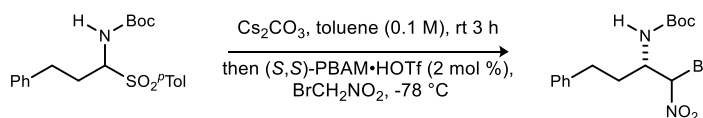
***N*-((2*R,Z*)-1-bromo-1-nitrooct-5-en-2-yl)-4-methylbenzenesulfonamide (206j)** Prepared according to the general procedure using ⁴MeO-StilbBAM•HOTf (3.4 mg, 5.0 μmol), (*E*)-*N*-((*Z*)-hept-4-en-1-ylidene)-4-methylbenzenesulfonamide (26.5 mg, 100 μmol), and bromonitromethane (11 μL, 150 μmol). Flash column chromatography (SiO₂ 5-10-20% ethyl acetate in hexanes) yielded the α-bromo nitroalkane (1:1 dr (¹H NMR)) as a yellow oil (37 mg, 91%). The diastereomers were determined to be 95 and 93% ee by chiral HPLC analysis (Chiralcel IC, 6% ⁱPrOH/hexanes, 1 mL/min, *t*_r(*d*₁, major) = 17.6 min, *t*_r(*d*₁, minor) = 19.1 min, *t*_r(*d*₂, minor) = 35.1 min, *t*_r(*d*₂, major) = 41.9 min); *R*_f = 0.31 (20% EtOAc/hexanes); IR (film) 3270, 2963, 1568 cm⁻¹; ¹H NMR (600 MHz, CDCl₃, 1:1 mixture of diastereomers) δ 7.80 (d, *J* = 8.3 Hz, 2H), 7.74 (d, *J* = 8.3 Hz, 2H), 7.34 (d, *J* = 8.0 Hz, 2H), 7.32 (d, *J* = 8.6 Hz, 2H), 6.13 (d, *J* = 4.1 Hz, 1H), 6.07 (d, *J* = 2.8 Hz, 1H), 5.42-5.32 (m, 2H), 5.13 (m, 1H), 5.10 (d, *J* = 9.5 Hz, 1H), 5.07-5.02 (m, 2H), 4.03-3.96 (m, 2H), 2.443 (s, 3H), 2.437 (s, 3H), 2.06-1.74 (m, 8H), 1.67-1.48 (m, 4H), 0.92 (t, *J* = 7.6 Hz, 3H), 0.89 (t, *J* = 7.6 Hz, 3H); ¹³C NMR (150 MHz, CDCl₃) ppm 144.4, 144.2, 137.0, 136.8, 134.0, 133.9, 129.93, 129.85, 127.1, 127.0, 125.8, 125.7, 84.8, 83.9, 57.7, 56.5, 31.7, 30.7, 23.1, 22.5, 21.6, 20.53, 20.47, 14.07, 14.05; HRMS (ESI): Exact mass calcd for C₁₅H₂₁BrNaN₂O₄S [M+Na]⁺ 427.0303, found 427.0299.

General procedure B for bromonitromethane additions: To a flame dried vial equipped with a stir bar was added *N*-benzyl quininium chloride **147** (10.8 mg, 24.0 μmol), *N*-Boc α-amidosulfone (200 μmol), toluene (0.6 mL), nitroethane (143 μL, 2.00 mmol), and bromonitromethane (22 μL, 300 μmol) and the reaction was cooled to -50 °C. CsOH•OH (40 mg, 260 μmol) was added and the reaction was stirred for 96 h. The mixture was quenched with 1 M HCl and extracted with dichloromethane. The organic phase was washed with 1 M HCl, dried and concentrated. The resulting solid was purified by flash column chromatography.

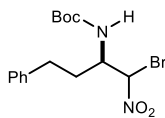
General procedure C for bromonitromethane additions: To a flame dried vial equipped with a stir bar was added *N*-Boc α-amidosulfone (100 μmol), toluene (1.0 mL) and Cs₂CO₃ (163 mg, 500 μmol). The reaction was stirred for 3 h at room temperature. The reaction was filtered through a plug of Celite and washed with toluene (0.5 mL). The filtrate was collected in a vial and (*S,S*)-PBAM•HOTf (1.3 mg, 2.0 μmol) was added. The vial was cooled to -78 °C and bromonitromethane (11 μL, 150 μmol) was added and the reaction was stirred for 24 h. The mixture was filtered through a plug of silica gel with ethyl acetate and then concentrated. The resulting solid was purified by flash column chromatography.



tert-Butyl ((2R)-1-bromo-1-nitro-4-phenylbutan-2-yl)carbamate (228). Prepared according to general procedure B using *tert*-butyl (3-phenyl-1-tosylpropyl)carbamate (77.8 mg, 200 μ mol). Flash column chromatography (SiO₂, 2.5-7.5-15% ethyl acetate in hexanes) yielded the α -bromo nitroalkane (1:1 dr (¹H NMR)) as a white solid (44 mg, 59%). The diastereomers were determined to be 96 and 96% ee by chiral HPLC analysis (Chiralcel OD-H, 3% ⁱPrOH/hexanes, 1 mL/min, $t_r(d_{1e1}$, major) = 16.8 min, $t_r(d_{1e2}$, minor) = 18.5 min, $t_r(d_{2e1}$, major) = 21.3 min, $t_r(d_{2e2}$, minor) = 24.0 min); R_f = 0.37 (10% EtOAc/hexanes); IR (film) 3334, 2977, 2929, 1705, 1565 cm⁻¹; ¹H NMR (600 MHz, CDCl₃, 1:1 mixture of diastereomers) δ 7.32-7.15 (m, 10H), 6.18 (d, J = 4.9 Hz, 1H), 6.16 (d, J = 2.8 Hz, 1H), 4.90 (d, J = 8.6 Hz, 1H), 4.80 (d, J = 9.0 Hz, 1H), 4.36 (m, 1H), 4.25 (m, 1H), 2.82-2.77 (m, 2H), 2.71-2.63 (m, 2H), 2.13-1.79 (m, 4H), 1.48 (s, 9H), 1.46 (s, 9H); ¹³C NMR (150 MHz, CDCl₃) ppm 154.9, 154.8, 140.0, 139.9, 128.68, 128.66, 128.3(2), 126.48, 126.45, 83.9, 82.7, 80.9, 80.8, 54.5, 54.0, 32.8, 32.1, 32.03, 31.96, 28.21, 28.17; HRMS (ESI): Exact mass calcd for C₁₅H₂₁BrN₂NaO₄ [M+Na]⁺ 395.0582, found 395.0588.

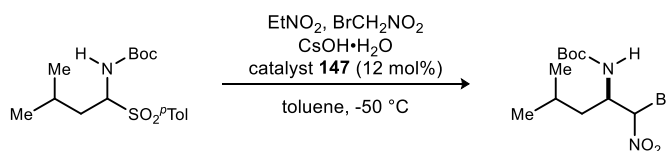


tert-Butyl ((2S)-1-bromo-1-nitro-4-phenylbutan-2-yl)carbamate (ent-228). Prepared according to general procedure C using *tert*-butyl (3-phenyl-1-tosylpropyl)carbamate (38.9 mg, 100 μ mol). Flash column chromatography (SiO₂, 2.5-7.5-15% ethyl acetate in hexanes) yielded the α -bromo nitroalkane (1:1 dr (¹H NMR)) as a white solid (26 mg, 70%). The diastereomers were determined to be 93 and 93% ee by chiral HPLC analysis (Chiralcel OD-H, 3% ⁱPrOH/hexanes, 1 mL/min, $t_r(d_{1e1}$, minor) = 16.8 min, $t_r(d_{1e2}$, major) = 18.5 min, $t_r(d_{2e1}$, minor) = 21.3 min, $t_r(d_{2e2}$, major) = 24.0 min).

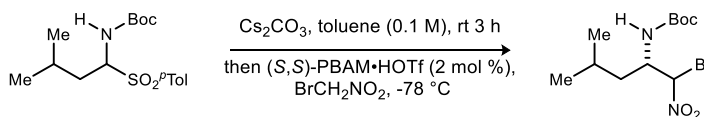


tert-Butyl ((2R)-1-bromo-1-nitro-4-phenylbutan-2-yl)carbamate (228). To a flame dried flask equipped with a stir bar was added *tert*-butyl (3-phenyl-1-tosylpropyl)carbamate (10.0 g, 25.7 mmol), toluene (270 mL) and Cs₂CO₃ (41.8 g, 128.5 mmol). The reaction was stirred for 3 h at room temperature. The reaction was

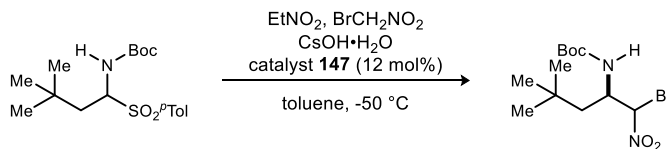
filtered through a plug of Celite and washed with toluene (135 mL). The filtrate was collected in a flask and (*R,R*)-PBAM·HOTf (169 mg, 257 μ mol) was added. The flask was cooled to -78 °C and bromonitromethane (2.69 mL, 38.6 mmol) was added and the reaction was stirred for 24 h. The mixture was filtered through a plug of silica gel with ethyl acetate and then concentrated. Flash column chromatography (SiO₂, 2.5-7.5-15% ethyl acetate in hexanes) yielded the α -bromo nitroalkane (1:1 dr (¹H NMR)) as a white solid (7.95 g, 83%). The solid was recrystallized from hexanes to afford 3.51 g (44% recovery). The diastereomers were determined to be 99 and 99% ee by chiral HPLC analysis.



tert-Butyl ((2R)-1-bromo-4-methyl-1-nitropentane-2-yl)carbamate (233). Prepared according to general procedure B using *tert*-butyl (3-methyl-1-tosylbutyl)carbamate (68.2 mg, 200 μ mol). Flash column chromatography (SiO₂, 2.5-7.5-15% ethyl acetate in hexanes) yielded the α -bromo nitroalkane (1:1 dr (¹H NMR)) as a white solid (37 mg, 57%). The diastereomers were determined to be 87 and 90% ee by chiral HPLC analysis (Chiralcel IC, 2% ⁱPrOH/hexanes, 0.4 mL/min, $t_r(d_{1e1}, \text{major}) = 19.2$ min, $t_r(d_{2e1}, \text{major}) = 20.3$ min, $t_r(d_{1e2}, \text{minor}) = 31.1$ min, $t_r(d_{2e2}, \text{minor}) = 31.6$ min); $R_f = 0.43$ (10% EtOAc/hexanes); IR (film) 3333, 2963, 2873, 1702, 1566 cm^{-1} ; ¹H NMR (600 MHz, CDCl₃, 1:1 mixture of diastereomers) δ 6.19 (d, $J = 4.4$ Hz, 1H), 6.15 (d, $J = 3.4$ Hz, 1H), 4.82 (d, $J = 8.6$ Hz, 1H), 4.74 (d, $J = 8.7$ Hz, 1H), 4.43-4.37 (m, 1H), 4.35-4.30 (m, 1H), 1.76-1.64 (m, 3H), 1.55-1.31 (m, 3H), 1.45 (s, 9H), 1.43 (s, 9H), 0.97 (d, $J = 6.7$ Hz, 3H), 0.95 (d, $J = 5.4$ Hz, 3H), 0.94 (d, $J = 5.0$ Hz, 3H), 0.93 (d, $J = 6.5$ Hz, 3H); ¹³C NMR (150 MHz, CDCl₃) ppm 154.9, 154.8, 84.3, 83.6, 80.7, 80.6, 53.3, 52.7, 39.7, 39.0, 28.19, 28.16, 24.8(2), 23.2, 22.9, 21.6, 21.4; HRMS (ESI): Exact mass calcd for C₁₁H₂₁BrN₂NaO₄ [M+Na]⁺ 347.0582, found 347.0582.

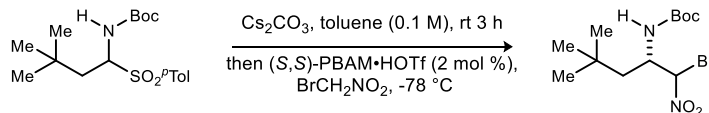


tert-Butyl ((2S)-1-bromo-4-methyl-1-nitropentane-2-yl)carbamate (ent-233). Prepared according to general procedure C using *tert*-butyl (3-methyl-1-tosylbutyl)carbamate (34.1 mg, 100 μ mol). Flash column chromatography (SiO₂, 2.5-7.5-15% ethyl acetate in hexanes) yielded the α -bromo nitroalkane (1:1 dr (¹H NMR)) as a white solid (27 mg, 83%). The diastereomers were determined to be 92 and 92% ee by chiral HPLC analysis (Chiralcel IC, 2% ⁱPrOH/hexanes, 0.4 mL/min, $t_r(d_{1e1}, \text{minor}) = 19.2$ min, $t_r(d_{2e1}, \text{minor}) = 20.3$ min, $t_r(d_{1e2}, \text{major}) = 31.1$ min, $t_r(d_{2e2}, \text{major}) = 31.6$ min).

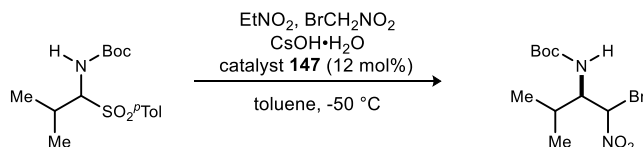


tert-Butyl ((2R)-1-bromo-4,4-dimethyl-1-nitropentane-2-yl)carbamate (234). Prepared according to general procedure B using *tert*-butyl (3,3-dimethyl-1-tosylbutyl)carbamate (71.0 mg, 200 μ mol). Flash column chromatography (SiO₂, 2.5-7.5-15% ethyl acetate in hexanes) yielded the α -bromo nitroalkane (1:1 dr (¹H NMR)) as a white solid (44 mg, 65%). The diastereomers were determined to be 92 and 93% ee by chiral HPLC analysis (Chiralcel OZ-H, 3% ⁱPrOH/hexanes, 0.6 mL/min, $t_r(d_{1e1}, \text{major}) = 8.0$ min, $t_r(d_{2e1}, \text{major}) = 8.7$ min, $t_r(d_{1e2}, \text{minor}) = 9.9$ min, $t_r(d_{2e2}, \text{minor}) = 12.0$ min); $R_f = 0.51$ (20% EtOAc/hexanes);

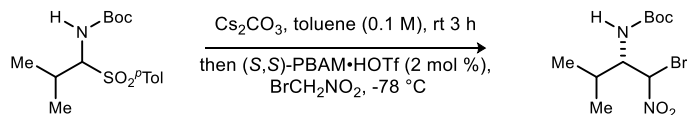
IR (film) 3416, 2959, 1692, 1563 cm^{-1} ; ^1H NMR (600 MHz, CDCl_3 , 1:1 mixture of diastereomers) δ 6.14 (d, $J = 4.3$ Hz, 1H), 6.12 (d, $J = 3.2$ Hz, 1H), 4.81 (d, $J = 8.6$ Hz, 1H), 4.78 (d, $J = 8.7$ Hz, 1H), 4.40-4.35 (m, 2H), 1.70 (d, $J = 14.6$ Hz, 1H), 1.51-1.31 (m, 3H), 1.44 (s, 9H), 1.42 (s, 9H), 0.96 (s, 9H), 0.93 (s, 9H); ^{13}C NMR (150 MHz, CDCl_3) ppm 154.53, 154.51, 84.7, 84.3, 80.7, 80.6, 52.6, 51.7, 43.8(2), 30.3, 30.2, 29.42, 29.40, 28.22, 28.19; HRMS (ESI): Exact mass calcd for $\text{C}_{12}\text{H}_{23}\text{BrN}_2\text{NaO}_4$ $[\text{M}+\text{Na}]^+$ 361.0739, found 361.0736.



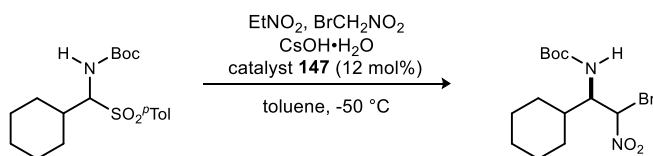
tert-Butyl ((2S)-1-bromo-4,4-dimethyl-1-nitropentan-2-yl)carbamate (ent-234). Prepared according to general procedure C using *tert*-butyl (3,3-dimethyl-1-tosylbutyl)carbamate (35.5 mg, 100 μmol). Flash column chromatography (SiO_2 , 2.5-7.5-15% ethyl acetate in hexanes) yielded the α -bromo nitroalkane (1:1 dr (^1H NMR)) as a white solid (30 mg, 88%). The diastereomers were determined to be 91 and 88% ee by chiral HPLC analysis (Chiralcel OZ-H, 3% i PrOH/hexanes, 0.6 mL/min, $t_r(d_1e_1, \text{minor}) = 8.0$ min, $t_r(d_2e_1, \text{minor}) = 8.7$ min, $t_r(d_1e_2, \text{major}) = 9.9$ min, $t_r(d_2e_2, \text{major}) = 12.0$ min).



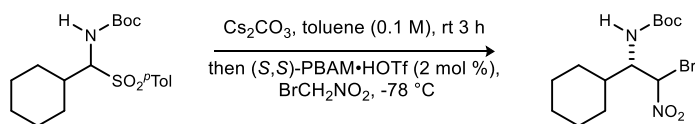
tert-Butyl ((2R)-1-bromo-3-methyl-1-nitrobutan-2-yl)carbamate (235). Prepared according to general procedure B using *tert*-butyl (2-methyl-1-tosylpropyl)carbamate (62.6 mg, 200 μmol). Flash column chromatography (SiO_2 , 2.5-7.5-15% ethyl acetate in hexanes) yielded the α -bromo nitroalkane (1:1 dr (^1H NMR)) as a white solid (27 mg, 44%). The diastereomers were determined to be 72 and 75% ee by chiral HPLC analysis (Chiralcel IA, 3% i PrOH/hexanes, 0.8 mL/min, $t_r(d_1e_1, \text{major}) = 11.4$ min, $t_r(d_2e_1, \text{major}) = 12.2$ min, $t_r(d_1e_2, \text{minor}) = 17.2$ min, $t_r(d_2e_2, \text{minor}) = 23.5$ min); $R_f = 0.44$ (20% EtOAc/hexanes); IR (film) 3300, 2969, 1682, 1564 cm^{-1} ; ^1H NMR (600 MHz, CDCl_3 , 1:1 mixture of diastereomers) δ 6.19 (d, $J = 2.9$ Hz, 1H), 6.06 (d, $J = 5.6$ Hz, 1H), 5.04 (d, $J = 9.8$ Hz, 1H), 4.71 (d, $J = 9.9$ Hz, 1H), 4.26 (dt, $J = 8.9, 2.9$ Hz, 1H), 4.13 (dt, $J = 10.6, 6.5$ Hz, 1H), 1.96 (m, 1H), 1.76 (m, 1H), 1.45 (s, 9H), 1.42 (s, 9H), 1.04 (d, $J = 9.7$ Hz, 3H), 1.02 (d, $J = 6.8$ Hz, 6H), 0.96 (d, $J = 6.7$ Hz, 3H); ^{13}C NMR (150 MHz, CDCl_3) ppm 155.4, 155.0, 85.2(2), 80.5, 80.4, 59.6, 59.3, 31.9, 30.3, 28.2, 28.1, 19.8, 19.3, 18.7, 18.1; HRMS (ESI): Exact mass calcd for $\text{C}_{10}\text{H}_{19}\text{BrN}_2\text{NaO}_4$ $[\text{M}+\text{Na}]^+$ 333.0426, found 333.0433.



tert-Butyl ((2S)-1-bromo-3-methyl-1-nitrobutan-2-yl)carbamate (ent-235). Prepared according to general procedure C using *tert*-butyl (2-methyl-1-tosylpropyl)carbamate (31.3 mg, 100 μ mol). Flash column chromatography (SiO₂, 2.5-7.5-15% ethyl acetate in hexanes) yielded the α -bromo nitroalkane (1:1 dr (¹H NMR)) as a white solid (18 mg, 58%). The diastereomers were determined to be 79 and 79% ee by chiral HPLC analysis (Chiralcel IA, 3% ⁱPrOH/hexanes, 0.8 mL/min, $t_r(d_{1e1}$, minor) = 11.4 min, $t_r(d_{2e1}$, minor) = 12.2 min, $t_r(d_{1e2}$, major) = 17.2 min, $t_r(d_{2e2}$, major) = 23.5 min).

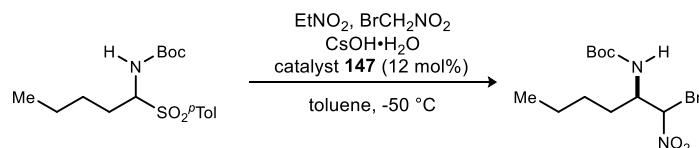


tert-Butyl ((1R)-2-bromo-1-cyclohexyl-2-nitroethyl)carbamate (236). Prepared according to general procedure B using *tert*-butyl (cyclohexyl(tosyl)methyl)carbamate (70.6 mg, 200 μ mol). Flash column chromatography (SiO₂, 2.5-7.5-15% ethyl acetate in hexanes) yielded the α -bromo nitroalkane (1:1 dr (¹H NMR)) as a white solid (19 mg, 36%). The diastereomers were determined to be 86 and 87% ee by chiral HPLC analysis (Chiralcel IC, 3% EtOH/hexanes, 1.0 mL/min, $t_r(d_{1e1}$, major) = 6.1 min, $t_r(d_{1e2}$, minor) = 6.8 min, $t_r(d_{2e1}$, major) = 8.1 min, $t_r(d_{2e2}$, minor) = 11.6 min); R_f = 0.50 (20% EtOAc/hexanes); IR (film) 3423, 2931, 2856, 1703, 1567 cm⁻¹; ¹H NMR (600 MHz, CDCl₃, 1:1 mixture of diastereomers) δ 6.20 (d, J = 2.6 Hz, 1H), 6.13 (d, J = 5.2 Hz, 1H), 5.09 (d, J = 10.2 Hz, 1H), 4.69 (d, J = 10.1 Hz, 1H), 4.32 (dt J = 9.1, 2.5 Hz, 1H), 4.12 (m, 1H), 1.86 (d, J = 12.8 Hz, 1H), 1.80-1.72 (m, 8H), 1.70-1.62 (m, 5H), 1.61-1.54 (m, 1H), 1.45 (s, 9H), 1.41 (s, 9H), 1.27-1.02 (m, 7H); ¹³C NMR (150 MHz, CDCl₃) ppm 155.5, 155.0, 85.1, 80.5, 80.3, 80.1, 58.58, 58.55, 40.9, 39.8, 30.1, 29.4, 28.8, 28.6, 28.2, 28.1, 25.8, 25.7, 25.62, 25.58, 25.54, 25.49; HRMS (ESI): Exact mass calcd for C₁₃H₂₃BrN₂NaO₄ [M+Na]⁺ 373.0739, found 373.0739.

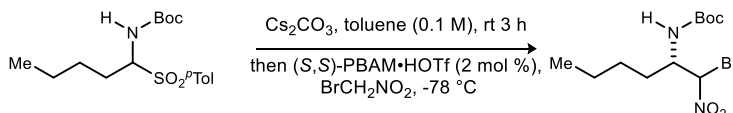


tert-Butyl ((1S)-2-bromo-1-cyclohexyl-2-nitroethyl)carbamate (ent-236). Prepared according to general procedure C using *tert*-butyl (cyclohexyl(tosyl)methyl)carbamate (35.3 mg, 100 μ mol). Flash column chromatography (SiO₂, 2.5-7.5-15% ethyl acetate in hexanes) yielded the α -bromo nitroalkane (1:1 dr (¹H NMR)) as a white solid (21 mg, 61%). The diastereomers were determined to be 92 and 92% ee by chiral

HPLC analysis (Chiralcel IC, 3% EtOH/hexanes, 1.0 mL/min, $t_r(d_1e_1, \text{minor}) = 6.1 \text{ min}$, $t_r(d_1e_2, \text{major}) = 6.8 \text{ min}$, $t_r(d_2e_1, \text{minor}) = 8.1 \text{ min}$, $t_r(d_2e_2, \text{major}) = 11.6 \text{ min}$).

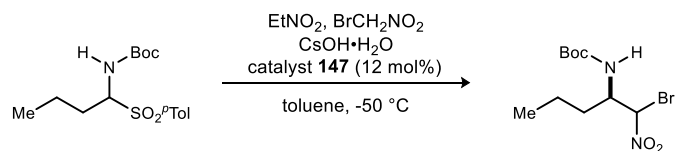


tert-Butyl ((2R)-1-bromo-1-nitrohexan-2-yl)carbamate (237). Prepared according to general procedure B using *tert*-butyl (1-tosylpentyl)carbamate (68.2 mg, 200 μmol). Flash column chromatography (SiO_2 , 2.5-7.5-15% ethyl acetate in hexanes) yielded the α -bromo nitroalkane (1:1 dr (^1H NMR)) as a white solid (35 mg, 54%). The enantiopurity was measured from the corresponding debrominated nitroalkane and determined to be 94% ee by chiral HPLC analysis¹³⁰ (Chiralcel AD, 10% *i*PrOH/hexanes, 0.8 mL/min, $t_r(e_1, \text{major}) = 7.7 \text{ min}$, $t_r(e_2, \text{minor}) = 8.1 \text{ min}$); $R_f = 0.53$ (20% EtOAc/hexanes); IR (film) 3333, 2962, 2869, 2873, 1697, 1555 cm^{-1} ; ^1H NMR (600 MHz, CDCl_3 , 1:1 mixture of diastereomers) δ 6.19 (d, $J = 4.3 \text{ Hz}$, 1H), 6.17 (d, $J = 2.5 \text{ Hz}$, 1H), 4.84 (d, $J = 8.3 \text{ Hz}$, 1H), 4.74 (d, $J = 8.6 \text{ Hz}$, 1H), 4.35-4.31 (m, 1H), 4.26-4.22 (m, 1H), 1.78-1.71 (m, 1H), 1.67-1.60 (m, 2H), 1.59-1.53 (m, 1H), 1.45 (s, 9H), 1.44 (s, 9H), 1.41-1.27 (m, 5H), 0.92 (t, $J = 6.4 \text{ Hz}$, 3H), 0.94 (d, $J = 7.0 \text{ Hz}$, 3H), 0.90 (d, $J = 6.5 \text{ Hz}$, 3H); ^{13}C NMR (150 MHz, CDCl_3) ppm 155.0, 154.9, 84.3, 83.1, 80.8, 80.6, 54.9, 54.4, 30.9, 30.0, 28.22, 28.19, 27.9, 27.8, 22.2, 22.1, 13.80, 13.79; HRMS (ESI): Exact mass calcd for $\text{C}_{11}\text{H}_{21}\text{BrN}_2\text{NaO}_4$ $[\text{M}+\text{Na}]^+$ 347.0582, found 347.0577.

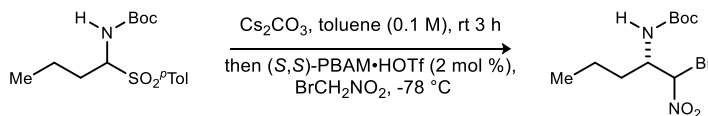


tert-Butyl ((2S)-1-bromo-1-nitrohexan-2-yl)carbamate (ent-237). Prepared according to general procedure C using *tert*-butyl (1-tosylpentyl)carbamate (34.1 mg, 100 μmol). Flash column chromatography (SiO_2 , 2.5-7.5-15% ethyl acetate in hexanes) yielded the α -bromo nitroalkane (1:1 dr (^1H NMR)) as a white solid (31 mg, 94%). The enantiopurity was measured from the corresponding debrominated nitroalkane and determined to be 88% ee by chiral HPLC analysis¹³⁰ (Chiralcel AD, 10% *i*PrOH/hexanes, 0.8 mL/min, $t_r(e_1, \text{minor}) = 7.7 \text{ min}$, $t_r(e_2, \text{major}) = 8.1 \text{ min}$).

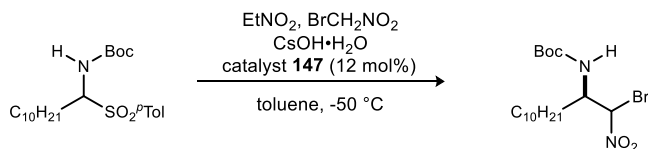
¹³⁰ Assay development of α -bromonitroalkane was difficult. α -Bromonitroalkane was treated with $\text{SnCl}_2 \cdot 2\text{H}_2\text{O}$ in THF to afford corresponding nitroalkane which was assayed to determine ee % of parent α -bromonitroalkane.



tert-Butyl ((2R)-1-bromo-1-nitropentan-2-yl)carbamate (238). Prepared according to general procedure B using *tert*-butyl (1-tosylbutyl)carbamate (65.4 mg, 200 μ mol). Flash column chromatography (SiO₂, 2.5-7.5-15% ethyl acetate in hexanes) yielded the α -bromo nitroalkane (1:1 dr (¹H NMR)) as a white solid (34 mg, 55%). The enantiopurity was measured from the corresponding debrominated nitroalkane and determined to be 87% ee by chiral HPLC analysis (Chiralcel AD, 10% ⁱPrOH/hexanes, 0.8 mL/min, $t_r(e_1, \text{major}) = 7.7$ min, $t_r(e_2, \text{minor}) = 8.6$ min); $R_f = 0.52$ (20% EtOAc/hexanes); IR (film) 3328, 2968, 2933, 1698, 1566 cm⁻¹; ¹H NMR (600 MHz, CDCl₃, 1:1 mixture of diastereomers) δ 6.19 (d, $J = 4.4$ Hz, 1H), 6.16 (d, $J = 2.7$ Hz, 1H), 4.84 (d, $J = 8.0$ Hz, 1H), 4.74 (d, $J = 8.9$ Hz, 1H), 4.35 (m, 1H), 4.26 (m, 1H), 1.74-1.67 (m, 2H), 1.61-1.52 (m, 4H), 1.45 (s, 9H), 1.43 (s, 9H), 1.43-1.34 (m, 2H), 0.97 (t, $J = 7.1$ Hz, 3H), 0.94 (t, $J = 7.4$ Hz, 3H); ¹³C NMR (150 MHz, CDCl₃) ppm 155.0, 154.9, 84.2, 83.1, 80.7, 80.6, 54.6, 54.1, 33.1, 32.3, 28.2, 28.1, 19.1, 19.0, 13.52, 13.46; HRMS (ESI): Exact mass calcd for C₁₀H₁₉BrN₂NaO₄ [M+Na]⁺ 333.0426, found 333.0439.

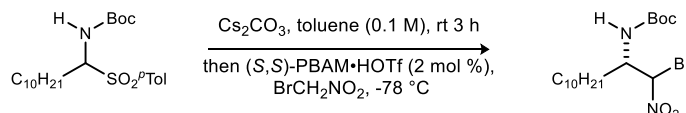


tert-Butyl ((2S)-1-bromo-1-nitropentan-2-yl)carbamate (ent-238). Prepared according to general procedure C using *tert*-butyl (1-tosylbutyl)carbamate (32.7 mg, 100 μ mol). Flash column chromatography (SiO₂, 2.5-7.5-15% ethyl acetate in hexanes) yielded the α -bromo nitroalkane (1:1 dr (¹H NMR)) as a white solid (27 mg, 87%). The enantiopurity was measured from the corresponding debrominated nitroalkane and determined to be 90% ee by chiral HPLC analysis (Chiralcel AD, 10% ⁱPrOH/hexanes, 0.8 mL/min, $t_r(e_1, \text{minor}) = 7.7$ min, $t_r(e_2, \text{major}) = 8.6$ min).

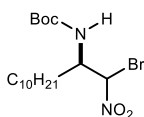


tert-Butyl ((2R)-1-bromo-1-nitrododecan-2-yl)carbamate (239). Prepared according to general procedure B using *tert*-butyl (1-tosylundecyl)carbamate (85.2 mg, 200 μ mol). Flash column chromatography (SiO₂, 2.5-7.5-15% ethyl acetate in hexanes) yielded the α -bromo nitroalkane (1:1 dr (¹H NMR)) as a white solid (41 mg, 51%). The diastereomers were determined to be 86 and 87% ee by chiral HPLC analysis (Chiralcel AD-H, 3% ⁱPrOH/hexanes, 1.0 mL/min, $t_r(d_{1e1}, \text{minor}) = 8.3$ min, $t_r(d_{1e2}, \text{major}) = 9.3$ min, $t_r(d_{2e1}, \text{minor}) = 10.3$ min, $t_r(d_{2e2}, \text{major}) = 11.0$ min); $R_f = 0.56$ (20% EtOAc/hexanes); IR (film)

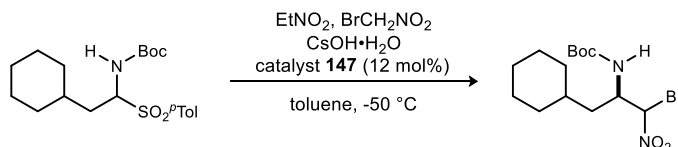
3342, 2927, 2856, 1703, 1566 cm^{-1} ; ^1H NMR (600 MHz, CDCl_3 , 1:1 mixture of diastereomers) δ 6.19 (d, J = 4.3 Hz, 1H), 6.16 (d, J = 2.3 Hz, 1H), 4.83 (d, J = 8.7 Hz, 1H), 4.73 (d, J = 9.0 Hz, 1H), 4.33 (m, 1H), 4.24 (m, 1H), 1.76-1.54 (m, 6H), 1.46 (s, 9H), 1.44 (s, 9H), 1.33-1.23 (m, 30H), 0.88 (t, J = 6.9 Hz, 6H); ^{13}C NMR (150 MHz, CDCl_3) ppm 155.0, 154.9, 84.3, 83.1, 80.7, 80.6, 54.9, 54.4, 31.9, 31.2, 30.3, 29.7, 29.5(2), 29.43(2), 29.36, 29.31(2), 29.26(2), 29.1, 29.02, 28.97, 28.21, 28.18, 25.8, 25.7, 22.7(2), 14.1(2); HRMS (ESI): Exact mass calcd for $\text{C}_{17}\text{H}_{33}\text{BrN}_2\text{NaO}_4$ $[\text{M}+\text{Na}]^+$ 431.1521, found 431.1538.



***tert*-Butyl ((2*S*)-1-bromo-1-nitrododecan-2-yl)carbamate (ent-239).** Prepared according to general procedure C using *tert*-butyl (1-tosylundecyl)carbamate (42.6 mg, 100 μmol). Flash column chromatography (SiO_2 , 2.5-7.5-15% ethyl acetate in hexanes) yielded the α -bromo nitroalkane (1:1 dr (^1H NMR)) as a white solid (36 mg, 88%). The diastereomers were determined to be 90 and 90% ee by chiral HPLC analysis (Chiralcel AD-H, 3% $^i\text{PrOH}$ /hexanes, 1.0 mL/min, $t_r(d_1e_1)$, major) = 8.3 min, $t_r(d_1e_2)$, minor) = 9.3 min, $t_r(d_2e_1)$, major) = 10.3 min, $t_r(d_2e_2)$, minor) = 11.0 min).

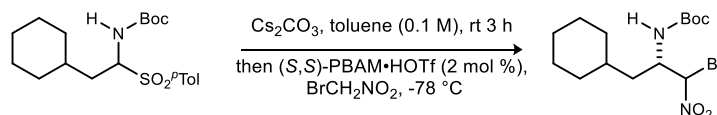


***tert*-Butyl ((2*R*)-1-bromo-1-nitrododecan-2-yl)carbamate (239).** To a flame dried flask equipped with a stir bar was added *tert*-butyl (1-tosylundecyl)carbamate (2.00 g, 4.70 mmol), toluene (47 mL) and Cs_2CO_3 (7.64 g, 23.5 mmol). The reaction was stirred for 3 h at room temperature. The reaction was filtered through a plug of Celite and washed with toluene (23 mL). The filtrate was collected in a flask and (*R,R*)-PBAM•HOTf (62.0 mg, 94.0 μmol) was added. The flask was cooled to -78 $^\circ\text{C}$ and bromonitromethane (517 μL , 7.05 mmol) was added and the reaction was stirred for 24 h. The mixture was filtered through a plug of silica gel with ethyl acetate and then concentrated. Flash column chromatography (SiO_2 , 2.5-7.5-15% ethyl acetate in hexanes) yielded the α -bromo nitroalkane (1:1 dr (^1H NMR)) as a white solid (1.41 g, 73%). The solid was recrystallized from ethanol and water to afford 412 mg (29% recovery). The diastereomers were determined to be 99 and 98% ee by chiral HPLC analysis.

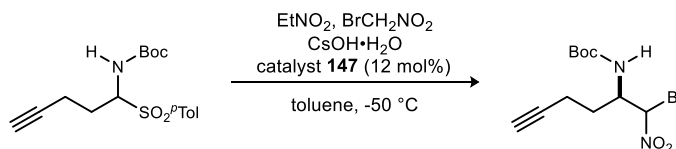


***tert*-Butyl ((2*R*)-1-bromo-3-cyclohexyl-1-nitropropan-2-yl)carbamate (240).** Prepared according to general procedure B using *tert*-butyl (2-cyclohexyl-1-tosylethyl)carbamate (76.4 mg, 200 μmol). Flash column chromatography (SiO_2 , 2.5-7.5-15% ethyl acetate in hexanes) yielded the α -bromo nitroalkane (1:1 dr (^1H NMR)) as a white solid (39 mg, 53%). The enantiopurity was measured from the corresponding debrominated nitroalkane and determined to be 96% ee by chiral HPLC analysis (Chiralcel AD, 10% $^i\text{PrOH}$ /hexanes, 0.8 mL/min, $t_r(e_1)$, minor) = 8.5 min, $t_r(e_2)$, major) = 9.2 min); R_f = 0.50 (20%

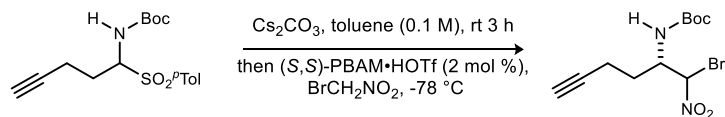
EtOAc/hexanes); IR (film) 3331, 2977, 2925, 2852, 1701, 1565 cm^{-1} ; ^1H NMR (600 MHz, CDCl_3 , 1:1 mixture of diastereomers) δ 6.18 (d, $J = 4.3$ Hz, 1H), 6.15 (d, $J = 2.8$ Hz, 1H), 4.81 (d, $J = 8.6$ Hz, 1H), 4.73 (d, $J = 8.9$ Hz, 1H), 4.43 (m, 1H), 4.36 (m, 1H), 1.81 (m, 2H), 1.73-1.53 (m, 10H), 1.40-1.09 (m, 9H), 1.45 (s, 9H), 1.43 (s, 9H), 1.05-0.80 (m, 5H); ^{13}C NMR (150 MHz, CDCl_3) ppm 154.9, 154.8, 84.4, 83.7, 80.7, 80.6, 52.6, 52.0, 38.4, 37.7, 34.0, 33.8, 33.5, 33.3, 33.2, 32.6, 32.3, 32.1, 28.2, 28.1, 26.2, 26.12, 26.08, 25.8; HRMS (ESI): Exact mass calcd for $\text{C}_{14}\text{H}_{25}\text{BrN}_2\text{NaO}_4$ $[\text{M}+\text{Na}]^+$ 387.0895, found 387.0891.



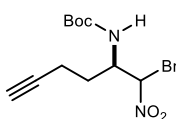
tert-Butyl ((2S)-1-bromo-3-cyclohexyl-1-nitropropan-2-yl)carbamate (ent-240). Prepared according to general procedure C using *tert*-butyl (2-cyclohexyl-1-tosylethyl)carbamate (38.2 mg, 100 μmol). Flash column chromatography (SiO_2 , 2.5-7.5-15% ethyl acetate in hexanes) yielded the α -bromo nitroalkane (1:1 dr (^1H NMR)) as a white solid (30 mg, 82%). The enantiopurity was measured from the corresponding debrominated nitroalkane and determined to be 85% ee by chiral HPLC analysis (Chiralcel AD, 10% i PrOH/hexanes, 0.8 mL/min, $t_r(e_1, \text{major}) = 8.5$ min, $t_r(e_2, \text{minor}) = 9.2$ min).



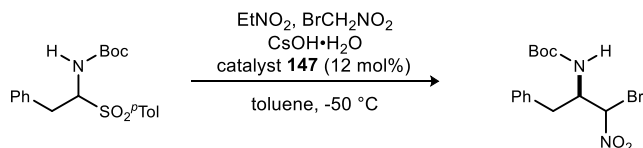
tert-Butyl ((2R)-1-bromo-1-nitrohex-5-yn-2-yl)carbamate (241). Prepared according to general procedure B using *tert*-butyl (1-tosylpent-4-yn-1-yl)carbamate (67.4 mg, 200 μmol). Flash column chromatography (SiO_2 , 2.5-7.5-15% ethyl acetate in hexanes) yielded the α -bromo nitroalkane (1:1 dr (^1H NMR)) as a white solid (27 mg, 42%). The diastereomers were determined to be 87 and 87% ee by chiral HPLC analysis (Chiralcel IC, 3% EtOH/hexanes, 1.0 mL/min, $t_r(d_1e_1, \text{major}) = 6.8$ min, $t_r(d_2e_1, \text{major}) = 7.3$ min, $t_r(d_1e_2, \text{minor}) = 9.1$ min, $t_r(d_2e_2, \text{minor}) = 10.2$ min); $R_f = 0.38$ (20% EtOAc/hexanes); IR (film) 3303, 2979, 1701, 1567 cm^{-1} ; ^1H NMR (600 MHz, CDCl_3 , 1:1 mixture of diastereomers) δ 6.27 (d, $J = 5.3$ Hz, 1H), 6.25 (d, $J = 2.6$ Hz, 1H), 4.95 (d, $J = 7.6$ Hz, 1H), 4.83 (d, $J = 8.4$ Hz, 1H), 4.48 (m, 1H), 4.35 (m, 1H), 2.38-2.30 (m, 4H), 2.05 (dd, $J = 2.6, 2.6$ Hz, 1H), 2.03 (dd, $J = 2.6, 2.6$ Hz, 1H), 1.97-1.87 (m, 2H), 1.80-1.72 (m, 2H), 1.44 (s, 9H), 1.43 (s, 9H); ^{13}C NMR (150 MHz, CDCl_3) ppm 154.79, 154.75, 83.3(2), 81.9, 81.7, 81.0, 80.9, 70.2, 70.1, 54.2, 53.9, 29.7, 28.8, 28.2(2), 15.4, 15.2; HRMS (ESI): Exact mass calcd for $\text{C}_{11}\text{H}_{17}\text{BrN}_2\text{NaO}_4$ $[\text{M}+\text{Na}]^+$ 343.0269, found 343.0284.



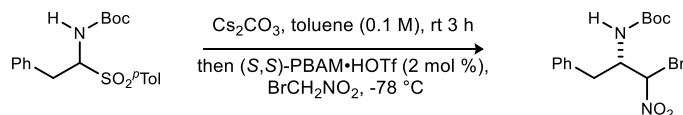
tert-Butyl ((2S)-1-bromo-1-nitrohex-5-yn-2-yl)carbamate (ent-241). Prepared according to general procedure C using *tert*-butyl (1-tosylpent-4-yn-1-yl)carbamate (33.7 mg, 100 μ mol). Flash column chromatography (SiO₂, 2.5-7.5-15% ethyl acetate in hexanes) yielded the α -bromo nitroalkane (1:1 dr (¹H NMR)) as a white solid (20 mg, 63%). The diastereomers were determined to be 85 and 86% ee by chiral HPLC analysis (Chiralcel IC, 3% EtOH/hexanes, 1.0 mL/min, $t_r(d_1e_1, \text{minor}) = 6.8$ min, $t_r(d_2e_1, \text{minor}) = 7.3$ min, $t_r(d_1e_2, \text{major}) = 9.1$ min, $t_r(d_2e_2, \text{major}) = 10.2$ min).



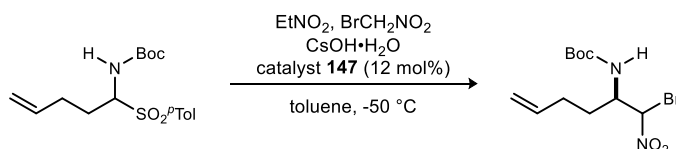
tert-Butyl ((2R)-1-bromo-1-nitrohex-5-yn-2-yl)carbamate (241). To a flame dried flask equipped with a stir bar was added using *tert*-butyl (1-tosylpent-4-yn-1-yl)carbamate (2.00 g, 5.90 mmol), toluene (60 mL) and Cs₂CO₃ (9.64 g, 29.7 mmol). The reaction was stirred for 3 h at room temperature. The reaction was filtered through a plug of Celite and washed with toluene (30 mL). The filtrate was collected in a flask and (*R,R*)-PBAM•HOTf (76.0 mg, 120.0 μ mol) was added. The flask was cooled to -78 °C and bromonitromethane (641 μ L, 8.85 mmol) was added and the reaction was stirred for 24 h. The mixture was filtered through a plug of silica gel with ethyl acetate and then concentrated. Flash column chromatography (SiO₂, 2.5-7.5-15% ethyl acetate in hexanes) yielded the α -bromo nitroalkane (1:1 dr (¹H NMR)) as a white solid (1.36 g, 72%). The solid was recrystallized from hexanes to afford 730 mg (54% recovery). The diastereomers were determined to be 98 and 99% ee by chiral HPLC analysis.



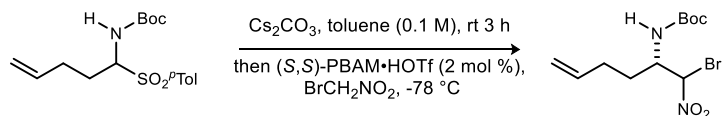
tert-Butyl ((2R)-1-bromo-1-nitro-3-phenylpropan-2-yl)carbamate (242). Prepared according to general procedure B using *tert*-butyl (2-phenyl-1-tosylethyl)carbamate (75.0 mg, 200 μ mol). Flash column chromatography (SiO₂, 2.5-7.5-15% ethyl acetate in hexanes) yielded the α -bromo nitroalkane (1:1 dr (¹H NMR)) as a white solid (20 mg, 28%). The enantiopurity was measured from the corresponding debrominated nitroalkane and determined to be 86% ee by chiral HPLC analysis (Chiralcel AD, 10% EtOH/hexanes, 0.8 mL/min, $t_r(e_1, \text{major}) = 10.8$ min, $t_r(e_2, \text{minor}) = 12.3$ min); R_f = 0.48 (20% EtOAc/hexanes); IR (film) 3362, 2979, 2929, 1693, 1549 cm⁻¹; ¹H NMR (600 MHz, CDCl₃, 1:1 mixture of diastereomers) δ 7.36-7.19 (m, 10H), 6.15 (d, $J = 5.3$ Hz, 1H), 6.00 (d, $J = 1.7$ Hz, 1H), 4.95 (d, $J = 8.0$ Hz, 1H), 4.86 (d, $J = 8.8$ Hz, 1H), 4.73-4.68 (m, 1H), 4.48-4.43 (m, 1H), 3.09-3.05 (m, 1H), 3.01-2.90 (m, 3H), 1.40 (s, 18H); ¹³C NMR (150 MHz, CDCl₃) ppm 154.7, 154.6, 135.4, 135.2, 129.2, 129.1, 129.0, 128.9, 127.5, 127.4, 84.2, 80.1, 80.94, 80.87, 80.7, 56.0, 55.8, 38.2, 36.5, 28.1; HRMS (ESI): Exact mass calcd for C₁₄H₁₉BrN₂NaO₄ [M+Na]⁺ 381.0426, found 381.0429.



tert-Butyl ((2S)-1-bromo-1-nitro-3-phenylpropan-2-yl)carbamate (ent-242). Prepared according to general procedure C using *tert*-butyl (2-phenyl-1-tosylethyl)carbamate (37.5 mg, 100 μ mol). Flash column chromatography (SiO₂, 2.5-7.5-15% ethyl acetate in hexanes) yielded the α -bromo nitroalkane (1:1 dr (¹H NMR)) as a white solid (14 mg, 39%). The enantiopurity was measured from the corresponding debrominated nitroalkane and determined to be 89% ee by chiral HPLC analysis (Chiralcel AD, 10% EtOH/hexanes, 0.8 mL/min, *t*_r(*e*₁, minor) = 10.8 min, *t*_r(*e*₂, major) = 12.3 min).

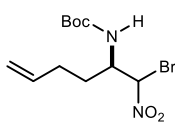


tert-Butyl ((2R)-1-bromo-1-nitrohex-5-en-2-yl)carbamate (243). Prepared according to general procedure B using *tert*-butyl (1-tosylpent-4-en-1-yl)carbamate (67.8 mg, 200 μ mol). Flash column chromatography (SiO₂, 2.5-7.5-15% ethyl acetate in hexanes) yielded the α -bromo nitroalkane (1:1 dr (¹H NMR)) as a white solid (37 mg, 57%). The enantiopurity was measured from the corresponding debrominated nitroalkane and determined to be 86% ee by chiral HPLC analysis (Chiralcel AD, 10% *i*PrOH/hexanes, 0.8 mL/min, *t*_r(*e*₁, major) = 7.6 min, *t*_r(*e*₂, minor) = 8.3 min); *R*_f = 0.38 (20% EtOAc/hexanes); IR (film) 3335, 2978, 2931, 1705, 1565 cm⁻¹; ¹H NMR (600 MHz, CDCl₃, 1:1 mixture of diastereomers) δ 6.19 (d, *J* = 4.7 Hz, 1H), 6.17 (d, *J* = 2.9 Hz, 1H), 5.81-5.72 (m, 2H), 5.09-5.03 (m, 4H), 4.88 (d, *J* = 7.4 Hz, 1H), 4.78 (d, *J* = 8.0 Hz, 1H), 4.36 (m, 1H), 4.25 (m, 1H), 2.25-2.18 (m, 2H), 2.17-2.09 (m, 1H), 1.87-1.59 (m, 4H), 1.45 (s, 9H), 1.43 (s, 9H); ¹³C NMR (150 MHz, CDCl₃) ppm 154.9, 154.8, 136.2, 136.1, 116.5, 116.4, 84.0, 82.8, 80.8, 80.7, 54.3, 53.8, 30.2, 29.8, 29.7, 29.5, 28.2, 28.1; HRMS (ESI): Exact mass calcd for C₁₁H₁₉BrN₂NaO₄ [M+Na]⁺ 345.0426, found 345.0439.



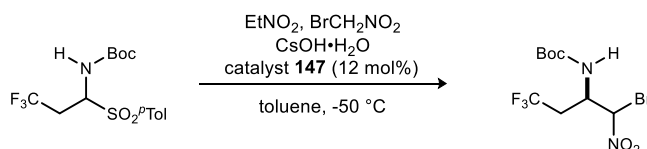
tert-Butyl ((2S)-1-bromo-1-nitrohex-5-en-2-yl)carbamate (ent-243). Prepared according to general procedure C using *tert*-butyl (1-tosylpent-4-en-1-yl)carbamate (33.9 mg, 100 μ mol). Flash column chromatography (SiO₂, 2.5-7.5-15% ethyl acetate in hexanes) yielded the α -bromo nitroalkane (1:1 dr (¹H NMR)) as a white solid (25 mg, 77%). The enantiopurity was measured from the corresponding

debrominated nitroalkane and determined to be 84% ee by chiral HPLC analysis (Chiralcel AD, 10% *i*PrOH/hexanes, 0.8 mL/min, $t_r(e_1, \text{minor}) = 7.6 \text{ min}$, $t_r(e_2, \text{major}) = 8.3 \text{ min}$).

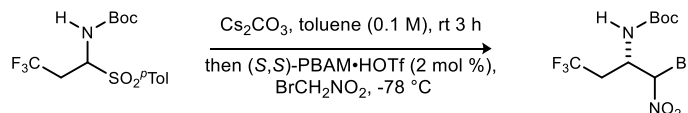


***tert*-Butyl ((2*R*)-1-bromo-1-nitrohex-5-en-2-yl)carbamate (243).** To a flame dried flask equipped with a stir bar was added using *tert*-butyl (1-tosylpent-4-en-1-yl)carbamate (1.95 g, 5.75 mmol), toluene (60 mL) and Cs₂CO₃ (9.36 g, 28.8 mmol).

The reaction was stirred for 3 h at room temperature. The reaction was filtered through a plug of Celite and washed with toluene (30 mL). The filtrate was collected in a flask and (*R,R*)-PBAM•HOTf (76.0 mg, 120.0 μmol) was added. The flask was cooled to -78 °C and bromonitromethane (630 μL, 8.60 mmol) was added and the reaction was stirred for 24 h. The mixture was filtered through a plug of silica gel with ethyl acetate and then concentrated. Flash column chromatography (SiO₂, 2.5-7.5-15% ethyl acetate in hexanes) yielded the α-bromo nitroalkane (1:1 dr (¹H NMR)) as a white solid (1.22 g, 66%). The solid was recrystallized from hexanes to afford 603 mg (59% recovery). The enantiopurity was measured from the corresponding debrominated nitroalkane and determined to be 99% ee by chiral HPLC analysis.

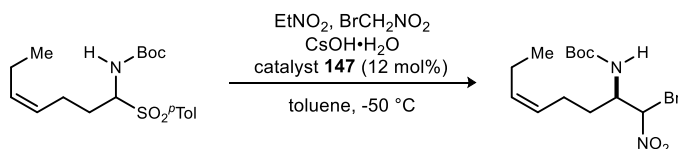


***tert*-Butyl ((2*R*)-1-bromo-4,4,4-trifluoro-1-nitrobutan-2-yl)carbamate (244).** Prepared according to general procedure B using *tert*-butyl (3,3,3-trifluoro-1-tosylpropyl)carbamate (75.0 mg, 200 μmol). Flash column chromatography (SiO₂, 2.5-7.5-15% ethyl acetate in hexanes) yielded the α-bromo nitroalkane (1:1 dr (¹H NMR)) as a white solid (32 mg, 46%). The enantiopurity was measured from the corresponding debrominated nitroalkane and determined to be 91% ee by chiral HPLC analysis (Chiralcel AD, 10% *i*PrOH/hexanes, 0.8 mL/min, $t_r(e_1, \text{major}) = 7.8 \text{ min}$, $t_r(e_2, \text{minor}) = 8.9 \text{ min}$); $R_f = 0.47$ (20% EtOAc/hexanes); IR (film) 3335, 2982, 2934, 1700, 1569 cm⁻¹; ¹H NMR (600 MHz, CDCl₃, 1:1 mixture of diastereomers) δ 6.35 (d, $J = 6.8 \text{ Hz}$, 1H), 6.29 (d, $J = 3.8 \text{ Hz}$, 1H), 5.04 (d, $J = 8.5 \text{ Hz}$, 1H), 4.98 (d, $J = 7.5 \text{ Hz}$, 1H), 4.64 (m, 1H), 4.45 (m, 1H), 2.86-2.74 (m, 2H), 2.64-2.52 (m, 2H), 1.44 (s, 9H), 1.43 (s, 9H); ¹³C NMR (150 MHz, CDCl₃) ppm 154.8, 154.3, 125.2 (¹ $J_{CF} = 276.8 \text{ Hz}$), 125.1 (¹ $J_{CF} = 276.8 \text{ Hz}$), 81.6, 80.5, 79.6, 50.5, 50.1, 34.6 (² $J_{CF} = 29.5 \text{ Hz}$), 33.5 (² $J_{CF} = 29.1 \text{ Hz}$), 28.0(2); HRMS (CI): Exact mass calcd for C₉H₁₅BrF₃N₂NaO₄ [M+H]⁺ 351.0162, found 351.0170.

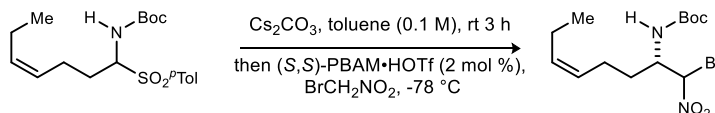


***tert*-Butyl ((2*S*)-1-bromo-4,4,4-trifluoro-1-nitrobutan-2-yl)carbamate (ent-244).** Prepared according to general procedure C using *tert*-butyl (3,3,3-trifluoro-1-tosylpropyl)carbamate (32.5 mg, 200 μmol). Flash column chromatography (SiO₂, 2.5-7.5-15% ethyl acetate in hexanes) yielded the α-bromo nitroalkane (1:1

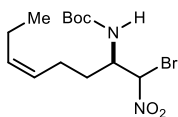
dr (^1H NMR)) as a white solid (20 mg, 57%). The enantiopurity was measured from the corresponding debrominated nitroalkane and determined to be 85% ee by chiral HPLC analysis (Chiralcel AD, 10% $^i\text{PrOH}$ /hexanes, 0.8 mL/min, $t_r(e_1, \text{minor}) = 7.8$ min, $t_r(e_2, \text{major}) = 8.9$ min).



***tert*-Butyl ((2*R*,*Z*)-1-bromo-1-nitrooct-5-en-2-yl)carbamate (245).** Prepared according to general procedure B using (*Z*)-*tert*-butyl (1-tosylhept-4-en-1-yl)carbamate (73.4 mg, 200 μmol). Flash column chromatography (SiO_2 , 2.5-7.5-15% ethyl acetate in hexanes) yielded the α -bromo nitroalkane (1:1 dr (^1H NMR)) as a white solid (40 mg, 57%). The enantiopurity was measured from the corresponding debrominated nitroalkane and determined to be 88% ee by chiral HPLC analysis (Chiralcel AD, 10% $^i\text{PrOH}$ /hexanes, 0.8 mL/min, $t_r(e_1, \text{major}) = 6.7$ min, $t_r(e_2, \text{minor}) = 7.4$ min); $R_f = 0.44$ (20% EtOAc/hexanes); IR (film) 3346, 2670, 2933, 1699, 1566 cm^{-1} ; ^1H NMR (600 MHz, CDCl_3 , 1:1 mixture of diastereomers) δ 6.20 (d, $J = 4.7$ Hz, 1H), 6.18 (d, $J = 2.9$ Hz, 1H), 5.45 (m, 2H), 5.26 (m, 2H), 4.87 (d, $J = 8.2$ Hz, 1H), 4.77 (d, $J = 8.6$ Hz, 1H), 4.33 (m, 1H), 4.23 (m, 1H), 2.15 (m, 4H), 2.01 (m, 4H), 1.66 (m, 2H), 1.58 (m, 2H), 1.45 (s, 9H), 1.43 (s, 9H), 0.96 (t, $J = 7.5$ Hz, 3H), 0.95 (t, $J = 7.5$ Hz, 3H); ^{13}C NMR (150 MHz, CDCl_3) ppm 154.9, 154.8, 133.9, 133.8, 126.3, 126.1, 84.0, 82.9, 80.7, 80.6, 54.4, 54.0, 30.9, 30.1, 28.2, 28.1, 23.3, 23.1, 20.50, 20.48, 14.1(2); HRMS (ESI): Exact mass calcd for $\text{C}_{13}\text{H}_{23}\text{BrN}_2\text{NaO}_4$ $[\text{M}+\text{Na}]^+$ 373.0739, found 373.0733.

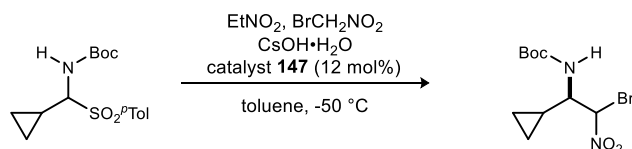


***tert*-Butyl ((2*S*,*Z*)-1-bromo-1-nitrooct-5-en-2-yl)carbamate (ent-245).** Prepared according to general procedure C using (*Z*)-*tert*-butyl (1-tosylhept-4-en-1-yl)carbamate (36.7 mg, 100 μmol). Flash column chromatography (SiO_2 , 2.5-7.5-15% ethyl acetate in hexanes) yielded the α -bromo nitroalkane (1:1 dr (^1H NMR)) as a white solid (28 mg, 80%). The enantiopurity was measured from the corresponding debrominated nitroalkane and determined to be 89% ee by chiral HPLC analysis (Chiralcel AD, 10% $^i\text{PrOH}$ /hexanes, 0.8 mL/min, $t_r(e_1, \text{minor}) = 6.7$ min, $t_r(e_2, \text{major}) = 7.4$ min).

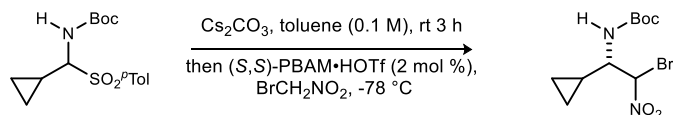


***tert*-Butyl ((2*R*,*Z*)-1-bromo-1-nitrooct-5-en-2-yl)carbamate (245).** To a flame dried flask equipped with a stir bar was added using (*Z*)-*tert*-butyl (1-tosylhept-4-en-1-yl)carbamate (2.00 g, 5.40 mmol), toluene (60 mL) and Cs_2CO_3 (8.84 g, 27.2 mmol). The reaction was stirred for 3 h at room temperature. The reaction was filtered through a plug of Celite and washed with toluene (30 mL). The filtrate was collected in a flask and (*R,R*)-PBAM·HOTf (71.0 mg, 110.0 μmol) was added. The flask was cooled to $-78\text{ }^\circ\text{C}$ and bromonitromethane (593 μL , 8.10 mmol) was added and the reaction was stirred for 24 h. The mixture was filtered through a plug of silica gel with ethyl acetate and then concentrated. Flash column chromatography (SiO_2 , 2.5-7.5-

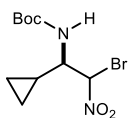
15% ethyl acetate in hexanes) yielded the α -bromo nitroalkane (1:1 dr (^1H NMR)) as a white solid (1.16 g, 61%). The solid was recrystallized from hexanes to afford 447 mg (39% recovery). The enantiopurity was measured from the corresponding debrominated nitroalkane and determined to be 99% ee by chiral HPLC analysis.



tert-Butyl ((1R)-2-bromo-1-cyclopropyl-2-nitroethyl)carbamate (246). Prepared according to general procedure B using *tert*-butyl (cyclopropyl(tosyl)methyl)carbamate (65.0 mg, 200 μmol). Flash column chromatography (SiO_2 , 2.5-7.5-15% ethyl acetate in hexanes) yielded the α -bromo nitroalkane (1:1 dr (^1H NMR)) as a white solid (31 mg, 50%). The diastereomers were determined to be 78 and 77% ee by chiral HPLC analysis (Chiralcel IC, 3% EtOH/hexanes, 0.8 mL/min, $t_r(d_{1e1}, \text{major}) = 8.3$ min, $t_r(d_{2e1}, \text{major}) = 9.5$ min, $t_r(d_{1e2}, \text{minor}) = 10.4$ min, $t_r(d_{2e2}, \text{minor}) = 11.7$ min); $R_f = 0.47$ (20% EtOAc/hexanes); IR (film) 3322, 2979, 2925, 1697, 1566 cm^{-1} ; ^1H NMR (600 MHz, CDCl_3 , 1:1 mixture of diastereomers) δ 6.34 (d, $J = 2.9$ Hz, 1H), 6.25 (s, 1H), 5.11 (d, $J = 6.0$ Hz, 1H), 4.97 (s, 1H), 3.73 (m, 1H), 3.66 (m, 1H), 1.45 (s, 9H), 1.43 (s, 9H), 1.08-1.01 (m, 2H), 0.72-0.69 (m, 1H) 0.67-0.61 (m, 2H), 0.60-0.56 (m, 1H), 0.51-0.47 (m, 2H), 0.43-0.39 (m, 1H), 0.38-0.33 (m, 1H); ^{13}C NMR (150 MHz, CDCl_3) ppm 154.9, 154.8, 84.3, 83.4, 80.71, 80.66, 59.1, 58.4, 28.2, 28.1, 13.3, 11.6, 4.8, 4.6, 3.3, 2.2; HRMS (ESI): Exact mass calcd for $\text{C}_{10}\text{H}_{17}\text{BrN}_2\text{NaO}_4$ $[\text{M}+\text{Na}]^+$ 331.0269, found 331.0260.



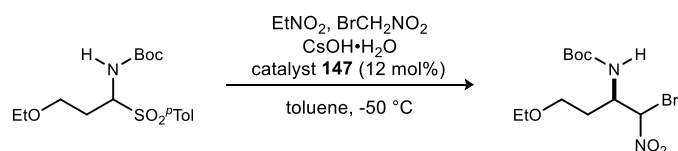
tert-Butyl ((1S)-2-bromo-1-cyclopropyl-2-nitroethyl)carbamate (ent-246). Prepared according to general procedure C using *tert*-butyl (cyclopropyl(tosyl)methyl)carbamate (32.5 mg, 100 μmol). Flash column chromatography (SiO_2 , 2.5-7.5-15% ethyl acetate in hexanes) yielded the α -bromo nitroalkane (1:1 dr (^1H NMR)) as a white solid (16 mg, 52%). The diastereomers were determined to be 83 and 85% ee by chiral HPLC analysis (Chiralcel IC, 3% EtOH/hexanes, 0.8 mL/min, $t_r(d_{1e1}, \text{minor}) = 8.3$ min, $t_r(d_{2e1}, \text{minor}) = 9.5$ min, $t_r(d_{1e2}, \text{major}) = 10.4$ min, $t_r(d_{2e2}, \text{major}) = 11.7$ min).



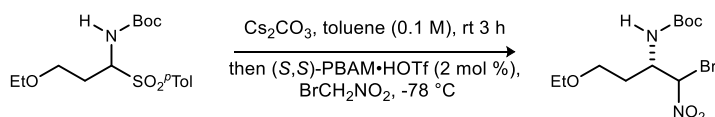
tert-Butyl ((1R)-2-bromo-1-cyclopropyl-2-nitroethyl)carbamate (246). To a flame dried flask equipped with a stir bar was added *tert*-butyl (cyclopropyl(tosyl)methyl)carbamate (1.95 g, 6.00 mmol), toluene (60 mL) and Cs_2CO_3 (9.75 g, 30.0 mmol). The reaction was stirred for 3 h at room temperature.

The reaction was filtered through a plug of Celite and washed with toluene (30 mL). The filtrate was collected in a flask and (*R,R*)-PBAM·HOTf (79.0 mg, 120.0 μmol) was added. The flask was cooled to $-78\text{ }^\circ\text{C}$ and bromonitromethane (660 μL , 9.00 mmol) was added and the reaction was stirred for 24 h. The

mixture was filtered through a plug of silica gel with ethyl acetate and then concentrated. Flash column chromatography (SiO₂, 2.5-7.5-15% ethyl acetate in hexanes) yielded the α -bromo nitroalkane (1:1 dr (¹H NMR)) as a white solid (949 mg, 51%). The solid was subjected to a recrystallization with ethanol and water to afford 578 mg (61% recovery) of an enantioenriched mother liquor. The diastereomers were determined to be 98 and 96% ee by chiral HPLC analysis.

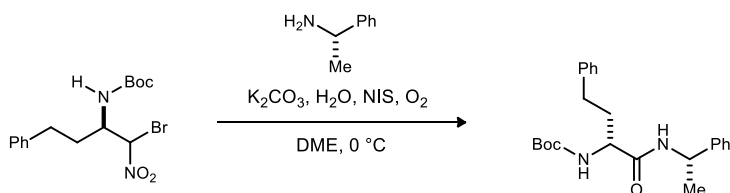


tert-Butyl ((2R)-1-bromo-4-ethoxy-1-nitrobutan-2-yl)carbamate (247). Prepared according to general procedure B using *tert*-butyl (3-ethoxy-1-tosylpropyl)carbamate (71.4 mg, 200 μ mol). Flash column chromatography (SiO₂, 10-20-30% ethyl acetate in hexanes) yielded the α -bromo nitroalkane (1:1 dr (¹H NMR)) as a white solid (25 mg, 37%). The enantiopurity was measured from the corresponding debrominated nitroalkane and determined to be 75% ee by chiral HPLC analysis (Chiralcel IA, 10% EtOH/hexanes, 1.0 mL/min, $t_r(e_1, \text{minor}) = 6.5$ min, $t_r(e_2, \text{major}) = 7.9$ min); $R_f = 0.25$ (20% EtOAc/hexanes); IR (film) 3333, 2977, 1705, 1566 cm⁻¹; ¹H NMR (600 MHz, CDCl₃, 1:1 mixture of diastereomers) δ 6.34 (d, $J = 2.6$ Hz, 1H), 6.29 (d, $J = 4.9$ Hz, 1H), 5.28 (d, $J = 8.4$ Hz, 1H), 5.04 (d, $J = 7.7$ Hz, 1H), 4.50 (m, 1H), 4.40 (m, 1H), 3.53-3.49 (m, 4H), 3.48-3.44 (m, 4H), 2.09-2.04 (m, 1H), 1.99-1.89 (m, 2H), 1.80-1.73 (m, 1H), 1.44 (s, 9H), 1.43 (s, 9H), 1.19 (t, $J = 7.0$ Hz, 6H); ¹³C NMR (150 MHz, CDCl₃) ppm 155.0, 154.9, 83.9, 82.1, 80.6, 80.5, 66.7, 66.5(2), 66.4, 53.5, 53.0, 31.2, 30.3, 28.2, 28.1, 15.0(2); HRMS (ESI): Exact mass calcd for C₁₁H₂₁BrN₂NaO₅ [M+Na]⁺ 363.0532, found 363.0515.

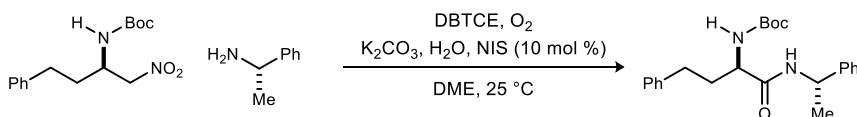


tert-Butyl ((2S)-1-bromo-4-ethoxy-1-nitrobutan-2-yl)carbamate (ent-247). Prepared according to general procedure C using *tert*-butyl (3-ethoxy-1-tosylpropyl)carbamate (35.7 mg, 100 μ mol). Flash column chromatography (SiO₂, 10-20-30% ethyl acetate in hexanes) yielded the α -bromo nitroalkane (1:1 dr (¹H NMR)) as a white solid (23 mg, 68%). The enantiopurity was measured from the corresponding debrominated nitroalkane and determined to be 76% ee by chiral HPLC analysis (Chiralcel IA, 10% EtOH/hexanes, 1.0 mL/min, $t_r(e_1, \text{major}) = 6.5$ min, $t_r(e_2, \text{minor}) = 7.9$ min).

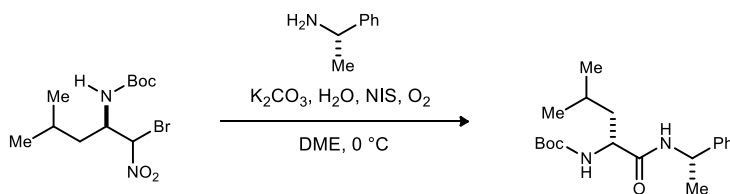
General procedure for Umpolung Amide Synthesis: To a vial equipped with a stir bar was added α -bromonitroalkane (1.0 equiv.), dimethoxyethane (0.5 M), H₂O (5 equiv.) and (*S*)- α -methylbenzylamine (1.2 equiv.). The reaction was cooled to 0 °C. K₂CO₃ (3 equiv.) and *N*-iodosuccinimide (0.1 equiv.) were added and the reaction mixture was placed under an O₂ atmosphere and stirred for 24 h. The mixture was quenched with 1 M HCl and extracted with dichloromethane. The organic phase was washed with sat. Na₂S₂O₃, dried and concentrated. The resulting solid was purified by flash column chromatography.



tert-Butyl ((R)-1-oxo-4-phenyl-1-(((S)-1-phenylethyl)amino)butan-2-yl)carbamate (248). Prepared according to the general procedure using *tert*-butyl ((2*R*)-1-bromo-1-nitro-4-phenylbutan-2-yl)carbamate (41.0 mg, 110 μ mol), DME (0.5 mL), H₂O (10 μ L, 550 μ mol), (*S*)- α -methylbenzylamine (17 μ L, 130 μ mol), *N*-iodosuccinimide (2.5 mg, 11 μ mol), K₂CO₃ (45.5 mg, 330 μ mol). Flash column chromatography (SiO₂, 10-15-20% ethyl acetate in hexanes) yielded the desired amide as a white solid (27 mg, 57%). The amide was determined to be 29:1 dr by HPLC analysis (Chiralcel AD-H, 10% *i*PrOH/hexanes, 1 mL/min, $t_r(d_1, \text{minor}) = 8.3$ min, $t_r(d_2, \text{major}) = 13.1$ min); $R_f = 0.16$ (20% EtOAc/hexanes); $[\alpha]_D^{20} -9.0$ (*c* .50, CHCl₃); IR (film) 3303, 2976, 2929, 1696, 1655 cm⁻¹; ¹H NMR (600 MHz, CDCl₃) δ 7.32-7.17 (m, 10H), 6.39 (br s, 1H), 5.09 (m, 1H), 4.95 (br s, 1H), 4.03 (br s, 1H), 2.72-2.66 (m, 2H), 2.17 (m, 1H), 1.91 (m, 1H), 1.48 (d, *J* = 7.0 Hz, 3H), 1.43 (s, 9H); ¹³C NMR (150 MHz, CDCl₃) ppm 170.6, 155.8, 143.0, 140.8, 128.6, 128.5, 128.4, 127.3, 126.1, 126.0, 80.2, 53.9, 48.8, 33.3, 31.9, 28.2, 22.0; HRMS (ESI): Exact mass calcd for C₂₃H₃₀N₂NaO₃ [M+Na]⁺ 405.2154, found 405.2159.

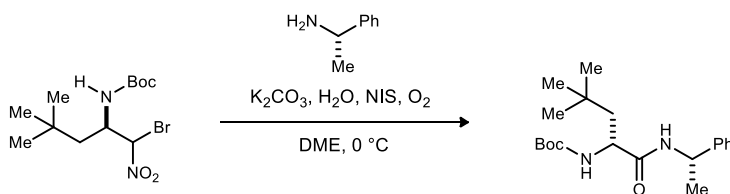


tert-Butyl ((R)-1-oxo-4-phenyl-1-(((S)-1-phenylethyl)amino)butan-2-yl)carbamate (248). Prepared according to the general procedure for nitroalkane amidation using *tert*-butyl (*R*)-1-(1-nitro-4-phenylbutan-2-yl)carbamate (29.4 mg, 100 μ mol) and (*S*)-1-phenylethylamine (26 μ L, 200 μ mol). Flash column chromatography (SiO₂, 10-40% ethyl acetate in hexanes) yielded the amide as a white solid (26 mg, 67%) in >20:1 dr (¹H NMR). Characterization data matched the literature.³⁹



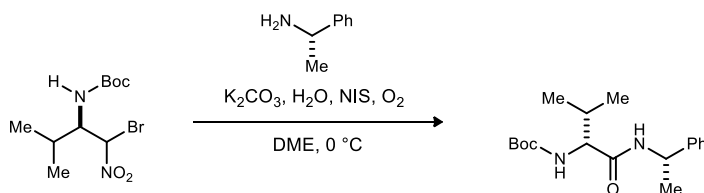
tert-Butyl ((R)-4-methyl-1-oxo-1-(((S)-1-phenylethyl)amino)pentan-2-yl)carbamate (249). Prepared according to the general procedure using *tert*-butyl ((2*R*)-1-bromo-4-methyl-1-nitropentan-2-yl)carbamate (26.0 mg, 80 μ mol), DME (0.4 mL), H₂O (7 μ L, 400 μ mol), (*S*)- α -methylbenzylamine (12 μ L, 100 μ mol), *N*-iodosuccinimide (1.8 mg, 8 μ mol), K₂CO₃ (33.1 mg, 240 μ mol). Flash column chromatography (SiO₂, 10-15-20% ethyl acetate in hexanes) yielded the desired amide as a white solid (15 mg, 58%). The amide was determined to be 18:1 dr by HPLC analysis (Chiralcel AD-H, 10% *i*PrOH/hexanes, 1 mL/min, $t_r(d_1, \text{minor}) = 5.6$ min, $t_r(d_2, \text{major}) = 9.5$ min); $R_f = 0.38$ (30% EtOAc/hexanes); $[\alpha]_D^{20} +4.0$ (*c* .35, CHCl₃); IR (film) 3282, 2960, 2930, 1679, 1651 cm⁻¹; ¹H NMR (600 MHz, CDCl₃) δ 7.32-7.21 (m, 5H), 6.50 (br s,

1H), 5.08 (m, 1H), 4.82 (br s, 1H), 4.08 (br s, 1H), 1.72-1.65 (m, 3H), 1.48 (d, $J = 6.9$ Hz, 3H), 1.42 (s, 9H), 0.94 (d, $J = 6.0$ Hz, 3H), 0.93 (d, $J = 5.8$ Hz, 3H); ^{13}C NMR (150 MHz, CDCl_3) ppm 171.3, 155.8, 143.1, 128.6, 127.2, 126.0, 80.1, 52.9, 48.7, 40.5, 29.7, 28.2, 24.7, 22.8, 22.0; HRMS (ESI): Exact mass calcd for $\text{C}_{19}\text{H}_{30}\text{N}_2\text{NaO}_3$ $[\text{M}+\text{Na}]^+$ 357.2154, found 357.2152.



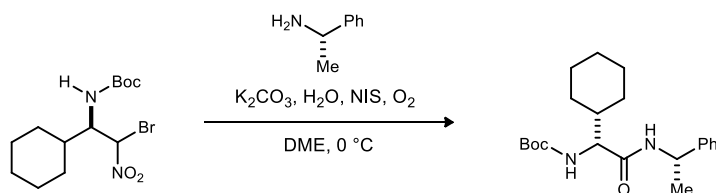
tert-Butyl ((R)-4,4-dimethyl-1-oxo-1-(((S)-1-phenylethyl)amino)pentan-2-yl)carbamate (250).

Prepared according to the general procedure using *tert*-butyl ((*2R*)-1-bromo-4,4-dimethyl-1-nitropentan-2-yl)carbamate (37.3 mg, 110 μmol), DME (0.5 mL), H_2O (10 μL , 550 μmol), (*S*)- α -methylbenzylamine (17 μL , 130 μmol), *N*-iodosuccinimide (2.5 mg, 11 μmol), K_2CO_3 (45.5 mg, 330 μmol). Flash column chromatography (SiO_2 , 10-15-20% ethyl acetate in hexanes) yielded the desired amide as a white solid (22 mg, 58%). The amide was determined to be 32:1 dr by HPLC analysis (Chiralcel AD-H, 10% $^i\text{PrOH}$ /hexanes, 1 mL/min, $t_r(d_1, \text{minor}) = 5.3$ min, $t_r(d_2, \text{major}) = 8.0$ min); $R_f = 0.41$ (30% EtOAc/hexanes); $[\alpha]_D^{20} +8.8$ (c .40, CHCl_3); IR (film) 3323, 2956, 1679, 1647 cm^{-1} ; ^1H NMR (600 MHz, CDCl_3) δ 7.29-7.20 (m, 5H), 6.60 (br s, 1H), 5.04 (m, 1H), 4.80 (d, $J = 6.8$ Hz, 1H), 4.09 (br s, 1H), 1.94 (d, $J = 11.4$ Hz, 1H), 1.45 (d, $J = 6.9$ Hz, 3H), 1.40 (s, 9H), 1.34 (dd, $J = 14.2, 7.7$ Hz, 1H), 0.93 (s, 9H); ^{13}C NMR (150 MHz, CDCl_3) ppm 171.7, 155.6, 143.2, 127.5, 127.1, 126.0, 80.1, 52.1, 48.7, 44.7, 30.2, 29.7, 28.3, 22.0; HRMS (ESI): Exact mass calcd for $\text{C}_{20}\text{H}_{32}\text{N}_2\text{NaO}_3$ $[\text{M}+\text{Na}]^+$ 371.2311, found 371.2310.

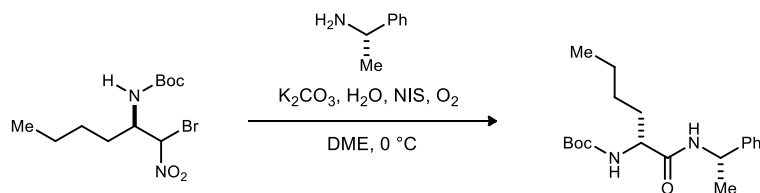


tert-Butyl ((R)-3-methyl-1-oxo-1-(((S)-1-phenylethyl)amino)butan-2-yl)carbamate (251).

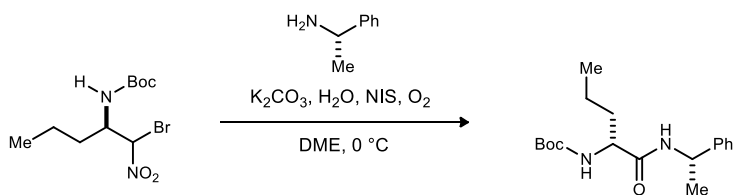
Prepared according to the general procedure using *tert*-butyl ((*2R*)-1-bromo-3-methyl-1-nitrobutan-2-yl)carbamate (23.9 mg, 77 μmol), DME (0.4 mL), H_2O (7 μL , 390 μmol), (*S*)- α -methylbenzylamine (12 μL , 93 μmol), *N*-iodosuccinimide (1.7 mg, 8 μmol), K_2CO_3 (31.7 mg, 230 μmol). Flash column chromatography (SiO_2 , 10-15-20% ethyl acetate in hexanes) yielded the desired amide as a white solid (18 mg, 73%). The amide was determined to be 5:1 dr by HPLC analysis (Chiralcel AD-H, 10% $^i\text{PrOH}$ /hexanes, 1 mL/min, $t_r(d_1, \text{minor}) = 6.2$ min, $t_r(d_2, \text{major}) = 9.2$ min); $R_f = 0.34$ (30% EtOAc/hexanes); $[\alpha]_D^{20} -30.5$ (c .42, CHCl_3); IR (film) 3325, 2968, 2927, 1649 cm^{-1} ; ^1H NMR (600 MHz, CDCl_3) δ 7.33-7.23 (m, 5H), 6.29 (d, $J = 7.7$ Hz, 1H), 5.11 (m, 1H), 4.07 (d, $J = 8.3$ Hz, 1H), 3.84 (dd, $J = 8.7, 6.8$ Hz, 1H), 2.15 (m, 1H), 1.48 (d, $J = 6.9$ Hz, 3H), 1.42 (s, 9H), 0.97 (d, $J = 6.8$ Hz, 3H), 0.92 (d, $J = 4.7$ Hz, 3H); ^{13}C NMR (150 MHz, CDCl_3) ppm 170.6, 155.9, 142.9, 128.6, 127.3, 126.0, 79.9, 60.2, 48.8, 30.5, 28.2, 21.9, 19.3, 17.9; HRMS (ESI): Exact mass calcd for $\text{C}_{18}\text{H}_{28}\text{N}_2\text{NaO}_3$ $[\text{M}+\text{Na}]^+$ 343.1998, found 343.1998.



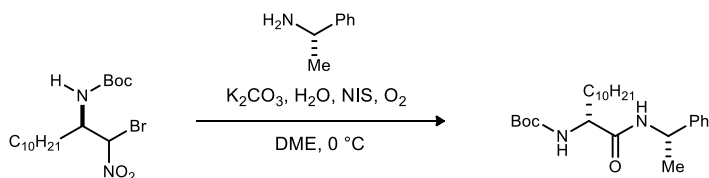
tert-Butyl ((R)-1-cyclohexyl-2-oxo-2-(((S)-1-phenylethyl)amino)ethyl)carbamate (252). Prepared according to the general procedure using *tert*-butyl ((1*R*)-2-bromo-1-cyclohexyl-2-nitroethyl)carbamate (17.6 mg, 50 μ mol), DME (0.3 mL), H₂O (5 μ L, 250 μ mol), (*S*)- α -methylbenzylamine (8 μ L, 60 μ mol), *N*-iodosuccinimide (1.2 mg, 5 μ mol), K₂CO₃ (20.7 mg, 150 μ mol). Flash column chromatography (SiO₂, 10-15-20% ethyl acetate in hexanes) yielded the desired amide as a white solid (10 mg, 56%). The amide was determined to be 14:1 dr by HPLC analysis (Chiralcel AD-H, 10% *i*PrOH/hexanes, 1 mL/min, $t_r(d_1, \text{minor}) = 7.0$ min, $t_r(d_2, \text{major}) = 10.5$ min); $R_f = 0.41$ (30% EtOAc/hexanes); $[\alpha]_D^{20} -12.6$ (c .34, CHCl₃); IR (film) 3409, 2926, 2853, 1649 cm⁻¹; ¹H NMR (600 MHz, CDCl₃) δ 7.33-7.24 (m, 5H), 6.19 (d, $J = 6.9$ Hz, 1H), 5.10 (m, 1H), 5.01 (br s, 1H), 3.83 (dd, $J = 7.4, 7.4$ Hz, 1H), 1.80-1.64 (m, 6H), 1.49 (d, $J = 6.9$ Hz, 3H), 1.42 (s, 9H), 1.30-0.94 (m, 5H); ¹³C NMR (150 MHz, CDCl₃) ppm 170.5, 155.9, 142.9, 128.6, 127.3, 126.1, 79.9, 59.7, 48.8, 40.0, 29.8, 29.7, 28.4, 28.3, 26.1, 25.9, 21.9; HRMS (ESI): Exact mass calcd for C₂₁H₃₂N₂NaO₃ [M+Na]⁺ 383.2311, found 383.2309.



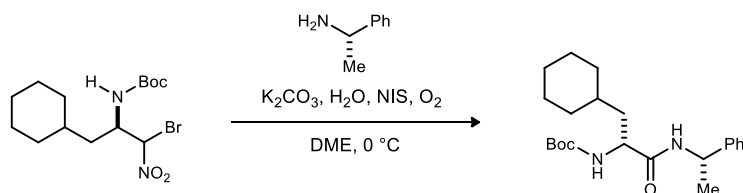
tert-Butyl ((R)-1-oxo-1-(((S)-1-phenylethyl)amino)hexan-2-yl)carbamate (253). Prepared according to the general procedure using *tert*-butyl ((2*R*)-1-bromo-1-nitrohexan-2-yl)carbamate (32.5 mg, 100 μ mol), DME (0.5 mL), H₂O (9 μ L, 500 μ mol), (*S*)- α -methylbenzylamine (16 μ L, 120 μ mol), *N*-iodosuccinimide (2.3 mg, 10 μ mol), K₂CO₃ (41.4 mg, 300 μ mol). Flash column chromatography (SiO₂, 10-15-20% ethyl acetate in hexanes) yielded the desired amide as a white solid (17 mg, 52%). The amide was determined to be 41:1 dr by HPLC analysis (Chiralcel AD-H, 10% *i*PrOH/hexanes, 1 mL/min, $t_r(d_1, \text{minor}) = 6.4$ min, $t_r(d_2, \text{major}) = 11.3$ min); $R_f = 0.22$ (20% EtOAc/hexanes); $[\alpha]_D^{20} -8.4$ (c .55, CHCl₃); IR (film) 3298, 2963, 2932, 1652 cm⁻¹; ¹H NMR (600 MHz, CDCl₃) δ 7.32-7.22 (m, 5H), 6.44 (br s, 1H), 5.08 (m, 1H), 4.93 (br s, 1H), 4.01 (br s, 1H), 1.84 (m, 1H), 1.57 (m, 1H), 1.48 (d, $J = 6.9$ Hz, 3H), 1.42 (s, 9H), 1.35-1.29 (m, 4H), 0.89 (t, $J = 6.8$ Hz, 3H); ¹³C NMR (150 MHz, CDCl₃) ppm 171.0, 155.8, 143.0, 128.6, 127.2, 126.0, 80.0, 54.6, 48.7, 31.6, 28.2, 27.8, 22.4, 22.0, 13.9; HRMS (ESI): Exact mass calcd for C₂₀H₃₂N₂NaO₃ [M+Na]⁺ 357.2154, found 357.2165.



tert-Butyl ((R)-1-oxo-1-(((S)-1-phenylethyl)amino)pentan-2-yl)carbamate (254). Prepared according to the general procedure using *tert*-butyl ((2*R*)-1-bromo-1-nitropentan-2-yl)carbamate (15.6 mg, 50 μ mol), DME (0.3 mL), H₂O (5 μ L, 250 μ mol), (*S*)- α -methylbenzylamine (8 μ L, 60 μ mol), *N*-iodosuccinimide (1.1 mg, 5 μ mol), K₂CO₃ (20.7 mg, 150 μ mol). Flash column chromatography (SiO₂, 10-15-20% ethyl acetate in hexanes) yielded the desired amide as a white solid (11 mg, 69%). The amide was determined to be 22:1 dr by HPLC analysis (Chiralcel AD-H, 10% ⁱPrOH/hexanes, 1 mL/min, $t_r(d_1, \text{minor})$ = 6.2 min, $t_r(d_2, \text{major})$ = 11.2 min); R_f = 0.34 (30% EtOAc/hexanes); $[\alpha]_D^{20}$ +10.3 (c .29, CHCl₃); IR (film) 3429, 2967, 2930, 1651 cm⁻¹; ¹H NMR (600 MHz, CDCl₃) δ 7.32-7.23 (m, 5H), 6.41 (br s, 1H), 5.09 (m, 1H), 4.91 (br s, 1H), 4.02 (br s, 1H), 1.82 (m, 1H), 1.56 (m, 1H), 1.48 (d, J = 7.0 Hz, 3H), 1.42 (s, 9H), 1.40-1.34 (m, 2H), 0.93 (t, J = 7.3 Hz, 3H); ¹³C NMR (150 MHz, CDCl₃) ppm 171.1, 155.8, 143.0, 128.6, 127.2, 126.0, 80.0, 54.4, 48.7, 33.0, 28.2, 22.0, 18.9, 13.7; HRMS (ESI): Exact mass calcd for C₁₈H₂₈N₂NaO₃ [M+Na]⁺ 343.1998, found 343.1985.

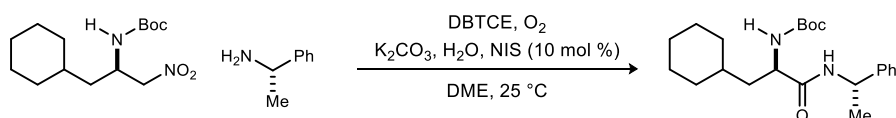


tert-Butyl ((R)-1-oxo-1-(((S)-1-phenylethyl)amino)dodecan-2-yl)carbamate (255). Prepared according to the general procedure using *tert*-butyl ((2*R*)-1-bromo-1-nitrododecan-2-yl)carbamate (34.8 mg, 85 μ mol), DME (0.4 mL), H₂O (8 μ L, 430 μ mol), (*S*)- α -methylbenzylamine (13 μ L, 100 μ mol), *N*-iodosuccinimide (1.9 mg, 9 μ mol), K₂CO₃ (35.9 mg, 260 μ mol). Flash column chromatography (SiO₂, 10-15-20% ethyl acetate in hexanes) yielded the desired amide as a white solid (23 mg, 65%). The amide was determined to be 28:1 dr by HPLC analysis (Chiralcel AD-H, 10% ⁱPrOH/hexanes, 1 mL/min, $t_r(d_1, \text{minor})$ = 4.8 min, $t_r(d_2, \text{major})$ = 8.4 min); R_f = 0.48 (30% EtOAc/hexanes); $[\alpha]_D^{20}$ -12.8 (c .36, CHCl₃); IR (film) 3284, 2926, 2855, 1653 cm⁻¹; ¹H NMR (600 MHz, CDCl₃) δ 7.31-7.22 (m, 5H), 6.51 (br s, 1H), 5.08 (m, 1H), 5.00 (d, J = 8.0 Hz, 1H), 4.03 (br s, 1H), 1.82 (m, 1H), 1.56 (m, 1H), 1.47 (d, J = 6.9 Hz, 3H), 1.42 (s, 9H), 1.33-1.23 (m, 16H), 0.88 (t, J = 7.1 Hz, 3H); ¹³C NMR (150 MHz, CDCl₃) ppm 171.2, 155.8, 143.0, 128.6, 127.2, 126.0, 80.0, 54.6, 48.7, 32.0, 31.8, 29.7, 29.52, 29.48, 29.4, 29.3, 28.2, 25.6, 22.6, 22.0, 14.1; HRMS (ESI): Exact mass calcd for C₂₅H₄₂N₂NaO₃ [M+Na]⁺ 441.3093, found 441.3100.



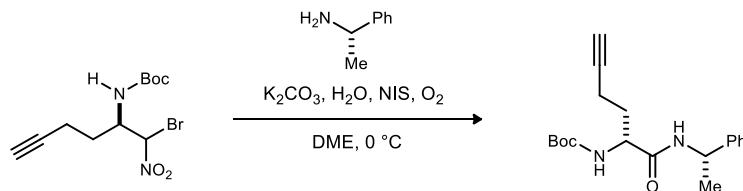
tert-Butyl ((R)-3-cyclohexyl-1-oxo-1-(((S)-1-phenylethyl)amino)propan-2-yl)carbamate (256).

Prepared according to the general procedure using *tert*-butyl ((*R*)-1-bromo-3-cyclohexyl-1-nitropropan-2-yl)carbamate (36.5 mg, 100 μ mol), DME (0.5 mL), H₂O (9 μ L, 500 μ mol), (*S*)- α -methylbenzylamine (16 μ L, 120 μ mol), *N*-iodosuccinimide (2.3 mg, 10 μ mol), K₂CO₃ (41.4 mg, 300 μ mol). Flash column chromatography (SiO₂, 10-15-20% ethyl acetate in hexanes) yielded the desired amide as a white solid (20 mg, 53%). The amide was determined to be 65:1 dr by HPLC analysis (Chiralcel AD-H, 10% *i*PrOH/hexanes, 1 mL/min, *t*_r(*d*₁, minor) = 8.0 min, *t*_r(*d*₂, major) = 13.7 min); R_f = 0.41 (30% EtOAc/hexanes); [α]_D²⁰ -3.4 (*c* .44, CHCl₃); IR (film) 3414, 2924, 2851, 1680, 1650 cm⁻¹; ¹H NMR (600 MHz, CDCl₃) δ 7.32-7.22 (m, 5H), 6.51 (br s, 1H), 5.08 (m, 1H), 4.83 (d, *J* = 6.3 Hz, 1H), 4.12 (br s, 1H), 1.78-1.63 (m, 6H), 1.56 (m, 1H), 1.48 (d, *J* = 7.0 Hz, 3H), 1.42 (s, 9H), 1.28-1.12 (m, 4H), 1.00-0.86 (m, 3H); ¹³C NMR (150 MHz, CDCl₃) ppm 171.4, 155.8, 143.1, 128.6, 127.2, 126.0, 80.1, 52.3, 48.7, 39.2, 34.1, 33.6, 32.8, 28.2, 26.4, 26.2, 26.0, 22.0; HRMS (ESI): Exact mass calcd for C₂₂H₃₄N₂NaO₃ [M+Na]⁺ 397.2467, found 397.2458.



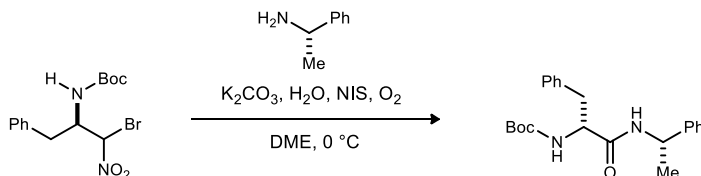
tert-Butyl ((R)-3-cyclohexyl-1-oxo-1-(((S)-1-phenylethyl)amino)propan-2-yl)carbamate (256).

Prepared according to the general procedure for nitroalkane amidation using *tert*-butyl (*R*)-(1-cyclohexyl-3-nitropropan-2-yl)carbamate (14.3 mg, 50 μ mol) and (*S*)-1-phenylethan-1-amine (13 μ L, 100 μ mol). Flash column chromatography (SiO₂, 10-40% ethyl acetate in hexanes) yielded the amide as a white solid (11 mg, 59%) in >20:1 dr (¹H NMR). Characterization data matched the literature.³⁹

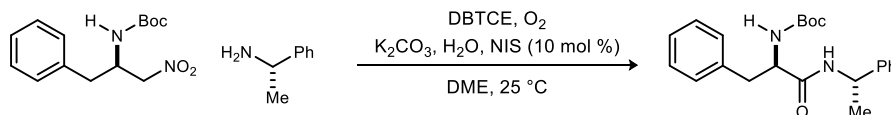


tert-Butyl ((R)-1-oxo-1-(((S)-1-phenylethyl)amino)hex-5-yn-2-yl)carbamate (257). Prepared according to the general procedure using *tert*-butyl ((*R*)-1-bromo-1-nitrohex-5-yn-2-yl)carbamate (16.1 mg, 50 μ mol), DME (0.3 mL), H₂O (5 μ L, 250 μ mol), (*S*)- α -methylbenzylamine (8 μ L, 60 μ mol), *N*-iodosuccinimide (1.1 mg, 5 μ mol), K₂CO₃ (20.7 mg, 150 μ mol). Flash column chromatography (SiO₂, 10-15-20% ethyl acetate in hexanes) yielded the desired amide as a white solid (8 mg, 48%). The amide was determined to be 31:1 dr by HPLC analysis (Chiralcel AD-H, 10% *i*PrOH/hexanes, 1 mL/min, *t*_r(*d*₁, minor) = 9.5 min, *t*_r(*d*₂, major) = 15.3 min); R_f = 0.28 (30% EtOAc/hexanes); [α]_D²⁰ -10.0 (*c* .27, CHCl₃); IR (film)

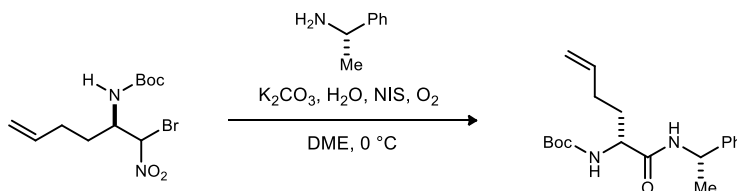
3413, 2976, 2929, 1652 cm^{-1} ; $^1\text{H NMR}$ (600 MHz, CDCl_3) δ 7.34-7.24 (m, 5H), 6.53 (br s, 1H), 5.09 (m, 2H), 4.24 (m, 1H), 2.36-2.24 (m, 2H), 2.06-2.00 (m, 2H), 1.86 (quint, $J = 7.1$ Hz, 1H), 1.49 (d, $J = 6.9$ Hz, 3H), 1.42 (s, 9H); $^{13}\text{C NMR}$ (150 MHz, CDCl_3) ppm 170.2, 155.7, 142.9, 128.6, 127.3, 126.0, 83.0, 80.2, 69.7, 53.5, 48.9, 29.7, 28.2, 22.0, 15.1; HRMS (ESI): Exact mass calcd for $\text{C}_{19}\text{H}_{26}\text{N}_2\text{NaO}_3$ $[\text{M}+\text{Na}]^+$ 353.1841, found 353.1844.



tert-Butyl ((R)-1-oxo-3-phenyl-1-(((S)-1-phenylethyl)amino)propan-2-yl)carbamate (258). Prepared according to the general procedure using *tert*-butyl ((2*R*)-1-bromo-1-nitro-3-phenylpropan-2-yl)carbamate (15.8 mg, 44 μmol), DME (0.3 mL), H_2O (4 μL , 220 μmol), (*S*)- α -methylbenzylamine (7 μL , 55 μmol), *N*-iodosuccinimide (1.0 mg, 4 μmol), K_2CO_3 (17.9 mg, 130 μmol). Flash column chromatography (SiO_2 , 10-15-20% ethyl acetate in hexanes) yielded the desired amide as a white solid (11 mg, 69%). The amide was determined to be 18:1 dr by HPLC analysis (Chiralcel AD-H, 10% *i*PrOH/hexanes, 1 mL/min, $t_r(d_1)$, minor) = 9.0 min, $t_r(d_2)$, major) = 14.3 min); $R_f = 0.34$ (30% EtOAc/hexanes); $[\alpha]_D^{20} -8.6$ (*c* .42, CHCl_3); IR (film) 3326, 2976, 2927, 1654 cm^{-1} ; $^1\text{H NMR}$ (600 MHz, CDCl_3) δ 7.31-7.16 (m, 10H), 5.87 (d, $J = 7.5$ Hz, 1H), 5.08 (br s, 1H), 5.00 (m, 1H), 4.28 (br s, 1H), 3.13 (dd, $J = 13.6, 6.0$ Hz, 1H), 2.99 (dd, 13.6, 8.0 Hz, 1H), 1.41 (s, 9H), 1.28 (d, $J = 4.1$ Hz, 1H); $^{13}\text{C NMR}$ (150 MHz, CDCl_3) ppm 169.9, 155.4, 142.7, 136.8, 129.34, 129.27, 128.9, 128.7, 128.6, 127.3, 126.9, 126.0, 80.1, 56.0, 48.8, 38.6, 29.7, 28.2, 28.1, 21.6; HRMS (ESI): Exact mass calcd for $\text{C}_{22}\text{H}_{28}\text{N}_2\text{NaO}_3$ $[\text{M}+\text{Na}]^+$ 391.1998, found 391.1988.

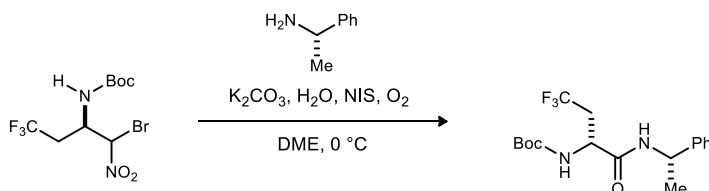


tert-Butyl ((R)-1-oxo-3-phenyl-1-(((S)-1-phenylethyl)amino)propan-2-yl)carbamate (258). Prepared according to the general procedure for nitroalkane amidation using *tert*-butyl (*R*)-(1-nitro-3-phenylpropan-2-yl)carbamate (28.0 mg, 100 μmol) and (*S*)-1-phenylethan-1-amine (26 μL , 200 μmol). Flash column chromatography (SiO_2 , 10-30% ethyl acetate in hexanes) yielded the amide as a white solid (28 mg, 76%) in >20:1 dr ($^1\text{H NMR}$). Characterization data matched the literature.³⁹



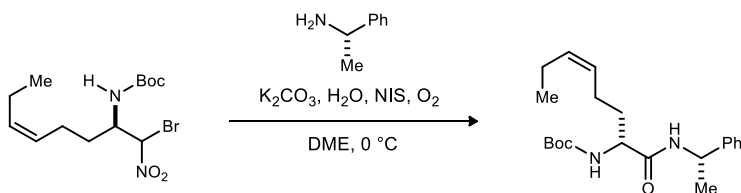
tert-Butyl ((R)-1-oxo-1-(((S)-1-phenylethyl)amino)hex-5-en-2-yl)carbamate (259). Prepared according to the general procedure using *tert*-butyl ((2*R*)-1-bromo-1-nitrohex-5-en-2-yl)carbamate (32.3 mg, 100 μmol), DME (0.5 mL), H_2O (9 μL , 500 μmol), (*S*)- α -methylbenzylamine (16 μL , 120 μmol), *N*-

iodosuccinimide (2.3 mg, 10 μ mol), K_2CO_3 (41.4 mg, 300 μ mol). Flash column chromatography (SiO₂, 10-15-20% ethyl acetate in hexanes) yielded the desired amide as a white solid (14 mg, 42%). The amide was determined to be 19:1 dr by HPLC analysis (Chiralcel AD-H, 10% *i*PrOH/hexanes, 1 mL/min, $t_r(d_1, \text{minor})$ = 6.8 min, $t_r(d_2, \text{major})$ = 11.4 min); R_f = 0.16 (20% EtOAc/hexanes); $[\alpha]_D^{20}$ -7.3 (*c* .83, CHCl₃); IR (film) 3309, 2976, 1697, 1658 cm⁻¹; ¹H NMR (600 MHz, CDCl₃) δ 7.32-7.23 (m, 5H), 6.43 (br s, 1H), 5.08 (m, 1H), 5.04 (dd, *J* = 17.2, 1.3 Hz, 1H), 5.01 (dd, *J* = 10.2, 1.3 Hz, 1H), 4.96 (br s, 1H), 4.73 (m, 1H), 4.04 (br s, 1H), 2.12 (m, 1H), 1.94 (m, 1H), 1.80 (m, 1H), 1.67 (m, 1H), 1.48 (d, *J* = 7.0 Hz, 3H), 1.42 (s, 9H); ¹³C NMR (150 MHz, CDCl₃) ppm 170.7, 155.0, 143.0, 137.2, 128.6, 127.2, 126.0, 115.7, 80.1, 53.9, 48.8, 29.8, 28.3, 23.4, 21.2; HRMS (ESI): Exact mass calcd for C₁₉H₂₈N₂NaO₃ [M+Na]⁺ 355.1998, found 355.2003.



***tert*-Butyl ((*R*)-4,4,4-trifluoro-1-oxo-1-((*S*)-1-phenylethyl)amino)butan-2-yl)carbamate (260).**

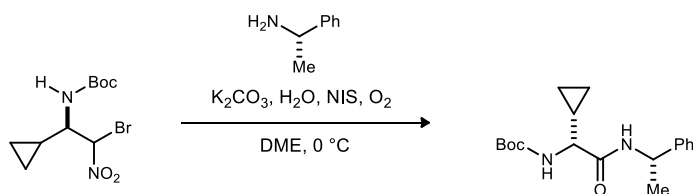
Prepared according to the general procedure using *tert*-butyl ((*2R*)-1-bromo-4,4,4-trifluoro-1-nitrobutan-2-yl)carbamate (31.6 mg, 90 μ mol), DME (0.5 mL), H₂O (8 μ L, 450 μ mol), (*S*)- α -methylbenzylamine (14 μ L, 110 μ mol), *N*-iodosuccinimide (2.0 mg, 9 μ mol), K_2CO_3 (37.3 mg, 270 μ mol). Flash column chromatography (SiO₂, 10-15-20% ethyl acetate in hexanes) yielded the desired amide as a white solid (12 mg, 38%). The amide was determined to be 22:1 dr by HPLC analysis (Chiralcel AD-H, 10% *i*PrOH/hexanes, 1 mL/min, $t_r(d_1, \text{minor})$ = 5.6 min, $t_r(d_2, \text{major})$ = 7.4 min); R_f = 0.38 (30% EtOAc/hexanes); $[\alpha]_D^{20}$ +12.3 (*c* .39, CHCl₃); IR (film) 3311, 2979, 2929, 1660 cm⁻¹; ¹H NMR (600 MHz, CDCl₃) δ 7.32-7.24 (m, 5H), 6.76 (br s, 1H), 5.06 (m, 2H), 4.42 (br s, 1H), 2.80 (m, 1H), 2.48 (m, 1H), 1.48 (d, *J* = 6.9 Hz, 3H), 1.42 (s, 9H); ¹³C NMR (150 MHz, CDCl₃) ppm 168.5, 155.4, 142.7, 128.6, 127.4, 125.9, 125.9 (¹*J*_{CF} = 276.9 Hz), 81.0, 49.4, 49.1, 35.07 (²*J*_{CF} = 29.0 Hz), 28.1, 21.8; HRMS (ESI): Exact mass calcd for C₁₇H₂₃F₃N₂NaO₃ [M+Na]⁺ 383.1558, found 383.1546.



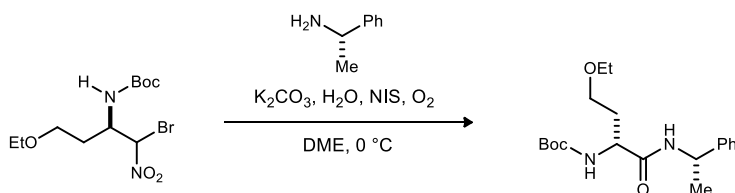
***tert*-Butyl ((*R,Z*)-1-oxo-1-((*S*)-1-phenylethyl)amino)oct-5-en-2-yl)carbamate (261).**

Prepared according to the general procedure using *tert*-butyl ((*2R,Z*)-1-bromo-1-nitrooct-5-en-2-yl)carbamate (21.1 mg, 60 μ mol), DME (0.3 mL), H₂O (6 μ L, 300 μ mol), (*S*)- α -methylbenzylamine (10 μ L, 70 μ mol), *N*-iodosuccinimide (1.4 mg, 6 μ mol), K_2CO_3 (24.8 mg, 180 μ mol). Flash column chromatography (SiO₂, 10-15-20% ethyl acetate in hexanes) yielded the desired amide as a white solid (8 mg, 38%). The amide was determined to be 17:1 dr by HPLC analysis (Chiralcel AD-H, 10% *i*PrOH/hexanes, 1 mL/min, $t_r(d_1, \text{minor})$ = 6.5 min, $t_r(d_2, \text{major})$ = 9.3 min); R_f = 0.41 (30% EtOAc/hexanes); $[\alpha]_D^{20}$ -3.7 (*c* .62, CHCl₃); IR (film) 3303, 2970, 2929, 1701, 1660 cm⁻¹; ¹H NMR (600 MHz, CDCl₃) δ 7.32-7.22 (m, 5H), 6.44 (br s, 1H), 5.41 (m, 1H), 5.30 (m, 1H), 5.09 (m, 1H), 4.92 (br s, 1H), 4.03 (br s, 1H), 2.11-1.90 (m, 4H), 1.65-1.59 (m, 2H), 1.48 (d, *J* = 7.0 Hz, 3H), 1.42 (s, 9H), 0.95 (t, *J* = 7.6 Hz, 3H); ¹³C NMR (150 MHz, CDCl₃) ppm 170.8,

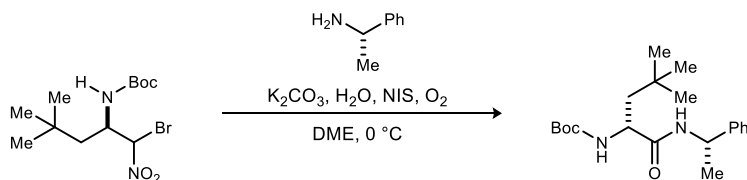
154.6, 143.0, 133.1, 128.6, 127.3, 126.1, 126.0, 80.1, 53.9, 48.7, 31.5, 30.1, 28.2, 23.2, 20.5, 14.2; HRMS (ESI): Exact mass calcd for $C_{21}H_{32}N_2NaO_3$ $[M+Na]^+$ 383.2311, found 383.2308.



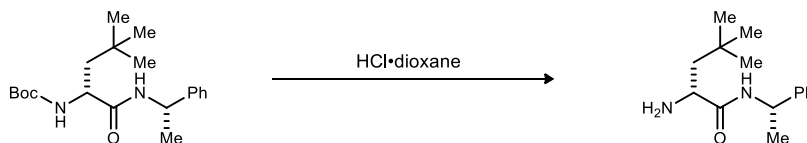
tert-Butyl ((R)-1-cyclopropyl-2-oxo-2-(((S)-1-phenylethyl)amino)ethyl)carbamate (262). Prepared according to the general procedure using *tert*-butyl ((1*R*)-2-bromo-1-cyclopropyl-2-nitroethyl)carbamate (27.8 mg, 90 μ mol), DME (0.5 mL), H₂O (8 μ L, 450 μ mol), (*S*)- α -methylbenzylamine (14 μ L, 110 μ mol), *N*-iodosuccinimide (2.0 mg, 9 μ mol), K₂CO₃ (37.3 mg, 270 μ mol). Flash column chromatography (SiO₂, 10-15-20% ethyl acetate in hexanes) yielded the desired amide as a white solid (14 mg, 49%). The amide was determined to be 8:1 dr by HPLC analysis (Chiralcel AD-H, 10% *i*PrOH/hexanes, 1 mL/min, $t_r(d_1, \text{minor}) = 7.5$ min, $t_r(d_2, \text{major}) = 11.3$ min); $R_f = 0.34$ (30% EtOAc/hexanes); $[\alpha]_D^{20} -29.6$ (*c* .50, CHCl₃); IR (film) 3300, 2976, 2929, 1651 cm^{-1} ; ¹H NMR (600 MHz, CDCl₃) δ 7.33-7.23 (m, 5H), 6.39 (br s, 1H), 5.19 (br s, 1H), 5.11 (m, 1H), 3.46 (br s, 1H), 1.49 (d, $J = 6.9$ Hz, 3H), 1.42 (s, 9H), 1.15 (br s, 1H), 0.63 (dd, $J = 9.0, 1.0$ Hz, 1H), 0.54 (dd, $J = 8.2, 0.8$ Hz, 1H), 0.43 (br s, 2H); ¹³C NMR (150 MHz, CDCl₃) ppm 170.4, 155.7, 143.0, 128.6, 127.2, 126.0, 80.0, 58.4, 48.7, 28.2, 21.9, 13.7, 3.7, 2.8; HRMS (ESI): Exact mass calcd for $C_{18}H_{26}N_2NaO_3$ $[M+Na]^+$ 341.1841, found 341.1836.



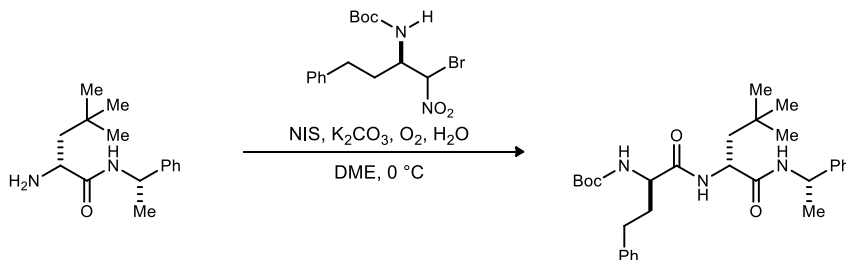
tert-Butyl ((R)-4-ethoxy-1-oxo-1-(((S)-1-phenylethyl)amino)butan-2-yl)carbamate (263). Prepared according to the general procedure using *tert*-butyl ((2*R*)-1-bromo-4-ethoxy-1-nitrobutan-2-yl)carbamate (23.9 mg, 70 μ mol), DME (0.4 mL), H₂O (6 μ L, 350 μ mol), (*S*)- α -methylbenzylamine (11 μ L, 80 μ mol), *N*-iodosuccinimide (1.6 mg, 7 μ mol), K₂CO₃ (29.0 mg, 210 μ mol). Flash column chromatography (SiO₂, 20-30-40% ethyl acetate in hexanes) yielded the desired amide as a white solid (14 mg, 61%). The amide was determined to be 8:1 dr by HPLC analysis (Chiralcel AD-H, 10% *i*PrOH/hexanes, 1 mL/min, $t_r(d_1, \text{minor}) = 9.7$ min, $t_r(d_2, \text{major}) = 12.2$ min); $R_f = 0.21$ (30% EtOAc/hexanes); $[\alpha]_D^{20} -5.9$ (*c* 1.25, CHCl₃); IR (film) 3299, 2975, 2930, 2869, 1693, 1656 cm^{-1} ; ¹H NMR (600 MHz, CDCl₃) δ 7.33-7.23 (m, 5H), 6.92 (br s, 1H), 5.73 (d, $J = 6.7$ Hz, 1H), 5.10 (br s, 1H), 4.23 (br s, 1H), 3.57-3.40 (m, 4H), 2.02 (q, $J = 5.5$ Hz, 2H), 1.48 (d, $J = 6.9$ Hz, 3H), 1.44 (s, 9H), 1.14 (t, $J = 6.9$ Hz, 3H); ¹³C NMR (150 MHz, CDCl₃) ppm 170.7, 155.8, 143.2, 128.6, 127.2, 126.0, 79.8, 68.0, 66.5, 53.3, 48.7, 32.2, 28.3, 21.9, 15.1; HRMS (ESI): Exact mass calcd for $C_{19}H_{30}N_2NaO_4$ $[M+Na]^+$ 373.2103, found 373.2092.



***tert*-Butyl ((*R*)-4,4-dimethyl-1-oxo-1-(((*S*)-1-phenylethyl)amino)pentan-2-yl)carbamate (269).** To a flask equipped with a stir bar was added *tert*-butyl ((*2R*)-1-bromo-4,4-dimethyl-1-nitropentan-2-yl)carbamate (1.00 g, 2.95 mmol), DME (15 mL), H₂O (270 μ L, 14.8 mmol), (*S*)- α -methylbenzylamine (470 μ L, 3.54 mmol). The reaction was cooled to 0 °C. K₂CO₃ (1.22 g, 8.85 mmol) and *N*-iodosuccinimide (66.4 mg, 295 μ mol) were added and the reaction mixture was placed under an O₂ atmosphere and stirred for 24 h. The mixture was quenched with 1 M HCl and extracted with dichloromethane. The organic phase was washed with sat. Na₂S₂O₃, dried and concentrated. The resulting solid was purified by flash column chromatography (SiO₂, 10-15-20% ethyl acetate in hexanes) yielded the desired amide as a white solid (585 mg, 57%). The amide was determined to be 20:1 dr by HPLC analysis.

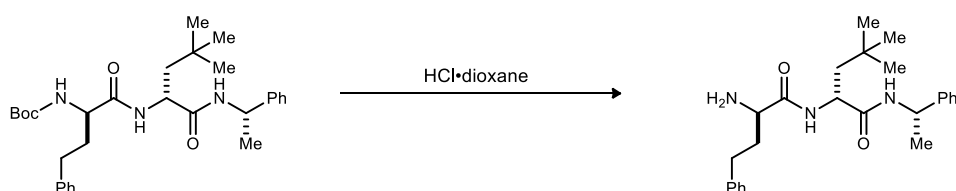


(*R*)-2-Amino-4,4-dimethyl-N-((*S*)-1-phenylethyl)pentanamide (270). To a flask equipped with a stir bar was added *tert*-butyl ((*R*)-4,4-dimethyl-1-oxo-1-(((*S*)-1-phenylethyl)amino)pentan-2-yl)carbamate (100.9 mg, 290 μ mol) and 4M HCl·dioxane (1 mL). The mixture was stirred for 30 minutes and then concentrated. The resulting solid was dissolved in dichloromethane and washed with sat. NaHCO₃. The organic layer was dried and concentrated to afford the desired free amine (70 mg, 97% yield). The product was carried on without further purification.

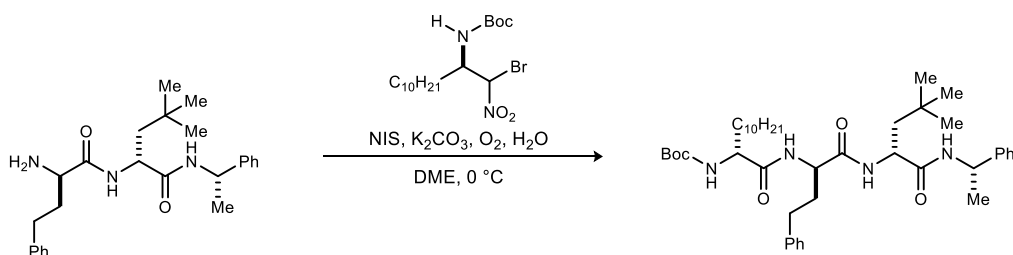


***tert*-Butyl ((*R*)-1-(((*R*)-4,4-dimethyl-1-oxo-1-(((*S*)-1-phenylethyl)amino)pentan-2-yl)amino)-1-oxo-4-phenylbutan-2-yl)carbamate (271).** To a vial equipped with a stir bar was added *tert*-butyl ((*2R*)-1-bromo-1-nitro-4-phenylbutan-2-yl)carbamate (78.3 mg, 210 μ mol), DME (1 mL), H₂O (19 μ L, 1.05 mmol), and (*R*)-2-amino-4,4-dimethyl-N-((*S*)-1-phenylethyl)pentanamide (71.0 mg, 250 μ mol). The reaction was cooled to 0 °C. K₂CO₃ (86.9 mg, 630 μ mol) and *N*-iodosuccinimide (4.7 mg, 21 μ mol) were added and the reaction was placed under an O₂ atmosphere and stirred for 24 h. The reaction mixture was quenched with

1 M HCl and extracted with dichloromethane. The organic phase was washed with sat. Na₂S₂O₃, dried and concentrated. The resulting solid was purified by flash column chromatography (SiO₂, 15-40% ethyl acetate in hexanes) to provide desired dipeptide as an orange solid (50 mg, 47%). *R_f* = 0.28 (30% EtOAc/hexanes); $[\alpha]_D^{20}$ +6.7 (*c* .36, CHCl₃); IR (film) 3282, 3064, 2955, 1691, 1643 cm⁻¹; ¹H NMR (600 MHz, CDCl₃) δ 7.30-7.10 (m, 10H), 6.69 (br s, 1H), 6.27 (d, *J* = 8.2 Hz, 1H), 5.04 (quint, *J* = 7.2 Hz, 1H), 4.87 (d, *J* = 5.2 Hz, 1H), 4.42 (m, 1H), 3.98 (br s, 1H), 2.59 (m, 2H), 2.03 (m, 2H), 1.82 (m, 2H), 1.47 (d, *J* = 7.0 Hz, 3H), 1.39 (s, 9H), 0.93 (s, 9H); ¹³C NMR (150 MHz, CDCl₃) ppm 171.5, 170.8, 143.1, 140.4, 128.5, 128.4, 127.1, 126.2, 126.0, 80.5, 54.5, 50.9, 48.9, 44.9, 44.4, 35.6, 31.9, 30.4, 30.3, 29.6, 28.2, 21.7; HRMS (ESI): Exact mass calcd for C₃₀H₄₃N₃NaO₄ [M+Na]⁺ 532.3151, found 532.3151.

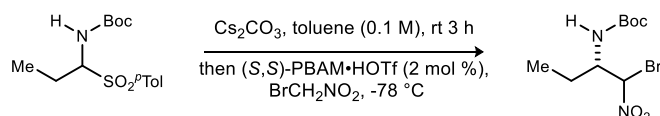


(*R*)-2-((*R*)-2-Amino-4-phenylbutanamido)-4,4-dimethyl-N-((*S*)-1-phenylethyl)pentanamide (272). To a flask equipped with a stir bar was added *tert*-butyl ((*R*)-1-(((*R*)-4,4-dimethyl-1-oxo-1-(((*S*)-1-phenylethyl)amino)pentan-2-yl)amino)-1-oxo-4-phenylbutan-2-yl)carbamate (40.2 mg, 79 μmol) and 4M HCl·dioxane (0.5 mL). The mixture was stirred for 30 minutes and then concentrated. The resulting solid was dissolved in dichloromethane and washed with sat. NaHCO₃. The organic layer was dried and concentrated to afford the desired free amine (30 mg, 94% yield). The product was carried on without further purification.

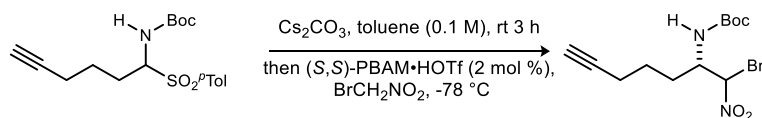


***tert*-Butyl ((*R*)-1-(((*R*)-1-(((*R*)-4,4-dimethyl-1-oxo-1-(((*S*)-1-phenylethyl)amino)pentan-2-yl)amino)-1-oxo-4-phenylbutan-2-yl)amino)-1-oxododecan-2-yl)carbamate (273).** To a vial equipped with a stir bar was added *tert*-butyl ((*R*)-1-bromo-1-nitrododecan-2-yl)carbamate (24.9 mg, 61 μmol), DME (0.4 mL), H₂O (6 μL, 350 μmol), and (*R*)-2-((*R*)-2-amino-4-phenylbutanamido)-4,4-dimethyl-N-((*S*)-1-phenylethyl)pentanamide (29.9 mg, 73.0 μmol). The reaction was cooled to 0 °C. K₂CO₃ (24.8 mg, 180 μmol) and *N*-iodosuccinimide (1.4 mg, 6 μmol) were added and the reaction was placed under an O₂ atmosphere and stirred for 24 h. The reaction mixture was quenched with 1 M HCl and extracted with dichloromethane. The organic phase was washed with sat. Na₂S₂O₃, dried and concentrated. The resulting solid was purified by flash column chromatography (SiO₂, 15-40% ethyl acetate in hexanes) to provide desired dipeptide as a brown solid (22 mg, 51%). *R_f* = 0.24 (30% EtOAc/hexanes); $[\alpha]_D^{20}$ +5.5 (*c* .51, CHCl₃); IR (film) 3277, 2928, 2857, 1640 cm⁻¹; ¹H NMR (600 MHz, CDCl₃) δ 7.33-7.12 (m, 10H), 7.02

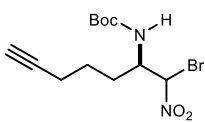
(d, $J = 7.8$ Hz, 1H), 6.48 (br s, 1H), 5.08-5.02 (m, 2H), 4.70 (m, 1H), 4.55 (td, $J = 8.0, 1.9$ Hz, 1H), 4.28 (m, 1H), 3.70 (m, 1H), 2.71-2.62 (m, 2H), 2.23-2.17 (m, 2H), 2.08 (d, $J = 13.7$ Hz, 1H), 1.93-1.86 (m, 2H), 1.84-1.75 (m, 2H), 1.48 (d, $J = 7.0$ Hz, 3H), 1.46 (s, 9H), 1.30-1.23 (m, 15H), 0.91 (s, 9H), 0.88 (t, $J = 6.7$ Hz, 3H); ^{13}C NMR (150 MHz, CDCl_3) ppm 172.8, 171.2, 170.7, 156.3, 143.9, 140.6, 128.7, 128.3, 128.2, 126.7, 126.3, 126.2, 81.0, 55.9, 54.6, 50.8, 48.9, 45.1, 32.8, 32.3, 31.8, 31.6, 30.5, 29.51, 29.49, 29.47, 29.4, 29.3, 29.2, 28.3, 25.6, 22.6, 21.8, 14.1; HRMS (ESI): Exact mass calcd for $\text{C}_{42}\text{H}_{66}\text{N}_4\text{NaO}_5$ $[\text{M}+\text{Na}]^+$ 729.4931, found 729.4954.



tert-Butyl ((2S)-1-bromo-1-nitrobutan-2-yl)carbamate (277). Prepared according to general procedure C using *tert*-butyl (1-tosylpropyl)carbamate (31.3 mg, 100 μmol). Flash column chromatography (SiO_2 , 2.5-7.5-15% ethyl acetate in hexanes) yielded the α -bromo nitroalkane (1:1 dr (^1H NMR)) as a white solid (27 mg, 90%). The enantiopurity was measured from the corresponding debrominated nitroalkane¹³⁰ and determined to be 81% ee by chiral HPLC analysis (Chiralpak AD, 10% $^i\text{PrOH}$ /hexanes, 0.8 mL/min, $t_r(e_1, \text{minor}) = 8.2$ min, $t_r(e_2, \text{major}) = 9.3$ min); $R_f = 0.48$ (20% EtOAc/hexanes); IR (film) 3412, 2977, 2932, 1697, 1567, 1513 cm^{-1} ; ^1H NMR (400 MHz, CDCl_3 , 1:1 mixture of diastereomers) δ 6.19-6.17 (m, 2H), 4.85 (d, $J = 6.9$ Hz, 1H), 4.74 (d, $J = 7.8$ Hz, 1H), 4.27 (m, 1H), 4.17 (m, 1H), 1.84-1.66 (m, 2H), 1.64-1.50 (m, 2H), 1.45 (s, 9H), 1.43 (s, 9H), 1.03 (t, $J = 6.5$ Hz, 3H), 1.02 (t, $J = 6.9$ Hz, 3H); ^{13}C NMR (100 MHz, CDCl_3) ppm 155.1, 155.0, 84.2, 82.8, 80.7, 80.6, 56.3, 55.9, 28.22, 28.18, 24.7, 23.7, 10.5, 10.3; HRMS (ESI): Exact mass calcd for $\text{C}_9\text{H}_{17}\text{BrN}_2\text{NaO}_4$ $[\text{M}+\text{Na}]^+$ 319.0269, found 319.0261.

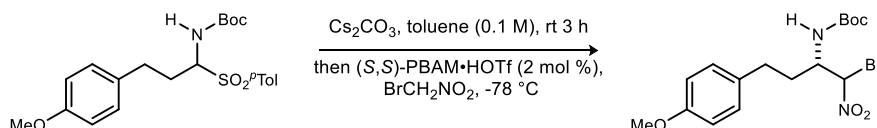


tert-Butyl ((2S)-1-bromo-1-nitrohept-6-yn-2-yl)carbamate (278). Prepared according to general procedure C using *tert*-butyl (1-tosylhex-5-yn-1-yl)carbamate (35.1 mg, 100 μmol). Flash column chromatography (SiO_2 , 2.5-7.5-15% ethyl acetate in hexanes) yielded the α -bromo nitroalkane (1:1 dr (^1H NMR)) as a white solid (24 mg, 73%). The enantiopurity was measured from the corresponding debrominated nitroalkane and determined to be 91% ee by chiral HPLC analysis (Chiralpak AD, 10% $^i\text{PrOH}$ /hexanes, 1.0 mL/min, $t_r(e_1, \text{minor}) = 8.9$ min, $t_r(e_2, \text{major}) = 9.5$ min); $R_f = 0.48$ (20% EtOAc/hexanes); IR (film) 3301, 2977, 2934, 1703, 1566, 1507 cm^{-1} ; ^1H NMR (400 MHz, CDCl_3 , 1:1 mixture of diastereomers) δ 6.20-6.17 (m, 2H), 4.93 (d, $J = 8.8$ Hz, 1H), 4.82 (d, $J = 8.6$ Hz, 1H), 4.36 (m, 1H), 4.26 (m, 1H), 2.26-2.22 (m, 4H), 1.99-1.96 (m, 2H), 1.97-1.92 (m, 2H), 1.68-1.58 (m, 6H), 1.44 (s, 9H), 1.42 (s, 9H); ^{13}C NMR (100 MHz, CDCl_3) ppm 154.9, 154.8, 83.9(2), 83.0, 82.7, 80.8, 80.7, 69.39, 69.35, 54.4, 53.9, 39.0, 29.1, 28.12, 28.09, 24.6, 24.4, 17.8(2); HRMS (ESI): Exact mass calcd for $\text{C}_{12}\text{H}_{19}\text{BrN}_2\text{NaO}_4$ $[\text{M}+\text{Na}]^+$ 357.0426, found 357.0409.

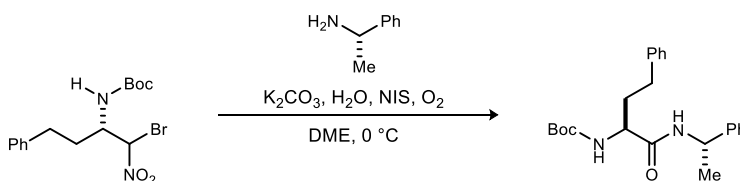


tert-Butyl ((2*R*)-1-bromo-1-nitrohept-6-yn-2-yl)carbamate (278). To a flame dried flask equipped with a stir bar was added using *tert*-butyl (1-tosylhex-5-yn-1-yl)carbamate (2.00 g, 5.70 mmol), toluene (60 mL) and Cs₂CO₃ (9.26 g, 28.0 mmol).

The reaction was stirred for 3 h at room temperature. The reaction was filtered through a plug of Celite and washed with toluene (30 mL). The filtrate was collected in a flask and (*R,R*)-PBAM•HOTf (37.0 mg, 57.0 μmol) was added. The flask was cooled to -78 °C and bromonitromethane (627 μL, 8.55 mmol) was added and the reaction was stirred for 24 h. The mixture was filtered through a plug of silica gel with ethyl acetate and then concentrated. Flash column chromatography (SiO₂, 2.5-7.5-15% ethyl acetate in hexanes) yielded the α-bromo nitroalkane (1:1 dr (¹H NMR)) as a white solid (1.51 g, 79%). The solid was recrystallized from hexanes to afford 1.01 g (67% recovery). The enantiopurity was measured from the corresponding debrominated nitroalkane and determined to be 98% ee by chiral HPLC analysis.

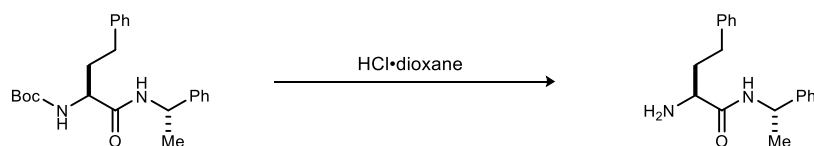


tert-Butyl ((2*S*)-1-bromo-4-(4-methoxyphenyl)-1-nitrobutan-2-yl)carbamate (279). Prepared according to general procedure using *tert*-butyl (3-(4-methoxyphenyl)-1-tosylpropyl)carbamate (42.0 mg, 100 μmol). Flash column chromatography (SiO₂, 10-20-30% ethyl acetate in hexanes) yielded the α-bromo nitroalkane (1:1 dr (¹H NMR)) as a white solid (27 mg, 68%). The diastereomers were determined to be 90 and 90% ee by chiral HPLC analysis (Chiralpak AD-H, 5% EtOH/hexanes, 0.8 mL/min, *t*_r(*d*₁*e*₁, minor) = 16.1 min, *t*_r(*d*₂*e*₁, minor) = 18.5 min, *t*_r(*d*₁*e*₂, major) = 20.0 min, *t*_r(*d*₂*e*₂, major) = 21.6 min); R_f = 0.36 (20% EtOAc/hexanes); IR (film) 3406, 2928, 1705, 1613, 1566, 1512 cm⁻¹; ¹H NMR (400 MHz, CDCl₃, 1:1 mixture of diastereomers) δ 7.12-7.06 (m, 4H), 6.85-6.82 (m, 4H), 6.18-6.13 (m, 2H), 4.90 (d, *J* = 8.3 Hz, 1H), 4.79 (d, *J* = 8.6 Hz, 1H), 4.34 (m, 1H), 4.23 (m, 1H), 3.79 (s, 6H), 2.78-2.68 (m, 2H), 2.66-2.58 (m, 2H), 2.08-1.98 (m, 1H), 1.96-1.86 (m, 1H), 1.84-1.75 (m, 1H), 1.62-1.56 (m, 1H), 1.47 (s, 9H), 1.45 (s, 9H); ¹³C NMR (100 MHz, CDCl₃) ppm 158.2(2), 132.0, 131.8, 129.4, 129.3, 114.08, 114.06, 114.0(2), 83.9, 82.7, 80.8, 80.7, 61.4, 55.2, 54.4, 53.9, 33.0, 32.3, 31.2, 31.0, 28.2(2); HRMS (ESI): Exact mass calcd for C₁₆H₂₃BrN₂NaO₅ [M+Na]⁺ 425.0688, found 425.0706.

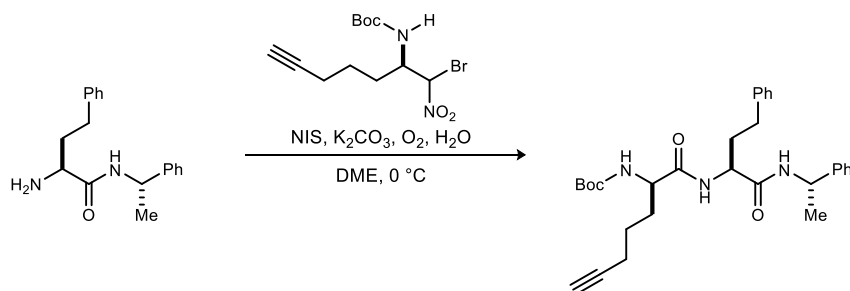


tert-Butyl ((*S*)-1-oxo-4-phenyl-1-((*S*)-1-phenylethyl)amino)butan-2-yl)carbamate (Boc-280). Prepared according to the general procedure for UmAS using *tert*-butyl ((2*S*)-1-bromo-1-nitro-4-phenylbutan-2-yl)carbamate (350.0 mg, 930 μmol), DME (5.0 mL), H₂O (84 μL, 4.65 mmol), (*S*)-α-

methylbenzylamine (150 μ L, 1.12 mmol), *N*-iodosuccinimide (20.9 mg, 93 μ mol), K_2CO_3 (258 mg, 1.87 mmol). Flash column chromatography (SiO_2 , 10-15-20% ethyl acetate in hexanes) yielded the desired amide as a white solid (225 mg, 63%). The amide was determined to be >20:1 dr by 1H NMR; R_f = 0.32 (20% EtOAc/hexanes); $[\alpha]_D^{20}$ -41.3 (*c* .90, $CHCl_3$); IR (film) 3295, 3062, 2975, 2929, 1653, 1533 cm^{-1} ; 1H NMR (400 MHz, $CDCl_3$) δ 7.35-7.08 (m, 10H), 6.46 (br s, 1H), 5.18-5.08 (m, 2H), 4.07 (br s, 1H), 2.64-2.60 (m, 2H), 2.12 (m, 1H), 1.90 (m, 1H), 1.47 (d, J = 7.0 Hz, 3H), 1.44 (s, 9H); ^{13}C NMR (100 MHz, $CDCl_3$) ppm 170.8, 155.7, 142.9, 140.8, 128.6, 128.4, 128.3, 127.3, 126.0(2), 80.0, 54.1, 48.7, 33.8, 31.7, 28.2, 21.7; HRMS (ESI): Exact mass calcd for $C_{23}H_{30}N_2NaO_3$ $[M+Na]^+$ 405.2154, found 405.2147.

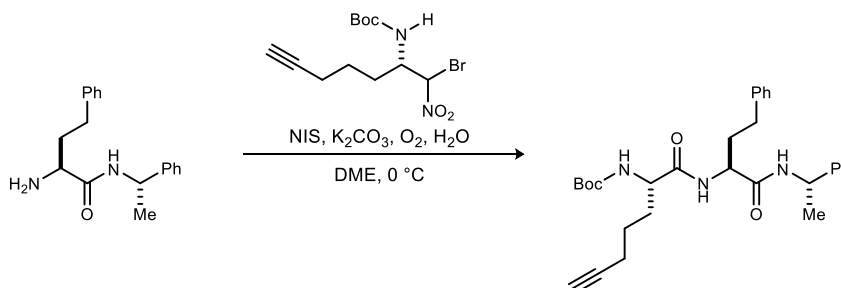


(*S*)-2-Amino-4-phenyl-*N*-((*S*)-1-phenylethyl)butanamide (280). To a flask equipped with a stir bar was added *tert*-butyl ((*S*)-1-oxo-4-phenyl-1-((*S*)-1-phenylethyl)amino)butan-2-ylcarbamate (200.0 mg, 520 μ mol) and 4M HCl·dioxane (2 mL). The mixture was stirred for 30 minutes and then concentrated. The resulting solid was dissolved in dichloromethane and washed with sat. $NaHCO_3$. The organic layer was dried and concentrated to afford the desired free amine (70 mg, 99% yield). The product was carried on without further purification.

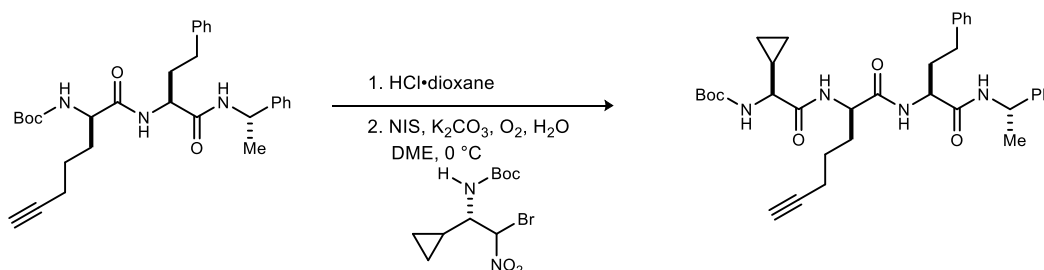


***tert*-Butyl ((*R*)-1-oxo-1-(((*S*)-1-oxo-4-phenyl-1-((*S*)-1-phenylethyl)amino)butan-2-yl)amino)hept-6-yn-2-ylcarbamate (281).** To a flask equipped with a stir bar was added *tert*-butyl ((*R*)-1-bromo-1-nitrohept-6-yn-2-yl)carbamate (87.1 mg, 260 μ mol), DME (2 mL), H_2O (23 μ L, 1.30 mmol), and (*S*)-2-amino-4-phenyl-*N*-((*S*)-1-phenylethyl)butanamide (73.0 mg, 260 μ mol). The reaction was cooled to 0 $^{\circ}C$. K_2CO_3 (71.8 mg, 520 μ mol) and *N*-iodosuccinimide (5.9 mg, 26 μ mol) were added and the reaction was placed under an O_2 atmosphere and stirred for 24 h. The reaction mixture was quenched with 1 M HCl and extracted with dichloromethane. The organic phase was washed with sat. $Na_2S_2O_3$, dried and concentrated. The resulting solid was purified by flash column chromatography (SiO_2 , 15-40% ethyl acetate in hexanes) to provide desired dipeptide as a white solid (71 mg, 54%). R_f = 0.38 (50% EtOAc/hexanes); $[\alpha]_D^{20}$ -21.7 (*c* .30, $CHCl_3$); IR (film) 3284, 3065, 2929, 1714, 1640, 1550 cm^{-1} ; 1H NMR (400 MHz, $CDCl_3$) δ 7.32-7.13 (m, 8H), 7.04-7.02 (m, 3H), 6.95 (d, J = 7.5 Hz, 1H), 5.22 (d, J = 5.2 Hz, 1H), 5.08 (quint, J = 7.0 Hz, 1H), 4.50 (m, 1H), 4.12 (m, 1H), 2.55 (m, 2H), 2.23-2.10 (m, 3H), 1.98-1.90 (m, 3H), 1.73 (m, 1H), 1.62-1.56 (m, 2H), 1.46 (d, J = 7.0 Hz, 3H), 1.41 (s, 9H); ^{13}C NMR (100 MHz, $CDCl_3$) ppm 172.2, 170.1, 155.5, 143.1, 140.7, 128.6, 128.4, 128.3, 127.2, 126.02, 125.98, 83.4, 80.2, 69.2, 54.5, 52.7, 48.9, 33.8, 31.6, 31.5,

28.2, 24.4, 21.8, 18.0; HRMS (ESI): Exact mass calcd for C₃₀H₃₉N₃NaO₄ [M+Na]⁺ 528.2838, found 528.2823.

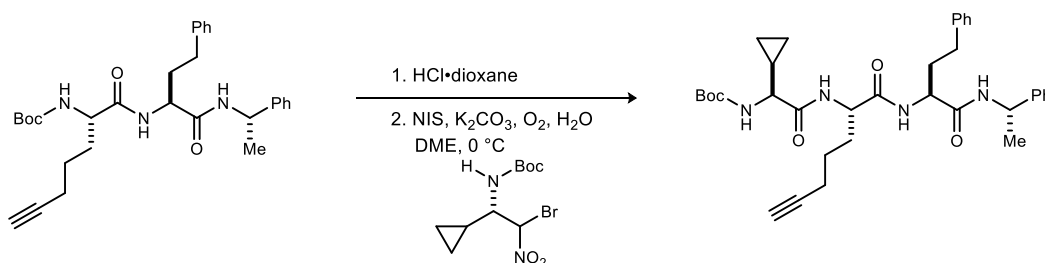


tert-Butyl ((S)-1-oxo-1-(((S)-1-oxo-4-phenyl-1-(((S)-1-phenylethyl)amino)butan-2-yl)amino)hept-6-yn-2-yl)carbamate (282). To a flask equipped with a stir bar was added *tert*-butyl ((2*S*)-1-bromo-1-nitrohept-6-yn-2-yl)carbamate (87.1 mg, 260 μmol), DME (2 mL), H₂O (23 μL, 1.30 mmol), and (*S*)-2-amino-4-phenyl-*N*-((*S*)-1-phenylethyl)butanamide (73.0 mg, 260 μmol). The reaction was cooled to 0 °C. K₂CO₃ (71.8 mg, 520 μmol) and *N*-iodosuccinimide (5.9 mg, 26 μmol) were added and the reaction was placed under an O₂ atmosphere and stirred for 24 h. The reaction mixture was quenched with 1 M HCl and extracted with dichloromethane. The organic phase was washed with sat. Na₂S₂O₃, dried and concentrated. The resulting solid was purified by flash column chromatography (SiO₂, 15-40% ethyl acetate in hexanes) to provide desired dipeptide as a white solid (74 mg, 56%). R_f = 0.38 (50% EtOAc/hexanes); [α]_D²⁰ -27.4 (c .80, CHCl₃); IR (film) 3285, 2929, 1687, 1640, 1529 cm⁻¹; ¹H NMR (600 MHz, CDCl₃) δ 7.32-7.10 (m, 9H), 7.07 (d, *J* = 7.5 Hz, 1H), 7.01 (d, *J* = 7.2 Hz, 2H), 5.13 (d, *J* = 6.8 Hz, 1H), 6.48 (br s, 1H), 5.08 (m, 1H), 4.51 (m, 1H), 4.16 (m, 1H), 2.58-2.49 (m, 2H), 2.21-2.10 (m, 2H), 1.98-1.87 (m, 3H), 1.66 (m, 1H), 1.57-1.52 (m, 2H), 1.46 (d, *J* = 7.0 Hz, 3H), 1.43 (s, 9H); ¹³C NMR (150 MHz, CDCl₃) ppm 172.1, 170.2, 155.6, 143.2, 140.9, 128.6, 128.4, 128.3, 127.3, 126.1, 126.0, 83.5, 80.2, 69.1, 54.3, 52.9, 48.9, 33.9, 31.6, 31.5, 28.3, 24.5, 21.9, 18.1; HRMS (ESI): Exact mass calcd for C₃₀H₃₉N₃NaO₄ [M+Na]⁺ 528.2838, found 528.2856.

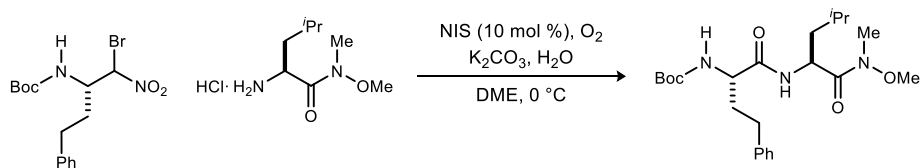


tert-Butyl ((S)-1-cyclopropyl-2-oxo-2-(((R)-1-oxo-1-(((S)-1-oxo-4-phenyl-1-(((S)-1-phenylethyl)amino)butan-2-yl)amino)hept-6-yn-2-yl)amino)ethyl)carbamate (283). To a flask equipped with a stir bar was added *tert*-butyl ((*R*)-1-oxo-1-(((*S*)-1-oxo-4-phenyl-1-(((*S*)-1-phenylethyl)amino)butan-2-yl)amino)hept-6-yn-2-yl)carbamate (45.0 mg, 90 μmol) and 4M HCl·dioxane (1 mL). The mixture was stirred for 30 minutes and then concentrated. The resulting solid was dissolved in dichloromethane and washed with sat. NaHCO₃. The organic layer was dried and concentrated to afford the desired free amine (36 mg, 99% yield). The product was carried on without further purification. To a flask equipped with a stir bar was added *tert*-butyl ((1*R*)-2-bromo-1-cyclopropyl-2-nitroethyl)carbamate (27.8 mg, 90.0 μmol), DME (1 mL), H₂O (9 μL, 450 μmol), and (*R*)-2-amino-*N*-((*S*)-1-oxo-4-phenyl-1-(((*S*)-1-phenylethyl)amino)butan-2-yl)hept-6-ynamide (36.0 mg, 90.0 μmol). The reaction was cooled to 0 °C.

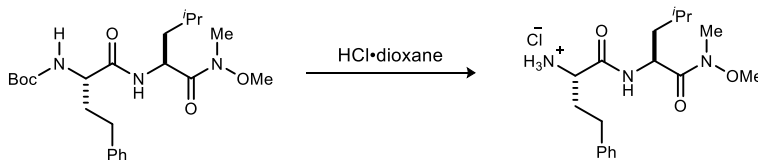
K_2CO_3 (24.8 mg, 180 μ mol) and *N*-iodosuccinimide (2.0 mg, 9 μ mol) were added and the reaction was placed under an O_2 atmosphere and stirred for 24 h. The reaction mixture was quenched with 1 M HCl and extracted with dichloromethane. The organic phase was washed with sat. $Na_2S_2O_3$, dried and concentrated. The resulting solid was purified by flash column chromatography (SiO_2 , 15-40% ethyl acetate in hexanes) to provide desired tripeptide as a white solid (28 mg, 52%). $R_f = 0.19$ (50% EtOAc/hexanes); $[\alpha]_D^{20} -6.0$ (c .20, $CHCl_3$); IR (film) 3281, 3081, 2928, 1714, 1632, 1546 cm^{-1} ; 1H NMR (600 MHz, $CDCl_3$) δ 7.29-7.13 (m, 10H), 7.08-7.02 (m, 3H), 5.40 (br s, 1H), 5.10 (m, 1H), 4.61-4.56 (m, 2H), 3.75 (br s, 1H), 2.57-2.54 (m, 2H), 2.22-2.14 (m, 3H), 2.02-1.93 (m, 3H), 1.80 (m, 1H), 1.62-1.57 (m, 2H), 1.46 (d, $J = 6.9$ Hz, 3H), 1.35 (s, 9H), 1.07 (m, 1H), 0.49-0.35 (m, 4H); ^{13}C NMR (150 MHz, $CDCl_3$) ppm 177.9, 171.8, 170.3, 155.7, 143.2, 140.8, 128.5, 128.4, 128.3, 127.2, 126.1, 126.0, 83.5, 79.9, 69.1, 53.1, 52.7, 48.7, 34.2, 31.7, 31.6, 29.6, 28.3, 24.4, 21.6, 18.1, 14.3, 3.0, 2.5; HRMS (ESI): Exact mass calcd for $C_{35}H_{46}N_4NaO_5$ $[M+Na]^+$ 625.3366, found 625.3347.



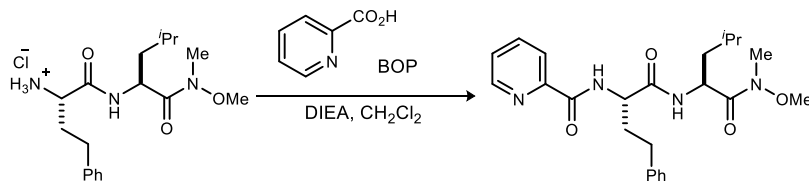
***tert*-Butyl ((*S*)-1-cyclopropyl-2-oxo-2-(((*S*)-1-oxo-1-(((*S*)-1-oxo-4-phenyl-1-(((*S*)-1-phenylethyl)amino)butan-2-yl)amino)hept-6-yn-2-yl)amino)ethyl)carbamate (284).** To a flask equipped with a stir bar was added *tert*-butyl ((*S*)-1-oxo-1-(((*S*)-1-oxo-4-phenyl-1-(((*S*)-1-phenylethyl)amino)butan-2-yl)amino)hept-6-yn-2-yl)carbamate (45.0 mg, 90 μ mol) and 4M HCl·dioxane (1 mL). The mixture was stirred for 30 minutes and then concentrated. The resulting solid was dissolved in dichloromethane and washed with sat. $NaHCO_3$. The organic layer was dried and concentrated to afford the desired free amine (36 mg, 99% yield). The product was carried on without further purification. To a flask equipped with a stir bar was added *tert*-butyl ((1*S*)-2-bromo-1-cyclopropyl-2-nitroethyl)carbamate (27.8 mg, 90.0 μ mol), DME (1 mL), H_2O (9 μ L, 450 μ mol), and (*S*)-2-amino-*N*-((*S*)-1-oxo-4-phenyl-1-(((*S*)-1-phenylethyl)amino)butan-2-yl)hept-6-ynamide (36.0 mg, 90.0 μ mol). The reaction was cooled to 0 $^{\circ}C$. K_2CO_3 (24.8 mg, 180 μ mol) and *N*-iodosuccinimide (2.0 mg, 9 μ mol) were added and the reaction was placed under an O_2 atmosphere and stirred for 24 h. The reaction mixture was quenched with 1 M HCl and extracted with dichloromethane. The organic phase was washed with sat. $Na_2S_2O_3$, dried and concentrated. The resulting solid was purified by flash column chromatography (SiO_2 , 25-50% ethyl acetate in hexanes) to provide desired tripeptide as a white solid (29 mg, 54%). $R_f = 0.19$ (50% EtOAc/hexanes); $[\alpha]_D^{20} -35.7$ (c .90, $CHCl_3$); IR (film) 3294, 2925, 1711, 1633, 1541 cm^{-1} ; 1H NMR (400 MHz, $CDCl_3$) δ 7.46 (d, $J = 7.3$ Hz, 1H), 7.34-7.11 (m, 10H), 7.04 (d, $J = 7.2$ Hz, 2H), 5.42 (br s, 1H), 5.10 (dt, $J = 7.2, 6.8$ Hz, 1H), 4.66-4.58 (m, 2H), 3.61 (m, 1H), 2.59-2.55 (m, 2H), 2.25-2.18 (m, 3H), 2.02-1.72 (m, 4H), 1.64-1.58 (m, 2H), 1.47 (d, $J = 7.0$ Hz, 3H), 1.39 (s, 9H), 1.05 (m, 1H), 0.52-0.40 (m, 4H); ^{13}C NMR (100 MHz, $CDCl_3$) ppm 171.9, 171.3, 170.3, 155.9, 143.5, 140.9, 128.4, 128.3, 128.2, 127.0, 126.1, 125.9, 83.5, 80.4, 69.3, 53.3, 52.9, 48.8, 33.8, 31.9, 31.5, 29.6, 28.2, 24.4, 22.1, 18.1, 14.0, 3.2, 3.1; HRMS (ESI): Exact mass calcd for $C_{35}H_{46}N_4NaO_5$ $[M+Na]^+$ 625.3366, found 625.3347.



***tert*-Butyl ((*S*)-1-(((*S*)-1-(methoxy(methyl)amino)-4-methyl-1-oxopentan-2-yl)amino)-1-oxo-4-phenylbutan-2-yl)carbamate (286).** To a flask equipped with a stir bar was added *tert*-butyl ((*2R*)-1-bromo-1-nitro-4-phenylbutan-2-yl)carbamate (186.5 mg, 500 μ mol), dimethoxyethane (2.5 mL), H₂O (45 μ L, 2.5 mmol) and (*S*)-2-amino-*N*-methoxy-*N*,4-dimethylpentanamide (126.0 mg, 600 μ mol). The reaction was cooled to 0 °C. K₂CO₃ (220.8 mg, 1.60 mmol) and *N*-iodosuccinimide (11.3 mg, 50 μ mol) were added and the reaction mixture was placed under an O₂ atmosphere and stirred for 24 h. The mixture was quenched with 1 M HCl and extracted with dichloromethane. The organic phase was washed with sat. Na₂S₂O₃, dried and concentrated. Flash column chromatography (SiO₂, 15-25-35% ethyl acetate in hexanes) yielded the desired dipeptide as a white solid (141 mg, 54%). The characterization data matched the literature.⁹³



(*S*)-1-(((*S*)-1-(Methoxy(methyl)amino)-4-methyl-1-oxopentan-2-yl)amino)-1-oxo-4-phenylbutan-2-aminium chloride (HCl-286). To a flask equipped with a stir bar was added *tert*-butyl ((*S*)-1-(((*S*)-1-(methoxy(methyl)amino)-4-methyl-1-oxopentan-2-yl)amino)-1-oxo-4-phenylbutan-2-yl)carbamate (78.5 mg, 180 μ mol) and 4M HCl·dioxane (1 mL). The mixture was stirred for 30 minutes and then concentrated to afford the desired amine salt (67 mg, 99% yield). The product was carried on without further purification.

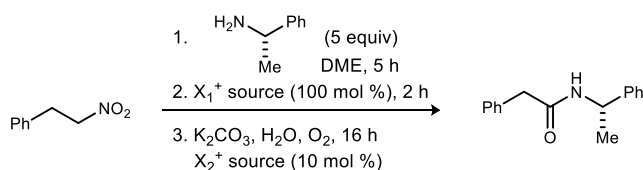


***N*-((*S*)-1-(((*S*)-1-(Methoxy(methyl)amino)-4-methyl-1-oxopentan-2-yl)amino)-1-oxo-4-phenylbutan-2-yl)picolinamide (287).** To a flame dried flask equipped with a stir bar was added picolinic acid (18.5 mg, 150 μ mol), CH₂Cl₂ (1.5 mL), diisopropylethylamine (66 μ L, 380 μ mol) and BOP (66.3 mg, 150 μ mol). (*S*)-2-((*S*)-2-amino-4-phenylbutanamido)-*N*-methoxy-*N*,4-dimethylpentanamide hydrochloride (66.8 mg, 180 μ mol) was added and the reaction mixture was stirred for 4 h. After completion, the reaction was diluted

with ethyl acetate and washed with 1M HCl, saturated NaHCO₃, and H₂O. The organic phase was dried and concentrated. Flash column chromatography (SiO₂, 30-40-50% ethyl acetate in hexanes) yielded the desired product as a white solid (43 mg, 65%). The characterization data matched the literature.⁹³

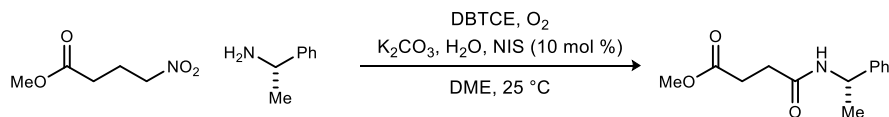
Method A for Bromination of nitroalkanes: According to the literature procedure¹²³, the nitroalkane (1 equiv.) was stirred with KOH (1 equiv.) in MeOH:H₂O (3:1, 0.4 M). After the mixture became homogenous (~5 h), the mixture was cooled to 0 °C and added to a separatory funnel containing the bromonium source (1 equiv.) and DCM (0.2 M) at -78 °C. The funnel was shaken vigorously and the layers separated. The aqueous layer was extracted with DCM. The combined organic layers were dried and concentrated. The residue was purified by flash column chromatography.

Method B for Bromination of nitroalkanes: Nitroalkane (1 equiv.), triethylamine (3 equiv.), and the bromonium source were stirred in DME (0.4 M) for 20 h at 25 °C. The mixture was quenched with 1 M HCl and extracted with DCM. The organic layer was dried and concentrated. The residue was purified by flash column chromatography.

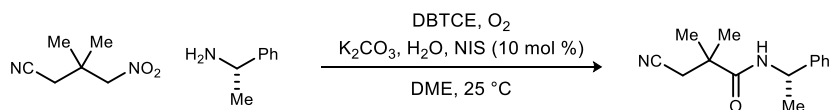


Procedure for step-wise protocol for one-pot halogenation of primary nitroalkanes

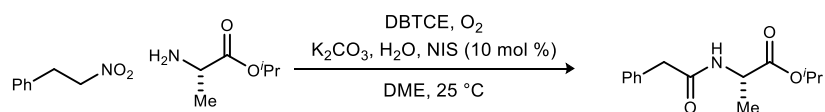
Nitroalkane **91** (1 equiv.) and (*S*)-1-phenylethan-1-amine (5 equiv.) were stirred at 25 °C in DME for 5 h. Halonium source X_1^+ (1 equiv.) was added and the mixture was allowed to stir for 2 h. Halonium source X_2^+ (0.1 equiv.), K_2CO_3 (2 equiv.), and H_2O (5 equiv.) were added to the reaction. The reaction setup was affixed with an O_2 balloon and allowed to stir for 16 h. The mixture was quenched with 1 M HCl and extracted with DCM. The organic layers were washed with satd aq $\text{Na}_2\text{S}_2\text{O}_3$, dried and concentrated. The resulting residue was purified by flash column chromatography.



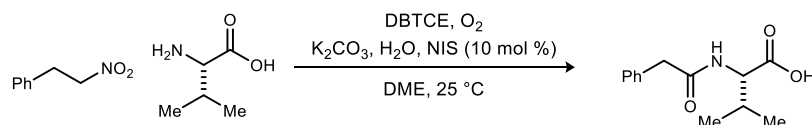
Methyl (S)-4-oxo-4-((1-phenylethyl)amino)butanoate (296). Prepared according to the general procedure for nitroalkane amidation using methyl 4-nitrobutanoate (14.7 mg, 100 μmol) and (*S*)-1-phenylethan-1-amine (26 μL , 200 μmol). Flash column chromatography (SiO₂, 20-40% ethyl acetate in hexanes) yielded the amide as a white solid (16 mg, 68%). Characterization data matched the literature.³⁴



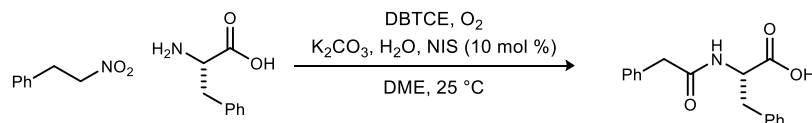
(S)-3-Cyano-2,2-dimethyl-N-(1-phenylethyl)propanamide (297). Prepared according to the general procedure for nitroalkane amidation using 3,3-dimethyl-4-nitrobutanenitrile (14.2 mg, 100 μ mol) and (*S*)-1-phenylethylamine (26 μ L, 200 μ mol). Flash column chromatography (SiO₂, 10-30% ethyl acetate in hexanes) yielded the amide as a white solid (15 mg, 65%). Characterization data matched the literature.³⁴



Isopropyl (2-phenylacetyl)-L-alaninate (298). Prepared according to the general procedure for nitroalkane amidation using (2-nitroethyl)benzene (15.1 mg, 100 μ mol) and isopropyl *L*-alaninate (26.2 mg, 200 μ mol). Flash column chromatography (SiO₂, 20-30% ethyl acetate in hexanes) yielded the amide as a white solid (18 mg, 72%). $R_f = 0.25$ (40% EtOAc/hexanes); $[\alpha]_D^{20} +9.7$ (*c* .35, CHCl₃); mp 56-60 °C; IR (film) 3297, 2981, 2926, 1735, 1650, 1546 cm⁻¹; ¹H NMR (600 MHz, CDCl₃) δ 7.38-7.35 (m, 2H), 7.31-7.27 (m, 3H), 6.03 (br s, 1H), 5.01 (m, 1H), 4.53 (m, 1H), 3.60 (s, 2H), 1.34 (d, *J* = 7.1 Hz, 3H), 1.23 (d, *J* = 6.2 Hz, 3H), 1.21 (d, *J* = 6.2 Hz, 3H); ¹³C NMR (150 MHz, CDCl₃) ppm 172.3, 170.3, 134.6, 129.4, 129.0, 127.3, 69.1, 48.3, 43.6, 21.62, 21.57, 18.4; HRMS (ESI) Exact mass calcd for C₁₄H₁₉NaNO₃ [M+Na]⁺ 272.1263, found 272.1258.



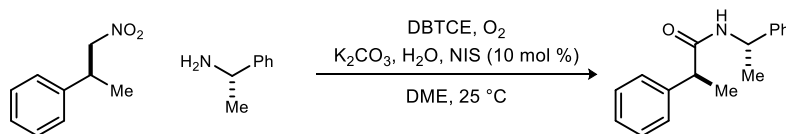
(2-Phenylacetyl)-L-valine (299). Prepared according to the general procedure for nitroalkane amidation using (2-nitroethyl)benzene (30.2 mg, 200 μ mol) and *L*-valine (46.8 mg, 400 μ mol). Flash column chromatography (SiO₂, 20-30% ethyl acetate in dichloromethane with 1% AcOH) yielded the amide as a white solid (27 mg, 57%). $R_f = 0.15$ (30% EtOAc/DCM, 1% AcOH); $[\alpha]_D^{20} -5.6$ (*c* 0.13, DMSO); mp 126-130 °C; IR (film) 3316, 2922, 1710, 1597, 1551 cm⁻¹; ¹H NMR (400 MHz, *d*₆-DMSO) δ 8.21 (d, *J* = 8.6 Hz, 1H), 7.32-7.26 (m, 4H), 7.22-7.20 (m, 1H), 4.15 (dd, *J* = 8.6, 5.8 Hz, 1H), 3.56 (d, *J* = 13.8 Hz, 1H), 3.48 (d, *J* = 13.8 Hz, 1H), 2.05 (dq, *J* = 13.6, 6.8, 6.8 Hz, 1H), 0.87 (d, *J* = 6.8 Hz, 3H), 0.85 (d, *J* = 6.8 Hz, 3H)¹³¹; ¹³C NMR (100 MHz, *d*₆-DMSO) ppm 173.1, 170.4, 136.6, 129.0, 128.1, 126.3, 57.2, 41.9, 29.9, 19.1, 18.0; HRMS (ESI) Exact mass calcd for C₁₃H₁₇NaNO₃ [M+Na]⁺ 258.1095, found 258.1106.



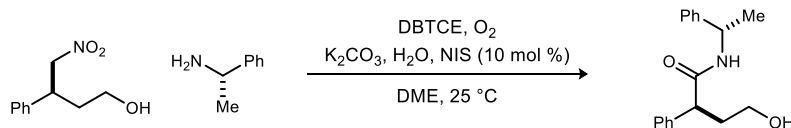
(2-Phenylacetyl)-L-phenylalanine (300). Prepared according to the general procedure for nitroalkane amidation using (2-nitroethyl)benzene (30.2 mg, 200 μ mol) and *L*-phenylalanine (66.0 mg, 400 μ mol). Flash column chromatography (SiO₂, 20-30% ethyl acetate in dichloromethane with 1% AcOH) yielded the amide as a yellow oil (30 mg, 53%). $R_f = 0.23$ (30% EtOAc/DCM, 1% AcOH); $[\alpha]_D^{20} +5.8$ (*c* 0.38, DMSO); IR (film) 3286, 3062, 3030, 2927, 2522, 2362, 1727, 1655, 1540 cm⁻¹; ¹H NMR (400 MHz, *d*₆-

¹³¹ Carboxylic acid ¹H not observed.

DMSO) δ 8.39 (d, $J = 8.0$ Hz, 1H), 7.27-7.16 (m, 8H), 7.13-7.11 (m, 2H), 4.44 (m, 1H), 3.44 (d, $J = 14.0$ Hz, 1H), 3.39 (d, $J = 14.0$ Hz, 1H), 3.07 (dd, $J = 13.8, 4.8$ Hz, 1H), 2.87 (dd, $J = 13.8, 9.6$ Hz, 1H)¹³¹; ¹³C NMR (100 MHz, *d*₆-DMSO) ppm 173.0, 170.0, 137.5, 136.2, 129.1, 129.0, 128.2, 128.1, 126.4, 126.2, 53.5, 42.0, 36.8; HRMS (ESI) Exact mass calcd for C₁₇H₁₇NO₃ [M]⁺ 284.1287, found 284.1280.



(S)-2-Phenyl-N-((S)-1-phenylethyl)propanamide (301). Prepared according to the general procedure for nitroalkane amidation using (*S*)-(1-nitropropan-2-yl)benzene (16.5 mg, 100 μ mol) and (*S*)-1-phenylethan-1-amine (26 μ L, 200 μ mol). Flash column chromatography (SiO₂, 10-30% ethyl acetate in hexanes) yielded the amide as a white solid (15 mg, 60%) in >20:1 dr (¹H NMR). $R_f = 0.35$ (40% EtOAc/hexanes); $[\alpha]_D^{20} +4.1$ (*c* 0.46, CHCl₃); mp 96-100 °C; IR (film) 3288, 2928, 1645, 1541 cm⁻¹; ¹H NMR (600 MHz, CDCl₃) δ 7.37-7.34 (m, 2H), 7.31-7.27 (m, 5H), 7.24-7.21 (m, 1H), 7.11 (d, $J = 7.2$ Hz, 2H), 5.56 (d, $J = 6.3$ Hz, 1H), 5.12 (m, 1H), 3.60 (q, $J = 7.2$ Hz, 1H), 1.54 (d, $J = 7.2$ Hz, 3H), 1.42 (d, $J = 6.9$ Hz, 3H); ¹³C NMR (150 MHz, CDCl₃) ppm 173.3, 143.4, 141.5, 129.0, 128.6, 127.8, 127.4, 127.2, 125.9, 48.8, 47.3, 22.0, 18.6; HRMS (ESI) Exact mass calcd for C₁₇H₁₉NaNO [M+Na]⁺ 276.1364, found 276.1357.



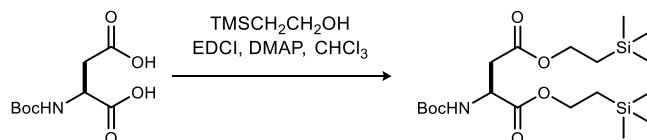
(S)-4-Hydroxy-2-phenyl-N-((S)-1-phenylethyl)butanamide (302). Prepared according to the general procedure for nitroalkane amidation using (*S*)-4-nitro-3-phenylbutan-1-ol (78.1 mg, 400 μ mol) and (*S*)-1-phenylethan-1-amine (102 μ L, 800 μ mol). Flash column chromatography (SiO₂, 1-5% methanol in dichloromethane) yielded the amide as a clear oil (59 mg, 52%) in >20:1 dr (¹H NMR). $R_f = 0.36$ (10% MeOH/CH₂Cl₂); $[\alpha]_D^{20} +7.2$ (*c* 0.25, CHCl₃); IR (film) 3287, 2931, 1648, 1544 cm⁻¹; ¹H NMR (600 MHz, CDCl₃) δ 7.35-7.32 (m, 2H), 7.29-7.19 (m, 6H), 7.08 (d, $J = 7.2$ Hz, 2H), 5.80 (d, $J = 7.4$ Hz, 1H), 5.08 (m, 1H), 3.71-3.67 (m, 2H), 3.63-3.59 (m, 1H), 2.42-2.36 (m, 1H), 2.02-1.97 (m, 1H), 1.41 (d, $J = 6.9$ Hz, 3H)¹³²; ¹³C NMR (150 MHz, CDCl₃) ppm 173.0, 142.9, 139.7, 128.9, 128.5, 128.0, 127.4, 127.1, 125.7, 60.7, 50.3, 48.9, 35.9, 21.9; HRMS (ESI) Exact mass calcd for C₁₈H₂₂NO₂ [M+H]⁺ 284.1651, found 284.1659.



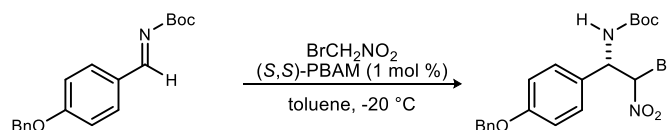
tert-Butyl ((1R)-1-(4-(benzyloxy)phenyl)-2-bromo-2-nitroethyl)carbamate (330). A 250-mL round-bottomed flask was charged with imine (6.80 g, 21.9 mmol), (*R,R*)-PBAM (540 mg, 1.10 mmol) and toluene

¹³² Alcohol ¹H not observed.

(120 mL) and cooled to $-78\text{ }^{\circ}\text{C}$. Bromonitromethane (1.81 mL, 26.1 mmol) was added over 1 minute and the reaction was stirred for 48 h at $-20\text{ }^{\circ}\text{C}$. The reaction was filtered through a silica gel plug using ethyl acetate, concentrated to a yellow solid (8.50 g, 86%), and determined to be 1:1 dr by ^1H NMR. The yellow solid was recrystallized from ethyl acetate. The diastereomers were determined to be 98% and 99% ee by chiral HPLC analysis (Chiralcel AD-H, 20% i PrOH/hexanes, 1 mL/min, $t_r(d_{1e1}, \text{minor}) = 15.6\text{ min}$, $t_r(d_{1e2}, \text{major}) = 19.3\text{ min}$, $t_r(d_{2e1}, \text{major}) = 20.4\text{ min}$, $t_r(d_{2e2}, \text{minor}) = 26.1\text{ min}$); All characterization data matched the literature.¹³³

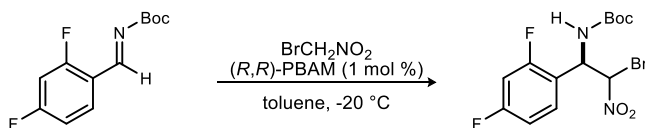


(S)-Bis(2-(trimethylsilyl)ethyl) 2-((tert-butoxycarbonyl)amino)succinate (Boc-336). To a solution of Boc aspartic acid (2.5 g, 10.7 mmol) in CHCl_3 (30 mL), EDC was added trimethylsilylethanol (3.4 mL, 23.5 mmol), EDC (5.1 g, 26.4 mmol), followed by DMAP (134 mg, 1.1 mmol). The resulting mixture was allowed to stir for 12 h before quenched by adding aq. NH_4Cl . The aqueous phase was extracted ethyl acetate, and the combined organic layers were washed with satd aq NaHCO_3 and brine, dried, filtered, and concentrated. The resulting residue was purified by column chromatography (SiO_2 , 10% EtOAc/hexanes) to provide 1.25 g (52 % yield) of the product as a clear oil. $R_f = 0.59$ (25% EtOAc/hexanes) $[\alpha]_D^{20} +14.1$ (c 1.4, CHCl_3); IR (film) 2955, 2900, 1728, 1652, 1251, 1172, 860, 838 cm^{-1} ; ^1H NMR (600 MHz, CDCl_3) δ 5.46 (d, $J = 9\text{ Hz}$, 1H), 4.48 (m, 1H), 5.10 (bs, 1H), 4.19 (m, 2H), 4.13 (m, 2H), 2.92 (dd, $J = 4.2, 16.8\text{ Hz}$, 1H), 2.74 (dd, $J = 4.8, 16.8\text{ Hz}$, 1H), 1.40 (s, 9H), 0.95 (m, 2H), 0.94 (m, 2H), -0.01 (s, 18H); ^{13}C NMR (150 MHz, CDCl_3) 171.1, 171.0, 155.3, 79.8, 64.0, 63.2, 50.0, 36.9, 28.2, 17.2, 17.2, -1.5, -1.6 ppm; HRMS (EI): Exact mass calcd for $\text{C}_{19}\text{H}_{39}\text{NO}_6\text{Si}_2$ $[\text{M}+\text{H}]^+$ 434.2394, found 434.2374.

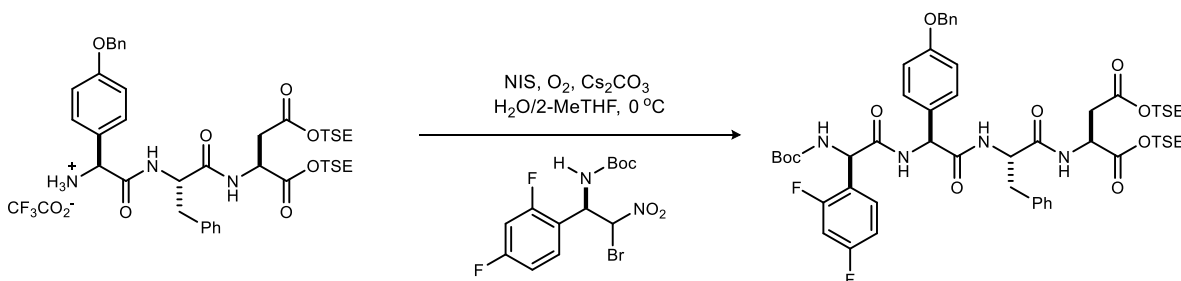


tert-Butyl ((1S)-1-(4-(benzyloxy)phenyl)-2-bromo-2-nitroethyl)carbamate (339). A 250-mL round-bottomed flask was charged with imine (6.80 g, 21.9 mmol), (S,S)-PBAM (540 mg, 1.10 mmol) and toluene (120 mL) and cooled to $-78\text{ }^{\circ}\text{C}$. Bromonitromethane (1.81 mL, 26.1 mmol) was added over 1 minute and the reaction was stirred for 48 h at $-20\text{ }^{\circ}\text{C}$. The reaction was filtered through a silica gel plug using ethyl acetate, concentrated to a yellow solid (8.90 g, 90%), and determined to be 1:1 dr by ^1H NMR. The yellow solid was recrystallized from ethyl acetate. The diastereomers were determined to be 98% and 99% ee by chiral HPLC analysis (Chiralcel AD-H, 20% i PrOH/hexanes, 1 mL/min, $t_r(d_{1e1}, \text{major}) = 15.6\text{ min}$, $t_r(d_{1e2}, \text{minor}) = 19.3\text{ min}$, $t_r(d_{2e1}, \text{minor}) = 20.4\text{ min}$, $t_r(d_{2e2}, \text{major}) = 26.1\text{ min}$); All characterization data matched the literature.¹³³

¹³³ Lim, V.; Tsukanov, S. V.; Doody, A. B.; Johnston, J. N. *Org. Synth.* **2016**, *93*, 88.

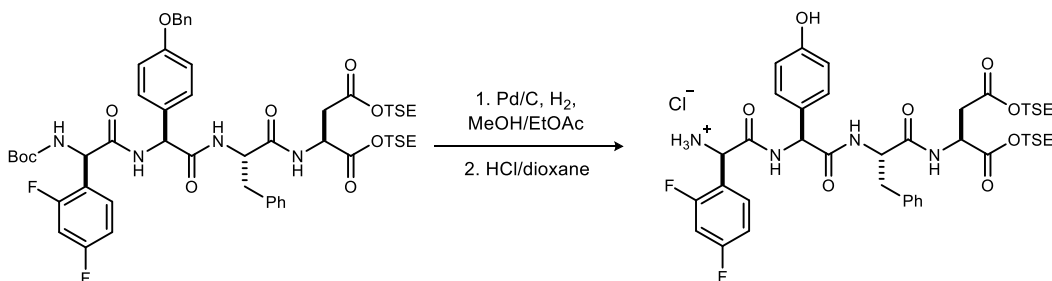


***tert*-Butyl ((1*R*)-2-bromo-1-(2,4-difluorophenyl)-2-nitroethyl)carbamate (346).** A 250-mL round-bottomed flask was charged with imine (22.92 g, 95.0 mmol), (*R,R*)-PBAM (482 mg, 950 μ mol) and toluene (482 mL) and cooled to -78 $^{\circ}$ C. Bromonitromethane (9.97 mL, 143.0 mmol) was added over 1 minute and the reaction was stirred for 48 h at -20 $^{\circ}$ C. The reaction was filtered through a silica gel plug using ethyl acetate, concentrated to a white solid (33.2 g, 92%), and determined to be 1:1 dr by 1 H NMR. The white solid was determined to be pure and required no further purification. The major diastereomer was determined to be 94% ee and the minor diastereomer was determined to be 97% ee by chiral HPLC analysis (Chiralcel AD-H, 4% i PrOH/hexanes, 1 mL/min, $t_r(d_{1e1}, \text{major}) = 20.7$ min, $t_r(d_{1e2}, \text{minor}) = 29.6$ min, $t_r(d_{2e1}, \text{major}) = 22.8$ min, $t_r(d_{2e2}, \text{minor}) = 25.5$ min); IR (film) 3355, 2985, 1690, 1607, 1566, 1506 cm^{-1} ; 1 H NMR (600 MHz, CDCl_3 , 1:1 mixture of diastereomers) δ 7.35-7.28 (m, 2H), 6.91 (dd, $J = 8.7, 8.7$ Hz, 2H), 6.88 (dd, $J = 9.7, 9.7$ Hz, 2H), 6.29 (br s, 2H), 5.81 (br s, 1H), 5.73 (br s, 1H), 5.65 (br s, 1H), 5.40 (br d, $J = 8.7$ Hz, 1H), 1.43 (s, 18 H); 13 C NMR (150 MHz, CDCl_3 , 1:1 mixture of diastereomers) ppm 163.41 (dd, $J_{\text{CF}} = 253, 12.1$ Hz), 163.37 (dd, $J_{\text{CF}} = 252, 12.6$ Hz), 160.4 (dd, $J_{\text{CF}} = 249, 12.2$ Hz), 154.4, 154.3, 130.5 (m), 118.5, 112.23 (dd, $J_{\text{CF}} = 21.6, 3.3$ Hz), 112.17 (dd, $J_{\text{CF}} = 21.5, 3.2$ Hz), 104.7 (dd, $J_{\text{CF}} = 25.8, 25.8$ Hz), 104.6 (dd, $J_{\text{CF}} = 25.5, 25.5$ Hz), 82.6, 81.4, 79.1, 53.9, 28.1; 19 F NMR (282 MHz, CDCl_3 , 1:1 mixture of diastereomers) ppm -106, -110, -111; HRMS (ESI): Exact mass calcd for $\text{C}_{13}\text{H}_{15}\text{BrF}_2\text{N}_2\text{NaO}_4$ $[\text{M}+\text{Na}]^+$ 403.0081, found 403.0065.

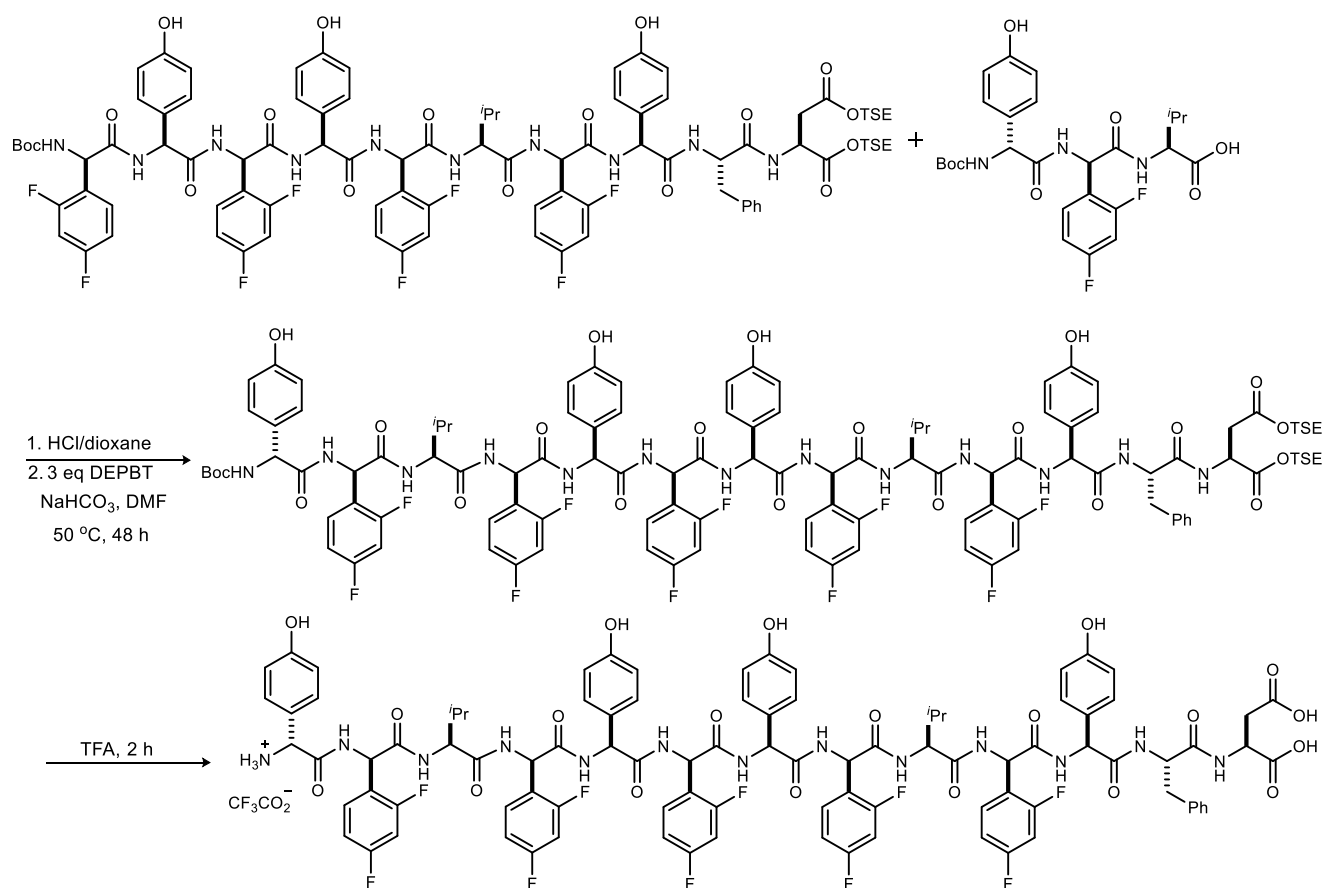


Bis(2-(trimethylsilyl)ethyl) ((*S*)-2-(4-(benzyloxy)phenyl)-2-((*R*)-2-((*tert*-butoxycarbonyl)amino)-2-(2,4-difluorophenyl)acetamido)acetyl)-*L*-phenylalanyl-*L*-aspartate (347). To a solution of the nitroalkane (115 mg, 302 μ mol) in 2-MeTHF (5.0 mL, 0.06 M) was added amine (277 mg, 332 μ mol). Cesium carbonate (344 mg, 1.056 mmol) and 50 eq of H_2O (15.3 mmol, 0.280 mL) were added in a sequence. The resulting mixture was cooled to 0 $^{\circ}$ C. NIS (68 mg, 0.302 mmol) was introduced and the flask was fitted with an oxygen balloon. The reaction mixture was stirred at 0 $^{\circ}$ C for 2 days. The resulting mixture was diluted with dichloromethane, washed with 1 M HCl, satd aq $\text{Na}_2\text{S}_2\text{O}_3$ and satd aq NaHCO_3 , dried with MgSO_4 and then filtered through Celite. The filtrate was concentrated and purified by column chromatography (SiO_2 , 25-32% EtOAc/hexanes) to provide 205 mg (69% yield) of the amide as white solid. $R_f = 0.37$ (30% EtOAc/hexanes); $[\alpha]_D^{20} +12.4$ (c 0.85, CHCl_3); IR (film) 3281, 3065, 2955, 1735, 1641, 1509, 1250, 1175 cm^{-1} ; 1 H NMR (400 MHz, CDCl_3) δ 7.43-7.20 (m, 10H), 7.15 (m, 2H), 7.10 (bs, 1H) 6.93 (m, 2H), 6.85 (bs, 1H), 6.79 (m, 3H), 6.69 (bs, 1H), 5.85 (bs, 1H), 5.50 (bs, 1H) 5.32 (d, $J = 6.4$ Hz, 1H),

4.98 (s, 2H), 4.72 (m, 2H) 4.20 (m, 2H), 4.12 (m, 2H), 3.20 (dd, $J = 4.4, 14.0$ Hz, 1H), 3.02 (dd, $J = 7.2, 14.0$ Hz, 1H), 2.85 (dd, $J = 4.4, 16.8$ Hz, 1H), 2.65 (dd, $J = 4.8, 16.8$ Hz, 1H), 1.41 (s, 9H), 0.97 (m, 4H), 0.03 (s, 9H), 0.02 (s, 9H); ^{13}C NMR (100 MHz, CDCl_3) 170.5, 170.2, 169.4, 169.0, 162.5 (dd, $^3J_{\text{CF}} = 11.2$ Hz, $^1J_{\text{CF}} = 249$ Hz), 160.2 (dd, $^3J_{\text{CF}} = 11.2$ Hz, $^1J_{\text{CF}} = 249$ Hz), 158.5, 155.1, 136.6, 136.1, 130.0, 129.4, 129.3, 129.0, 128.6, 128.5, 128.4, 127.9, 127.7, 127.4, 126.8, 121.7 (d, $^3J_{\text{CF}} = 17.5$ Hz), 114.7, 111.5, (d, $^2J_{\text{CF}} = 20$ Hz), 103.8 (t, $^2J_{\text{CF}} = 26$ Hz), 80.0, 69.8, 64.0, 63.3, 56.2, 54.2, 51.6, 48.6, 38.9, 36.3, 28.3, 17.3, 17.2, -1.4, -1.9 ppm; ^{19}F NMR (376 MHz, CDCl_3) ppm -109.4, -113.2; HRMS (EI): Exact mass calcd for $\text{C}_{55}\text{H}_{66}\text{F}_2\text{N}_4\text{O}_{10}\text{Si}_2$ $[\text{M}+\text{Na}]^+$ 1011.4183, found 1011.4238.



(8*S*,11*S*,14*S*,17*R*)-11-Benzyl-17-(2,4-difluorophenyl)-14-(4-hydroxyphenyl)-2,2-dimethyl-6,10,13,16-tetraoxo-8-((2-(trimethylsilyl)ethoxy)carbonyl)-5-oxa-9,12,15-triaza-2-silaheptadecan-17-aminium chloride (349). To a solution of tetrapeptide (330 mg, 336 μmol) in the mixture of EtOAc/MeOH (50 mL, 1:1) was added Pd/C (330 mg). The reaction mixture was evacuated and refilled with hydrogen twice. After flask was fitted with hydrogen balloon and stirred at rt for 24 h. The resulting solution was filtered through Celite and solvent was removed in vacuo. The complete removal of the benzyl group was confirmed using NMR spectroscopy. Then to the resulting crude Boc amine (300 mg, 334 μmol) was added HCl in dioxane (4M, 10 mL). The mixture was stirred at rt for 2 h and solvent was removed in vacuo to provide 260 mg (93% yield) of the free amine salt as grey solid. $[\alpha]_D^{20} +5.8$ (c 0.86, MeOH); IR (film) 3232, 3026, 2952, 1725, 1654, 15119, 1248, 1177 cm^{-1} ; ^1H NMR (600 MHz, MeOD) δ 7.42 (m, 1H), 7.23 (m, 5H), 7.12 (dt, $J = 2.0, 8.0$ Hz, 1H), 7.03 (dt, $J = 2.0, 8.0$ Hz, 1H), 6.89 (m, 2H), 6.64 (dt, $J = 3.0, 8.0$ Hz, 1H), 5.35 (s, 1H), 5.32 (d, $J = 4.0$ Hz, 1H) 4.71 (m, 2H), 4.20 (m, 4H), 3.21 (m, 1H), 3.00 (m, 1H), 2.80 (m, 2H), 1.00 (m, 4H), 0.05 (s, 9H), 0.04 (s, 9H); ^{13}C NMR (150 MHz, MeOD) Behavior associated with multiple conformations was observed by ^{13}C NMR, preventing an accurate peak listing beyond those provided here. Please see the ^{13}C NMR image provided in Supporting Information II; ^{19}F NMR (376 MHz, CDCl_3) ppm -110.9, -115.4; HRMS (EI): Exact mass calcd for $\text{C}_{39}\text{H}_{53}\text{F}_2\text{N}_4\text{O}_8\text{Si}_2$ $[\text{M}]^+$ 799.3370, found 799.3389.

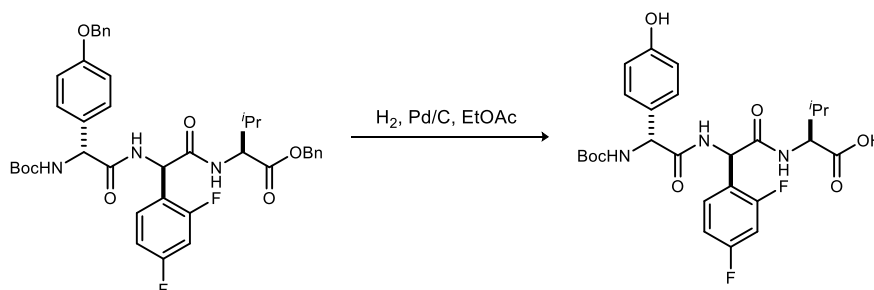


Bis (1*R*,4*R*,7*S*,10*R*,13*S*,16*R*,19*S*,22*R*,25*S*,28*R*,31*S*,34*S*,37*S*)-34-benzyl-37,38-dicarboxy-4,10,16,22,28-pen-takis(2,4-difluorophenyl)-1,13,19,31-tetrakis(4-hydroxyphenyl)-7,25-diisopropyl-2,5,8,11,14,17,20,23,26,29,32,35-dodecaoxo-3,6,9,12,15,18,21,24,27,30,33,36-dodecaazaoctatriacontan-1-aminium 2,2,2-trifluoroacetate (353).

Boc decapeptide (57 mg, 32 μmol) was treated with 2 mL of 4M HCl in dioxane. The reaction was stirred for 2 h at rt and the solvent was removed in vacuo. The crude hydrochloride salt of decapeptide was dissolved in DMF (300 μL) then was added sodium bicarbonate (4.0 equiv; 11.0 mg, 128 μmol) and DEPBT (3.0 equiv., 29 mg, 96 μmol). The resulting mixture was stirred at rt for 6 h. Then tripeptide (1.2 equiv., 20 mg, 38 μmol) was added in DMF (100 μL), reaction mixture was heated to 50-55 $^{\circ}\text{C}$ and stirred for 48 h. The resulting solution was cooled to rt and solvent was removed in vacuo. Then the resulting crude mixture was dissolved in MeCN and purified by HPLC (C18, 55-95% $\text{CH}_3\text{CN}/\text{H}_2\text{O}$) to provide 29 mg (40% yield) of the product as a white solid.

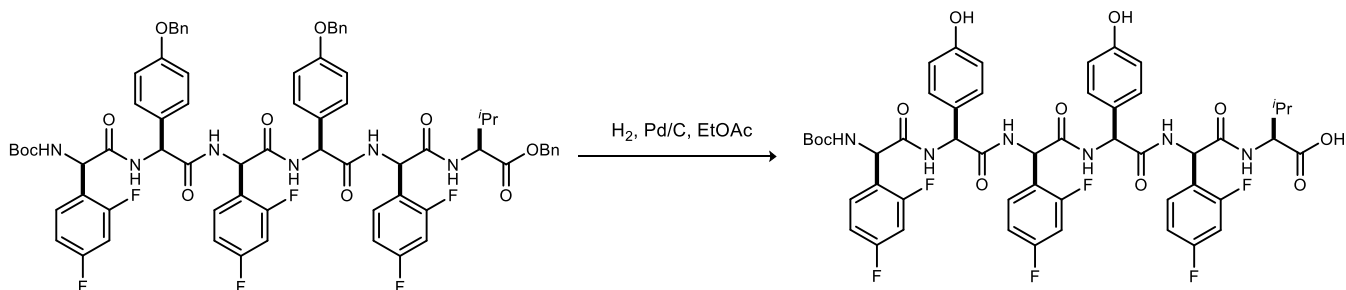
Global deprotection. The resulting tridecapeptide was dissolved in TFA (1 mL), stirred for 2 hours. TFA was removed in vacuo, then to the resulting crude mixture was dissolved in MeCN and purified by HPLC (C18, 40-95% $\text{CH}_3\text{CN}/\text{H}_2\text{O}$) to provide 15 mg (55% yield) of the product as a transparent oil. $[\alpha]_D^{20}$ -5.8 (c 0.70, CH_3CN); IR (film) 3293, 2928, 2857, 1681, 1640, 1505, 1433, 1206, 1138. cm^{-1} ; ^1H NMR (400 MHz, DMSO) δ 9.76 (m, 1H), 9.40 (m, 4H), 9.15 (d, J = 6.6 Hz, 1H), 8.89 (m, 2H), 8.72 (d, J = 6.8 Hz, 2H), 8.66 (m, 2H), 8.53 (m, 1H), 8.33 (m, 1H), 8.21 (d, J = 8.9 Hz, 1H), 7.93 (d, J = 7.9 Hz, 1H), 7.45-6.80 (m, 28H), 6.63-6.58 (m, 8H), 5.81 (m, 3H), 5.54 (m, 2H), 5.35 (d, J = 8.2 Hz, 1H), 4.96 (m, 1H), 4.56 (m, 2H), 4.46 (m, 1H), 4.33 (m, 1H), 4.25 (m, 1H), 4.04 (m, 1H), 3.56 (m, 1H), 3.51-3.25 (m, 1H), 3.02 (m, 1H), 2.84 (m, 1H), 1.88 (m, 2H), 0.60 (d, J = 9.6 Hz, 3H), 0.54 (d, J = 9.6 Hz, 3H), 0.49 (d, J = 10.2 Hz, 3H); ^{13}C NMR (100 MHz, DMSO) Presence of multiple fluorine atoms and also behavior associated with multiple

conformations was observed by ^{13}C NMR resulting in multiple overlaps of the signals and preventing an accurate assignment and listing of the peaks. Please see the ^{13}C NMR image provided in Supporting Information II; ^{19}F NMR (376 MHz, DMSO) ppm -110.2, -110.6, -110.8, -110.8, -110.9, -111.4, -111.5, -111.6, -111.7 -112.2; HRMS (MALDI): Exact mass calcd for $\text{C}_{95}\text{H}_{88}\text{F}_{10}\text{N}_{13}\text{O}_{20}^+$ $[\text{M}]^+$ 1920.6103, *submitted*.



((R)-2-((R)-2-((tert-Butoxycarbonyl)amino)-2-(4-hydroxyphenyl)acetamido)-2-(2,4-difluorophenyl)acetyl)-L-valine (354).

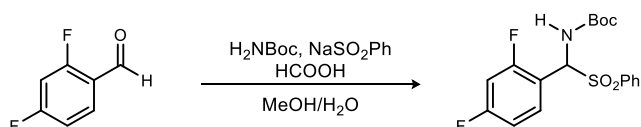
To a round bottom flask containing tripeptide (180 mg, 252 μmol) in ethyl acetate (15.0 mL) was added Pd/C (180 mg). The flask was fitted with balloon containing hydrogen gas. The mixture was purged two times under reduced pressure. The resulting heterogeneous mixture was stirred at rt for 24 h. The mixture was filtered through Celite and concentrated under reduced pressure to provide 120 mg (89%) of free acid as a white solid. $[\alpha]_D^{20}$ -72 (*c* .84, MeOH); IR (film) 3292, 2969, 1660, 1509 cm^{-1} ; ^1H NMR (400 MHz, MeOD) δ 7.51 (dt, $J = 6.0, 9.0$ Hz, 1H), 7.23 (d, $J = 8.0$ Hz, 2H), 7.02-6.94 (m, 2H), 6.75 (d, $J = 8.0$ Hz, 2H), 5.76 (br s, 1H), 5.58 (d, $J = 6.1$ Hz, 1H), 5.53 (br s, 1H), 5.12 (br s, 1H), 4.29 (br s, 1H), 2.09 (m, 1H), 1.44 (s, 9H), 0.83 (d, $J = 6.0$ Hz, 3H), 0.79 (d, $J = 6.0$ Hz, 3H); ^{13}C NMR (125 MHz, MeOD) ppm 174.5, 173.5, 171.2, 164.4 (dd, $^1J_{\text{CF}} = 250.0$ Hz, $^3J_{\text{CF}} = 12.0$ Hz), 162.3 (dd, $^1J_{\text{CF}} = 250.0$ Hz, $^3J_{\text{CF}} = 12.0$ Hz), 158.7, 157.6, 132.1 (m, pattern is not clear), 129.8, 129.2, 122.3 (dd, $^2J_{\text{CF}} = 13.0$ Hz, $^4J_{\text{CF}} = 4.0$ Hz), 116.7, 112.5 (d, $^2J_{\text{CF}} = 21.0$ Hz), 104.9 (t, $^2J_{\text{CF}} = 26.0$ Hz), 81.0, 59.7, 59.3, 52.7, 30.7, 28.7, 19.6, 18.2; ^{19}F NMR (376 MHz, CDCl_3) ppm -111.6, -113.7; HRMS (ESI): Exact mass calcd for $\text{C}_{26}\text{H}_{31}\text{F}_2\text{N}_3\text{O}_7\text{Na}$ $[\text{M}+\text{Na}]^+$ 558.2028, found 558.2025.



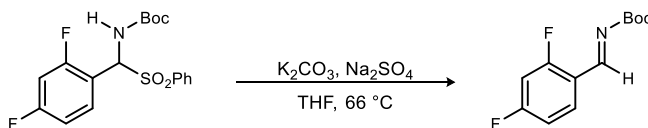
((R)-2-((S)-2-((R)-2-((S)-2-((R)-2-((tert-Butoxycarbonyl)amino)-2-(2,4-difluorophenyl)acetamido)-2-(4-hydroxyphenyl)acetamido)-2-(2,4-difluorophenyl)acetamido)-2-(4-hydroxyphenyl)acetamido)-2-(2,4-difluorophenyl)acetyl)-L-valine (356).

To a round bottom flask containing hexapeptide (287 mg, 222 μmol) in ethyl acetate (30.0 mL) was added Pd/C (300 mg). The flask was fitted with balloon containing hydrogen gas. The mixture was purged two times under reduced pressure. The resulting heterogeneous mixture was stirred at rt for 24 h. The mixture was filtered through Celite and concentrated under reduced pressure to provide 201 mg (89%) of free acid as a white solid. $[\alpha]_D^{20}$ -1.3 (*c* 1.15, MeOH); IR (film) 3287, 2975, 1640, 1509 cm^{-1} ; ^1H NMR (400 MHz, MeOD) δ 7.37 (dd, $J = 8.2, 15.0$ Hz, 1H), 7.16 (m, 4H), 7.07 (d, $J = 8.5$ Hz, 2H), 6.90 (m, 4H), 6.79 (m, 2H), 6.68 (d, $J = 8.0$ Hz, 2H), 6.63 (d, $J = 8.5$ Hz, 2H),

5.94 (s, 1H), 5.82 (s, 1H), 5.53 (s, 1H), 5.48 (3 bs, 3H), 5.95 (d, $J = 6.6$ Hz, 1H), 5.81 (d, $J = 9.3$ Hz, 1H), 5.63 (d, $J = 11.8$ Hz, 1H), 5.24 (d, $J = 11.8$ Hz, 1H), 5.10 (s, 2H), 4.41 (bs, 1H), 2.08 (m, 1H), 1.41 (s, 9H), 0.81 (d, $J = 6.5$ Hz, 3H), 0.80 (d, $J = 6.3$ Hz, 3H); ^{13}C NMR (150 MHz, MeOD) ppm 173.0, 172.6, 172.6, 171.5, 171.1, 171.0, 164.2 (dd, $^1J_{\text{CF}} = 248$ Hz, $^3J_{\text{CF}} = 12.0$ Hz), 164.1 (dd, $^1J_{\text{CF}} = 248$ Hz, $^3J_{\text{CF}} = 12.0$ Hz), 164.1 (dd, $^1J_{\text{CF}} = 248$ Hz, $^3J_{\text{CF}} = 12.0$ Hz), 162.1 (dd, $^1J_{\text{CF}} = 250$ Hz, $^3J_{\text{CF}} = 12.0$ Hz), 162.0 (dd, $^1J_{\text{CF}} = 250$ Hz, $^3J_{\text{CF}} = 12.0$ Hz), 161.9 (dd, $^1J_{\text{CF}} = 250$ Hz, $^3J_{\text{CF}} = 12.0$ Hz), 158.9, 158.8, 157.1, 131.5, 131.5, 131.3, 130.2, 130.1, 128.0 (3C), 122.8 (dd, $^2J_{\text{CF}} = 15.0$ Hz, $^4J_{\text{CF}} = 3.0$ Hz), 122.5 (dd, $^2J_{\text{CF}} = 15.0$ Hz, $^4J_{\text{CF}} = 3.0$ Hz), 122.0 (dd, $^2J_{\text{CF}} = 15.0$ Hz, $^4J_{\text{CF}} = 3.0$ Hz), 116.5, 116.4, 112.4 (d, $^2J_{\text{CF}} = 22$ Hz), 112.1 (d, $^2J_{\text{CF}} = 22$ Hz), 104.7 (t, $^2J_{\text{CF}} = 26$ Hz), 104.5 (t, $^2J_{\text{CF}} = 26$ Hz), 81.2, 59.4, 58.8, 58.4, 53.0, 52.6, 52.3, 30.7, 28.6, 19.5, 18.2; ^{19}F NMR (376 MHz, MeOD) ppm -112.0, -112.1 (d, $^1J_{\text{FF}} = 4$ Hz), -112.2 (d, $^2J_{\text{FF}} = 8$ Hz), -114.0 (bs), -114.1 (d, $^3J_{\text{FF}} = 6$ Hz), -114.4 (bs); HRMS (ESI): Exact mass calcd for $\text{C}_{50}\text{H}_{48}\text{F}_6\text{N}_6\text{NaO}_{11}\text{Na}$ $[\text{M}+\text{Na}]^+$ 1045.3182, found 1045.3159.

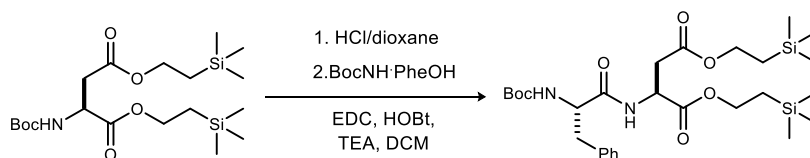


tert-Butyl ((2,4-difluorophenyl)(phenylsulfonyl)methyl)carbamate (359). A 1-L round-bottomed flask was charged with 2,4-difluorobenzaldehyde (29.8 g, 210 mmol), benzenesulfinic acid sodium salt (45.9 g, 280 mmol), *tert*-butyl carbamate (16.4 g, 140 mmol), formic acid (10.6 mL, 280 mmol), methanol (130 mL), and water (260 mL) and stirred for 3 days. The solid was filtered and rinsed with water. The washed solid was added to diethyl ether and stirred overnight. Filtration and washing with diethyl ether afforded the pure product as a white solid (47.2 g, 88% yield). Mp 144-146 °C; IR (film) 3342, 2979, 1705, 1619, 1505 cm^{-1} ; ^1H NMR (600 MHz, CDCl_3) δ 7.93 (d, $J = 7.3$ Hz, 2H), 7.66 (t, $J = 7.3$ Hz, 1H), 7.55 (d, $J = 7.6$, 7.6 Hz, 2H), 7.45 (ddd, $J = 7.9$, 7.9, 7.9 Hz, 1H), 6.96 (ddd, $J = 8.1$, 8.1, 1.9 Hz, 1H), 6.87 (ddd, $J = 10.6$, 8.7, 2.5 Hz, 1H), 6.19 (d, $J = 10.9$ Hz, 1H), 5.90 (d, $J = 10.5$ Hz, 1H), 1.27 (s, 9H); ^{13}C NMR (150 MHz, CDCl_3) ppm 163.9 (dd, $J_{\text{CF}} = 253$, 12.3 Hz), 161.4 (dd, $J_{\text{CF}} = 252$, 11.7 Hz), 153.4, 136.5, 134.2, 131.3 (d, $J_{\text{CF}} = 10.3$ Hz), 129.4, 129.2, 114.1 (d, $J_{\text{CF}} = 14.5$ Hz), 112.1 (d, $J_{\text{CF}} = 20.0$ Hz), 104.6 (dd, $J_{\text{CF}} = 25.7$, 25.7 Hz), 81.5, 68.7, 28.0; ^{19}F NMR (282 MHz, CDCl_3) ppm -104, -109 (d, $J_{\text{HF}} = 8.5$ Hz); HRMS (ESI): decomposed to imine during analysis ($M = 242$).

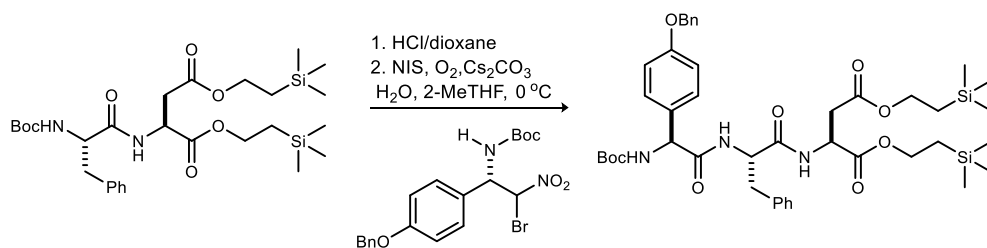


tert-Butyl 2,4-difluorobenzylidencarbamate (360). A 500-mL round-bottomed flask was charged with *tert*-butyl ((2,4-difluorophenyl)(phenylsulfonyl)methyl)carbamate (36.8 g, 96.0 mmol), K_2CO_3 (92.7 g, 672 mmol), Na_2SO_4 (109.1 g, 768 mmol) and THF (300 mL). The pot was refluxed for 4 h until completion (checked by ^1H NMR). The reaction mixture was filtered through Celite, washed with diethyl ether and concentrated on low heat to yield the title compound as a colorless oil [23.1 g, 99% (<2% aldehyde)]. IR (film) 3079, 2982, 2936, 1718, 1619, 1502 cm^{-1} ; ^1H NMR (600 MHz, CDCl_3) δ 9.08 (s, 1H), 8.16 (ddd,

$J = 8.5, 8.5, 6.7$ Hz, 1H), 6.96 (ddd, $J = 8.9, 8.9, 2.3$ Hz, 1H), 6.88 (ddd, $J = 10.7, 8.8, 2.4$ Hz, 1H), 1.58 (s, 9H); ^{13}C NMR (150 MHz, CDCl_3) ppm 166.5 (dd, $J_{\text{CF}} = 258, 12.5$ Hz), 164.4 (dd, $J_{\text{CF}} = 260, 12.8$ Hz), 162.3, 161.7 (d, $J_{\text{CF}} = 4.6$ Hz), 130.2 (dd, $J_{\text{CF}} = 10.5, 3.1$ Hz), 118.7 (dd, $J_{\text{CF}} = 8.9, 3.5$ Hz), 112.6 (dd, $J_{\text{CF}} = 22.0, 3.3$ Hz), 104.4 (dd, $J_{\text{CF}} = 25.0, 25.0$ Hz), 82.7, 27.9; ^{19}F NMR (282 MHz, CDCl_3) ppm -98, -112; HRMS (ESI): Exact mass calcd for $\text{C}_{12}\text{H}_{14}\text{F}_2\text{NO}_2$ $[\text{M}+\text{H}]^+$ 242.0987, found 242.0989.

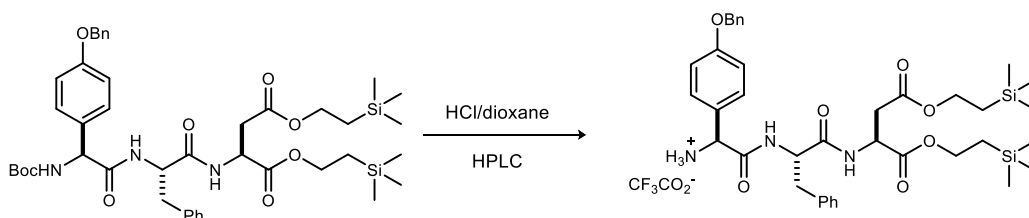


(S)-Bis(2-(trimethylsilyl)ethyl) 2-((S)-2-((tert-butoxycarbonyl)amino)-3-phenylpropanamido)succinate (363). Boc aspartic acid (1.57 g, 3.62 mmol) was treated with 15 mL of 4M HCl in dioxane. The reaction was stirred for 2 h at rt and the solvent was removed in vacuo. The crude amino acid was redissolved in CH_2Cl_2 (10 mL). In a separate flask BocPheOH (1.00 g, 3.77 mmol) was dissolved in CH_2Cl_2 (50 mL), EDC (0.728 g, 3.80 mmol) and HOBt (0.527 g, 3.90 mmol) were added followed by Et_3N (769 mg, 7.60 mmol, 1.05 mL). After 15 min at rt the solution of aspartic acid was added and the resulting mixture was allowed to stir for 15 h before quenched by adding H_2O . The organic phase was washed with 1M HCl, satd aq NaHCO_3 and brine, dried, filtered, and concentrated to provide 1.90 g (90 % yield) of the product as a clear oil. $R_f = 0.53$ (25% EtOAc/hexanes) $[\alpha]_D^{20} +14.4$ (c 0.98, CHCl_3); IR (film) 3317, 2955, 2900, 1734, 1667, 1251, 1221, 1174, 860, 838 cm^{-1} ; ^1H NMR (600 MHz, CDCl_3) δ 7.22 (m, 2H), 7.15 (m, 3H), 6.97 (d, $J = 7.8$ Hz, 1H), 5.06 (d, $J = 7.2$ Hz, 1H), 4.70 (m, 1H), 4.37 (bs, 1H), 4.15 (m, 2H), 4.10 (m, 2H), 2.92 (dd, $J = 6.0, 13.8$ Hz, 1H), 3.00 (bs, 1H), 2.90 (dd, $J = 4.8, 17.4$ Hz, 1H), 2.74 (dd, $J = 4.8, 17.4$ Hz, 1H), 1.34 (s, 9H), 0.93 (m, 4H), -0.02 (s, 18H); ^{13}C NMR (150 MHz, CDCl_3) 170.9, 170.6, 170.2, 155.0, 136.3, 129.2, 128.3, 126.6, 79.7, 63.9, 63.0, 55.2, 48.5, 38.1, 36.1, 28.0, 17.3, 17.2, -1.5, -1.6 ppm; HRMS (EI): Exact mass calcd for $\text{C}_{19}\text{H}_{39}\text{NO}_6\text{Si}_2$ $[\text{M}+\text{Na}]^+$ 603.2898, found 603.2890.



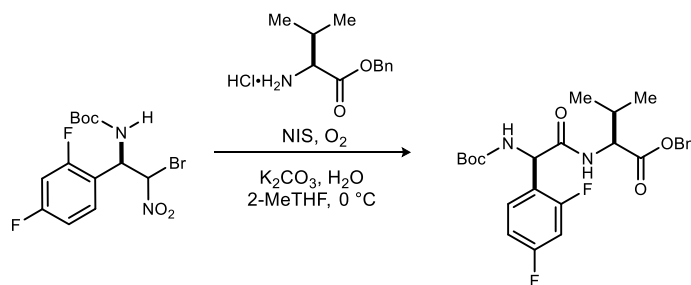
(S)-Bis(2-(trimethylsilyl)ethyl) 2-((S)-2-((S)-2-(4-(benzyloxy)phenyl)-2-((tert-butoxycarbonyl)amino)-acetamido)-3-phenylpropanamido)succinate (364). Boc dipeptide (0.657 g, 1.16 mmol) was treated with 10 mL of 4M HCl in dioxane. The reaction was stirred for 2 h at rt and the solvent was removed in vacuo. The crude hydrochloride salt was redissolved in 2-MeTHF (8.0 mL, 0.14 M). To a solution were added nitroalkane (438 mg, 0.970 mmol), cesium carbonate (1.1 g, 3.395 mmol) and 50 eq of H_2O (48.5 mmol, 0.90 mL). The resulting mixture was cooled to 0 °C. NIS (217 mg, 0.970 mmol) was introduced and the flask was fitted with an oxygen balloon. The reaction mixture was stirred at 0 °C for 2 days. The resulting mixture was diluted with dichloromethane, washed with 1 M HCl, satd aq $\text{Na}_2\text{S}_2\text{O}_3$ and satd aq NaHCO_3 , dried with MgSO_4 and then filtered through Celite. The filtrate was concentrated and purified by column chromatography (SiO_2 , 15-25% EtOAc/hexanes) to provide 440 mg

(55% yield) of the amide as yellow foam. $R_f = 0.18$ (25% EtOAc/hexanes); $[\alpha]_D^{20} +36.5$ (c 1.5, CHCl_3); IR (film) 3285, 3065, 2954, 2900, 1734, 1647, 1510, 1249, 1173 cm^{-1} ; ^1H NMR (400 MHz, CDCl_3) δ 7.44-7.14 (m, 12H), 6.91 (m, 2H), 6.84 (bs, 1H), 6.49 (d, $J = 7.6$ Hz, 1H) 5.55 (bs, 1H), 5.05 (s, 2H), 4.72 (m, 2H) 4.24 (m, 2H), 4.17 (m, 2H), 3.18 (dd, $J = 6.4, 14.0$ Hz, 1H), 3.06 (dd, $J = 6.8, 14.0$ Hz, 1H), 2.90 (dd, $J = 4.4, 16.8$ Hz, 1H), 2.70 (dd, $J = 5.2, 16.8$ Hz, 1H), 1.42 (s, 9H), 1.01 (m, 4H), -0.06 (s, 9H) -0.05 (s, 9H); ^{13}C NMR (100 MHz, CDCl_3) 170.7, 170.2, 170.1, 170.0, 158.8, 155.2, 136.7, 136.0, 129.9, 129.3, 128.6, 128.5, 128.4, 128.0, 127.4, 127.0, 115.3, 80.1, 69.9, 64.2, 63.3, 58.4, 54.1, 48.7, 37.8, 36.2, 28.2, 17.3, 17.2, -1.5, -1.6 ppm; HRMS (EI): Exact mass calcd for $\text{C}_{55}\text{H}_{66}\text{F}_2\text{N}_4\text{O}_{10}\text{Si}_2$ $[\text{M}+\text{Na}]^+$ 842.3844, found 842.3825.



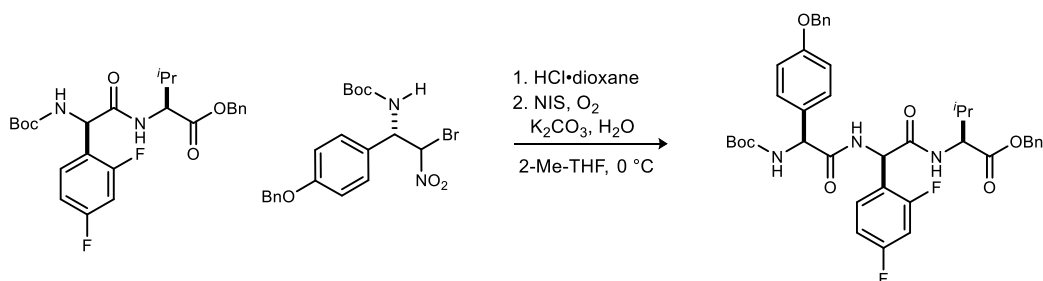
(8*S*,11*S*,14*S*)-11-Benzyl-14-(4-(benzyloxy)phenyl)-2,2-dimethyl-6,10,13-trioxo-8-((2-(trimethylsilyl)ethoxy)carbonyl)-5-oxa-9,12-diaza-2-silatetradecan-14-aminium 2,2,2-trifluoroacetate (TFA-364).

To a Boc amine (65 mg, 79 μmol) was added HCl in dioxane (4M, 3 mL). The resulting mixture was stirred at rt for 1 h and solvent was removed in vacuo. The resulting residue was purified by HPLC (C18, 55-95% $\text{CH}_3\text{CN}/\text{H}_2\text{O}$) to provide 55 mg (85 % yield) of the product as a white foam. $[\alpha]_D^{20} +34.7$ (c 1.24, CHCl_3); IR (film) 3378, 3245, 3067, 2955, 1741, 1652, 1516, 1252, 1182 cm^{-1} ; ^1H NMR (400 MHz, CDCl_3) δ 7.40-7.26 (m, 7H), 7.14 (m, 3H), 7.07 (d, $J = 6.8$ Hz, 2H), 6.91 (d, $J = 8.0$ Hz, 2H), 5.10 (bs, 1H), 4.94 (s, 2H), 4.61 (m, 2H), 4.10 (m, 4H), 3.03 (dd, $J = 6.4, 14.0$ Hz, 1H), 2.95 (dd, $J = 6.4, 14.0$ Hz, 1H), 2.72 (dd, $J = 4.8, 16.8$ Hz, 1H), 2.63 (dd, $J = 4.8, 16.8$ Hz, 1H), 0.94 (m, 4H), 0.01 (s, 9H), 0.00 (s, 9H); ^{13}C NMR (100 MHz, CDCl_3) 170.9, 170.4, 170.2, 168.1, 160.0, 136.4, 135.8, 129.7, 129.3, 128.5, 128.4, 128.0, 127.5, 126.9, 124.0, 115.6, 77.2, 69.9, 64.3, 63.4, 56.6, 55.1, 48.9, 37.4, 36.0, 17.2, 17.1, -1.6, -1.7 ppm; HRMS (EI): Exact mass calcd for $\text{C}_{38}\text{H}_{54}\text{N}_3\text{O}_7\text{Si}_2$ $[\text{M}]^+$ 720.3500, found 720.3492.

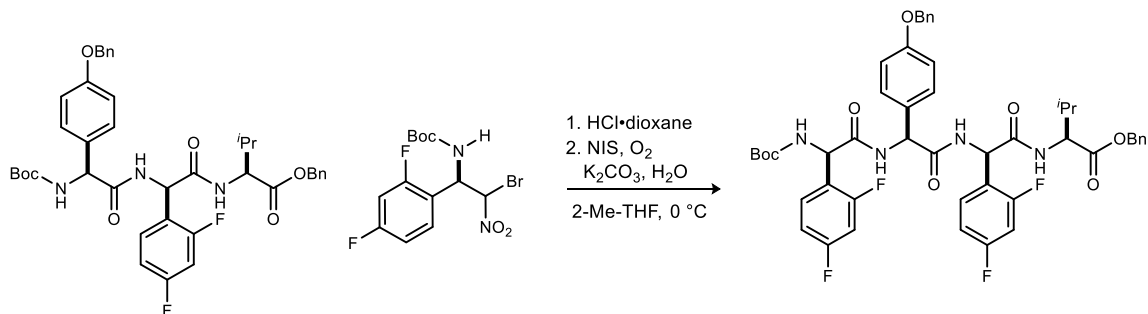


Benzyl ((*R*)-2-((*tert*-butoxycarbonyl)amino)-2-(2,4-difluorophenyl)acetyl)-*L*-valinate (365). To a round bottom flask was added *tert*-butyl ((1*R*)-2-bromo-1-(2,4-difluorophenyl)-2-nitroethyl)carbamate (1.02 g, 2.70 mmol), HCl-Val-OBn (790 mg, 3.24 mmol), H_2O (1.2 mL, 67.5 mmol) and 2-MeTHF (13 mL). The flask was cooled to 0 °C. K_2CO_3 (1.19 g, 8.64 mmol) and NIS (610 mg, 2.70 mmol) were added to the reaction mixture. An O_2 balloon was placed on the reaction and it was allowed to stir for 48 h at 0 °C. The reaction mixture was quenched with 1 M HCl and extracted with CH_2Cl_2 . The organic phase was washed with sat. Na_2SO_3 , dried and concentrated. The resulting solid was purified by flash column chromatography (SiO_2 , 2.5-15% ethyl acetate in hexanes) to provide desired dipeptide as a white foam (980 mg, 76%). $R_f = 0.36$ (20% EtOAc/hexanes); $[\alpha]_D^{20} -36.8$ (c .71, CHCl_3); IR (film) 3327, 2971, 1718, 1679,

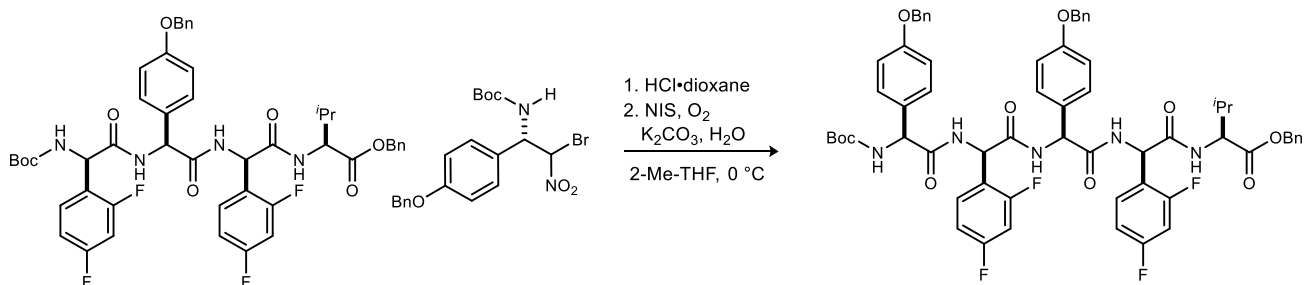
1613 cm^{-1} ; ^1H NMR (400 MHz, CDCl_3) δ 7.38-7.32 (m, 6H), 6.88-6.80 (m, 2H), 6.47 (d, $J = 6.4$ Hz, 1H), 5.84 (d, $J = 4.5$ Hz, 1H), 5.48 (d, $J = 3.8$ Hz, 1H), 5.20 (d, $J = 12.2$ Hz, 1H), 5.13 (d, $J = 12.2$ Hz, 1H), 4.56 (dd, $J = 8.8, 4.6$ Hz, 1H), 2.12 (m, 1H), 1.40 (s, 9H), 0.72 (d, $J = 6.9$ Hz, 3H), 0.70 (d, $J = 6.9$ Hz, 3H); ^{13}C NMR (150 MHz, CDCl_3) ppm 171.3, 169.1, 162.7 (dd, $^1J_{\text{CF}} = 250.2$ Hz, $^3J_{\text{CF}} = 12.0$ Hz), 160.3 (dd, $^1J_{\text{CF}} = 247.6$ Hz, $^3J_{\text{CF}} = 12.0$ Hz), 154.9, 135.2, 129.7, 128.64, 128.55, 128.4, 121.9, 112.0 (d, $^3J_{\text{CF}} = 21.1$ Hz), 104.2 (t, $^2J_{\text{CF}} = 25.4$ Hz), 80.4, 67.2, 57.1, 52.5, 31.3, 28.2, 18.8, 17.1; ^{19}F NMR (376 MHz, CDCl_3) ppm -109.4, -113.6; HRMS (ESI): Exact mass calcd for $\text{C}_{25}\text{H}_{30}\text{F}_2\text{N}_2\text{NaO}_5$ $[\text{M}+\text{Na}]^+$ 499.2020, found 499.2027.



Benzyl ((R)-2-((S)-2-(4-(benzyloxy)phenyl)-2-((tert-butoxycarbonyl)amino)acetamido)-2-(2,4-difluorophenyl)acetyl)-L-valinate (366). To a round bottom flask containing benzyl ((R)-2-((tert-butoxycarbonyl)amino)-2-(2,4-difluorophenyl)acetyl)-L-valinate (980 mg, 2.06 mmol) was added $\text{HCl}\cdot\text{dioxane}$ (5 mL, 4.0 M) and stirred for 1 h. The reaction mixture was concentrated and taken on without further purification. To a round bottom flask containing the amine HCl salt was added *tert*-butyl ((1S)-1-(4-(benzyloxy)phenyl)-2-bromo-2-nitroethyl)carbamate (929 mg, 2.06 mmol), H_2O (1.85 mL, 103 mmol) and 2-MeTHF (10 mL). The flask was cooled to 0 $^\circ\text{C}$. K_2CO_3 (853 mg, 6.18 mmol) and NIS (464 mg, 2.06 mmol) were added to the reaction mixture. An O_2 balloon was placed on the reaction and it was allowed to stir for 48 h at 0 $^\circ\text{C}$. The reaction mixture was quenched with 1 M HCl and extracted with CH_2Cl_2 . The organic phase was washed with sat. Na_2SO_3 , dried and concentrated. The resulting solid was purified by flash column chromatography (SiO_2 , 5-20% ethyl acetate in hexanes) to provide desired tripeptide as an off-white foam (951 mg, 65%). $R_f = 0.16$ (20% EtOAc /hexanes); $[\alpha]_D^{20} +31.5$ (c .33, CHCl_3); IR (film) 3299, 3066, 2967, 1736, 1651, 1612 cm^{-1} ; ^1H NMR (400 MHz, CDCl_3) δ 7.43-7.31 (m, 11H), 7.20 (d, $J = 8.6$ Hz, 2H), 7.12 (d, $J = 5.9$ Hz, 1H), 6.92 (d, $J = 8.7$ Hz, 2H), 6.85 (m, 1H), 6.79 (td, $J = 10.8, 2.4$ Hz, 1H), 6.66 (td, $J = 8.2, 2.0$ Hz, 1H), 6.36 (d, $J = 7.4$ Hz, 1H), 5.69 (d, $J = 6.7$ Hz, 1H), 5.57 (d, $J = 5.1$ Hz, 1H), 5.20 (d, $J = 12.1$ Hz, 1H), 5.14 (d, $J = 12.1$ Hz, 1H), 5.06 (s, 2H), 4.52 (dd, $J = 8.8, 4.6$ Hz, 1H), 2.08 (m, 1H), 1.40 (s, 9H), 0.65 (d, $J = 6.9$ Hz, 6H); ^{13}C NMR (150 MHz, CDCl_3) ppm 171.0, 169.6, 168.3, 162.6 (dd, $^1J_{\text{CF}} = 250.3$ Hz, $^3J_{\text{CF}} = 12.2$ Hz), 160.1 (dd, $^1J_{\text{CF}} = 247.9$ Hz, $^3J_{\text{CF}} = 11.9$ Hz), 158.8, 155.0, 136.7, 135.0, 130.1, 128.9 (d, $^4J_{\text{CF}} = 4.8$ Hz), 128.8 (d, $^4J_{\text{CF}} = 4.6$ Hz), 128.62, 128.59, 128.57, 128.4, 128.0, 127.4, 121.0 (dd, $^2J_{\text{CF}} = 13.4$ Hz, $^4J_{\text{CF}} = 3.3$ Hz), 115.3, 111.0 (d, $^3J_{\text{CF}} = 21.1$ Hz), 104.1 (t, $^2J_{\text{CF}} = 25.7$ Hz), 80.1, 70.0, 67.3, 58.1, 57.2, 50.9, 31.2, 28.2, 18.7, 17.0; ^{19}F NMR (376 MHz, CDCl_3) ppm -109.2, -113.7; HRMS (ESI): Exact mass calcd for $\text{C}_{40}\text{H}_{43}\text{F}_2\text{N}_3\text{NaO}_7$ $[\text{M}+\text{Na}]^+$ 738.2967, found 738.2935.

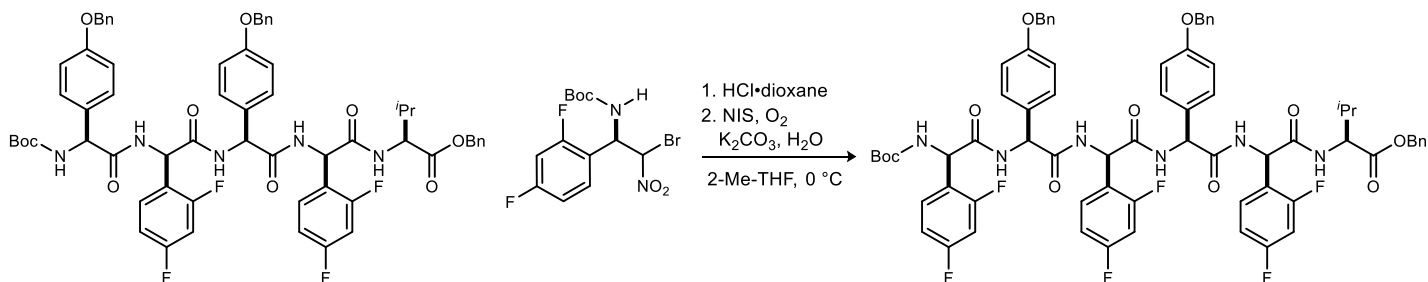


Benzyl ((R)-2-((S)-2-(4-(benzyloxy)phenyl)-2-((R)-2-((tert-butoxycarbonyl)amino)-2-(2,4-difluorophenyl)acetamido)acetamido)-2-(2,4-difluorophenyl)acetyl)-L-valinate (367). To a round bottom flask containing benzyl ((R)-2-((S)-2-(4-(benzyloxy)phenyl)-2-((tert-butoxycarbonyl)amino)acetamido)-2-(2,4-difluorophenyl)acetyl)-L-valinate (951 mg, 1.33 mmol) was added HCl·dioxane (5 mL, 4.0 M) and stirred for 1 h. The reaction mixture was concentrated and taken on without further purification. To a round bottom flask containing the amine HCl salt was added *tert*-butyl ((1*R*)-2-bromo-1-(2,4-difluorophenyl)-2-nitroethyl)carbamate (495 mg, 1.33 mmol), H₂O (1.2 mL, 66.5 mmol) and 2-MeTHF (6.5 mL). The flask was cooled to 0 °C. K₂CO₃ (551 mg, 3.99 mmol) and NIS (299 mg, 1.33 mmol) were added to the reaction mixture. An O₂ balloon was placed on the reaction and it was allowed to stir for 48 h at 0 °C. The reaction mixture was quenched with 1 M HCl and extracted with CH₂Cl₂. The organic phase was washed with sat. Na₂SO₃, dried and concentrated. The resulting solid was purified by flash column chromatography (SiO₂, 10-30% ethyl acetate in hexanes) to provide desired tetrapeptide as an off-white solid (612 mg, 52%). *R*_f = 0.48 (40% EtOAc/hexanes); [*α*]_D²⁰ +10.5 (*c* .40, CHCl₃); IR (film) 3301, 2968, 1734, 1643 cm⁻¹; ¹H NMR (400 MHz, CDCl₃) δ 7.43-7.26 (m, 12H), 7.17 (m, 1H), 7.05 (d, *J* = 8.2 Hz, 2H), 6.81 (d, *J* = 8.7 Hz, 2H), 6.79-6.75 (m, 4H), 6.62 (m, 1H), 6.54 (m, 1H), 6.15 (s, 1H), 5.71 (d, *J* = 6.9 Hz, 1H), 5.55 (m, 2H), 5.26 (d, *J* = 12.1 Hz, 1H), 5.15 (d, *J* = 12.1 Hz, 1H), 5.04 (s, 2H), 4.60 (dd, *J* = 8.9, 4.3 Hz, 1H), 2.12 (m, 1H), 1.38 (s, 9H), 0.67 (d, *J* = 6.6 Hz, 6H); ¹³C NMR (125 MHz, CDCl₃) ppm 171.5, 168.9, 168.3, 162.6 (dd, ¹*J*_{CF} = 250.3 Hz, ³*J*_{CF} = 12.1 Hz), 160.38 (dd, ¹*J*_{CF} = 247.0 Hz, ³*J*_{CF} = 16.3 Hz), 160.37 (dd, ¹*J*_{CF} = 250.5 Hz, ³*J*_{CF} = 16.3 Hz), 160.0 (dd, ¹*J*_{CF} = 248.0 Hz, ³*J*_{CF} = 12.0 Hz), 158.8, 155.2 (d, ⁴*J*_{CF} = 3.8 Hz), 155.2 (d, ⁴*J*_{CF} = 4.1 Hz), 136.7, 135.1, 129.9 (d, ⁴*J*_{CF} = 7.1 Hz), 129.8 (d, ⁴*J*_{CF} = 6.7 Hz), 129.0, 128.62, 128.61, 128.57, 128.5, 128.3, 128.1, 127.4, 121.5 (dd, ²*J*_{CF} = 10.8 Hz, ⁴*J*_{CF} = 3.6 Hz), 121.0 (dd, ²*J*_{CF} = 11.8 Hz, ⁴*J*_{CF} = 3.1 Hz), 115.2, 111.8 (d, ³*J*_{CF} = 21.1 Hz), 111.6 (d, ³*J*_{CF} = 22.9 Hz), 104.0 (t, ²*J*_{CF} = 26.2 Hz), 103.9 (t, ²*J*_{CF} = 25.9 Hz), 80.3, 69.9, 67.4, 57.1, 56.5, 52.3, 50.7, 31.4, 28.2, 18.8, 16.8; ¹⁹F NMR (376 MHz, CDCl₃) ppm -109.4, -110.0 -113.0, -113.8; HRMS (ESI): Exact mass calcd for C₄₈H₄₈F₄N₄NaO₈ [M+Na]⁺ 907.3306, found 907.3319.



Benzyl ((R)-2-((S)-2-(4-(benzyloxy)phenyl)-2-((R)-2-((S)-2-(4-(benzyloxy)phenyl)-2-((tert-butoxycarbonyl)amino)acetyl)-L-valinate)-2-(2,4-difluorophenyl)acetamido)acetamido)-2-(2,4-

difluorophenyl)acetyl)-L-valinate (368). To a round bottom flask containing benzyl ((R)-2-((S)-2-(4-(benzyloxy)phenyl)-2-((R)-2-((tert-butoxycarbonyl)amino)-2-(2,4-difluorophenyl)acetamido)acetamido)-2-(2,4-difluorophenyl)acetyl)-L-valinate (612 mg, 0.69 mmol) was added HCl·dioxane (4 mL, 4.0 M) and stirred for 1 h. The reaction mixture was concentrated and taken on without further purification. To a round bottom flask containing the amine HCl salt was added *tert*-butyl ((1*S*)-1-(4-(benzyloxy)phenyl)-2-bromo-2-nitroethyl)carbamate (312 mg, 0.69 mmol), H₂O (1.2 mL, 69.0 mmol) and 2-MeTHF (5.5 mL). The flask was cooled to 0 °C. K₂CO₃ (286 mg, 2.07 mmol) and NIS (155 mg, 0.69 mmol) were added to the reaction mixture. An O₂ balloon was placed on the reaction and it was allowed to stir for 48 h at 0 °C. The reaction mixture was quenched with 1 M HCl and extracted with CH₂Cl₂. The organic phase was washed with sat. Na₂SO₃, dried and concentrated. The resulting solid was purified by flash column chromatography (SiO₂, 20-40% ethyl acetate in hexanes) to provide desired pentapeptide as an off-white solid (349 mg, 45%). *R*_f = 0.43 (40% EtOAc/hexanes); $[\alpha]_D^{20} +48.5$ (*c* .39, CHCl₃); IR (film) 3285, 3067, 2969, 1710, 1641 cm⁻¹; ¹H NMR (400 MHz, CDCl₃) δ 8.45 (br s, 1H), 8.30 (br s, 1H), 8.12 (br s, 1H), 7.63 (br s, 1H), 7.45-7.32 (m, 16H), 7.01 (d, *J* = 8.0 Hz, 2H), 6.85 (d, *J* = 8.4 Hz, 4H), 6.73 (td, *J* = 9.7, 2.2 Hz, 1H), 6.64 (d, *J* = 8.0 Hz, 2H), 6.58 (d, *J* = 8.0 Hz, 2H), 6.49 (td, *J* = 8.1, 1.8 Hz, 1H), 6.36 (m, 2H), 5.94 (d, *J* = 6.1 Hz, 2H), 5.80 (s, 2H), 5.47 (d, *J* = 11.8 Hz, 1H), 5.19 (d, *J* = 12.0 Hz, 1H), 5.06 (s, 2H), 5.00 (d, *J* = 2.5 Hz, 2H), 4.75 (dd, *J* = 8.0, 3.6 Hz, 1H), 2.06 (m, 1H), 1.43 (s, 9H), 0.65 (d, *J* = 6.9 Hz, 3H), 0.58 (d, *J* = 6.8 Hz, 3H); ¹³C NMR (150 MHz, CDCl₃) ppm 173.1, 170.2, 169.6, 168.6, 162.4 (dd, ¹*J*_{CF} = 248.1 Hz, ³*J*_{CF} = 10.8 Hz), 162.3 (dd, ¹*J*_{CF} = 249.6 Hz, ³*J*_{CF} = 12.3 Hz), 162.2 (dd, ¹*J*_{CF} = 246.6 Hz, ³*J*_{CF} = 11.1 Hz), 160.2 (dd, ¹*J*_{CF} = 249.0 Hz, ³*J*_{CF} = 11.7 Hz), 158.8, 158.2, 155.9, 136.9, 136.8, 135.4, 131.2, 128.83, 128.77, 128.74, 128.72, 128.64, 128.61, 128.56, 128.5, 128.3, 128.2, 128.1, 128.0, 127.5, 127.4, 127.3, 122.1 (d, ²*J*_{CF} = 14.3 Hz), 121.4 (d, ²*J*_{CF} = 15.5 Hz), 115.0, 114.7, 111.0(2) (d, ³*J*_{CF} = 18.7 Hz), 103.8 (t, ²*J*_{CF} = 25.6 Hz), 103.5 (t, ²*J*_{CF} = 25.8 Hz), 80.2, 70.0, 69.7, 67.7, 56.9, 56.7, 56.1, 51.4, 50.2, 32.1, 28.5, 18.4, 17.0; ¹⁹F NMR (376 MHz, CDCl₃) ppm -109.4, -110.0 -113.0, -113.8; HRMS (ESI): Exact mass calcd for C₆₃H₆₁F₄N₅NaO₁₀ [M+Na]⁺ 1146.4252, found 1146.4271.



Benzyl ((R)-2-((S)-2-(4-(benzyloxy)phenyl)-2-((R)-2-((S)-2-(4-(benzyloxy)phenyl)-2-((R)-2-((tert-butoxycarbonyl)amino)-2-(2,4-difluorophenyl)acetamido)acetamido)-2-(2,4-

difluorophenyl)acetamido)acetamido)-2-(2,4-difluorophenyl)acetyl)-L-valinate (369). To a round bottom flask containing Benzyl ((R)-2-((S)-2-(4-(benzyloxy)phenyl)-2-((R)-2-((S)-2-(4-(benzyloxy)phenyl)-2-((tert-butoxycarbonyl)amino)acetamido)-2-(2,4-

difluorophenyl)acetamido)acetamido)-2-(2,4-difluorophenyl)acetyl)-L-valinate (349 mg, 0.31 mmol) was

added HCl·dioxane (3 mL, 4.0 M) and stirred for 1 h. The reaction mixture was concentrated and taken on

without further purification. To a round bottom flask containing the amine HCl salt was added tert-butyl

((1R)-2-bromo-1-(2,4-difluorophenyl)-2-nitroethyl)carbamate (118 mg, 0.31 mmol), H₂O (0.56 mL, 31.0

mmol) and 2-MeTHF (2 mL). The flask was cooled to 0 °C. K₂CO₃ (128 mg, 0.93 mmol) and NIS (70.0

mg, 0.31 mmol) were added to the reaction mixture. An O₂ balloon was placed on the reaction and it was

allowed to stir for 48 h at 0 °C. The reaction mixture was quenched with 1 M HCl and extracted with

CH₂Cl₂. The organic phase was washed with sat. Na₂SO₃, dried and concentrated. The resulting solid was

purified by flash column chromatography (SiO₂, 20-40% ethyl acetate in hexanes) to provide desired

hexapeptide as an off-white solid (152 mg, 38%). R_f = 0.57 (40% EtOAc/hexanes); [α]_D²⁰ +97.6 (c .59,

CHCl₃); IR (film) 3283, 2966, 1638 cm⁻¹; ¹H NMR (400 MHz, CDCl₃) δ 8.80 (br s, 1H), 8.48 (br s, 1H),

8.34 (br s, 1H), 7.66 (br s, 1H), 7.52-7.30 (m, 20H), 6.92 (d, J = 8.4 Hz, 2H), 6.84 (td, J = 9.6, 2.4 Hz, 1H),

6.79-6.64 (m, 6H), 6.55-6.45 (m, 3H), 6.50 (d, J = 8.3 Hz, 2H), 6.36 (td, J = 8.1, 1.7 Hz, 1H), 6.27 (d, J =

8.5 Hz, 1H), 6.10 (d, J = 8.2 Hz, 1H), 5.95 (d, J = 6.6 Hz, 1H), 5.81 (d, J = 9.3 Hz, 1H), 5.63 (d, J = 11.8

Hz, 1H), 5.24 (d, J = 11.8 Hz, 1H), 5.10 (s, 2H), 4.99 (d, J = 1.8 Hz, 2H), 4.75 (d, J = 6.6 Hz, 1H), 2.13 (m,

1H), 1.38 (s, 9H), 0.65 (d, J = 6.8 Hz, 3H), 0.62 (d, J = 6.7 Hz, 3H); ¹³C NMR (150 MHz, CDCl₃) ppm

172.8, 170.8, 170.5, 170.3, 169.9, 169.6, 162.4 (dd, ¹J_{CF} = 249.2 Hz, ³J_{CF} = 11.3 Hz), 162.3 (dd, ¹J_{CF} = 249.6

Hz, ³J_{CF} = 11.1 Hz), 162.2 (dd, ¹J_{CF} = 248.2 Hz, ³J_{CF} = 11.3 Hz), 160.8 (dd, ¹J_{CF} = 245.4 Hz, ³J_{CF} = 11.8

Hz), 159.99 (dd, ¹J_{CF} = 249.4 Hz, ³J_{CF} = 12.1 Hz), 159.95 (dd, ¹J_{CF} = 249.7 Hz, ³J_{CF} = 13.0 Hz), 158.6,

158.2, 155.8, 136.9, 136.8, 135.2, 130.1, 129.7 (d, ⁴J_{CF} = 6.7 Hz), 129.6 (d, ⁴J_{CF} = 4.4 Hz), 129.0, 128.62(2),

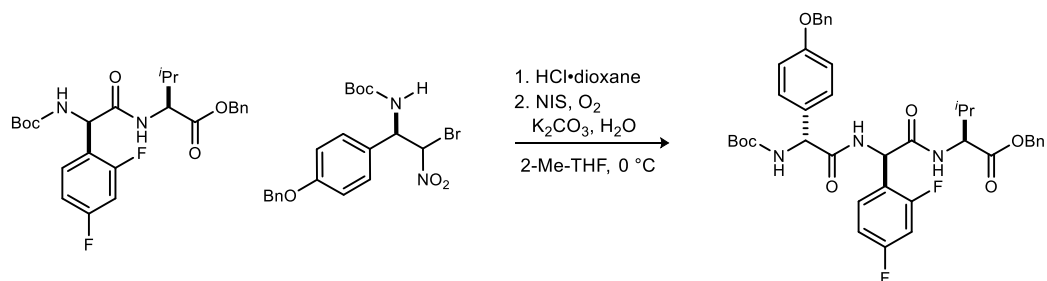
128.57(2), 128.4, 128.1, 127.9, 127.4(2), 127.2(2), 127.0, 121.8(2) (d, ²J_{CF} = 14.1 Hz), 121.3 (d, ²J_{CF} = 16.0

Hz), 114.8, 114.6, 111.0 (d, ³J_{CF} = 18.8 Hz), 110.9 (d, ³J_{CF} = 20.0 Hz), 110.6 (d, ³J_{CF} = 20.9 Hz), 103.9 (t,

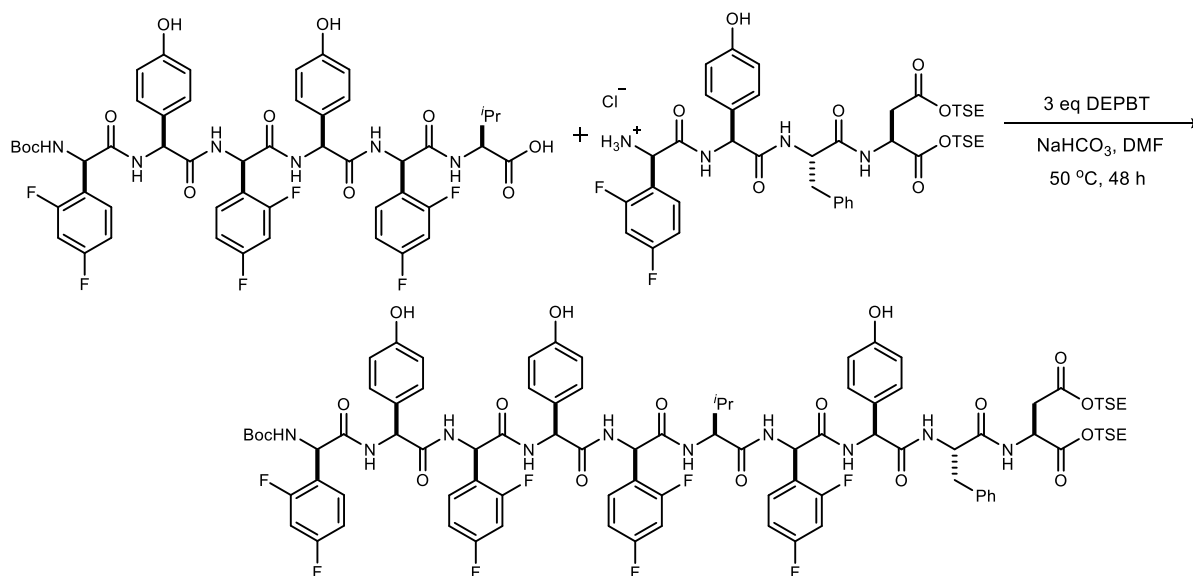
²J_{CF} = 25.4 Hz), 103.1 (t, ²J_{CF} = 24.3 Hz), 103.0 (t, ²J_{CF} = 25.1 Hz), 80.2, 69.8, 69.6, 68.2, 57.0, 56.5, 54.3,

51.8, 51.0, 49.4, 32.8, 28.2, 18.8, 16.3; ¹⁹F NMR (376 MHz, CDCl₃) ppm -110.2, -111.4, -111.7, -111.9, -

112.6, -113.4; HRMS (ESI): Exact mass calcd for C₇₁H₆₆F₆N₆NaO₁₁ [M+Na]⁺ 1315.4591, found 1315.4618.



Benzyl ((R)-2-((R)-2-(4-(benzyloxy)phenyl)-2-((tert-butoxycarbonyl)amino)acetamido)-2-(2,4-difluorophenyl)acetyl)-L-valinate (370). To a round bottom flask containing benzyl ((R)-2-((tert-butoxycarbonyl)amino)-2-(2,4-difluorophenyl)acetyl)-L-valinate (980 mg, 2.06 mmol) was added HCl·dioxane (5 mL, 4.0 M) and stirred for 1 h. The reaction mixture was concentrated and taken on without further purification. To a round bottom flask containing the amine HCl salt was added *tert*-butyl ((1*R*)-1-(4-(benzyloxy)phenyl)-2-bromo-2-nitroethyl)carbamate (929 mg, 2.06 mmol), H₂O (1.85 mL, 103 mmol) and 2-MeTHF (10 mL). The flask was cooled to 0 °C. K₂CO₃ (853 mg, 6.18 mmol) and NIS (464 mg, 2.06 mmol) were added to the reaction mixture. An O₂ balloon was placed on the reaction and it was allowed to stir for 48 h at 0 °C. The reaction mixture was quenched with 1 M HCl and extracted with CH₂Cl₂. The organic phase was washed with sat. Na₂SO₃, dried and concentrated. The resulting solid was purified by flash column chromatography (SiO₂, 5-20% ethyl acetate in hexanes) to provide desired tripeptide as an off-white solid (633 mg, 43%). *R*_f = 0.57 (40% EtOAc/hexanes); $[\alpha]_D^{20}$ -74 (*c* .90, CHCl₃); IR (film) 3308, 2968, 1736, 1652, 1612 cm⁻¹; ¹H NMR (400 MHz, CDCl₃) δ 7.42-7.27 (m, 13H), 7.09 (d, *J* = 5.9 Hz, 1H), 6.94 (d, *J* = 8.7 Hz, 1H), 6.85 (m, 2H), 6.32 (br s, 1H), 5.58 (d, *J* = 6.1 Hz, 1H), 5.53 (br s, 1H), 5.17 (d, *J* = 12.2 Hz, 1H), 5.11 (d, *J* = 12.2 Hz, 1H), 5.03 (s, 2H), 4.51 (dd, *J* = 8.7, 4.7 Hz, 1H), 2.10 (m, 1H), 1.40 (s, 9H), 0.69 (d, *J* = 6.8 Hz, 3H), 0.66 (d, *J* = 6.8 Hz, 3H); ¹³C NMR (125 MHz, CDCl₃) ppm 171.1, 169.8, 168.3, 162.9 (dd, ¹*J*_{CF} = 250.7 Hz, ³*J*_{CF} = 12.0 Hz), 160.3 (dd, ¹*J*_{CF} = 248.9 Hz, ³*J*_{CF} = 12.1 Hz), 159.0, 155.2, 136.7, 135.0, 129.94 (d, ⁴*J*_{CF} = 4.5 Hz), 129.87 (d, ⁴*J*_{CF} = 5.1 Hz), 128.61, 128.59, 128.53, 128.46, 128.4, 128.0, 127.5, 121.1 (dd, ²*J*_{CF} = 12.5 Hz, ⁴*J*_{CF} = 2.5 Hz), 115.4, 112.1 (d, ²*J*_{CF} = 18.6 Hz), 104.3 (t, ²*J*_{CF} = 25.5 Hz), 80.3, 70.0, 67.2, 58.4, 57.3, 51.6, 31.2, 28.2, 18.7, 17.1; ¹⁹F NMR (376 MHz, CDCl₃) ppm -108.9, -113.3; HRMS (ESI): Exact mass calcd for C₄₀H₄₃F₂N₃NaO₇ [M+Na]⁺ 738.2967, found 738.2955.



Bis(2-(trimethylsilyl)ethyl) ((S)-2-((R)-2-((S)-2-((R)-2-((S)-2-((R)-2-((S)-2-((R)-2-((tert-butoxycarbonyl)-amino)-2-(2,4-difluorophenyl)acetamido)-2-(4-hydroxyphenyl)acetamido)-2-(2,4-difluorophenyl)acetamido)-2-(4-hydroxyphenyl)acetamido)-2-(2,4-difluorophenyl)acetamido)-3-methylbutanamido)-2-(2,4-difluorophenyl)acetamido)-2-(4-hydroxyphenyl)acetyl)-L-phenylalanyl-L-aspartate (371).

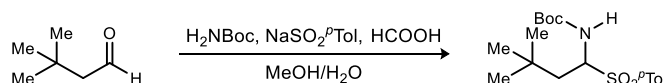
To a solution of hexapeptide (40 mg, 39 μ mol) in DMF (1.0 mL) was added sodium bicarbonate (4.0 equiv; 13.0 mg, 156 μ mol) and DEPBT (3.0 equiv; 35 mg, 117 μ mol). The resulting mixture was stirred at rt for 3 h. Precipitate formation was observed. Then tetrapeptide (1.2 equiv, 39 mg, 47 μ mol) was added, reaction mixture was heated to 50-55 °C and stirred for 48 h. The resulting solution was cooled to rt and solvent was removed in vacuo. Then the resulting crude mixture was redissolved in MeCN and purified by HPLC (C18, 55-95% CH₃CN/H₂O) to provide 12 mg (17 % yield) of the product as a white solid. 29 mg of deprotected amine (the product without Boc group) was also isolated in 44% yield.

Boc protected decapeptide: $[\alpha]_D^{20} +4.2$ (*c* 1.1, MeOH); IR (film) 3293, 1718, 1505, 1273, 1250 cm⁻¹; ¹H NMR (600 MHz, DMSO) δ : 9.37 (m, 3H, PhOH), 8.94 (m, 2H), 8.74 (d, *J* = 6.1 Hz, 1H), 8.70 (d, *J* = 8.0 Hz, 1H), 8.54 (d, *J* = 8.9 Hz, 1H), 8.44 (m, *J* = 7.4 Hz, 2H), 8.41 (d, *J* = 7.9 Hz, 1H), 8.35 (m, 1H), 8.27 (d, *J* = 7.8 Hz, 1H), 7.38-6.82 (m, 23H), 6.65-6.56 (m, 6H), 5.82 (m, 2H), 5.75 (d, *J* = 7.4 Hz, 1H), 5.56 (d, *J* = 7.4 Hz, 1H), 5.47 (d, *J* = 7.2 Hz, 2H), 5.34 (d, *J* = 7.4 Hz, 1H), 4.59-4.49 (m, 2H), 4.32 (m, 1H), 4.08 (m, 4H), 3.02 (m, 1H), 2.87-2.60 (m, 3H), 1.85 (m, 1H), 1.36 (s, 9H), 0.90 (m, 4H), 0.59 (m, 6H), 0.01 (m, 18H). ¹³C NMR (150 MHz, DMSO) Presence of multiple fluorine atoms and also behavior associated with multiple conformations was observed by ¹³C NMR resulting in multiple overlaps of the signals and preventing an accurate assignment and listing of the peaks. Please see the ¹³C NMR image provided in Supporting Information II; ¹⁹F NMR (376 MHz, DMSO) ppm -110.7 (d, *J* = 7.4 Hz), -110.8 (d, *J* = 7.3 Hz), -110.8 (d, *J* = 4.6 Hz), -111.1 (d, *J* = 8.2 Hz), -111.4 (d, *J* = 7.4 Hz), -111.6 (d, *J* = 5.9 Hz), -112.0 (d, *J* = 6.4 Hz), -112.3 (d, *J* = 5.3 Hz); HRMS (ED): Exact mass calcd for C₈₉H₉₈F₈N₁₀O₁₈Si₂Na [M+Na]⁺ 1826.6398, found 1826.6407.

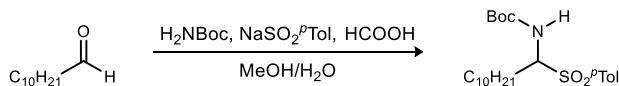
Free amine decapeptide: $[\alpha]_D^{20} +10.6$ (*c* 1.0, MeOH); IR (film) 3294, 1641, 1504 cm⁻¹; ¹H NMR (600 MHz, DMSO) δ : 9.39 (m, 3H), 9.24 (d, *J* = 7.8 Hz, 1H), 9.03 (d, *J* = 8.0 Hz, 1H), 8.84 (d, *J* = 7.4 Hz, 1H), 8.73 (d, *J* = 7.6 Hz, 1H), 8.69 (d, *J* = 7.9 Hz, 1H), 8.63 (m, 3H), 8.52 (d, *J* = 7.6 Hz, 1H), 8.43 (d, *J* = 7.9 Hz, 1H), 8.38 (d, *J* = 8.1 Hz, 1H), 8.18 (d, *J* = 8.8 Hz, 1H), 7.34-7.29 (m, 3H) 7.24-7.10 (m, 11H), 7.05-6.86 (m, 9H), 6.62-6.55 (m, 6H), 5.83 (m, 2H), 5.74 (d, *J* = 6.8 Hz, 1H), 5.65 (d, *J* = 7.9 Hz, 1H), 5.53 (d, *J* =

7.7 Hz, 1H), 5.33 (d, $J = 7.6$ Hz, 1H), 5.26 (d, $J = 4.7$ Hz, 1H), 4.57-4.53 (m, 2H), 4.31 (m, 1H), 4.09 (m, 4H), 3.03 (dd, $J = 5.0, 13.8$ Hz, 1H), 2.83 (dd, $J = 8.7, 13.8$ Hz, 1H), 2.65 (dd, $J = 6.9, 16.5$ Hz, 1H), 2.55 (dd, $J = 6.1, 16.5$ Hz, 1H), 1.88 (m, 1H), 0.93-0.84 (m, 4H), 0.61 (d, $J = 6.7$ Hz, 6H), 0.00 (m, 18H). ^{13}C NMR (150 MHz, DMSO) Presence of multiple fluorine atoms and also behavior associated with multiple conformations was observed by ^{13}C NMR resulting in multiple overlaps of the signals and preventing an accurate assignment and listing of the peaks. Please see the ^{13}C NMR image provided in Supporting Information II; ^{19}F NMR (376 MHz, DMSO) ppm -107.6 (d, $J = 8.5$ Hz), -109.3 (d, $J = 8.7$ Hz), -110.6 (d, $J = 7.6$ Hz), -110.7 (d, $J = 7.7$ Hz), -110.8 (d, $J = 7.4$ Hz), -111.4 (d, $J = 7.5$ Hz), -111.5 (d, $J = 7.3$ Hz), -111.9 (d, $J = 7.2$ Hz); HRMS (EI): Exact mass calcd for $\text{C}_{84}\text{H}_{91}\text{F}_8\text{N}_{10}\text{O}_{16}\text{Si}_2\text{Na}^+$ $[\text{M}+\text{Na}]^+$ 1726.5918, found 1726.5751.

General procedure for preparation of *N*-Boc α -amidosulfones: According to literature procedure,⁶⁸ to a round bottomed flask equipped with a stir bar was added *tert*-butyl carbamate (1 equiv.), *p*-toluenesulfinic acid sodium salt (2 equiv.), MeOH and water. The corresponding aldehyde (1.5 equiv.) was then added, followed by formic acid (2 equiv.). The mixture was stirred for 96 h at room temperature. The resulting precipitate was filtered and washed with water and hexanes to afford the desired α -amidosulfone without further purification.

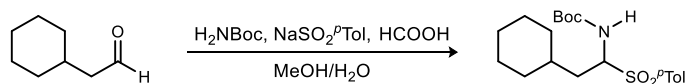


***tert*-Butyl (3,3-dimethyl-1-tosylbutyl)carbamate (S1).** Prepared according to the general procedure using *tert*-butyl carbamate (1.17 g, 10.0 mmol), *p*-toluenesulfinic acid sodium salt (3.90 g, 20.0 mmol), 3,3-dimethylbutanal (1.89 mL, 15.0 mmol), formic acid (0.8 mL, 20.0 mmol), MeOH (10 mL) and H_2O (20 mL). Filtration yielded the α -amidosulfone as a white solid (3.35 g, 94%). $R_f = 0.28$ (20% EtOAc/hexanes); IR (film) 3430, 2959, 1706, 1520 cm^{-1} ; ^1H NMR (400 MHz, CDCl_3) δ 7.79 (d, $J = 8.2$ Hz, 2H), 7.32 (d, $J = 8.0$ Hz, 2H), 4.93-4.83 (m, 2H), 2.41 (s, 3H), 2.24 (dd, $J = 14.5, 1.1$ Hz, 1H), 1.57-1.48 (m, 1H), 1.20 (s, 9H), 0.97 (s, 9H); ^{13}C NMR (100 MHz, CDCl_3) ppm 153.3, 144.8, 133.5, 129.6, 129.5, 80.6, 68.9, 39.3, 30.6, 29.4, 27.9, 21.6; HRMS (ESI): Exact mass calcd for $\text{C}_{18}\text{H}_{29}\text{NNaO}_4\text{S}$ $[\text{M}+\text{Na}]^+$ 378.1715, found 378.1698.

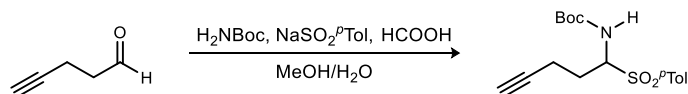


***tert*-Butyl (1-tosylundecyl)carbamate (S2).** Prepared according to the general procedure using *tert*-butyl carbamate (1.17 g, 10.0 mmol), *p*-toluenesulfinic acid sodium salt (3.90 g, 20.0 mmol), undecanal (3.09 mL, 15.0 mmol), formic acid (0.8 mL, 20.0 mmol), MeOH (10 mL) and H_2O (20 mL). Filtration yielded the α -amidosulfone as a white solid (2.84 g, 66%). $R_f = 0.36$ (20% EtOAc/hexanes); IR (film) 3429, 2926, 2855, 1706, 1645 cm^{-1} ; ^1H NMR (400 MHz, CDCl_3) δ 7.78 (d, $J = 8.2$ Hz, 2H), 7.32 (d, $J = 8.1$ Hz, 2H), 4.93 (d, $J = 10.9$ Hz, 1H), 4.79 (td, $J = 10.8, 3.3$ Hz, 1H), 2.41 (s, 3H), 2.26-2.19 (m, 1H), 1.61 (s, 5H), 1.25 (s, 12H), 1.22 (s, 9H), 0.88 (t, $J = 6.9$ Hz, 3H); ^{13}C NMR (100 MHz, CDCl_3) ppm 153.8, 144.8, 133.9,

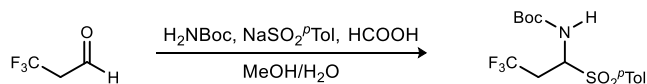
129.6, 129.3, 80.6, 70.8, 31.8, 29.5, 29.4, 29.3, 29.0, 27.9, 27.6, 26.4, 25.3, 22.6, 21.6, 14.1; HRMS (ESI): Exact mass calcd for C₂₃H₃₉NNaO₄S [M+Na]⁺ 448.2498, found 448.2495.



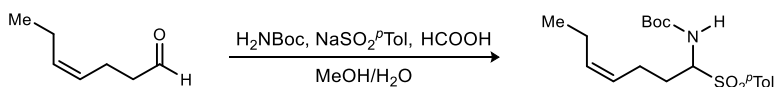
tert-Butyl (2-cyclohexyl-1-tosylethyl)carbamate (S3). Prepared according to the general procedure using *tert*-butyl carbamate (1.17 g, 10.0 mmol), *p*-toluenesulfonic acid sodium salt (3.90 g, 20.0 mmol), 2-cyclohexylacetaldehyde (1.89 g, 15.0 mmol), formic acid (0.8 mL, 20.0 mmol), MeOH (10 mL) and H₂O (20 mL). Filtration yielded the α -amidosulfone as a white solid (2.08 g, 55%). *R_f* = 0.28 (20% EtOAc/hexanes); IR (film) 3425, 2926, 1705, 1646 cm⁻¹; ¹H NMR (400 MHz, CDCl₃) δ 7.78 (d, *J* = 8.2 Hz, 2H), 7.32 (d, *J* = 8.0 Hz, 2H), 4.91-4.89 (m, 2H), 2.41 (s, 3H), 2.09-2.02 (m, 1H), 1.75-1.65 (m, 8H), 1.45-1.37 (m, 2H), 1.22 (s, 9H), 1.10-0.86 (m, 2H); ¹³C NMR (100 MHz, CDCl₃) ppm 153.7, 144.7, 133.9, 129.6, 129.3, 80.6, 69.0, 33.9, 33.8, 33.3, 31.7, 27.9, 26.2, 26.1, 25.8, 21.6; HRMS (ESI): Exact mass calcd for C₂₀H₃₁NNaO₄S [M+Na]⁺ 404.1872, found 404.1868.



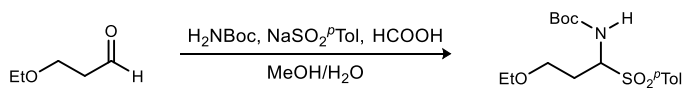
tert-Butyl (1-tosylpent-4-yn-1-yl)carbamate (S4). Prepared according to the general procedure using *tert*-butyl carbamate (1.17 g, 10.0 mmol), *p*-toluenesulfonic acid sodium salt (3.90 g, 20.0 mmol), pent-4-ynal (1.23 g, 15.0 mmol), formic acid (0.8 mL, 20.0 mmol), MeOH (10 mL) and H₂O (20 mL). Filtration yielded the α -amidosulfone as a white solid (2.11 g, 62%). *R_f* = 0.16 (20% EtOAc/hexanes); IR (film) 3426, 2954, 1703, 1643, 1518 cm⁻¹; ¹H NMR (400 MHz, CDCl₃) δ 7.79 (d, *J* = 8.2 Hz, 2H), 7.33 (d, *J* = 8.0 Hz, 2H), 4.99-4.96 (m, 2H), 2.52-2.36 (m, 3H), 2.41 (s, 3H), 2.01 (t, *J* = 2.4 Hz, 1H), 1.98-1.92 (m, 1H), 1.23 (s, 9H); ¹³C NMR (100 MHz, CDCl₃) ppm 153.6, 145.0, 133.7, 129.7, 129.3, 81.6, 80.8, 70.0, 69.8, 27.9, 25.9, 21.6, 15.0; HRMS (ESI): Exact mass calcd for C₁₇H₂₃NNaO₄S [M+Na]⁺ 360.1245, found 360.1232.



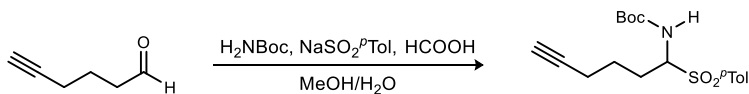
tert-Butyl (3,3,3-trifluoro-1-tosylpropyl)carbamate (S5). Prepared according to the general procedure using *tert*-butyl carbamate (784 mg, 6.7 mmol), *p*-toluenesulfonic acid sodium salt (2.61 g, 13.4 mmol), 3,3,3-trifluoroacetaldehyde (0.86 mL, 10.0 mmol), formic acid (0.5 mL, 13.4 mmol), MeOH (7 mL) and H₂O (14 mL). Filtration yielded the α -amidosulfone as a white solid (503 mg, 20%). *R_f* = 0.24 (20% EtOAc/hexanes); IR (film) 3390, 2934, 1701, 1526 cm⁻¹; ¹H NMR (400 MHz, CDCl₃) δ 7.80 (d, *J* = 8.2 Hz, 2H), 7.36 (d, *J* = 8.1 Hz, 2H), 5.19 (td, *J* = 11.1, 2.1 Hz, 1H), 5.07 (d, *J* = 10.8 Hz, 1H), 3.16-3.04 (m, 1H), 2.59-2.50 (m, 1H), 2.43 (s, 3H), 1.23 (s, 9H); ¹³C NMR (100 MHz, CDCl₃) ppm 153.1, 145.8, 132.2, 129.9, 129.6, 125.2 (¹*J_{CF}* = 274.7 Hz), 81.4, 65.5, 30.3 (²*J_{CF}* = 30.3 Hz), 27.9, 21.7; HRMS (ESI): Exact mass calcd for C₁₅H₂₀F₃NNaO₄S [M+Na]⁺ 390.0963, found 390.0958.



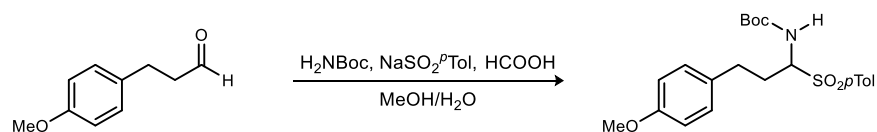
(Z)-tert-Butyl (1-tosylhept-4-en-1-yl)carbamate (S6). Prepared according to the general procedure using *tert*-butyl carbamate (1.17 g, 10.0 mmol), *p*-toluenesulfinic acid sodium salt (3.90 g, 20.0 mmol), (*Z*)-hept-4-enal (1.98 mL, 15.0 mmol), formic acid (0.8 mL, 20.0 mmol), MeOH (10 mL) and H₂O (20 mL). Filtration yielded the α -amidosulfone as a white solid (3.21 g, 87%). $R_f = 0.24$ (20% EtOAc/hexanes); IR (film) 3358, 2970, 1706, 1517 cm^{-1} ; ¹H NMR (400 MHz, CDCl₃) δ 7.78 (d, $J = 8.2$ Hz, 2H), 7.32 (d, $J = 8.0$ Hz, 2H), 5.48-5.41 (m, 1H), 5.30-5.24 (m, 1H), 4.93 (d, $J = 10.5$ Hz, 1H), 4.81 (td, $J = 10.8, 2.8$ Hz, 1H) 2.62 (s, 3H), 2.34-2.19 (m, 1H), 1.99 (dq, $J = 7.4, 7.4$ Hz, 2H), 1.83-1.75 (m, 1H), 1.45-1.37 (m, 2H), 1.22 (s, 9H), 0.93 (t, $J = 7.5$ Hz, 3H); ¹³C NMR (100 MHz, CDCl₃) ppm 153.7, 144.8, 134.0, 133.9, 129.6, 129.3, 126.1, 80.6, 70.2, 27.9, 26.4, 22.8, 21.6, 20.5, 14.2; HRMS (ESI): Exact mass calcd for C₁₉H₂₉NNaO₄S [M+Na]⁺ 390.1715, found 390.1707.



***tert*-Butyl (3-ethoxy-1-tosylpropyl)carbamate (S7).** Prepared according to the general procedure using *tert*-butyl carbamate (585 mg, 5.0 mmol), *p*-toluenesulfinic acid sodium salt (1.95 g, 10.0 mmol), 3-ethoxypropanal (765 mg, 7.5 mmol), formic acid (0.4 mL, 10.0 mmol), MeOH (5 mL) and H₂O (10 mL). Filtration yielded the α -amidosulfone as a white solid (1.45 g, 81%). $R_f = 0.16$ (20% EtOAc/hexanes); IR (film) 3345, 2978, 2930, 1716, 1598, 1518 cm^{-1} ; ¹H NMR (400 MHz, CDCl₃) δ 7.79 (d, $J = 8.1$ Hz, 2H), 7.32 (d, $J = 8.0$ Hz, 2H), 5.28 (d, $J = 10.2$ Hz, 1H), 5.00 (td, $J = 10.0, 3.7$ Hz, 1H), 3.70-3.58 (m, 2H), 3.49-3.42 (m, 2H), 2.53-2.47 (m, 1H), 2.41 (s, 3H), 2.06-1.98 (m, 1H), 1.23 (s, 9H), 1.17 (t, $J = 7.0$ Hz, 3H); ¹³C NMR (100 MHz, CDCl₃) ppm 153.7, 144.8, 134.0, 129.7, 129.4, 80.5, 68.9, 66.5, 66.1, 28.0, 27.2, 21.6, 15.0; HRMS (ESI): Exact mass calcd for C₁₇H₂₇NNaO₅S [M+Na]⁺ 380.1508, found 380.1504.

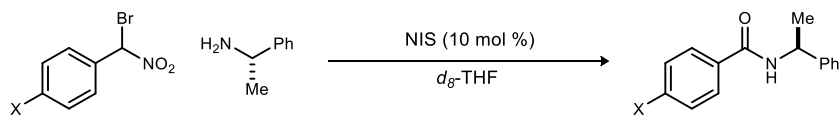


***tert*-Butyl (1-tosylhex-5-yn-1-yl)carbamate (S8).** Prepared according to the general procedure using *tert*-butyl carbamate (2.34 g, 20.0 mmol), *p*-toluenesulfinic acid sodium salt (7.80 g, 40.0 mmol), hex-5-ynal (1.92 g, 20.0 mmol), formic acid (1.6 mL, 40.0 mmol), MeOH (20 mL) and H₂O (40 mL). Filtration yielded the α -amidosulfone as a white solid (3.29 g, 47%). $R_f = 0.28$ (20% EtOAc/hexanes); IR (film) 3305, 2976, 2934, 1715, 1597, 1517 cm^{-1} ; ¹H NMR (400 MHz, CDCl₃) δ 7.77 (d, $J = 8.2$ Hz, 2H), 7.31 (d, $J = 8.1$ Hz, 2H), 5.03 (d, $J = 10.8$ Hz, 1H), 4.82 (td, $J = 10.8, 3.5$ Hz, 1H), 2.40 (s, 3H), 2.38-2.18 (m, 3H), 1.97 (t, $J = 2.6$ Hz, 1H), 1.91-1.59 (m, 3H), 1.21 (s, 9H); ¹³C NMR (100 MHz, CDCl₃) ppm 153.8, 144.9, 133.8, 129.7, 129.3, 83.0, 80.7, 70.3, 69.4, 27.9, 25.6, 24.3, 21.6, 17.9; HRMS (ESI): Exact mass calcd for C₁₈H₂₅NNaO₄S [M+Na]⁺ 374.1402, found 374.1386.



***tert*-Butyl (3-(4-methoxyphenyl)-1-tosylpropyl)carbamate (S9).** Prepared according to the general procedure using *tert*-butyl carbamate (585 mg, 5.0 mmol), *p*-toluenesulfinic acid sodium salt (1.95 g, 10.0 mmol), 3-(4-methoxyphenyl)propanal (820 mg, 5.0 mmol), formic acid (0.4 mL, 10.0 mmol), MeOH (5 mL) and H₂O (10 mL). Filtration yielded the α -amidosulfone as a white solid (970 mg, 46%). R_f = 0.32 (20% EtOAc/hexanes); IR (film) 3430, 2953, 1640, 1513 cm⁻¹; ¹H NMR (400 MHz, CDCl₃) δ 7.75 (d, J = 8.3 Hz, 2H), 7.31 (d, J = 8.1 Hz, 2H), 7.08 (d, J = 8.6 Hz, 2H), 6.82 (d, J = 8.6 Hz, 2H), 4.95 (d, J = 10.8 Hz, 1H), 4.79 (td, J = 10.9, 3.2 Hz, 1H), 3.78 (s, 3H), 2.84-2.77 (m, 1H), 2.70-2.62 (m, 1H), 2.58-2.48 (m, 1H), 2.40 (s, 3H), 2.06-1.96 (m, 1H), 1.23 (s, 9H); ¹³C NMR (100 MHz, CDCl₃) ppm 158.2, 153.7, 144.8, 133.8, 131.8, 129.7, 129.4, 129.3, 114.0, 80.7, 70.2, 55.2, 30.6, 28.4, 27.9 21.6; HRMS (ESI): Exact mass calcd for C₂₂H₂₉NNaO₅S [M+Na]⁺ 442.1664, found 442.1657.

General procedure for determination of initial rate: Bromonitroalkane (1.0 equiv., 100 μmol) was dissolved in 0.5 mL d_8 -THF in a vial. NIS (0.1 equiv., 10 μmol) and CH_2Br_2 (0.5 equiv., 50 μmol) (internal standard) were added to the vial. The solution was transferred to an NMR tube. (*S*)- α -methyl benzylamine (3.0 equiv., 300 μmol) was added to the NMR tube, which was immediately placed in NMR spectrometer. The reaction was monitored by NMR every 5 min for 1 h charting the yield of amide. Data was collected twice for each substrate. The percent yield of amide was plotted against time. The slope of the line was used as the initial rate (k) of the reaction.



X	run 1 k	run 2 k	avg. k	$\log(k_x/k_h)$	σ
OMe	0.124	0.148	0.136	0.114	-0.27
Me	0.112	0.116	0.114	0.0375	-0.17
H	0.0941	0.115	0.105	0	0.0
Cl	0.0808	0.0929	0.0869	-0.0805	0.23
CF_3	0.0611	0.0622	0.0617	-0.229	0.54
CN^*	0.0889	0.0286	0.0567	-0.265	0.66
NO_2	0.0424	0.0329	0.0377	-0.443	0.78

*a third set of data was collected for this substrate: $k = 0.0527$

